

# LOAN DOCUMENT

PHOTOGRAPH THIS SHEET

AD-A262 023



DTIC ACCESSION NUMBER

LEVEL



INVENTORY

AEOSR-YR-93-0125

DOCUMENT IDENTIFICATION

Dec 92

~~DISTRIBUTION STATEMENT~~

Approved for public release  
Distribution Unlimited

DISTRIBUTION STATEMENT

ACCESSION BY

NTIS ☒ GRAB

DTIC ☐ TRAC

UNANNOUNCED

JUSTIFICATION

BY

DISTRIBUTION/

AVAILABILITY CODES

DISTRIBUTION

AVAILABILITY AND/OR SPECIAL

A-1

DISTRIBUTION STAMP

**DTIC**  
**ELECT**  
**MAR 10 1993**  
**S C D**

DATE ACCESSIONED

DATE RETURNED

98 3 10 009

DATE RECEIVED IN DTIC

93-05127



REGISTERED OR CERTIFIED NUMBER

PHOTOGRAPH THIS SHEET AND RETURN TO DTIC-FDAC

H  
A  
N  
D  
L  
E  
  
W  
I  
T  
H  
  
C  
A  
R  
E

# REPORT DOCUMENTATION PAGE

1. AGENCY USE ONLY (Leave blank)

28 Dec 92

Annual 1 Sep 91 - 31 Aug 92

3. TITLE AND SUBTITLE

1992 Summer Faculty Research Program (SFRP)  
Volumes 1 - 16

F49620-90-C-0076

V-15

Mr Gary Moore

4. PERFORMING ORGANIZATION NAME(S) AND ADDRESS(ES)

Research & Development Laboratories (RDL)  
5800 Uplander Way  
Culver City CA 90230-6600

AFOSR-77 00 01 95

5. MONITORING AGENCY NAME(S) AND ADDRESS(ES)

AFOSR/NI  
110 Duncan Ave., Suite B115  
Bldg 410  
Bolling AFB DC 20332-0001  
Lt Col Claude Cavender

6. SUPPLEMENTARY NOTES

7. DISTRIBUTION AVAILABILITY STATEMENT

UNLIMITED

8. ABSTRACT (Maximum 200 words)

The purpose of this program is to develop the basis for continuing research of interest to the Air Force at the institution of the faculty member; to stimulate continuing relations among faculty members and professional peers in the Air Force to enhance the research interests and capabilities of scientific and engineering educators; and to provide follow-on funding for research of particular promise that was started at an Air Force laboratory under the Summer Faculty Research Program.

During the summer of 1992 185 university faculty conducted research at Air Force laboratories for a period of 10 weeks. Each participant provided a report of their research, and these reports are consolidated into this annual report.

9. SUBJECT TERMS

10. SECURITY CLASSIFICATION OF REPORT

UNCLASSIFIED

11. SECURITY CLASSIFICATION OF THIS PAGE

UNCLASSIFIED

12. SECURITY CLASSIFICATION OF ABSTRACT

UNCLASSIFIED

UL

13. DISTRIBUTION STATEMENT

UNITED STATES AIR FORCE  
SUMMER RESEARCH PROGRAM -- 1992  
HIGH SCHOOL APPRENTICESHIP PROGRAM (HSAP) REPORTS

VOLUME 15  
WRIGHT LABORATORY

RESEARCH & DEVELOPMENT LABORATORIES  
5800 Uplander Way  
Culver City, CA 90230-6608

Program Director, RDL  
Gary Moore

Program Manager, AFOSR  
Lt. Col. Claude Cavender

Program Manager, RDL  
Billy Kelley

Program Administrator, RDL  
Gwendolyn Smith

Submitted to:

AIR FORCE OFFICE OF SCIENTIFIC RESEARCH  
Bolling Air Force Base  
Washington, D.C.  
December 1992

## PREFACE

This volume is part of a 16-volume set that summarizes the research accomplishments of faculty, graduate student, and high school participants in the 1992 Air Force Office of Scientific Research (AFOSR) Summer Research Program. The current volume, Volume 15 of 16, presents part one of the final research reports of high school (HSAP) participants at Wright Laboratory.

Reports presented herein are arranged alphabetically by author and are numbered consecutively -- e.g., 1-1, 1-2, 1-3; 2-1, 2-2, 2-3. Research reports in the 16-volume set are organized as follows:

VOLUME	TITLE
1	Program Management Report
2	Summer Faculty Research Program Reports: Armstrong Laboratory
3	Summer Faculty Research Program Reports: Phillips Laboratory
4	Summer Faculty Research Program Reports: Rome Laboratory
5A	Summer Faculty Research Program Reports: Wright Laboratory (part one)
5B	Summer Faculty Research Program Reports: Wright Laboratory (part two)
6	Summer Faculty Research Program Reports: Arnold Engineering Development Center; Civil Engineering Laboratory; Frank J. Seiler Research Laboratory; Wilford Hall Medical Center
7	Graduate Student Research Program Reports: Armstrong Laboratory
8	Graduate Student Research Program Reports: Phillips Laboratory
9	Graduate Student Research Program Reports: Rome Laboratory
10	Graduate Student Research Program Reports: Wright Laboratory
11	Graduate Student Research Program Reports: Arnold Engineering Development Center; Civil Engineering Laboratory; Frank J. Seiler Research Laboratory; Wilford Hall Medical Center
12	High School Apprenticeship Program Reports: Armstrong Laboratory
13	High School Apprenticeship Program Reports: Phillips Laboratory
14	High School Apprenticeship Program Reports: Rome Laboratory
15	High School Apprenticeship Program Reports: Wright Laboratory
16	High School Apprenticeship Program Reports: Arnold Engineering Development Center; Civil Engineering Laboratory



## 1992 HIGH SCHOOL APPRENTICESHIP REPORTS

### Wright Laboratory

<u>Report Number</u>	<u>Report Title</u>	<u>Author</u>
1	Summer Research Including Hypermedia Documents	Lori L. Anderson
2	Monte Carlo Star Detectability and Micro-G Calibration Studies	Eric A. Apfel
3	Video Documentation of EPIC Capabilities	Jennifer R. Bautista
4	Evaluation of the Sensitivity and Performance of Insensitive Composite Booster Explosives	Brad Blanchard
5	Expanded Study of Computer Software and Inventory Control	J. Stacey Bond
6	Inventory Control for the Solid State Electronics Directorate	Helen Chou
7	The Creation of an Automatic Electronic Monitoring System	Claudius W. Christmas, Jr.
8	Wrap-Around Fins	Theresa J. Cook
9	A Study of Heat Transfer Simulation and Simulation Software User-Friendliness	Gerald Dalley
10	Development of a Pressure Transducer Calibration Device	Elizabeth C. Day
11	Fractal Geometry: An Explanation and Application	Lesha Denega
12	Automated Testing of High Performance Heterojunction Bipolar Transistors	Christopher Dodsworth
13	Geometric Modeling and Finite Element Mesh Generation Using PATRAN	Thomas J. Fraites, Jr.
14	Reflections of Ramjet Research	Kimberly A. Frank
15	A Model of the Operating Temperature Range of Ester-Based Lubricants	Erin Lynn Glaser
16	Stress Gage Algorithm Development	Daniel R. Grayson
17	Flow Visualization of a Jet in a Crossflow	Amy Hancock
18	High Surface Area Conductive Polymers	Deanna Harrison
19	A Study of the Fragmentation of Graphite/Epoxy Panels Under High Velocity Impact	Steven R. Hart
20	A Study of an Unbalanced Shaft due to Oil Leakage	David B. Hartsock
21	Infrared Laser Polarimetry	Chad Houghton
22	Development of a Graphical User Interface for the AVATAR/ESP Simulation	John H. Kahrs

## Wright Laboratory (cont'd)

<u>Report Number</u>	<u>Report Title</u>	<u>Author</u>
23	An Investigation of the APTAS System	Daniel A. Kelley
24	Evaluation of Hydrocode Strain Contours by Microhardness testing	Jason A. Kitchen
25	A Study of the C and BASIC Computer Languages as well as an In Depth Discussion of Certain Mathematical Concepts	Barry J. Koestler II
26	Electrical Analysis of $\text{YBa}_2\text{Cu}_3\text{O}_{7-x}$ Superconducting Thin Films and Bulk Samples	Peter G. Kozlowski
27	Computer Resources: Examining the Workings of a Computer Network	Daniel J. Kramer
28	Forced Liquid Cooling of a Non-Flush Simulated Electronic Chip	Joel Kulesa
29	Using Mathematical Concepts to Produce Three Dimensional Computer Graphics	Allen L. Lefkovitz
30	Image Analysis: A Fractal Application	Jason Eric Lindsey
31	Analysis of Fractal Image Compression and Decompression	Daran J. Mason
32	Video Documentation of the Patran to Epic Link	Elliott Moore II
33	Construction and Design of a Regulated Power Supply	Robert Baird Murray, IV
34	Preparing High Tech Aircraft for Testing	Thomas M. Owsley
35	Using Computer Applications	M. Cristina Pacheco
36	The Creation of a Graphics Workstation	Eric J. Powers
37	A Comparison of Concept Recognition Skills	Melvin K. Richardson
38	Characterization and Analysis of 1,3,5,5-Tetranitrohexahydropyrimidine	David A. Rosenbaum
39	A Study of the Importance of Sled Tests to Crew Escape Engineers	Kimberly D. Royalty
40	A Second Year Study on the Implementation of the Recirculating Optic Delay Line Concept in a Coherent Radar System	Dennis W. Scott, Jr.
41	Discovering and Exploring Supercritical Fluid Chromatography	Tiffany M. Selmon
42	From Thermocouples to Multi-Million Dollar Chunks of Titanium Matrix Composite	Jonathan D. Servaites
43	Using Computers for IP-3 Intermodulation Analysis	Michael A. Shaffer

## Wright Laboratory (cont'd)

<u>Report Number</u>	<u>Report Title</u>	<u>Author</u>
44	A Mass Spectroscopic Study of Diamond Growth for Low-Pressure Chemical Vapor Deposition	David J. Spry
45	Sensor Computation Analysis	Christina M. Trossbach
46	GaAs Ohmic Contacts at High Currents	Darcie Tutin
47	Evaluation of Engineering and Scientific Software Tools for Use in Electronic Warfare and Digital Signal Processing Applications	David L. Watson
48	The Temperature Dependence of Intrinsic Defect Levels in GaAs Semiconductors	Jeffrey A. Yerian
49	Software Development for the Aerosol Test Chamber	James E. Youngblood

SUMMER RESEARCH  
INCLUDING HYPERMEDIA DOCUMENTS

Lori L. Anderson

Final Report for:  
Summer Research Program  
Avionics Laboratory

Sponsored by:  
Air Force Office of Scientific Research  
Bolling Air Force Base, Washington, D.C.

August 1992

SUMMER RESEARCH  
INCLUDING HYPERMEDIA DOCUMENTS

Lori L. Anderson

Abstract

The following report is a description of the work I performed during my participation in the Air Force Office of Scientific Research (AFOSR) High School Apprenticeship Program. During my second summer of employment at Wright-Patterson Air Force Base (WPAFB), I worked with a number of software packages, including word processors, spreadsheets and graphics packages. These software packages were hosted on a Gateway 2000 80486 personal computer. In addition, I utilized hypermedia software packages on both the 486 computer and a Macintosh Iix and evaluated the usability of these packages. I also resumed an empirical study of the Ada programming language which I had commenced during my previous summer of employment at WPAFB. The Ada compiler I used for this effort was the Digital Equipment Corporation (DEC) Ada Compiler, hosted on a DEC VAX computer.

## SUMMER RESEARCH INCLUDING HYPERMEDIA DOCUMENTS

Lori L. Anderson

### INTRODUCTION

My first summer of employment at Wright Laboratory (WL) Avionics Directorate had been educational, both from the standpoint of practical experience that I gained from using various computer systems and software packages, and from the ability of programming in a computer language which I acquired during the apprenticeship. I consequently applied for a second summer of employment, with the understanding that I would work again with the same mentor, Marc Pitarys in the Software Concepts Group of the Avionics Logistics Branch (WL/AAAF). Upon my arrival, I discovered that the office had traded their Zenith 80286 microcomputers for new 486s, complete with windows and software with which I was unfamiliar. I therefore was able to learn to use many new commercial software packages, such as word processors and spreadsheet software which were superior to the programs I had used last summer. I also continued to learn the Ada programming language which I had studied during my first summer of employment. My main objective for the summer was to learn and evaluate hypermedia software which is currently being tested for use in avionics documentation applications.

### DISCUSSION

I quickly became aware of the short life of technology and the ever present need for improvement in both software and hardware when I used the 486 system for the first time. The most notable difference in the computer systems which I had used last year and the new systems which were installed was the ease of executing functions. I had not worked with

Microsoft Windows before and was amazed at the increase in access which this program enabled. I discovered that the elimination of manually typed commands not only conserves time, but also eliminates much frustration over misplaced files.

My previous experiences with word processors had included Wordstar and WordPerfect, with my preference being WordPerfect, because of the feature of pulldown menus. The word processor currently being used in the office is AmiPro, and I had to re-orient myself to the commands and features of this new software. I found that AmiPro was preferable to either of the programs I had previously used, merely because it was much more simple to operate. The availability of many options and ease of accessing them with either pulldown menus or displayed icons was far superior to either WordPerfect or WordStar.

I also became aware of the inferiority of the spreadsheet and presentation software which I had previously used. My previous experiences with Quattro Pro, creating spreadsheets that would calculate and chart the billings, payments and earnings of various contractors, were simplified by the availability of Lotus 1-2-3 for windows. The quality of output and ease of construction of presentation materials created using Freelance was also significantly superior to that of Harvard Graphics, which I had used on the 286 computer.

The utilization of a program called Expert Animator also introduced me to the basics of computer graphics and animation. This software enabled the user to create a series of drawings of an object, or 'sprite', which when combined and cycled in sequence appeared to make the drawing move. The program, while rather simple, still offered the basic ability of animation, and presented the user with a glimpse into the world of computer graphics.

During my previous summer of apprenticeship, I had spent the majority of my time programming in the Ada computer language. I had learned the history and basics of the language and utilized a VAX networking system to create programs with the use of the Language Sensitive Editor (LSE). I was later introduced to functions and packages and thus

was able to write more complicated routines such as the game of NIM, a random number generator using the linear congruence method, and programs using Newton's method to compute a square root and the root of any polynomial equation. Although not I did not focus on programming this summer, I continued to study and create programs in the Ada language.

The most interesting program that I wrote used a modification of the Gaussian Elimination Method to solve a series of simultaneous linear equations. The use of a computer in such a calculation can be time conserving, but also inaccurate, because of the computer's representation of floating point numbers. Not all floating point numbers can be precisely described in binary. As a result, numbers are rounded or truncated to a specific number of significant digits. This process causes the computer to be unable to distinguish between zero and numbers very close to zero. In an effort to minimize the error due to roundoff, the Gaussian Elimination Method was modified for use in this program. Given a set of equations such as the one below,

$$A_1x + B_1y + C_1z = a$$

$$A_2x + B_2y + C_2z = b$$

$$A_3x + B_3y + C_3z = c$$

these can be represented in matrix notation as  $Ax = b$ , where

$$A = \begin{bmatrix} A_1 & B_1 & C_1 \\ A_2 & B_2 & C_2 \\ A_3 & B_3 & C_3 \end{bmatrix} \quad x = \begin{bmatrix} x \\ y \\ z \end{bmatrix} \quad b = \begin{bmatrix} a \\ b \\ c \end{bmatrix}$$

The goal of the Gaussian elimination method is to perform operations on A in order to obtain the values of the Identity matrix, I, where I is equal to

$$I = \begin{bmatrix} 1 & 0 & 0 \\ 0 & 1 & 0 \\ 0 & 0 & 1 \end{bmatrix}$$



The first step in the modified Gaussian Elimination Method is to identify the pivot equation, or equation in which the specified variable has the highest absolute value. For example, if the value of the coefficient  $A_2$  in  $A$  were higher than that of either  $A_1$  or  $A_3$ , the second row would be interchanged with the first row to place  $A_2$  in the pivot position, yielding

$$\begin{array}{ccc} A_2 & B_2 & C_2 \\ A_1 & B_1 & C_1 \\ A_3 & B_3 & C_3 \end{array}$$

It is necessary that the coefficient of  $x$  in the pivot equation is equal to 1 in order to achieve the desired identity matrix. This is accomplished by dividing the row one by the pivot coefficient, obtaining

$$\begin{array}{ccc} 1 & (B_2/A_2) & (C_2/A_2) \\ A_1 & B_1 & C_1 \\ A_3 & B_3 & C_3 \end{array}$$

The first row is then multiplied by  $A_1$ , the coefficient of  $x$  in the second row, and the resulting equation is subtracted from the line two, thus eliminating  $x$  from this line. The first row is then multiplied by the coefficient of  $x$  in line three,  $A_3$ , and the resulting equation is subtracted from the third row, thus eliminating  $x$  from line three. The resulting matrix is

$$\begin{array}{ccc} 1 & (B_2/A_2) & (C_2/A_2) \\ 0 & (B_1 - A_1 B_2/A_2) & (C_1 - A_1 C_2/A_2) \\ 0 & (B_3 - A_3 B_2/A_2) & (C_3 - A_3 C_2/A_2) \end{array}$$

The second row now becomes the pivot equation, with  $(B_1 - A_1 B_2/A_2)$  being the pivot coefficient. The procedure is repeated in order to eliminate the variable  $y$  from rows one and three, and the process is repeated for the number of variables which the set of equations contains. In this example the number of variables is three. Finally, the identity matrix is achieved, and the equation  $Ax = b$  yields the values for the variables  $x$ ,  $y$  and  $z$  by matrix multiplication.

My main project for the eight weeks of employment was to learn and evaluate several hypertext and hypermedia software packages. Hypertext enables the construction of documents in multi-level 'stacks', in which each level offers the option of viewing more detailed

Information pertaining to a topic discussed in the current level. Hypertext software packages, such as HyperCard, also offer the option of cross referencing text within a document. Hypertext offers a template in which to store data electronically, while maintaining and expanding on the ease of access of a book or reference manual using familiar features such as an outline, index, glossary and table of contents. Hypermedia also has the ability to enable access between sections of text, but can include other types of media such as movies and sound. The SuperCard software package generates an environment in which the user is able to create hypermedia applications using a variety of tools. One particular application in SuperCard which I worked with was Knowledge Information Technology (KIT), which allows the user to transfer existing text and digital information to hypermedia documents. Within KIT, the reader has the option of viewing a laser disc movie as a supplement to the text by simply clicking on a window. Hypermedia and hypertext software enables the user to quickly and correctly access information from any section of a document by scrolling on the monitor or using the mouse. In the future, hypermedia documents have the potential to become commonplace alternatives to the mass of information available in books and reference manuals.

## CONCLUSION

When I decided to work in the Software Concepts Group for another summer, I realized that I would gain valuable computer-related experience which would be useful in college and in the workplace. I had no expectations that my experiences would apply to the major which I have decided to study in college, environmental engineering. From my viewpoint, computers utilized tremendous quantities of paper and created a large mass of paper waste, and therefore were causing environmental problems. Throughout my study of hypermedia documents, I realized that the electronic representation of information

which this software enables is in many ways superior to traditional methods of documentation, such as books and reference materials. Not only does electronic documentation allow easier access to information, but it also enables rapid transfer of materials through electronic mailing networks. Because this method is paperless, the damage caused to the environment by the production and disposal of paper is eliminated. In effect, computers allow the entire world to become a small community in which all resources can be easily utilized and conserved.

Monte Carlo Star Detectability & Micro-G Calibration Studies

Eric A. Apfel  
High School Apprentice  
Guided Interceptor Technology Branch

Wright Laboratory Armament Directorate  
WL/MNSI  
Eglin AFB, FL 32542-5434

Final Report for:  
High School Apprenticeship Program  
Wright Laboratory Armament Directorate

Sponsored by:  
Air Force Office of Scientific Research  
Bolling Air Force Base, Washington, D.C.

August 1992

## Monte Carlo Star Detectability & Micro-G Calibration Studies

Eric A. Apfel  
High School Apprentice  
Guided Interceptor Technology Branch  
WL/MNSI

### Abstract

Several programs were written to determine whether various startracker sensor designs, at any point in their orbit around the earth, will be able to detect a sufficient number of stars. The known locations of these stars would then be used to correct the heading of host guided projectiles if necessary. Another program was developed to calibrate an accelerometer in a micro-gravity environment with the aid of a Kalman filter. The program filtered out measurement noise and random acceleration noise to determine the actual accelerometer bias error. Both tasks serve to aid the guidance and navigation of interceptors such as a ground-based kinetic energy weapon. The positive results received from the programs provides incentive for further studies.

# Monte Carlo Star Detectability & Micro-G Calibration Studies

Eric A. Apfel

## Introduction

Stellar navigation (using the stars to determine attitude and position) continues to prevail as one of the most reliable methods for navigation aiding. Indeed, in exoatmospheric conditions, the stars are just about all a navigator can rely on for good reference. The studies detailed in this report support the guidance and navigation of a guided interceptor by the use of startrackers (such as MiniOWLS: the miniature optical wide-angle lens startracker) and by determining linear accelerometer bias errors. All work done is primarily in reference to ground-based kinetic energy weapons.

## Background

Before detailing this year's work as a high school apprentice, I will briefly describe last year's projects from which most of my work stemmed. Primarily, I modelled possible startracker designs by varying pertinent sensor design parameters: bandwidth, aperture area, transmission efficiency, quantum efficiency, dark current noise, signal integration time, pixel spread, and required signal to noise ratio. Using a star catalog consisting of over 240,000 stars, I determined exactly how many stars should be detectable for specific startracker designs. From this software I was able to determine sensitivities of these various sensor design parameters. Sensitivity plots are shown in figures 1-a, 1-b, and 1-c (note: the baseline values referenced are shown in table 1). The three separate charts (each differing only in quantum efficiency) may mislead some readers into believing that the sensitivity of quantum efficiency was of primary concern. In actuality, quantum efficiency does not have any more effect in star detection than, for example, transmission efficiency. The reason for the three charts is that a single baseline quantum efficiency could not be decided upon, so three quantum efficiencies were chosen as baseline values.

## Probability of Availability

To complement my previous star detectability studies, I implemented the second major aspect of stellar navigation: star availability. The original star detection programs tested the startracker sensor's ability to detect

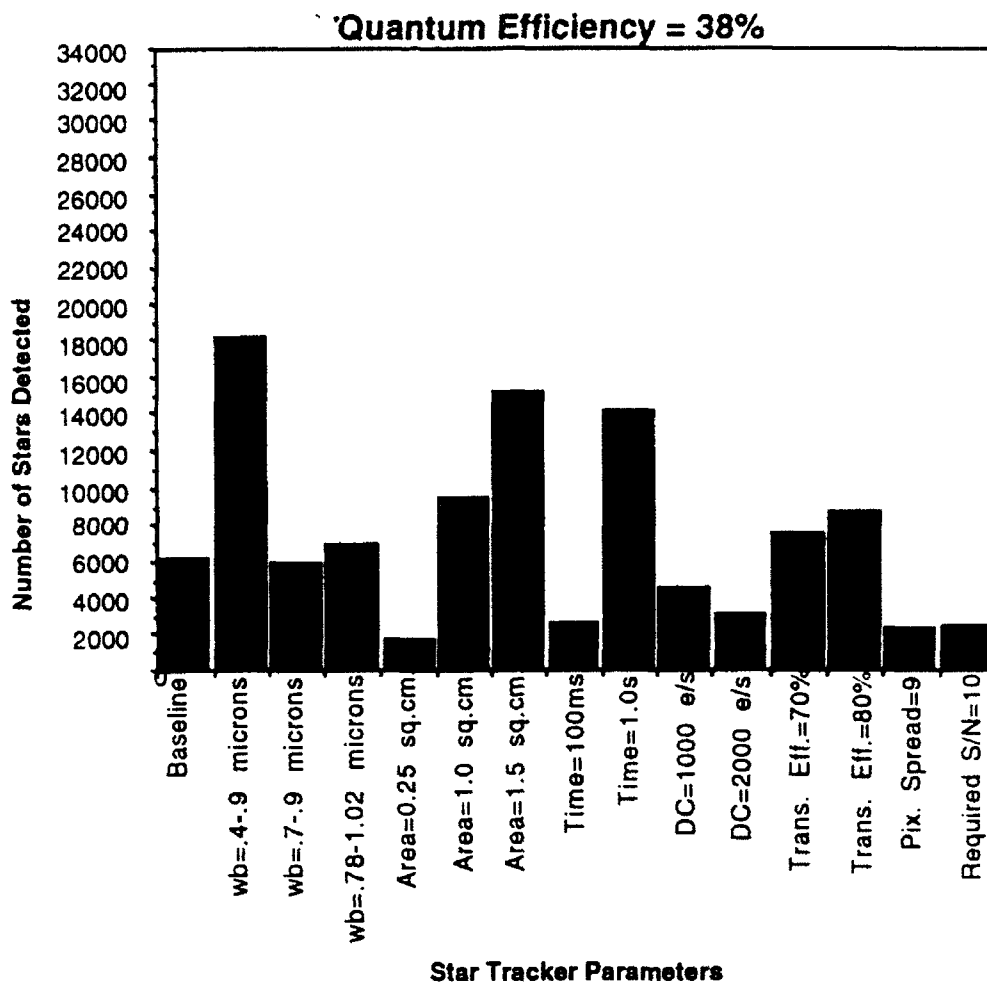


Figure 1-a

any of the stars in the celestial sphere. The updated software takes many more factors into consideration. First, the startracker is simulated in random positions in an orbit around the earth. The field of view of its telescopes (three telescopes in the case of MiniOWLS) is then clearly defined, limiting the available number of stars in the celestial sphere. Proximity of the sun and the moon is also taken into account (the extreme luminosity of these bodies in effect hides starlight within a certain distance: 20 arcseconds for the sun, and 5 arcseconds for the moon). The number of stars within this smaller catalog detected by the startracker is then counted, and a new random location is chosen. This process is continued until a total of 1000 locations (or "shots") has been chosen. Star scene simulation software was used to simulate this random process.

Two other programs use the information obtained from the random "shots"

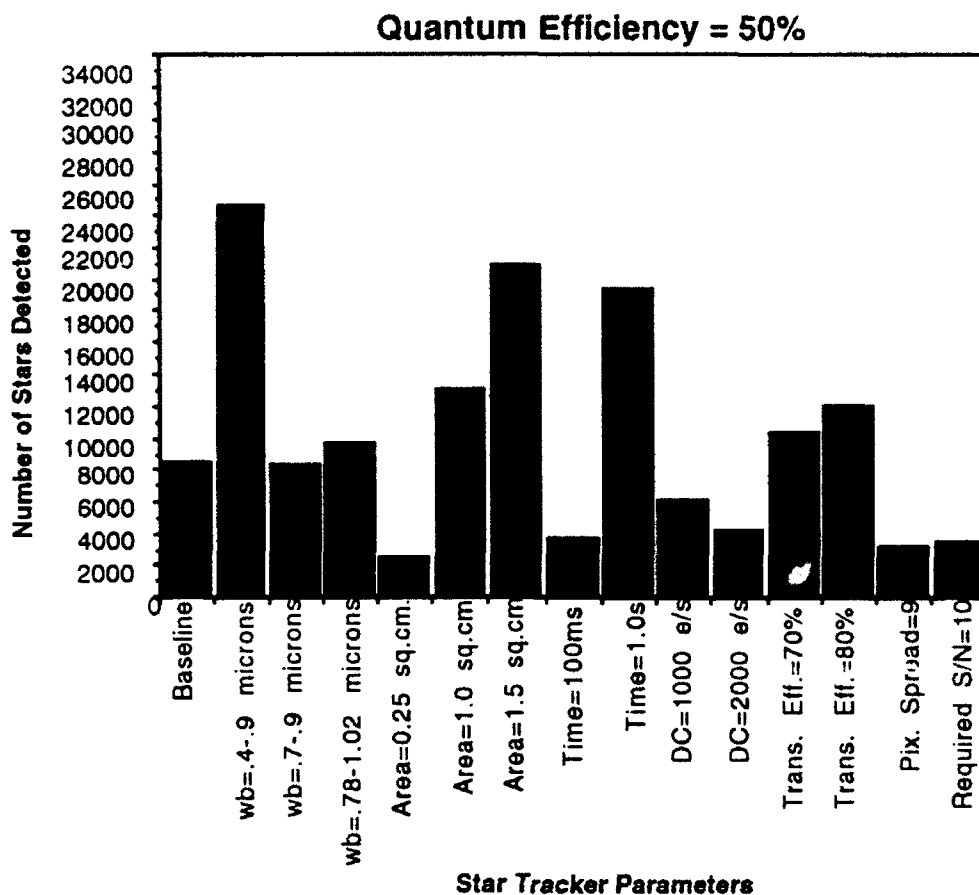


Figure 1-b

(number of possible detectable stars, magnitude of brightest star, right ascension, and declination) and determines both the probability of detecting a specific number of stars and the probability of detecting stars up to a specific magnitude (brightness). This step can be done simply by counting the total number of shots that detected a specific number of stars (or the total number of shots that detected stars up to a specific magnitude) and divide by 1000. Examples of the program output have been graphed in figure 2.  $P(N)$  refers to the probability of detecting a given number of stars and  $P(M_m)$  refers to the probability of detecting stars up to a given magnitude. The Monte Carlo study completed my work with the startracker sensor analysis, and I proceeded to another method of interceptor navigation.



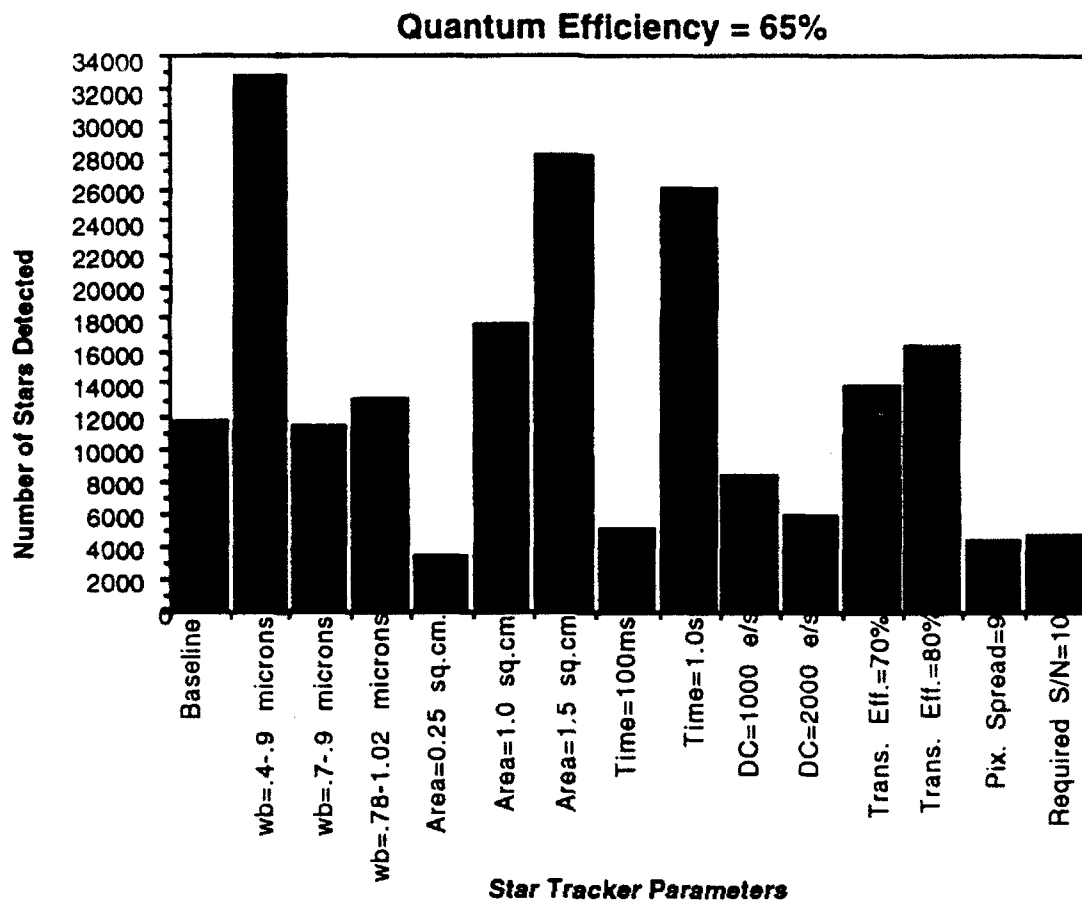


Figure 1-c

Baseline Parameters	
Waveband (wb)	.6-.8 microns
Aperture Area	.7 cm <sup>2</sup>
Signal Integration Time	300 milliseconds
Dark Current	500 e-/sec
Transmission Efficiency	60%
Pixel Spread	4
Required Signal to Noise Ratio	5.5

Table 1

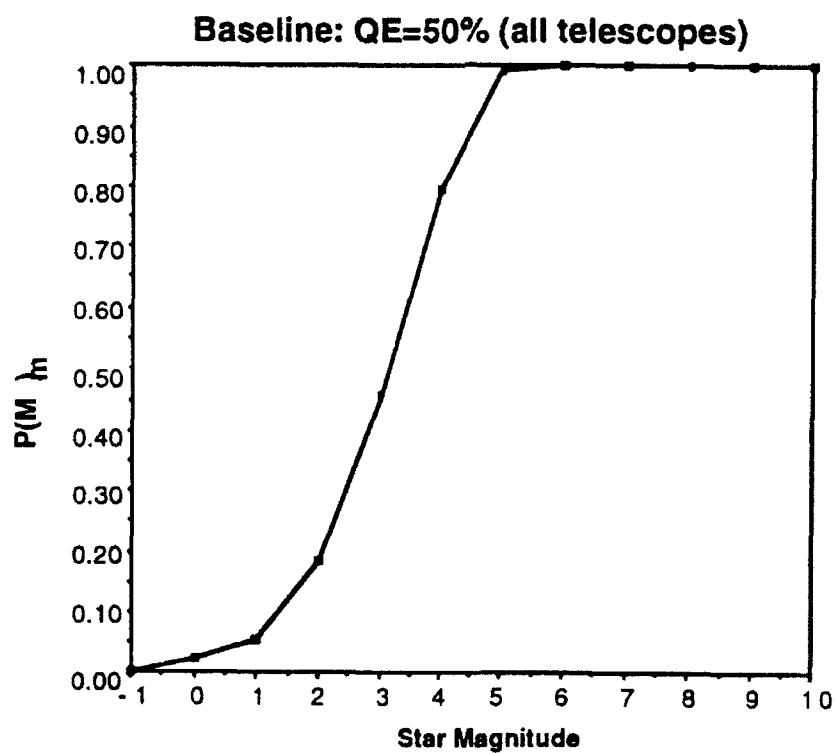
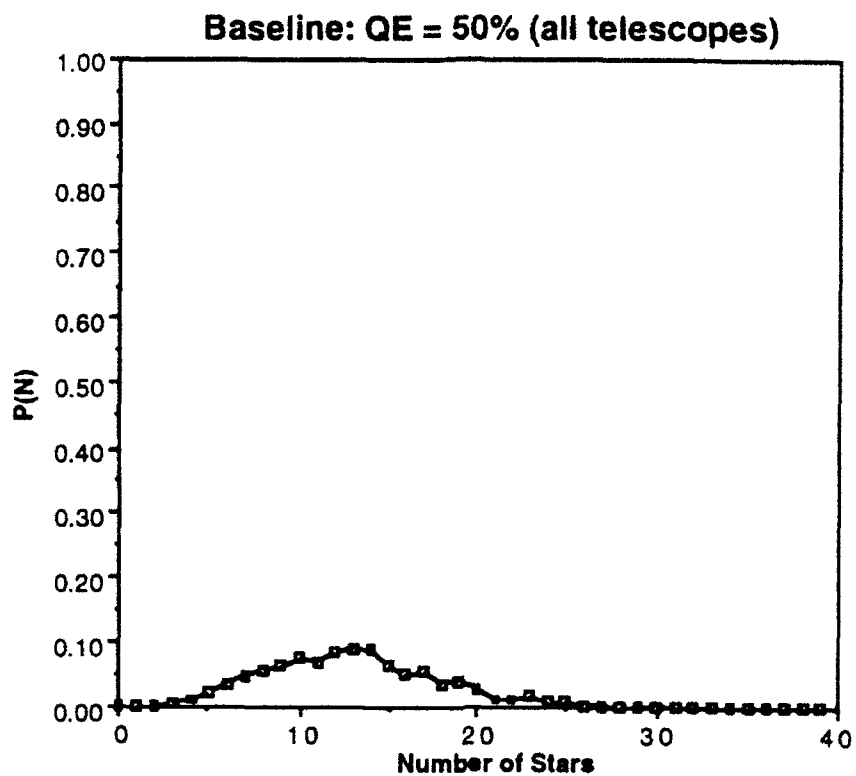


Figure 2

### Micro-G Calibration

Last year, I briefly wrote a program which modelled an interceptor's flight history as would be sensed by three gyros (for rotational acceleration measurement in three-dimensional space) and three accelerometers (for linear acceleration measurement). The program took several factors into account including force of thrust in each direction, the mass of the interceptor, and errors in accelerometer bias. While in ballistic exo-atmospheric flight, however, accelerometer bias is observable and may be calibrated even in the presense of measurement noise and random acceleration noise. A method was required to filter out the noise and home in on the bias error.

A Kalman filter was chosen to aid in the determination of accelerometer bias. I wrote a program which initially estimates the accelerometer bias error. It then reads the accelerometer measurement and updates the error state. Next, it loops back to the beginning and makes another estimate. This process continues a predetermined number of times. Studies were then performed to see how the Kalman filter would behave with a detuned process noise matrix. It managed to

#### **Accelerometer Bias Estimation Error vs. Time**

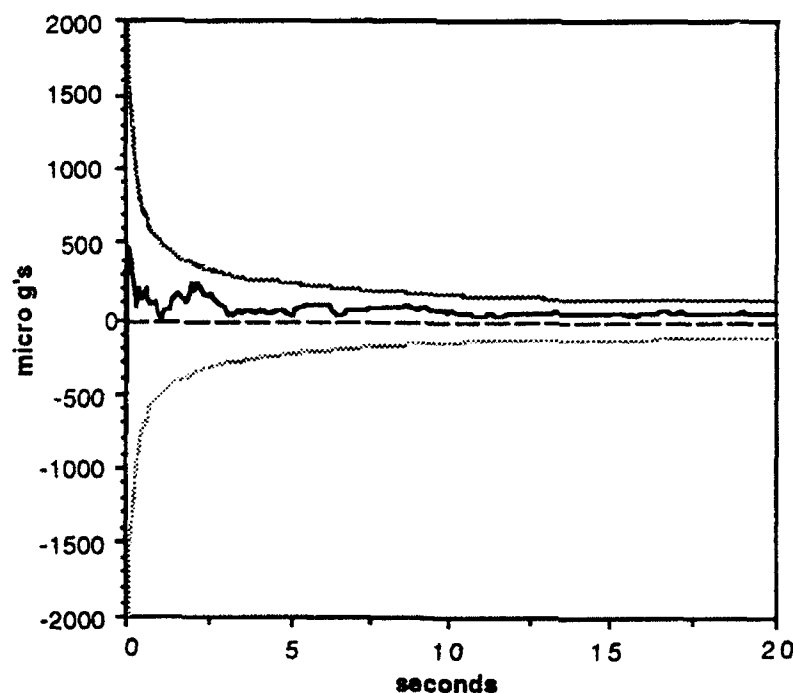


Figure 3

successfully converge in all cases (though the time to convergence depended on how tuned the process noise matrix was). Figure 3 shows an example of the iterated accelerometer bias error estimation error versus time. The two outer curves represent the third standard deviation of the estimation accuracy computed from the covariance matrix in the Kalman filter. Computer runs showed that the filter is stable and converges properly.

### Conclusion

The data accumulated throughout the summer was used to plot dozens of detailed graphs and charts, which serve not only to provide a visual reference of the programs' behavior, but also to compare with information received from other sources.

These studies also served to educate me further with the VAX/VMS environment. Extensive ForTran programming was useful for programming practice, although I did not have time to use C++ (a real language!). Using the Cray Supercomputer again was an enjoyable experience, though.

I also gained valuable experience in systems modelling and Kalman filtering (WOW!).

### Acknowledgements

To conclude this report I would like to thank the following who made a great impact upon my life:

My mentor Captain Tim Poth (the few times I saw him were a blast.), my other mentor Randy Wells (I really admire a full-fledged physicist, but I am going into computer science. Sorry!), Don Harrison (great program; you really did a lot to make it work.), Mike Deiler (who always was ready to think up new activities for the HSAP's), Mike Couvillon ("The answer is no, now what's the question."), Alice McRae (who had to hunt down us HSAP's cause we were never at our desk), Mel Nagel (for letting me use the MelMac), Ron Rapp (I loved the tour of KHILS), Clif Nees (love the hammer and dart gun), Rick Miller( never seen a bigger heavy metal fan), Mark McClure (you've got the greatest models and posters), Paul McCarley (I swear everytime I see your name plate it says Paul McCartney), Bob LeBeau (need I say more?), Daran Mason (we've worked together for two years!), Christina Trossbach (thanks for letting me listen to your CD's, thanks for the mail, etc. You won't have as much fun next year 'cause I won't be here.), John Henry Kahrs (love that middle name! Street Fighter II was interesting.), Jennifer Bautista (for the mail messages and letting me borrow her annual), Torrey Baines (no one else knows the VAX as well as we do. What more do you want?), Chad Houghton (had to put your name in here somewhere), Michael Coleman (my best friend, though you did ruin my life.), Kathryn Platt and Macon Harris (the FSU Salley Hall duo), Jonathan Roper (for making me feel smart at FSU), Megan Taylor (for putting up with Jonathan), Leslie Duers (for introducing me to the Cure. I keep forgetting to go to Big Kahunas), The Cure (of course I had to put y'all in here. The greatest, greatest, greatest group of all time. And I'm not just saying that.), Metallica (nice job with "Wherever I May Roam")., Lionel Richie (not!), OMD (if Christina likes them, they must be pretty good.), MTV (mostly trashy videos, but some aren't so bad.), Duff (for doing such a great job hosting MTV), Steve Isaacs (for doing an okay job hosting MTV), Michael Jackson (the "Jam" video is great, but get rid of Kris Kros), Weird Al Yankovic (great stuff.), Pop Tarts (my early morning breakfast), Burger King (love those employees on the night shift), Amy at Eglin Lane's lane 30 (sorry, don't know your last name. Wood, maybe?), Babbage's (just 'cause I know everybody who works there.), Peter

Norton (I couldn't live without Norton Utilities.), IBM (the best machines made.), Gene Roddenberry (Star Trek is the greatest TV show made. May your image live long and prosper), George Lucas and Steven Spielberg (get on the ball! I've been waiting forever for the Star Wars saga to continue.), Robin Williams (you're an outstanding actor and comedian!), Chevy Chase (Torrey recommended you.), Johnny Carson (you'll always be better than Jay Leno), Julia Roberts (great job in Hook!), Steven Seagal (my martial arts inspiration), my sister Sheryl (why did I put you in here?), my parents (can I borrow some money?), Research and Development Laboratories (thanks for the funding.).

Too bad this is my last year, because I'm going to miss it. This is Eric Apfel signing off.

## Appendix A: Algorithm for Accelerometer Bias Estimation

Note: The following was extracted from a memo entitled "Introduction to Kalman Filtering and Accelerometer Bias Error Estimation in a Micro-Gravity Environment" written by Randy Wells.

### I. Initialization

Set initial values for:

- $\Delta v_0$  (initial filter velocity error)
- $\Delta a_{B0}$  (initial filter accelerometer bias error)

Set constant values for:

- LSB (incremental velocity represented by one pulse)
- $\sigma_Q$  (compute  $\sigma_Q = \frac{LSB}{\sqrt{12}}$ )
- $\sigma_{VRW}$  (standard deviation of velocity random walk)
- $\sigma_{RA}$  (compute  $\sigma_{RA} = \frac{\sigma_{VRW}}{\sqrt{T_S}}$ )
- $a_{TRUE}$  (true acceleration)
- $\Delta a_{BTRUE}$  (actual accelerometer bias error)
- (filter sampling period)

Initialize Kalman filter matrices and vectors:

$$X_0 = \begin{bmatrix} \Delta v_0 \\ \Delta a_{B0} \end{bmatrix} \quad \Phi = \begin{bmatrix} 1 & T_S \\ 0 & 1 \end{bmatrix} \quad H = [1 \ 0]$$

$$R = \sigma_Q^2 \quad P_0 = \begin{bmatrix} (\Delta v_0)^2 & 0 \\ 0 & (\Delta a_{B0})^2 \end{bmatrix} \quad Q = \begin{bmatrix} T_S(\sigma_{VRW})^2 & 0 \\ 0 & 0 \end{bmatrix}$$

### II. Simulation of Accelerometer (Computation of $\Delta V$ )

Draw a random (Gaussian) acceleration noise data point,  $\eta_{RA}$ , with standard deviation,  $\sigma_{RA}$ .

Draw a random (Gaussian) measurement noise data point,  $\eta_Q$ , with standard deviation,  $\sigma_Q$ .

Compute  $\Delta V$ :

$$\Delta V = (a_{TRUE} + \Delta a_{BTRUE} + \eta_{RA}) * T_S + \eta_Q$$

### III. Simulation of Kalman Filter

Propagate the Error State Estimate Vector:

$$\mathbf{X}_{k/k-1} = \Phi \mathbf{X}_{k-1/k-1}$$

Propagate the Error Covariance Matrix:

$$\mathbf{P}_{k/k-1} = \Phi \mathbf{P}_{k-1/k-1} \Phi^T + \mathbf{Q}$$

where  $\mathbf{P}_{k-1/k-1}$  is the updated error covariance at the previous iteration.

Update the Kalman Gain Matrix:

$$\mathbf{K}_k = \mathbf{P}_{k/k-1} \mathbf{H}^T (\mathbf{H} \mathbf{P}_{k/k-1} \mathbf{H}^T + \mathbf{R})^{-1}$$

Update the Error State Estimate Vector:

$$\mathbf{X}_{k/k} = \mathbf{X}_{k/k-1} + \mathbf{K}_k (\mathbf{Z}_k - \mathbf{H} \mathbf{X}_{k/k-1})$$

where  $\mathbf{X}_{k/k}$  is the updated error state vector estimate at the previous iteration and  $\mathbf{Z}_k$  is the current accelerometer measurement,  $\Delta V$ .

Update the Error Covariance Matrix:

$$\mathbf{P}_{k/k} = \mathbf{P}_{k/k-1} - \mathbf{K}_k \mathbf{H} \mathbf{P}_{k/k-1}$$

Extract  $\Delta a_B$  from  $\mathbf{X}_{k/k}$ :

$$\Delta a_B = \mathbf{X}_{k/k}(2)$$

Compute the Error in Accelerometer Bias Estimation:

$$\epsilon \Delta a_B = \Delta a_{B\text{TRUE}} - \Delta a_B$$

### IV. Reiteration

Begin simulation loop again (go back to step II).

(This step would usually include a condition to check to see if a predetermined number of iterations have been completed.)



Video Documentation of EPIC  
Capabilities

Jennifer R. Bautista  
High School Apprentice  
Warheads Branch  
Mentor: Mr. Mike Nixon

Wright Laboratory Armament Directorate  
WL/MNMW  
Eglin AFB, FL 32542-5434

Final Report for:  
High School Apprenticeship Program  
Wright Laboratory Armament Directorate

Sponsored by:  
Air Force Office of Scientific Research  
Bolling Air Force Base, Washington D.C.

August 1992

## Video Documentation of EPIC Capabilities

Jennifer R. Bautista  
High School Apprentice  
Warheads Branch  
Wright Laboratory Armament Directorate

### Abstract

I spent the summer working as a high school apprentice in the Computational Mechanics Section of the Warhead Branch (WL/MNMW) at the Wright Laboratory Armament Directorate on Eglin Air Force Base. I worked with Mr. Mike Nixon, my mentor, and a fellow apprentice, Elliot Moore II. My project for the summer was video documentation of EPIC capabilities. Using a Silicon Graphics Iris Indigo, I ran the EPIC code, created graphics using the RSCORS graphics program, captured the .rgb files, and then animated the files to create simulation videos of what the EPIC code is capable of representing and simulating.

## Video Documentation of EPIC Capabilities

Jennifer Bautista

### Introduction

In recent years, the development of faster and more capable hydrocodes has become increasingly important. It has long been the practice in warhead research and development to construct prototypes of new concepts and designs. However, this process can be costly and time consuming, since many ideas are neither functional nor practical. The hydrocodes, if accurate, offer a capability of simulating new designs and their reactions, thus reducing time and money spent on research and development.

The particular hydrocode that I worked with, EPIC, can be used to simulate warhead formation, penetration, and target response. My task for the summer was to graphically document the capabilities of EPIC for future use in exhibiting the hydrocode's capabilities.

### Methodology

As EPIC 91 (which stands for Elastic Plastic Impact Computations, 1991 version) is distributed, it contains 13 different input files, demonstrating the different capabilities of the hydrocode. My project for the summer involved using this information to run EPIC and create a series of videos that would illustrate just what the code is capable of doing. This includes capturing screen images which are generated through RSCORS, a graphics program developed by Sandia National Laboratories.

The first major step in making a movie is the preprocessor step. Here is where the user chooses any desired options, and determines the number of frames involved in the movie. It is necessary to instruct EPIC when the data from the test is to be saved, and these "time dumps" are calculated by dividing the TMAX (maximum time, in seconds, for the test to run) by the number of frames in the movie. The EPIC code is capable of producing state and time history plots of

EPIC results. The "time dumps" are increments of this time where EPIC will output the data. The smaller the time increments, the smoother the movie will be. **Figure One** shows an example of part of a preprocessor input card.

The second step is running the main processor. EPIC will write information about each element of the model for each "time dump." This information is routed to different places—into neutral files (*ExxPxx.MDL*) for use with PATRAN (an engineering program) and into output (*epic.out*) and restart (*epic.res*) files for use with the postprocessing step. The *epic.out* file provides a type of "play-by-play" on what goes on during the execution of the program. It tells what information was used, where the resulting data was written to, and points out any errors that occur. It is a useful troubleshooting tool for the user. The *epic.res* restart file is instrumental in the postprocessing step in that it contains all geometric and variable data necessary to do the plots.

Once the main processor step is complete and error-free, the next step is to run the postprocessor, called POST1. The postprocessor's function is to create the graphics using *epic.res* and an input deck (*post1.in*). The same "time dumps" that were programmed into *epic.in* are input into *post1.in*. **Figure Two** shows an example of a *post1.in* file. The output from the post processor program is two files named *post1.out* and *POPIN.40*. Like *epic.out*, *post1.out* supplies information on the execution and any information about errors that occur. *POPIN.40* is the metafile that holds the data for graphic generation in RSCORS. The graphics program has the capability to create one-, two-, and three-dimensional graphics in black and white or color. **Figure Three** shows an example of the RSCORS graphics. RSCORS allows you to select and look at each individual frame of the picture. It is especially useful in determining if the scale of the picture is correct and if the graphic is of good quality and suitability for animation.

Once it is determined that the frames are ready to be animated, QMOUSE (developed by Darren Boisjolie of Sverdrup Corporation) is used to capture each frame from the metafile and create an individual ".rgb" file. The QMOUSE program is a mouse activated program that

captures images presented to the screen to a data file usually called *xxx.rgb*. The next step was executed on Silicon Graphics Power Series 210. In order to animate the *xxx.rgb* files into a single movie, the user utilizes a program called ANIMATE (developed by Randy Anderson, also of Sverdrup Corporation.) ANIMATE controls a U-MATIC VTR (Video Tape Recorder) that uses large tapes much like the tapes used in television broadcast stations. The user instructs the program on the location of the input, and how many frames, and other options, and it animates the *.rgb* files.

### Results

The result of the entire process was twofold. First, I created six black and white simulation videos for future use in WL/MNMW:

1. 2D Shaped Charge with Standard Elements
2. 2D Explosively Formed Penetrator
3. 2D Multipoint Detonation with Wave Shaper
4. 2D Penetrator Perforation with Erosion and Behind Armor Debris (B.A.D.)
5. 2D Projectile Penetration into a Concrete/Soil Target
6. 3D Oblique Perforation

I have also gained knowlege in the field of computers: a little programming, how to use DOS and UNIX operating systems, and a little knowlege on the way that computers and their memory systems operate.

### Acknowledgments

I would like to thank many people for giving me the opportunity to work this summer in a research and development environment. Most of all, I'd like to thank my mentor, Michael Nixon, for guiding me and giving me invaluable instruction on my task at hand, as well as the joys of government service. He has done an excellent job, in my opinion, in teaching the high school

students, as well as instilling in them a sense of responsibility and independence. I'd like to thank Elliot Moore, another high school apprentice, for helping me and being my companion during the course of the summer. I'd like to thank Ken Gage, for answering my questions and helping me out when I had problems with the Silicon Graphics or the animation process. The Sverdrup employees in our office, Bizhan Aref, Darren Boisjolie, Randy Anderson, and Pam Cortner, were always there with an answer to my question or a smile for me, and I'd like to say thanks for their help. I'd also like to thank anyone else in MNMW for their assistance and helpfulness. I'd like to thank the Air Force and Research and Development Laboratories for creating and sponsoring the High School Apprenticeship Program, and Don Harrison and Mike Deiler for their help and direction.

TDROP	NNDE	NNAB	NELE	NSLD	NRG	NCNK	NPLT	LPLT	IRTZ	FAIL			
0.000041	144	0	240	0									
TIME	ECHECK		NCHECK		RDAMP	SAVE	BURN	YPRT	NDAT	SLPR	PROJ	PAT	RZNE
0.000001	1111.		0.0		0.0	1	0	0	10			4	
0.000002	1111.		0.0		0.0	1	0	0	10			4	
0.000003	1111.		0.0		0.0	1	0	0	10			4	
0.000004	1111.		0.0		0.0	1	0	0	10			4	
0.000005	1111.		0.0		0.0	1	0	0	10			4	
0.000006	1111.		0.0		0.0	1	0	0	10			4	
0.000007	1111.		0.0		0.0	1	0	0	10			4	
0.000008	1111.		0.0		0.0	1	0	0	10			4	
0.000009	1111.		0.0		0.0	1	0	0	10			4	
0.000010	1111.		0.0		0.0	1	0	0	10			4	
0.000011	1111.		0.0		0.0	1	0	0	10			4	
0.000012	1111.		0.0		0.0	1	0	0	10			4	
0.000013	1111.		0.0		0.0	1	0	0	10			4	
0.000014	1111.		0.0		0.0	1	0	0	10			4	
0.000015	1111.		0.0		0.0	1	0	0	10			4	
0.000016	1111.		0.0		0.0	1	0	0	10			4	
0.000017	1111.		0.0		0.0	1	0	0	10			4	
0.000018	1111.		0.0		0.0	1	0	0	10			4	
0.000019	1111.		0.0		0.0	1	0	0	10			4	
0.000020	1111.		0.0		0.0	1	0	0	10			4	
0.000021	1111.		0.0		0.0	1	0	0	10			4	
0.000022	1111.		0.0		0.0	1	0	0	10			4	
0.000023	1111.		0.0		0.0	1	0	0	10			4	
0.000024	1111.		0.0		0.0	1	0	0	10			4	
0.000025	1111.		0.0		0.0	1	0	0	10			4	
0.000026	1111.		0.0		0.0	1	0	0	10			4	
0.000027	1111.		0.0		0.0	1	0	0	10			4	
0.000028	1111.		0.0		0.0	1	0	0	10			4	
0.000029	1111.		0.0		0.0	1	0	0	10			4	
0.000030	1111.		0.0		0.0	1	0	0	10			4	
0.000031	1111.		0.0		0.0	1	0	0	10			4	
0.000032	1111.		0.0		0.0	1	0	0	10			4	
0.000033	1111.		0.0		0.0	1	0	0	10			4	
0.000034	1111.		0.0		0.0	1	0	0	10			4	
0.000035	1111.		0.0		0.0	1	0	0	10			4	
0.000036	1111.		0.0		0.0	1	0	0	10			4	
0.000037	1111.		0.0		0.0	1	0	0	10			4	
0.000038	1111.		0.0		0.0	1	0	0	10			4	
0.000039	1111.		0.0		0.0	1	0	0	10			4	
0.000040	1111.		0.0		0.0	1	0	0	10			4	
0.000041	1111.		0.0		0.0	1	0	0	10			4	
0.000042	1111.		0.0		0.0	1	0	0	10			4	
0.000043	1111.		0.0		0.0	1	0	0	10			4	
0.000044	1111.		0.0		0.0	1	0	0	10			4	
0.000045	1111.		0.0		0.0	1	0	0	10			4	
0.000046	1111.		0.0		0.0	1	0	0	10			4	
0.000047	1111.		0.0		0.0	1	0	0	10			4	
0.000048	1111.		0.0		0.0	1	0	0	10			4	
0.000049	1111.		0.0		0.0	1	0	0	10			4	
0.000050	1111.		0.0		0.0	1	0	0	10			4	

Figure One: Preprocessor input card

```

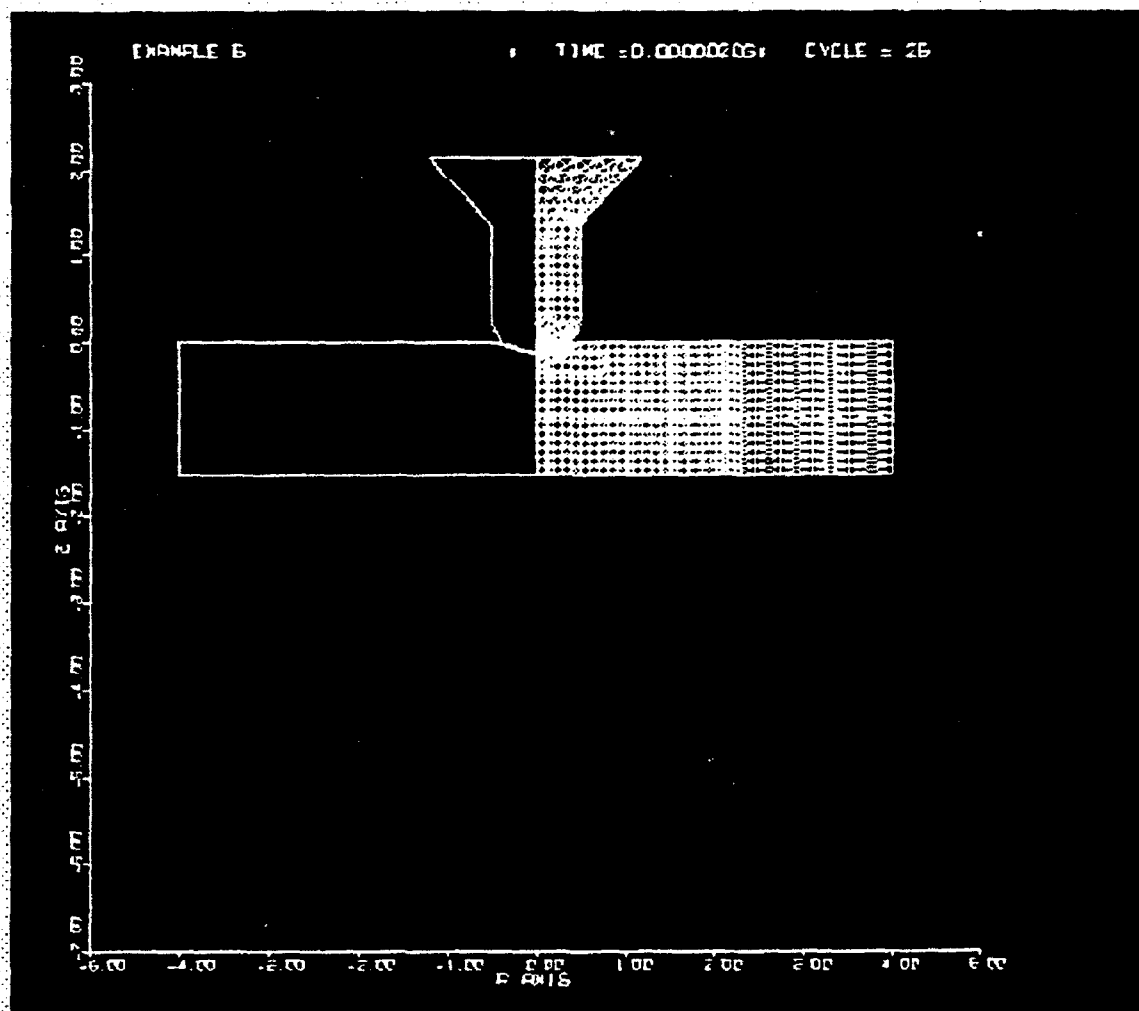
$ 1 CYCL TIME A V O S E F N P F F C F R A G ...TITLE.....
  1  0 .00000120101000 EXAMPLE 1
$ X/RMAX YMAX ZMAX X/RMIN YMIN ZMIN E1 EN M
   5.0   0.0  16.0  -5.0   0.0   0.0
$ 1 CYCL TIME A V O S E F N P F F C F R A G ...TITLE.....
  1  0 .00000120101000 EXAMPLE 1
$ X/RMAX YMAX ZMAX X/RMIN YMIN ZMIN E1 EN M
   5.0   0.0  16.0  -5.0   0.0   0.0
$ 1 CYCL TIME A V O S E F N P F F C F R A G ...TITLE.....
  1  0 .00000120101000 EXAMPLE 1
$ X/RMAX YMAX ZMAX X/RMIN YMIN ZMIN E1 EN M
   5.0   0.0  16.0  -5.0   0.0   0.0
$ 1 CYCL TIME A V O S E F N P F F C F R A G ...TITLE.....
  1  0 .00000120101000 EXAMPLE 1
$ X/RMAX YMAX ZMAX X/RMIN YMIN ZMIN E1 EN M
   5.0   0.0  16.0  -5.0   0.0   0.0
$ 1 CYCL TIME A V O S E F N P F F C F R A G ...TITLE.....
  1  0 .00000120101000 EXAMPLE 1
$ X/RMAX YMAX ZMAX X/RMIN YMIN ZMIN E1 EN M
   5.0   0.0  16.0  -5.0   0.0   0.0
$ 1 CYCL TIME A V O S E F N P F F C F R A G ...TITLE.....
  1  0 .00000120101000 EXAMPLE 1
$ X/RMAX YMAX ZMAX X/RMIN YMIN ZMIN E1 EN M
   5.0   0.0  16.0  -5.0   0.0   0.0
$ 1 CYCL TIME A V O S E F N P F F C F R A G ...TITLE.....
  1  0 .00000120101000 EXAMPLE 1
$ X/RMAX YMAX ZMAX X/RMIN YMIN ZMIN E1 EN M
   5.0   0.0  16.0  -5.0   0.0   0.0
$ 1 CYCL TIME A V O S E F N P F F C F R A G ...TITLE.....
  1  0 .00000120101000 EXAMPLE 1
$ X/RMAX YMAX ZMAX X/RMIN YMIN ZMIN E1 EN M
   5.0   0.0  16.0  -5.0   0.0   0.0
$ 1 CYCL TIME A V O S E F N P F F C F R A G ...TITLE.....
  1  0 .00000120101000 EXAMPLE 1
$ X/RMAX YMAX ZMAX X/RMIN YMIN ZMIN E1 EN M
   5.0   0.0  16.0  -5.0   0.0   0.0
$ 1 CYCL TIME A V O S E F N P F F C F R A G ...TITLE.....
  1  0 .00000120101000 EXAMPLE 1
$ X/RMAX YMAX ZMAX X/RMIN YMIN ZMIN E1 EN M
   5.0   0.0  16.0  -5.0   0.0   0.0

```

Figure Two: Postprocessor input card



Figure Three: RSCORS generated graphic  
(as seen on screen)



## References

Johnson, G.R. and R.A. Stryk, User Instructions for the 1991 Version of the EPIC Code

Alliant Techsystems, Inc. Brooklyn Park, MN, March 1991

Johnson, G.R. and R.A. Stryk, User Instructions for the 1991 Version of the EPIC

Research Code Alliant Techsystems, Inc. Brooklyn Park, MN, October 1991

EVALUATION OF THE SENSITIVITY AND PERFORMANCE OF  
INSENSITIVE COMPOSITE BOOSTER EXPLOSIVES

BRAD BLANCHARD

FINAL REPORT

HIGH SCHOOL APPRENTICESHIP PROGRAM

WRIGHT LABORATORY

HIGH EXPLOSIVES RESEARCH AND DEVELOPMENT FACILITY

WL/MNME

SPONSORED BY :

RESEARCH AND DEVELOPMENT LABORATORIES  
CULVER CITY, CA

AUGUST 19, 1992

## CONTENTS

I. INTRODUCTION

II. BACKGROUND

III. PROCEDURES AND RESULTS

IV. CONCLUSION

V. ACKNOWLEDGMENTS

VI. REFERENCES

## Introduction

PBX-9502 is an insensitive composite booster explosive that has been used for years in both conventional and nuclear weapons applications. This explosive is a composite of 2,4,6-trinitro-1,3,5-triaminobenzene and KEL F 800 at a 95/5 weight percentage (95% Explosive/5% KEL F). PBX-9502 was originally developed for use in nuclear applications, but since it allows weapons to be handled with much greater safety, and has recently been adapted for use in conventional applications. Test results have shown TATB to be an extremely safe explosive, but it does have one major disadvantage-cost. Because this explosive is expensive and its supply is less abundant, attempts are being made to replace PBX-9502 as an insensitive booster explosive.

7-Amino-4, 6-dinitrobenzofuroxan (ADNBF); 7-,5-diamino-4, 6-dinitrobenzofuroxan(CL-14); and 1,4-dinitroglycoluril (DINGU) are possible replacements for PBX-9502. ADNBF, CL-14, and DINGU, which are high density, high energy explosives, contain several advantages over PBX-9502. In order to utilize these explosives as insensitive boosters, characterization and performance tests must be conducted.

First the explosives were coated with a polymer binder to allow pressing of the materials. Characterization of the explosives was then conducted by thermal analysis and sensitivity tests. Fabrication of the materials was done with a hydraulic press. The main objective was to determine the proper pressing conditions for each composite explosive, enabling small scale performance tests to be run.

## Background

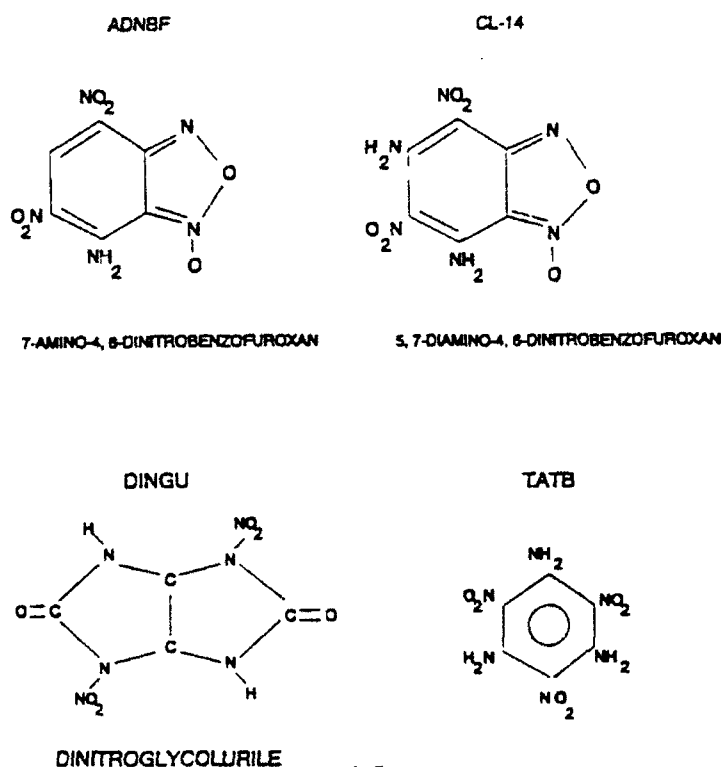
PBX-9502, a composite of TATB and KEL F 800 95/5, is used as an insensitive composite booster explosive. TATB (2,4,6-Trinitro-1,3,5-Triaminobenzene) has excellent thermal stability and extreme resistance to accidental initiation by impact or shock, which allow it to be used effectively for special applications. Even though the utilization of TATB as an insensitive booster explosive is practical, the cost of this explosive is relatively high (Ref.1).

The problem at hand is to find insensitive explosives that are less costly, but have equal performance. By utilizing 7-Amino-4, 6-Dinitrobenzofuroxan (ADNBF); 5,7-diamino-4, 6-Dinitrobenzofuroxan (CL-14), and 1,4-Dinitroglycoluril (DINGU) several advantages can be attained. These high energy, high density explosives are less expensive, and at the same time have 15% higher performance and smaller critical diameters. A smaller critical diameter will result in higher reliability for these materials.

ADNBF, the aminodinitro derivative of benzofuroxan, has been evaluated at the Naval Weapons Center, China Lake, and has been found to have potential application as a cookoff resistant booster explosive. It shows good performance and low sensitivity. ADNBF also exhibits mild cookoff reactions, high shock initiation threshold, and is easily synthesized. The first step in the preparation of ADNBF is the production of 2,3,4,6-tetranitroaniline (TNA). TNA is synthesized by the nitration of m-nitroaniline, and then it is converted to ADNBF by adding sodium azide and acetic acid. The final product, ADNBF, then crystallizes out of the acetic acid and is filtered from the medium and washed. This explosive has been prepared successfully at the Naval Weapons Center (Ref.3).

CL-14, which is also a thermally stable, high density, high performance explosive, has been evaluated at the Naval Weapons Center, China Lake. Performance tests demonstrated that this explosive has a failure diameter of less than one-half inch, which makes it useful in many ordnance applications. CL-14 is also much less sensitive to impact than either TNT or RDX, is much more powerful than TNT, and approaches RDX in power. Several routes have been taken for the synthesis of CL-14, and a new improved method of synthesis has been discovered (This method will be discussed in this part of the report.) Through this route of synthesis, CL-14 is prepared by amination of 7-amino-4,6-dinitro benzofuroxan (ADNBF) with hydroxylamine in presence of potassium hydroxide. ADNBF is used as the starting material mainly because it is currently available in large quantities (Ref.4).

DINGU is another high energy, high density explosive of an insensitive nature, yet its sensitivity to shock remains undefined. Even though DINGU has a disadvantage of low thermal stability, its starting materials are readily available at low cost. The synthesis of this explosive involves two steps. First glycoluril is produced from glyoxal and urea. DINGU is then prepared by nitration of the glycoluril (Ref.2).



Once these materials are synthesized, they must then be formulated with a polymer binder. KEL F 800 was the binder used at a 95/5 weight percentage (95% explosive/5% KEL F). ADNBF, CL-14, and DINGU will not compact under high pressure without KEL F 800. The coating of these explosives was done here at the High Explosives Research and Development Facility, EGLIN AFB.



## Procedures and Results

Thermal analysis of ADNBF/KEL F, CL-14/KEL F, and DINGU/KEL F was performed with the Differential Scanning Calorimeter (DSC). This test was run to confirm the compatibility of KEL F 800 with the explosive. ADNBF/KEL F and CL-14/KEL F were both heated to 400 degrees Celsius to evaluate the exothermic onset. The samples were placed in unvented aluminum pans and sealed prior to their exposure to elevated temperature. DINGU/KEL F was also done in an unvented pan, only it was heated to 300 degrees Celsius.

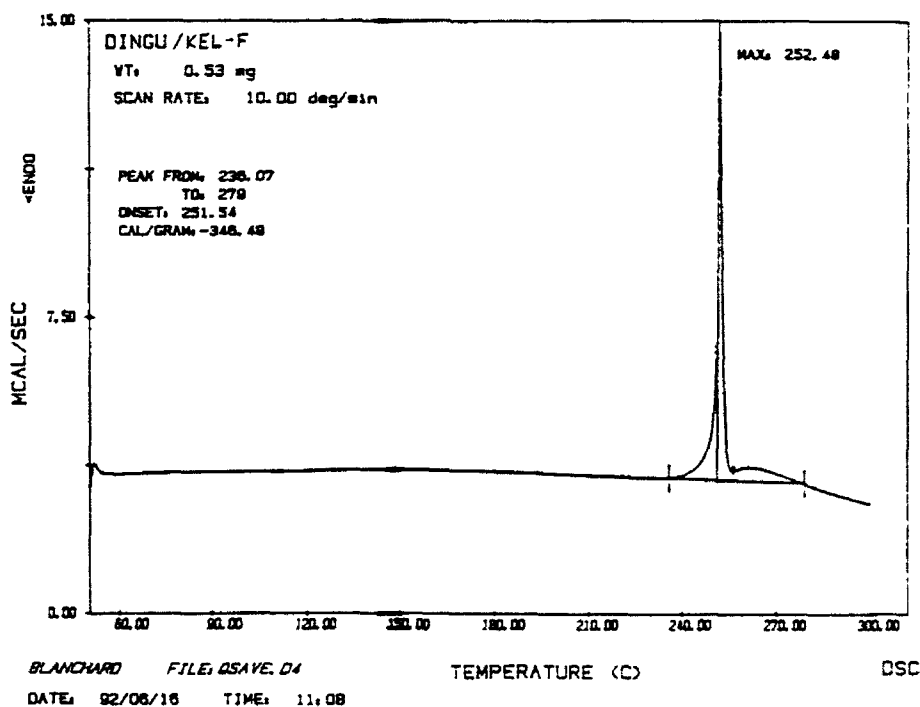
The results from the DSC revealed that ADNBF/KEL F had an exothermic onset of 273.32 degrees. The exothermic onset of the neat material was 270.43 degrees Celsius, which is relatively close to the results of the explosive with the binder. From these results it was concluded that KEL F 800 had no significant effect on the explosive's character. DSC results from CL-14/KEL F and DINGU/KEL F also indicated that KEL F 800 had no chemical incompatibility with the materials. However, the exothermic onsets were all higher with the presence of KEL F 800. The exothermic onset of CL-14/KEL F was found to be 308.4 degrees, as compared to CL-14 at 296.75 degrees. DINGU/KEL F had an onset of 251.56 degrees, and DINGU has an onset of 243.18 degrees. One might agree that the increase in exothermic onset indicates that KEL F 800 stabilizes the decomposition of the materials. (See figures 2 and 3)

Figure 2.

# DSC RESULTS

MATERIAL	EXOTHERM PEAK (°C )	ONSET (°C )
ADNBF	297.67	270.43
ADNBF/KEL F	286.31	273.32
CL-14	300.59	296.75
CL-14/KEL F	309.33	308.4
DINGU	245.48	243.18
DINGU//KEL F	252.48	251.56

Figure 3.- Example spectrum from the DSC results.



The sensitivity was then evaluated for ADNBF/KEL F, CL-14/KEL F, and DINGU/KEL F. It is important to evaluate the sensitivity of these explosives because they are exposed to pinching and extrusion during the pressing procedures. Pressing an explosive before determining its sensitivity can result in a disastrous event. Impact sensitivity was first determined with a Bureau of Mines type 12B drophammer. For these particular explosives a 2.5 kg weight was dropped onto the samples from various heights. The average height at which the explosives detonated was figured and then recorded. The results showed that the impact sensitivity of ADNBF/KEL F was at 69.5 cm, DINGU KEL F was at 82.7 cm, and CL-14/KEL F at 151.2 cm. Using RDX as a reference, with an impact sensitivity at 22 cm, we can tell that these three explosives are insensitive (CL-14/KEL F being the least sensitive).

#### IMPACT SENSITIVITY RESULTS

MATERIAL	H50 (cm)
ADNBF/KEL F	69.5
CL-14/KEL F	151.2
DINGU/KEL F	82.7
RDX	22

Friction sensitivity was then determined for these composite explosives. A BAM friction tester was used for this part of the experiment. Samples weighing 20 mg are prepared and placed on a porcelain plate. The porcelain plate is then clamped into position on the specimen stage. A porcelain pin is dragged across the sample at different levels of friction (measured in kg). The highest level at which no reaction occurs is considered to be its sensitivity to friction. The results of this test showed ADNBF/KEL F and CL-14/KEL F to be

highly insensitive to friction. However, DINGU/KEL F was more sensitive, with results similar to those of TNT.

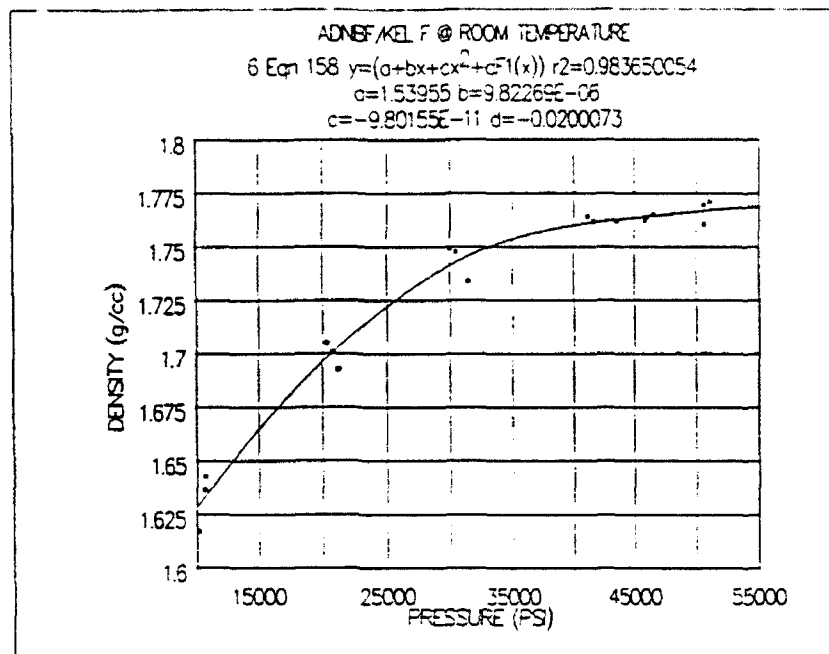
#### FRICTION SENSITIVITY

ADNBF/KEL F	6.0 kg
CL-14/KEL F	6.4 kg
DINGU/KEL F	3.2 kg
TNT	3.6 kg

A pressing study was conducted to determine the optimum pressing conditions for the fabrication of ADNBF/KEL F, CL-14/KEL F, and DINGU/KEL F pellets. These 1/2 inch pellets were fabricated with a Carver 11 ton hydraulic press. Before pressing was done, the explosive samples were dried in an oven at 70 degrees Celsius. Also, a vacuum was attached to the die during pressing procedures to remove any residual air in the materials. After each pellet was fabricated, the density was determined by pellet weight and measurements.

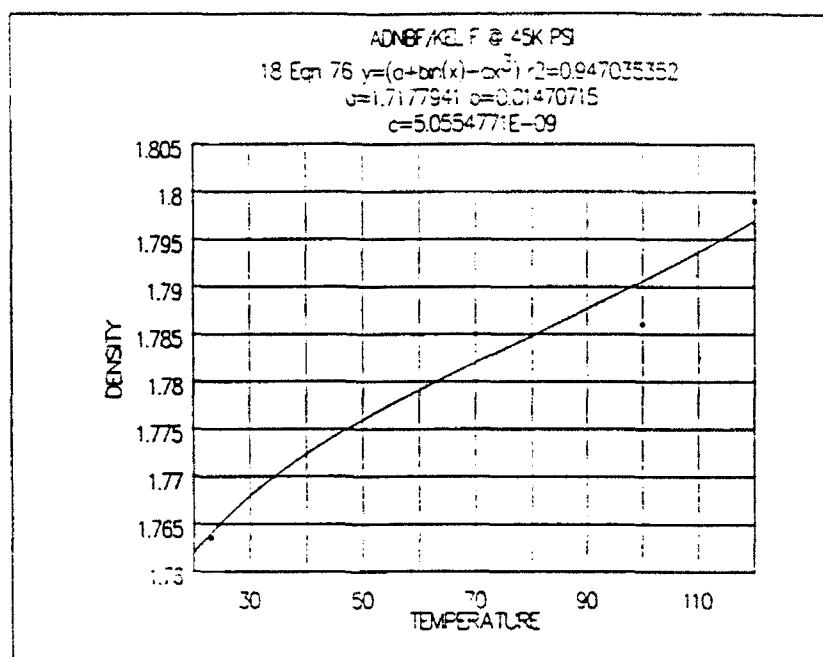
In an attempt to achieve a density of 96-98% of the Theoretical Maximum Density, the explosives were pressed at room temperature with varied pressure, and then at constant pressure with varied temperature. A dwell time of 5.0 minutes was found to be sufficient for successful pressing. It was increased to 10.0 and 15.0 minutes, but no increase in density was achieved. Each explosive was pressed at a pressure of 10,000 pounds/ square inch and increased at intervals of 10,000. At room temperature ADNBF/KEL was maximized at 45,000 PSI; CL-14/KEL F at 45,000 PSI; and DINGU/KEL F at 55,000 PSI. With an increase in pressure there was a direct increase of density up to these maximum densities. (see next page)

Sample graph.



The final variable factor was an increase in temperature during pressing. The following procedure was used to increase the temperature: Explosive materials and die were heated to desired temperature with an oven. The die and materials were subjected to heated environment for approximately 30 minutes. Pressing was then performed at elevated temperatures of 70, 100, 120 degrees Celsius. Each explosive was then pressed at a constant pressure: ADNBF/KEL F @ 45,000 PSI, CL-14/KEL F @ 45,000 PSI and DINGU/KEL F @ 55,000 PSI. AT 70 degrees Celsius all three explosives exhibited an increase in density, but not enough to achieve 96-92% of TMD. At 100 degrees Celsius ADNBF/KEL F and CL-14/KEL showed further increase in density but still did not reach the desired density. However, DINGU/KEL F @ 100 degrees Celsius reached a density if 96.07% TMD. In attempts to further increase the densities for ADNBF/KEL F and CL-14/KEL F they were pressed at a temperature of 120 degrees Celsius. The results still did not meet the desired density of 96-98% TMD. (see next page)

Sample graph.



The final results of the pressing study (shown below) indicate that DINGU/KEL F was pressed to an acceptable level. On the other hand ADNBF/KEL F and CL-14/KEL F will require further pressing study.

#### PRESSING RESULTS

	TMD	MAXIMUM DENSITY	%TMD
ADNBF/KEL F	1.91 g/cc	1.799 g/cc	94.35%
CL-14/KEL F	1.95 g/cc	1.815 g/cc	93.20%
DINGU/KEL F	1.94 g/cc	1.864 g/cc	96.07%

The following performance calculations were figured for ADNBF/KEL F, CL-14/KEL F, and DINGU/KEL F using Kamlet Finger, Hardesty and Kennedy, Doherty, Short and Kamlet, and Gurney methods.

	ADNBF/KEL F @ 1.907 g/cc	CL-14/KEL F @1.948 g/cc	DINGU/KEL F @ 1.944 g/cc
$V_8$ (mm/usec)	1.515	1.55	1.56
$V_{19}$ (mm/usec)	1.8739	1.709	1.721
$E_8$ (kJ/g)	1.1478	1.2012	1.2168
$E_{19}$ (kJ/g)	1.4011	1.4603	1.4809
$E_g$ (kJ/cc)	6.73	7.04	7.13
$\rho E^{1/2}$ (mm/usec)	2.67	2.71	2.73

## Conclusion

Compatibility of explosive with KEL F binder was evaluated. According to the DSC results of ADNBF/KEL F, CL-14/KEL F, and DINGU/KEL F, there was no incompatibility of KEL F 800 with the explosives.

Sensitivity of the composite materials was also evaluated. In order to test the explosives' sensitivity to pinching and extrusion, impact and friction sensitivity tests were performed. The results showed CL-14/KEL F and ADNBF/KEL F to be highly insensitive to friction. DINGU/KEL F with a friction sensitivity of 3.2 kg, was slightly more sensitive than TNT (3.6 kg).

Pressing studies were completed for DINGU/KEL F, ADNBF/KEL F, and CL-14/KEL F. A density of 96.07% TMD was achieved at the following conditions: 55,000 PSI @ 100 degrees Celsius. This is an acceptable density to continue on with cylinder tests of this composite explosive. The maximum density achieved for ADNBF/KEL F was 1.799g/cc (94.35%TMD). CL-14/KEL F was pressed to a density of 1.815g/cc (93.20%TMD). Further pressing study will be required in order to achieve greater densities for both of these explosives. It is suggested that the corrective action for CL-14 is the recrystallization of the neat material. This will enable a bimodal distribution of particles of KEL F and the explosive. An increase in space packing will result in a higher density of the pressed material.

A possible explanation of ADNBF/KEL F not reaching 96% TMD is that it contains a 1% acetic acid impurity. This impurity will be removed by recrystallization of ADNBF in xylene and butyrolactone before pressing. The pressing materials will then yield a higher density.



## Acknowledgments

My summer project would not have been such a success without the guidance and support I received from the personnel at the HERD facility. First of all I would like to thank Mr. Stephen Aubert for creating a step-by-step project that involved hands on operation of different types of lab equipment. I would also like to thank Ms. Susan Cooke for training me to use the equipment in the labs. I appreciate everyone's cooperation and eagerness to assist me at all times. It was most definitely a pleasure to be a part of this program.

## References

1. LASL Explosive Property Data  
Berkeley: University of California Press, 1980  
Regents of University of California.
2. M.M. Stinecipher, L.A. Stretz: Sensitivity and Performance Characterization of  
DINGU, New Mexico: Los Alamos National Laboratory.
3. Norris. W.P. 7-Amino-4, 6-Dinitrobenzofuroxan, an Insensitive High Explosive Naval  
Weapons Center: China Lake, California.
4. Norris, William P., Michael P. Kramer and David J. Vanderal CL-14, A High-  
Performance Insensitive Explosive Naval Weapons Center: China Lake,  
California.

EXPANDED STUDY OF COMPUTER SOFTWARE  
AND INVENTORY CONTROL

J. Stacey Bond  
Summer Apprentice  
Wright Laboratory

Final Report for:  
AFOSR Summer Research Program  
Wright Laboratory

Sponsored by: AFOSR

August 1992

EXPANDED STUDY OF COMPUTER SOFTWARE  
AND INVENTORY CONTROL

J. Stacey Bond  
Summer Apprentice  
Wright Laboratory, W.P.A.F.B.

Abstract

This summer I worked on two different types of projects. First, I learned many various types of computer software. I was introduced to most of them for the first time, and the others I expanded my knowledge of them. The other major project I did included taking inventory of all the computers in the entire WL/EL, the electronics department.

The solid state electronics directorate is responsible for electronic device research and development in the areas of microelectronics, microwaves, and electrooptics. Research extends from fundamental growth and device fabrication through integrated circuits. In the electrooptics area, lasers, detectors, and integrated focal plane arrays are developed. The solid state electronics directorate is divided into 5 parts -- microelectronics, microwave technology, electro-optics technology, research, and operations. The microelectronics division develops the technology base for advanced microelectronics. This division develops, demonstrates, and applies microelectronic concepts to provide the technological foundation for high performance and reliable Air Force weapons system electronics. The microwave division conducts research and advanced programs for microwave and millimeter wave devices, integrated circuits, components and subsystems. The division is responsible for the transition of microwave products into Air Force Weapon systems. The electrooptics division conducts research and advanced programs with electro-optical component technology, including the development of lasers and incoherent light sources, non-linear optical devices and interactions, optical processing, beam deflection detectors and focal plane arrays. The research division conducts research and development programs on semi-conductor and electro-magnetic materials and devices. They explore new device concepts and conduct demonstration efforts on devices with potential for high frequency microwave/millimeter wave, high speed electronics and electro-optical applications. The operations division provides policy and guidance for directorate corporate planning and programs and management advice. It evaluates the programs and recommends changes. They direct, manage, and

implement administrative support programs and conduct specialized training programs.

This summer I worked in the microelectronics directorate. The main areas of concentration include new device approaches to logic and electronic processing, ultra-high speed digital switching devices, advanced semiconductor fabrication technology, high speed/density integrated circuit packaging, power/thermal management techniques, and computer based tools for electronic equipment design. There were four main programs going on in the ELE division, including:

#### ADVANCED INTEGRATED MICROSENSORS

The objective of this effort is to demonstrate monolithic microsensors by developing the IC fabrication, micro-machining, and packaging techniques necessary to meet the requirements of advanced aircraft sensor systems. Achieving this will result in the reduction of the system size, weight, power, and cost while increasing system reliability and performance.

#### RESONANT TUNNELING TRANSISTOR MSI

The objective of this program is to optimize resonant tunneling transistor or diode technology and to apply it to advanced compressed MSI Logic functions including real and complex multipliers. A significant increase in processing and a reduction device count is expected as a result of RTT's technology investment plan.

#### VHDL BEHAVIORAL SIMULATION ACCELATOR

The objective of this proposed effort is to develop a hardware and software system that provides 3 to 4 orders of magnitude greater simulation performance over software simulators on engineering workstations for very high speed integrated circuits hardware description language behavioral descriptions. This accelerator would allow hardware and software to be

developed concurrently and reduce redesigns at all levels. VHDL is the industry and government standard description language and the development of VHDL models is a DOD mandated acquisition practice.

#### ADVANCED CAD TOOLS FOR RAPID DESIGN OF ELECTRONICS

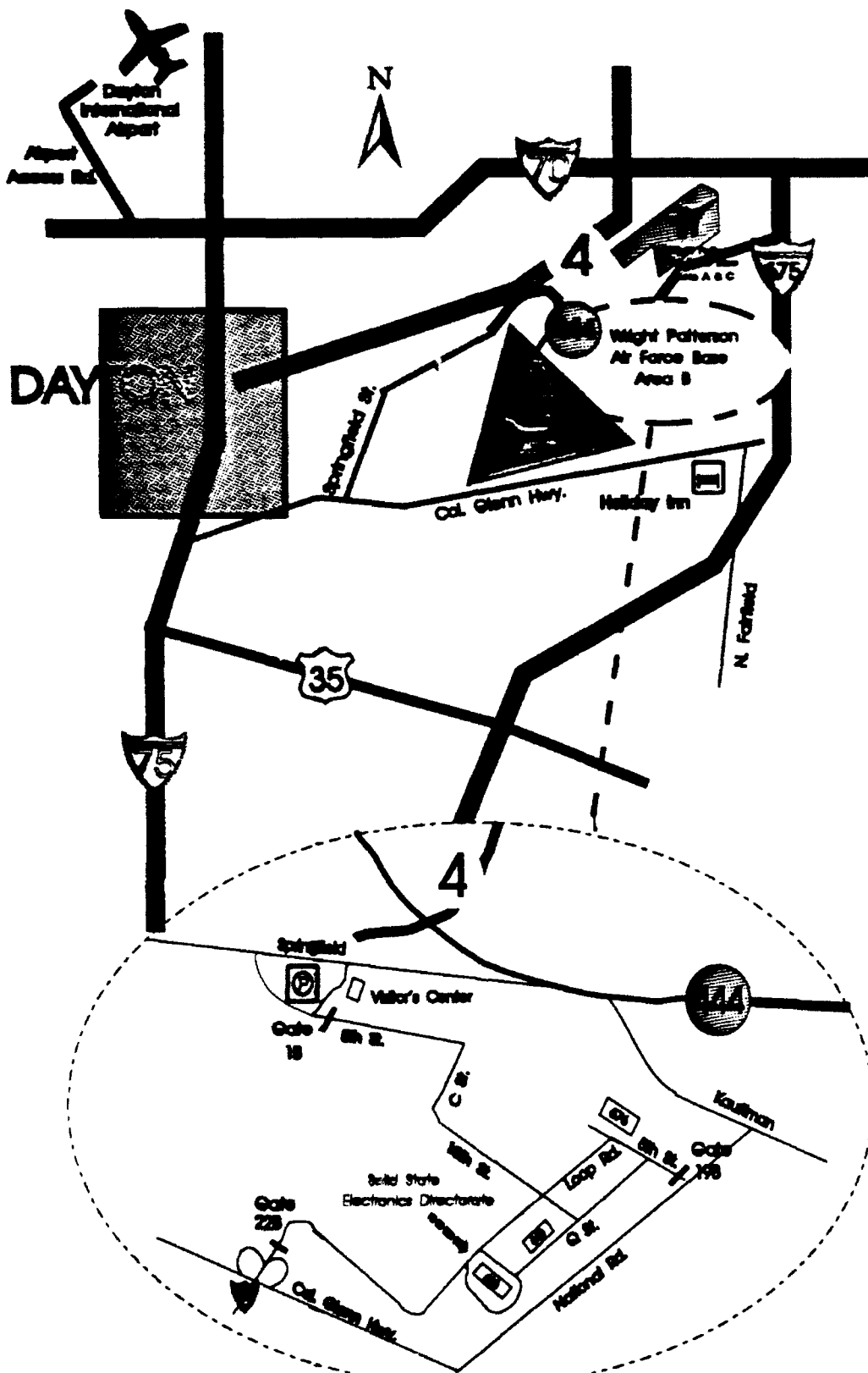
The objective of this proposed effort is to advance the tools, methods, and techniques for the computer aided design (CAD) of electronics. A second objective is to integrate advanced tools into CAD systems and design environments that are widely used by DOD and it's contractors. The end result will be a transfer of technology from basic research to DOD weapon system and system component developers. The ability to put leading edge CAD technology into the hands of designers is critical to the success of the DOD and the U.S. electronics industry.

This summer, before I worked on my final project, I enhanced my knowledge of 5 different computer software. My mentor, Luis Concha, did not just tell me how to run these software, he made me read or skim through the manuals, take down notes, and practice on the tutorials. The first software I learned was MS-DOS. Some of the important commands I learned was how to copy files, change directories, delete files, format, and make new directories. Multilevel directories can contain numerous files using paths from one file to another. Wildcards (\*) and (?) are used in place of characters to locate files you don't know the name of. Internal commands use paths while external commands load from a disk or partition. EDLIN creates text files that can be save and updates existing files that can delete, edit, insert, and display lines. Link creates executable programs from object files. Next, I briefly used Microsoft Windows. Windows are the interface between the user and the operating system -- it is "user friendly". It allows you to click on

executable files to run them. It also allows/provides you to use icons for file management. Next I worked with Wordperfect, which is a word processor. I used this in which to make a memorandum and to type this report. Corel Draw was the software in which I became most familiar with. There are 9 different tools you are given to create and design illustration. The arrow tool, the arc tool, the magnification tool, the pencil tool, the square tool, the ellipse tool, the fountain pen tool, and the painting tool. I worked with Corel Draw for a couple of weeks, and one of things I created includes the map on the following page. This map was made primarily for visitors that need to come on base. [This map was made in color] Microsoft Excel is the last software I learned. Learning this was crucial to completing my summer project. I needed to create spreadsheets to store data that I compiled from the project. Excel showed me how to make data worksheets, graphs, and charts to import graphics onto the spreadsheet.

My project for the summer was to create a data base on Micro Soft Excel spreadsheet to store information we collected and then to make bar code labels that you can scan with the Percon bar code scanner. This project was worked on by both Helen Chou and myself. The first thing I had to do was learn how to construct a pocket reader application. I first needed to make 3 frames titled Main Menu, Data Collection, and Upload the Data. Then I went into the data collection frame to create nodes. Each node contains details of the task to be performed. There are 7 types of nodes and you work with almost all of them. The display node displays information on the Pocketreaders display. Input allows you to import data into the pocketreader itself. Verify tests the data for content. Copy duplicates data within the pocketreader. Modify changes the data. Math performs mathematical operations and output exports data from the pocketreader. Link connects the nodes together so they might





function as one unit. To load the program into the pocketreader, you need to connect the scanners cable to the adaptor. Then select Download and the pocketreader will reset and run your application when it has finished programming. Now your program is in the scanner. Next data was collected from the entire electronics directorate. We went to every office to take inventory of all the computers and computer related equipment. For each piece of equipment, we wrote down the room number, name of the responsible party, division, description of equipment, serial and model numbers and/or bar code numbers, EMAS number, and whether it was marked with a security identification sticker. After this we typed the data onto the spreadsheet and loaded it into the Percon scanner. Next our task was to make bar codes for all of the equipment, so that everything would be labeled. This way, by scanning the bar code, you would know immediately who was responsible for it. This was necessary because equipment gets moved around so much and there is constantly new equipment coming in. I felt this project was a learning experience because I got to travel throughout the entire electronics directorate, seeing the many different things people do. I believe that our inventory control has helped the solid state electronic department.

In conclusion, I would like to thank RDL for allowing me the opportunity to work in the AFOSR High School Apprenticeship Program. My experience this summer taught me more about the Air Force and computers and has been enjoyable. I'd also like to thank my mentor, Luis Concha, and Don Peacock for being there for me every day. Thanks!

**Inventory Control For The Solid  
State Electronics Directorate**

Helen Chou  
Summer Apprentice  
Division: ELA-Operations  
Wright Patterson Air Force Base

Final Report For:  
AFOSR Summer Research Program  
Wright Laboratories

AFOSR Sponsorship

August 1992

## **Inventory Control For The Solid State Electronics Directorate**

Helen Chou  
Summer Apprentice  
Division: ELA-Operations  
Wright Laboratories, WPAFB

### **Abstract**

The main project was to devise an efficient method of bar coding all Air Force equipment in the Solid State Electronics Directorate. The main purpose of this project was to be able to inventory all equipment in the lab, select a responsible party for each piece of equipment, and to make the data file able to update quickly and efficiently whenever a change is needed. The approach plan is to first collect all the necessary information and then input it into a spreadsheet. Next, generate bar codes from the data in the spreadsheet and post on each corresponding piece of equipment. Lastly, program the bar code reader to display the individual data listings whenever the bar code on the equipment is scanned.

**Inventory Control For The Solid  
State Electronics Directorate  
and Other Projects**

**Helen Chou**

This summer I worked in the Operations Division (ELA) of the Solid State Electronics Directorate at Wright Patterson Air Force Base. This division is in charge of the operations of the other four counterparts of the directorate: Electro-optics Technology, Microelectronic Technology, Microwave Technology, and Electronic Device Research.

As a summer apprentice in this directorate, I utilized my computer skills to complete numerous projects. My accomplishments include creating two government forms on PerFORM Pro, recreating the new Air Force Materiel Command logo on CorelDraw, and devising a system to keep track of all capital equipment in the Solid State Electronics Directorate using Microsoft Excel, PerFORM Pro, and a programmable bar code reader.

The first software package I familiarized myself with was PerFORM Pro. PerFORM Pro Designer and Filler is a two-part package made specifically for designing, managing, filling in, and printing business forms. It allows the user to design forms with sophisticated fill-in features, and then, using the Filler application, fill in the created forms. The goal of this exercise was to provide secretaries with an efficient method of form generation and to develop an understanding of relational databases. The Filler portion is easy for the secretaries to utilize and eliminates fill-in errors and tedium. It also allows the fill in of volumes of data records quickly and efficiently.

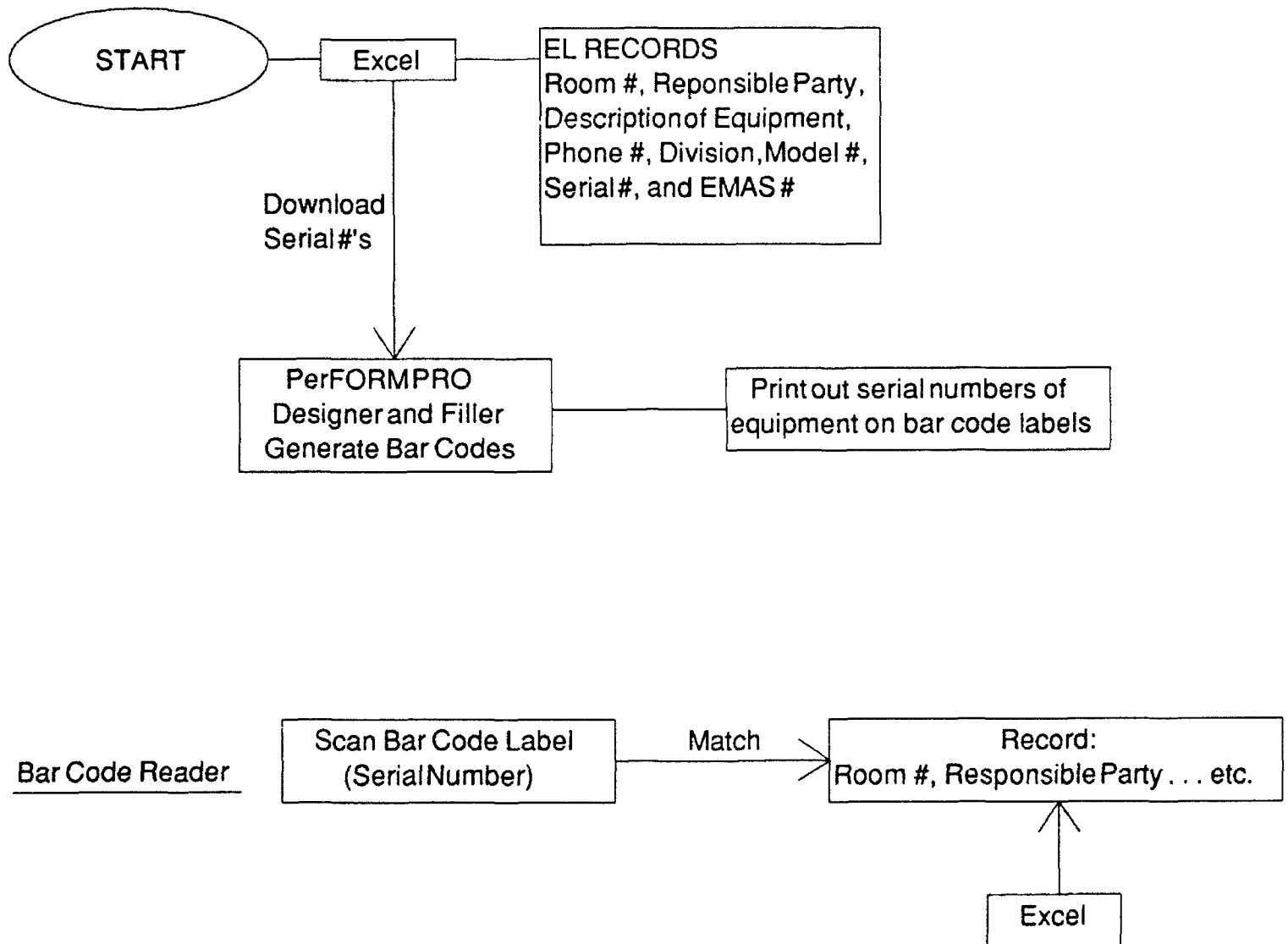
The two forms I created with the Designer were the Standard Form 120 rev. Report of Excess Personal Property and a Micro-computer Registration Form (both included in report). To create these forms, I used the design tools available and defined fill-in fields (records) of specified fonts, lengths, and other attributes. These two forms are related to the third project I

worked on having to do with inventory control.

My second task was to create the new Air Force Materiel Command logo using the design program CorelDraw. The purpose of this project was to optimize the logo for minimum computer requirements. The Directorate already possessed various logo files consisting of around 500K bytes each. My goal was to compose from scratch a logo file with a reduction in file size. The objective of creating a file with less bytes is to enable the future user to save memory space and disk space, and to read, display, and store the file quickly and easily. This allows for an overall better performance. My completed logo file was 17K bytes which was a significant reduction in file size (created logo included in report--one in color and one in black and white).

The final project of my summer apprenticeship was devising an efficient method of bar coding all Air Force equipment in the Solid State Electronics Directorate. The main purpose of this project was to be able to inventory all equipment in the lab, select a responsible party for each piece of equipment, and to make the data file able to update quickly and efficiently whenever a change is needed.

First, a plan of approach was necessary. The following flow chart was designed:



The first step was to go office-to-office and compile all the information needed to properly identify and locate all equipment. The information collected was the following: Room number, responsible party, phone number, division, description of equipment, model number, serial number and EMAS number. This data was then input into Microsoft Excel 3.0. Excel is a powerful integrated spreadsheet for Microsoft Windows. It gives the user advanced calculating ability, along with the convenience of using windows to organize tasks and documents on the screen. It allows the user to possess automated business tools for projections, calculations, and data analysis as well as the presentation tools needed for reporting results. The purpose of using Excel was that in the future, Excel enables us to report changes and updates in equipment and allows us to sort the file by serial numbers.

Once all the data was input, I created a file using PerFORM Pro Designer to allow us to download the serial numbers from Excel and generate bar codes out of them. We placed the generated bar code stickers on the corresponding computer equipment in each office. Then, using the Percon bar code programmer, programmed the bar code reader to scan the bar codes and display all the data associated with that particular piece of equipment onto the bar code reader's display screen. Using a bar code system speeds data entry and eliminates errors. The particular program we used is called Percon Program Generator. It is a system for creating custom application programs for the PocketReader. This program generator allows the user to use tools to create and label a flowchart of an application. The Percon Program Generator converts it into a program for the PocketReader. The user must first sketch the steps needed and then create the flowchart.

Lastly, I would like to take an opportunity to thank the following people: RDL and WPAFB for offering me another great opportunity to acquire valuable and memorable working



experience. I truly learned a lot through this high school apprenticeship program. What I learned will be very useful and valuable for me in my future endeavors. I would also like to thank Mr. Don Peacock for his time and effort in organizing this summer's division tours. Many thanks also goes to my mentor Mr. Dave Cartmell for his guidance and expertise in helping me accomplish my projects this summer.

---

# PERFORM PRO

- FAMILIARIZATION WITH TWO-PART DESIGNER AND FILLER PACKAGES
  - FAMILIARIZATION WITH PROGRAM DESIGN TOOLS
  - WALK THROUGH USER'S MANUAL EXAMPLES
  - TAKE STANDARD FORM AND DESIGN STRUCTURE OF FORM WITH PERFORM DESIGNER PACKAGE
  - DEFINE FIELDS AND FILL-IN ATTRIBUTES FOR FORM
-

## 1. REPORT NO.

2. DATE MAILED

3. TOTAL COST	
---------------	--

4. TYPE  
OF REPORT

(Check one only of  
"a," "b," "c," or "d")

a. ORIGINAL

b. CORRECTED

c. PARTIAL W/D

d. TOTAL W/D

(Also check "e" and/or "T"  
if appropriate)

e. OVERSEAS

f. CONTRACTORS INV

5. TO (Name and Address of Agency to which report is made) THRU

6. APPROP. OR FUND TO BE REIMBURSED (if any)
--

7. FROM (Name and Address of Reporting Agency)

8. REPORT APPROVED BY (Name and Title)

9. FOR FURTHER INFORMATION CONTACT (Title, Address, and Telephone No.)

10. AGENCY APPROVAL (If applicable)

11. SEND PURCHASE ORDERS OR DISPOSAL INSTRUCTIONS TO (Title, Address and Telephone No.)

12. GSA CONTROL NO.

13. FSC GROUP  
NO.

14. LOCATION OF PROPERTY (If location is to be abandoned give date)

15. REIM/REQD	
YES	NO

YES	NO
-----	----

16. AGENCY CONTROL NO.

17. SURPLUS RELEASE DATE	
-----------------------------	--

### 1d. EXCESS PROPERTY LIST

**ПЕМ**

### DESCRIPTION

(b)

COND.

UNIT

(b)

NUMBER  
OF UNITS  
(e)

ACQUISITION COST

PER UNIT

(1)

TOTAL

(g)

**FAIR**

VALUE

%  
(%)

# MICRO-COMPUTER REGISTRATION

NAME:

OFFICE (CHECK ONE):

EL ☐ ELA ☐ ELE ☐ ELM ☐ ELO ☐ ELR ☐  
 TSSI ☐ WS ☐ UES ☐

ROOM LOCATION OF EQUIPMENT:  
 (Including clean room)

CPU TYPE (CHECK ONE):

Z-100 ☐ Z-248 ☐ UNISYS 386 ☐  
 MAC SE/30 ☐ MAC II ☐ MAC IIx ☐  
 MAC IId ☐ MAC IIx ☐ OTHER:

SERIAL NUMBER:

MODEL NUMBER:

PERIPHERALS:

	TYPE	SERIAL	MODEL
PRINTER			
SCANNER			
OTHER			
OTHER			
OTHER			

SOFTWARE:  
 DOS SYSTEMS  
 (check all that apply)

NAME	
BASIC	
CALL	
CHART	
COREL DRAW	
DBASE	
DRAWPERFECT	
ENABLE	
EUREKA	
FORTRAN	
FREELANCE	
GEMDRAW	
GRAFTALK	
GRAMATIK	
HARV GRAPH	
LOTUS	
MATHCAD	
MS DATABASE	
MS DOS	
MS EXCEL	
MS FORTRAN	
MS WINDOWS	
MS WORD	
NEWSMASTER	
NORTON UTIL	

NAME	
PCTOOLS	
PRO COMM	
PROFILE	
PSPICE	
PUFF	
QBASIC	
SLIDE WRITE	
SMARTERM	
SUPER CALC	
TIMELINE	
TURBO C++	
TURBO PASCAL	
WINDOWS	
WINDOWS DRAW	
WORDPERFECT	
WORDSTAR	
ZSTEM	
OTHER:	

MACINTOSH  
 (check all that apply)

NAME	
C	
CRICKET GRAPH	
DATADESK	
DELTA GRAPH	
EXCEL	
EXPRESSIONIST	
FORTRAN	
MAC 241	
MAC WRITE II	
MACDRAFT	
MACDRAW	
MACLINK	
MACPAINT	
MACWRITE	
MATHEMATICA	
MATHWRITE	
MINICAD	
MS WORD	
ORACLE	
THINK PASCAL	
POWERPOINT	
PSPICE	
QBASIC	

NAME	
QUED/M	
SOFT PC	
STATWORKS	
SUPER 3D	
SUPERPAINT	
SWIVEL 3D	
TOPS	
VERSATERM	
WORDPERFECT	
WORKS	
OTHER:	

---

# CORELDRAW

- DIGITIZE LOGO VIA PAGE SCANNER
- IMPORT BITMAP FILE INTO CORELDRAW
- CONVERT BITMAP IMAGES INTO OBJECT  
ORIENTED IMAGES TO CREATE NEW FILE THAT  
OPTIMIZES THE LOGO FOR MINIMUM COMPUTER  
REQUIREMENTS



---

# INVENTORY CONTROL

- DEVELOPED STRATEGY BY FLOW CHART FORMAT
- COLLECT ALL NECESSARY INFORMATION ABOUT EQUIPMENT AND ITS LOCATION
- FAMILIARIZE WITH MICROSOFT EXCEL 3.0 AND INPUT EQUIPMENT DATA INTO SPREADSHEET
- DESIGN BARCODE FILE IN PERFORM PRO DESIGNER
- DOWNLOAD SERIAL NUMBERS FROM EXCEL EQUIPMENT FILE AND GENERATE BAR CODES FROM DATA

- 
- POST GENERATED BAR CODE STICKERS ON  
CORRESPONDING EQUIPMENT
  - DESIGN FLOWCHART OF APPLICATION USING  
PERCON PROGRAM GENERATOR
  - PERCON PROGRAM GENERATOR CONVERTS  
FLOWCHART INTO A PROGRAM FOR POCKETREADER  
AND DOWNLOADS PROGRAM INTO POCKETREADER
  - ROUTINELY SCAN EQUIPMENT AND UPDATE DATA  
FILE OF ANY CHANGES
-



# Safeguard government items

By SSGT. ROBERT P. HENSON

BASE RESOURCES PROTECTION MANAGER

"When was the last time a complete inventory was conducted of all government belongings within your organization? This question should be asked by everyone — command supervisors, civilian and military personnel.

Especially during these times, when the Air Force is streamlining and merging organizations, confusion and carelessness can lead to the loss of organizational belongings. Whether by theft or negligence, government equipment can be easily taken and can add up to millions of dollars in losses. Police reports at Wright-Patterson have shown that employees have taken government equipment from their work areas or simply ignored requirements to account for necessary items.

As the Air Force downsizes its workforce, some unhappy employees may find it an opportune time to take with them a small token from their job. Maybe a pen or paper, or

worse, maybe several computers or expensive tools.

When the Air Force relocates several organizations to different locations, it also offers an excellent opportunity for employees to hide government equipment or remove its property secretly from packaging before shipment or arrival. Regardless of how the equipment is taken, the Wright-Patterson community needs to be conscious of its obligation and responsibility to safeguard government items.

Keeping this in mind, there are some recommendations to follow.

Ensure that an organizational equipment list is maintained and kept up-to-date.

Conduct a complete physical inventory of all equipment anytime someone from the organization is being transferred or relieved of duty.

Don't overlook small items which are easily pilfered,

such as picture frames, books, pens, etc.

Look for anyone who may be concealing items in large gym bags or duffel bags.

Make periodic checks of people who work nights or odd hours. The fall of darkness will greatly enhance the chances of someone concealing items.

Keep all entrances and exits to the facility at a minimum.

Ensure all government equipment is released or destroyed in the proper manner and not just thrown out in the garbage.

If an organization is moving, ensure all equipment is properly packaged and shipping documents reflect the exact contents.

By using these recommendations and good security awareness, the loss of government equipment can be kept to a minimum. Remember, it's everyone's responsibility to safeguard government items.

# Example of Microsoft Excel Inventory Spreadsheet

91-9

Room #	Responsible Party Last Name, First	Phone #	Division	Description	Model #	Serial #	EMAS #	ADPE ID (y or n)
B221A	AGRESTA, D.	53804	ELO	Z-248	MN200	3WH13569		
B221A	AGRESTA, D.	53804	ELO	ALPS	P2000			
S2Y57	BACON, R.	58646	ELE	Z-248	ZBO-2503-EK	849CC000872		
S2Y48	BARKER, D.	58639	ELE	Z-248	ZBO-2503-EK	850CC001699		
C2-V72	BEST, L.	52159	ELA	Z-248	ZBO-2503-EK	904CE003029		
C2-V72	BEST, L.	52159	ELA	PANASONIC	KX-P1124	9FMAQHF90479		
C2V71	BLASINGAME, J.	57693	ELA	Z-248		6340021		
C2V71	BLASINGAME, J.	57693	ELA	ALPS-P2000G				
C2V71	BLASINGAME, J.	57693	ELA	MODEM	CTS-2424-ADH	10116FEE		
C2V71	BLASINGAME, J.	57693	ELA	MOUSE	LOGITECH C7-3F-9F	4BULT3A1063		
S2Z51	BOBB, R.	58645	ELE	UNISYS 386	PW820COP	406591412		
S2Z51	BOBB, R.	58645	ELE	KEYTRONIC KEY	E0343ZEUS	0095035		
S2Z51	BOBB, R.	58645	ELE	LOGITECH MO	M-MC13	LU149101291		
S2Z51	BOBB, R.	58645	ELE	NEC MULTISYN	JC-1403HMA	87M006405		
NE2G15	BOZADA, C.	58650	ELR	MAC IICI	MAC IICI	F9391J8740		
NE2DD1	CHAMPAGNE, E.	57689	CA-E	Z-248	ZWX-248-62	634AE0407		
S2-P68	CHENEY, M.		ELR	Z-248	ZWX-248-62	638AF0537		
S2U48	CONCHA, L.	58662	ELE	UNISYS 386		406591354		
NE2DD1	COOK, D.	57689	CA-E	Z-248	ZENITH	638AF0492		
NE2DD1	COOK, D.	57689	CA-E	APPLE	6000 LASERWRITER II	CA844TM5%M6000		
NE2DD1	COOK, D.	57689	CA-E	MONITOR	ZENITH	646-95310047		
S2L53	COOK, J.	57681	ELM	Z-248	ZBO-2503-EK	920AH007487		
S2L53	COOK, J.	57681	ELM	PANASONIC	KX-P1124	9FMAQHF86742		
NE2X11	COOPER, T.	53643	WSU	Z-248	ZWX-248-62	649AC2883		
NE2X11	COOPER, T.	53643	WSU	Z-248	ZWX-248-62	649AC2884		
NE2X11	COOPER, T.	53643	WSU	OKIDATA	U83A8222A	283422		
S2Z52	COUTURIER, E.	58667	ELE	Z-248	ZBO-2503-EK	850CC001677		
C106	CRESPO, A.	55536	ELO	Z-248	ZWX248	638AF0294		
C106	CRESPO, A.	55536	ELO	ALPS P2000G	ALPS20	7A6222265Y		
MOD A	CUMMINS, S.	51728	ELR/WSU	MAC SE/30	IDE BY ELM FOR MIN	F94277AK02		
NE2U2	DAVIS, E.	52169	ELR	386 UPGRADE BOARD	3RD PARTY C	05378		
NE2U2	DAVIS, E.	52169	ELR	DOT MATRIX	EPSON FX-85			

THE CREATION OF AN AUTOMATIC  
ELECTRONIC MONITORING SYSTEM

Claudius W. Christmas, Jr.  
High School Apprentice

Final Report for:  
Summer Research Program  
Wright Laboratory

Sponsored by:  
Air Force Office of Scientific Research  
Bolling Air Force Base, Washington, D.C.

August 1992

# THE CREATION OF AN AUTOMATIC ELECTRONIC MONITORING SYSTEM

Claudius W. Christmas, Jr.  
High School Apprentice

## Abstract

A computer system that would electronically monitor and control electric current during experiments was created. To accomplish computer-controlled monitoring, it was necessary to find a program that would meet the requirements and demands of such a system. Upon finding such a program, the problem of deciding which type of computer system (80286, 80386, or 80486) to run the application software on had to be solved. In solving this problem, the efficiency of the final system had to be taken into consideration. The final result was a slightly modified Zenith 20286 computer system that quickly and effectively regulated the various electrical activity used in conducting experiments.

# THE CREATION OF AN AUTOMATIC ELECTRONIC MONITORING SYSTEM

Claudius W. Christmas, Jr.  
High School Apprentice

## INTRODUCTION

In the past, experiments conducted at the Wright Laboratory Structures Test Facility involving the use of electric current have required that all circuit breakers in use be manned by an operator. The person controlling the circuit breaker had to wait for instructions from the engineer telling him to close or open the circuit. These experiments also required that someone be placed at a monitoring station to monitor the volts, amps, watts, etc. This person was also responsible for communicating with the demand monitor who controlled the amount of current being drawn from the power source. The whole procedure proved to be long and tedious when an experiment required that a large amount of current be used. Therefore, the task at hand was to create a system that would successfully complete all of these jobs performed by individual workers faster and without the loss of quality.

## METHODOLOGY

The application software used in the structuring of this system was IMPACC, published by Westinghouse. This program, along with the installation of a Digitrip circuit controller in each circuit breaker and a CONI (computer Operated Network

Interface) card into an empty expansion port of the Central Processing Unit, converted an IBM compatible Zenith 286 computer into a powerful control system. In order to run this application, there were many other requirements that had to be met. First and most importantly, to operate the system at its most minimal degree, Microsoft Windows had to be installed on the computer's 20 megabyte hard drive. Second, the IMPACC program had to be installed on the hard drive. The third and final step was the most technical, this was the step in which all of the system components, including the CONI card, the AEM (Automatic Electronic Monitor through which the Digitrip units and the computer communicated), and the IMPACC program, had to be connected. Although there were only three major steps, each step had its own set of requirements which also had to be fulfilled, thus making this project extremely challenging.

The installation of Microsoft Windows was the most challenging part of the whole process. The first challenge was that of deciding which version to use. In the beginning, there was the compatibility factor. First of all, what version of Windows did the IMPACC software require? The answer to this question was version 2.01. Discussion with my co-worker and mentor revealed that 2.01 was an archaic version of Windows that was slow and consumed a large amount of random access memory (RAM). To increase the likeliness of successful operation of the system, I followed the directions and installed Windows version 2.01. To make the operating system more efficient and

user-friendly, I also installed a Logitech mouse. Another specification of Windows was the Disk Operating System (DOS) version. Initially, I had installed DOS version 4.01. However, Windows required a version of DOS earlier than 4.00. Therefore, to correct this problem, I installed version 3.01 of Microsoft DOS. I then tested Windows and it worked.

Naturally, I moved on to step two. For the most part, the installation of the CONI card into the CPU and IMPACC onto the hard drive was simple. I just removed the cover from the CPU, found an open expansion port and slid the CONI card into place. Then, I installed IMPACC on the hard drive. I seemed to be making great progress on the system. Upon completion of these two steps, I again proceeded to test the system. I ran IMPACC and the program began loading Windows. This was a normal part of the loading process. After Windows was loaded into memory, the IMPACC application itself began to load. About half way through the load of IMPACC, a message appeared on the screen. The message said "Not enough memory to run IMPACC!" What had happened was that I overlooked the fact that both programs were large and would need to reside in memory at the same time. Therefore, the system needed more than just the base memory of 640 kilobytes (K). To correct this problem, I installed 2 Mb of expansion memory. Although not all of this memory would be used in the running of these two applications, it would allow room for the use of larger programs in the future. The installation of this memory required that memory chips be installed on a memory

expansion board. The process was simple. After I installed this new memory, I tested the system again. There was still a conflict somewhere in the operation of the system. My co-worker and I discussed the problem and together we decided that we would try to upgrade the system using the most recent program versions available. This decision meant that I would have to reformat and totally erase the 20 Mb hard drive. I did this and I called Westinghouse publications to obtain the latest version of IMPACC. This upgrade was given to us at no cost because the representatives of Westinghouse that had previously installed the Digitrip units and the AEM had provided us with the latest version of the AEM which was the AEM II. The new AEM was not compatible with the version of IMPACC that Westinghouse had provided us. Therefore, they simply sent us the latest version of the program at no charge. I was also able to find DOS version 5.00 and Windows version 3.00. I then reinstalled all three of these programs on the hard drive and the system was extremely fast and successful and almost complete.

The final step was connecting the AEM to the computer and testing the system as a whole. To connect the system to the AEM, I had to relocate the computer and its components to their final destination. Following this relocation a few members of the High Voltage Maintenance team at the laboratory ran the wire that would be the final connecting point of the system to the AEM. I connected the wire to the system through the CONI card. I then completed the final test, running IMPACC and monitoring each



breaker. The test was successful! Weeks of work had finally yielded results and the automatic electronic monitoring system was complete. I made a few minor adjustments and modifications to aid in the use of the program and the system became a major enhancement in the productivity of the electricians to whom this system now belonged.

### CONCLUSION

In the creation of this system, only one minor discovery was made. This discovery involved the phases or sub-units controlled by the breakers. Since the control of the breakers had been controlled by humans since the systems setup, any error made in the setup would not have been found without close examination. However, when the first test was run and monitored on the computer an error in the conventional setup was discovered. In this test, only two phases, phases A & B, were being run. On the computer, phases B & C were the ones that were being monitored. This could only mean one thing. It meant that for the 25 years that this conventional system had been used, phases A & C on channel 57 had been plugged in to opposite ports. Although this discovery was not critical and had no bearing on the previous tests using this channel, it was nice to know that the system that I had constructed will serve many meaningful purposes. All of the tasks it will perform, I do not know. One thing I do know is that this High School Apprenticeship program allowed me the opportunity to be a part of it. I learned a tremendous amount

about teamwork, computers and dealing with people. I would just like to send out thanks to the Air Force Office of Scientific Research and to my supervisor and co-workers that I had the privilege to work with this summer. It was a great learning experience and one that I will never forget.

## Bibliography

1. IMPACC version 6.08 monitor and control software, (c) 1990, available from Westinghouse. Requires an IBM compatible computer with an Enhanced Graphics Adapter and Microsoft Windows.
2. Microsoft DOS versions 3.01, 4.01 & 5.00 disk operating systems, (c) 1986, 89, 91, available from Microsoft. Requires an IBM compatible computer.
3. Microsoft Windows versions 2.01 & 3.00, (c) 1986, 1991 available from Microsoft. Requires an IBM compatible computer with an Enhanced Graphics Adapter.

## **WRAP-AROUND FINS**

Theresa J. Cook  
High School Apprentice  
Aerodynamics Branch

Wright Laboratory Armament Directorate  
WL/MNAA  
Eglin AFB, FL 32542

Final Report for:  
High School Apprenticeship Program  
Wright Laboratory Armament Directorate

Sponsored by:  
Air Force Office of Scientific Research  
Bolling Air Force Base, Washington, D.C.

August 1992

## WRAP-AROUND FINS

Theresa J. Cook  
High School Apprentice  
Aerodynamics Branch  
Wright Laboratory Armament Directorate

### Abstract

The computer-simulated aerodynamics of missiles with wrap-around fin configurations were studied. The fins were modeled both with and without thickness on an infinitely long cylindrical body. The thick fins were bi-convex airfoils with a thickness of ten percent of the chord and the thin fins were infinitely thin. Computed trends of the thick-finned models closely resembled the trends of experimental data. The wrap-around fin configuration caused a roll reversal through Mach 1, a side force at angle of attack, and a roll moment at zero degrees angle of attack. The thick fins also created a lift force that was a constant amount more than the force created by the thin fins.

## WRAP-AROUND FINS

Theresa J. Cook

### Introduction

The need for greater storage ability of munitions has created a demand for more compact missile configurations. Many different methods have been tried, but the most effective is the wrap-around fin, which is a fin that is bent to match the curvature of the missile body. This allows the missiles to be stored more conveniently and also allows them to be tube-launched. Currently, missiles are bulky and take up large amounts of space in storage shelters or cargo bays. Also, care must be taken to ensure that the fins are not damaged. With the wrap-around fin, the fins fold up flush with the body, so that the missile only takes up as much space as the actual body and the fins are more protected from scrapes and dings that may occur during shipment and handling. Having a wrap-around fin configuration also allows the missile to be tube-launched, eliminating the need for sophisticated propellant systems or sabots. These are both tremendous advantages.

There are drawbacks to the wrap-around fin configuration, however. The curved fins create an asymmetrical body in which the forces created on one fin are not counteracted by the fin on the opposite side of the body. This creates a number of aerodynamic oddities, such as roll reversal through Mach 1, a side force (yaw) at certain angles of attack (pitch), and a roll moment at zero degrees angle of attack. These occurrences, combined with the lift force generated at angle of attack, make for a very unstable flight. If this continues undamped, the missile becomes less accurate and the results could be catastrophic.

The roll reversal through Mach 1 is an unexplained phenomenon. The missile rolls positively, or clockwise, through its subsonic flight, but then rolls negatively, or counterclockwise, through its supersonic flight. This may be caused by the different forces acting on the fins at these speeds, but this is an uninvestigated occurrence. However, the transition from positive to negative rolling moment does not occur exactly at Mach 1. The positive rolling trend actually crosses zero around Mach .95.

The side force at angle of attack causes the missile to have greater yaw. This can lead to erratic flight patterns and loss of accuracy. A small side force is to be expected from various launch effects, but it should damp out during the course of the flight. In some cases, the side force does not damp out, and the missile is inaccurate.

The roll moment at zero degrees angle of attack is unexpected because there should not be forces that would act more on one side than on the other at no angle of attack. This effect may be caused by the different pressure zones created by the curvature of the fins.

### Methodology

Using Computational Fluid Dynamics (CFD) codes, missiles and fins can be modeled on the computer for testing purposes. The process for modeling these objects is extensive. First, the parameters for each piece of each surface must be defined and the surface created. There are usually errors, and the surfaces must be checked thoroughly to ensure that everything matches up and all the parts are there. Then the surface code is run through a grid generator to create all the points for the computer to analyze. This also has frequent errors and must be checked. When the surfaces and the grid are error-free, the code is put into a flow-solver, which simulates airflow around the body. This is a very large task and is usually run on a super computer. Different aerodynamic conditions, such

as Mach number, angle of attack, and roll angle, can be specified to get the desired results. These runs give a variety of output in several forms. One form is actual numbers, which represent the aerodynamic coefficients, and the other form is the computer code that is made. This output can be converted into graphics and the effects of the configuration can be demonstrated visually. The output data can also be compared to experimental data and the aerodynamic trends observed.

The models in this analysis were a set of four fins modeled on an infinite cylinder. The fins were modeled with and without thickness, in order to test the capabilities of the CFD codes. The thick fins are bi-convex airfoils with a thickness of ten percent of the chord, while the thin fins are infinitely thin, that is, they are only a line. The reason for the two different types of fins was to determine whether or not the fins must have thickness to get accurate results. The fins were not modeled on an actual missile body because there are other factors and problems created by the effects of the nose and the body ahead of the missile.

Once the models were prepared, they were run under several different conditions. Tests were run at Mach numbers .3 through 3.5, angles of attack ranging from -4 degrees to +4 degrees, and at roll angles from -45 degrees to +45 degrees. The alteration of these variables helps to analyze many different situations that may occur during the missile's flight. The Mach numbers helped to investigate the difference in roll moment subsonically and supersonically. The varying angles of attack and roll angles can simulate the effects of an unstable flight on the path of the missile. The results from these test runs were then checked for reliability and compared to experimental results.

## Results

The output data from these tests runs was used in many ways. The tests were run on



the set of four fins as a group and on each fin individually. On the individual fins, the pressure contours were examined. The supersonic cases (Fig. 1) exhibited regions of high pressure, particularly against the body on the upper side of the fin and under the fin, while the subsonic cases (Fig. 2) showed more low pressure trends. If the pictures were viewed in color, the high pressure areas would be lighter colors (white, pink, red), and the lower pressure areas would be darker colors (blue, purple, black). These differences in pressure may explain the change in the roll moment through Mach 1.

The pressure contours observed on the four fins as a whole are affected by angle of attack and roll angle. The regions of high pressure are repeated on all four fins similarly at zero degrees angle of attack and zero degrees roll angle (Fig. 3), but become more and more dissimilar as angle of attack and roll angle are increased. At negative two degrees angle of attack and zero degrees roll (Fig. 4), for example, The pressure on the top and bottom fins remains the same, but the pressure on the left and right fins changes drastically. This change in pressure increases the roll moment. Another case, at negative two degrees angle of attack and forty-five degrees roll (Fig. 5), the pressure contours on all four fins change. The two pairs of fins on either side of the body are completely unbalanced by the fins on the other side, creating an even greater roll moment.

The roll moment reversal was also studied. The runs were started at Mach .3 and run up to Mach 3.5. Through the plot of the roll moments generated at each test run (Fig. 6), the roll moments steadily rose up to Mach .85, where it seemed to peak. After this point, the roll moments drop sharply through Mach 1.5, when they seem to stabilize. Then the roll moments rise slowly through Mach 2.5, where they level out and there does not seem to be a large effect on rolling moment at speeds higher than this. This trend is similar qualitatively to the trends observed in experimental results. Several cases were also run at Mach 1.5 and varying degrees of roll and angle of attack to determine if there

was a large difference caused by these factors. While there was an effect caused by the roll angle and angle of attack, it was not significant.

There is also a lift force created by the fins at angle of attack. The force created by the thin fins is almost linear from negative four to positive four degrees angle of attack and is zero at zero degrees angle of attack. The thick fin, however, is also very close to linear, but is shifted vertically a small amount.

### Conclusions

This project was an important step in determining the usefulness of Computational Fluid Dynamics in simulating airflow patterns around various missiles and fin configurations. The CFD codes emulated the trends observed in experimental tests accurately, proving that CFD is a useful tool in the analysis of asymmetrical fin configurations. It properly illustrated the aerodynamic trends such as a roll moment at zero degrees angle of attack, a roll reversal through Mach 1, and a side moment at any angle of attack. There is a difference, however, between the thick and the thin finned models. Only the thick fins demonstrated the similar aerodynamic trends that were observed in experimental data. The thin fins were ineffective in analysis and did not show similar forces or trends. The computer needs to have that thickness in the fins to differentiate that there is actually a body there. Although the thin fins are much easier to model, the data acquired from those tests runs was unusable.

This is an ongoing project and much more work can be done on it. Some recommendations for future studies would be to add viscous effects to the test runs. Viscosity is the 'stickiness' of air and may have some effect on the flight of the missile. This factor was left out of these tests because of time restraints and complexity. Another suggestion would be to model the fins on an actual missile body to see if the disturbance

caused by the nose and the rest of the body has any effect on the way the fins behave. A third possible improvement would be to compare the results quantitatively to experimental data. These tests were only compared qualitatively because of the lack of comparable information in both the analytical and experimental areas.

The wrap-around fin configuration is not just stuck in labs and on drawing boards. This technology is currently being used in several missiles, but much more can be done to improve upon it. All four branches of the Armed Services of the United States and other countries all around the world are conducting experiments on wrap-around fins, and hopefully a reliable configuration will be found soon.

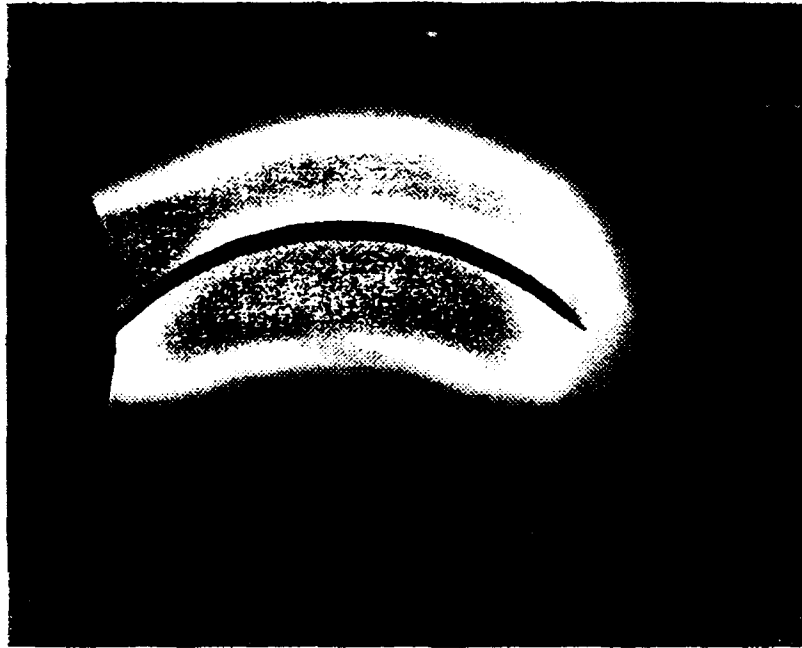


Fig. 1  
Pressure at Mach 1.5



Fig. 2  
Pressure at Mach 7



Fig. 3  
0 deg. Angle of attack  
0 deg. Roll

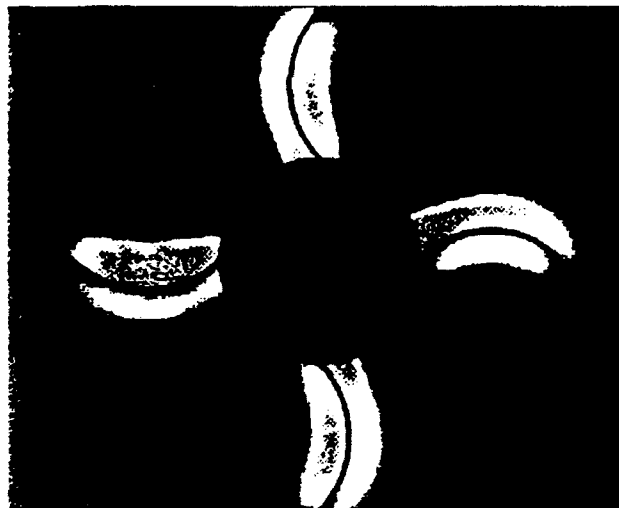


Fig. 4  
-2 deg Angle of attack  
0 deg. Roll

Fig. 5  
-2 deg. Angle of attack  
45 deg. Roll



# Roll Moment vs. Mach Number

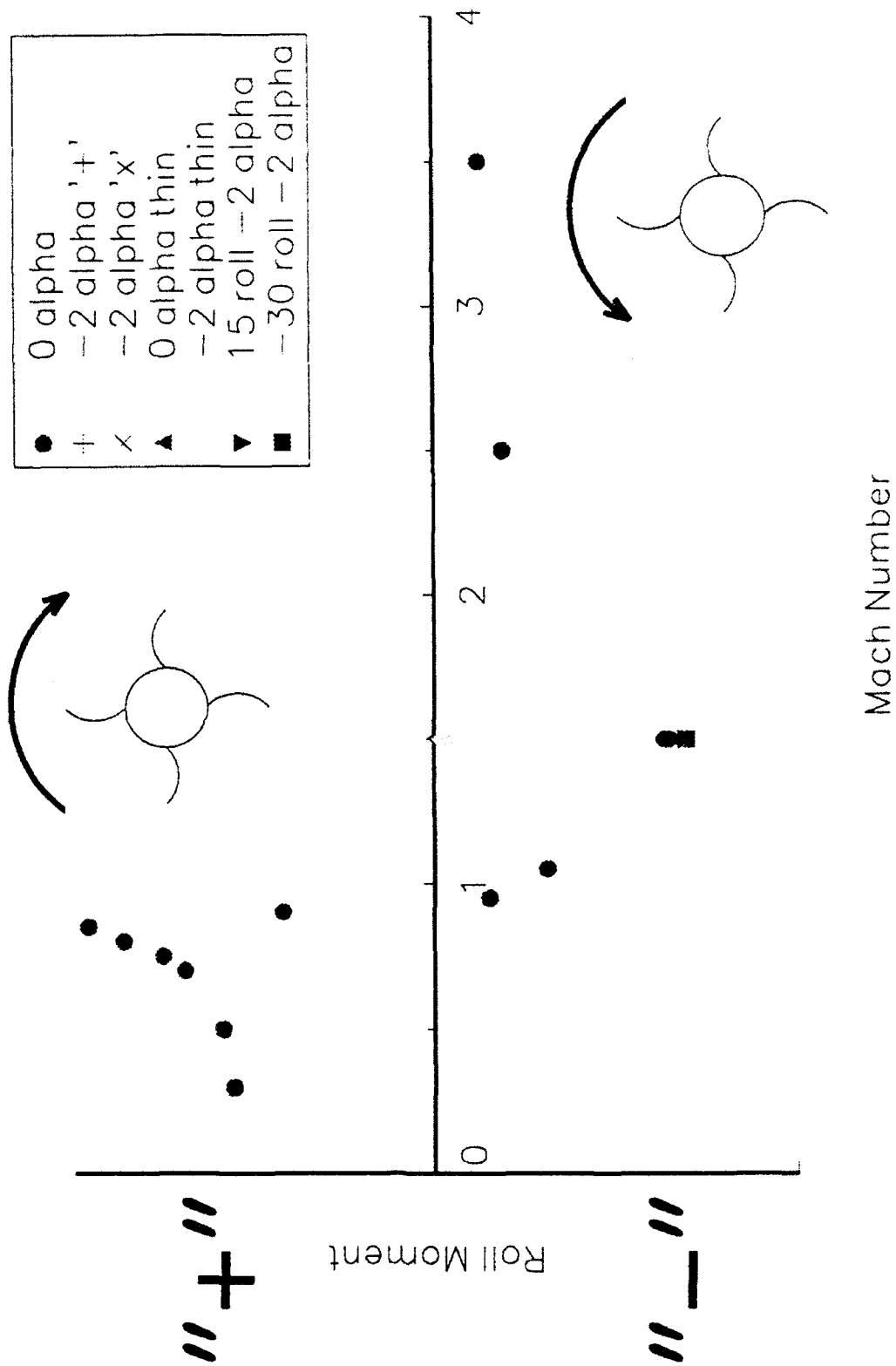


Fig. 6

A STUDY OF HEAT TRANSFER SIMULATION AND  
SIMULATION SOFTWARE USER-FRIENDLINESS

Gerald Dalley  
Student

Beavercreek High School  
2490 Dayton-Xenia Road  
Beavercreek, OH 45385

Final Report For:  
Summer Research Program  
Wright Laboratory

Sponsored by:  
Air Force Office of Scientific Research  
Wright-Patterson Air Force Base, Dayton, Ohio

September 1992

A STUDY OF HEAT TRANSFER SIMULATION AND  
SIMULATION SOFTWARE USER-FRIENDLINESS

Gerald Dalley  
Student

Abstract

In the course of studying the user-friendliness of the Kappa-PC expert-shell software, simulations for two heat exchanger systems were produced. The first, part of the AHXE (Advanced Helical-loop eXchanger Evaluation), simulates a new high efficiency heat exchanger. Originally designed for use on NASP (National Aerospace Plane), the exchanger will be used to absorb high levels of heat quickly and efficiently. Specifically, it is designed to cool hypersonic aircrafts' leading edges. The actual testing of the heat exchanger is scheduled for later this year.

The second project, micro-encapsulated PCM(Phase Change Material), studies the use of microscopically encased globules of paraffin in a coolant. The simulation, nearing completion, will help determine the increased efficiency and possible weight reductions for cooling systems aboard advanced aircraft. The results found the Kappa-PC program, used to create these two simulations, to be a powerful simulation shell capable of building highly user-friendly simulations. The software itself, in creating simulations, lacks some of the elements of user-friendliness that its simulations hold.



# A STUDY OF HEAT TRANSFER SIMULATION AND SIMULATION SOFTWARE USER-FRIENDLINESS

Gerald Dalley

## INTRODUCTION

Simulations in today's scientific world provide a much needed capability for enhancing experiments and generating higher test reliability. Given initial mathematical data, a scientist can then model the test appropriately and compare the empirical findings to the theoretical ones. A better understanding of the experiment is achieved through the intimate knowledge of the problem required to complete the simulation. Then, when the actual test stands are actually built, the debugging time and costs are greatly reduced through comparison of the stand to the simulation results at appropriate checkpoints.

## DESCRIPTION OF PROBLEM

The AHXE simulation was originally designed for the National Aerospace Plane project. The helical-coil evaporator provides a method of applying heat to a coolant more effectively. This is accomplished by spinning the fluid such that the cooling liquid is forced outside, onto the heated surface. Possible applications for similar evaporators are the NASP wingtips and other locations where high heat transfer is required.

More recently begun is the PCM Initiative, designed for use in advanced aircraft. The PCM used is a type of micro-encapsulated paraffin suspended in a PAO (Polyalphaolefins) coolant. Since the PCM material absorbs more than three times more heat by latent heat absorption when melting than the PAO fluid does through a simple temperature increase, it raises the heat absorption capacity of the overall fluid. This results in more efficient cooling systems that can be smaller, lighter, and more effective. The empirical tests will determine to what extent various potential problems are a concern. Some possible problems include the release of paraffin into the PAO due to shear forces in a pump ripping away the encapsulation. Neutral buoyancy

must be maintained to avoid settling of the PCM in the lines and pump while not in operation. The simulation provides a mean of foreseeing some of the results of these and other concerns to the programs.

## METHODOLOGY

In order to produce the simulations required for the AHXE and PCM programs, Kappa-PC, by IntelliCorp, was used. Kappa is a graphically-oriented, object-based expert shell. By representing the various elements of heat exchanger loops as objects, a flexible and intuitive relationship among the them was made, from user as well a programmers' standpoint. The AHXE system was modeled first. With it, the setup for a basic Freon and water loops was made and the individual objects in the loop such as a pump, evaporator, and condenser. Much of the mathematics involved with AHXE were accomplished through external communication with other programs. Data from a pre-made Excel spreadsheet was acquired through the MS Windows DDE (Dynamic Data Exchange), and I/O files provided the exchange with a program written in FORTRAN. After completion with AHXE, the program was modified to accommodate a PCM/PAO loop instead of a Freon circuit. Having used the object-based methodology, few methods were made necessary to be modify.

## RESULTS

Using Kappa-PC, the AHXE and PCM simulations were written. The abilities to import images created in Harvard Graphics and Windows Paintbrush greatly enhance the user-friendliness capabilities. The ability to use many of the Windows "gadgets" such as buttons, scroll bars, and radio boxes also add to the ease of use. However, this ease is not achieved within the the simulation setup and programming. Kappa lacks several design elements and keyboard shortcuts, such as graphical element grouping, often making the front-end take far longer to create than the actual simulation mathematics.

Here are some example screens from the AHXE and PCM simulations:

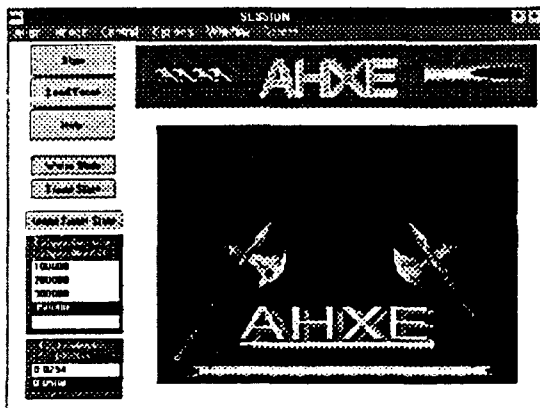


Figure 3: AHXE Simulation Initial Screen

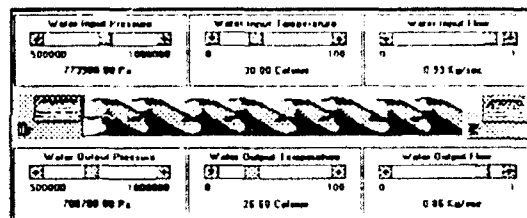


Figure 2: AHXE Water Loop Output

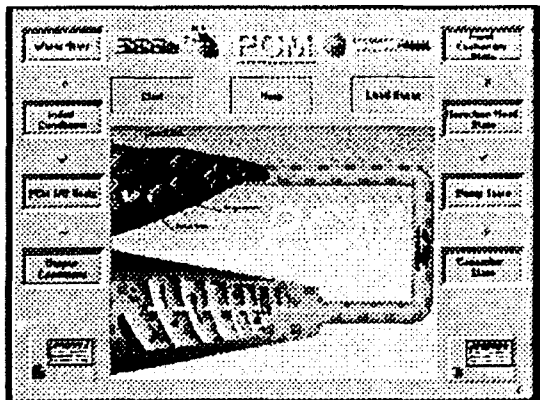


Figure 1: PCM Simulation Initial Screen

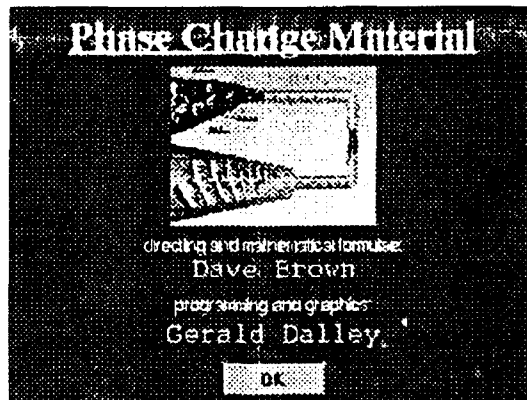


Figure 4: PCM "About Dialog"

## CONCLUSIONS

Kappa-PC has proven to be a powerful simulation tool capable of displaying detailed and informative front-ends with a polished appearance. However, more polish could be put into the programmer's graphical interface.

The experiences gained through the RDL High School Apprenticeship program have helped me to better understand what is involved in an engineering and research career. I have gained valuable work experience with it, as well as experience with several state-of-the-art and industry standard software.

DEVELOPMENT OF A PRESSURE TRANSDUCER  
CALIBRATION DEVICE

Elizabeth C. Day  
Summer Apprentice  
Compressor Aero Research Lab  
Technology Branch  
Turbine Engine Division  
Aero Propulsion and Power Directorate

WL/POTX  
Wright-Patterson AFB, OH 45433

Final Report for:  
AFOSR Summer Research Program  
Wright Laboratory

Sponsored by:  
Air Force Office of Scientific Research  
Bolling Air Force Base, Washington, D.C.

August 1992

DEVELOPMENT OF A PRESSURE TRANSDUCER  
CALIBRATION DEVICE

Elizabeth C. Day  
Summer Apprentice  
Technology Branch  
Turbine Engine Division  
Aero Propulsion and Power Directorate  
Wright Laboratory  
Wright-Patterson Air Force Base

**Abstract**

*In order to obtain the most accurate measurements possible, a measuring device must be compared to a standard, or calibrated. The measuring device cannot be calibrated to an accuracy greater than that of the standard. Generally, the calibration standard should be at least ten times more accurate than the instrument being calibrated. It is imperative that pressure transducers used in axial compressor research be carefully calibrated in order to allow for accurate experimental results, as the results may affect expenditures, new design plans, and even human lives. A device used to calibrate pressure transducers for the Air Force Aero Research Lab was needed. A thorough description of the design process is presented.*

## DEVELOPMENT OF A PRESSURE TRANSDUCER CALIBRATION DEVICE

Elizabeth C. Day

During Air Force axial compressor research, a need developed for a device that could be used to periodically calibrate pressure transducers. Pressure transducers electronically transmit pressure measurements. Calibration ensures the acquisition of accurate experimental results. Having two types of cylindrical pressure measurement systems with different diameters, the device needed to capacitate each system at different times. The smaller transducer measured static pressure, while the larger instrument measured total pressure. In order to preserve time efficiency, multiple transducers needed to be calibrated at the same time, although only one type of transducer would be processed at a time. A static calibration technique fulfilled the requirements in the development of the device.

The first step in the development was to determine a method for maintaining temperature, volume, and the moles of gas at constant values. An enclosed volume such as a box would suffice. Variable pressure would be supplied by pressurized air entering the airtight box through an opening containing a compression fitting. The pressure could be monitored by a pressure gauge fitted in the same manner. To allow the tubes connected to the transducers to remain unobstructed, only the sensor portion of the transducers could penetrate the box. This was accomplished by lowering the measurement devices through holes in the top of the box and sealing them with compression fittings. Two tops for the calibration box were necessary. One would contain sixteen holes to compensate for the smaller transducers, while the other would contain ten holes for the larger instruments. The two tops could be easily interchanged as needed.

The next step in the development was to choose the material and to calculate the dimensions for the construction of the calibration box. The calibration box needed to withstand pressures up to 30 pounds per square inch.



At the same time, the practicality of the box needed to be maintained. Weight, portability, and convenience were considered. Aluminum seemed to be the logical choice, as it could withstand low pressures and was a lightweight material. The aluminum could also be welded to seal any cracks that might leak air. In determining the size of the box, the dimensions of the transducers were measured. The width and length were derived by allowing room for the larger measuring instruments, their fittings, a wrench for adjustments, and clearance from the sides of the box. The length of the larger instruments also delineated the height of the box.

All of the edges of the box could be welded together, but the lids, being interchangeable, could not be welded to the box. Instead, an alternative method of sealing the lid to the rest of the box was needed. A gasket placed in between the lid and box sides was a possibility, but the question of whether the gasket would leak at 30 psi remained. To ensure a permanent pressure-withstanding seal, a groove for an O-Ring was placed in the top of the sides of the box. The tops of the sides of the box were extended to accommodate a standard size O-Ring. The circumference of the O-ring and the need for adequate clearance from the edges determined the length of the extension and the placement of the groove. The interchangeable lids were attached to the box with standard screws in six places around the edges. The holes in the box were threaded, while the lids contained clearance holes in alignment with the threaded holes.

The inlets for the pressurized air and pressure gauge were placed low upon one side of the box. This would prevent the inlets from obstructing the paths of the pressure transducers. To prevent over-pressurization of the box, which would result in damage to the pressure transducers, a relief valve was added to the side opposite the air and gauge inlets. The relief valve was placed on the opposite side in order to protect the user if the valve were to release.

After deciding upon the dimensions, the materials, an O-Ring, and opening placements, the design was drawn using a computer aided drafting program. The program made dimensioning, tolerancing, and editing faster and easier. The machine shop that constructed the calibration box was able to clearly understand

the drawings and reproduced the calibration box precisely as it was conceived.

The practicality of the calibration box is overwhelming. It is inexpensive, portable, and time efficient. The device can even be used to check for leaks in the pressure transducers. Other lids may be designed to accommodate different sizes of pressure transducers as needed. The resulting calibration device serves as a quick, convenient way to calibrate pressure transducers.

### References

- Doebelin, Ernest O. Measurement Systems. New York: McGraw-Hill Book Company, 1966.
- Holman, J. P. Experimental Method for Engineers. New York: McGraw-Hill Book Company, 1966.

SECTION A-A

O-RING GROOVE  
0.185 ± 0.005 WIDE  
0.106 ± 0.003 DEEP

6.000

7.250

0.250 ± 0.002 TYP

0.250 ± 0.002 TYP

0.250 ± 0.002 TYP

0.125 RAD TYP

0.125 RAD TYP

10.32 THD THRU TYP

1/2 X 1/2 IN ALUMINUM  
WELDED, TYP

1/4 NPT

NOTE: ALL DIMENSIONS  $\pm$  0.005 UNLESS OTHERWISE INDICATED

**NOTE. ALL PIECES FROM 1/2 IN. ALUMINUM STOCK WELDED TOGETHER**

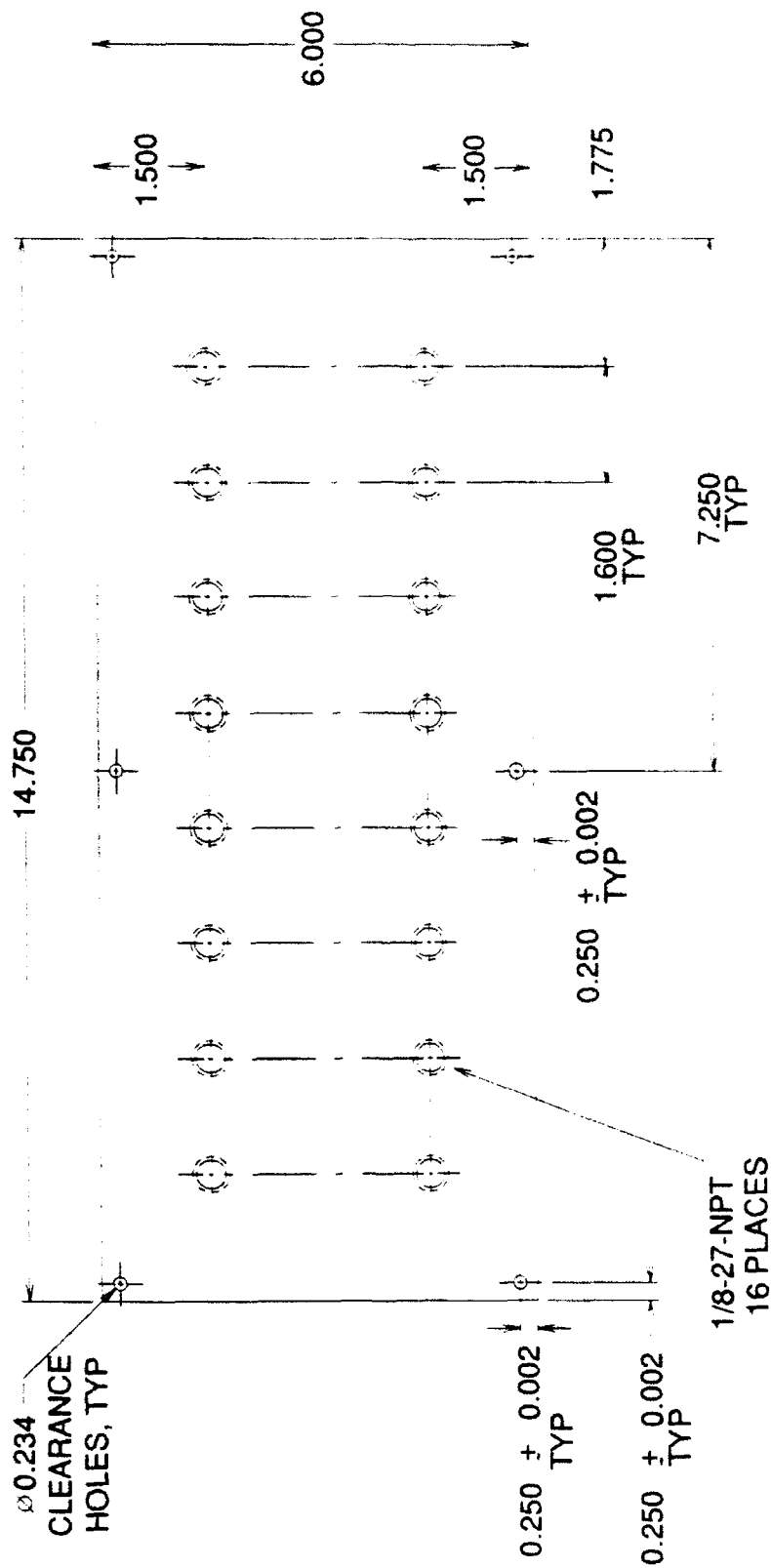
**NOTE: O-RING 277**

Technical drawing of a 10-8 plate showing dimensions and hole locations. The drawing includes the following specifications:

- Overall Dimensions:**
  - Width: 6.000
  - Height: 14.750
- Clearance Holes:**
  - Size:  $\phi 0.234$
  - Location: 1.875 from the top and bottom edges.
- Main Holes:**
  - Size: 3/4-NPT
  - Quantity: 10 PLACES
  - Location: 2.750 TYP from the centerline.
- Other Dimensions:**
  - 0.250  $\pm$  0.002 TYP (multiple locations)
  - 0.250  $\pm$  0.002 TYP (multiple locations)

NOTE: ALL DIMENSIONS ± 0.005 UNLESS OTHERWISE INDICATED

# KULITE LID FOR CALIBRATION BOX



10-9

NOTE: FROM 1/2 IN. ALUMINUM STOCK

NOTE: ALL DIMENSIONS ± 0.005 UNLESS OTHERWISE INDICATED

FRACTAL GEOMETRY: AN EXPLANATION AND APPLICATION

Lesha Denega  
High School Apprentice  
Advanced Guidance Branch

Wright Laboratory Armament Directorate  
WL/MNGA  
Eglin AFB, FL 32542-5434

Final Report for:  
High School Apprenticeship Program  
Wright Laboratory Armament Directorate

Sponsored by:  
Air Force Office of Scientific Research  
Bolling Air Force Base, Washington, D.C.

August 1992  
FRACTAL GEOMETRY: AN EXPLANATION AND APPLICATION

Lesha Denega  
High School Apprentice  
Advanced Guidance Branch  
Wright Laboratory Armament Directorate

Abstract

Increased awareness of the study of chaos in the past twenty years has brought into focus a new and different type of geometry. Fractal geometry is a product of chaos study and the study of turbulent systems. The practical applications of fractal geometry and fractal dimension have also found an use in seeker systems as a means of detecting man-made objects in clutter. We discovered that it was possible to write code to perform this function on the ATLAS LADAR system.



## INTRODUCTION

For many hundreds of years science has concerned itself with the problems of life as we know it; strangely enough, the models of classical systems are often very different from the natural phenomenon they mimic. The imperfections and chaotic tendencies of natural systems have forced scientific models to rely heavily on guesswork. Until recent years, the mathematics and geometry of turbulent and natural systems were non-linear, and therefore theoretically unsolvable. Yet with the study of chaos and chaotic systems came a new geometry, and a new way of studying natural systems and objects - fractals. This summer, I studied the science of fractals; in doing so I was able to understand and help apply that science to the LADAR (Laser Radar) imaging system for the ATLAS (Advanced Technology LADAR System) program. Under the guidance Lt. Matt Whiteley, John Wolverton, and Bill Eardley, I studied how and why fractal geometry could be applied to this system. I then assisted a fellow apprentice in writing code for a program to utilize this knowledge. The following are explanations of the geometry and calculations behind fractal applications to LADAR.

## APPARATUS

For my research I used a 386 desktop and a 248 Zenith laptop. I also utilized several references books and articles on the subject, as well as speaking extensively with personnel familiar with the LADAR system.

## BACKGROUND

There is, to date, no definitive explanation of what a fractal is exactly. The study of this peculiar branch of geometry was a result of increased scientific interest in chaos and chaotic systems. For many years before Benoit Mandelbrot's paper "How Long is the Coast of Britain?" was published, there was extensive, if little known, research about chaotic systems. In his paper, Mandelbrot explains the seeming paradox of infinite perimeter and finite area. Consider a coastline, any coastline in the world. If you measure the coastline with a yardstick, by laying yardsticks along the twists and curves of the coast, you will reach a certain number. But if you measured the coastline again, this time laying down one-foot rulers, you would reach another number, a larger number. The smaller the measuring stick you use, the more curves and twists you can accurately measure. Potentially, this scaling could continue ad infinitum, yet the area

the land mass remains finite. Modern science would have us believe that at some point these values would converge to one finite perimeter. As James Gleick says "Mandelbrot found that as the scale of measurement becomes smaller, the measured length of a coastline rises without limit, bays and peninsulas revealing ever smaller subbays and subpeninsulas," (1987).

The realization that coastlines, in this fashion of measurement, were infinite created another question in the minds of scientists. Was there another way, a qualitative way, to measure these infinite perimeters? The answer was "Yes." Coastlines, or any curve that is "fractal" in nature can be measured by their "fractal dimension." In our everyday lives, we usually perceive objects in dimensions of integer values. Dimensions, though, might not really be so simple. Briggs and Peat explain: (see figure 1) "What, for example, is the dimension of a ball of string? From far away the ball looks like a point and therefore has zero dimension. But from a few feet away everything is back to normal and the ball is three dimensional. But what happens if we come very close? We see an individual thread that is twisted up and wrapped around. The ball is composed of a twisted line, and is therefore one dimensional. Even closer this line turns into a column of finite thickness, and the thread becomes three

dimensional" (1989).

This lengthy discussion about a ball of string illustrates how the effective dimension of an object or surface can change at differing scales. What, then, is the true dimension? Fractal dimension is simply the fractional value applied to the dimension of a curve. The closer this value is to one, the smoother the curve is. But as the curve acquires greater detail and irregularity, the dimension approaches that of a plane, and the fractal dimension approaches the integer two. The coastline of Great Britain, for example, has a fractal dimension of 1.26 (Briggs and Peat, 1989). The Koch snowflake, first described in 1904 by Helge von Koch, is another example of infinite perimeter with a finite area. An equilateral triangle (side length 1) is inscribed in a circle. To the three sides of the triangle, in the middle of each side, place another triangle one third the size of the original, and so forth. If the original triangle (see Figure 2) is inscribed in a circle, even after a million iterations, the area will still remain in the circle. Not only is the curve infinite, it is also self similar, a property Mandelbrot observed in his coastline question. No matter what scale you look at the Koch curve, it looks the same as the iteration before. (Gleick, 1987).

Mandelbrot was discovering a whole new way of

looking at seemingly impossible and random curves and shapes. Looking back at cotton prices of the past century and the heights of rivers of the world, Mandelbrot found the same "order within chaos" that he observed in the coastlines. While the prices of cotton and the heights of the rivers were erratic and random, Mandelbrot found that the pattern of randomness was extremely similar at different scales. The curve for changes in one month was remarkably alike the curve for one year. Self-similarity at differing scales was found not just in the strange constructs of von Koch, but in the chaotic systems of natural flux as well (Gleick, 1987).

What exactly are fractals, then? Briggs and Peat offer this definition: "In general fractals are characterized by infinite detail, infinite length, no slope or derivative, fractional dimension, self-similarity, and (as was done to produce the Koch coastline) they can be generated by iteration" (1989). Gleick says of the subject: "Above all, fractal meant self-similar," and that "self-similarity is symmetry across scale. It implies recursion, pattern inside of a pattern" (1987). Fractals became a way of describing the shapes and systems of nature in a uniquely qualitative fashion, rather than a quantitative method.

## METHODOLOGY

Once an understanding of fractals and fractal dimension was established, I concentrated on applying that knowledge to image processing, with the ATLAS LADAR system specifically in mind (see figure 3). One of the key problems involved in image processing is reducing background clutter. An airplane in the middle of the desert is much easier for an autonomous system to detect than an airplane in the middle of dense brush or vegetation. How could this new mathematics of chaos aid in the reduction of background clutter? After speaking with other ATLAS team members, we hypothesized that natural objects, being more fractal fundamentally, would have fractional dimensions. Man-made objects like bridges, buildings and aircraft would have dimensions closer to integer values. Any fractal properties that man-made objects possess at one level of magnification would tend to disappear when looking at said object at any other scale.

This idea, we discovered, was not entirely new. Kim T. Constantines, a senior staff engineer in APL's Fleet Systems Department, published an article in Johns Hopkins APL Technical Digest in November of 1991 regarding the same idea. The title, "Using Fractal Dimension for Target Detection in Clutter" fairly well summarized what we were trying to accomplish. There was

a fundamental difference, though. Constantikes' article focused on target detection using infared radar. The ATLAS system uses LADAR, or laser radar, so that the returns give not only x and y data, but z values as well. The algorithm we eventually developed using, in part, data from Constantikes' findings, was able to function using either type of return.

The fundamental premise of what we were attempting was based on the assumption I mentioned earlier - natural objects are more fractal in nature than man made objects. By segmenting the image return and determining the fractal dimension of each bin, it is possible to differentiate between areas of differing fractal dimension. Lt. Whiteley, one of my mentors, explained the portions of the algorithm that we were unable to understand. We were now ready to write code that would perform the functions outlined in the original plan. I assisted fellow apprentice Jason Lindsey in writing code in Pascal to perform the algorithm.

## REFERENCES

Briggs, John and F.David Peat, Turbulent Mirror. Harper  
New York; 1990.

ar

Constantikes, Kim T. "Using Fractal Dimension for  
Target Detection in Clutter," Johns Hopkins APL  
Technical Digest. Vol. 12 No. 4, 1991.

Gleick, James, Chaos: Making a New Science. Peguin  
Books, New york;  
1987.



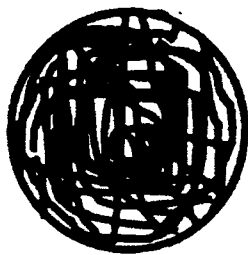
# Fig 1 Fractal Dimension (& a ball of yarn)

Viewed from far away.....



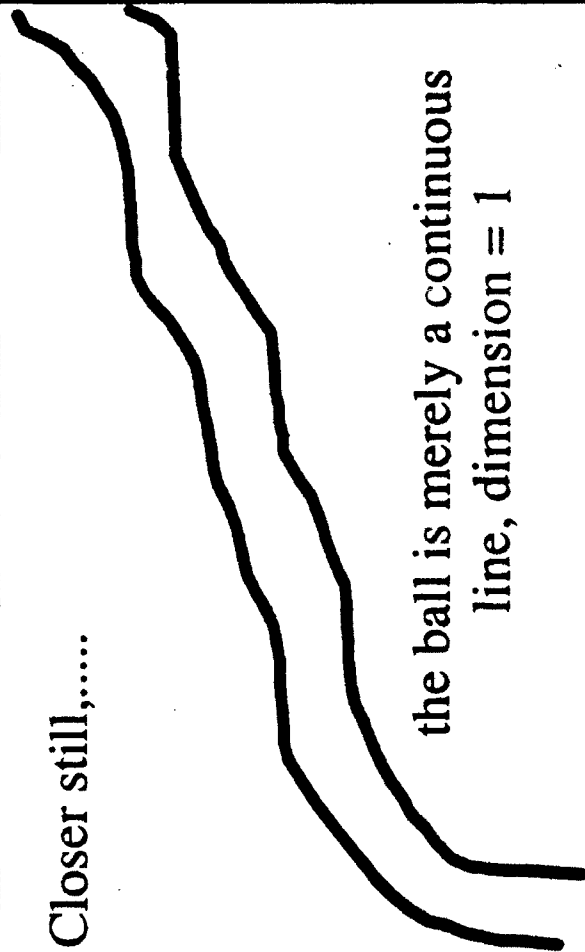
the ball is a point, dimension = 0

Upon closer inspection.....



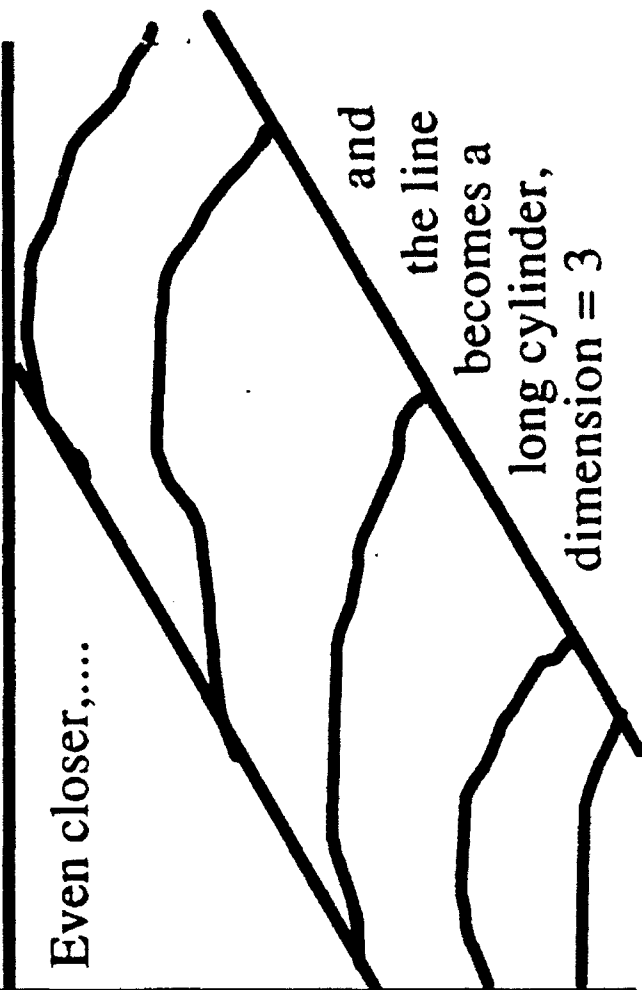
the ball is a sphere, dimension = 3

Closer still,....



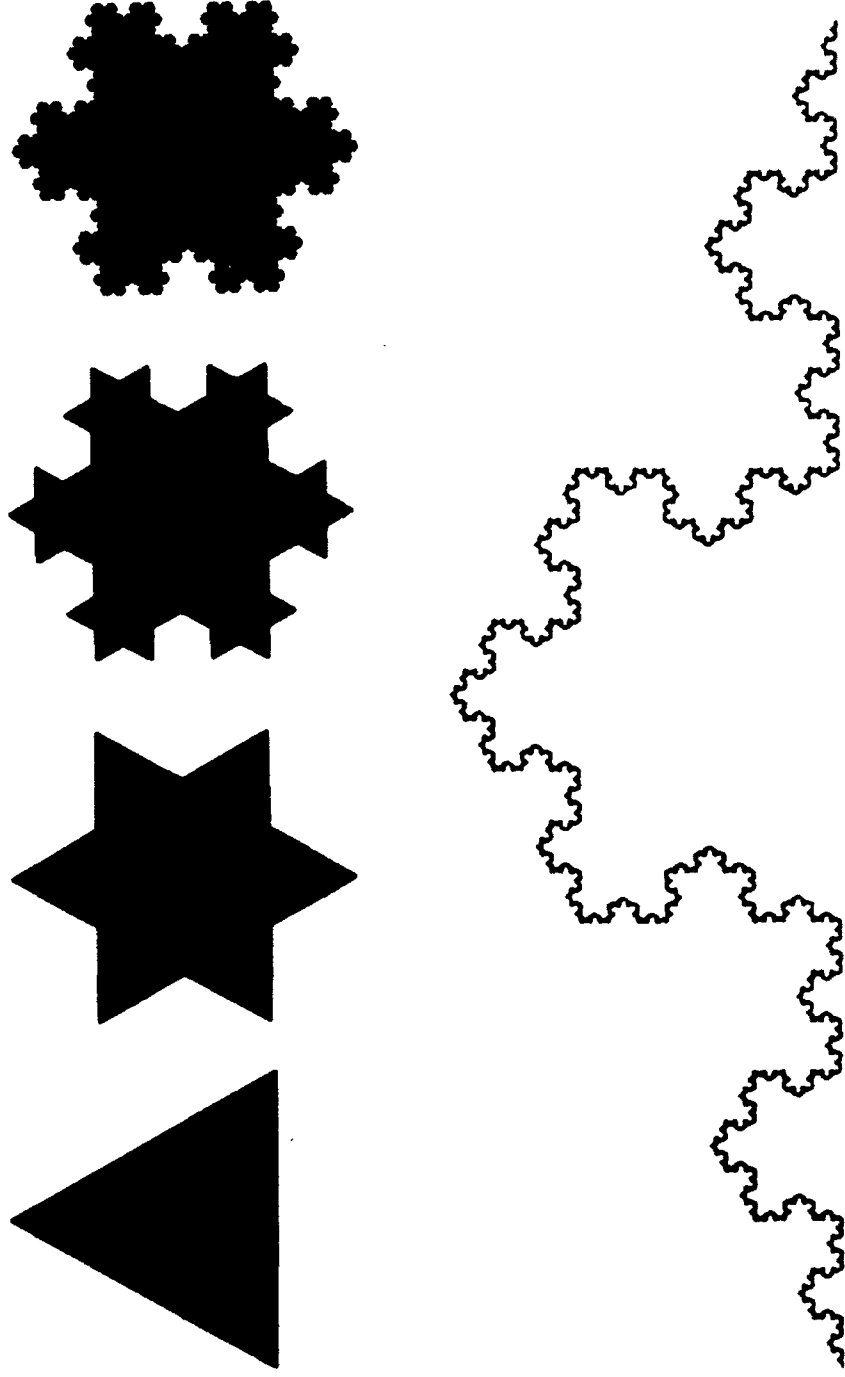
the ball is merely a continuous  
line, dimension = 1

Even closer,....



and  
the line  
becomes a  
long cylinder,  
dimension = 3

Fig 1  
**The Koch Snowflake**  
a finite area with an infinite perimeter



Automated Testing of High Performance  
Heterojunction Bipolar Transistors

Christopher Dodsworth  
WL/ELR  
Wright Patterson Air Force Base

Final Report for:  
AFOSR Summer Research Program  
Wright Laboratories

Sponsored by:  
Air Force Office of Scientific Research  
Bolling Air Force Base, Washington, D.C

August 1992

# Automated Testing of High Performance Heterojunction Bipolar Transistors

Christopher Dodsworth

## Abstract

In order to speed up the research and development process, the use of automated computer testing of transistors was studied. Five major tests were developed, along with an interface program to help the user control the computer. When tests were performed, an 80% increase in speed was found. Moreover, the accuracy of the results was 100%. Researchers were able to start testing, work on another project, and come back, their testing completed.

## Automated Testing of High Performance Heterojunction Bipolar Transistors

Christopher Dodsworth

### Introduction

Since the beginning of the modern computer era, transistors have revolutionized our lives. They have done away with vacuum tubes and have given us a method for making computers smaller and faster than ever. As technology continues to advance, engineers are constantly finding new ways to miniaturize transistors. In this process, materials other than silicon are being used. Some of today's fastest transistors are being fabricated on Gallium-Arsenide (GaAs) wafers. GaAs transistors offer several advantages over silicon ICs "in speed,(propagation delay and clock rate), power consumption,...operating temperature range, and radiation hardness" (Sclater 96). In addition, optical lithography allows for sub-micron precision during fabrication. When all these factors come into play, it becomes possible to fabricate over 10,000 transistors on a single GaAs wafer. While this ability to minimize the space used by transistors presents obvious benefits, it will inevitably create certain problems, particularly during the testing phase. A major part of research and development, the testing phase is more than a simple quality check; it helps the researcher to revise more accurately his processing steps. Because of this, multiple tests run on all the transistors would be of great benefit to the researcher. However, to perform those tests manually on a single wafer would take at least a week, and the result to effort ratio would be so out of proportion that it would be impossible to justify the testing. Although manual testing would be not be worthwhile, the use of a computer to automate the testing would not only dramatically reduce the amount of time spent, but would insure the accuracy of the results by eliminating human error.

### Apparatus

In order to facilitate computer controlled testing, the use of a manual probe station was abandoned in favor of the Keithley Yieldmax 450 MiniVax System. The Keithley system has two probe stations as well as a dedicated minivax computer used to control the probe stations. As a result, the prober can be controlled on-site or remotely over a network. The actual control of the prober is implemented in task-specific Fortran programs written by the user. These programs call machine language subroutines supplied by Keithley Instruments, Inc. to control testing. The

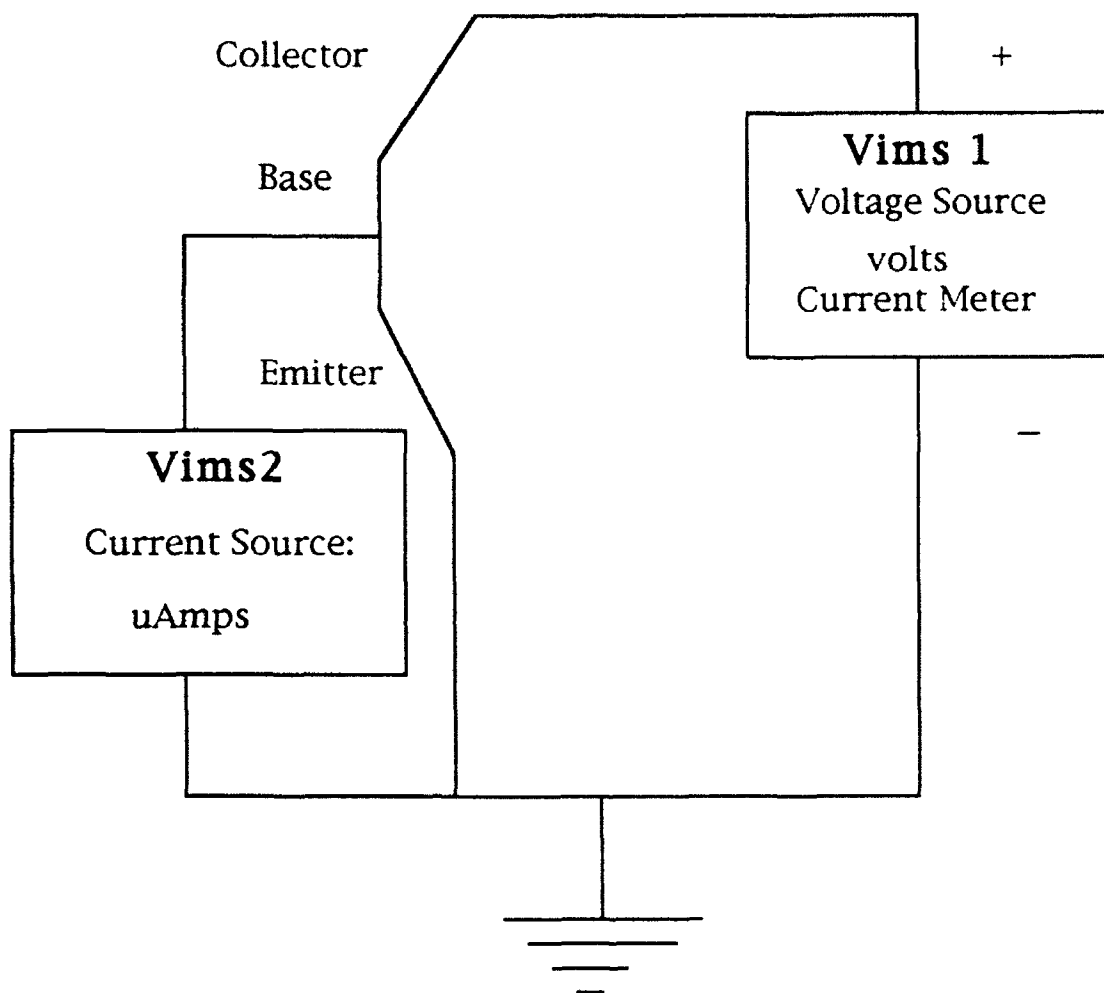
prober itself consists of a probe card, which has pins that extend down to touch the emitter, base, and collector contacts of transistors on the wafer, and the prober itself, on which the wafer lies. The prober has the capability of moving the wafer in any direction, thus allowing the probe card pins to connect with any part of the wafer. Once the probe card tips are connected with a transistor, the Keithley uses a VIMS (voltage, current measurement system) to perform tests. The VIMS is capable of sending different amounts of voltage and current through any part of the transistor. In addition, a VIMS can also measure voltage and current within a transistor. This arrangement allows the researcher to perform a variety of tests on a transistor. Moreover, once the test has been developed, the user can instruct the system to test every single transistor on the wafer and then to record the measured data to disk for later use.

### Methodology

While automated computer testing can greatly improve the testing process, the programming necessary to utilize these capabilities can also consume large amounts of time each time a slightly new process needs to be developed. Therefore, in developing the testing program, five major tests were created, each flexible enough to be used over and over again in different situations. These five programs were then tied together by a main program called *HBTSHELL*, which lets the user select which test he wants to run. In addition, since some of the tests can use the data collected from other tests, *HBTSHELL* insures that the necessary data is transferred between tests. Moreover, the program also provides two other utility programs that help the user in configuring the prober for different tests. When *HBTSHELL* is run, it guides the user through the preliminary procedures to testing, and then provides a menu of the five tests available to be run.

Of the five major tests created, the functionality test (*figure 1*) is the most basic. Designed to determine whether or not a transistor works, it forces voltage across the collector-emitter junction while forcing current through the base. The collector current is then measured, and the beta (common emitter current gain) of the transistor is calculated using the formula

$$\text{beta} = \frac{\text{Collector current}}{\text{Base current}} \quad (1)$$



Functionality Test

*Figure 1*

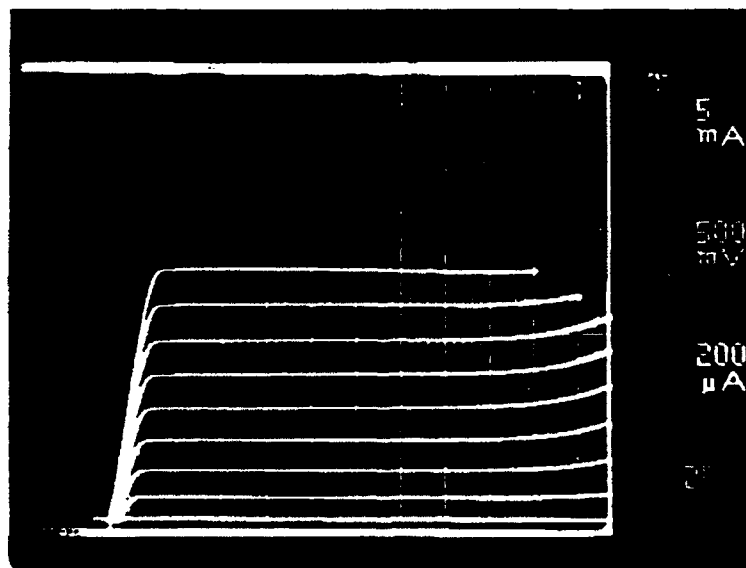
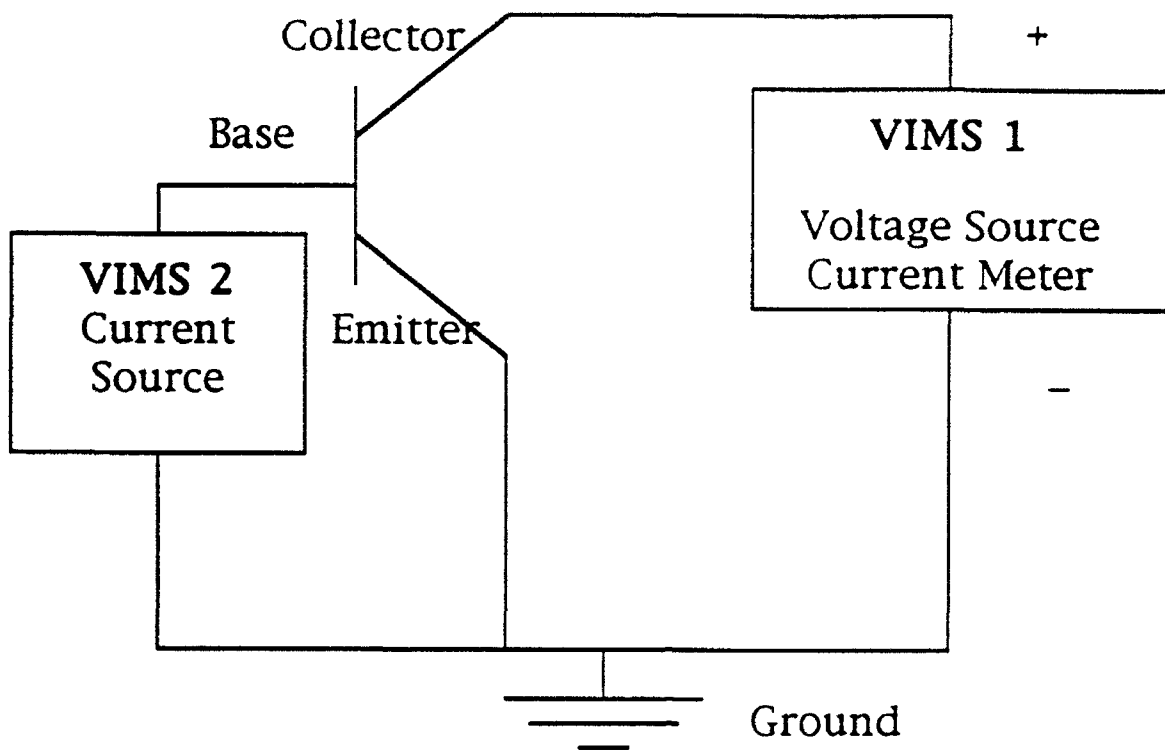
The user specifies the amount of collector voltage and base current. Then the program measures beta at two different values of collector current and compares them. If they are within a certain user-defined percentage of each other, the transistor is considered good. At the end of the testing, the program provides a breakdown of good and bad transistors and the percentage of each. In this way, it can provide the researcher with statistics on his yield. Moreover, the information collected in this test can be ported over to other tests. There, before the program tests a transistor, it will first check to see if the transistor is bad; if it is, that particular transistor will be skipped, and time will be saved.

The second of the five major tests created, the IV curve test, (*figure 2*) is similar to the functionality test in its schematic but is different in purpose. The IV Curve test forces voltage across the collector-emitter junction and current through the base, just as the functionality test does, but does not calculate beta. Instead, it uses the data to plot an IV curve (*figure 2*). An IV curve shows the researcher how well the transistor works; at what point it turns on (the peak) and how stable it is. Once it is on, it should show a flat line from there on, indicating that current is not leaking from one part of the device to another. It also shows that the transistor holds up under higher voltages and does not allow the current to fluctuate. Thus, it acts like a switch (as it should). This information is critical to how well the transistor would perform as part of an IC (integrated circuit).

Another aspect of a transistor is its amplifying ability. In a bipolar transistor, current flows into the collector and is stopped by the base until the transistor is turned on. This occurs when current is forced through the base by another source. Then the transistor is turned on and the collector current flows through to the emitter. In this process, the collector current is amplified up to forty times its original value. The Gummel Plot test (*figure 3*) measures this amplification ability. In this test, voltage is forced across the base-emitter junction and across the collector-emitter junction, with the emitter grounded. The base and collector currents are then measured. When this is plotted, one can compare the gain of the device at various base-emitter voltages. This is useful for determining the probable amplification ability of the device.

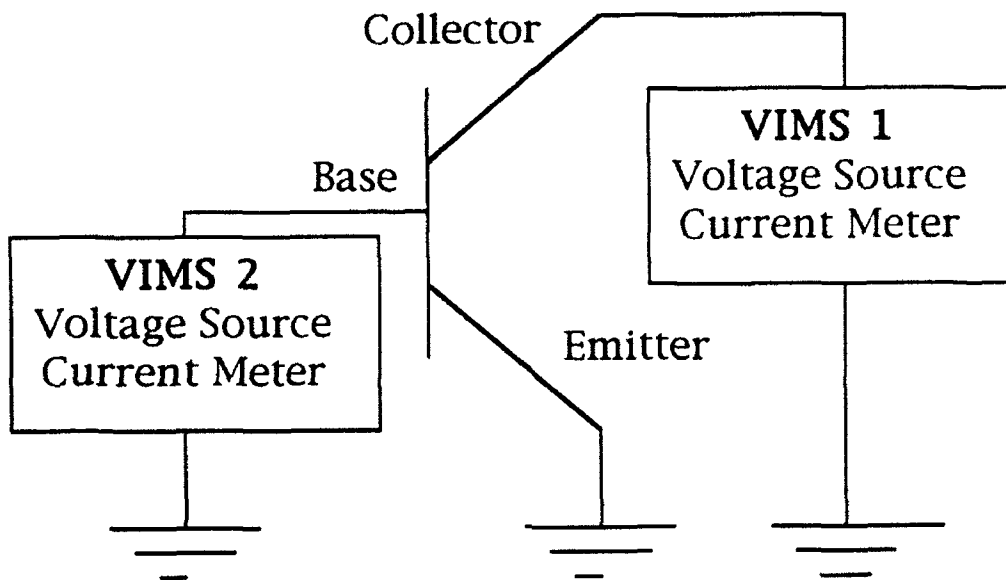
A diode, by definition, is a junction of an n-type and a p-type material. In a good diode, current only flows from the p material to the n material. A bipolar transistor is really nothing more than two diodes put together: a p-n-p or an n-p-n structure. Therefore, analyzation of the individual diodes that make up a transistor would provide information as to how well it is working. More specifically, it would





IV Curve Test schematic and IV Curve graph

Figure 2



Gummel Plot Schematic

*Figure 3*

help trace any leakage shown by an IV curve graph. The final two tests created, the base-emitter and the base-collector characteristics tests, (*figure 4*) are designed to analyze their respective diodes. Both force voltage across the base and measure the base current. This can then provide the researcher with information about the effectiveness of the transistor.

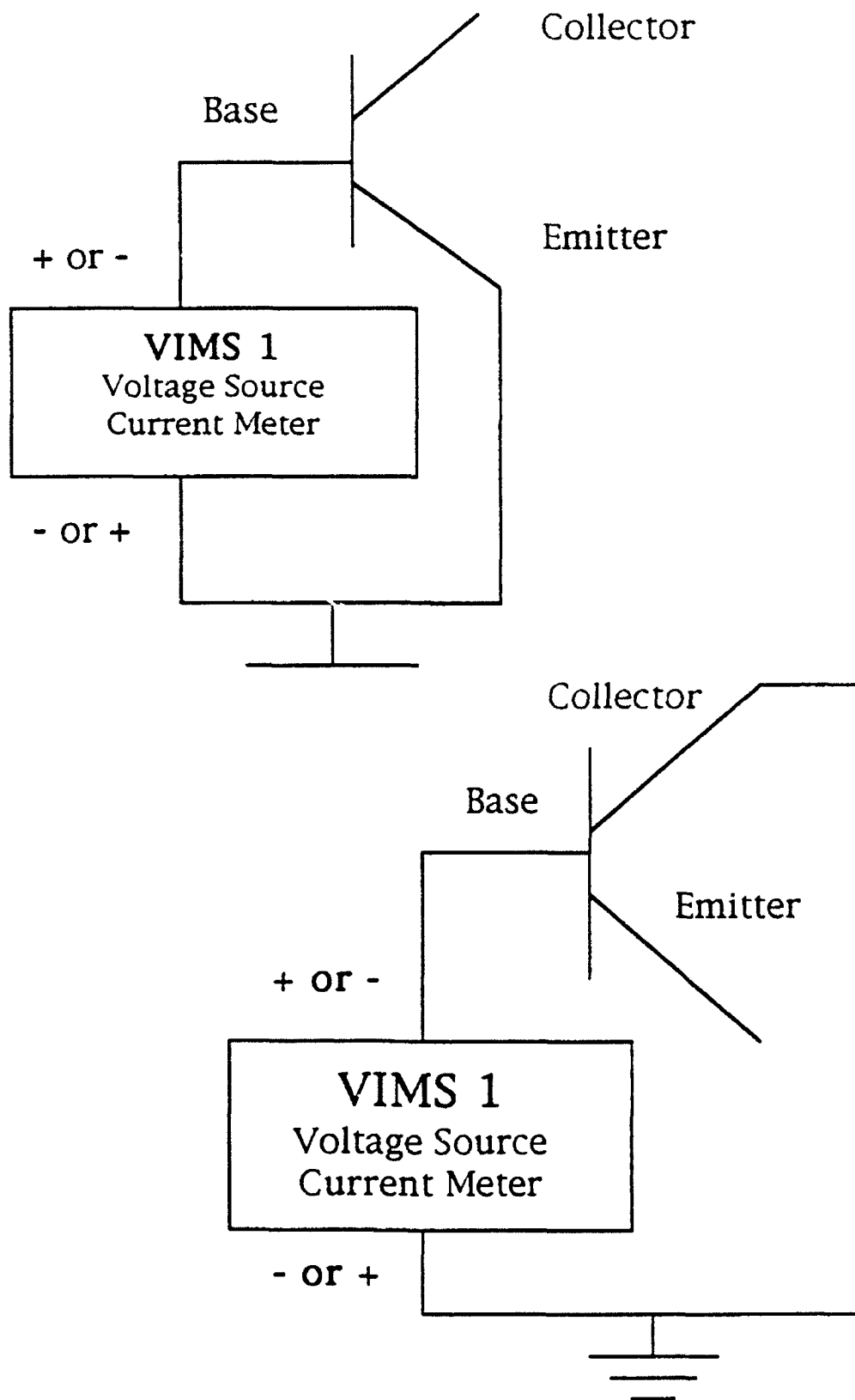
The final two programs written, *program defaults* and *site file creator*, are not tests but applications designed to help with configuring the prober for a test. The *program defaults* routine sets basic defaults for the entire program, such as which prober station to use and which type of prober card is being used. The *site file creator* helps the user to create the data file which controls the prober; when testing starts, the Keithley minvax system looks for this file to show it where to go. In this manner, the user is able to have total control over the prober itself.

### Results

Overall, performance was excellent. Based upon times taken to perform different tests, the program should be able to test 700 transistors (the amount on one wafer) in about 35 minutes. On a manual probe station, a researcher could test about 150 transistors for functionality in that amount of time. The data collected paralleled the results found using the manual probe station.

### Conclusion

Based upon the results of all the tests, and the time taken to perform them, the contribution made by computer controlled testing was significant. The time spent testing was reduced 80%. In addition, the accuracy was found to be 100%. Therefore, in lieu of these results, it is obvious that computer controlled testing can be of great benefit to research.



Base-emitter and base-collector characterization tests

Figure 4

### Selected Bibliography

Sclater, Neil GALLIUM ARSENIDE IC Technology: Principles and Practice. TAB Books, Inc. Blue Ridge Summit, PA 1988.

**GEOMETRIC MODELING AND FINITE ELEMENT  
MESH GENERATION USING PATRAN**

Thomas J. Fraites, Jr.  
High School Apprentice

WL/MNSA  
Eglin Air Force Base, Florida 32542-5434

Final Report for:  
High School Apprenticeship Program  
Wright Laboratory/Armament Directorate

Sponsored by:  
Air Force Office of Scientific Research  
Bolling Air Force Base, Washington, D.C.

August 1992

GEOMETRIC MODELING AND FINITE ELEMENT  
MESH GENERATION USING PATRAN

Thomas J. Fraites, Jr.  
High School Apprentice

Abstract

The mission of the Technology Assessment Branch (WL/MNSA) is to assess the lethality of hypervelocity kinetic energy weapons (KEWs) against foreign aerospace threats. To fulfill this mandate, WL/MNSA uses various analytical tools. Among these tools are Eulerian finite difference codes (hydrocodes), which are useful for initial impact results, and finite element codes, which are better for late-time structural response analyses. The goal of WL/MNSA, then, is to combine these two codes to provide a good representation of a hypervelocity impact event from start to finish (or critical time step). In order to accomplish this goal, an efficient finite element modeler is required to set up finite element problems based on hydrocode results. One such modeler is PATRAN. During the summer of 1992, the usefulness of PATRAN in comparison to code-specific model generation techniques was studied, and the results of that study are the basis for this report.

# GEOMETRIC MODELING AND FINITE ELEMENT MESH GENERATION USING PATRAN

Thomas J. Fraites, Jr.

## INTRODUCTION

The Technology Assessment Branch (WL/MNSA) has a charter from the Defense Nuclear Agency to assess the lethality of hypervelocity kinetic energy weapons (KEWs) against foreign aerospace targets. WL/MNSA uses several assessment techniques to fulfill this mandate, including subscale tests and analytical analyses. There are three primary analytical tools that the branch uses. Eulerian finite difference codes, or hydrocodes, are effective in observing the initial impact results of a hypervelocity impact event, when strong shocks and large deformations occur. Finite element codes are more reliable for observing late-time structural response. The third analytical tool, semi-empirical codes, are codes created on the bases of multiple test results. The purpose of my work this summer is to support the goal of combining hydrocodes and finite element codes into a single analytical system that can be used to observe and predict the properties of a hypervelocity event, as accurately as possible, from start to finish. This combined system will be known in this document as **linked analysis**. The basic requirement for linked analysis is an efficient, easy-to-use modeler that enables the user to create geometric models and meshes for finite element problems, based on the results of hydrocode output data. By using the output from hydrocodes as the basis for input for finite element codes, the closest, most feasible analysis can be performed. WL/MNSA decided to test PATRAN as such a modeler. The main purpose of my work was to demonstrate and evaluate the effectiveness of PATRAN by using its modeling and mesh generation features to create models of various test items and generic targets, and to compare its



capabilities as a modeler to the code-specific techniques that are currently in use within WL/MNSA. This was not my only task for the summer, however, and my other duties will also be discussed in this document.

### PATRAN

The obvious question for the general information-seeker is "What is PATRAN?" PATRAN is an open-ended, general purpose, 3D mechanical computer-aided engineering software package (MCAE) that uses interactive graphics in a windows environment to link engineering design, analysis, and results evaluation functions. It can be used for geometric model generation, finite element mesh generation, pre and post-processing, and a host of graphics applications. In addition, it can be adapted and interfaced to include materials libraries and animation features. Of primary interest to WL/MNSA have been the model and finite element mesh generator functions of PATRAN. WL/MNSA has been using PATRAN 2.5 interactively on the Cray Y-MP supercomputer at Eglin AFB through a Silicon Graphics workstation and several X terminals within the WL/MNSA.

### TRAINING

My summer began with a training and familiarization phase that included refreshing my UNIX operating system skills as well as training in PATRAN. My PATRAN training included viewing a 15-hour videotape short-course acquired from PDA Engineering, running practice problems using PATRAN, and skimming through various PATRAN manuals and update pages. I also was required to gain a very basic understanding of how to manipulate DYNA, a finite element code used by WL/MNSA and the primary code targeted for linked analysis this summer. With these basic skills and an account on the Cray Y-MP in hand, I was ready to begin

working on the assigned tests and models.

#### GEOMETRIC MODELING

The first step in producing an analytical assessment or pre-test prediction is a requirement. From the requirement stage the engineer moves into the "idea" mode, and tries to find innovative and effective solutions that will fulfill the requirement. Once a possible solution is selected, it is modeled using some kind of geometric modeler. PATRAN serves as an effective tool by automating much of this process. It enables the engineer to create complex geometry using a minimum of commands. In fact, much of the process can be done using a series of menus, which are accessed with a mouse. The user does have the option of using text command input only, however. Geometry in PATRAN is structured according to dimensions, that is, commands are given on levels of points, lines, surfaces, and solids (in PATRAN syntax, grids, lines, patches (PAT(s)), and hyperpatches (HPAT(S)), respectively). These are called Phase 1 Geometry commands, as opposed to commands for Phase 2 Geometry, which includes elements and nodes for finite element analysis. Commands for Phase 1 range from simply plotting an object based on its dimensions and location in either a rectangular or cylindrical coordinate system, to generation of a line or lines, by the computer, based on the intersection(s) of two or more solid objects. Models can be rotated, cross-sectioned, and solid shaded to give exact views of the progress and results of the engineer's work. Automated commands, a reference manual set, and a quick reference card make both simple and complex models easier to generate. A schematic of the command structure for geometric entities is included on the next page as Figure 13-1. The command structure is hierarchical in nature, with commands for three-dimensional objects being greater in number and scope than

Figure 13-1

# SUMMARY OF PDA/PATRAN GEOMETRY CONSTRUCTION OPTION

TYPE OF ITEM(S) TO BE BUILT	METHOD OF CREATION					
	DIRECT INPUT	CONSTRUCT FROM—				
		GRID(S)	LINE(S)	PAT(S)	HPAT(S)	OTHER
GRID	BLANK FRAME DZ SP	TRANSLATE ROTATE MIRROR SCALE MSCALE GRID VSUM	LINE CL INTERSECT	PATCH CP	HPAT	PIERCE
LINE	ALG GEOM POINT GAUSS BLANK DZ	STRAIGHT 3 GRID 4 GRID PWL FIT SPLINE ARC ARC3 CONIC INVC CURSOR BEZIER BSPLINE	EXTEND MSCALE BREAK BLEND LABEL TRANSLATE ROTATE MIRROR SCALE MERGE NUP VSUM REVERSE FILLET TANL	INTERSECT PATCH 4L	HPAT	PROJECT 2 NODE 3 NODE 4 NODE F NODE TANG
PATCH	ALG GEOM POINT GAUSS BLANK	QUAD 16 GRID CURSOR BEZIER BSPLINE	2 LINE 3 LINE 4 LINE EDGE ARC GLIDE NORM	MSCALE BREAK BLEND LABEL TRANSLATE ROTATE MIRROR SCALE NUP VSUM REVERSE FILLET MATCH	HPAT 4P	
HPAT	ALG GEOM POINT GAUSS BLANK	HEX 64 GRID CURSOR BSPLINE BEZIER	EDGE 16L	2 PATCH 3 PATCH 4 PATCH ARC GLIDE NORM FACE EXTRUDE	MSCALE BLEND LABEL TRANSLATE ROTATE MIRROR SCALE NUP VSUM REVERSE	

those for basic points. This system of commands makes it easy to analyze, manipulate, alter, and improve models with a minimum of commands in a user-friendly, windows environment.

#### FINITE ELEMENT ANALYSIS

Finite element codes are essential for studying structural response. In hypervelocity impact events, there are certain properties and phenomena that the engineer wishes to observe. In order to generate useful results from a finite element code, the engineer must know where to put high concentrations of nodes and small-sized elements, and where to put a minimal number of nodes and allow large element sizes. Once these parameters have been determined, PATRAN can generate these entities in a number of ways. The quickest method is an automated mesh generator called automesh. In this application, the user sets certain parameters, such as how many nodes length by width by height. PATRAN will then automatically place the nodes proportionally throughout the model for which these parameters have been defined. Nodes and elements can be generated and defined for lines, patches (surfaces), and hyperpatches (solids). The user can also isolate various critical areas of a model and create any desired number of nodes and elements for those specific areas, in order to get more detailed and accurate results. The benefits of these features will be further discussed in the section of this document entitled "Comparison". PDA Engineering also offers its own finite element analysis code with certain packages, but it is not included in the license under which WL/MNSA is currently operating PATRAN.

#### ANALYSIS SYSTEM WITH PATRAN

A modeling and analysis system involving PATRAN has a basic flow pattern,

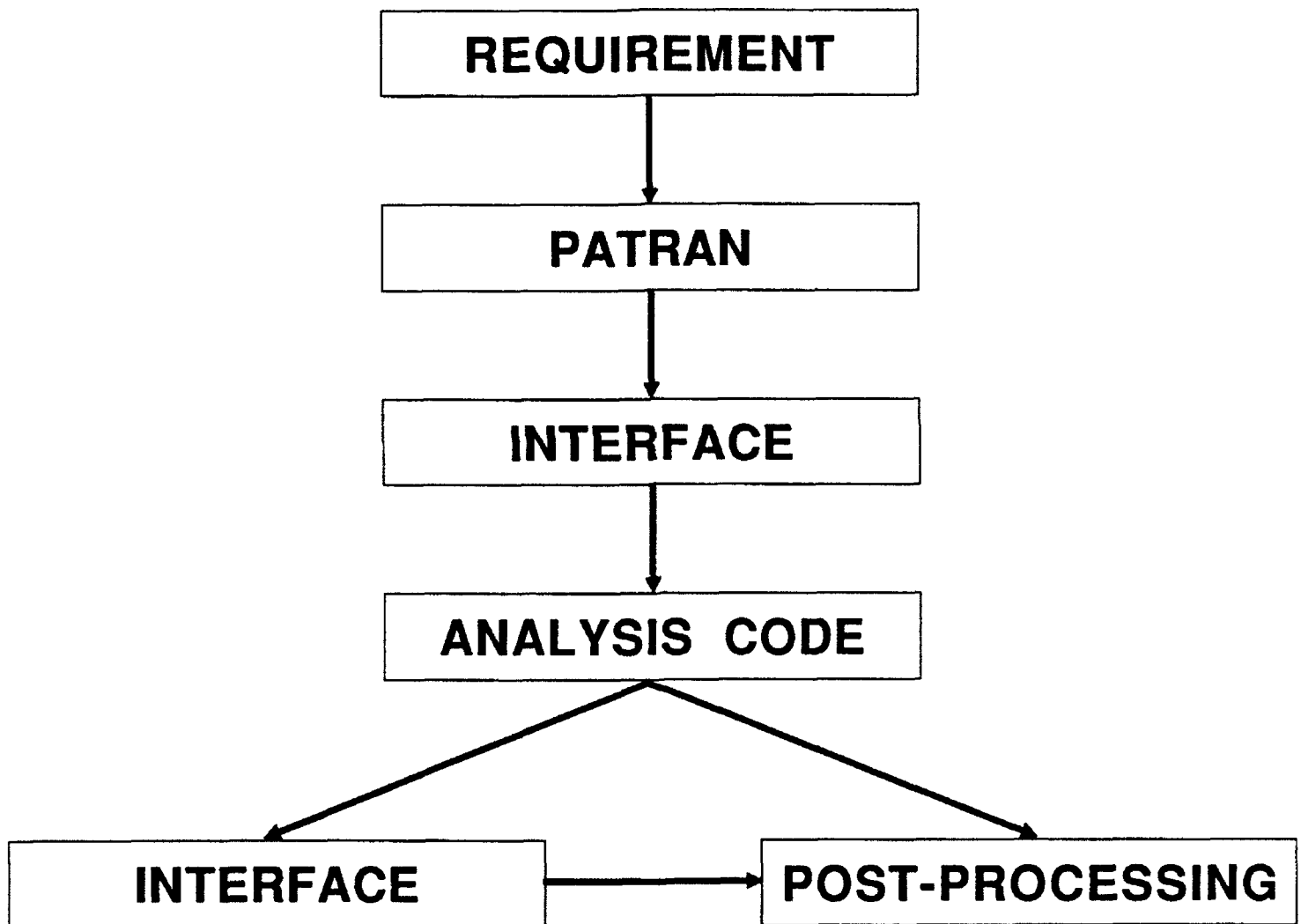
but it can be altered in several different ways. The system begins with a requirement, perhaps a pretest prediction or simulated target. The engineer designs the problem in PATRAN and creates a finite element mesh. He/she then sends the data through an interface, which translates the data from PATRAN format to a code-specific format. The problem is then entered into the code and runs to completion. The data is then passed through another interface, being translated this time from the code-specific format to PATRAN format. This basic outline appears on the next page as Figure 13-2. Again, this process can be varied in several ways. A few of these iterations will now be discussed.

The first option situation occurs after the finite element mesh has been produced (before loads, boundary conditions, etc. have been set). Several options come to the fore, depending on the software configuration being used. If a sophisticated PATRAN-to-analysis code interface is being used, loads, boundary conditions, degrees of freedom, shear, tension, and a variety of other problem parameters can now be set, before the data is passed to an interface. If, however, the price of interfaces and/or other issues have caused the user to acquire/create an in-house interface, or if an interface for the desired analysis code does not exist, the data may have to go through the interface at this point, and the aforementioned parameters usually must be set after the interface stage.

Another possible function that has some degree of flexibility is post-processing. It was mentioned earlier that after the problem has run to completion it passes through an interface back into PATRAN format. This process is not necessarily mandatory, as the post-processing phase can be executed by means of the post-processor specific to the particular analysis code being used.

Other alterations are possible, and the ones mentioned can be altered to varying degrees. WL/MNSA does not currently possess any PDA Engineering inter

## **MODELING SYSTEM USING PATRAN**



faces; therefore, an in-house PATRAN/DYNA interface is currently being used.

### COMPARISON

I mentioned earlier that one of the main objectives of this summer's work was to compare PATRAN to code-specific modeling techniques in an effort to assess the usefulness of PATRAN in our environment. The modeler that we used for comparison this summer was INGRID, the modeler for the DYNA and NIKE families of codes. All three packages are produced and disseminated by Lawrence Livermore National Laboratory. A chart on the next page (Figure 13-3) briefly outlines the issues that were evaluated and the results of our observations. Several topics are of particular interest, so I will expand upon them here.

1. Command input: PATRAN allows for both mouse-driven, menu input or standard text input, whereas INGRID allows only text.

2. Mesh generation: I mentioned the automesh feature of PATRAN earlier in this document. Finite element problems often require a great number of nodes and elements. Using INGRID, each node must be assigned its own specific geometric location within the model. With hundreds of nodes to place on a model, this can be the most time-consuming portion of the modeling process. With PATRAN, it can take as little time as a few minutes. Nodes can also be set in groups or sections of the model, allowing for greater accuracy and detail in critical areas and points of interest.

3. Technical support: The chart is misleading in that it says there is "no" tech support for INGRID. While this is not literally true, the difference in support for INGRID and PATRAN is marked. Few people can be called expert INGRID users, and its originators have little time to spend giving help due to their large number of other duties and tasks. PDA Engineering, on the other

# PATRAN / INGRID COMPARISON

ISSUE	INGRID	PATRAN
-------	--------	--------

KEYPAD INPUT	YES	YES
MENU INPUT	NO	YES
AUTOMATED MODEL GENERATION	NO	YES
AUTOMATED MESH GENERATION	NO	YES
NODE ASSIGNMENT	INDIVIDUAL NODES	SET PARAMETERS
ELEMENT ASSIGNMENT	INDIVIDUAL ELEMENTS	AUTOMESH
MANUAL	OUTDATED	DETAILED
TECH SUPPORT	NO	YES
COMMAND SYNTAX	CRYPTIC	LOGICAL
TRAINING	NONE	VIDEO COURSE
OVERALL	DIFFICULT	USER-FRIENDLY



hand, maintains a technical hotline at their corporate headquarters for those users who have purchased this service as part of their licensing agreement. Engineers are available to answer questions about a variety of PATRAN issues. WL/MNSA has used this service and has found it to be efficient and effective.

4. Overall assessment: The overall assessment of PATRAN versus INGRID leads to a conclusion that while INGRID is the original modeler for DYNA, PATRAN actually enables the user to use DYNA in a more efficient, less time-consuming manner. It also enables the user to change components or sections of a model with accuracy and ease. The cost of a PATRAN license, at the present time, is more than offset by the reduction in model preparation time. The assessment, therefore, is that because of its extensive capabilities and user-friendliness, PATRAN is the current modeler of choice for the branch.

#### SAMPLE TEST CASE

In order to have a complete PATRAN system, a working interface is needed. WL/MNSA has developed an in-house PATRAN to DYNA interface, and we tested it this summer. The interface only translates data concerning geometry and meshes; it does not translate loads, boundary conditions, etc. We had to set those parameters after the interface stage. I designed a sample test in order to test our system. The model consisted of a thin, solid rod, with a square base, and a length by width by height ratio of one-one-five. Nodes and elements were auto-meshed onto the model and it passed through the interface with no problems. We did encounter problems somewhere in our DYNA calculations, but these problems were independent of the interface. Therefore, the capability of creating an effective, working in-house interface was demonstrated.

### PERIPHERY DUTIES

I had several other duties within the branch this summer, some of them related to my central project, some of them completely different. The first of my tasks included procuring two finite element codes and one hydrocode for the branch from Sandia and Lawrence Livermore National Laboratories. This task included correspondence with the originators of the codes and arranging for points of contact within WL/MNSA. Some of the codes required protection procedures, and I observed the layout of those procedures by members of the WL/MNSA. Another task I was assigned was to do some advance work for the acquisition of PATRAN 3, the latest version of the package, from PDA Engineering. This included finding out what hardware configurations it was capable of running on, what is new in version 3, what license agreements are necessary, and many other significant issues. Finally, I was tasked with scanning into a computer and editing a paper copy of a computer program that WL/MNSA wanted to test. The completion of these tasks broadened my work experience and gave me new insights into procurement and acquisition.

### CONCLUSION

My work these past two summers has given me a whole new perspective into working in a research environment, government work, and career opportunities. I have gained invaluable computer knowledge and training, and I have become familiar with a variety of hardware devices. I am pleased with the results of my work this summer, and I think my assessment of PATRAN versus INGRID will prove valuable to the branch and the United States Air Force.

#### ACKNOWLEDGEMENTS

I would like to thank first and foremost my mentor, Mr Dan Brubaker, for his patience and guidance these past two summers. Thanks are also in order for John Bailey, Bruce Patterson, and the other engineers and program managers in WL/MNSA who helped me whenever I needed it. I extend a warm thank you to Major Paul Coutee, my branch chief, and Mr George Kirby, the MNS division chief. A final thank you is offered to Mr Don Harrison and Mr Mike Deiler for their hard work in coordinating the High School Apprenticeship Program at Wright Laboratory, Armament Directorate, to Research and Development Laboratories for their support, and to the Air Force Office of Scientific Research for sponsoring this program. It has been a truly invaluable and rewarding experience for me.

## REFERENCES

Hallquist, J.O. and D.W. Stillman. INGRID: A three-dimensional mesh generator for modeling nonlinear systems. Lawrence Livermore National Laboratory. December, 1981. Revised July, 1985. UCID-20506

PDA Engineering. Introduction to PATRAN Plus: PAT101N Course Notes/Exercise Workbook. Revised 6/89.

Reflections of Ramjet Research

Kimberly A. Frank  
Research Apprentice  
Advanced Propulsion Division

Wright-Patterson Air Force Base  
Area B, Building 18  
WL/POPT  
Wright-Patterson AFB, OH 45433-6563

Final Report for:  
Summer Research Program  
Wright Laboratory

Sponsored by:  
Air Force Office of Scientific Research  
Bolling Air Force Base, Washington, D.C.

August 1992

## Reflections of Ramjet Research

Kimberly A. Frank  
Research Apprentice  
Advanced Propulsion Division  
Wright Laboratory  
Wright-Patterson Air Force Base

### Abstract

The objective of Test Cell 22 currently is to test the performance of various ram components for a ramjet engine, such as the combustor or nozzle. In order to test the accuracy of the ram rig, data was taken at two different states: the natural state (nothing was being done to the rig-- no pressurized air, no vacuum pulling on the rig) and the simulated high altitude, high flight speed state (high pressurized unheated air being passed through the rig and/or an exhaust vacuum pulling on the engine components). The results of the data taken at both states were closely studied and compared. Through studying the data from the experiment it was learned that there were vibrations in and on the ram equipment that influenced the force reading from the load cell. True mechanical solutions to eliminate the problems found in the ram rig are very complicated and not practical; for now, electrical filtering has been found to solve the problems. Vibration frequencies on the thrust stand were easily identified using a special instrument that measures both the amplitude and frequency of the disturbance. A series of capacitors were attached across the load cell to filter higher frequency vibrations. The experiments proved very valuable because it identified both the frequency and amplitude of the vibrations, as well as identifying solutions that could be made practically.

## Reflections of Ramjet Research

Kimberly A. Frank

### INTRODUCTION

Over a period of fifty years, ramjet engines have gone from a mere idea to a reality. In the early 1950's, when Wright-Patterson Air Force Base (WPAFB) established their first ramjet facilities, many people were hopeful for ramjet research, but doubtful that ramjets would ever become a reality. WPAFB worked very hard in their ramjet facilities and in the mid 1970's when ramjet research had reached a high point in Wright Laboratory, discoveries were made about ramjet engines that are now being used as accuracy standards in Test Cell 22's research. Shortly after the accuracy standards were set (within 2% variation), one of WPAFB's ramjet facilities was shut down for 15 years. In order to reopen Test Cell 22, the ramjet facility that was shut down, a complete modernization of the facility was required. Many new systems were installed so that the research could be conducted on direct-connect combustion and on new advanced propulsion concepts. In a ground test facility like Test Cell 22, engine components are mounted on a thrust stand to measure how efficiently the components are operating. Along with the thrust stand there are two other major elements that are a must in ramjet ground testing. First is the air, air that is heated to 1600 °R is passed through the components to simulate flight speeds of over Mach 3.0. Secondly is a type of vacuum, an exhaustor system that produces subatmospheric conditions simulates high altitude operation for the ramjet exhaustor nozzle.

Before component testing can begin, the accuracy of the thrust stand needs to be measured. With all of the new equipment installed, the tests were

conducted to measure the variables that could influence the thrust stand output. With only a ram rig (see APPARATUS for detailed description) set up in the testing area, the accuracy of the system was well below the accuracy standard set in 1974. Since there was a low accuracy in the test cell with only the ram parts to a ramjet engine, it was certain that if other components were added, such as turbine engine equipment the accuracy of the system would become even lower. [A complete ramjet engine must have some type of boosting system in order to allow the rig to obtain a speed of about Mach 2, the speed at which ram equipment can take over and be efficient.] Tests were conducted and the results were studied to determine what influenced the accuracy of the system most. Once everything becomes fairly accurate and the efficiency of the system is improved, only a strong future will remain for ramjet engines. Ramjet and advanced airbreathing propulsion systems could be used in a broad range of tactical missions in the future: air-to-air and air-to-ground missile systems operating in the Mach range of two to six at altitudes from sea level to above 30 kilometers (hypersonic vehicles are also being considered for development that will operate beyond Mach six to altitudes that far exceed 30 kilometers).

#### EXPERIMENTATION

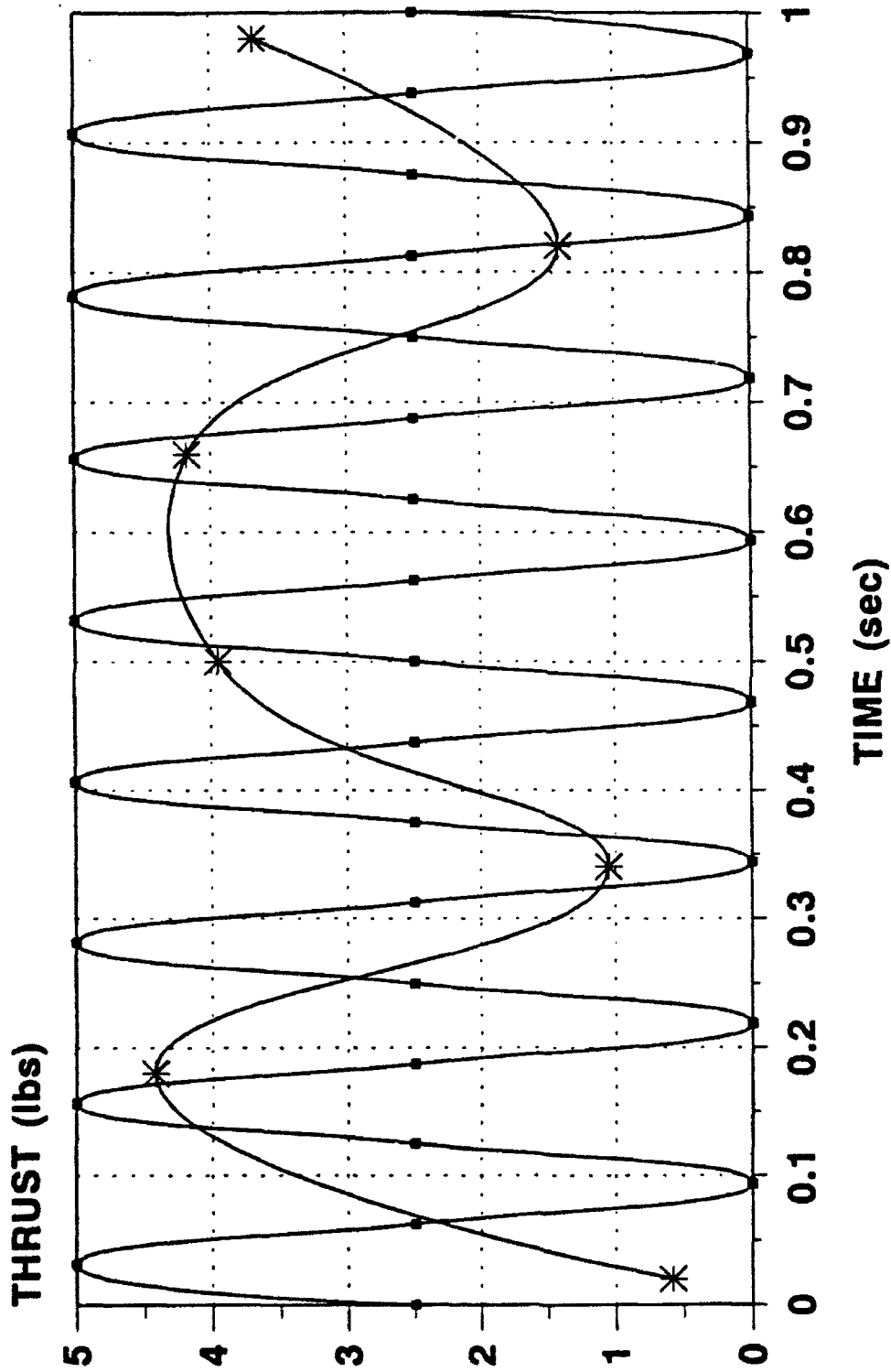
The easiest way of checking the efficiency of a ramjet system is to check the accuracy of the equipment and instruments; the best way to check the accuracy of equipment and instruments is through experimentation. When taking data from a certain measuring instrument, the values of the data generally should be relatively close to each other. If the values of the data vary over a wide range, most of the time this is an indication of some type of problem



within the instrument or within the equipment. If the data values are within a reasonable range, then one can presuppose that the system is fairly accurate.

As tests were being run, it was discovered that a few instruments were reading data values at a wide range. Cause-and-effect relationships were considered, but nothing was conclusive. A sonic wave relationship was also considered (see Figure A), but again nothing was conclusive. So in a desperate effort to find the problem of equipment vibration, a few instruments were chosen to be closely observed. The main piece of equipment studied was the load cell, because it is the main measuring element of the thrust stand. The load cell is a device that converts mechanical motion, that is, proportional to a thrust force, to an electrical signal which is recorded on a computer based data acquisition system. [The load cell is a six inch long cylinder with a three inch diameter used to determine the amount of push or pull on the thrust stand. The thrust stand is a twenty-five foot long, seven feet wide platform that sits approximately seven feet from the ground to the top of the combustor. The thrust stand holds the piping for the ram rig and is suspended by a flexure at each of the four corners.] The load cell is located inside the thrust stand and is attached to the data acquisition computer; each "card" in the computer system contains thirty-two channels. Every eight channels there was a wire attached to the load cell so that the data values could be reviewed on an even interval (this computer setup was used in all of the load cell testing). First, data was collected with no pressurized air passing through the rig and no exhaustor pulling on the rig; also, the load cell was taken out of the thrust stand (the results of this data can be viewed in

Figure A



Data Values from No Air with No Exhausters, Load Cell in the Thrust Stand  
Values Being Compared to a Sinusoidal Curve

Figure B and Figure C). Figure B is the data in a narrow band view. Figure C is the same data as Figure B (the difference between them is the range). The seven pound range difference in Figure C will be used later to compare these results to results of tests run later. [The accuracy results of this first test are the results that are being looked for in the tests to follow.]

Secondly, the load cell was replaced back into the thrust stand and more tests were run with the same air and exhaust situations (and the same accuracy was expected). When comparing the results of the second test (Figure D) to the results of the first test (Figure B), it was logical to conclude that the thrust stand was experiencing some type of vibration. Next the exhausters were turned on in the basement (the exhausters cause a pull on the ram components) and a series of data were again taken. The interesting results of these data values can be viewed in Figure E. Lastly a thought was pondered, that with the pressurized air in the ram rig some of the vibrations may disappear. So 8 lbm/s of air was sent through the rig but the load cell results were not what was hoped. The depressing Figure F shows what was learned after this test. The problem was sighted (vibrations in the ramjet system and a possibility of unsteady air flow) and a series of trial and errors would be attempted in order to find a workable solution. One idea that was tried was the use of rubber to pad the load cell from the metal-to-metal contact within the thrust stand. Most metal-to-metal connections can magnify a vibration and hopes were formed that the rubber would reduce the vibration amplitude of the thrust stand. A rubber mat and rubber washers were placed on one side of the load cell; later, a second set of rubber mats and washers were added to the second side of the load cell. Each time the rubber was added, the amplitudes

No Air with No Exhausters, Load Cell not in Thrust Stand

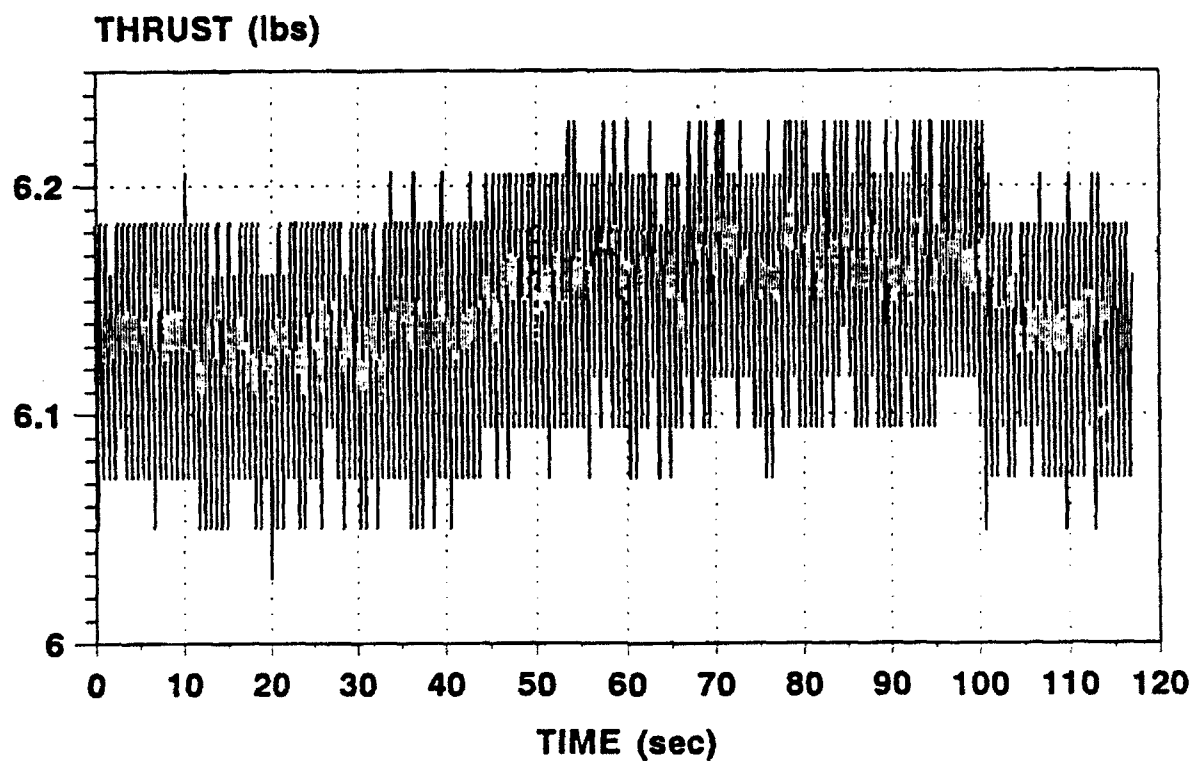


Figure B

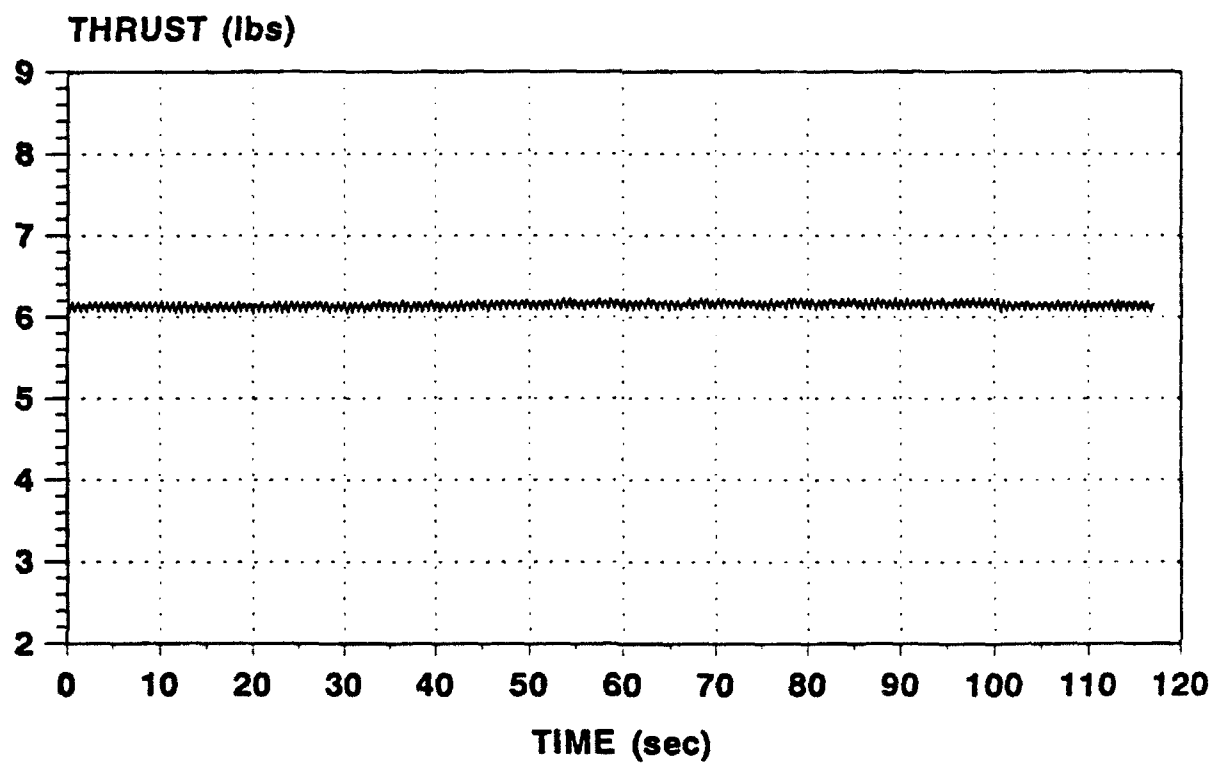
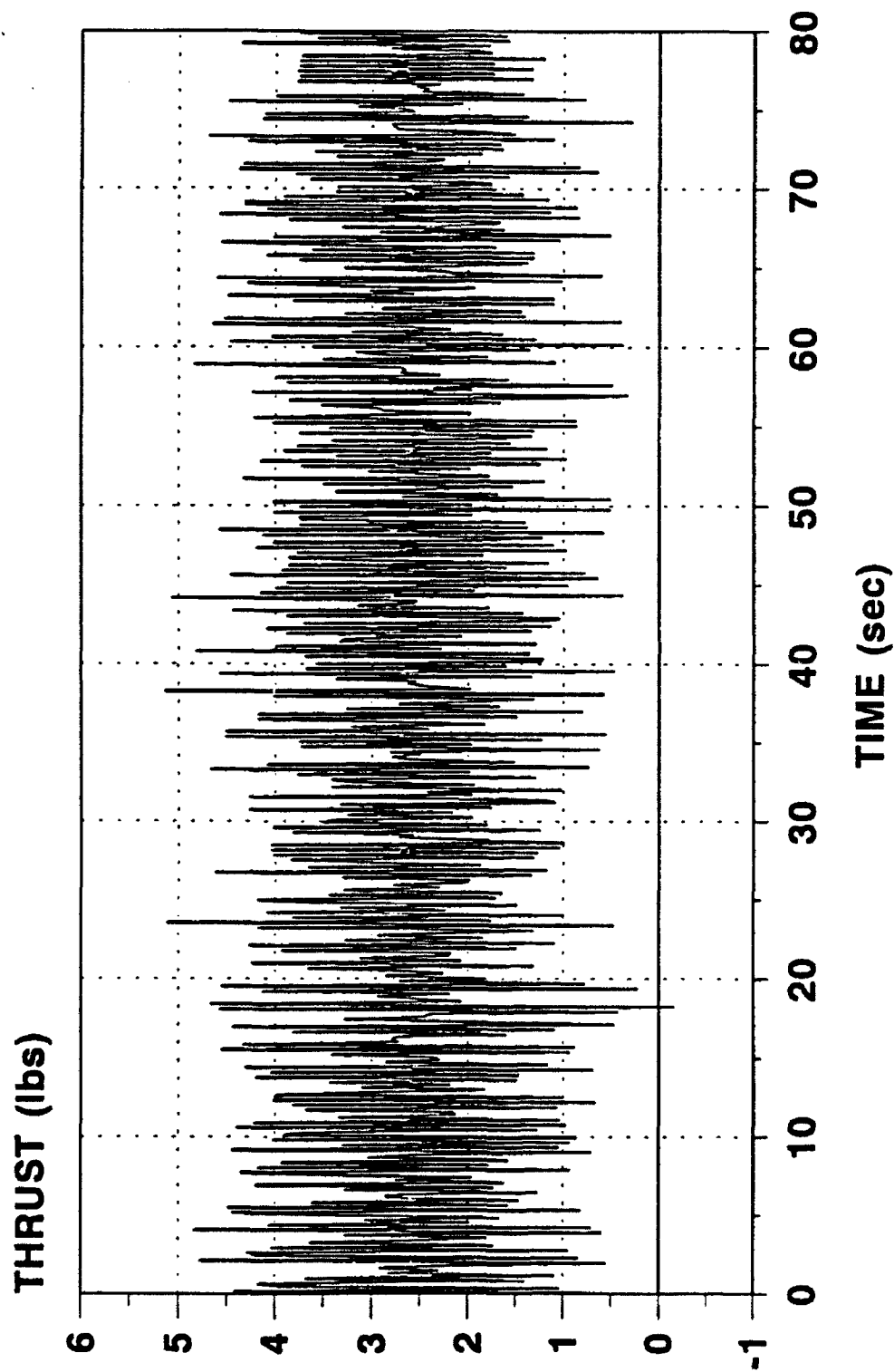


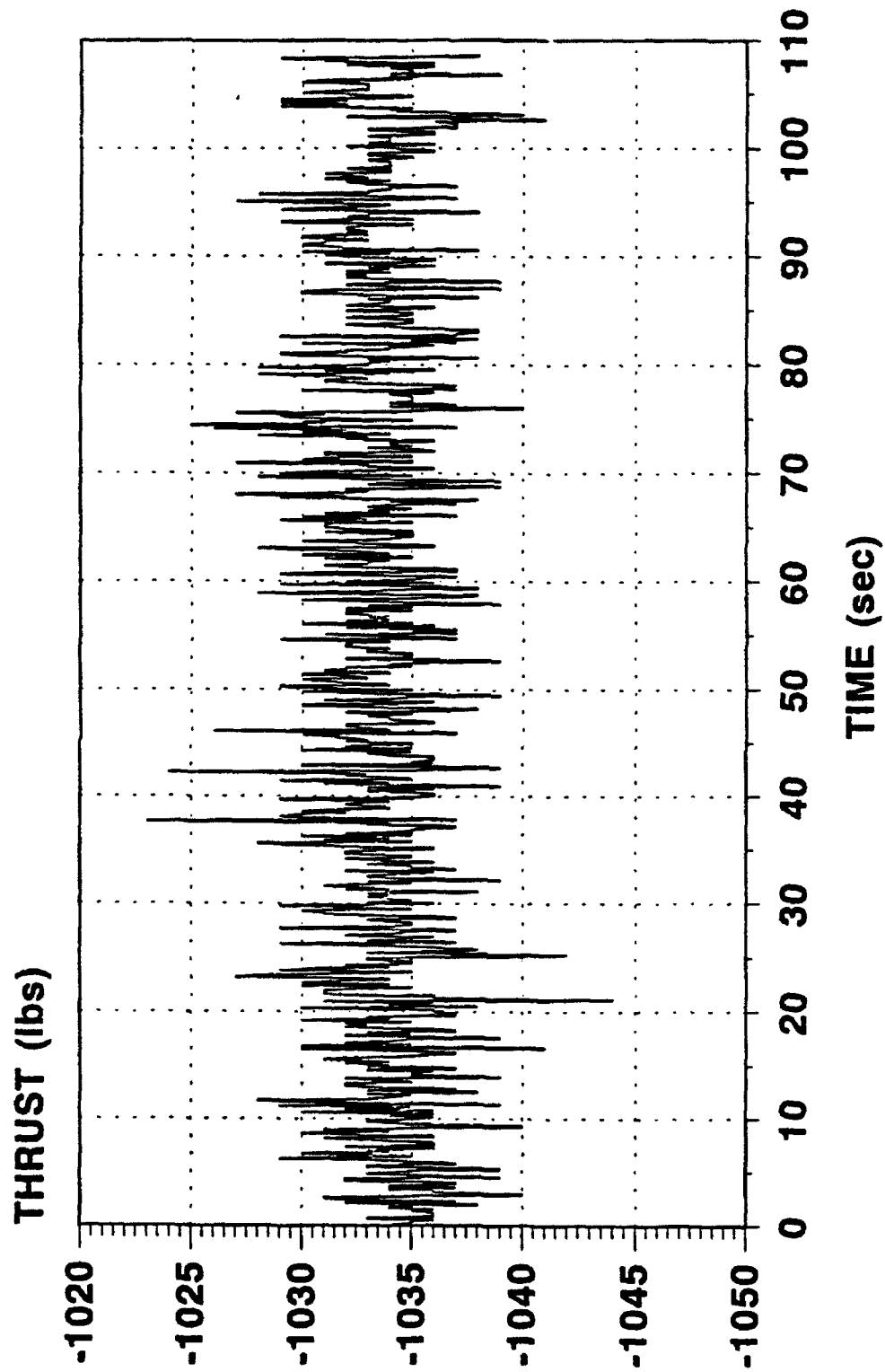
Figure C

Figure D



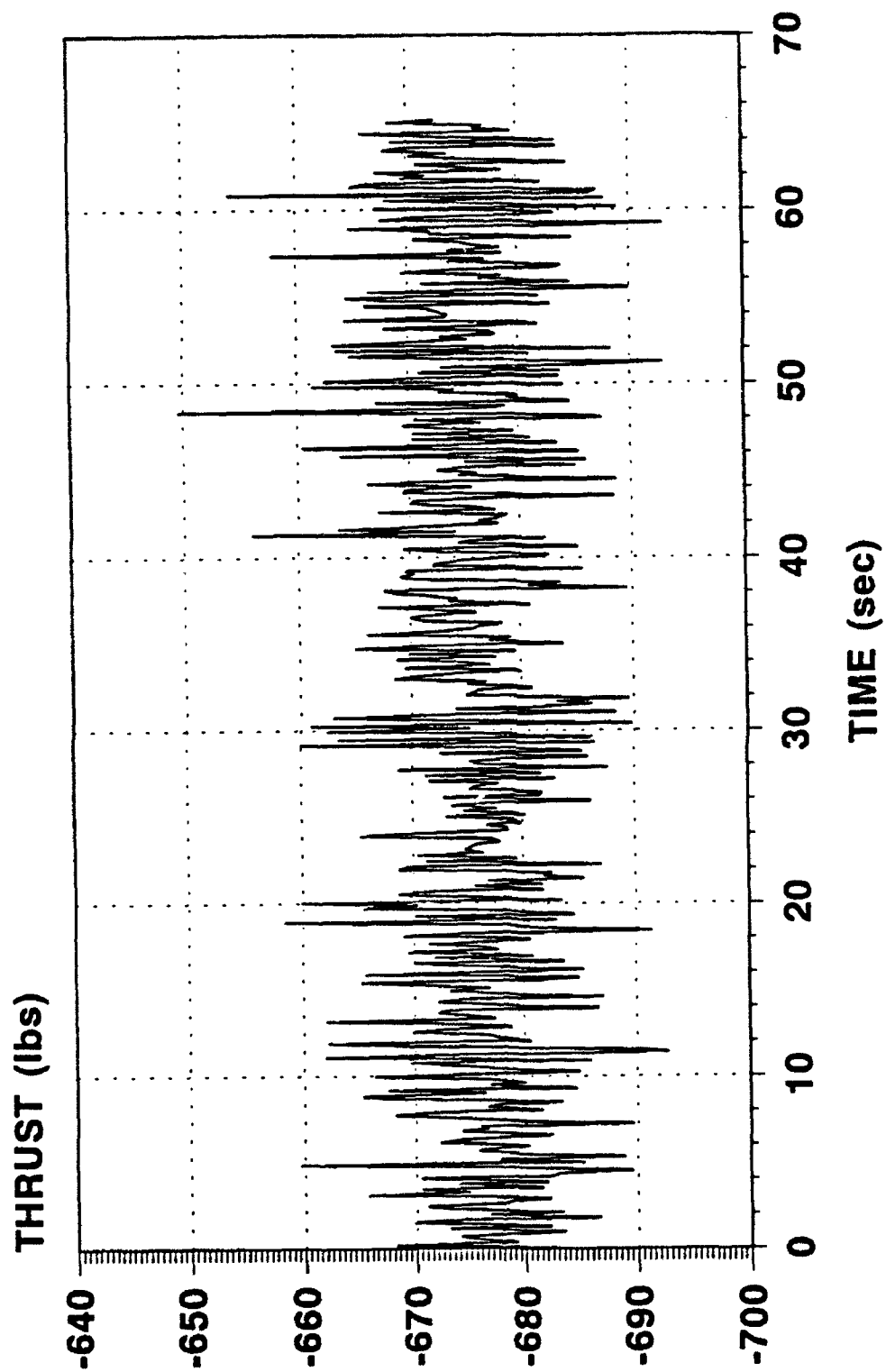
No Air with No Exhausters, Load Cell is in the Thrust Stand

Figure E



Exhausters on with Nc Air, Load Cell is in the Thrust Stand

Figure F



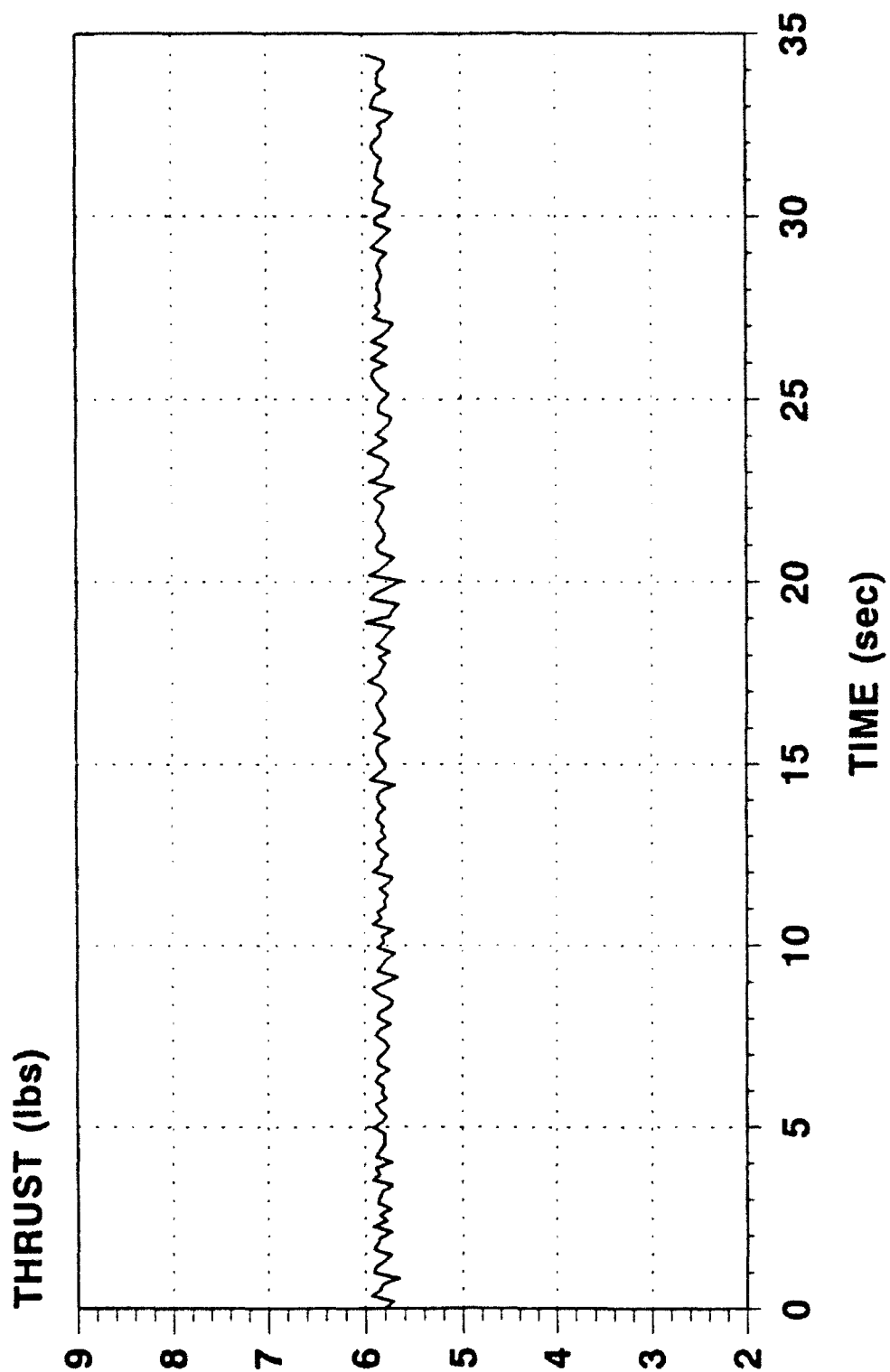
Exhausters On with Air Flowing, Load Cell is in the Thrust Stand

of some of the noise frequencies were reduced; however, the vibrations were not reduced. Extending from the results of the rubber mats and washers, an idea was introduced to use a series of capacitors. The capacitors were tuned at what was thought to be the natural frequencies of some of the ram equipment. The capacitors were attached to the wires leading out of the load cell and into one of the thirty-two channel cards in the acquisition computer. The same basic tests were run as before: no pressurized air with no exhaust vacuum (Figure G), exhaust vacuum with no pressurized air (Figure H), and pressurized air with exhaust vacuum (Figure I). Results of the two sets of tests were compared: no pressurized air with no exhaust vacuum (see 14-16), exhaust vacuum with no pressurized air (see 14-17), and pressurized air with exhaust vacuum (see 14-18). The capacitors filtered out the electrical vibrational noises to the computer; however, the capacitors did not reduce the actual mechanical vibrations in the ram rig. Capacitors are being used in other testing facilities and they are okay as long as the combustor dynamics of the system are not being studied, because the capacitors increase the system time response. Since the exact future of Test Cell 22 is unknown, a decision was made to look for an answer that would mechanically filter out the vibrations (as opposed to electrically filtering). Several different designs of Dynamic Vibration Isolators (DVI) are being considered. Only the future will tell how this problem will be effectively solved.

This section only gives one example of the experiments that went on in Wright Laboratory's Test Cell 22. If a similar section were to be written about the experiments that were done on the other instruments that were examined and re-calibrated, this paper would take me well into October of 1992 to

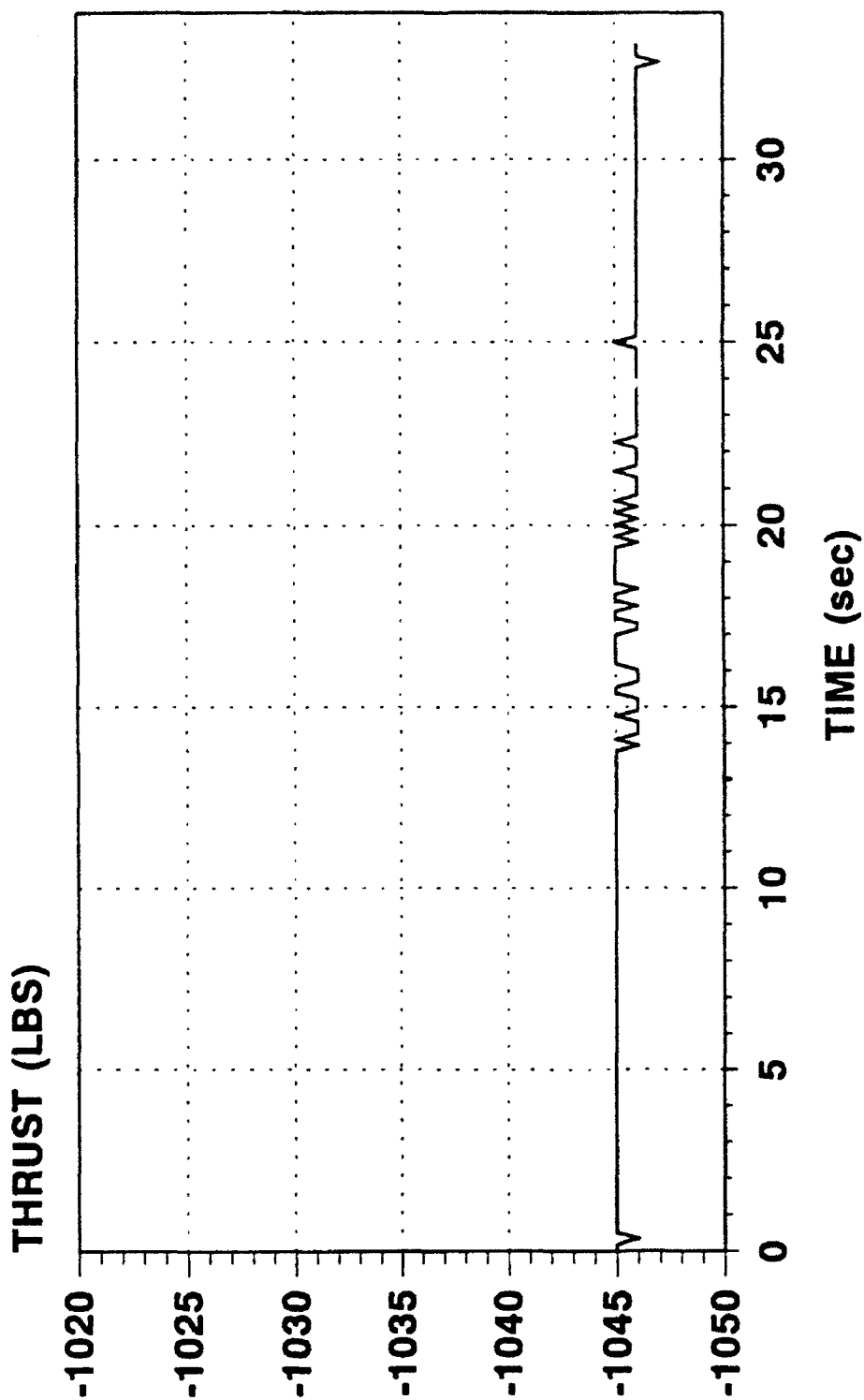


Figure G



No Exhausters with No Air, Load Cell is in the Thrust Stand  
Capacitors are mounted to data  
Acquisition System from Load Cell

Figure H

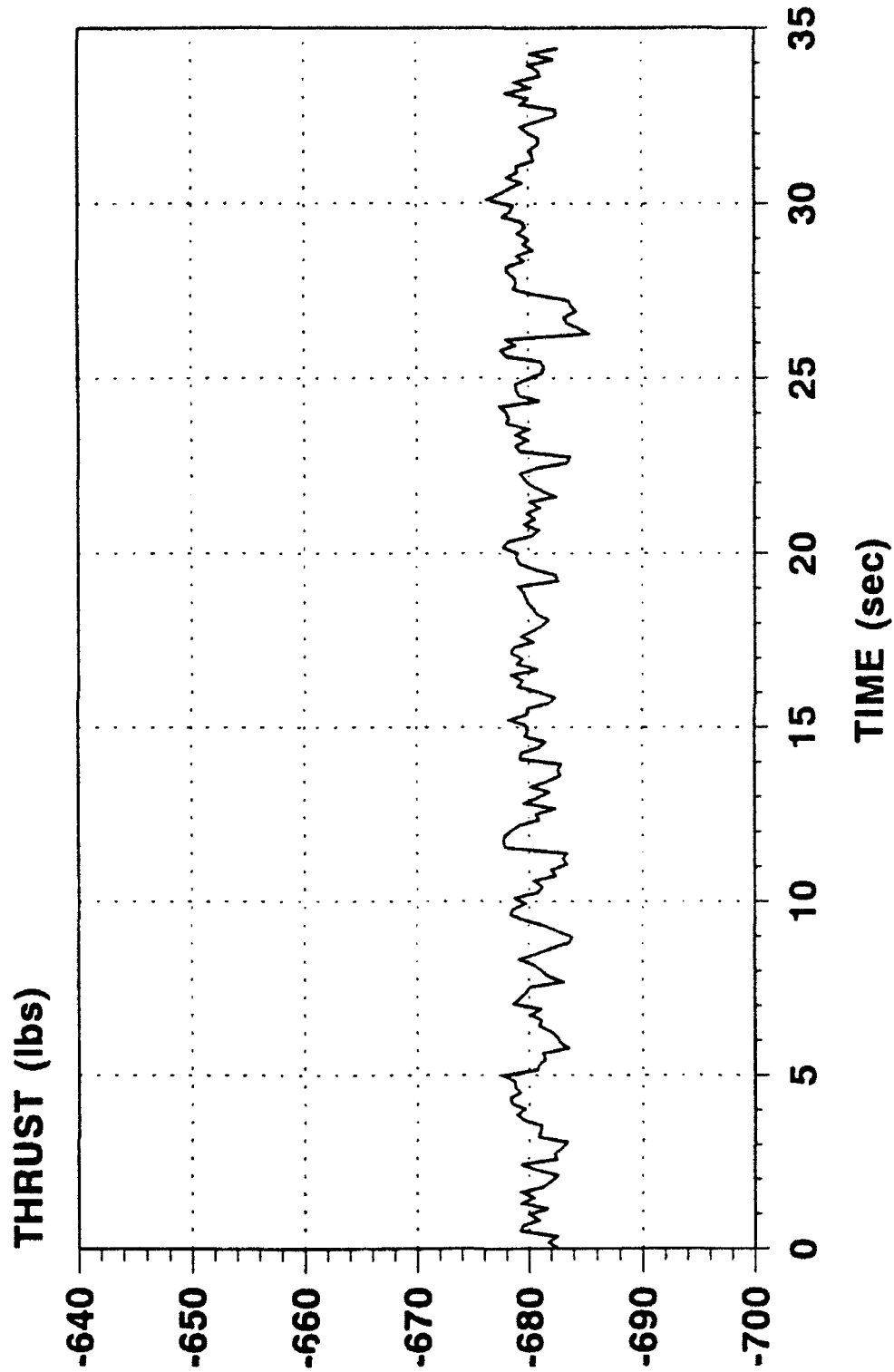


Exhausters On with No Air, Load Cell is in the Thrust Stand

Capacitors are mounted to the data

Acquisition System from the Load Cell

Figure I



Exhausters On with Air Flow, Load Cell is in the Thrust Stand  
Capacitors are mounted to the Data  
Acquisition System from the Load Cell

No Air with No Exhausters, Load Cell is in the Thrust Stand

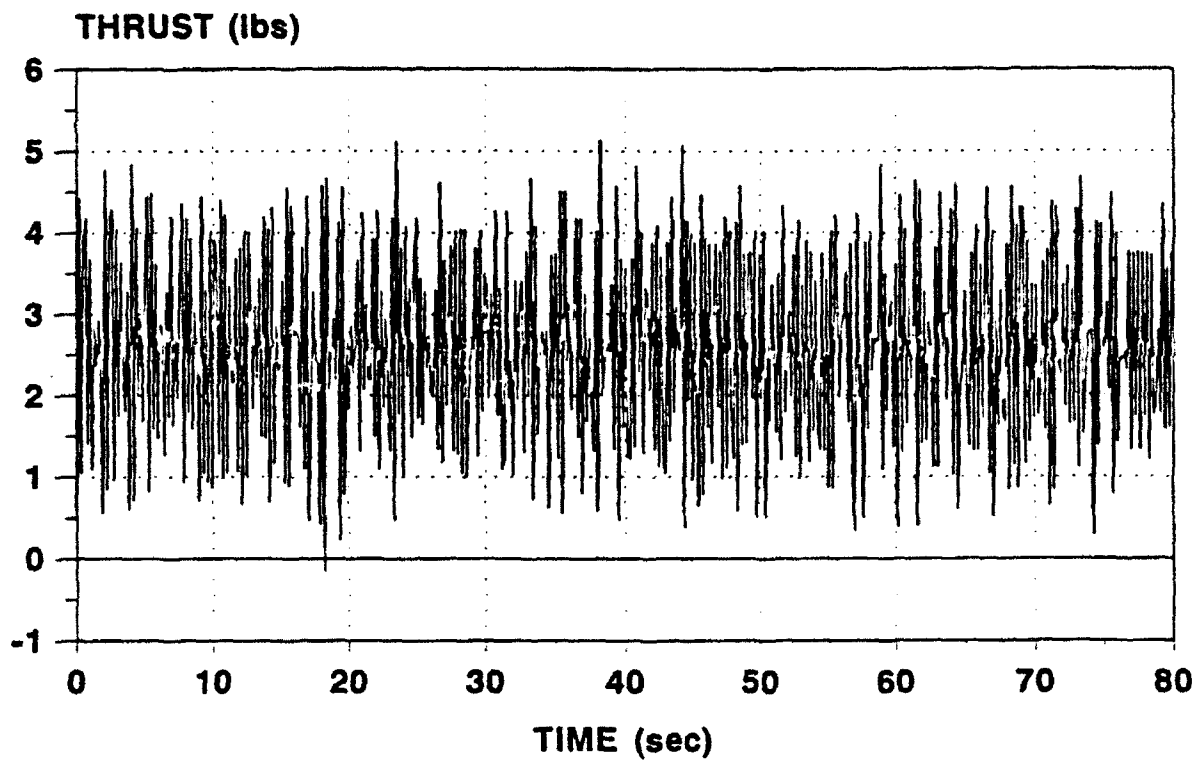


Figure D  
Load Cell without Capacitors

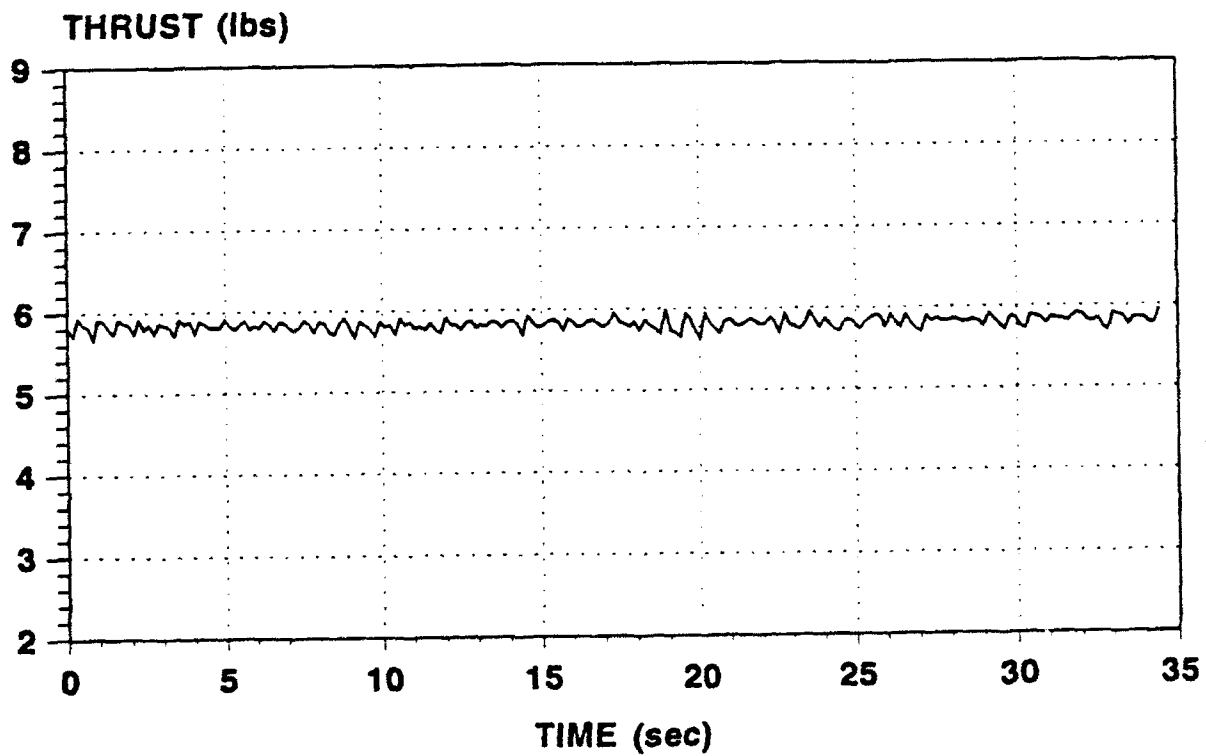
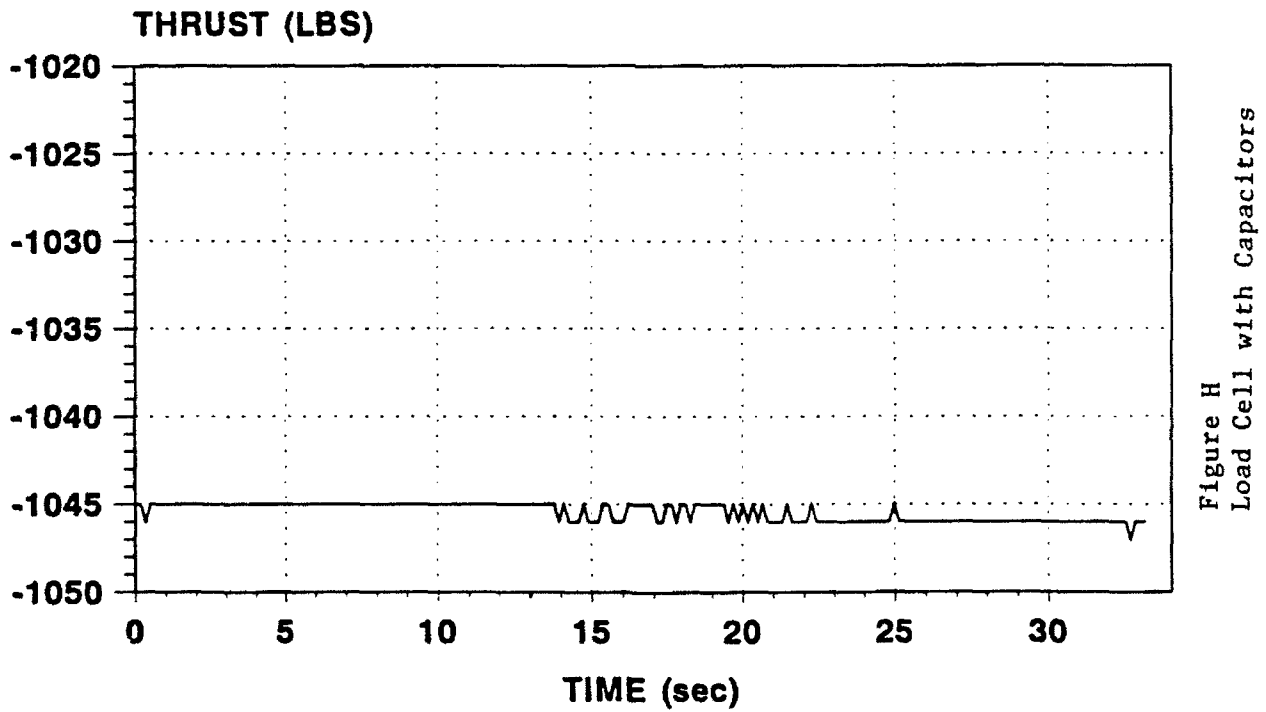
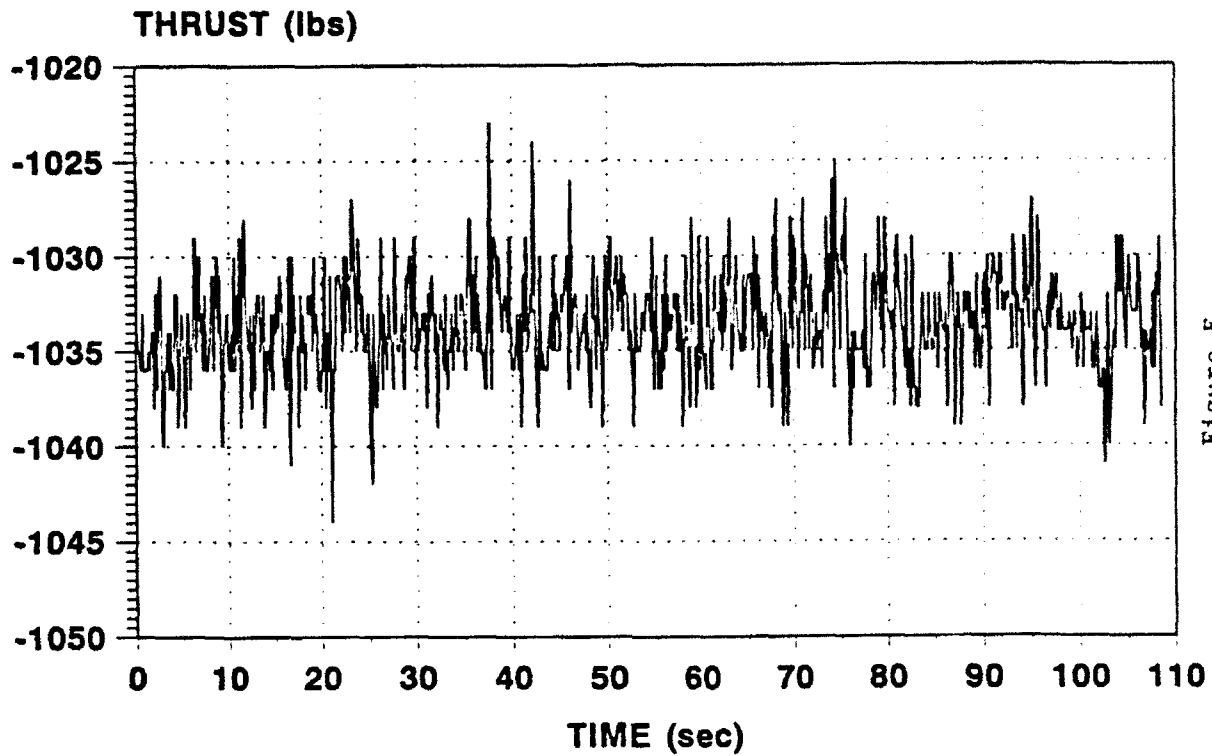


Figure G  
Load Cell with Capacitors

Exhausters with No Air, Load Cell is in the Thrust Stand



Air Flow with Exhausters, Load Cell is in the Thrust Stand

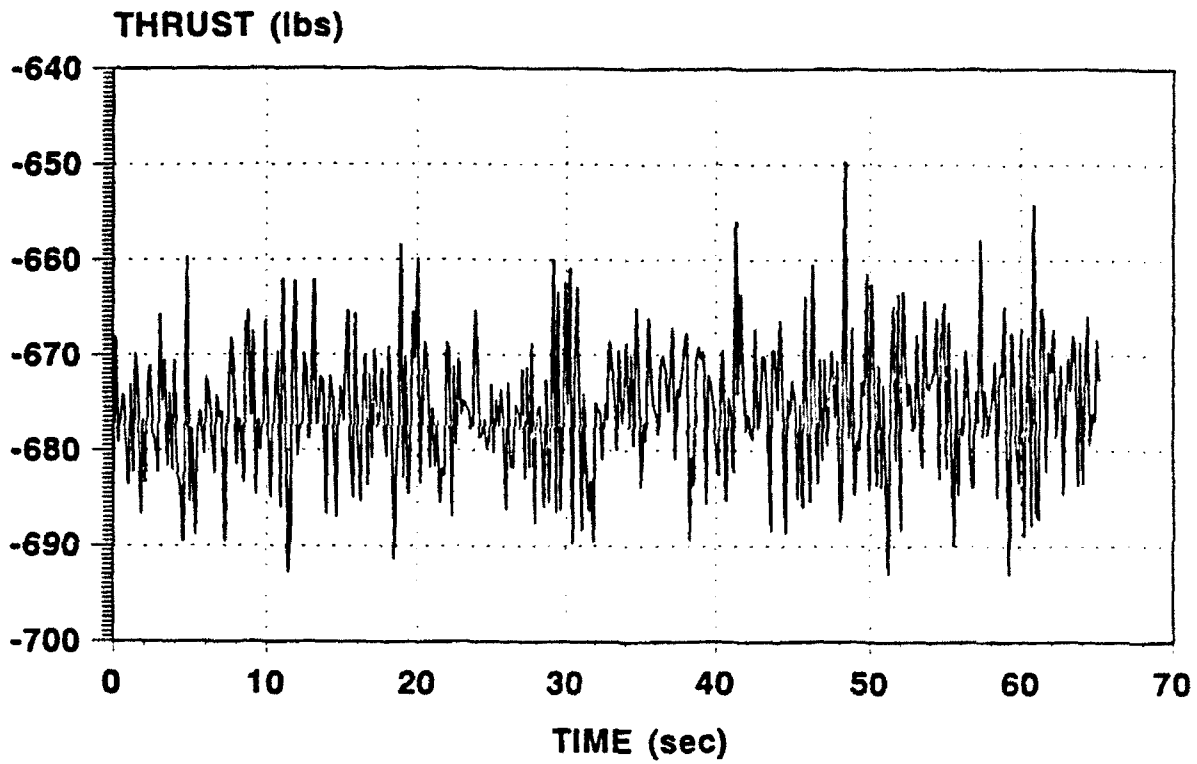


Figure F  
Load Cell without Capacitors

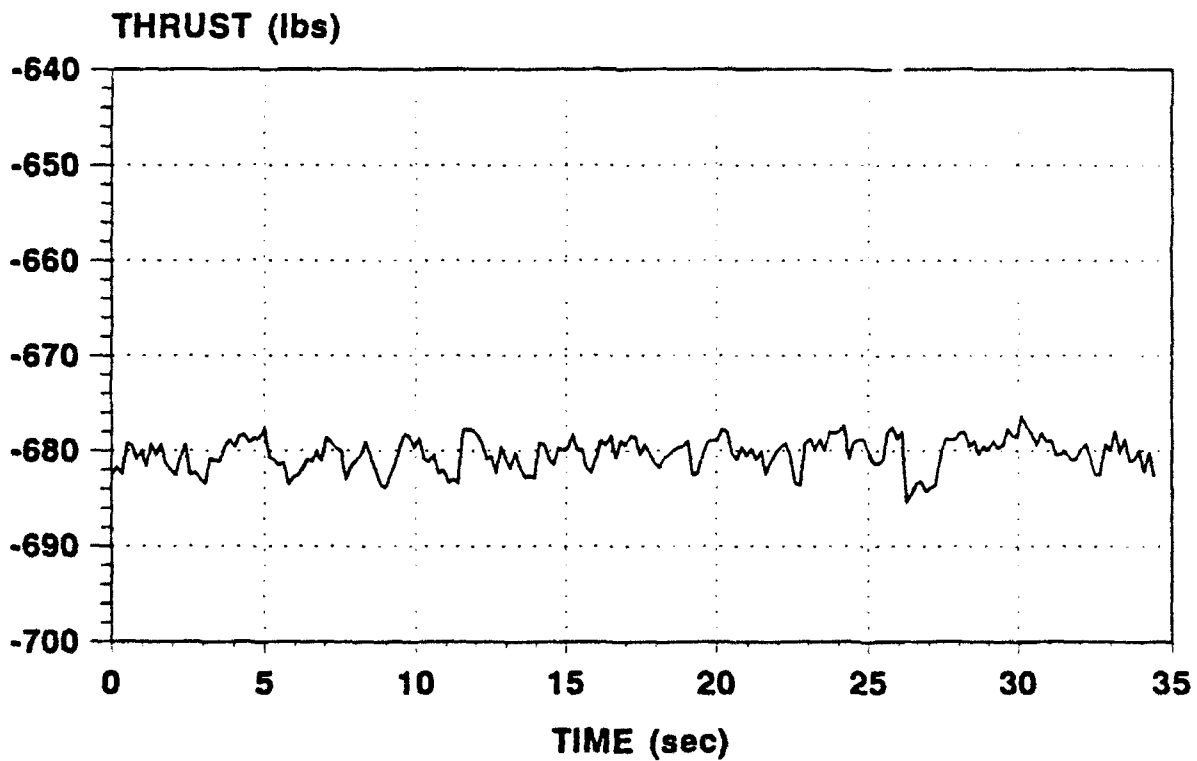


Figure I  
Load Cell with Capacitors

complete. The experiences that I had, the experiments that I helped on, the people that I had an opportunity to work with and the people that I got to know were all so numerous that I had a hard time deciding what to write this paper about; however, the problems with the load cell and the thrust stand were primarily what I worked on and so I wrote about what I know most. I worked with many computers and had the chance to make the data plots that are in this paper. My knowledge has increased about computers, airplanes, ramjet engines, effective research, college, and life in general. Everyone had some words of advice for me and had the time to talk to me about the different projects that they were working on. I would never have made it through the summer without the people that I worked with. An engineering experience at a high school level is very valuable and I am now ready for college so that I can learn more of the skills that are needed to be a successful engineer. I would not have traded this summer job or the friends that I made for anything or anybody. I truly hope that everyone else who had the opportunity to do the summer research learned as much as I did and will value the chances given to them as much as I know that I will.

#### APPARATUS

The ram rig primarily consists of the thrust stand and all that is on or in it. The thrust stand is a twenty-five foot long, seven feet wide, and seven feet tall from the floor to the top of the combustor. The actual ram components are suspended above the base of the thrust stand. The load cell is in the first foot of the front of the base of the thrust stand. The air pipes leading up to the ram rig are attached at one end of the thrust stand and the exhaustor pipes are attached at the other end. The thrust stand itself is

primarily free standing so that it can properly simulate all the motions of a ramjet engine. There are several indicators placed throughout the ram rig that allow a read-out of the simulated situations. The indicators mostly lead into the data acquisition system and the cards within it. There are about eight cards in the data acquisition that can each read thirty-two different measurements. The technology of Wright Laboratory's facilities is amazing and the possibilities for the future are endless.



**A MODEL OF THE OPERATING TEMPERATURE RANGE  
OF ESTER-BASED LUBRICANTS**

**Erin Lynn Glaser  
High School Apprentice  
Research and Development Laboratories**

**Final Report for:  
Summer Research Program  
Wright Laboratory**

**Sponsored by:  
Air Force Office of Scientific Research  
Wright-Patterson Air Force Base, Dayton, Ohio**

**August 1992**

**A MODEL OF THE OPERATING TEMPERATURE RANGE  
OF ESTER-BASED LUBRICANTS**

Erin Lynn Glaser  
High School Apprentice Program  
Research and Development Laboratories

Abstract

The densities and viscosities of four Mobil ester-based lubricants were measured at four different temperatures. The data points obtained were then used along with Walther's viscosity equation to create a mathematical model which could be used to predict the kinematic viscosity of any of these four lubricants over a wide range of temperatures. The models were then graphed, and the graphs were used to determine the operating temperature range of each of the four lubricants based upon a 2-cSt to 20,000-cSt operable viscosity range.

# A MODEL OF THE OPERATING TEMPERATURE RANGE OF ESTER-BASED LUBRICANTS

Erin Lynn Glaser

## INTRODUCTION

It is well-documented that the single most important property of a lubricating fluid is its viscosity. This quality, defined as the resistance of a liquid to flow, plays a major part in the selection of appropriate lubricants for particular engines and for particular functions within an engine. A fluid with an exceedingly low viscosity will not adequately protect contacting metal components and will result in short machine life; at the other extreme, an exceptionally viscous fluid will be impossible to pump at cold temperatures. Bearing lubricant film-thickness analysis shows that, to prolong bearing life, the kinematic viscosity of an acceptable aircraft lubricant must not fall below 2 cSt, nor may it rise above 20,000 cSt.

This report will refer to two types of viscosity: kinematic viscosity (symbol  $\nu$ ), measured in centistokes (cSt), a unit equal to 1 millimeter squared per second; and absolute or dynamic viscosity (symbolized by the Greek letter eta,  $\eta$ ), measured in centipoise (cP), a unit equal to 1/100 of a dyne-second per centimeter squared. Dynamic viscosity is defined as "that property of a liquid by virtue of which it offers resistance to shear stress" (Streeter 5). It can further be simplified as the ratio between an applied shear stress and the resultant rate of shear (ASTM 170):

$$\eta = \frac{\tau}{du/dy}$$

where  $\eta$  = dynamic viscosity, cP;

$\tau$  = applied shear stress, dynes/cm<sup>2</sup>; and

$du/dy$  = the motion of one layer of liquid relative to an adjacent layer, s<sup>-1</sup>.

Kinematic viscosity, on the other hand, is the ratio of the dynamic viscosity of a fluid to its mass density (symbolized by the Greek letter rho,  $\rho$ ):

$$\nu = \frac{\eta}{\rho}$$

where  $\rho$  = density, g/cm<sup>3</sup>.

This is a useful quantity, as many viscosity measurements (including the one

outlined in this report) utilize an indirect method in order to determine the kinematic viscosity, from which the dynamic viscosity may be calculated.

The property of viscosity is highly dependent on the temperature of the fluid in question; thus, an oil at 40° C is more viscous than the same oil at 100° C. The relationship between temperature and viscosity of most lubricating oils is a logarithmic function. Several methods of mathematical modeling exist to calculate viscosity over a range of temperatures. The method employed here uses Walther's viscosity equation

$$v = \log^{-1}[\log^{-1}(a - m \log T_A)] - 0.7$$

where  $v$  = kinematic viscosity in cSt,

$T_A$  = absolute temperature in degrees Kelvin, and

$a$  and  $m$  are constants to be determined for each individual fluid  
(Walther 419).

The purpose of this investigation was to determine a set of data points upon which a mathematical model could be established for each of four similar Mobil lubricating oils blended to obtain different viscosities. The data could then be extrapolated to determine the operating temperature range of the four lubricants, based upon a 2-cSt to 20,000-cSt viscosity requirement.

## EQUIPMENT

### A. Constant Temperature Baths

In order to ensure that the test samples would remain at a constant desired temperature during the procedure, a temperature bath was employed for each test run. In most cases the bath was the Model H-1 high temperature bath manufactured by the Cannon Instrument Company, and the bath fluid was a common mineral oil. At temperatures above 100° C (212° F), however, to avoid thermal decomposition of the bath fluid, a poly(phenyl ether)-based fluid was used. This is much more stable at high temperatures. At 18° C (64.4° F), the Neslab LTV-40 low temperature bath was used along with a bath fluid of isopropyl alcohol, which has a lower viscosity than oil and a lower freezing point than water. In each of the above cases, equipment could be suspended in the liquid by means of specially designed rubber stoppers fitted into holes in the lid of the bath. At 70° C (158° F), the mineral oil bath was heated instead by an element manufactured by the Koehler Instrument Co., controlled by a Cannon thermoregulator; and equipment was suspended in the bath by clamps.

Each bath contained a stainless steel panel behind the instrument area to provide a uniform background against which to view the instruments.

All baths employed a stirrer to ensure uniformity of temperature throughout the bath and a thermoregulator to control the desired temperature.

### B. Temperature Measurement and Control

The Cannon thermoregulators are accurate and precise to approximately  $\pm 0.1^{\circ}\text{C}$  ( $\pm 0.2^{\circ}\text{F}$ ), which is sufficiently consistent for density and viscosity measurements at elevated temperatures. These thermoregulators utilize a manually operated rotating magnet and a mercury column to adjust the setpoint. The Cannon baths may also be cooled with a slight flow of water through a cooling coil immersed in the bath fluid.

The Neslab LTV-40 low temperature bath employs a different method of thermal regulation. The setpoint is adjusted electronically, and the instantaneous temperature is displayed on a digital screen. In addition to the heat control, there is also a refrigeration function and an extra, manually operated "boost heater" should the temperature need to be brought up quickly by a few tenths of a degree. The temperature control on this bath tends to wander a bit if left alone; therefore, it must be constantly monitored to ensure that the temperature remains consistent. For the duration of the testing, the temperature was precise to an average of  $\pm 0.3^{\circ}\text{C}$  ( $\pm 0.5^{\circ}\text{F}$ ) with a maximum displacement of  $\pm 0.5^{\circ}\text{C}$  ( $\pm 0.9^{\circ}\text{F}$ ). Unfortunately, at low temperatures, the precision of thermal control is extremely important for proper results in

viscosity tests; therefore, the average error was significantly increased for viscosity measurements at 18° C (64.4° F).

At least two (2) recently calibrated mercury-column thermometers were immersed in each bath to ensure uniformity of temperature throughout.

#### C. Timing Devices

The timer employed in all cases was the Model S-10 Precision Timer manufactured by the Standard Electric Time Corporation. An electric clock with a sweep-hand display, it measures elapsed time up to 1000 seconds with precision to the nearest 0.01 seconds. These timers undergo a calibration check twice yearly, with the most recent calibration in June 1992, two weeks before the start of the eight-week testing period.

#### D. Viscometers

All viscometers used were the Cannon-Manning Semi-Micro viscometer for transparent liquids. This is the glass-capillary type and the most accurate. They are calibrated at the Cannon Instrument Company in State College, PA and assigned viscometer constants for 40° C (100° F) and for 100° C (210° F), from which the constant at other temperatures may be calculated.

## PROCEDURES

### A. Preliminary Measurements and Calculations

In accordance with published data (Touloukian 1372), the thermal expansion of Pyrex glass containers standardized by the manufacturer at 293 K (20° C, 68° F) was calculated over the range of temperatures to be tested, from 18° C (64.4° F) to 150° C (302° F). The maximum volumetric expansion was found to be +0.13% at 150° C (302° F), or an error of -0.0325 mL when using a 25-mL Pyrex volumetric flask, the type employed in the density measurements. This is an experimentally insignificant value and may be ignored.

The density of distilled water was measured first, using a 10-mL sample at 40° C (104° F), and was found to be  $0.988 \pm 0.011$  g/mL. The accepted value (Weast F-11) is 0.992 g/mL @ 40° C, which yields an experimental error of 0.4%. Possible sources of error such as contamination of the flasks or barometric pressure drops were ruled out as insignificant or improbable. To increase the resolution, the experiment was repeated using a 25-mL sample of distilled water. This time, the density was measured to be  $0.992 \pm .004$  g/mL, which agrees well with the accepted value. All future density measurements were made using a 25-mL sample.

The kinematic viscosity of distilled water was measured at 18° C (64.4° F) and found to have a value of approximately  $1.08 \pm 0.01$  cSt, which yields an absolute viscosity of 1.08 cP. The accepted value (Weast F-42) for the absolute viscosity of distilled water at 18° C is 1.05 cP; at 17° C, 1.08 cP. This results in an error of 2.86%, almost certainly caused by fluctuations in the bath temperature--which at this low level can result in large fluctuations in viscosity measurements. Although 2.86% is a relatively minor experimental error, it suggests that values obtained for viscosity in the low end of the temperature range should be subject to more intense scrutiny than values obtained at higher temperatures. In addition, it should be noted that the viscosity/temperature curves of liquids more viscous than water (including, of course, most lubricating oils) will deform even more drastically at higher temperatures, making their measurable viscosities even more sensitive to minor fluctuations in temperature.

A kinetic energy correction was calculated for the trial run of oil sample TEL-92013 through viscometer #C3, size 100, as suggested in specification D 446 of the 1990 ASTM (ASTM 176): "For viscometers whose constants are 0.05 cSt/s or less, a kinetic energy correction may be significant if the minimum 200-s flow time is not observed. Where this is not possible, [the kinetic energy equation  $v = Ct$ ] takes on the following form:

$$\text{Kinematic viscosity, cSt,} = Ct - E/t^2$$

where:

$E$  = kinetic energy factor,

$C$  = viscometer constant, and

t = flow time, s."

The average flow time for this sample was 117.42 s, so it was deemed worthwhile to check the necessity of a kinetic energy correction. The kinetic energy factor was calculated and taken into consideration when calculating the kinematic viscosity; then this value was compared with the value obtained for kinematic viscosity without incorporating the kinetic energy term  $E/t^2$ . This term proved to be so small, on the order of 0.0000009 cSt/s, that kinetic energy corrections on this scale of measurement would be impractical. Few were even applicable, since most of the viscosity flow times were in excess of 200 s.

#### B. Density Measurements

All density measurements were made using the basic technique of mass divided by volume. The standard ASTM hydrometer method was not used because it employs a larger sample than was practical for use in this particular laboratory setting.

The mass of an empty, chemically clean 25-mL volumetric flask was determined; then the flask was filled to the 25-mL mark and suspended in a temperature bath for a sufficient amount of time to allow the system to reach thermal equilibrium. The level of the liquid was then adjusted with a pipette, after which the temperature was again allowed to stabilize. This was repeated until the level of the meniscus remained steady at the 25-mL mark. The flask was removed from the bath, stoppered, and the outside was cleaned thoroughly with acetone and toluene; the flask was then allowed to dry in an oven. After drying, the flask was weighed again. Four trials were made, and the average mass of the flask's contents was divided by 25.0 mL to obtain the density of the fluid.

Care was taken to avoid contamination of the flasks before weighings. Latex gloves were worn during most stages of the measuring process, and excess bath oil was completely removed before the flasks were put to dry.

#### C. Kinematic Viscosity Measurements

Kinematic viscosity measurements were taken using the standard ASTM technique outlined in Designation D 445-88, "Standard Test Method for Kinematic Viscosity of Transparent and Opaque Liquids" (ASTM 170-175).

The glass capillary tube is filled to a marked level by first inverting it with the filling arm (the narrow end) immersed in the sample to be tested, and then drawing the liquid into it by means of a vacuum line. The viscometer is then suspended (in a normal vertical position) in the temperature bath and allowed to come to thermal equilibrium.

A vacuum line is applied to the mouth of the filling arm to draw the level of the sample above the higher of the two timing marks above and below the timing bulb. The sample is then allowed to flow freely past the two timing marks, and



the time elapsed as the meniscus passes from the higher to the lower mark is measured. Six trials were taken of each sample at each temperature, with the exception that, due to high fluctuations in measured values, at 18° C (64.4° F) twelve trials were taken in an attempt to find a truer average.

The kinematic viscosity is then calculated using the viscometry equation

$$v = Ct$$

where  $v$  = kinematic viscosity, cSt,

$C$  = the viscometer constant, cSt/s, and

$t$  = average flow time, s.

## RESULTS

Experimental findings were as follows:

### A. Lubricant Density vs. Temperature

Lubricant #	<u>Density, g/mL</u>			
	18° C	40° C	70° C	100° C
TEL-92013	0.958	0.943	0.923	0.898
TEL-92014	0.995	0.979	0.958	0.934
TEL-92017	0.997	0.981	0.961	0.937
TEL-92016	1.012	0.996	0.974	0.952

All data were known to an accuracy of  $\pm 0.001$  g/mL.

### B. Kinematic Viscosity vs. Temperature

Lubricant #	<u>Kinematic Viscosity, cSt</u>			
	18° C	40° C	70° C	100° C
TEL-92013	33.5 $\pm 0.9$	14.51 $\pm 0.02$	6.50 $\pm 0.01$	3.46 $\pm 0.01$
TEL-92014	81 $\pm 3$	29.20 $\pm 0.02$	11.74 $\pm 0.03$	5.55 $\pm 0.01$
TEL-92017	133 $\pm 4$	45.24 $\pm 0.06$	16.80 $\pm 0.02$	7.66 $\pm 0.03$
TEL-92016	186 $\pm 6$	60.93 $\pm 0.34$	21.41 $\pm 0.07$	9.34 $\pm 0.02$

## ANALYSIS OF RESULTS

The data obtained in the course of the test was used to find the two constants  $a$  and  $m$  needed to plot Walther's viscosity equation for each oil. This was done with a computer program previously used in an earlier set of experiments, published as "Physical Properties of High Temperature Synthetic Lubricants" (Forster, n.p.). The set of calculated points were then graphed to show the operating temperature ranges of each oil.

### A. Ester Lubricant Data Analysis using Walther's Equation:

$$A := \begin{bmatrix} 33.55 & 80.73 & 132.61 & 185.98 \\ 14.15 & 29.2 & 45.24 & 60.93 \\ 6.5 & 11.74 & 16.802 & 21.41 \\ 3.462 & 5.55 & 7.66 & 9.34 \end{bmatrix} \quad T := \begin{bmatrix} 18 \\ 40 \\ 70 \\ 100 \end{bmatrix} \quad T_0 := \begin{bmatrix} 291 \\ 313 \\ 343 \\ 373 \end{bmatrix}$$

Matrix A:

Column 0 - Viscosity of exp Mobil 3 cSt (TEL-92013) @ corresponding row in matrix T  
 Column 1 - Viscosity of exp Mobil 5 cSt (TEL-92014) @ corresponding row in matrix T  
 Column 2 - Viscosity of exp Mobil 7 cSt (TEL-92017) @ corresponding row in matrix T  
 Column 3 - Viscosity of exp Mobil 9 cSt (TEL-92016) @ corresponding row in matrix T

Matrix T:

Column 0 - Temperature deg. C

Matrix T<sub>0</sub>:

Column 0 - Temperature deg. K

Index I. Number of temperature data points (Rows in matrices A, T, and T<sub>0</sub>)

Index J. Number of lubricants tested (Columns in matrix A)

Algebraic solution for Walther's viscosity equation:

$$Z_{\min_j} := A_{3,j} + .7$$

$$Z_{\max_j} = A_{0,j} + .7$$

$$m_j = \frac{\log[\log[Z_{\min_j}]] - \log[\log[Z_{\max_j}]]}{\log[Ta_0] - \log[Ta_3]}$$

$$m = \begin{bmatrix} 3.655 \\ 3.528 \\ 3.362 \\ 3.297 \end{bmatrix}$$

$$a_j := \log[\log[Z_{\min_j}]] + m_j \cdot \log[Ta_3]$$

$$v_{1,j} := \left[ 10^{\left[ 10^{\left[ a_j - [m_j \cdot \log[Ta_1]] \right]} \right]} \right]^{-.7}$$

$$a = \begin{bmatrix} 9.193 \\ 8.974 \\ 8.612 \\ 8.48 \end{bmatrix}$$

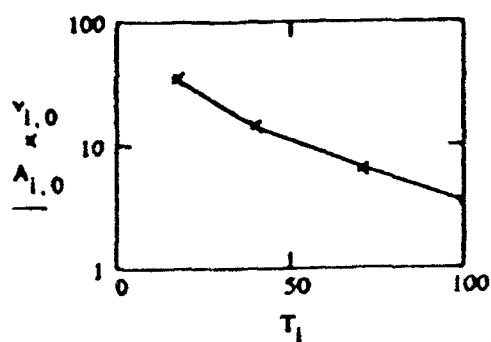
Calculated values

$$v = \begin{bmatrix} 33.55 & 80.73 & 132.61 & 185.98 \\ 14.288 & 29.331 & 45.333 & 60.392 \\ 6.241 & 11.044 & 15.993 & 20.228 \\ 3.462 & 5.55 & 7.66 & 9.34 \end{bmatrix}$$

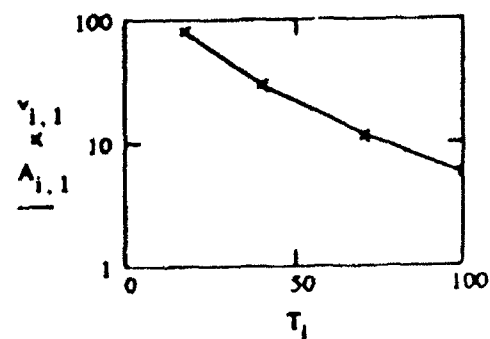
Data

$$A = \begin{bmatrix} 33.55 & 80.73 & 132.61 & 185.98 \\ 14.15 & 29.2 & 45.24 & 60.73 \\ 6.5 & 11.74 & 16.802 & 21.41 \\ 3.462 & 5.55 & 7.66 & 9.34 \end{bmatrix}$$

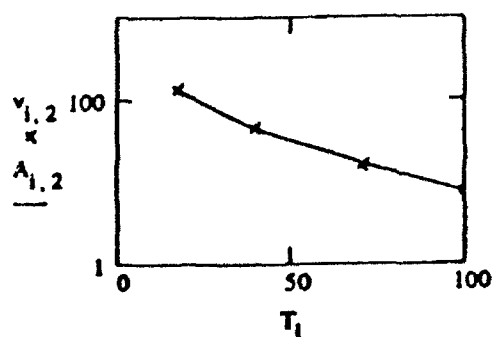
Walther's Eq: 3cSt Ester



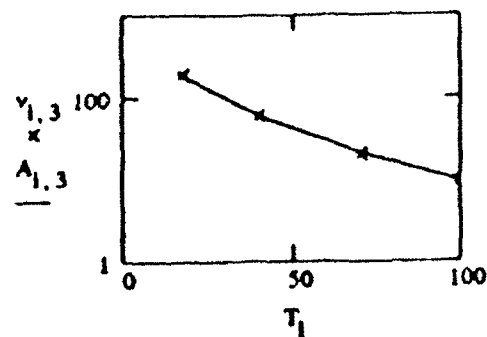
Walther's Eq: 4cSt Ester



Walther's Eq: 5 cSt Ester



Walther's Eq: 7.5 cSt Ester



# Analysis of Results using Algebraic solution to Walther's equation :

Input variables:

Difference between data and calculated results

$$\delta_{i,j} := A_{i,j} - v_{i,j}$$

$$n := 6$$

$$\kappa := 3$$

$$A_{avgj} := \frac{\sum_i A_{i,j}}{n}$$

$$\delta = \begin{bmatrix} -1.208 \cdot 10^{-13} & -1.137 \cdot 10^{-13} & -2.075 \cdot 10^{-12} & 1.279 \cdot 10^{-12} \\ -0.138 & -0.131 & -0.093 & 0.538 \\ 0.259 & 0.696 & 0.809 & 1.182 \\ 4.885 \cdot 10^{-15} & 1.776 \cdot 10^{-14} & -2.753 \cdot 10^{-14} & 1.599 \cdot 10^{-14} \end{bmatrix}$$

Mean of Residuals

$$S_j := \left[ \frac{\sum_i [\delta_{i,j}]^2}{[n - \kappa]} \right]^{.5}$$

$$S = \begin{bmatrix} 0.169 \\ 0.409 \\ 0.47 \\ 0.75 \end{bmatrix}$$

Average value of % Deviation:

$$D_j := \frac{100}{n} \cdot \sum_i \left| \frac{\delta_{i,j}}{A_{i,j}} \right|$$

$$D = \begin{bmatrix} 0.827 \\ 1.062 \\ 0.837 \\ 1.067 \end{bmatrix}$$

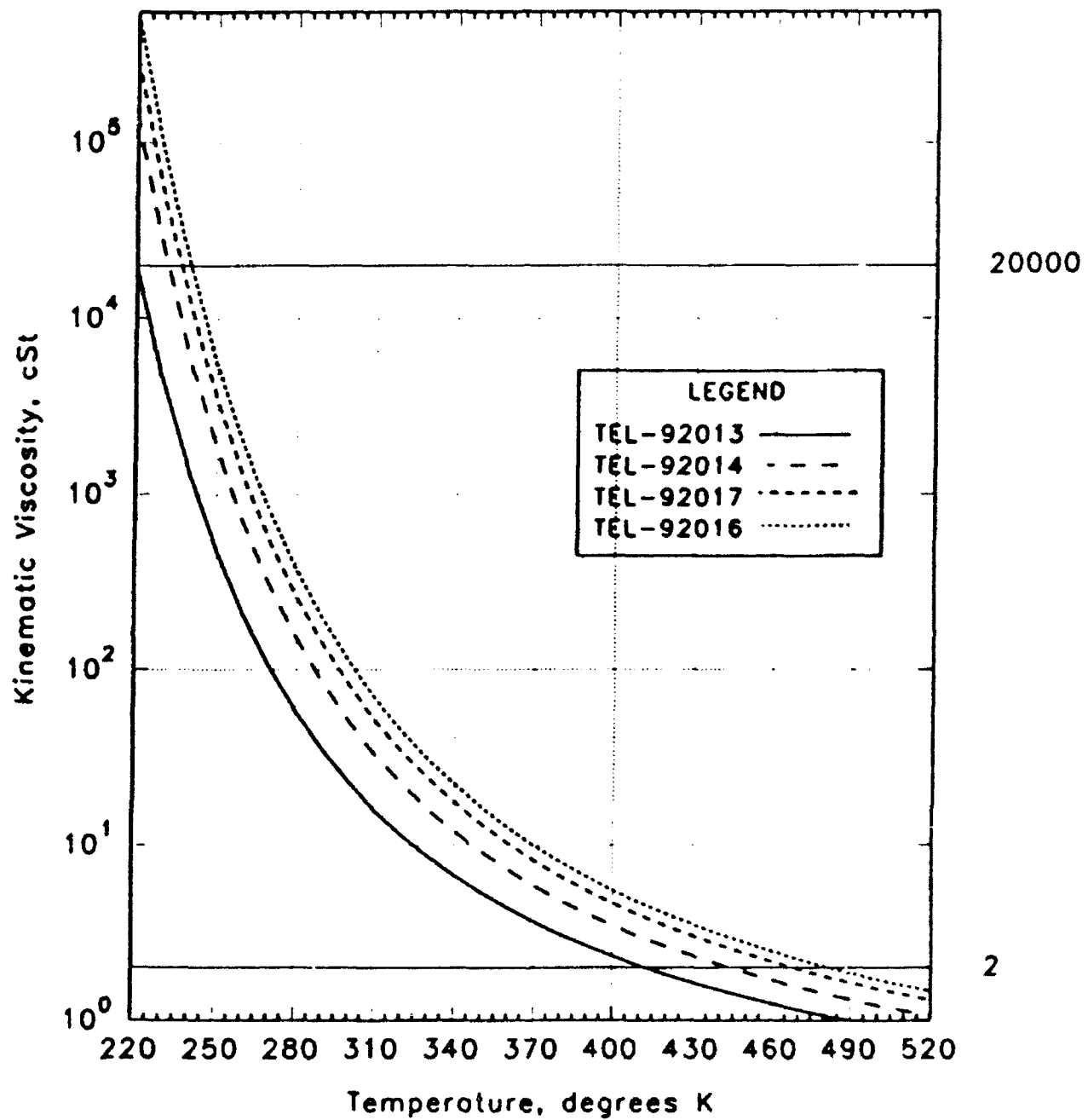
Correlation:

$$R_j := \left[ 1 - \frac{\sum_i [\delta_{i,j}]^2}{\sum_i [v_{i,j} - A_{avgj}]^2} \right]^{.5}$$

$$R = \begin{bmatrix} 1 \\ 1 \\ 1 \\ 1 \end{bmatrix}$$

# Projected Kinematic Viscosity

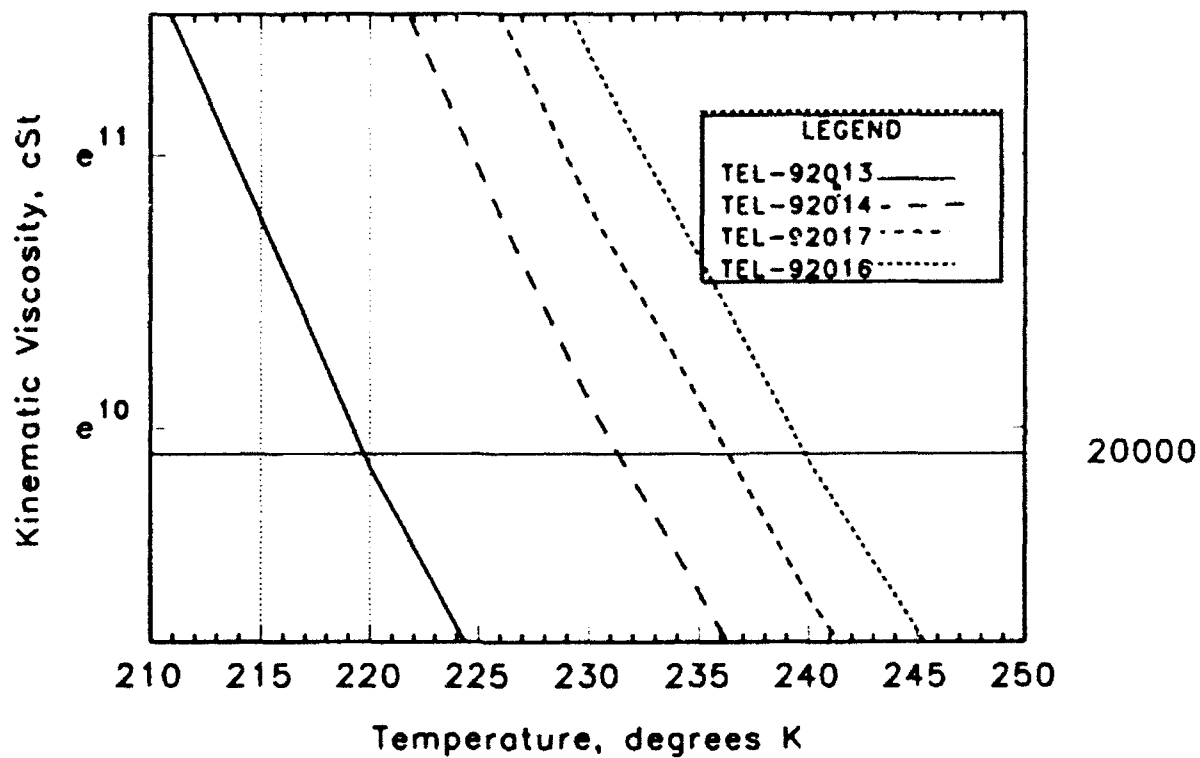
Walther's Equation Curve-fit



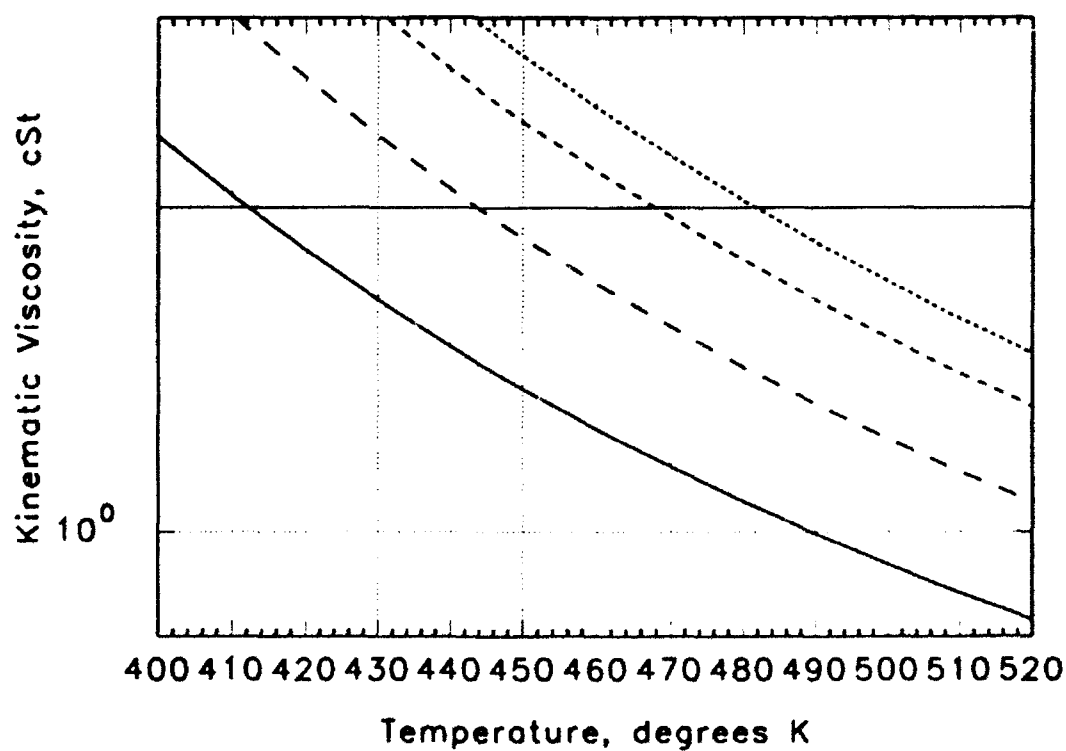
# Projected Kinematic Viscosity

(1) Upper and (2) Lower Limits of Use

1



2



### CONCLUSION

The mathematical model predicts that the four oils have usable temperature ranges of 195 to 242 Celsius degrees. The operating temperatures of the four oils are as follows:

TEL-92013: operable from -54 C to 141 C (-65 F to 286 F), a range of 195 Celsius degrees (351 F ).

TEL-92014: operable from -41 C to 173 C (-42 F to 343 F), a range of 214 Celsius degrees (385 F ).

TEL-92017: operable from -36 C to 195 C (-33 F to 383 F), a range of 231 Celsius degrees (416 F ).

TEL-92016: operable from -33 C to 209 C (-27 F to 408 F), a range of 242 Celsius degrees (435 F ).



#### REFERENCES

1. American Society for Testing and Materials, "Standard Specifications and Operating Instructions for Glass Capillary Viscometers." ASTM Designation D446-89a, 1990 Annual Book of ASTM Standards, Section 5, ASTM, Philadelphia. (1990)
2. American Society for Testing and Materials, "Standard Test Method for Kinematic Viscosity of Transparent and Opaque Liquids." ASTM Designation D445-88, 1990 Annual Book of ASTM Standards, Section 5, ASTM, Philadelphia. (1990)
3. Forster, Nelson H., "Physical Properties of High Temperature Synthetic Lubricants," Spring Semester 1992.
4. Streeter, Victor L., Fluid Mechanics. McGraw-Hill Book Company, Inc., New York. (1965)
5. Touloukian, Y. S., ed. Thermophysical Properties of Matter, vol. 13, Thermal Expansion of Nonmetallic Solids. Purdue Research Foundation. IFI/Plenum Data Company, div. of Plenum Publishing Corporation, New York. (1977)
6. Walther, C., Proc. World Petroleum Congress, London, p. 419. (1933)
7. Weast, Robert C., Ph.D., ed. CRC Handbook of Chemistry and Physics, 62nd edition. CRC Press, Inc., Boca Raton, Florida. (1981-1982)

## **STRESS GAGE ALGORITHM DEVELOPMENT**

Daniel R. Grayson  
High School Apprentice

WL/MNGI  
Eglin Air Force Base, Florida 32542-5434

Final Report for:  
High School Apprenticeship Program  
Wright Laboratory/Armament Directorate

Sponsored by:  
Air Force Office of Scientific Research  
Boiling Air Force Base, Washington, D.C.

August 1992

## STRESS GAGE ALGORITHM DEVELOPMENT

Daniel R. Grayson  
High School Apprentice  
WL/MNGI  
Eglin Air Force Base

### ABSTRACT

Research this summer centered on the creation of an algorithm for certain piezoelectric stress gages. The algorithm's function was to give accurate output values for shock velocity, particle velocity, and pressure from time of arrival data. Project work included range tests, use of scientific graphical software, mathematical calculations, and software development. The algorithm will be used to measure the effectiveness of the tested piezoelectric gages as stress sensors.

## STRESS GAGE ALGORITHM DEVELOPMENT

Daniel R. Grayson

### INTRODUCTION

Accurate measurement of weapon effectiveness and performance is necessary for conventional weapon technology development. The existing state of measurement techniques and sensors for munitions is inadequate. Investigation into the utilization of innovative sensor materials such as piezoelectric gages may remedy current problems. In addition to usage as stress sensors, certain piezoelectric gages have been found to possibly serve as detonation verifiers during wartime. Determination of the effectiveness of the piezoelectric PVF2 gage was studied and performed.

### METHODOLOGY

The development of an algorithm for the PVF2 gage was the primary concern of project work. Tests were conducted at the C64A range to collect time of arrival data. A shock wave was propagated through plexiglass targets of known width with a PVF2 gage on the alternate side to sense the arrival of the wave. Forty-one waveforms were examined for time of arrival data points. The points were then entered into arrays on the scientific software packages of Graftool and Curvfit. It was later found that the program Graftool was more powerful and efficient than the program Curvfit. Graftool was therefore used more extensively.

A series of mathematical manipulations were done on the forty-one point data array in Graftool. Firstly, a second-degree polynomial regression was done on the scatter plot derived from the point data array. The derivative of the time versus distance equation regression was then taken to give an equation and curve in time versus velocity format (The derivative of displacement is velocity). The equation in time versus velocity format was in terms of velocity so the equation was solved for time. The equation now in terms of time was then substituted into the original time versus distance equation to give an equation of distance versus velocity. At this point a variable distance for the shock wave to travel through a plexiglass target could be inputted to find the velocity of at that point.

The next step involved the use of QuickBasic 4.5 to write a software package that would use the Hugoniot relationship and the Law of Conservation of Momentum to find particle velocity and pressure from the outputted shock velocity. The two equations stated above were incorporated into the program. By simply inputting a shock velocity value, an accurate particle velocity and pressure are outputted.

#### APPARATUS

The first step in the evaluation of the PVF2 gage involved tests at Eglin Air Force Base's C64A range. Gages were mounted on either plexiglass targets or metal canisters. An explosive, either pentolite or tritonal was involved in the target setup.

When the sensing element in the gage is squeezed by a phenomenon such as the shock wave propagated from an explosion it causes the gage to give off an electrical pulse. The electrical pulse may be measured directly with coaxial cables attached to the gage or monopole antennas may be used to transmit and receive the pulse. RTD710 and RTD720 digitizers were used to capture waveforms from gage signals. Data collected for mathematical analyzation was taken from antenna tests used to determine time of arrival.

One Waveform on One Graph

03/31/92 09:42:24

5153 Pts.

Cha 1, Rec 1

100.0mV

50.00mV

0.000 V

-50.00mV

-100.0mV

-150.0mV

Two PVF2-11-0.25-EK gages on top and middle 127 Mhz antenna

Two RG58 coax connected to gages (10 feet long) no connectors

-6us

-2us

2us

6us

10us

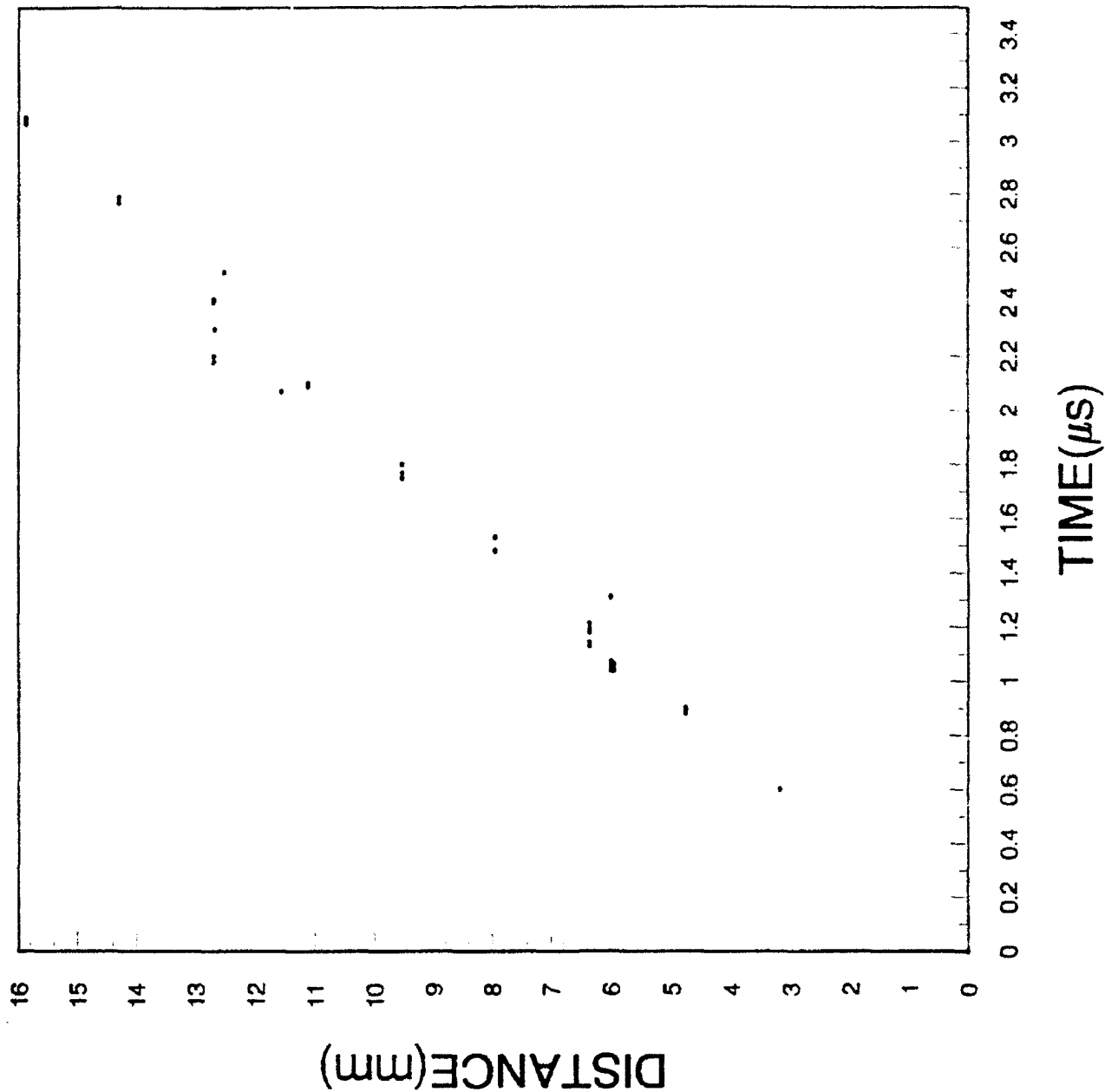
14us

18us

Shot 1, Target 2 (PMMA), target on wood table 5-6 ft above ground.

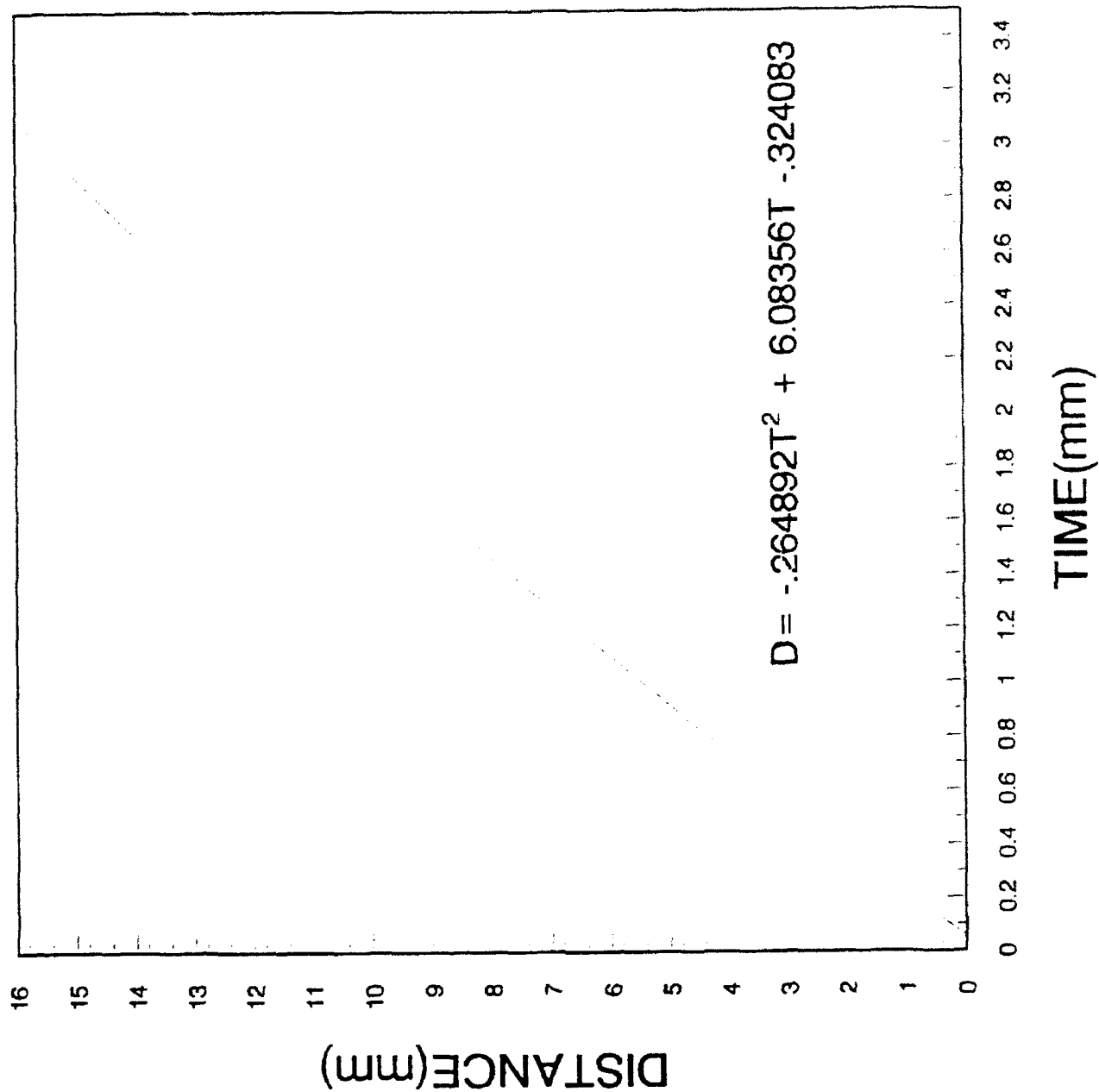
Two 1/2 inch discs

# PMMA TIME OF ARRIVAL SCATTER PLOT.

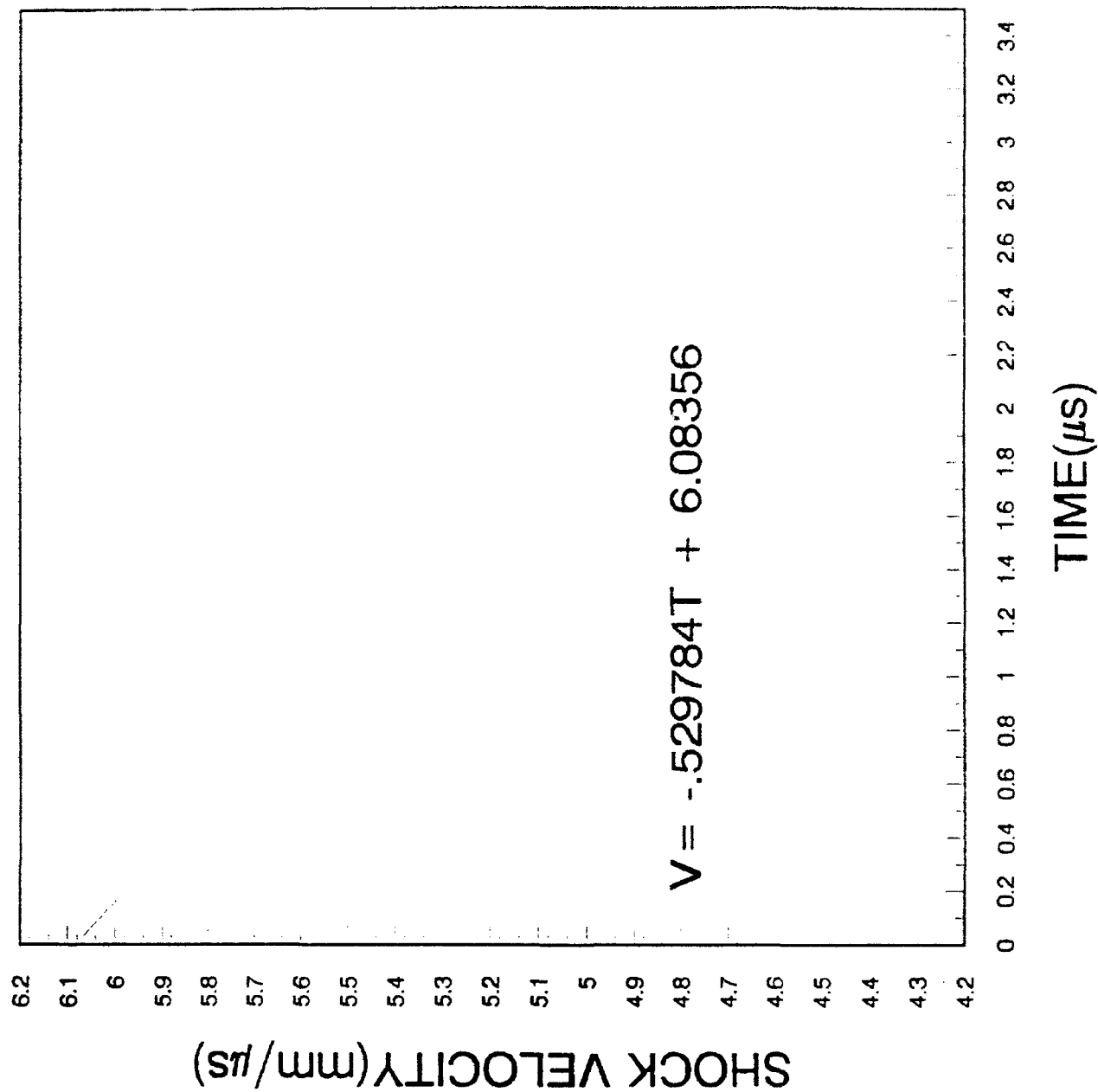




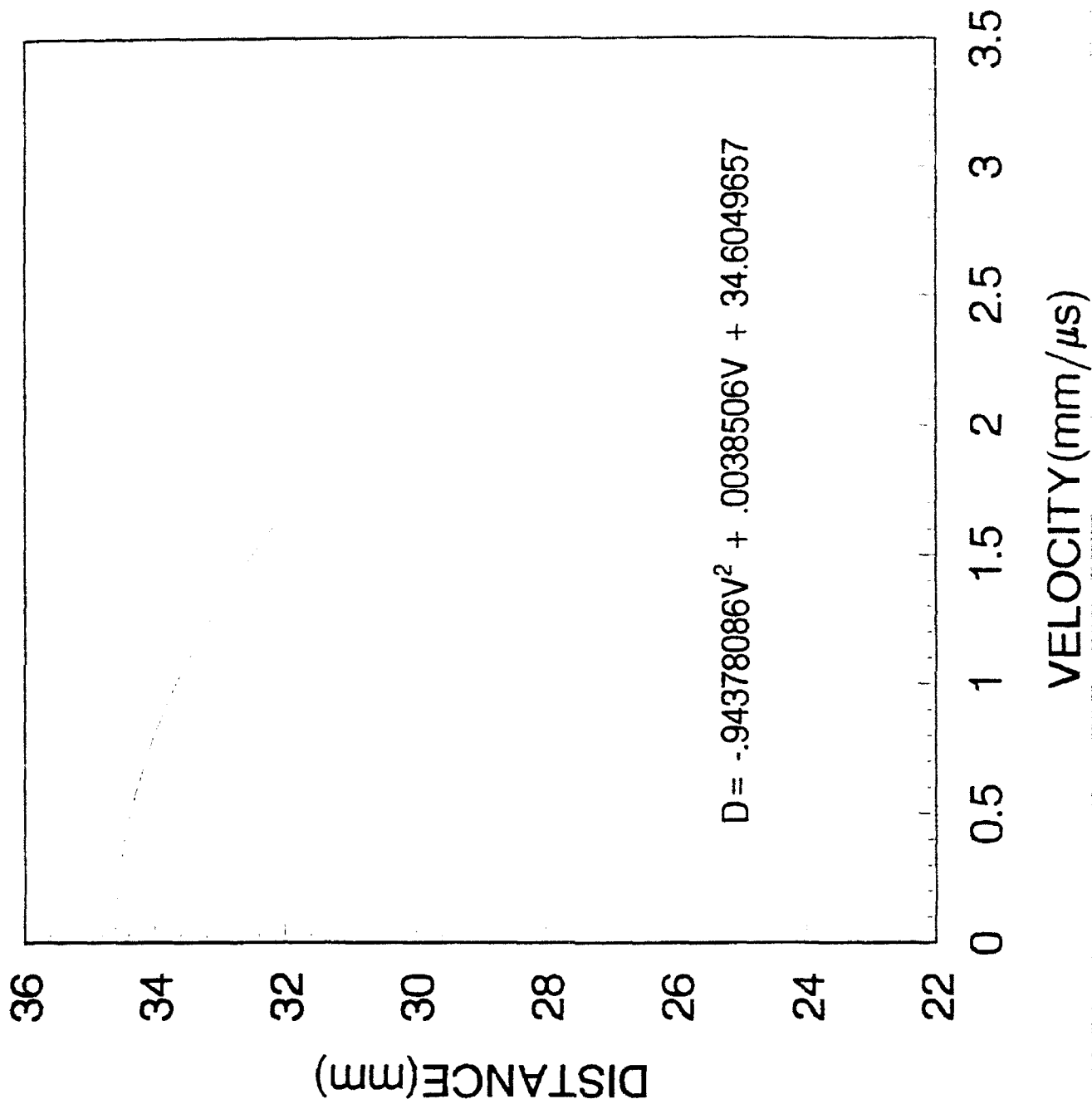
# PMMA TIME OF ARRIVAL CURVE



# PMMA SHOCK VELOCITY CURVE



# PMMA VELOCITY VERSUS DISTANCE CURVE



FLOW VISUALIZATION OF A  
JET IN A CROSSFLOW

Amy Hancock  
HSAP Student  
Roy High School  
Roy, UT 84067

Final Report for:  
Scientific High School Apprenticeship Program  
Wright Laboratory

Sponsored by:  
Air Force Office of Scientific Research HSAP  
Wright-Patterson Air Force Base, Ohio

August 1992

## FLOW VISUALIZATION OF A JET IN A CROSSFLOW

Amy Hancock

### Abstract

A qualitative study of the mixing of a jet in a crossflow, or freestream, was conducted using a flow visualization technique known as Reactive Mie Scattering. To visualize this mixing process, the jet is seeded with titanium tetrachloride ( $\text{TiCl}_4$ ) vapor and the freestream is seeded with water vapor. The  $\text{TiCl}_4$  and the water vapor react at the interface of the two streams forming micron-sized titanium dioxide ( $\text{TiO}_2$ ) particles. The particles are small enough to follow the gaseous flow and are illuminated by a light sheet from a pulsed Nd:YAG laser. Piezoelectric actuator blades are located on the four inside surfaces of the square jet conduit to provide a means of imparting energy disturbances into the jet to enhance mixing. The blades are driven at their natural frequency of 500 Hz. The piezoelectric actuators were found to significantly enhance mixing of the jet with the freestream. This study provides preliminary qualitative data for use in establishing a more complete test matrix for characterization of a driven jet in a crossflow.

# FLOW VISUALIZATION OF A JET IN A CROSSFLOW

Amy Hancock

## Introduction

This paper discusses the application of the Reactive Mie Scattering Visualization technique to a fluid dynamic system involving a jet in a crossflow.<sup>1</sup> This technique is useful in obtaining qualitative data that will give a better understanding of the behavior of a jet in a crossflow and help to determine which tests should be pursued in greater detail.

The frequency doubled output (532-nm light) of a Nd:YAG laser is formed into a light sheet. The laser pulses at a frequency of 10 Hz with a pulse length of 10 ns. The short pulse length allows instantaneous snapshots of the flow to be collected. The laser sheet slices through the flow illuminating only the TiO<sub>2</sub> particles within the sheet. Various positions within the flow can be observed by moving the light sheet to the two-dimensional surface of interest.

Reactive Mie Scattering is a visualization technique in which water vapor in one flow reacts with TiCl<sub>4</sub> in another flow spontaneously forming TiO<sub>2</sub> particles ( $\text{TiCl}_4 + 2\text{H}_2\text{O} = \text{TiO}_2 + 4\text{HCl}$ ). Each micro-meter sized TiO<sub>2</sub> particle is small enough to accelerate rapidly to the velocity of the carrier gas but is too large to diffuse readily. When hit with the Nd:YAG laser, the TiO<sub>2</sub> particles scatter light, revealing the gaseous fluid structures. Standard 35mm color photographs are then collected, recording the details of the flow for evaluation.

## Methodology

Titanium tetrachloride is a colorless to light yellow liquid with a pungent acid smell. It gives off dense white fumes and smoke when brought in contact with water vapor. According to Freymuth, the brightness of the scattered light off the smoke consisting of TiO<sub>2</sub> particles is an advantage in flow visualization when compared to other smokes.<sup>2</sup> One disadvantage of TiCl<sub>4</sub>, however, is the corrosive hydrochloric acid (HCl) byproduct generated in the reaction with H<sub>2</sub>O. This requires conducting experiments where TiO<sub>2</sub> and HCl can be vented out of the laboratory through an overhead hood.

Piezoelectric actuators are used to drive many types of flows. In this study, the piezoelectric blades were used to drive the jet. Piezoelectricity is defined in the

dictionary as charges of electricity induced in crystalline substances by pressure. When piezoelectric blades, or actuators, are driven at their natural frequency, large physical oscillations result despite very low electrical input. The natural frequency of the blades was found to be approximately 500 Hz.

There have been many prior investigations of a jet in a crossflow. Some studies have looked at the process of film cooling, and others have focused on the entrainment of the jet. Many high temperature parts require film cooling. Rivir, et al. have studied the need of better film cooling methods in parts of a turbine engine. They state that the efficient use of film cooling flows becomes increasingly important as turbine inlet temperatures increase and coolant flows decrease.<sup>3</sup> Jet entrainment and mixing studies are also made with a jet in a crossflow. Several items require quick and efficient mixing of two airflows in order to operate. Coal furnaces, ramjets, and gas turbine combustors are all examples of such items. Vermeulen, et al. found that pulsing the air jet causes significant increases in jet spread, penetration (up to 92% increase), and mixing.<sup>4</sup> Although a different jet modulation technique was used in their experiment, similar enhanced mixing results were found.

This paper looks at the effects of driving only the leading edge blade, identified as blade 1, or the upstream edge of the jet. A comparison of driven and undriven flows are studied in this experiment.

### Apparatus

The apparatus used in this experiment is illustrated in Figure 1. Water vapor is entrained into the freestream air and the dry air jet is seeded with  $\text{TiCl}_4$  vapor. The velocity of both flows can be controlled independently. When the two flows interact, the interface is marked by the newly formed  $\text{TiO}_2$  particles. The apparatus can be rotated, allowing both the side view and the transverse view to be visualized and studied. The base of the plexiglas chimney representing the confined cross section of the jet is 8.9 cm square, and is 61 cm long. The opening of the square jet into the flow is 1.5 cm on each side. This apparatus enables us to study the behavior of a jet in a crossflow at a large enough scale to be visualized easily.

The square jet used in this study contains four piezoelectric actuators. They are located along each of the four inner walls of the jet. Tests can be made without any driving of the jet, or they can be driven in different methods. Each piezoelectric blade can be controlled individually. This study focuses on the leading edge upstream blade. Throughout the paper, this blade is identified as Blade 1.

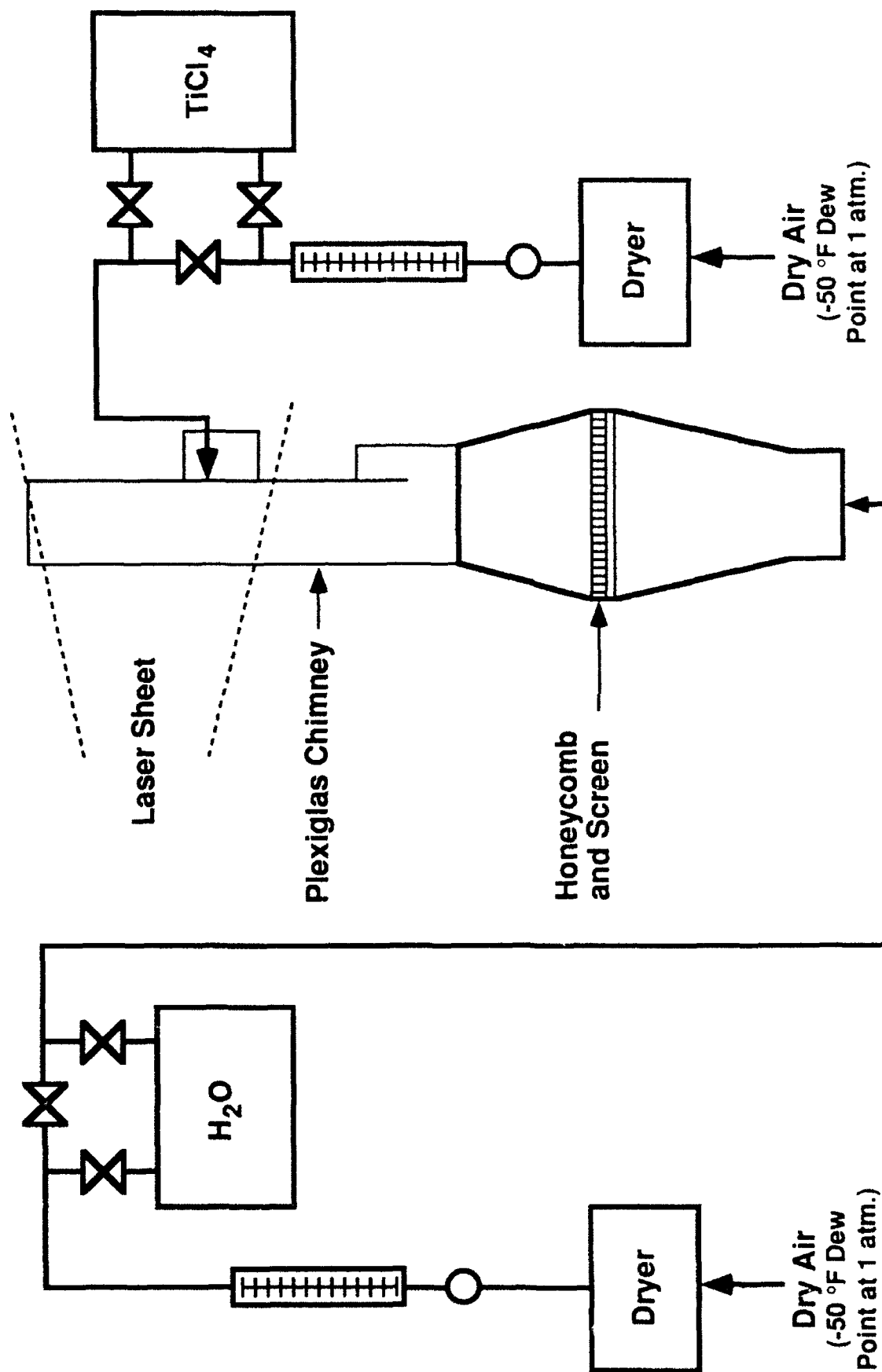


Fig. 1. Jet in a Crossflow Facility Schematic



## Results

In this study, it was found that driving the square jet with piezoelectric actuators had a significant effect on the airflows and enhanced mixing. Figure 2 shows the close-ups of the side views of the undriven and driven jet in a crossflow. Both were ran at the same conditions with the freestream velocity at 1.19 m/s and a jet velocity of 1.01 m/s. The flow shown in Fig. 2a. did not have any driving of the piezoelectric actuators, where in Fig. 2b., the jet was driven by the upstream blade. Figure 3 and Fig. 4 give different views of the flow. These views are of the rotated cross section, also known as the transverse view. The laser slices the flow 1 mm off the surface of the wall from which the jet issues. In these views, the jet would be coming out of the page toward the reader. The bottom of this close-up frame is just below the entrance of the jet. Both Fig. 3 and Fig. 4 have a main flow velocity of 1.19 m/s and a jet velocity of 1.01m/s. Figure 3 is not driven, while Fig. 4 is driven by the piezoelectric blade 1 at 500 Hz. Comparison of the driven and undriven flows indicate that mixing, penetration of the jet into the freestream, and jet spread is significantly enhanced by the driving of the blades. This preliminary study gives us qualitative data that shows that driving the jet with piezoelectric actuators enhances mixing and is worthy of further, more in depth, investigation.

## Conclusion

In conclusion, the Reactive Mie Scattering technique gave effective visualizations of the interaction of a jet in a crossflow. By slicing the flow in various planes, the effect of driving the jet was evaluated qualitatively. The data shows that driving the jet flow definitely has an effect on the flow. Specifically, when the leading edge blade was driven, it resulted in *increased jet spread, deeper penetration of the jet into the freestream, and enhanced mixing*. This preliminary study provided qualitative data for a better understanding of the behavior of a jet in a crossflow. It also helped to establish the test conditions for future, more in depth studies to determine optimal driving conditions to enhance mixing of a jet in a crossflow.



Fig. 2a.

UNDRIVEN

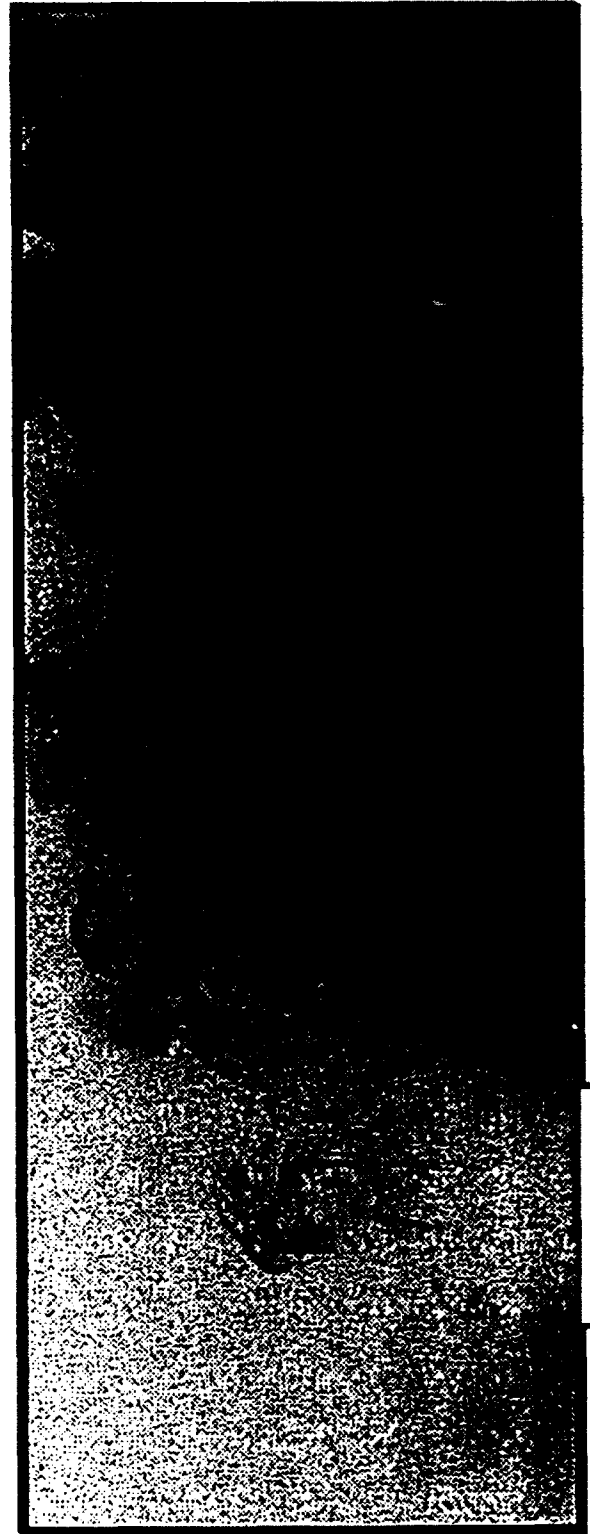


Fig. 2b.

DRIVEN by Blade 1 at 500 Hz

Conditions - Freestream at 1.194 m/s and Jet at 1.016 m/s.

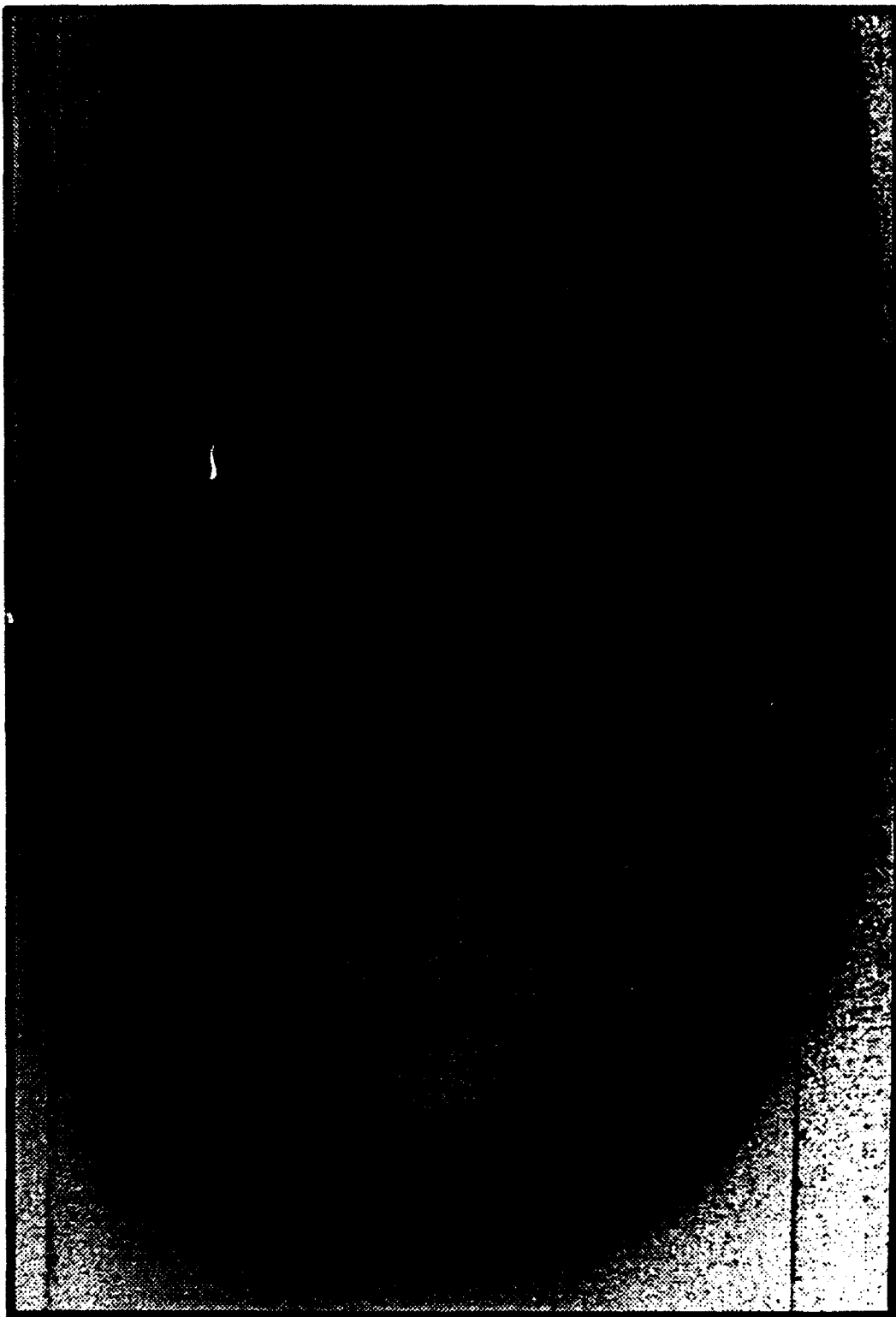


Fig. 3. UNDRIVEN

Conditions - Freestream at 1.19 m/s and Jet at 1.01 m/s



Fig. 4. DRIVEN by Blade 1 at 500 Hz  
Conditions - Freestream at 1.19 m/s and Jet at 1.01 m/s

### References

1. L.-D. Chen and W.M. Roquemore, "Visualization of Jet Flames," *Combust. Flame* **66**, 81-86 (1986).
2. P. Freymuth, "Air Flow Visualization Using Titanium Tetrachloride," *Advances in Fluid Mechanics Measurements*, M. Gad-el-Hak, ed., Springer-Verlag, Berlin Heidelberg, 1989.
3. R.B. Rivir, W.M. Roquemore, and J.W. McCarthy, "Visualization of Film Cooling Flows Using Laser Sheet Light," AIAA-87-1914 (1987).
4. P.J. Vermeulen, C.-F. Chin, and W.K. Yu, "Mixing of an Acoustically Pulsed Air Jet with a Confined Crossflow," *J. Propulsion* **6**, 777-783 (1990).

## **HIGH SURFACE AREA CONDUCTIVE POLYMERS**

**Deanna Harrison  
High School Apprentice  
Fuzes Branch**

**Wright Laboratory Armament Directorate  
WL/MNMF  
Eglin AFB, FL 32542-5434**

**Final Report for:  
High School Apprentice Program  
Wright Laboratory Armament Directorate**

**Sponsored by:  
Air Force Office of Scientific Research  
Bolling Air Force Base, Washington, D. C.**

**August 1992**

## HIGH SURFACE AREA CONDUCTIVE POLYMERS

Deanna Harrison  
High School Apprentice  
Fuzes Branch  
Wright Laboratory Armanent Directoate

### Abstract

Most polymers are insulators, such as plastics, but a few that have been recently developed are conductive. In the past few years there has been much research done on conductive polymers because of their many practical applications.

There are some significant advantages to using conductive polymers instead of metals. They are very light weight and relatively easy to make. It is also possible to alter their physical and electrical properties by changing the conditions at which the polymer films are deposited [3]. The focus of this project was to find ways to increase the surface area of conductive polymer films. A textured anode proved to increase the surface area of the PPY/DBS films without making them brittle. Although this is an effective way of creating high surface area films, the use of a pulsed current was also investigated. Depositing a base coat of smooth PPY/DBS allows there to be more flexibility, thus it is an essential part of this process. A base current of 40 mA was used for the first 45 minutes of deposition. After this period the current was pulsed for 15 minutes. It is still to be determined what type of effect these films will have when used in capacitors.

# HIGH SURFACE AREA CONDUCTIVE POLYMERS

Deanna Harrison

## INTRODUCTION

Most polymers are insulators , such as plastics, but a few that have been recently developed are conductive. In the past few years there has been much research done on conductive polymers because of their many practical applications. They can be used to make rechargeable batteries that do not work by chemical reactions. This process eliminates the problem of corrosion. Smart windows are another recent development in which conductive polymers are used to block out sunlight and heat by turning opaque. This reaction is triggered as light or heat passes through the windows. Double layer capacitors can also be made using conductive polymer films as electrodes [1]. These films can be used with nonaqueous electrolytes and can sustain higher voltages than other materials commonly used in capacitors [2].

There are some significant advantages to using conductive polymers instead of metals. They are very light weight and relatively easy to make. It is also possible to alter their physical and electrical properties by changing the conditions at which the polymer films are deposited [3].

## DISCUSSION OF PROBLEM

Most capacitors have high surface area metal oxide electrodes, which are ideal. The texture creates more area in which the electrodes and electrolyte come in contact with each other, increasing capacitance [4]. Those made with polymer films as electrodes work well, except for the fact that the low surface area greatly inhibits capacitance [5]. The focus of this project was to find ways to increase the surface area of conductive polymer films. Since capacitors are used in fuzes, any research in this field is also pertinent to the development and improvement of weapons.



## METHODOLOGY

The conductive polymer used in this research was polypyrrole (PPY), which was doped with dodecylbenzenesulfonate (DBS) (Figure 1). DBS has been reported to give more order to polypyrrole films. Research has also been done stating that films made with this large dopant anion have higher conductivities [6].

I first made films with a steady current in order to determine the best molarity, current, electrode configuration and type, and length of deposition time. Part of the task would be to determine the best concentrations of ppy and DBS. Since there was no noticeable difference in the conductivity of films made from different molar solutions, 0.05M PPY and 0.05M DBS were used throughout the study as constants. For normal low surface area films, a steady current of 40 mA (6.3 V) was used. Several types of electrodes were tried, including zirconium and chrome plated steel, but nickel electrodes were used as a standard for the subject experiments. The anode was polished so that texture created by its surface would not be confused with texture created by altering other variables. Each of the electrodes were 9x16cm. They were placed approximately 15cm apart in a container that was 17x12x8cm. One liter of solution was used for each experiment. This immersed an area of 9x5cm on each nickel electrode. A deposition time of one hour was also set as a constant.

After these constants had been set, two methods of achieving enhanced surface area were evaluated. The first, most logical, method was to use a textured anode during deposition. The second method was the application of a pulsed current. When the current was pulsed from the start at levels high enough to increase texture, the resulting film was too brittle for practical use in capacitors. To eliminate this problem a smooth film was deposited for the initial three-fourths of the process, and pulsed film material was grown on this base for the remainder of the time. A circuit was set up that enabled a steady current to be switched to a pulsed current (Figure 2).

To test the films for resistance, a four point probe and an LCR meter were used. The values were then converted to resistivity and conductivity using formulas and correction factors. A scanning electron microscope (SEM) was used to analyze and compare the surface areas of the PPY/DBS films (Figures 3 & 4).

## RESULTS

A textured anode proved to increase the surface area of the PPY/DBS films without making them brittle. Although this is an effective way of creating high surface area films, the use of a pulsed current was also investi-

gated. Depositing a base coat of smooth PPY/DBS allows there to be more flexibility, thus it is an essential part of this process. A base current of 40 mA was used for the first 45 minutes of deposition. After this period the current was pulsed for 15 minutes. Varying the pulsed current had a significant effect on the texture as well as the flexibility of the films. Results from many depositions showed that pulsed currents under 90 mA did not noticeably increase the texture. Films deposited above 115 mA were too brittle to be used in capacitors. A pulsed current waveform of 90-115 mA at 8.33 mHz (Figure 5) was used to grow the ideal film upon a smooth PPY/DBS substrate material. Films made using this procedure were more textured than films made at a steady current, but not as brittle as films made at a pulsed current for the entire deposition time.

When the films were analyzed using the SEM, the increase in surface area was easily seen (Figures 3 & 4). Magnifications of 50x and 400x were used to compare the films. The films made using a steady current throughout their deposition had smaller and less concentrated texture than the films made using a pulse.

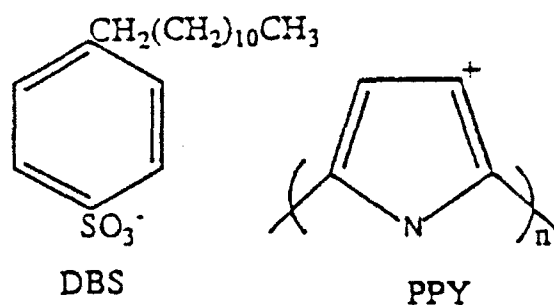
The films that were made at a steady current (40 mA) had conductivities of about 70 siemens. Films that were textured by using a pulsed current had conductivities of about 50 siemens. The highest conductivities measured for PPY/DBS films [7] are approximately  $10^2$  siemens (Figure 6).

## CONCLUSION

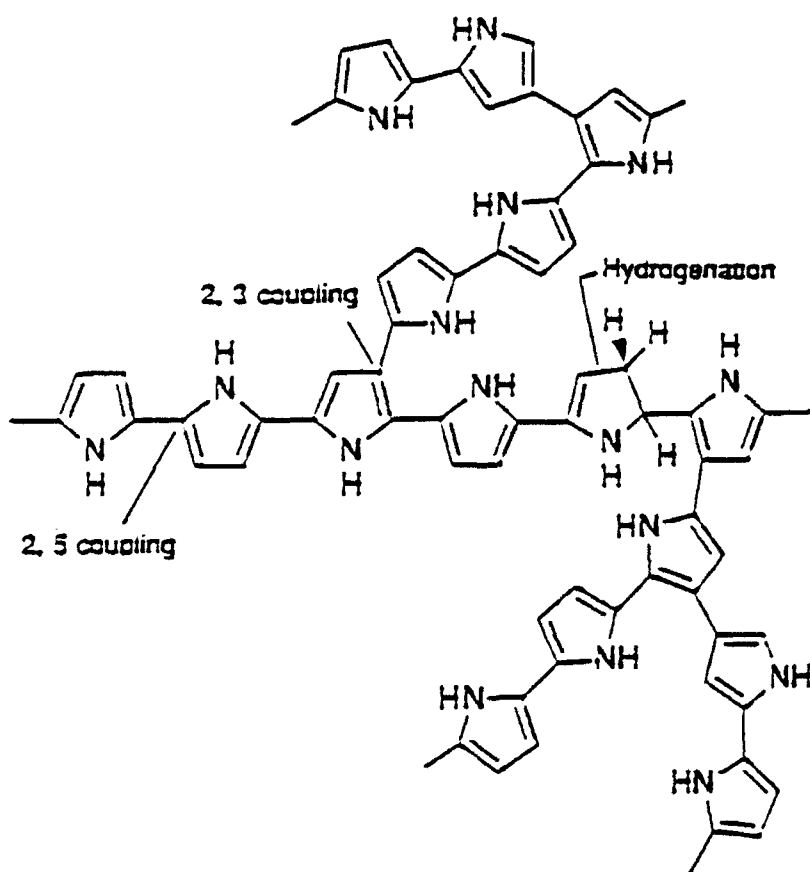
The surface area of PPY/DBS films can be increased by using a pulsed current. This results in some loss of flexibility and a slight decrease in conductivity. It is still to be determined what type of effect these films will have when used in capacitors. If the surface area of the PPY/DBS is high enough, it should increase capacitance, despite the slightly reduced conductivity. I also found that using a textured anode increases surface area. These two methods of texturing films could conceivably be combined to create an even higher surface area. It is also noteworthy that both methods are adaptable to a continuous type of manufacturing process. Indeed, it has been suggested by J. R. Reynolds [8] that a high surface area, cylinder shaped anode could be rotated in order to allow one to peel off a continuous strip of textured conductive polymer material.

## REFERENCES

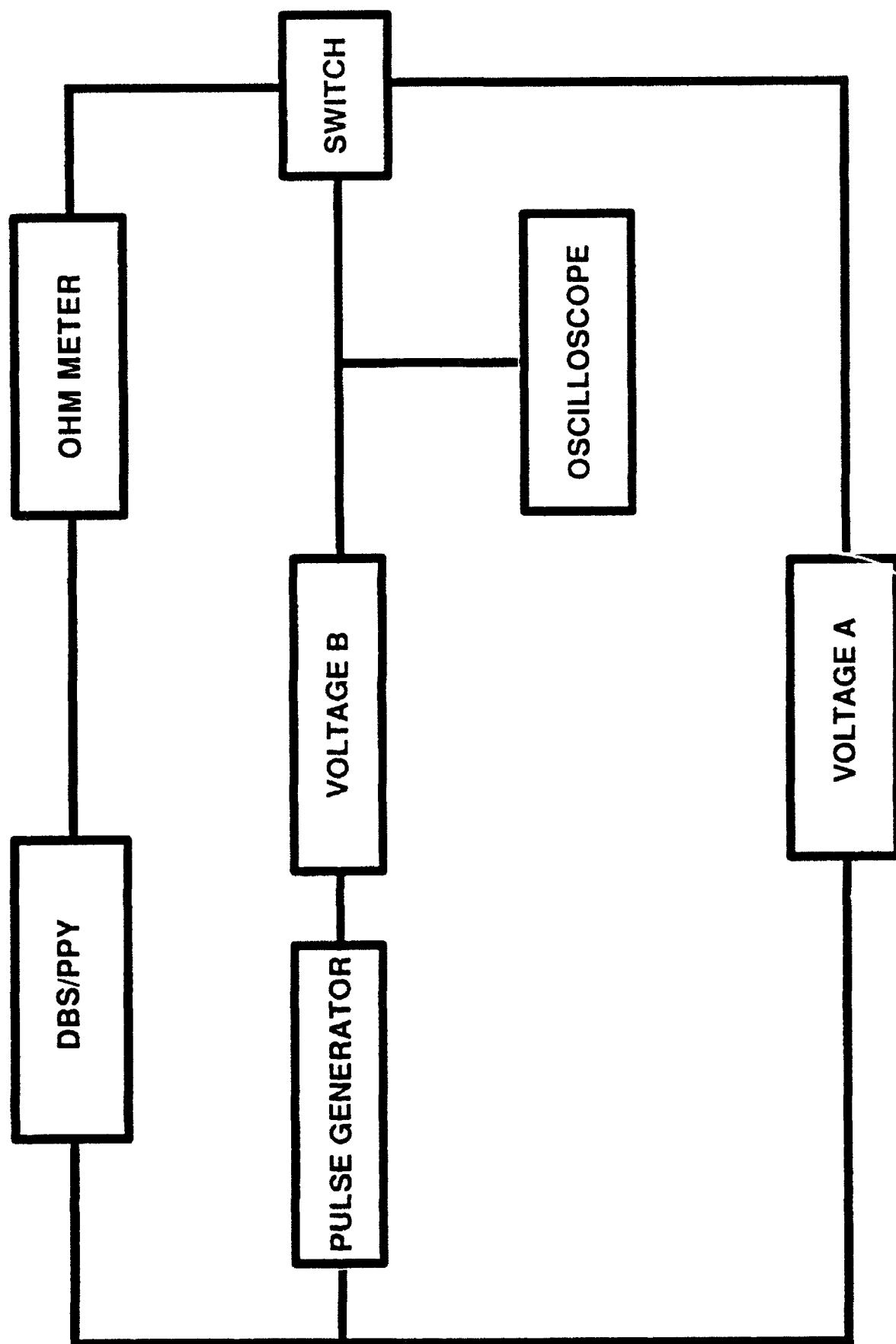
1. M. G. Kanatzidis, "Conductive Polymers," Chemical and Engineering News, Dec. 3, 1990.
2. D. DiStefano, "Conducting Polymers for Thermoplastic Electrodes," JPL Task Plan No. 80-3201, Air Force Armament Laboratory, August 1991.
3. Same as above
4. D. Finello, "Solid Laminated Double Layer Capacitor," AFATL-TR-90-72, Air Force Armament Laboratory, July 1990.
5. R. K. Bunting, "Interpenetrating Polymer Network Capacitors," WL-TR-92-7009, Air Force Armament Laboratory, Feb. 1992.
6. L.F. Warren and D.P. Anderson, "Polypyrrole Films from Aqueous Electrolytes," J. Electrochem. Soc., **134**, 101 (1987).
7. J. O. Laakso, Acta Poly. Scand., (Chem. Tech. & Metal. Series No. 184), Helsinki 1988, 48 pp.
8. J.R. Reynolds, "Advances in the Chemistry of Conducting Organic Polymers: A Review J. of Molecular Electronics, Vol. 2, pp 1-21 (1986).

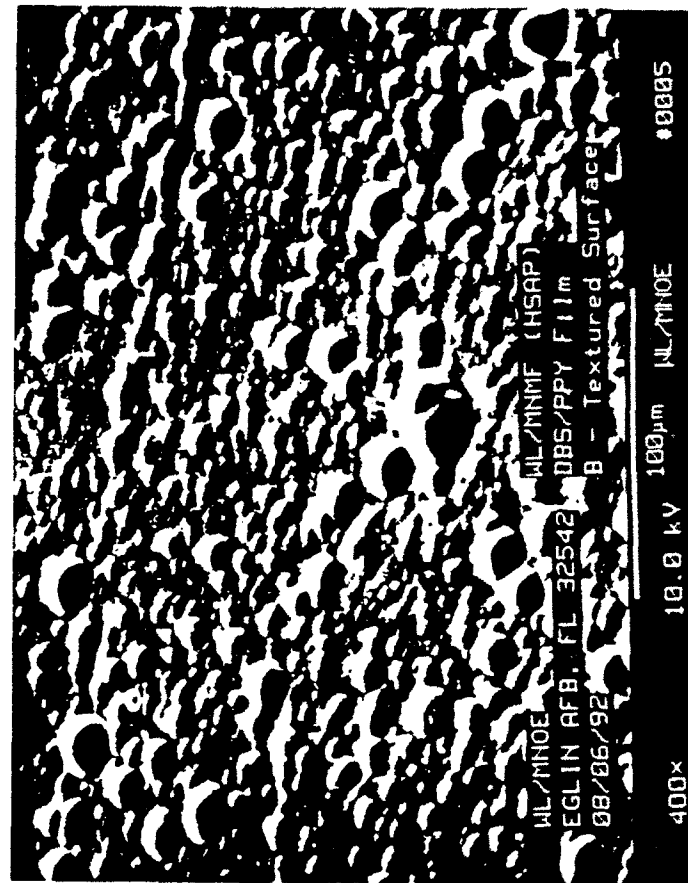
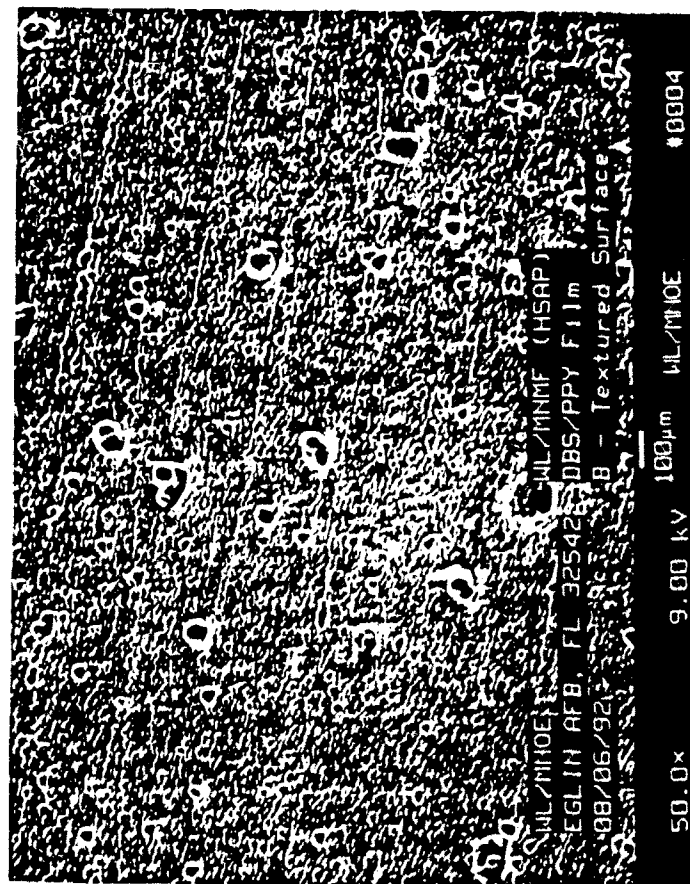
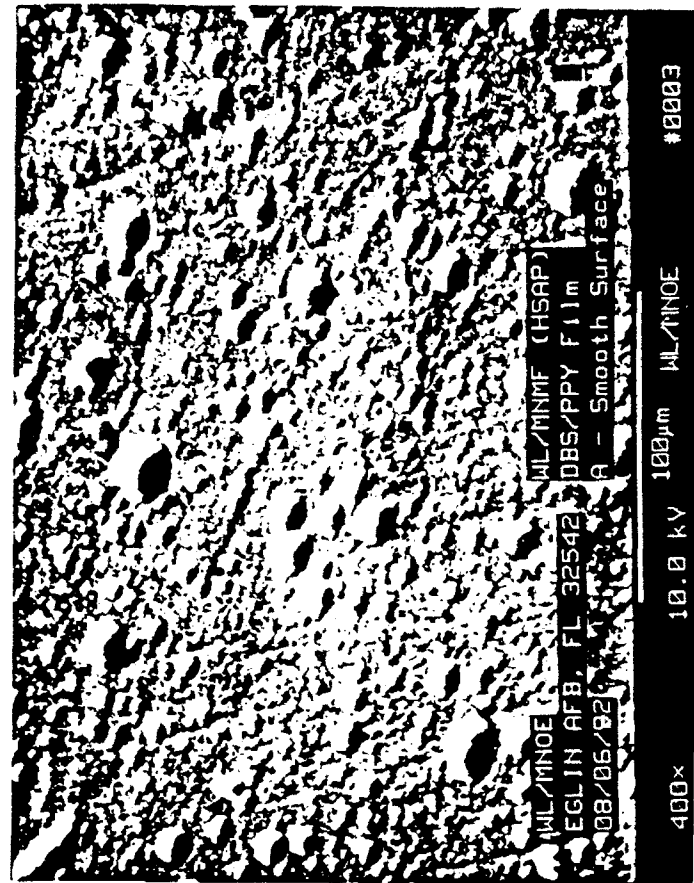
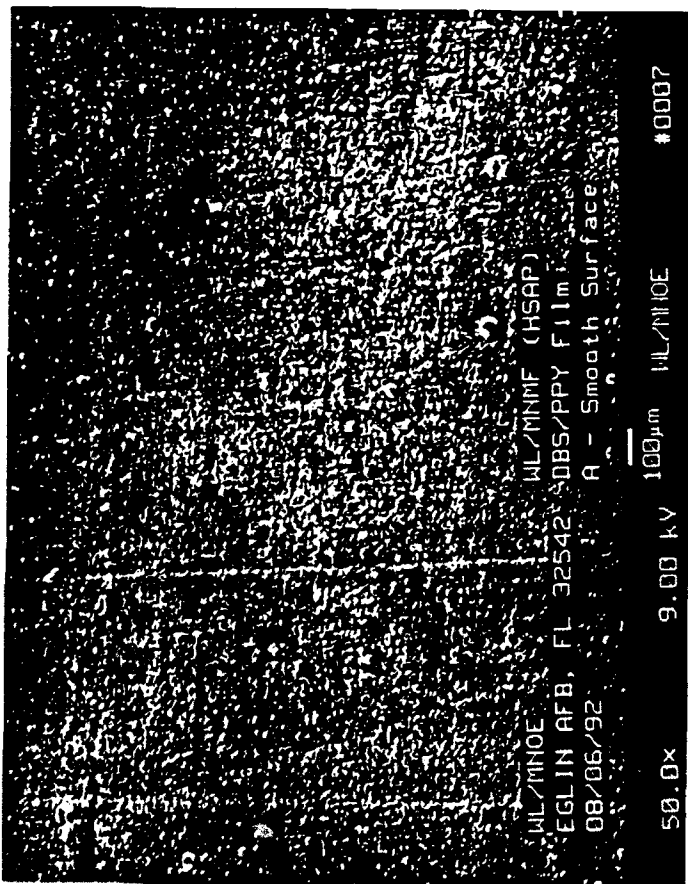


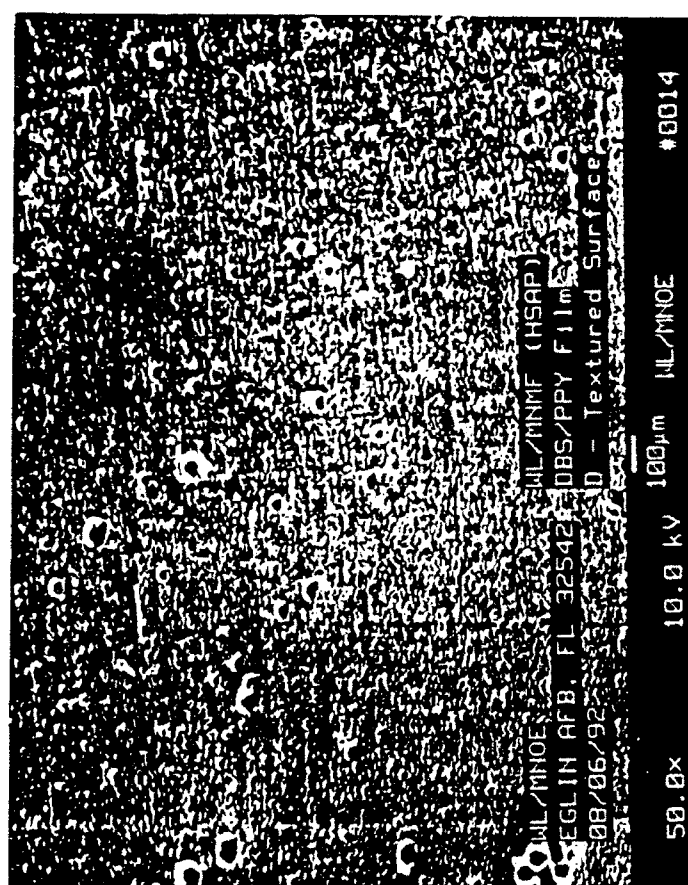
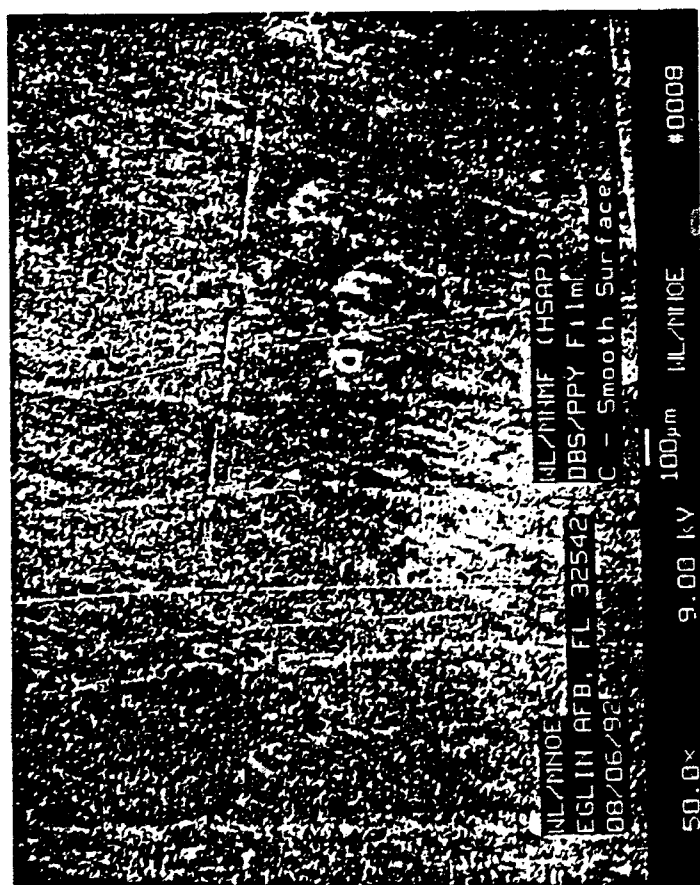
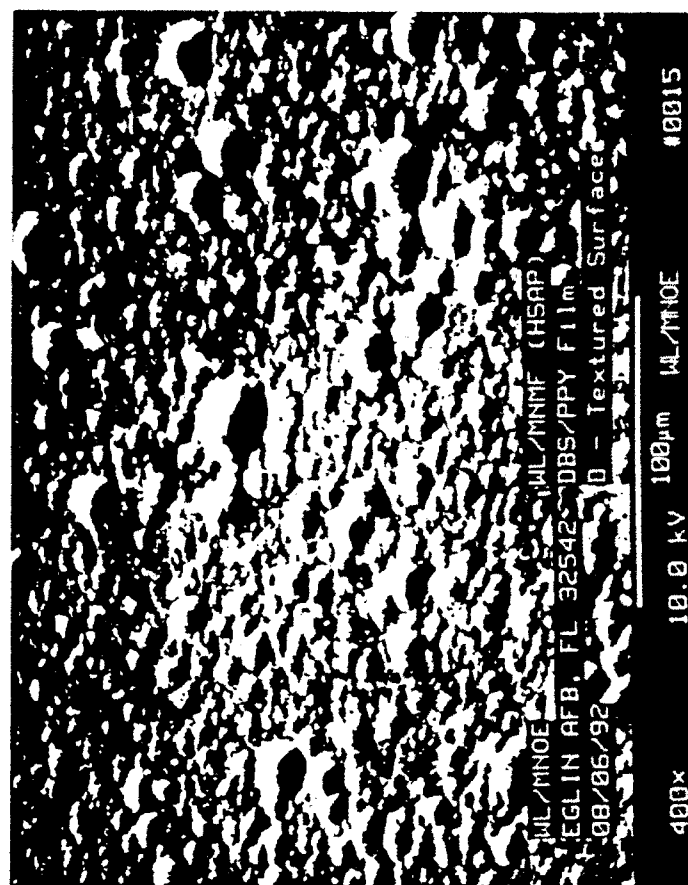
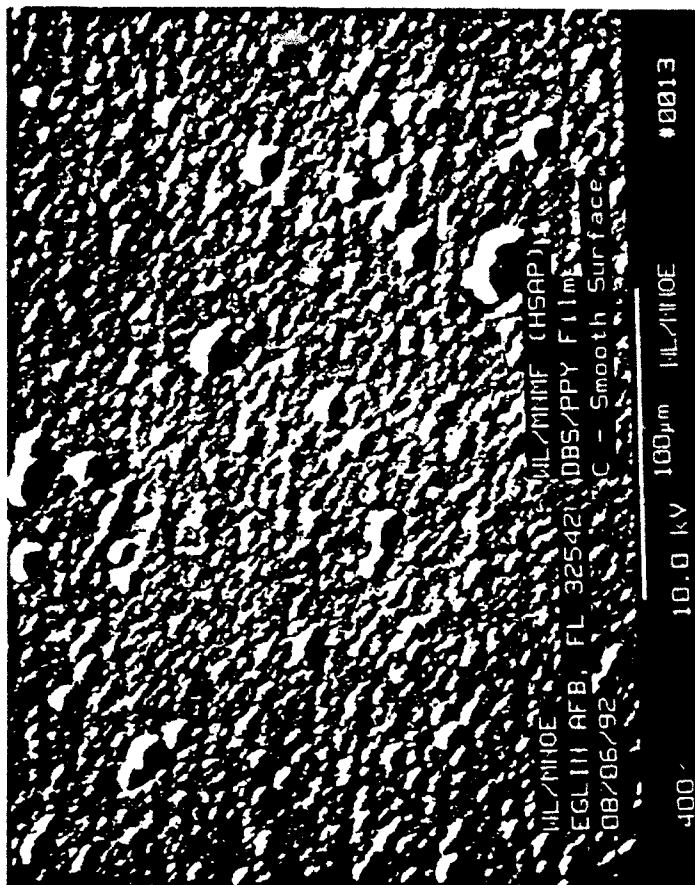
Chemical structure of polypyrrole PPY with dodecylbenzenesulfonate DBS counterion

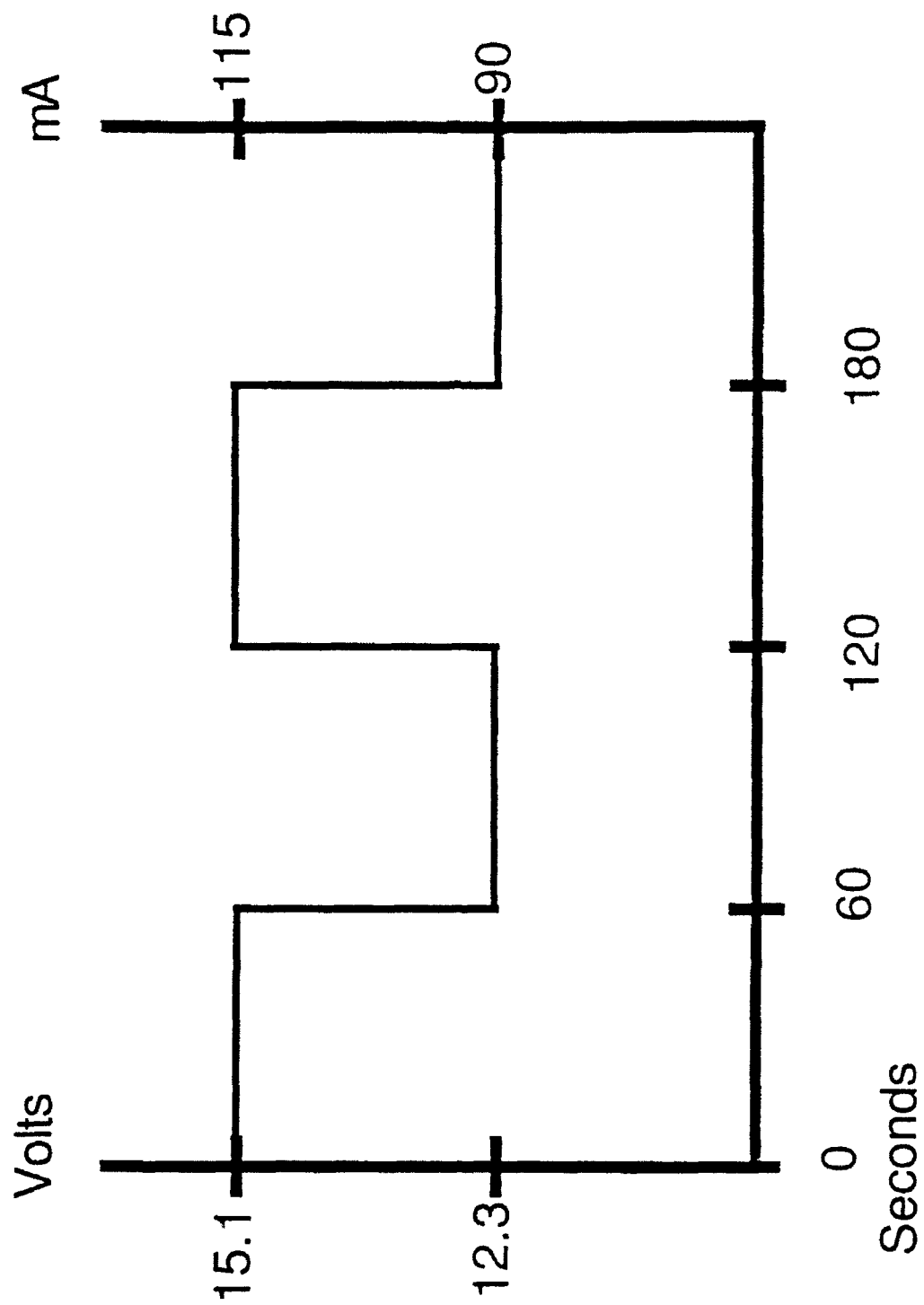


Proposed disordered structural model for polypyrrole

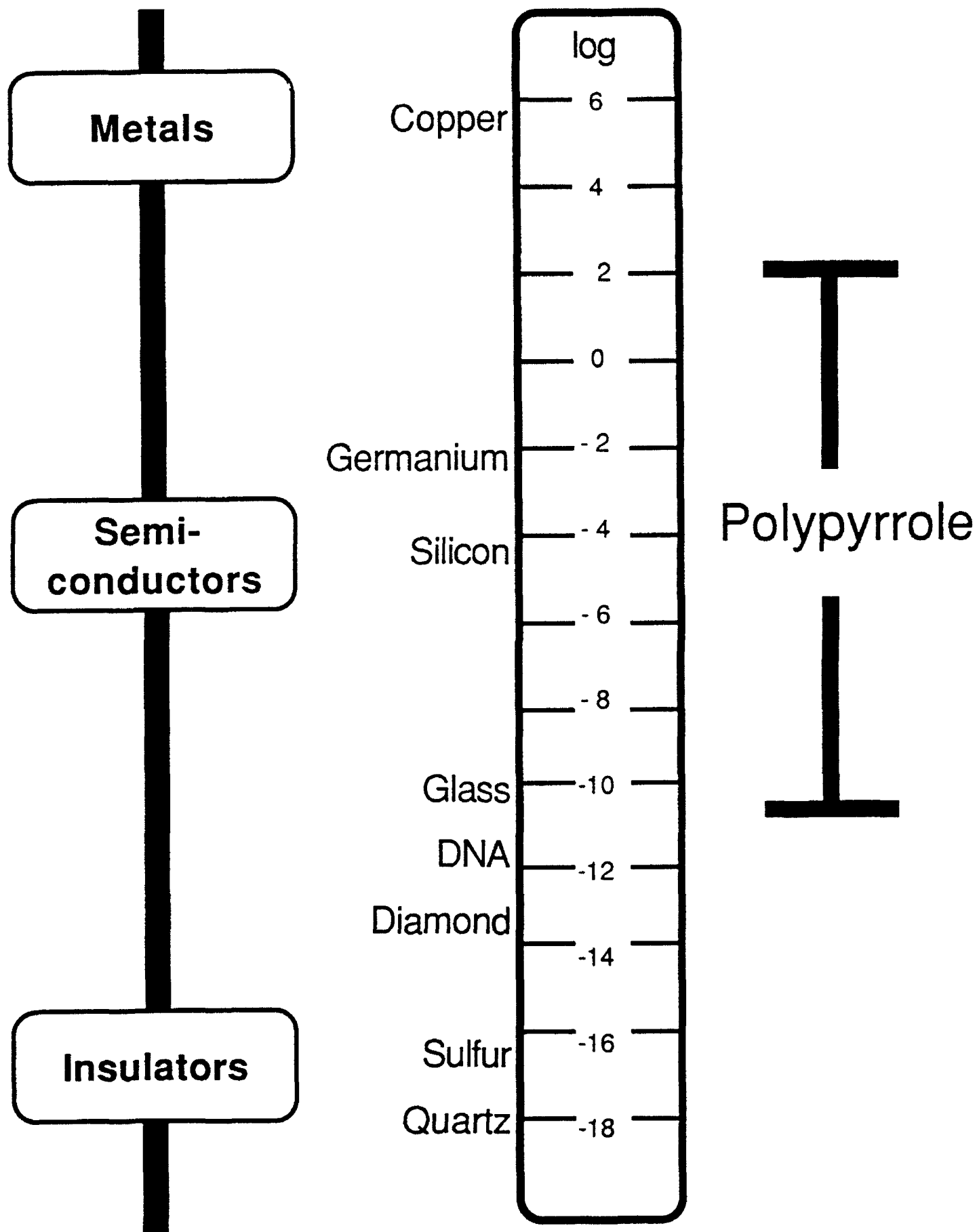












**A STUDY OF THE FRAGMENTATION OF GRAPHITE/EPOXY  
PANELS UNDER HIGH VELOCITY IMPACT**

**Steven R. Hart**

**West Carrollton Senior High School  
5833 Student Street  
West Carrollton, Ohio 45449**

**Final Report for:  
Summer Research Program  
Wright Laboratory  
Flight Dynamics Directorate  
Vehicle Subsystems Division  
Survivability Enhancement Branch**

**Sponsored by:  
Air Force Office of Scientific Research**

**August 1992**

**A STUDY OF THE FRAGMENTATION OF GRAPHITE/EPOXY  
PANELS UNDER HIGH VELOCITY IMPACT**

Steven R. Hart  
West Carrollton Senior High School  
5833 Student Street  
West Carrollton, Ohio 45449

Abstract

The fragmentation characteristics of unidirectional composite panels was studied. The composite panels were impacted at a range of high velocities with half inch diameter steel spheres to cause fragmentation. The fragments were collected and later analyzed. Results from this analyzation were then used to establish a quantitative description of the fragmentation characteristics of the composite panels. Specifically, the size distribution of the fragments and the mean fragment size.

# **A STUDY OF THE FRAGMENTATION OF GRAPHITE/EPOXY PANELS UNDER HIGH VELOCITY IMPACT**

Steven R. Hart

## **INTRODUCTION**

Research on the quantitative description of fragmentation characteristics is not a new area of study. However, this type of research pertaining specifically to composite panels has never before been done. The experimental portion of this research includes the impacting of composite panels, the collection of the fragments created by this impacting and, the calculating of the velocity of the projectile before and after impact with the panel. The overall goal of this research, in general, is to understand the energy partitioning of composite panels or in other words, to ascertain the amount of energy lost by the projectile after impact and absorbed by the panel that goes into the damage of the composite panel. When energy is transferred from projectile to panel on impact, four types of damage occur, delamination, matrix cracking, fiber breaking, and fragmentation. However, this particular study is only concerned with damage from fragmentation. The analytical side of the study includes the collection and reduction of data for the use of drawing conclusions about patterns in fragmentation in the areas of size distribution of fragments and the mean fragment size. The utilization of unidirectional composite panels rather than multidirectional panels and steel spheres rather than actual ammunition is made to simplify the experiment.

## EXPERIMENTAL

### METHODOLOGY

The following is a description of the test setup used in this experiment. A schematic illustration is also provided to help visualize the testing procedure (Figure 1).

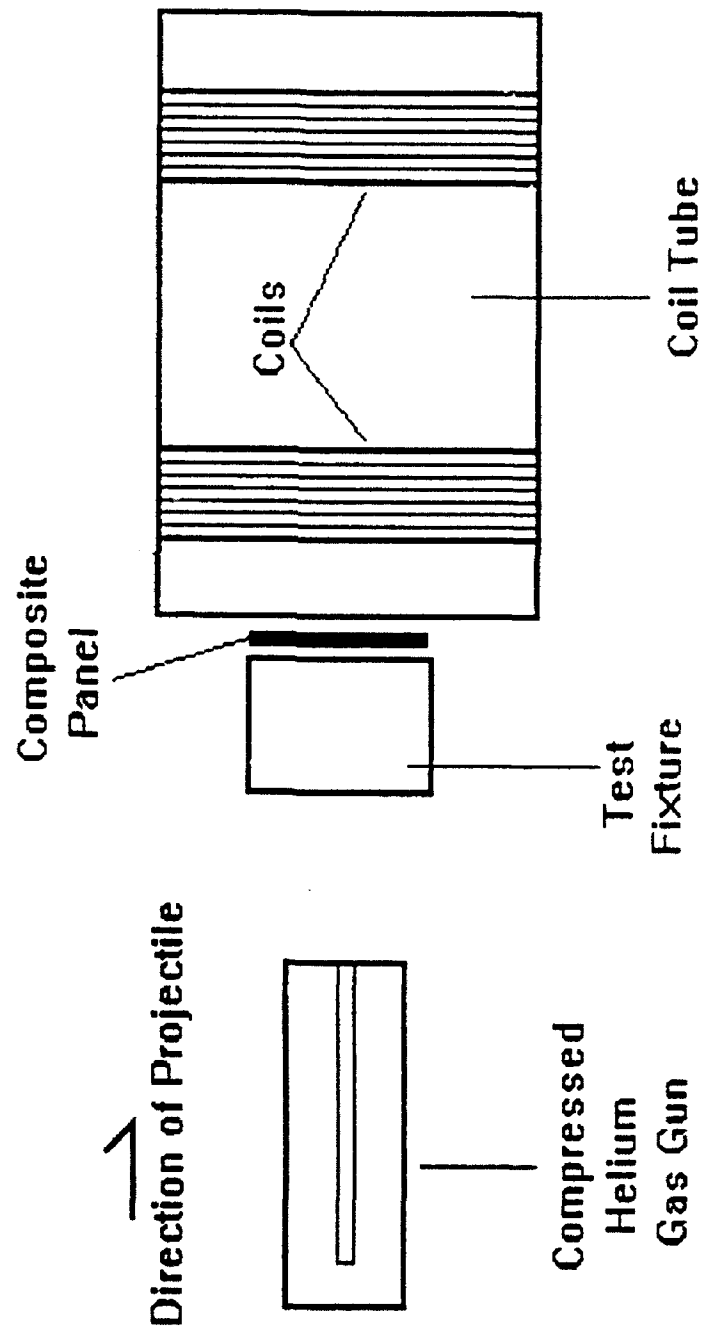
A half inch diameter steel sphere is fired at a predetermined velocity from a compressed helium gas gun. The projectile then passes through the test fixture and impacts the graphite epoxy panel which is composed of eight, sixteen, or thirty-two unidirectional lamina. (To see a combination of velocities and ply thicknesses, refer to Table 1a). In turn, this causes fragmentation of the composite panel.

Table 1a

Test I.D.	No. Plies	Init.Vel. (fps)	Res. Vel. (fps)	Proj. Wt. (grams)	Mass Loss (grams)
1	32	533.2	265.7	8.6080	6.2581
2	16	530.1	350.9	8.5935	3.4892
3	16	4122.1	3829.1	-----	0.8456
4	8	4088.6	3870.6	8.4724	0.3578
5	8	533.2	440.9	8.5516	1.5605
6	16	1993.5	1862.2	8.5295	1.0758
7	32	1985.8	1821.5	-----	1.5769
8	32	4113.7	3687.2	-----	1.8809

The fragments are collected with a special type of paper that has an adhesive applied to one side. Three individual pieces of the adhesive paper are placed in different positions along the

Figure 1  
Test Setup



test setup. The first piece of the paper, approximately 12"x21", is rolled into the shape of a cylinder (open at both ends). This cylinder is then placed inside the test fixture and therefore, directly in front of the panel to the gun side. Any fragments exiting the panel toward the gun after impact of the projectile will be caught by this paper. The second paper, approximately 48"x49", is again made into an open cylinder. However, this piece is placed in the coil tube directly behind the test fixture that holds the epoxy panel to be impacted. The responsibility of this piece of adhesive is that of apprehending the majority of the fragments that escape from the rear of the panel or the side opposite of the gun. A final 18"x18" square of the adhesive paper is then fixed to the posterior end of the coil tube. This paper prevents any fragments that would have otherwise exited from the end of the coil tube entirely.

The conclusive step in the fragmentation collection process is the removal of the used adhesive paper from the various locations along the test setup. Later an analysis is performed on the adhesive paper to compile data pertaining to the fragments. This process will be explained later within the analytical section.

Velocity is an important component in the analysis of the data and also in determining the validity of the results and the conclusions that are made utilizing these results. Therefore, great care is taken in the calculation of the velocity before the projectile impacts the panel, or initial velocity, and the velocity of the projectile after exiting the composite panel, or residual velocity.

To measure the initial velocity, a wire or small piece of graphite is placed across the opening of the barrel of the gun, and likewise, the same is done at the opening to the test fixture. When the projectile is fired, the wires are broken as the projectile quickly makes its way downrange. At the breaking of each wire, a signal is sent to a high speed digital oscilloscope (KONTRON). Then the KONTRON is used to determine the time between the breakage of the two wires. After this is established, the initial velocity can be calculated using the distance between the breakwires, with the time between breakage in the formula,  $V=s/t$ .

The residual velocity can be determined utilizing two different methods. The first method uses the coils that are wrapped around the coil tube in relation with the KONTRON to calculate a velocity. The coils create two separate magnetic fields within the coil tube. When the steel ball passes through each field, it causes a disturbance in the field that sends a signal to the KONTRON. Using the difference in the time between disturbances, along with the distance separating the coils, a residual velocity can be calculated using the formula,  $V=s/t$ .

The second method of acquiring the residual velocity, makes use of break papers. These are papers that have a continuous line of silver ink that almost cover them but do not overlap. Each of the two papers is then connected to a circuit. When the steel ball breaks through the each paper, it sends a signal to the KONTRON. The difference in time between these two signals is then used with the distance between the papers to calculate residual velocity using the formula,  $V=s/t$ .

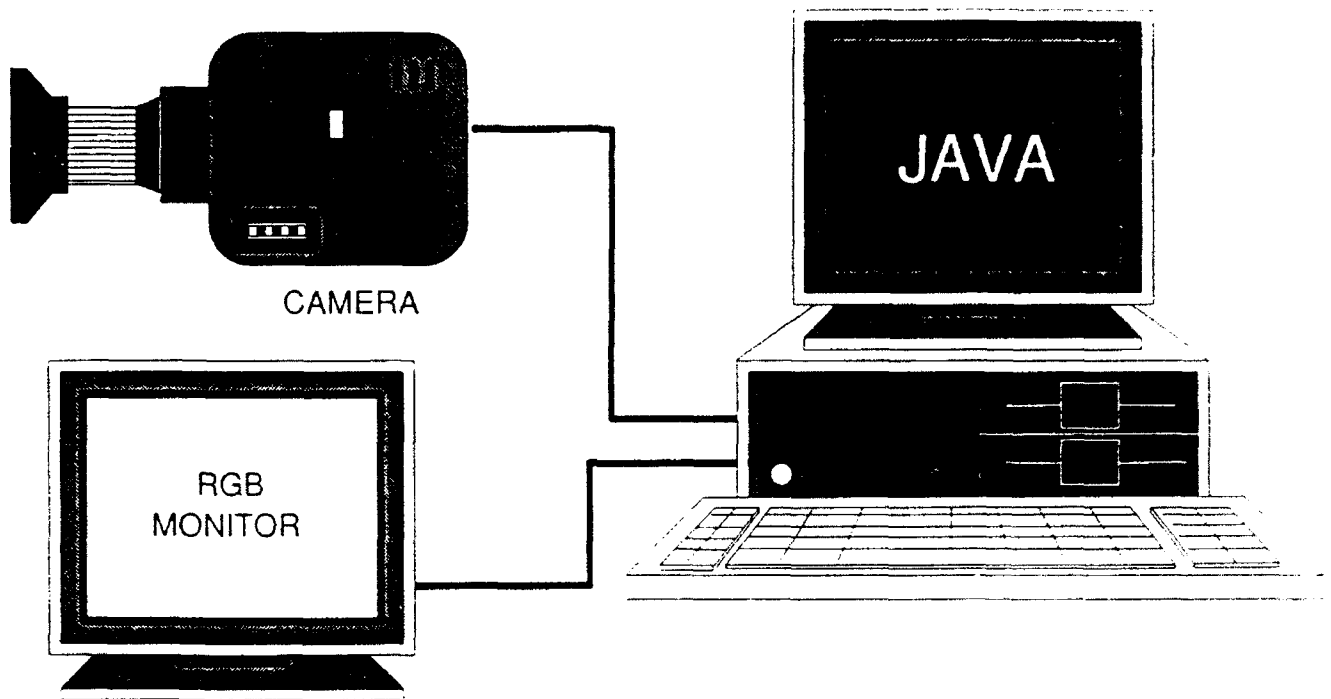


## ANALYTICAL

### METHODOLOGY

The collection adhesive papers that were used in the earlier experimental portion are now cut into equal sections either 2"x3" or 3"x4". Next the sections are analyzed individually utilizing the JAVA (Jandel Video Analysis software) system (Figure 2). This step includes many different procedures. First a specimen is placed under the video camera and an image of this is displayed on the high resolution monitor. After capturing the image on the monitor, a series of steps must be taken in order to maximize the accuracy of the data compilation. This includes the counting and measuring of all of the fragments on an individual specimen. The first step once the image is frozen is to apply a clearfield to the image. The purpose of this step is to compensate for uneven lighting across an image. Next, the contrast enhancement is used to help separate the dark fragments from the lighter background. Following this step, the image is cleaned up using the paint feature to separate overlapping objects and to remove unwanted dirt and smudges from the specimen. Intensity levels are then set using the threshold feature of the system. Finally, using the count feature, the fragments are counted and measured. After the fragmentation data is transferred to disks, reduction of the data is begun to ease the analyzation process.

Figure 2  
JAVA (Jandel Video Analysis Software)



### CONCLUSIONS

Due to restrictions on time, only the first two shots have been analyzed (see Table 1a). However, this analysis has produced many encouraging pathways from which to speculate. Within the introduction, the statement was made that when a transfer of energy occurs from a projectile to a panel upon impact, the energy absorbed by the panel goes toward four types of damage. These types are delamination, matrix cracking, fiber breaking, and fragmentation. From the data that has been analyzed, panel #1 (Table 1a), which is thirty-two (32) plies thick and therefore twice as thick as panel #2 (Table 1a), absorbed only twenty-six

percent (26%) more energy than panel #2, while almost twice as many fragments were created upon impact of the projectile (24,066 fragments from panel #1 as opposed to only 12,367 fragments for panel #2). However, the total projected area of the fragments generated from panel #1 ( $28.572\text{in}^2$ ) is only about nineteen percent (19%) greater than that of panel #2 ( $23.231\text{in}^2$ ). This results in a smaller average fragment size for the first panel than for the second which suggests that a greater percentage of the energy absorbed by panel #1 is spent in the creation of fragments.

Figure 3 displays the size distribution of fragments from both tests, where  $n(s)$  is the percent of fragments in the size increment  $s=2^i \times 10^{-4}\text{in}^2$ ,  $i=1,2,3,\dots$ . The data is plotted in this manner to reduce statistical fluctuations. In both cases, it can be seen that over ninety-nine and one half percent (99.5%) of the total amount of fragments created are less than one-tenth of one square inch ( $0.10\text{in}^2$ ). This leads us to believe that fragments larger than one tenth of one square inch are created only by the last one or two plies as a result of some type of peeling process that takes place upon impact of the projectile, and that the large majority of the fragments, those smaller than one tenth of one square inch ( $0.10\text{in}^2$ ), originate from of the hole created by the projectile upon impact, and therefore, these fragments are a combination of all of the plies.

Figure 4 shows the same data plotted for  $s < 0.10\text{in}^2$ . This graph displays the inverse relationship between the size of the fragments and the number that are created for that size. The graph

also suggests that the greater the thickness of the panel, the more small fragments are created.

Figure 3

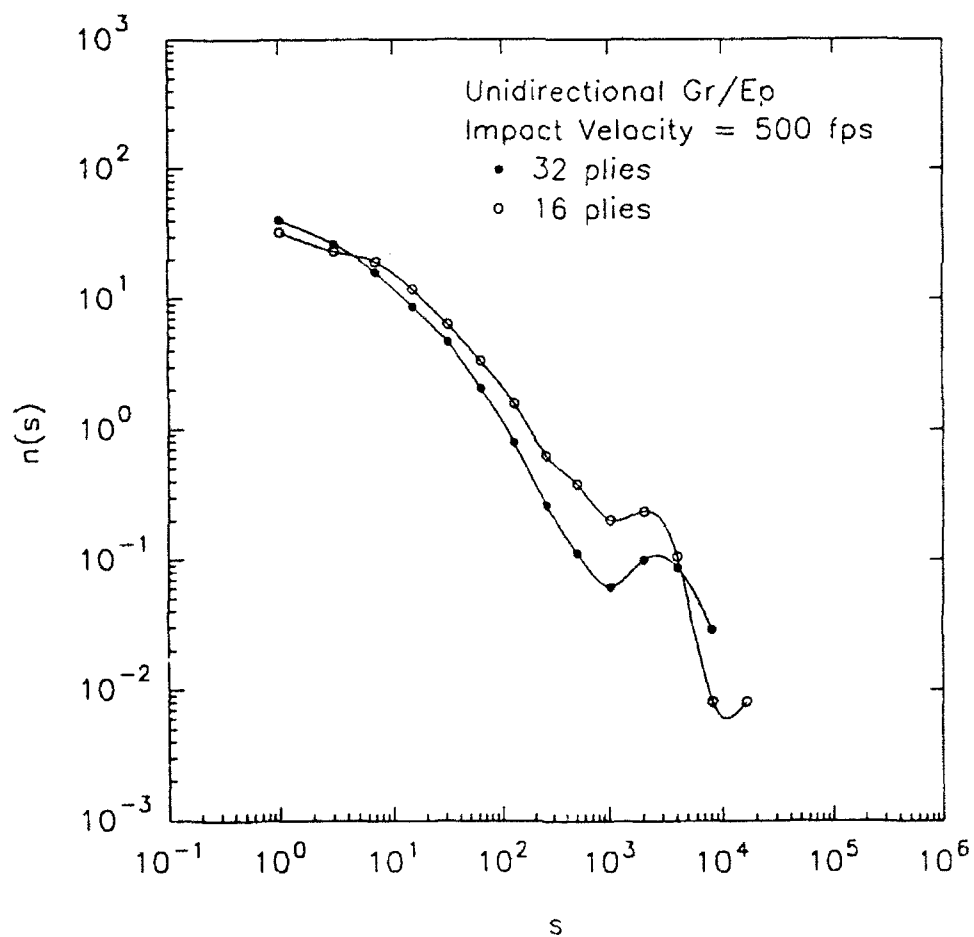
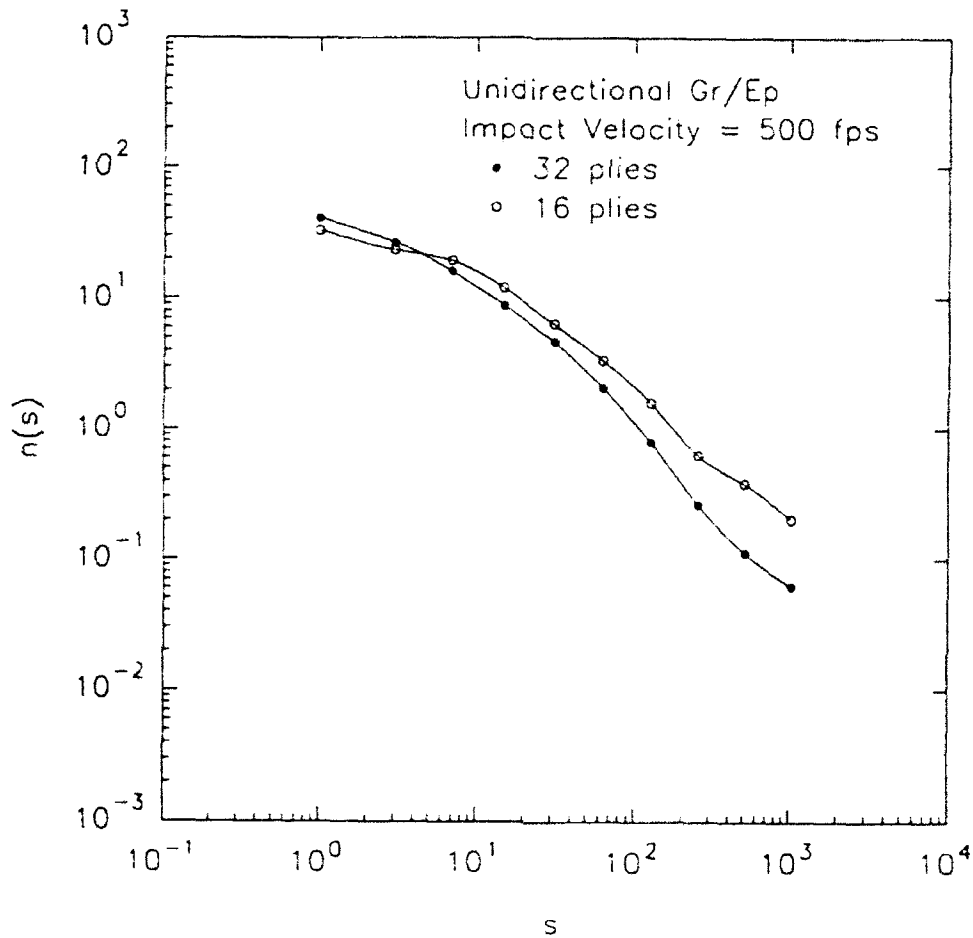


Figure 4



ACKNOWLEDGEMENTS

For the past eight weeks, I have worked at the WL/FIVS branch at Wright Patterson Air Force Base. However, in many ways, my time spent these past few weeks has been more of a learning experience than a form of summer employment. There are many individuals to whom I am grateful for making the experience possible and also for

allowing me to participate in the research done at this branch. I would first like to thank my mentor, Larry Coulthard for the time he has invested into the High School Apprenticeship Program (HSAP). I would also like to thank Mark Morgan, John Lair, and Mohammed Samad for allowing me to be a part of the data collection of their individual projects. Finally, I would like to express my sincere gratitude to Kristina Pawlikowski for making me part of her individual research, about which this paper is written.

A STUDY OF AN UNBALANCED  
SHAFT DUE TO OIL LEAKAGE

DAVID B. HARTSOCK

STUDENT

BELLBROOK HIGH SCHOOL

BELLBROOK HIGH SCHOOL  
3491 UPPER BELLBROOK RD  
BELLBROOK OH 45305

FINAL REPORT FOR:  
SUMMER RESEARCH PROGRAM  
COMPRESSOR RESEARCH FACILITY

SPONSORED BY:  
AIR FORCE OFFICE OF SCIENTIFIC RESEARCH WRIGHT PATTERSON AIR  
FORCE BASE, DAYTON OH

JULY 1992

A STUDY OF AN UNBALANCED  
SHAFT DUE TO OIL LEAKAGE

DAVID B. HARTSOCK  
STUDENT  
BELLBROOK HIGH SCHOOL

ABSTRACT

At the Compressor Research Facility fans to be used in jet engines are tested. On May 11, 1992 oil from a PRATT & WHITNEY test article leaked into the jackshaft which runs the compressor, which powers the test article. This oil sat in the bottom of a coupling that is connected to the jackshaft. Eventually, enough oil collected in the coupling that it caused uneven rotations of the shaft. This unbalance of the shaft caused the shaft to vibrate while rotating. Due to the vibration, the seals surrounding the shaft were broken. No major damage was done to the shaft or the test article. Fortunately the engine was shut down before any serious damage could occur.



A STUDY OF AN UNBALANCED  
SHAFT DUE TO OIL LEAKAGE

DAVID B. HARTSOCK

INTRODUCTION

The Aero Propulsion and Power Directorate's Compressor Research Facility (CRF) was constructed and is operated to provide detailed evaluations of fans and compressors for gas turbine engines. Through the CRF, the Air Force can independently evaluate full-scale, multi-stage, single-spool fans and compressors under operating conditions similar to actual flight. The CRF is capable of evaluating most of the fans/compressors currently in the Air Force inventory or anticipated as a future development item. Since becoming fully operational in 1984, the CRF has been used to investigate aerodynamic and mechanical performance of many compressor configurations. Research into high stageloading in both straight and swept blades have been performed with several rotor designs. Detailed inner blade flow field analysis has been performed with Laser Transmit Anemometry on an advanced fan design. Also, performance characteristics of a prototype Advanced Tactical

Fighter engine fan have been obtained by the use of the CRF.

#### DRIVE SYSTEM

The drive-system at the CRF is what is used to power the compressor and the fans that are being tested. The fan makes a substantial contribution to the total thrust. It accelerates the air passing through it. In a jet engine, the drive-shaft that runs the compressor is greatly reduced. The drive-system at the CRF consist of five major components: the jackshaft, the high speed gearbox, the low speed gearbox, the high speed motor, and the low speed motor, so that the CRF can produce the desired power or speed that is needed to satisfy the test article. The high speed motor has 30,000 horse-power and can be run up to 30,000 RPM. Since the high speed motor can reach such a high RPM, it allows the motor to run at high speeds. The low speed motor also has a 30,000 horse-power engine, but is geared very low and is only capable of running at 17,000 RPM. Running at a maximum of 17,000 RPM, the low speed motor can obviously not run at high speeds, but is capable of producing considerably more power than the high speed motor. The low speed gearbox is a permanent 65,000 pound gearbox that is more than twice the size of high speed gearboxes. The low speed gearbox runs at lower speeds but has a higher voltage capacity than the high speed

gearbox. There are three interchangeable high speed gearboxes, a 25,000 pound, a 27,000 pound, and a 29,000 pound gearbox. These gearboxes have a lower voltage capacity, but can run at faster speeds. The gearbox rotates the jackshaft. The jackshaft is responsible for running the compressor in a test article. Whoever owns the test article has to supply their own compressor for the test. The fan that is being tested is directly run by the compressor. The test article (fan) is installed in the test chamber, and is driven from one of the two rear motors. Air enters through the inlet filter house, which is directly in front of the test chamber, and passes through the test article. The air then exits the test article through the fan discharge systems and then exhaust to the atmosphere through the discharge stack. Data for the testing is acquired in the signal conditioning room. It is then processed by equipment in the computer room and displayed into graphical form in the control room.

#### OIL LEAKAGE

The CRF received the PRATT & WHITNEY test article on November 12, 1991. It took about five months to install the article and prepare it for testing. After getting through a lot of minor problems the CRF began testing, they made their first

run on March 26, 1992. Everything was going smoothly the first month of testing other than some minor errors that were coming up at times. On the second shift of the evening Monday May 11, 1992 a major problem arose while testing. The computers in the control room began picking up heavy vibration signals. The vibrations were so high that the computer called for an automatic shut down. The vibration problems of the shaft appeared to be very serious. No one seemed to know what the problem could be, and without finding the cause of the vibration the CRF testing would have to be put on hold for an indefinite amount of time.

The probable problem was found when they were taking the jackshaft apart. When it was taken apart to be looked at, traces of oil were found in it. When the coupling on the end of the jackshaft was taken off, about one quart of oil poured out. It was a good probability that it was the excess oil causing the vibrations of the shaft, so the next step was to find out where the excess oil had come from. Samples of the oil were taken to be examined. By examining the oil, they found that the oil was 7808 oil, 7808 was the oil that was in the slipring. By knowing where the oil came from, they could solve their problem by just fixing the slipring. After studying the slipring they found that there was no easy way of temporarily fixing the slipring. So instead delaying the testing for a long period of time, they

simply decided to remove the slipring altogether from the test. Although not all data could be acquired without the slipring they were still able to complete the testing of the fan for PRATT & WHITNEY. The vibration of the shaft didn't cause any serious damage to the test article or the shaft because the drive motor was shut down in time. The vibration of the shaft did cause some minor damage directly around it. The five bearings were thoroughly inspected by the engineer in charge of the drive-system. After inspecting the bearings, it was concluded that the vibrations had done nothing to the bearings. The labyrinth seal, which is used to keep the oil from leaking, was ruined because of the vibration. The labyrinth seal was not fixable and a replacement was needed in order to get the jackshaft in its original condition to continue the testing.

#### PROJECT

The project was my major priority while working at the CRF this summer. My mentor and I simulated the oil leakage problem that had happened on May 11<sup>th</sup> to the Pratt & Whitney test article. My mentor is the engineer who is in charge of the drive system, so he had all of the information about the test that was needed. There were a couple things hoped to be accomplished by the simulated testing. When looking back at the tape of the

May 11<sup>th</sup> testing, we found that someone had taped over all of the taping of that day. Without that tape the CRF has no record or data from the oil leakage test. By simulating the test we hoped to receive accurate data so that the CRF would have some type of data on oil leakage into the jackshaft. We hoped to figure out when or how the oil got in the coupling. Whether it was a massive dumping from the slipring, or was it a very gradual process where the oil leaked so slow that it was unnoticeable until enough oil buildup in the bottom of the coupling. We also wanted to get an accurate account as to how much oil it would take to cause the shaft to vibrate, and at what RPM and mass would the vibrations get worse.

#### EXPERIMENT

When doing the experiment we used all of the same equipment that we could. We had to order a new coupling for the jackshaft, but we did use the same jackshaft, gearbox, and motor. We simplified the experiment by taking off everything between the coupling and the end of the test article. We simplified the experiment so that we could still get accurate results, but without taking the chance of having more problems and technicalities by using unneeded parts. We added the amount of oil we wanted directly into the coupling rather than going to the

trouble of putting on a slipring and then making the slipring leak the oil into the coupling. Also by removing some of the unneeded articles we cause less wear and tear on the jackshaft. When the runs are being done, we aren't going to be running at the high RPM's that the test article was run at. We also will not add as much oil to the coupling as was found during the testing. Due to these circumstances we will not get the exact results as it happened during the test, but they should be similar, just on a smaller scale. If we were to run at the high speeds and with high amounts of oil in the coupling we would run the risk of tearing up something in the jackshaft.

#### DATA

When we did our no-load runs in our experiments we ran at four different speeds. The minimum speed was 6,540 RPM; the other speeds were 8,000 RPM, 10,000 RPM, and the highest we ran was at 12,000 RPM. We did ten runs before coming up with our final results.

RUN #1: This was our first no-load run that was done. There was no oil put in the coupling on this run. We needed a run without oil so that when the oil is in the coupling we would be able to tell when there is a change in the vibration levels.

Our first run went very smoothly, we have the coupling attached and we came up with very low vibration levels at our four trial speeds.

RUN #2: On our second run was also with no oil in the coupling. A bolt was taken out of the coupling for this run. The bolt that was taken out weighed 13.74 grams. The reason for doing a run with a bolt taken out of the coupling is to get a feel for the sensitivity of the system. We only got to run this at our minimum speed because of the high vibration level we received at minimum speed.

RUN #3: We had no idea of how much oil we needed to put in the coupling to get our results so on our first run with oil in the coupling we added one-half an ounce. We received basically the same vibration levels as our first run, meaning that the oil had no effect on the shaft.

RUN #4: After having no results in run #3 another one-half ounce of oil was added to the coupling. Again the oil had no effect on the vibration of the shaft.

RUN #5: For this run we added one full ounce rather than just a half oz., hoping to get some results with 2 ounces of oil



in the coupling. At this point in the testing we were having no luck at all in seeing any type of vibrations. After having done three runs with oil in the coupling, I made the prediction that the oil would never have an effect on the vibration of the shaft. When the test was going on for Pratt & Whitney, the oil was leaking into the coupling while the shaft was moving at high RPM's. We were adding the oil to the coupling while everything was shut down. For this reason I thought the oil was just moving around the shaft evenly and not causing an unbalance.

RUN #6: Since my prediction was just another guess of what would happen we added another ounce of oil to the coupling. Again the oil had no effect on the vibration of the shaft.

RUN #7: We added a fourth ounce of oil to the coupling, and we still received the same vibration levels as the earlier runs. At this point we began raising and lowering the speed very quickly. We hoped that by doing that we would slosh the oil around in the coupling and maybe receive some signs of vibration.

RUN #8: Again one ounce of oil was added to the coupling. We received no signs of vibration at first, but on our way up to 10,00 RPM we did get some small vibrations. At 9,763 RPM was our first sign of vibration in our experiment.

RUN #9: On our #9 we added our sixth ounce of oil to the coupling. Again there was no sign of vibration at 6,540 or 8,000. At 10,000 RPM we all of a sudden got high vibrations. The vibration level in bearings three and four more than doubled what they had been in the past. The oil is very unpredictable. After slowing down and going back up to 10,000 RPM where we had our high vibrations, we no longer received any trace of vibrations at the level. Sometimes the oil catches and keeps up with the rotation of the shaft, and sometimes it sloshes around and can't keep up with the shaft which is what causes the vibration. When we increase the speed of the shaft slowly we don't receive any vibration. That's because we're not starting out quick enough for the shaft to go faster than the oil.

RUN #10: We added our seventh and final ounce of oil to the coupling. At 6,540 or 8,000 RPM no vibrations occurred. At 10,000 RPM we received very high vibrations, only four tenths away from any automatic shut down. We went back down to minimum speed and raised quickly to 10,000 RPM. Vibrations absolutely skyrocketed. Bearings 1, 2, and 3 went way over their maximum limit. The computer automatically shut us down.

RUN #	Amount of Oil	VIBRATION LEVELS IN RPM			
		6,540	8,000	10,000	12,000
1	None	2,3	3,1	3,3	3,1
2	Bolt taken out	4,5	---	---	---
3	1/2 oz	2,1	3,1	3,2	3,0
4	1 oz	2,3	3,2	3,1	3,0
5	2 oz	2.2	3.1	3.1	3.0
6	3 oz	2.2	3.2	3.1	2.9
7	4 oz	2.2	3.0	3.0	2.9
8	5 oz	2.4	3.1	---	3.0
9	6 oz	2.4	3.0	4.6	2.9
10	7 oz	2.2	2.9	4.6	---

Throughout the simulated testing there was no change in the vibration levels at 6,540 RPM, 8,000 RPM, or 12,000 RPM. AT 10,000 RPM is where we received all of our vibration levels. There is no specific reason why all the vibrations happened at 10,000 RPM other than the fact that 10,000 RPM seems to be the critical point for this shaft.

This project was not only a good learning experience, but it was also very enjoyable. We accomplished everything we had hoped to accomplished and more. This project not only allowed me to learn about this subject, it also gave me a hands on look at the field I'd like to go into later in life.

INFRARED LASER POLARIMETRY

CHAD HOUGHTON

HIGH SCHOOL APPRENTICE

SEEKER TECHNOLOGY BRANCH

WRIGHT LABORATORY ARMAMENT DIRECTORATE

WL\ MNGS

FINAL REPORT FOR:

HIGH SCHOOL APPRENTICESHIP PROGRAM

WRIGHT LABORATORY ARMAMENT DIRECTORATE

SPONSORED BY:

AIR FORCE OFFICE OF SCIENTIFIC RESEARCH

BOLLING AIR FORCE BASE, WASHINGTON D.C.

AUGUST 1992

## INFRARED LASER POLARIMETRY

CHAD D. HOUGHTON

HIGH SCHOOL APPRENTICE

WRIGHT LABORATORY ARMAMENT DIRECTORATE

WLMNGS

### **ABSTRACT**

A polarimeter is an optical instrument used in testing and calculating various polarization and retardance properties of light and different materials. The field of laser polarimetry has been advanced by improvements made in calibration techniques, alignment, accuracy, as well as the further testing of optical materials. The infrared polarimeter was realigned and recalibrated using enhanced software and a new sample mount was prepared to test the material Gallium Arsenide.

## INFRARED LASER POLARIMETRY

CHAD D. HOUGHTON

HIGH SCHOOL APPRENTICE

WRIGHT LABORATORY ARMAMENT DIRECTORATE

WL\MNCS

# INTRODUCTION

Throughout the last two summers, research in the field of laser polarimetry has been conducted and advanced under the guidance and administration of Dr. Dennis Goldstein who first developed the polarimeter. During my first summer in the High School Apprenticeship Program I built, calibrated, and tested materials in a visible polarimeter which operated with a Helium Neon laser source. Working with two graduate students, I became familiar with the field of laser polarimetry and the calculations involved in data reduction that included Fourier analysis and Mueller calculus. Compiling what I had learned from last summer and the documented work already completed on the polarimeters, I began realigning and recalibrating the infrared polarimeter that operates with a carbon dioxide tunable laser source.

The infrared laser polarimeter was first designed and developed by Dr. Dennis Goldstein and later assembled with the assistance of Mr. David Chenault. The first stages of assembly and development as well as the first tests administered on the polarimeter can be found in Mr. Chenault's final report.<sup>1</sup> A successive series of improvements as well as further data collection was compiled by Mr. Randy Gove and Mr. Randall Hodgson. Follow up research, data collection,

and calibration procedures are documented in Mr. Gove's final report.<sup>4</sup> Until last summer all research on the polarimeters was in conjunction with the infrared polarimeter; my final report to RDL 1991 documents the extent of research and development of the visible polarimeter designed by Dr. Dennis Goldstein.<sup>3</sup> In the time span of my second summer, I have been able to use the experience obtained from working on the visible polarimeter to initiate recalibration and alignment as well as more sample testing on the infrared polarimeter.

Additional information on polarimetry or electrooptic modulator materials can be found in Dr. Goldstein's dissertation.<sup>2</sup> Improvements on the polarimeters are in constant formulation and would improve inconsistent or nonexistent information on potentially good electrooptic modulators. By compiling a list of data on various samples, improvements on these electrooptic modulators would enhance target simulation systems, optical processing systems, image processing systems, and eventually optical computing.

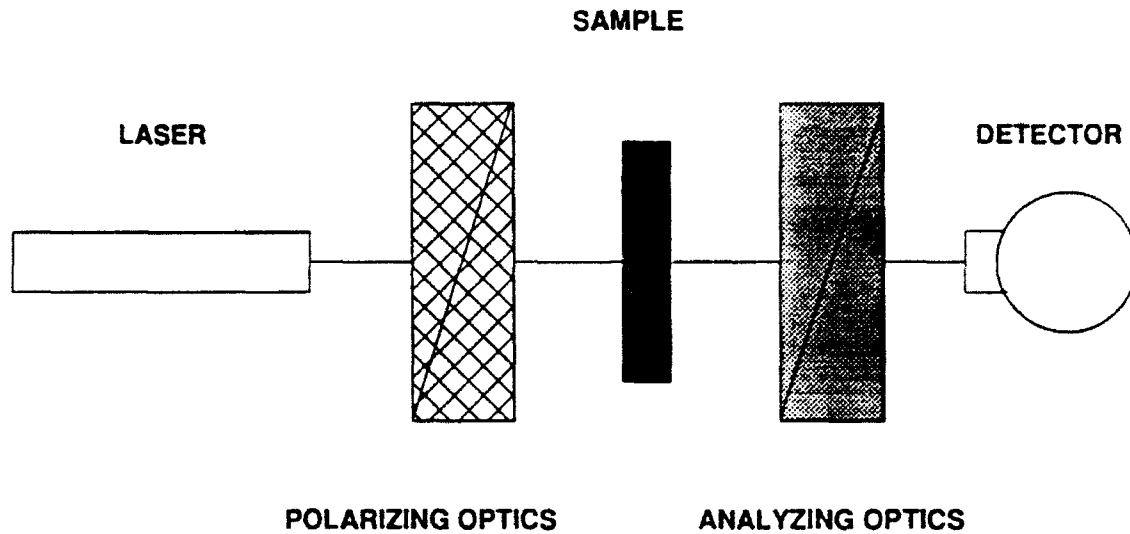
# **BACKGROUND**

A polarimeter is an optical instrument used to test polarizing and retardance properties of light and different materials. The basic fundamental approach of the polarimeter operates on the idea that if the behavior of the source light is known then the polarization change produced by inserting a sample into the polarimeter may be determined. The results obtained from the polarimeter are expressed by a mathematical formulation that uses Mueller calculus. In Mueller calculus a four-element column vector called the Stoke's vector represents the polarized light beam of the source; the emerging beam from the polarimeter is also expressed by a Stoke's vector. The result of a mathematical comparison between these two vectors is a four-by-four matrix called the Mueller matrix which contains information about properties of the light and the material tested in the polarimeter.

As an effective tool of analysis the polarimeter functions to test certain samples for material and electrooptic properties. To test the sample, a source beam is passed through the sample and measurements are taken to determine the properties of the emerging light. Using the Mueller calculus, a Mueller matrix for the sample can be found. The principle of the polarimeter rests on the idea that a beam of known properties can be propagated through a sample and into a detection device that will produce results which can then be compared to the those properties of the original beam. The actual basis for the system is a set of dual rotating retarders that the beam must travel through. In Figure 1 a block diagram explains the components of the polarimeter system.



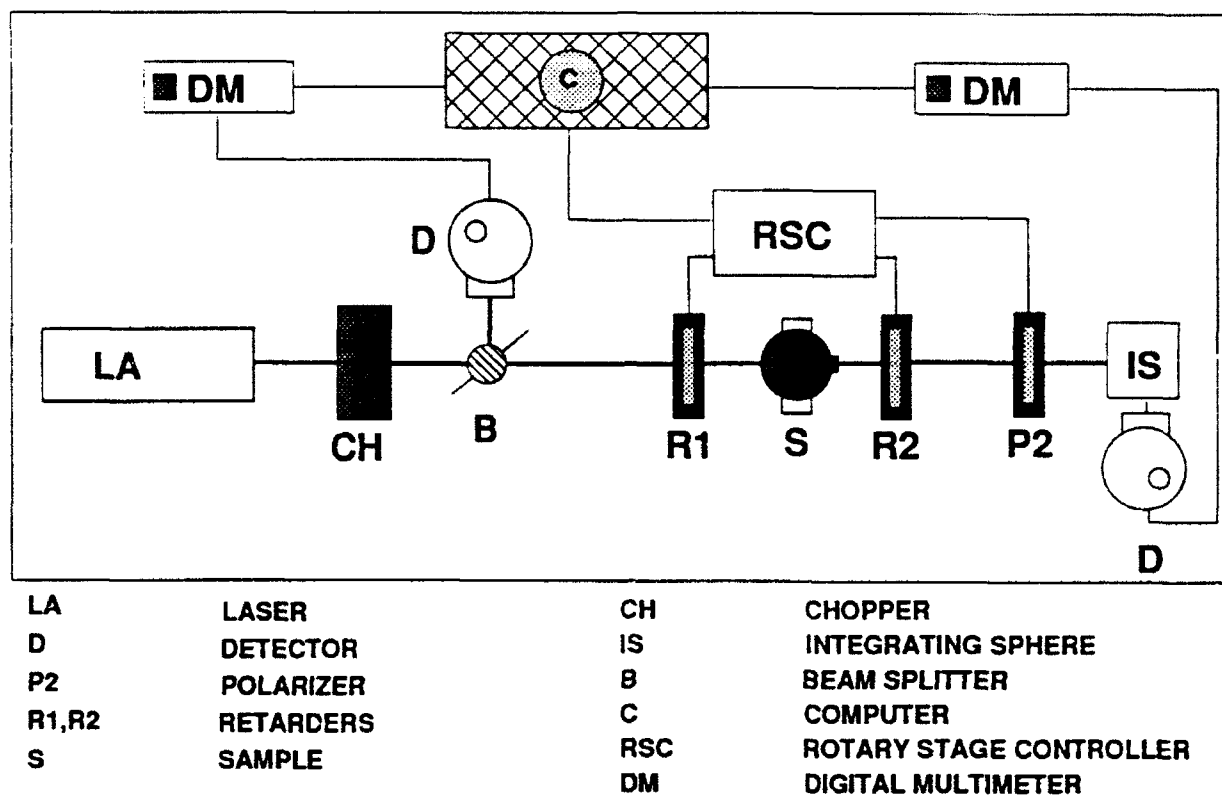
## BLOCK DIAGRAM



D. Goldstein, 12 April 1990

Figure 1

The system can be divided into five different sections: the source, the polarizing optics, the analyzing optics, and the detector. Each of these sections contains individual elements that comprise the entire polarimeter setup. Figure 2 displays the actual setup of the infrared polarimeter including the hardware that operates the system.



## INFRARED LASER POLARIMETER

Figure 2

The source is a carbon dioxide tunable infrared laser which enables its controller to adjust the wavelength of the beam. The polarizing optics consists of only one quarter wave retarder because the light from the laser is already linearly polarized so the first polarizer is ideally unnecessary. The retarder is mounted in a rotation stage controlled by the computer which makes calibration and test procedures more efficient. The sample area consists of a specially designed sample mount to accommodate the material and the actual sample to be

tested. The analyzing optics consist of both a quarter wave retarder and a linear polarizer. Each of these are mounted in computer controlled rotation stages as well. The detector measures the intensity of the beam emerging from the analyzing optics; a programmable multimeter which is integrated into the computer software reads the detector and collects the information. A dewar filled with liquid nitrogen is used to cool the detector, and a chiller set at twelve degrees centigrade provides a cooling system for the laser. Since the detector is designed to read very small intensities for better accuracy, a beam splitter must be inserted to decrease the power of the beam entering the detector to prevent saturation. The beam is chopped by a device that rotates at a set rate of about 1kHz due to the fact that the detector electronics require a modulated signal.

Data is collected from the polarimeter by the computer controller software. Each test run whether calibration or sample testing involves rotating each of the retarders at different increments and collecting the intensities at each of these increments. The computer graphs these intensities into a modulated intensity pattern and then reduces the data into a set of Fourier coefficients which produce effectively the Mueller matrix.

## **RESEARCH/DISCUSSION**

The basic experimental pattern operating the polarimeter begins with the alignment of the setup. The process aims at making sure that the laser beam propagates parallel to the optical track and is centered onto the detector aperture. One technique used was simply an eye value estimation which involved the use of infrared detection plates to locate the beam. To make fine tune adjustments we maximized the laser's output intensity into the detector using a digital multimeter and an oscilloscope. After the beam and laser source were secured and aligned into place, each optical element was then adjusted so that the beam propagated through the center of the element. The end result was an aligned setup that was ready to be calibrated for testing procedures.

The second step in the experimental procedure involving sample testing was the calibration of the polarimeter. The concept behind calibration rests on the idea that by initiating a data run on the polarimeter without a sample, a set of retardance and orientation errors can be generated for the three optical elements. These errors generated by the calibration run can be used to compensate the actual sample data. The errors are generated by the normal functioning process of the software that controls the computer during a sample test. The Mueller matrix of the calibration run is what produces the orientation errors and should ideally resemble the identity matrix as shown in Figure 3.

$$\begin{pmatrix} 1 & 0 & 0 & 0 \\ 0 & 1 & 0 & 0 \\ 0 & 0 & 1 & 0 \\ 0 & 0 & 0 & 1 \end{pmatrix}$$

Figure 3

These azimuthal orientation errors originated with misalignments of the first and second retarders and the second polarizer. Since the error terms for the retarders and the polarizers are a function of the Mueller matrix and the Fourier coefficients, they can be calculated given one or the other. In Figure 4 the data sheet for a typical calibration run displays the calculation of the orientation errors. The graph of the laser intensities at different retarder increments is called the modulated intensity pattern, and it is found at the bottom of the sheet. At the top of the data sheet is the run number which allows the controller to keep track of each element's orientation due to the fact that calibration is a repetitive process and requires several different runs. In the center of the sheet is a list of Fourier coefficients calculated from the modulated intensity pattern and a Mueller matrix based on the calculated Fourier coefficients. The final product of a sample run would have been the compensated Mueller matrix; however, in the calibration run the error terms generated from the matrix are the end result. Through a repetitive process of adjusting each element to compensate for the errors, the final product is a set of orientation errors as close to zero as possible. The minimal error terms obtained are then recorded and used in the sample testing to compensate the actual data.

After the polarimeter was aligned and calibrated, I began sample testing

procedures. The first step was to create a sample mount appropriate for the Gallium Arsenide crystal. In the data tests on the crystal a voltage was applied to the sample that allowed the index of refraction in the crystal structure to be changed. By changing the index of refraction the electro-optic tensor coefficient could be calculated from the data reduction. The sample mount was comprised of a large rotation mount with horizontal plates fastened to the side. This setup gave the user three different degrees of freedom for alignment of the crystal. The Gallium Arsenide sample was then placed in between two metal plates allowing a voltage to be applied across the crystal during a sample test run.

Each data run on the polarimeter took approximately four hours and involved increasing the voltage by increments of 200 volts and taking a sample run at each voltage. The voltage was increased from 0 to 3000 volts in random order to allow for detection of biased factors changing over time and to differentiate these factors from the voltage increase.

The Mueller calculus can reveal many properties of a sample, however, the electro-optic characteristic that I was concerned with in the tests on the Gallium Arsenide crystal was calculated from the retardance value of the crystal. In each of the test runs, I focused my attention on Mueller matrix element number 4-4 due to the fact that it was the only element expressed solely in terms of retardance.

Figure 4

## INFRARED POLARIMETER

CALIBRATION RUN #5

09:16:40 7 Aug 1992

ANGLE INCREMENT IS 5 DEGREES

POWER FLUCTUATION MEASURED ON HgCdTe Photoconductor 109.8

.0069643769825 SUBTRACTED FROM EACH INTENSITY READING.

A 0 = +3.09461734E-01	B 0 = +0.00000000E+00
A 1 = +5.49402973E-04	B 1 = +1.29832639E-03
A 2 = +6.36342927E-02	B 2 = +8.80549504E-04
A 3 = +6.02216022E-04	B 3 = +8.45710674E-04
A 4 = -1.24172638E-01	B 4 = -6.38341195E-05
A 5 = +1.80906221E-04	B 5 = -2.11037944E-04
A 6 = +1.24733239E-01	B 6 = +7.50283120E-04
A 7 = -9.17991789E-05	B 7 = +3.62651775E-04
A 8 = +6.14434697E-02	B 8 = +6.65750057E-04
A 9 = +6.87251072E-04	B 9 = +3.02924356E-04
A10 = +6.15311792E-02	B10 = +8.08571142E-04
A11 = -2.05391665E-05	B11 = +3.05949650E-04
A12 = +1.18293276E-03	B12 = +2.01408808E-04

.968	-.010	.006	.005
-.009	1.000	-.011	0.000
-.002	.018	.962	.006
.006	-.009	-.005	.978

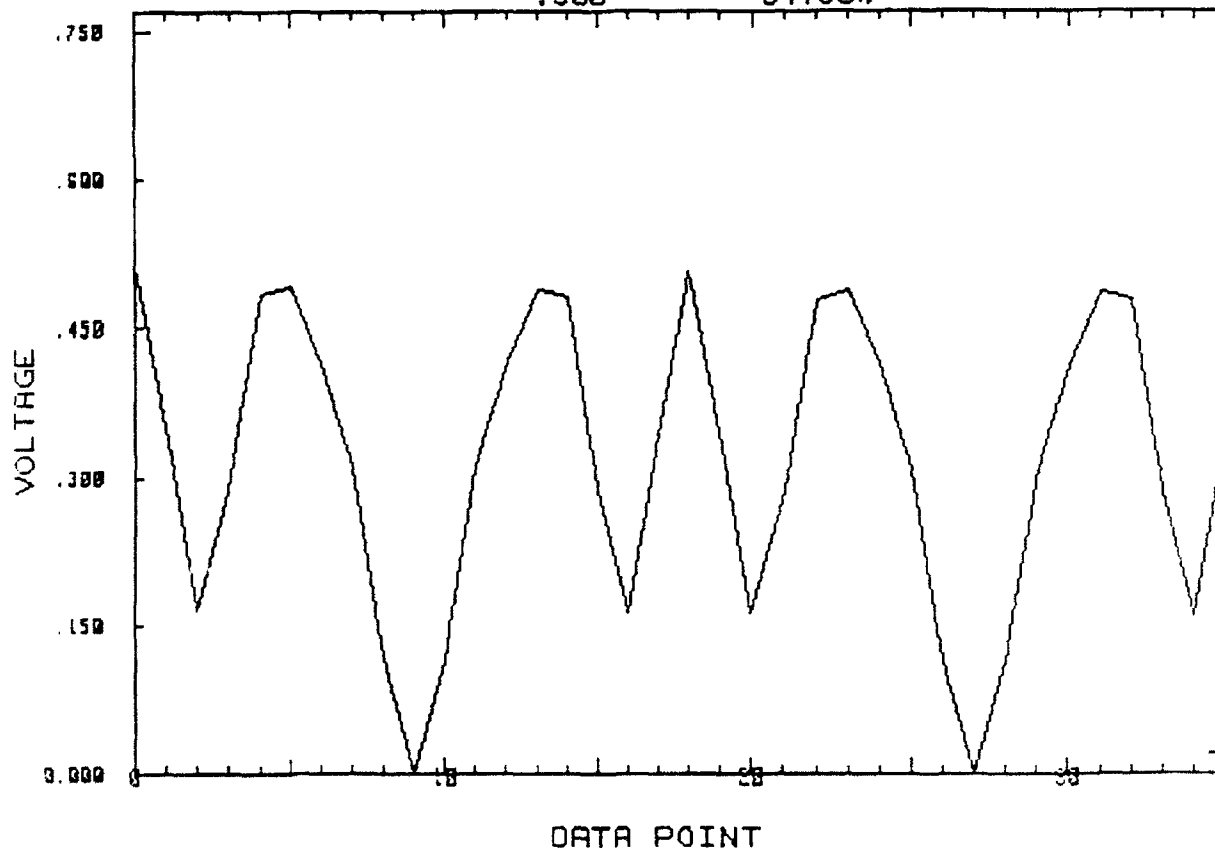
THIS MATRIX IS COMPENSATED WITH THE FOLLOWING ERROR TERMS

RET ORIENT 1    RET ORIENT 2    POL2    RETARD 1    RETARD 2

-.033	.191	.330	89.959	88.994
-------	------	------	--------	--------

09:16:40  
7 Aug 1992

**VOLTAGE VS. TIME**  
 DATA DETECTOR STABILITY  
 .500 54.90%



## CONCLUSION

The data from each of the runs was averaged and compiled into a graph which represents the matrix element value verses the applied voltage. Figure 5 shows the first graph. Matrix element number 4-4 is the only element that expresses solely the retardance property of the crystal. By taking the arcosine of the element, the retardance value can be calculated. The arcosine of each matrix element in Figure 5 was taken and plotted against the same voltage over time. To reduce the data more clearly, a linear regression was completed on the data and compiled into a second graph. Figure 6 shows the second graph. As a final analysis of the data, the slope of the linear regression curve was calculated and used to find the electro-optic characteristic of the Gallium Arsenide crystal. Figure 7 shows the method by which the electro-optic characteristic was calculated.

$$\delta = \frac{2\pi}{\lambda} n^3 r_{41} V \frac{l}{d}$$
$$SLOPE = \frac{\frac{2\pi}{\lambda} n^3 r_{41} V \frac{l}{d}}{V}$$

Figure 7

The results of the calculations are tabulated and shown in Figure 8.



**EXPERIMENTAL ELECTRO-OPTICAL CHARACTERISTIC VALUE:**

$$n^3r_{41}=5.975 \times 10^{-11}$$

**TABULATED ELECTRO-OPTICAL CHARACTERISTIC VALUE:**

$$n^3r_{41}=5.426 \times 10^{-11}$$

**Figure 8**

To use as a standard comparison, a set of data from a tabulated materials chart was integrated into the electro-optical characteristic's formula and a somewhat ideal comparison was given for the real data.

The data was completed and compiled in an effort to complete a full list of electro-optic characteristics of the Gallium Arsenide crystal. The characteristics chart would be able to tell researchers whether or not Gallium Arsenide would be a potentially good electro-optic modulator for the infrared. A great deal more data has yet to be collected from the sample and further tests will be administered to research other properties of the sample.

Figure 6

MM44

GaAs Aug. 1997

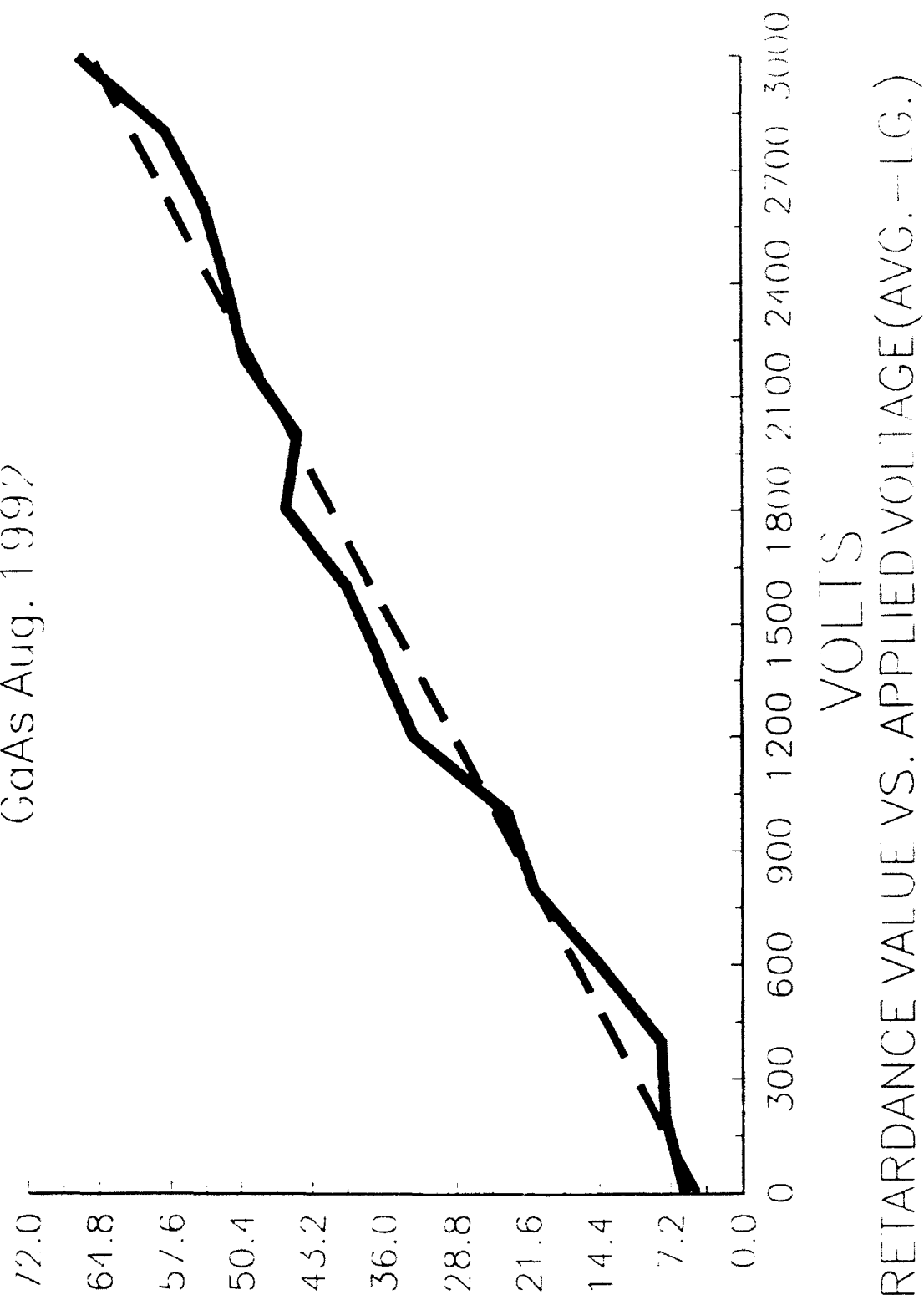
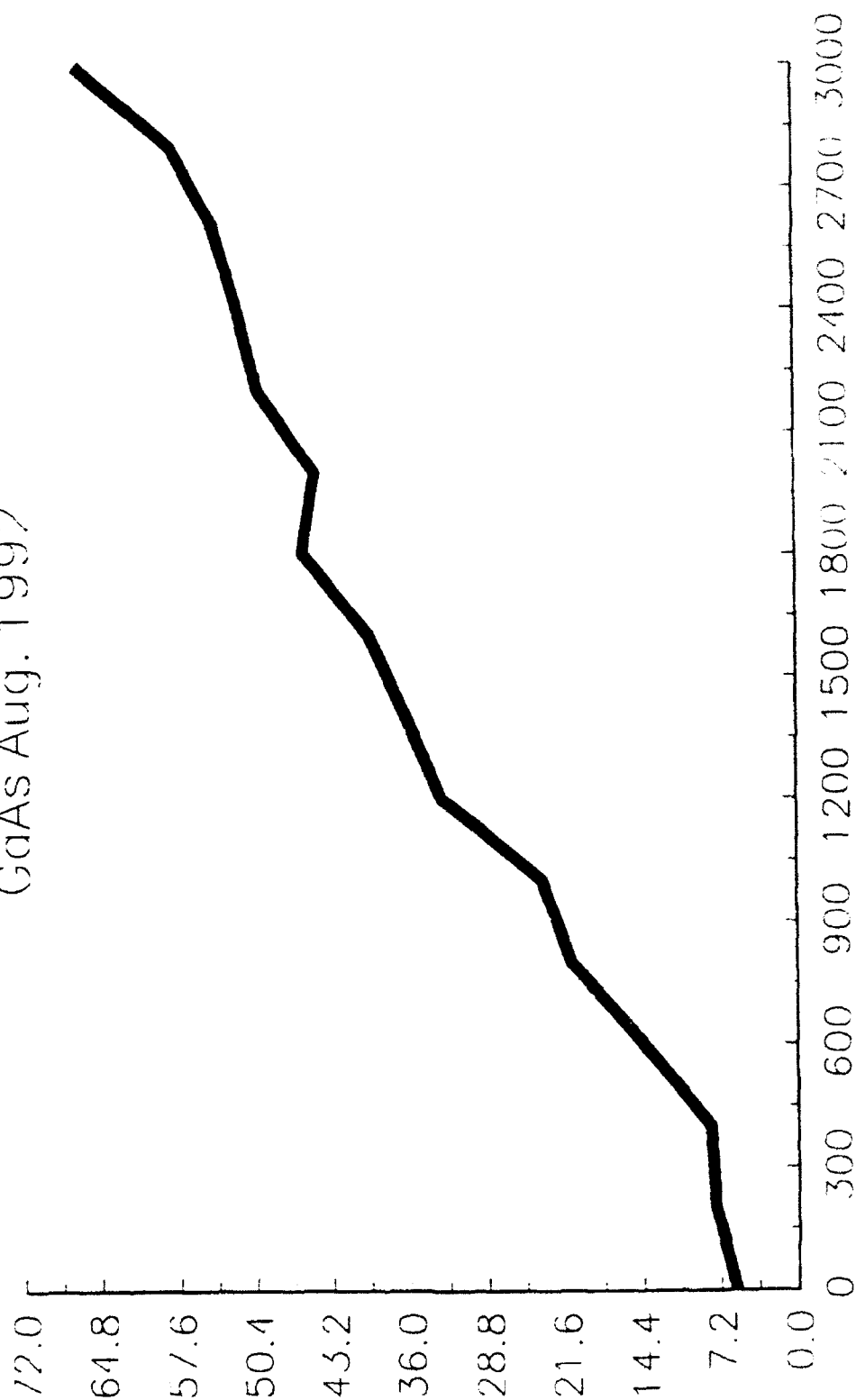


Figure 5

MM44

GaAs Aug. 1992



MATRIX ELEMENT VALUE VS. APPLIED VOLTAGE (AVG. - LG.)

# **SUMMER EXPERIENCES/LESSONS**

## **LEARNED**

In the last two summers under the guidance of Dr. Goldstein and the many college co-ops and graduate students in the lab, I have gained experience and knowledge unavailable to many students and that would normally require years of college to understand or have access to. The many doors opened include those of possible career choices, knowledge accumulated for further college study, valuable work experience, and incentive to continue a career in engineering. The High School Apprenticeship Program provided a chance for me to extend my perimeters and benefit from ideal study resources without losing sight of their practical applications. Each day's tasks and challenges required me to collectively use everything I had learned in school and the processes and experiences of last summer.

Last summer I started off by learning the basics of optics from the definition of a light wave and its primary components to its mathematical representation. The fundamental concepts of laser polarimetry were later introduced which then gave preface to the understanding of the actual physical setup of the polarimeters. By familiarizing myself with the controller software necessary to run the polarimeters and utilizing other software for data expression, I gained valuable computer programming experience.

Throughout the previous summer, I took the foundation of what I had learned the summer before and applied it to the new tasks assigned to me. I

researched the polarimeters further which allowed me to gain a more complete understanding of them and a broader view of their purpose and formulation. I became familiar with more enhanced software and studied the development of new equipment and systems.

The experience of working on the polarimeters two consecutive summers has given me an advantage in the field I hope to pursue. The program has been without a doubt a unique and prosperous experience. Every aspect has been rewarding and advantageous and the unlimited horizon that it has presented tops that of any other student internship program.

# **ACKNOWLEDGMENTS**

I would like to acknowledge first and foremost the staff at Wright Laboratories for opening their doors to the High School Apprenticeship Program and for providing an ideal working environment to all of the students. I would like to thank the Air Force Office of Scientific Research for their funding of the program and Research and Development Laboratories for their excellent administration.

Perhaps most of all I would like to extend gratitude to my mentor, Dr. Dennis Goldstein, for not only guiding me through every aspect of my summer research and teaching me more than I ever thought possible in two summers, but for also putting up with me and having the astronomical amount of patience that it took. The branch chain of command must also be thanked for their support and help in everything from the smallest of problems to the largest: Lt. Col. DeLorenzo, Major Santiago, and Mr. Lynn Deibler. The technicians in the special projects laboratories deserve thanks for their assistance: Voncile Houston, Michael VanTassel, Howard McCormick, and Linda Lau.

Finally, I would like to thank Lisa Collins for being there to help me through both summers, making work more fun than thought possible, and for keeping security top notch in the office. Without a doubt I must acknowledge my comrade Danielle Walker for just about everything: keeping me sane, opening my eyes to SO MUCH, helping to document all the AMS and PMS files, assisting in fixing all scheduling errors, helping sort through mountains of paperwork in the technical library, snapping the hose to always keep me in line, teaching me the fine art of chicken dancing, being an INTEGRAL figure in the end of the summer

supply auction, sharing with me the secrets of decorative paper shredding, helping enhance all signal processing from the D.D.G.(uh...huh, uh...uh), impromptu covering, teaching me how to be a K.E.E.G., and most of all for keeping me updated on all the Harlequin's of her life. Thanks Danielle, Lisa, and Dennis for making the last two summers not only bearable but one of my most memorable experiences as well.

# **REFERENCES**

1. Chenault, David B. "Mueller Matrix Infrared Polarimetry." Final report for the 1988 USAF-UES Graduate Student Research Program. 22 Aug. 1988.
2. Houghton, Chadwick D. "Visible Laser Polarimetry." Final report to RDL for 1991 summer. High School Apprenticeship Program. 24 Aug. 1991.
3. Gove, Randy. "Infrared Laser Polarimetry." Final report for the 1990 USAF-UES Graduate Student Research Program. 22 Aug. 1990.
4. Goldstein, Dr. Dennis H. "Polarization Modulation in Infrared Electrooptical Materials." Dissertation proposal submitted to Department of Physics, University of Alabama in Huntsville. 1989.
5. Gove, Randy. "Laser Polarimetry." Final Report to RDL. Graduate Student Research Program. 24 Aug. 1991.



Development of a Graphical User Interface  
for the AVATAR/ESP Simulation

John H. Kahrs  
High School Apprentice  
Guided Interceptor Technology Branch

Wright Laboratory Armament Directorate  
WL/MNSI  
Eglin AFB, FL 32542-5434

Final Report for:  
High School Apprenticeship Program  
Wright Laboratory Armament Directorate

Sponsored by:  
Air Force Office of Scientific Research  
Bolling Air Force Base, Washington, D.C.

August 1992

Reproduced From  
Best Available Copy

Development of a Graphical User Interface  
for the AVATAR/ESP Simulation

John H. Kahrs  
High School Apprentice  
Guided Interceptor Technologies Branch  
Eglin AFB

Abstract

The AVATAR/ESP is a simulation for almost any Kinetic Kill Vehicle. The simulation is in the process of being put into the Xwindows environment. Several utilities are also being incorporated into the simulation. The scope of this study centered around utilities for managing the variable database that is read into the ESP aspect of the simulation. The first being a program to sort feasible interceptors by a selected engagement parameter, and the second, a program for alphabetizing a selected database by variable name. Finally, the database for the Brilliant Pepples scenario was converted to a database for the Ground-Based Interceptor scenario.

# Development of a Graphical User Interface for the AVATAR/ESP Simulation

John H. Kahrs

## Introduction

The Kinetic Kill Vehicle (KKV) is an interceptor in development for use in the Strategic Defense Initiative (SDI). A KKV is an interceptor much like a bullet in that it destroys by impact rather than a missile that destroys by detonation. A KKV may be a Space Based Interceptor (SBI) or a Ground Based Interceptor (GBI). In both cases the KKV is deployed to intercept approaching Inter-Continental Ballistic Missiles (ICBM).

## Simulation

This simulation is composed of two parts, AVATAR and ESP. AVATAR provides a one-to-one end-to-end engagement capability. It models the interceptor, target, and any external trackers. It provides miss distance sensitivity to subsystem parameters such as the focal plane array. The main function of AVATAR is act as a 3DOF or 6DOF (Degrees Of Freedom) simulation environment. The 3DOF simulation provides three degrees of freedom along the X, Y, and Z axis. The 6DOF simulation adds to the 3DOF by providing rotation about each axis. AVATAR can model both space and ground based interceptors.

The Engagement Setup Program or ESP is a front-end driver for

the AVATAR aspect of the simulation. ESP first reads in the selected interceptor database. This database provides all of the different aspects and variables of the interceptor. ESP then takes in the deployment of the interceptors and the selected target of the simulation. From that information, ESP then generates a launch envelope for the interceptor. It takes into account the kinematic accessibility of the interceptor and the overall system effectiveness. It then passes to AVATAR an array of numbers for it to work with that it has generated from the parameters given to it.

The original version of ESP was a menu driven text program, but it is now being developed for the Xwindows environment. Xwindows provides several advantages over the previous version. It is a full blown graphical user interface which makes it more user friendly. Multiple application can be run under it and each can be viewed easily.

#### Retrospect

Within the AVATAR/ESP simulation are a number of utilities for managing data. It was this aspect of the simulation that I primarily dealt with. The first utility that I developed was a program to sort feasible interceptors by selected engagement parameters. The program was written in C so that it could be incorporated directly into the main simulation which is written in C as well. The sort was a Bubble sort that utilized a linked list.

A linked list is a list of data in memory which is kept track of through the use of pointers. The code utilized the malloc command to acquire memory space for data as it need it. This has advantages over the dimensioning of memory in that it does not take unnecessary space and frees up the space in memory for other tasks. Both of these methods take advantage of the versatility of the C programming language. The use of a linked list speeds up the sort routine. Instead of moving the entire block of data in memory, it just sets the pointer to point the other blocks of data in sorted order.

The second program that I developed was a program for alphabetizing the interceptor database by variable name. The database was first read into memory using routines that were already in existence. Once in memory, the variable names were then sorted and then outputted in sorted formatted to the screen. This program utilized the same code techniques that the first used.

Finally, to assist in widening the scope of the simulation, I converted the database for the brilliant pebbles scenario to a database for the ground based interceptor.

### Results

These utilities that I have developed have now been incorporated into the main AVATAR/ESP simulation. The pure meat of my code was taken out of these programs and then combined with Xwindows routines in C to control all of the input and output. My

original utilities were ascii versions that used modified versions of the standard database routines as drivers. I have come to the conclusion that these utilities have been successfully incorporated into the main simulation, and are functioning without error.

### References

Dale, Neil and Lilly, Susan C. Pascal Plus Data Structures,  
Algorithms, and Advanced Programming. C.C. Heath and Co.  
Lexington, Mass. 1985.

Schildt, Herbert. C: The Complete Reference. Osborn, McGraw-Hill.  
Berkeley, CA. 1987.

### Acknowledgments

I would like to thank the following people who helped me during the course of my project. Craig Ewing, who was my mentor. John Shearer who thought up those fascinating projects for me to do. Melissa Vaughan, my source of information about the being a computer scientist. She was one who informed my that I was a computer geek. She also pointed my in new direction in computers that I had not considered. Thank you for everything. Anne Carstens, for having that shoulder to complain on. Mike Couvillion, for getting me two good terminals and taking the time to explain the wonders of VAX/VMS. Bob LaBeu for giving me advice about life, the universe, and everything. Thanks to Darren Mason (the nick), Eric Apfel (Elmer Fudd), and Christina Trossbach (the redhead) for the memorable conversations and lunch breaks in our branch. I'd Like to thank all of the folks down in MNGA for putting up with my occasional visits. I'd like to thank all of the GRC people that are working at SAIC. I'm sorry about the VAX. Finally, I's like to thank all of the people in the NSAC program who made this possible.



AN INVESTIGATION OF THE APTAS SYSTEM

Daniel A. Kelley

Final Report for:  
AFOSR Summer Research Program  
Wright Laboratory

Sponsored by:  
Air Force Office of Scientific Research  
Bolling Air Force Base, Washington, D.C.

August 1992

## AN INVESTIGATION OF THE APTAS SYSTEM

Daniel A. Kelley

### Abstract

The Automatic Programming Technologies for Avionics Software (APTAS) system was studied. This system's purpose is to streamline the process of target tracker design by making it possible for a tracking expert without programming expertise to do computer-based prototyping.

The system's current structure and functionality were investigated. This process included the creation of test programs with APTAS. Modifications were made in order to judge the amount of labor required to make meaningful expansions to the system. Current problems with the system were identified as well as possible solutions and improvements.

# AN INVESTIGATION OF THE APTAS SYSTEM

Daniel A. Kelley

## 1.0 BACKGROUND

When I began my apprenticeship I was given the option of either working with a Multiple Hypothesis Tracking (MHT) Algorithm programmed in MATLAB design language or working with the APTAS system. To familiarize myself with advanced target tracking (ATRA) concepts and decide to which task I would apply myself, I studied the tracking and data association texts of Bar-Shalom [1] and S. S. Blackman [2], a paper by my mentor on MHT [3], a Hughes Aircraft Company paper on MHT [4], an ATRA In-House proposal prepared by WL/AART-1 [5], and the APTAS system program final report [6]. Based on this reading, and a sampling of both the APTAS system and MATLAB based MHT simulation, I decided to work on the APTAS effort.

2.0 INTRODUCTION: The Lockheed Palo Alto Research Laboratory is developing an environment which allows users to create software by specifying the characteristics of an application instead of coding the software directly. This system, the Lockheed Environment for Automatic Programming (LEAP), would be used by experts in fields throughout industry who need to develop software, but who lack professional programming expertise. The APTAS system is one application of the LEAP technology.

The APTAS system applies LEAP technology to the domain of multiple target tracking. The designer specifies the structure of the tracker by completing a set of interactive forms. Each form provides a set of options for tracker design and simulation conditions, such as type of radar, target acceleration, and false alarm rate. Depending on which options are chosen, other forms may be provided for the user to fill out to further define the tracking system. When this process is completed, the system generates a representation of the software architecture which can be further modified. APTAS provides the Graphical User Interface (G.U.I.) as an environment for making such changes. Once the definition

process is completed, the architecture is synthesized in Common Intermediate Design Language (CIDL). This can later be translated to LISP, Ada, or C for run-time analysis.

The APTAS system synthesizes a tracker architecture using predefined CIDL routines. These routines, which carry out various tracker functions, are collectively called primitives. Existing primitives can be modified and new primitives can be created, thus expanding the knowledge base.

### 3.0 METHODOLOGY

The APTAS System study was divided into three major tasks:

1. Confirming the correct functioning of the system.
2. Accumulating general data about the workings of the APTAS system.
3. Attempting to modify an existing CIDL primitive.

### 4.0 Task 1: APTAS Test Procedures

Correct functioning of the APTAS system was confirmed using Lockheed's specification for testing the system [7]. These test procedures step through the synthesis of a default tracker design, modification of the design, generation of a new design, and customization of the runtime display for the modified design.

#### 4.1 Test Procedure #1: Default Tracker Synthesis

The synthesis of a default design as explained in the Test Description proceeded as written through the stages of synthesis and execution of tracker code and display of the results using the Runtime Interface. However, attempts to translate the tracker to an Ada implementation failed. The menu system used to access this function performed acceptably. The problem with translation is that our test station was set up with Ada version 4.1. Though the test specifications call for "Ada" without specifying a version, Lockheed used Telesoft Telegen2 Ada Development System, Version 1.4. Through communication with Lockheed it will be determined whether we can initiate successful Ada translation on our current platform, and if not, what changes are necessary to achieve this goal (probably acquisition of a compatible Ada version or a modified APTAS system).

#### 4.2 Test Procedure #2: Modification of the Default Design

Modification of the default design was achieved as specified. Modifications made at the form level required little effort. Those made at the graphical editor level were somewhat inconvenient. In particular, the "target\_specs" parameter required too much effort to change because the entire equation describing the target trajectory did not fit into the allocated display area. Synthesis and execution worked as the text described. Again, Ada implementation failed for the reasons given above.

#### 4.3 Test Procedure #3: New Tracker Architecture Generation

The procedure for generating a new tracker architecture worked as described. The procedure is not difficult, however it appears that due to the way the forms are displayed, it is possible to not realize how large a form is and therefore incompletely fill it out.

Since the "new tracker" requires primitives that do not have CIDL implementations, tracker design synthesis was not possible. However, the generated architecture is consistent with the test specifications.

#### 4.4 Test Procedure #4: Customizing the Runtime Display

The test of the runtime display had two parts: configuration and execution. For the test, the execution results of the modified tracker (see 4.2), currently stored to a file, were used for data. Configuring the display required little effort. However, the runtime interface could not be executed as this option was not present on the main user menu. Eventually it was determined that a file path had been defined incorrectly due to an ambiguity in the specification text [7]. After redefining the file path, the interface operated as expected.

### 5.0 Task 2: General Findings for Various APTAS Components

#### 5.1 Forms Interface

The forms defined for the tracker domain include many options that have not yet been coded. However, these forms provide a logical direction to take when further coding is initiated.

Some parameters can only be modified at the Graphical User Interface level. For example, if the "Ground" option is chosen as the "Platform Type" on form 1.9 and then applied, it is still possible to

enter values for "Maximum Altitude", "Minimum Altitude", et cetera. Though relevant for fighter platforms, these variables are obviously meaningless for a ground radar system.

## 5.2 Graphical User Interface

When there are a large number of modules in a project, not all of them will fit in the main window (even if the window is screen size), and those modules that are completely cut off can't always be relocated so that they are visible.

Variables, such as Probability\_of\_Detection, that are of type REAL or INT can't be prompted for a self-description with the "Describe Type" function. In order to get a description of these variables, the user must leave the APTAS system and read the "global.desc" file. This is very inconvenient.

Some variables are located in two different modules within the Graphical User Interface. If the user changes a value in one of these modules, the change will not be reflected at the other location. If the user goes back later to check on the value of that variable, he or she must remember where the changed value resides. Otherwise, it may be difficult to tell which value is the active one.

## 5.3 Runtime Display

The runtime display is inconvenient to use. Observations of the runtime display include:

1. Panning and zooming functions would be more convenient if they were accessible while the display is running.
2. If the user could display data from more than one test run it would improve the analysis of experimental data.
3. The user should be able to control the time frame of the tracking display. This would include pause, fast-forward, and reverse functions, as well as specification of time  $t$ .
4. The track history length control operates illogically. If it is set from 0 to 10 it acts normally, but if it is set at 11, it displays all the track points regardless of the size of the track buffer. As a consequence, the user cannot set

the length to 17 or 22, for example, unless that is the maximum size of the track buffer.

#### 5.4 The Current Tracking System

##### 5.4.1 Existing Primitive Modules

Lockheed has only coded the primitives for the default tracking system. The primitives are shown below:

##### PRIMITIVES

- a. Generate\_Search\_Gates
- b. Initiate\_Tentative\_Tracks
- c. Output\_Display
- d. Presentation\_Process
- e. Process\_Gate\_Contact\_Association
- f. Resolve\_Extra\_Contacts
- g. Resolve\_Missing\_Contacts
- h. Scan\_to\_Track\_Correlation
- i. Sensor\_Model
- j. Track\_Database
- k. Update\_Tracks

##### 5.4.2 Adjustable Simulation Parameters

The complete list of algorithm parameters which may be adjusted are shown below along with a short description of each variable.

- a. **Initial\_Gate\_Deltas**-Determines the size of the normal track gate.
- b. **Reduced\_Delta\_Factors**-Determines the reduction in gate size.
- c. **Increased\_Delta\_Factors**-Determines the increase in gate size.
- d. **Perturbation Factor**-Determines the amount of noise added to the target trajectories.
- e. **Tentative\_to\_Regular\_Threshold**-Determines the number of detections required to pass a track from tentative to regular status.
- f. **Terminated\_Reg\_Track\_Save**-Determines the number of scan periods a terminated regular track is kept in the database.
- g. **Termination\_Thresholds**-Determines the number of missed detections before a regular track is terminated and the number of missed detections before a tentative track is terminated.

- h. **Terminated\_Tent\_Track\_Save\_Limit**-Determine the number of scan periods a terminated tentative track is kept in the database.
- i. **Test Iterations Count**-Number of cycles/scan periods in the simulation.
- j. **Maximum Number of Targets**
- k. **Target\_Specs**-Mathematically defined target trajectories.
- l. **Required\_Application\_Memory**-This parameter value is calculated during synthesis. A value given to it in the graphical editor will be overwritten by the synthesis engine. It's visibility in the graphical editor is merely to provide information after synthesis.

#### 5.4.3 The Simulated Environment

The default tracker is a nearest-neighbor system that uses a least-squares polynomial fit [8] method for approximating new target positions. All operations occur within a simulated 2-dimensional space.

The system does not include functional modeling of ownship altitude, velocity, or maneuvering. Many other options are also absent, such as control of scan volume, number of bars per scan, frame update interval, time tagging of individual detections, jammers, clutter (sea, land),  $P_{FA}$ ,  $P_D$ , and platform. Control of target specifications is limited to trajectory (defined mathematically) and number of targets.

#### 5.4.4 Miscellaneous Observations

##### Tracker Project Files

When there are more than forty projects on the system, the menu for project files will not open, making it impossible to start a new project without first relocating or deleting one or more projects through the operating system.

#### 6.0 Task 3: Modification of an Existing CIDL Module

In the course of investigating the APTAS system it was discovered that "adaptive" gating was implemented by allowing the user to define three gate sizes: "initial", "reduced", and "increased". In the course of tracking a target the algorithm simply varies the gate size between these choices.

To further my understanding of the APTAS system, I worked to add an incremental gating mechanism to the tracking algorithm. This modification redefined the **increased\_delta\_factors** variable so that it



represented the changes in length and width of the gate at each incrementation. The **reduced\_delta\_factors** variable was redefined analogously for each decrementation.

The module modified was the **Generate\_Search\_Gates** primitive. This module is a submodule of the **Scan\_to\_Track\_Correlation** module, which is a submodule of the **Tracker** module, which in turn is a submodule of the **Tracker\_Environment** module. The CIDL code for the **Generate\_Search\_Gates** primitive is located in the file "Generate\_Search\_Gates.cdl".

The beginning of the module is shown in figure 1.

```
1| module Generate_Search_Gates
2|Parameters
3|database : Track_Database;
4|initial_gate_deltas : tuple real, real end;
5|reduced_delta_factors : tuple real, real end;
6|increased_delta_factors : tuple real, real end;
7|platform : PlatformType;
8|target_trajectory : TargetTrajectoryType;
```

Figure 1

Line 1 identifies the module. Line 2 begins the parameters section. The values to which these parameters are set when the module is "plugged" into the main program determine the exact characteristics the module has in that instance. For example, line 4 defines the parameter **initial\_gate\_deltas** as type "tuple real, real end". In CIDL a tuple type is a "record" composed of various types, in this case it is two real numbers [9]. The word "end" signifies the end of the tuple construct. When the user sets the value of **initial\_gate\_deltas** using the Graphical Editor, he or she determines the two real numbers that the **Generate\_Search\_Gates** module will use when the module utilizes **initial\_gate\_deltas** in its code.

To achieve the desired effect, it was necessary to change the structure section of the module. The section of

"generate\_search\_gates.cdl" shown in figure 2 contains the local declarations that define how the module works.

```
38| increased_deltas : tuple real, real end
39| =(initial_gate_deltas@0 * increased_delta_factors@0,
40|   initial_gate_deltas@1 * increased_delta_factors@1);
41|
42| reduced_deltas : tuple real, real end
43| =(initial_gate_deltas@0 * reduced_delta_factors@0,
44|   initial_gate_deltas@1 * reduced_delta_factors@1);
```

Figure 2

The code in Figure 2 from the original module defines the variables **increased\_deltas** and **reduced\_deltas**. Line 38 defines **increased\_deltas** as having type "tuple real, real", the two real numbers representing the x-axis and y-axis displacements. Lines 39 and 40 give **increased\_deltas** a value in terms of the user defined parameters **initial\_gate\_deltas** and **increased\_delta\_factors**. The @x notation--as in "@1"--specifies a single component of the tuple (the numbering begins at 0, i.e., "@4" specifies the fifth component of a tuple) therefore, line 39 sets the first (x) component of **increased\_deltas** to equal the first (x) value of **initial\_gate\_deltas** multiplied by the first (x) value of **increased\_delta\_factors**. Line 40 acts analogously for the y values, and lines 42 through 44 define the same process for **reduced\_deltas**.

In the original module the values of **increased\_deltas** or **reduced\_deltas** define the sizes of the increased and reduced gates. A new gate is made by adding these values to, and subtracting these values from, the predicted target position to define the upper and lower bounds of the gate. To incorporate incremental gating into the module, the procedure is changed so that **increased\_deltas** is simply added to the already existing gate size and **reduced\_deltas** is subtracted from that size. To accomplish this, the code was rewritten as in figure3 below.

```

38| increased_deltas : tuple real, real end
39| =(increased_delta_factors@0,
40| increased_delta_factors@1);
41|
42| reduced_deltas : tuple real, real end
43| =(-reduced_delta_factors@0,
44| -reduced_delta_factors@1);

```

Figure 3

This modification sets the x-component of **increased\_deltas** equal to the x-component of **increased\_delta\_factors**, and does the same with the y-components and the corresponding values of **reduced\_deltas**. Next, the code that actually creates the gates (fig. 4) had to be modified.

```

131|Generate_New_Gate(Track_ID : TrackID;
132| new_track : bool;
133| last_contact : GenericContact;
134| last_gate : GenericSearchGate) : GenericSearchGate

```

Figure 4

Lines 131-134 begin the procedure **Generate\_New\_Gate**. **Track\_ID**, **new\_track**, **last\_contact**, and **last\_gate** are values passed to the procedure when it is called. **Track\_ID** is of the type **TrackID**, an integer identifying the track in question. **new\_track** is of the type **bool**, which means it is a boolean variable with a value of either "true" or "false". **last\_contact** is of the type **GenericContact**, a type defined as a theory composed of one component ("pos") which is made of a two-valued real tuple:

```
GenericContact : type = theory pos : tuple real, real end end;
```

**last\_contact** contains the last position where the target was detected or the extrapolated last position if there have been missed

detections. **last\_gate** is of the type **GenericSearchGate**, a type defined as in figure 5. **last\_gate** contains the parameters of the last search gate generated for the target. The second occurrence of "GenericSearchGate" on line 134 indicates that the procedure returns a value of that type.

```
GenericSearchGate : type = theory
predicted : GenericContact;
high : GenericContact
low : GenericContact
shape : SearchGateShape;
empty : int
end;
```

Figure 5

```

135|let
136|   error_string : store(string)
137|   new_gate :
store(GenericSearchGate)
138|in
139|   if new_track
140|   then new_gate := struct
141|predicted=last_contact
142|high=add_delta
143|(last_contact,
144| struct pos =
initial_gate_deltas end);
145|low=subtract_delta
146|   (last_contact,
147|   struct pos =
initial_gate_deltas end);
148|shape=$rectangular;
149|empty=0
150| end;
151|error_string :=
database.Process.Assertion
152|(struct
153|assertion_id=24;
154|args=struct
155|   TID=Track_ID;
156|   TrackType="";
157|   Index_Degree_or_MissionID=-1;
158|
MissionHeader=NULLMissionHeader;
159|   Contact=NULLContact;
160|   TrackState=NULLTargetState;

161|   SearchGate=content(new_gate);
162|
PlatformPosition=NULLPlatformPos
163|end
164|end)
165| else
166|let
167| predicted_pt : GenericContact
168|=Get_Next_Pt(Track_ID,
last_contact);
169| deltas : store(tuple real, real
end)
170|   in
171| if last_gate.empty>0
then deltas := increased_deltas
172| else deltas := reduced_deltas
173| fi;
174|   new_gate := struct
175|   predicted=predicted_pt;
176|   high=add_delta
177|   (predicted_pt,
178|   struct pos=content(deltas)
end);
179|   low=subtract_delta
180|   shape=$rectangular;
181|   empty=0
182|end
183|   end
184| fi;
185| content(new_gate)
186|   end;

```

Figure 6

Line 135 in figure 6 begins a *let expression*. The value returned by this expression will set the value of the **GenericSearchGate** that the **Generate\_New\_Gate** procedure passes back.[9] Line 137 defines the construct that ultimately returns the new gate generated by the procedure.

The *if expression* that starts on line 139 checks to see if the track is a new one. If it is, lines 140 through 164 generate an initial gate of the size that the user has defined. If the track is not new, lines 166 through 187 set the gate to either the increased or reduced size.

The original process gets the next predicted point and stores it (line 167). Then it defines the variable **deltas**. Next it checks on whether the last gate was empty. If it was, **deltas** is set to **increased\_deltas**, otherwise it is set to **reduced\_deltas**. The new gate's upper bounds are set equal to the predicted position of the target plus **deltas**, while the lower bounds are set to this position minus **deltas**. Finally, line 188 stores the new gate before the procedure ends.

In adding incremental gating lines 167 through 169 (fig. 7) were augmented.

```
167|Last_Delta : store(GenericContact);
168|Up_Delta : store(GenericContact);
169|Down_Delta : store(GenericContact);
170|predicted_pt : GenericContact
171|    =Get_Next_Pt(Track_ID, last_contact);
172|deltas : store(tuple real, real end)
```

Figure 7

**Last\_Delta** stores the size of the last gate. **Up\_Delta** stores the value of the old gate displacement plus the new position, while **Down\_Delta** stores the value of the new position minus the old displacement. Lines 170 through 186 were also modified as shown in figure 8.

```

173|in
174| Last_Delta := subtract_delta(last_gate.high, last_contact);
175| Up_Delta := add_delta(predicted_pt, content(Last_Delta));
176| Down_Delta := subtract_delta(predicted_pt, content(Last_Delta));
177| if last_gate.empty>0
178| then deltas := increased_deltas
179| else deltas := reduced_deltas
180| fi;
181| new_gate := struct
182|predicted=predicted_pt;
183|high=add_delta
184|(content(Up_Delta),
185| struct pos = content(deltas) end);
186|low=subtract_delta
187|(content(Down_Delta),
188|struct pos=content(deltas) end);
189|shape=$rectangular;
190|empty=0
191| end
192|end
193|
194|content(new_gate)

```

Figure 8

Line 174 in figure 8 calculates the size of the last gate by subtracting the position of the last target contact from the position of the upper bound of the last gate. This size is attached to the new predicted point in lines 175 and 176. Line 177 checks whether the gate is enlarged or reduced. The enlargement or reduction displacement is combined with the old gate size in lines 183 through 188. Finally line 194 stores the new gate.

Another procedure in "generate\_search\_gates.cdl" that was modified is **Store\_Update\_Track\_and\_Gate\_in\_DB**. Figure 9 shows original code from this procedure.

```
285|when length(track_data.cluster)=0
286|=>new_target_state
287|:=struct
288|id=track_data.id
289|state=gate.predicted;
290|cluster : sequence(GenericContact)=[]
291|end;
292|next_predicted := Get_Next_Pt(track_data.id, gate.predicted);
293|new_gate := struct
294|predicted=content(next_predicted);
295|high=add_delta
296|(content(next_predicted),
297 struct pos = increased_deltas end);
298|low=subtract_delta
299|(content(next_predicted),
300|struct pos = increased_deltas end);
301|shape=$rectangular;
302|empty=gate.empty+1
303| end
```

Figure 9

This code sets the gate at the larger size if the last gate was empty. To change the code so that the procedure *increases* the gate size, the following code shown in figure 10 was added between 292 and 293:

```
blue_gate := Generate_New_Gate(track_data.id, false
    content(new_target_state).state,
    gate);
```

Figure 10



This line calls the now modified **Generate\_New\_Gate** procedure which increases the gate size. The lines that give values to **high** and **low** (lines 295 and 298) were changed to store this new gate and are shown in figure 11:

```
high=content(blue_gate).high  
low=content(blue_gate).low  
blue_gate : store(GenericSearchGate);
```

Figure 11

After defining the **blue\_gate** object, the incorporation of incremental gating was complete.

## 7.0 Results and Conclusions

### 7.1 Task 1

The test of the APTAS system was successful. Except for the aforementioned bugs the APTAS system functioned correctly. In addition, Lockheed's testing specifications provided a good way to familiarize a new user with the system.

### 7.2 Task 2

Since the only way to do fast tracker runs is to translate to Ada, and since Ada translation takes approximately two hours, doing studies where one or more variables are incremented through a range of values will take more time than is practical in a real-world situation. However, with the new version of the APTAS system Ada translation will be much faster.

The current version of the APTAS system is not sophisticated enough for real-world tracker applications. The framework for a system that can someday be used for this purpose exists but it will take large quantities of time and effort to bring the system forward to this point. The current system is better suited for investigation of the technology's potential.

### 7.3 Task 3

The relatively basic procedural change accomplished in this task required more than 20 trials to code correctly. The nature of CIDL

makes relatively high demands on a programmer new to the language. CIDL's flexibility is accomplished through a syntax that has very specific constraints but wide latitude within those constraints. Therefore the user must precisely learn the syntactic working of several constructs. Correctly using these constructs means avoiding errors that are often subtle, especially to a CIDL neophyte. The CIDL literature provided with the APTAS system has a high learning curve. To understand the text, basic concepts of CIDL must be grasped. These concepts are not always directly conveyed. When they are, the explanation often resides in technical jargon. While it gives a complete description of CIDL, the text does so in a compact way. Even understanding the examples requires much effort. To make the mastery of the language easier a general, nontechnical explanation of what objects, constructs, types, etc. actually mean in CIDL would be helpful. The addition of several well documented examples would also be useful.

Based on the difficulty of this task, it is reasonable to assume that creating an entirely new functional module will require a long and intense effort. The effort previously outlined did not require a working knowledge of every aspect of the code. Also, additional syntax must be learned in order to incorporate the module into the existing framework by modifying the "global.form", "global.gsdl-1", "global.gsdl-t", and "global.synth" files. This knowledge will be vital to the creation of a new module.

## 8.0 REFERENCES

- [1] Yaakov Bar-Shalom, "Tracking and Data Association" Academic Press, 1988.
- [2] S.S. Blackman, "Multiple Target Tracking with Radar Applications", Artech House, 1986.
- [3] J. Werthmann, "A Step-by-Step Description of a Computationally Efficient Version of MHT", 1992.

- [4] G.C. Demos, R.A. Ribas, T.J. Broida, S.S. Blackman, "Applications of MHT to Dim Moving Targets", SPIE Vol. 1305, Signal and Data Processing of Small Targets 1990.
- [5] J. Werthmann "Advanced Tracking Algorithms In-House Analysis Proposal", WL/AART-1, 15 APR 92.
- [6] Paul S. Jensen, Lori Ogata, "Final Report For Automatic Programming Technologies for Avionics Software (APTAS)", Lockheed Software Technology Center, 1991.
- [7] Software Test Description for the Automatic Programming Technologies for Avionics Software (APTAS) System, Lockheed Software Technology Center, 1991.
- [8] Paul S. Jensen, Avionics Tracking System Specification for Automatic Code Synthesis, Lockheed Software Technology Center, 1990.
- [9] Wolfgang Polak, Henson Graves, "The Cidl Language User Manual", 1992
- [10] Software User's Manual for the Automatic Programming Technologies for Avionics Software (APTAS) System, Lockheed Software Technology Center, 1991.

Evaluation of Hydrocode Strain Contours by  
Microhardness Testing

Jason A. Kitchen  
High School Apprentice  
Warhead Branch

Wright Laboratory Armament Directorate  
WL/MNMW  
Eglin AFB, FL 32542-5434

Final Report for:  
High School Apprenticeship Program  
Wright Laboratory Armament Directorate

Sponsored by:  
Air Force Office of Scientific Research  
Bolling Air Force Base, Washington D.C.

August 1992

Evaluation of Hydrocode Strain Contours by  
Microhardness Testing

Jason A. Kitchen  
High School Apprentice  
Warhead Branch  
Wright Laboratory Armament Directorate

Abstract

For this research project, microhardness plots of metal test specimens were compared to hydrocode strain contour plots. The microhardness values of copper, aluminum, and steel Taylor-Anvil specimens were measured by the use of a microhardness testing apparatus. The apparatus consists of a microscope for viewing the metal test specimen and a diamond tipped indenter placed under a load for determining the hardness value for a specific point in the specimen. The diamond indentations were repeated at regular intervals across the specimen, and a microhardness value plot for the specimen was created. This plot of values was analyzed for trends where values significantly changed. The trend lines were then compared to hydrocode strain contour plots.

The results of microhardness testing were encouraging. While the range of hardness values on copper and aluminum Taylor specimens did not vary enough to exhibit trends, the wide-spread values of the steel plots allowed trends to be observed. These trend lines were compared to steel strain contour plots from hydrocodes and similarities were seen in the hardness values and corresponding strain contours. While the validity of hydrocode predictions cannot yet be determined by microhardness testing, future work is planned to further investigate microhardness testing as a means for hydrocode evaluation.

## Evaluation of Hydrocode Strain Contours by Microhardness Testing

Jason A. Kitchen

### Introduction

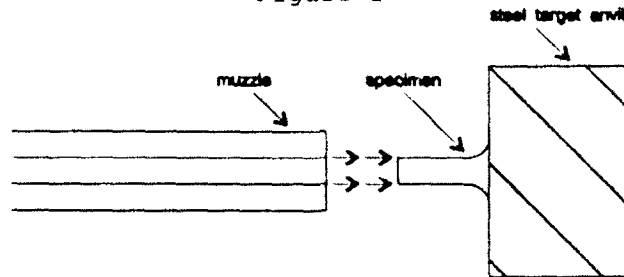
My research for the past two summers has been in the Warhead Branch of Wright Laboratory's Armament Directorate. The current objectives of the Warhead Branch are to enhance the performance of warhead penetration by researching the mechanical and material properties of different materials impacting a target at high velocities. Computer hydrodynamic codes, or hydrocodes, have been programmed in order to accurately predict warhead performance under variable circumstances. By the use of accurate hydrocodes, many answers about mechanical and material properties of a material impacting a target can be answered quickly and inexpensively. The validity of these continuum dynamic codes are evaluated by comparing their predictions with real data from experimental testing. My work has centered on measuring the mechanical property of strain on metals during high-velocity impact with a target and comparing it with hydrocode predictions.

### Methodology

In order to measure mechanical and material properties of metals during high velocity impact, an experiment called a Taylor-Anvil test is performed. In this test, a 1-inch long plane-ended cylindrical rod is shot from a .30 caliber rifle into a steel target, called the anvil (see Figure 1). This test allows a specimen of any suitable material for analysis to be shot at a large range of velocities. As the specimen impacts with the steel anvil, mechanical properties, such as stress, strain, pressure and temperature are measured. The deformed post-impact specimen can be analyzed to determine material

properties, such as grain size and void formation. My research project dealt with measuring the material aspect of hardness in a metal and comparing this data with hydrocode strain contour plots.

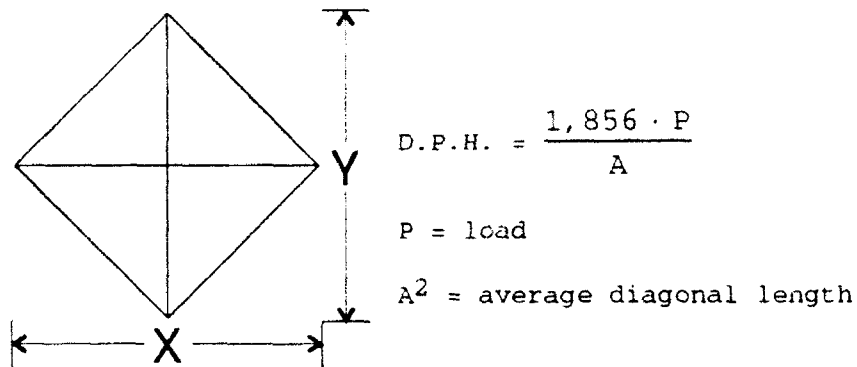
Figure 1



In order to analyze the varying hardness values of the impact specimen, the specimen first had to be halved down its cylindrical axis. This was accomplished using a metal cutting saw with a diamond wafering blade. One half of the specimen was then mounted flat-side-down in a cold-set epoxy. The mounted specimen was then finely polished and etched to further flatten the exposed surface. A Buehler Microhardness testing apparatus was used to measure the hardness values. This apparatus consists of a powerful microscope and a diamond indenter. The metal specimen is brought into focus under the microscope and then subjected to indentation by the loaded diamond indenter for a set amount of time. The resultant diamond-shaped indentation in the specimen is viewed through the microscope. The diagonal lengths of the indentation are measured and these two lengths are averaged (see Figure 2). The average diagonal length is then entered with the load on the diamond indenter into the Diamond Pyramid Hardness equation for determining the microhardness value of that point of the sample. The indentation and measurement process is repeated at regular intervals along the surface of the specimen. After obtaining a

matrix of microhardness values, a two-dimensional plot of the specimen with its microhardness values is created.

Figure 2



#### Procedure

For my research project, Taylor specimens of copper, aluminum, and steel were analyzed. The microhardness values of these specimens were plotted and analyzed in order to map regions of varying hardness in the specimen. Hydrocode strain contour plots for Taylor impact tests with the same testing conditions as with the real Taylor samples were produced and compared with microhardness value plots.

#### Results

By analyzing the microhardness plots of copper, aluminum, and steel, several observations were noted. First, as expected, microhardness values of the specimen near to the impact interface between the specimen and target were greater than values towards the back of the specimen. This range of values was due to work hardening of the deformed area of the specimen caused by the tremendous energy transferred there during impact. Second, the microhardness value plots of copper and aluminum did not have a significant range of values



from the front of the specimen to the back to mark trends showing where changes in hardness occurred. The smaller hardness ranges on the copper and aluminum specimens are due to their thermal conductivity. Estimates have been made that 95% of the energy to deform a material is radiated as heat energy, the remaining energy being stored in the material as internal, or strain energy. This strain energy is reflected in the hardness values of a material. Because of the heat capacity and density relationships of copper and aluminum, less total energy was stored as strain and more was added to the volume of heat energy, thus resulting in a lower range of hardness values along the length of the specimen. The main objective of comparing trend lines of copper and aluminum Taylor specimens with hydrocode plots could not be accomplished, so a means is necessary to negate the affects of temperature on them. One way to accomplish this in the future would be to normalize the hardness data by applying the strain to the following equation which takes temperature affects into account:

$$\Delta T = \frac{0.95}{\rho \cdot C_p} \int_0^{\epsilon} \sigma d\epsilon, \text{ where}$$

$\rho$  is density,

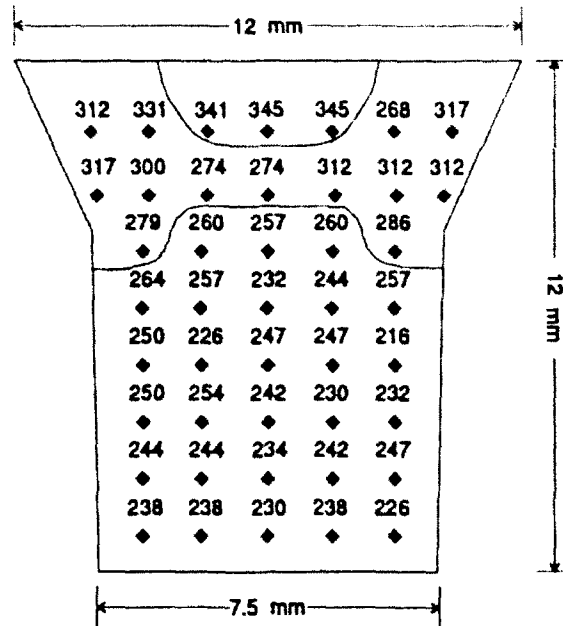
$C_p$  is heat capacity,

$\sigma$  is engineering stress, and

$\epsilon$  is engineering strain.

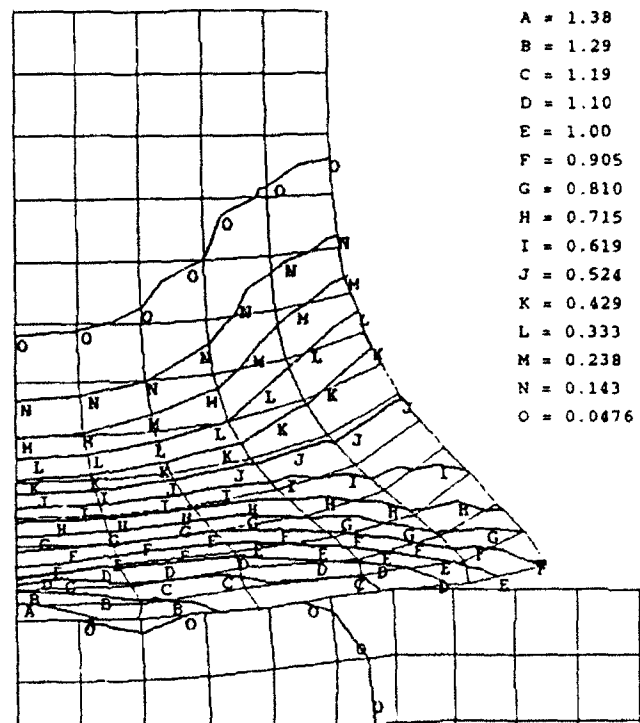
The microhardness plots from the steel Taylor samples were most beneficial in determining trends where hardness values significantly changed (see Figure 3).

Figure 3



When compared to hydrocode strain contour plots, similarities were noted in the shape of those trend lines. Figure 4 is a hydrocode strain contour plot for a steel Taylor impact specimen.

Figure 4



At this time the validity of hydrocode strain predictions cannot be assessed by the use of microhardness testing. Future work is planned to gain more information on the strain occurring on Taylor specimens during impact. Hydrocode predictions may be compared with temperature-normalized microhardness plots from copper and aluminum Taylor samples for further evaluation and refinement of hydrocode models.

## References

Buehler, Adolph I. Instructions for Micromet Microhardness Tester. Buehler LTD., Evanston, IL. 1977.

Carrington, W.E. and Mary L.V. Gaylor, D.Sc. "Changes in microstructure caused by deformation under impact at high-striking velocities." The Use of Flat-Ended Projectiles for Determining Dynamic Yield Stress 24 July 1947.

### Acknowledgments

I would like to express my sincere thanks to Joel House, my mentor for the past two summers at the Armament Directorate. He did his best to introduce me to his research in material science and allowed me to do work that was important for everyone involved. I would also like to thank Don Harrison and Mike Deiler, the High School Apprenticeship Program coordinators at the Armament Directorate this summer. They did a great job leading the program and were always there to answer any questions. Thanks also goes to my laboratory co-workers, Jessica Mayes, Steve Hatfield, and Thaddeus Wallace, who have become good friends over the past two summers. I am very happy and thankful to have been able to participate in this program. I know that the knowledge and skills I have learned here will continue to benefit me at college and in my future career.

A STUDY OF THE C AND BASIC COMPUTER LANGUAGES AS WELL AS AN  
IN DEPTH DISCUSSION OF CERTAIN MATHEMATICAL CONCEPTS

Barry J. Koestler II

Beavercreek High School  
2660 Dayton-Xenia Road  
Beavercreek, OH 45434

Final Report for:  
Summer Research Program  
Wright Laboratory

Sponsored by:  
Air Force Office of Scientific Research  
Wright Patterson Air Force Base, Dayton, Ohio

August 1992

A STUDY OF THE C AND BASIC COMPUTER LANGUAGES AS WELL AS AN  
IN DEPTH DISCUSSION OF CERTAIN MATHEMATICAL CONCEPTS

Barry J. Koestler  
Valedictorian  
Beaver Creek High School

Abstract

My summer apprenticeship entailed first reviewing some difficult BASIC programming, and then applying this knowledge to neural networks and matrices. Next I began learning and researching the C programming language and its mathematical implementations. Included in my study of these applications was the examination of the use of C to describe and work with sets and set theory. I also studied matrices and their properties in conjunction with neural networks. After becoming somewhat familiar with these two languages and their uses in mathematics, I examined several model programs (figs. 1-2 from Rietman 156-7, 164-5) written in BASIC and also looked at some mathematical C code (fig 3).

Figure 1

NEURON8F

```

10 CLS
20 INPUT "INPUT RANDOM SEED ": SEED
30 RANDOMIZE SEED
40 INPUT "ENTER THE NUMBER OF NEURONS (100 MAXIMUM) "; N
50 INPUT "INPUT THE THRESHOLD VALUE (0 TO 2 ARE REASONABLE VALUES) "; IO
60 INPUT "ENTER THE VALUE OF THE INFORMATION (0 TO 1 IS A GOOD VALUE ) "; INFO
70 INPUT "YOU WANT TO ENTER THE INPUT VECTOR YOURSELF (1/YES 0/NO)? "; VECTOR
80 INPUT "DO YOU WANT TO INPUT THE T MATRIX (1/YES 0/NO) "; MATRIX
90 DIM T(100, 100), V(100), U(100)
100 REM FILL T(I,J) MATRIX
110 IF MATRIX = 0 THEN 190
120 FOR I = 1 TO N
130 FOR J = 1 TO N
140 PRINT "T("; I; ", "; J; ") "
150 INPUT T(I, J)
160 NEXT J
170 NEXT I
180 GOTO 360: 'FILL INPUT VECTOR
190 FOR I = 1 TO N
200 FOR J = 1 TO N
210 R = RND(1)
220 IF R < .8 THEN R = 0 ELSE R = 1: REM DILUTE MATRIX
230 T(I, J) = R
240 NEXT J
250 PRINT
260 NEXT I
270 FOR I = 1 TO N
280 FOR J = 1 TO N
290 IF I = J THEN T(I, J) = 0
300 T(J, I) = T(I, J)
310 PRINT T(I, J);
320 NEXT J
330 PRINT
340 NEXT I
350 PRINT : PRINT : PRINT
360 REM FILL INPUT VECTOR U
370 IF VECTOR = 0 THEN 430
380 FOR I = 1 TO N
390 PRINT "INPUT U("; I; ") "
400 INPUT U(I)
410 NEXT I
420 GOTO 470: 'BEGIN CALCULATIONS OF OUTPUT VECTOR
430 FOR I = 1 TO N
440 GOSUB 790
450 U(I) = R
460 NEXT I
470 REM BEGIN CALCULATION
480 FOR ITERATE = 1 TO 8: REM THIS ALLOWS THE OUTPUT VECTOR TO BE FEED BACK

```



Figure 1 cont.

NEURONBP cont.

```
490 FOR I = 1 TO N
500 FOR J = 1 TO N
510 SIGMA = T(I, J) * U(J) + SIGMA
520 NEXT J
530 SIGMA = SIGMA + INFO
540 IF SIGMA > 10 THEN SIGMA = 1 ELSE SIGMA = 0
550 V(I) = SIGMA
560 SIGMA = 0
570 NEXT I
580 FOR I = 1 TO N
590 PRINT U(I);
600 NEXT I
610 PRINT
620 FOR I = 1 TO N
630 PRINT V(I);
640 NEXT I
650 PRINT
660 ENERGY = 0
670 FOR I = 1 TO N: REM ENERGY CALCULATION
680 ENERGY = ENERGY + (U(I) * V(I))
690 NEXT I
700 ENERGY = -.5 * ENERGY
710 PRINT "          ENERGY "; ENERGY: PRINT
720 FOR I = 1 TO N
730 U(I) = V(I): REM FOR FEEDBACK
740 NEXT I
750 ENERGY = 0
760 NEXT ITERATE
770 PRINT : PRINT : PRINT : PRINT
780 GOTO 360
790 R = RND(1)
800 IF R < .5 THEN R = 0 ELSE R = 1
810 RETURN
```

Figure 2

HEBB3P

```

10 CLS
20 INPUT "INPUT RANDOM SEED "; SEED
30 RANDOMIZE SEED
40 INPUT "ENTER THE NUMBER OF NEURONS (100 MAXIMUM) "; N
50 INPUT "DO YOU WANT TO ENTER THE INPUT VECTOR YOURSELF (1/YES 0/NO)? "; VECTOR
60 DIM T(100, 100), V(100), U(100)
70 REM FILL T(I,J) MATRIX
80 PRINT : PRINT : PRINT
90 INPUT "INPUT THE NUMBER OF MEMORY VECTORS (M=INT(.15*N) "; M
100 FOR MEMS = 1 TO M
110 PRINT "INPUT THE MEMORY VECTOR "; MEMS; "FOR THE HEBB MATRIX."
120 FOR I = 1 TO N
130 PRINT "V("; I; ")"
140 INPUT V(I)
150 U(I) = V(I)
160 NEXT I
170 FOR I = 1 TO N
180 FOR J = 1 TO N
190 T(I, J) = T(I, J) + V(I) * U(J)
200 IF I = J THEN T(I, J) = 0
210 IF T(I, J) > 1 THEN T(I, J) = 1
220 PRINT T(I, J);
230 NEXT J
240 PRINT
250 NEXT I
255 PRINT : PRINT : PRINT : PRINT : PRINT
260 NEXT MEMS
270 PRINT : PRINT : PRINT
280 REM FILL INPUT VECTOR U
290 IF VECTOR = 0 THEN 350
300 FOR I = 1 TO N
310 PRINT "INPUT U("; I; ")"
320 INPUT U(I)
330 NEXT I
340 GOTO 390: 'BEGIN CALCULATIONS OF OUTPUT VECTOR
350 FOR I = 1 TO N
360 GOSUB 640
370 U(I) = R
380 NEXT I
390 REM BEGIN CALCULATION
400 FOR ITERATE = 1 TO 8: REM THIS ALLOWS THE OUTPUT VECTOR TO BE FEED BACK
410 FOR I = 1 TO N
420 FOR J = 1 TO N
430 SIGMA = T(I, J) * U(J) + SIGMA
440 NEXT J
450 SIGMA = SIGMA

```

Figure 2 cont.

HEBB3P

```
460 IF SIGMA > 0 THEN SIGMA = 1 ELSE SIGMA = 0
470 V(I) = SIGMA
480 SIGMA = 0
490 NEXT I
500 IF ITERATE = 1 THEN 510 ELSE 550
510 FOR I = 1 TO N
520 PRINT U(I);
530 NEXT I
540 PRINT
550 FOR I = 1 TO N
560 U(I) = V(I): REM FOR FEEDBACK
570 NEXT I
580 NEXT ITERATE
590 FOR I = 1 TO N
600 PRINT V(I)
610 NEXT I
620 PRINT : PRINT : PRINT : PRINT
630 GOTO 280
640 R = RND(1)
650 IF R < .5 THEN R = 0 ELSE R = 1
660 RETURN
```

Figure 3  
Sample C code

```

/*****
/* Multiplication of two matrices */
/*****/
void Matrix_Multiply (float mat1[4][4], float mat2[4][4], float mat3[4][4])
{
    static int i, j, k;
    static float sum;
    for (i = 0; i < 4; i++)
    {
        for (j = 0; j < 4; j++)
        {
            sum = 0;
            for (k = 0; k < 4; k++)
            {
                sum += mat1[i][k] * mat2[k][j];
                mat3[i][j] = sum;
            }
        }
    }
} /* Matrix_Multiply(mat[4][4], mat2[4][4], mat3[4][4]) */
/*****
/* Make an identity matrix */
/*****/
void Make_Identity (float mat[4][4])
{
    static int i, j;
    for (i=0; i < 4; i++)
    {
        for (j = 0; j < 4; j++)
        {
            if (i == j)
            {
                mat[i][j] = 1;
            }
            else
                mat[i][j] = 0;
        }
    }
} /* Make_Identity(mat[4][4]) */
/*****
/* Cross product of two vectors */
/*****/
void Cross_Product (float x1, float y1, float z1,
                    float x2, float y2, float z2,
                    float *x3, float *y3, float *z3)
{
    *x3 = y1 * z2 - y2 * z1;
    *y3 = x2 * z1 - x1 * z2;
    *z3 = x1 * y2 - x2 * y1;
} /* Cross_Product(x1, y1, z1, x2, y2, z2, *x3, *y3, *z3) */

```

# STUDY OF THE C AND BASIC COMPUTER LANGUAGES AS WELL AS AN IN-DEPTH DISCUSSION OF CERTAIN MATHEMATICAL CONCEPTS

BARRY G. ROESTLER

## INTRODUCTION

The C programming language is often called a middle-level computer language because it combines elements of a high-level language with the functionalism of an assembler. As a middle-level language, C manipulates the bits, bytes, and addresses that the computer uses to function. Unlike BASIC, which can operate directly on strings of characters to perform a multitude of string functions, C can operate directly on characters. In BASIC, there are built-in statements to read and write disk files, while in C these procedures are performed by functions that are not part of the C language proper, but are contained in the C standard library. One benefit of C is that it has only 18 keywords to remember. Thus, C compilers can be easily written, so there is generally one available for the machine being used. Also, since C operates on the same data types as the computer, the code output is efficient and C can be used in place of an assembler for most tasks.

Neurons are living nerve cells and neural networks are networks of these cells. One example of a natural neural network is the cerebral cortex of the brain because it thinks, feels, learns, and remembers. In attempts to build

model. To study neural networks, two types of modeling have become prevalent. These two types are biological modeling and technical modeling. Because technical modeling allows for scenarios and components that may not be biologically possible, it is the type of modeling generally accepted by investigators working in areas of artificial neural networks and neurocomputers. The objectives of researching artificial neural networks are twofold. First, scientists wish to comprehend how the brain imparts abilities like perceptual interpretation, associative recall, common sense, learning, and reasoning. Also, researchers desire to understand and work with a subclass of neural network models that emphasize "computational power" rather than biological fidelity. Similar to the objectives of research, the motivations for artificial neural network research are also twofold. Foremost is the want to build a new breed of powerful computers (6th generation computers). Also very important is the desire to develop cognitive models that can provide a strong base for artificial intelligence. In figure 2 is a program known as Hebb3c (Rietman 164-5) that demonstrates a fundamental rule dealing with neurons. This rule, the Hebbian Learning Rule, was developed by psychologist Donald Hebb and states that changes in synaptic strengths are proportional to the activations of the neurons.

## METHODOLOGY

As this project had no specific objectives and was more research oriented, I spent most of the time reading programming books, trying sample programs, and learning about neural networks, set theory, and matrices. I spent many hours at the library reading, and the rest of the time I spent at the computer that was provided for me, a Zenith 125.

## RESULTS

During my eight weeks in the Avionics Laboratory, I learned much about the C programming language and some of the high level mathematics that go along with it. It has been a very worthwhile program, and I am glad that I have had the opportunity to participate in it the past two summers. I feel that it has given me invaluable experience in the mathematics and engineering fields as well as experience with the military and its structure.

## REFERENCES

- Berry, R.E. and B.A.E. Meekings. A Book on C. London, England: Macmillan Education Ltd., 1984.
- Blum, Adam. Neural Networks in C++. New York: John Wiley & Sons, Inc., 1992.
- Breuer, Josef. The Theory of Sets. Englewood Cliffs, New Jersey: Prentice-Hall, Inc., 1958.
- Fraenkel, Abraham A. Abstract Set Theory. Amsterdam: North-Holland Publishing Company, 1953.
- Lien, David A. The BASIC Handbook. San Diego, California: Compusoft Publishing, 1978.
- Purdum, Jack. C Programming Guide. Indianapolis, Indiana: Que Corporation, 1983.
- Rietman, Ed. Experiments in Artificial Neural Networks. Blue Ridge Summit, Pennsylvania: Tab Books, 1988.
- Schildt, Herbert. C Made Easy. Berkeley, California: McGraw-Hill, 1985.
- Vamuri, V. Artificial Neural Networks: Theoretical Concepts. Washington, D.C.: Computer Society Press, 1988.



ELECTRICAL ANALYSIS OF  $\text{YBa}_2\text{Cu}_3\text{O}_{7-x}$  SUPERCONDUCTING  
THIN FILMS AND BULK SAMPLES

Peter G. Kozlowski

Centerville High School  
500 East Franklin Street  
Centerville, Ohio

Final Report for :  
AFOSR Summer Research Program  
Materials Directorate  
Wright Laboratory  
Wright Patterson Air Force Base, Ohio

Sponsored by :  
Air Force Office of Scientific Research  
Boiling Air Force Base, Washington, D.C.

August 1992

# ELECTRICAL ANALYSIS OF $\text{YBa}_2\text{Cu}_3\text{O}_{7-x}$ SUPERCONDUCTING THIN FILMS AND BULK SAMPLES

Peter G. Kozlowski  
Centerville High School

## Abstract

High temperature superconducting thin films and bulk samples of the Y-Ba-Cu-O system were studied in order to characterize their electrical properties. The preparation of high critical temperature  $\text{YBa}_2\text{Cu}_3\text{O}_{7-x}$  films on single crystalline  $\text{SrTiO}_3$  and  $\text{Al}_2\text{O}_3$  was done by laser ablation. In all cases, c-axis oriented films with critical temperature of about 90 K were obtained. On patterned films we obtained a critical current density of  $10^6 \text{ A/cm}^2$ . Bulk samples, having a much larger cross-sectional area, exhibit lower critical current densities, approximately  $10^3 \text{ A/cm}^2$ . Both thin films and bulk samples were measured by a four point technique and were tested through a range of temperature from 77 K (liquid nitrogen) to 300 K (room temperature).

# ELECTRICAL ANALYSIS OF $\text{YBa}_2\text{Cu}_3\text{O}_{7-x}$ SUPERCONDUCTING THIN FILMS AND BULK SAMPLES

Peter G. Kozlowski

## INTRODUCTION

The electrical resistance of high temperature superconducting materials falls to zero when they are cooled to temperatures below critical which are still above the temperature of liquid nitrogen (77 K). This makes the superconductive transport properties of high critical temperature superconductors an important aspect for future applications. The electrical properties of these materials in both bulk and thin film form were measured by using a four-point technique capable of measuring very low values of resistance. The properties which were measured include the normal state resistivity as a function of temperature, the temperature at which the transition to superconductive properties occurs (critical temperature), and the maximum current (critical current) which can be carried by the material in the superconducting state before the material begins to show resistance.

## METHODOLOGY

Superconducting thin films were grown on  $\text{SrTiO}_3$  substrates by using an ArF excimer laser operating at a wavelength of 193 nanometers, pulse duration of 15 nanoseconds, and a repetition rate of 20 Hertz. The focussed laser beam was rastered across a rotating, stoichiometric  $\text{YBa}_2\text{Cu}_3\text{O}_{7-x}$  target with an energy density at the target of approximately  $1.5 \text{ J/cm}^2$ . The surface of the target was cleaned, prior to film growth, by ablating the target in situ for 5 minutes with excimer radiation. The target to substrate distance was 6 centimeters [1].

The single crystal  $\text{SrTiO}_3$  substrates were cleaned by rinsing in trichloroethylene, acetone, and methanol, after which they were subjected to a 30 minute ultraviolet-ozone treatment. After being loaded into the growth chamber, the substrates were heated to approximately  $850^\circ\text{C}$  in  $\text{O}_2$  (100 mTorr) for 30 minutes. Film growth was carried out at approximately  $750^\circ\text{C}$  in  $\text{O}_2$  (100 mTorr) and required 30 minutes [2]. The deposition rate was typically  $0.4 \text{ nm/s}$ , and the resultant film thickness ranged from  $0.6$  to  $0.9 \text{ }\mu\text{m}$ , as measured with a stylus profilometer. Immediately after deposition, the growth chamber was backfilled with  $\text{O}_2$  to a final pressure of 1 atmosphere. The resulting films were superconducting as grown and were wet-chemically patterned into a 4-probe structure which allows measurements of resistivity ( $\rho$ ) and critical current densities ( $J_c$ ). Then, four gold wires were attached to the sample with silver paint and it was annealed for 1 hour

at 400°C. The transport properties were then measured by this 4-point technique with the current leads and voltage leads being attached to the thin film as shown in Figure 1.

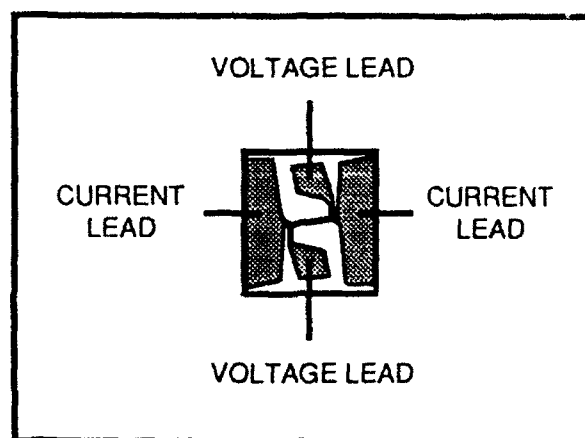


Figure 1. Schematic layout of a thin film prepared for transport measurements.

Bulk samples made of yttrium barium copper oxide were first prepared in a tube furnace under flowing oxygen. This procedure varies according to how long the sample is treated and at what temperature. The particular samples that we measured were made of 1-2-3 ( $\text{YBa}_2\text{Cu}_3\text{O}_{7-x}$ ) + 5 weight percent of  $\text{Y}_2\text{BaCuO}_{7-x}$  (2-1-1), and silver. The pelletized sample underwent a melt-process procedure consisting of many steps at different parameters. First, the sample was heated to 1055°C and remained at this temperature for approximately 30 minutes. Second, the temperature was lowered to 1015°C and remained there for 20 minutes. Then at the rate of 2°C/hr, temperature was rapidly lowered to 960°C. Finally, at a rate of 240°C/hr the temperature was ramped to room temperature. Annealing of sample took place for two days at 450°C under flowing oxygen. The pellet was then cut into a rectangular small bar using a diamond saw. On average, a bulk sample has the dimensions of approximately 5 mm (length) by 2 mm (width) by 1 mm (thickness). The four leads attached to the bulk sample may have different configurations as shown in Figure 2.

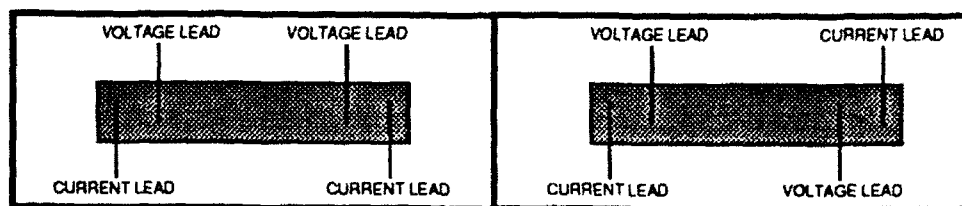


Figure 2. Schematic layout of bulk sample prepared for transport measurements.

The transport measurements were carried out by using the four probe technique on both the bulk samples and thin films. In both cases, a voltmeter showed the readings between the two voltage leads and a current source of 10 mA was applied across the superconductor with an ammeter which took readings through the current leads. A thin film connected in this way is shown in Figure 3.

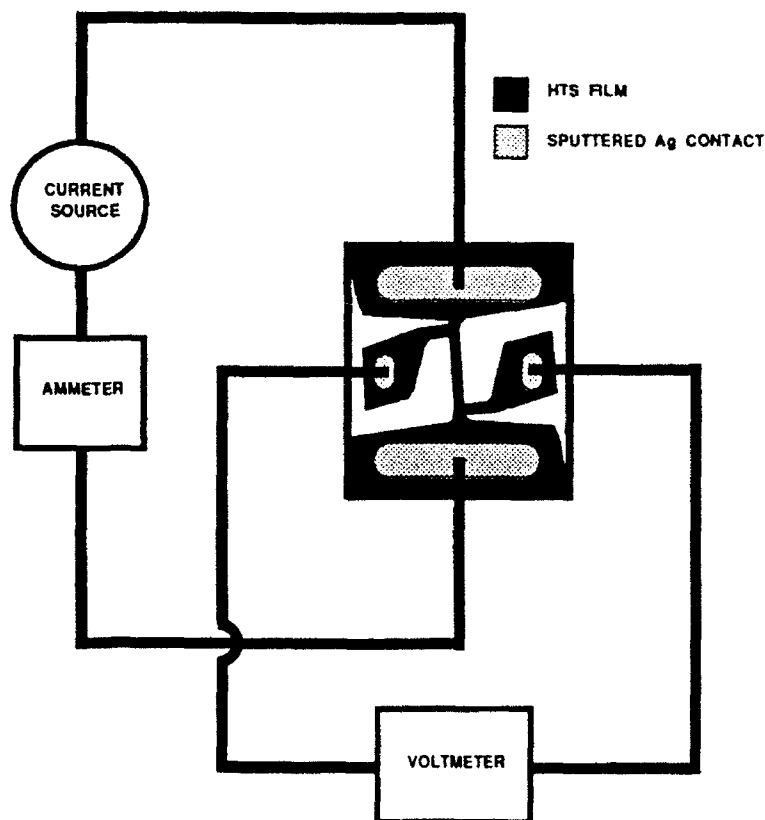


Figure 3. Four-probe technique for transport measurements.

This four wire measurement technique is capable of measuring very low values of resistance [3]. All experiments are completely automated with computer control to set the sample temperature, set the sample current, and collect all current and voltage readings. The properties which are measured include the normal state resistivity, the critical temperature, and the critical current density.

## RESULTS

The normal state resistivity were measured as a function of temperature from room temperature down to the temperature at which the transition to superconductive behavior occurs

(the critical temperature). High-quality  $\text{YBa}_2\text{Cu}_3\text{O}_{7-x}$  thin films grown in-house by pulsed laser ablation with transition widths of about 1 K have been measured. The resistivity curve (Figure 4) of one of the measured samples shows a critical temperature of 90 K.

## RESISTIVITY

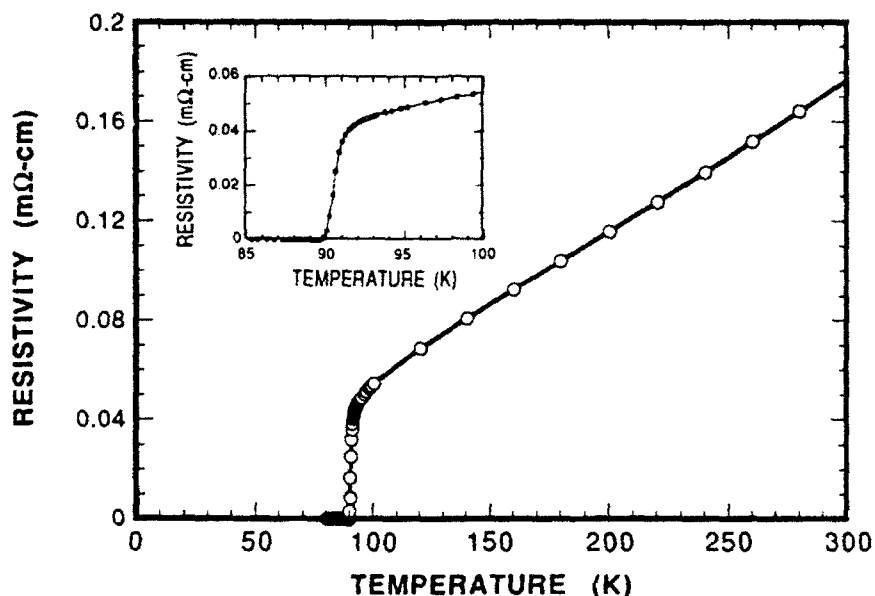


Figure 4. Resistivity versus temperature dependence.

To calculate the resistivity of a thin film or bulk sample, the formula :

$$\text{Resistivity} = \frac{R \cdot A}{l}$$

was used where  $R$  is the resistance of the sample in  $\text{m}\Omega$ ,  $A$  is the cross-sectional area, and  $l$  is the distance between the voltage leads [4]. Again, the resistivity curve is used for indicating the critical temperature of the sample.

The voltage as a function of current was measured at different temperatures to determine the maximum current (the critical current) which can be carried by the material in the superconductivity state before the material begins to show resistance. High quality thin films grown in-house have critical current densities of  $5 \cdot 10^6 \text{ A/cm}^2$  at 77 K (Figure 5) shows a typical voltage versus current graph of a sample. Keeping the temperature constant at 20 K, 40 K, 60 K, 70 K, 77 K, 85 K, and

89.5 K, the current value is increased and voltage is measured. In superconducting state, the material has no voltage and thus explains the primary superconducting principle that the material's resistance also equals zero. According to Ohm's Law,  $V=IR$  and thus  $R=V/I$ . When different current values are run through the sample at and below its critical temperature, the voltage is zero. And so, mathematically, when voltage equals zero in the equation  $R=V/I$  ( $I>0$ ), any value of current will give a resistance of zero [5]. At temperatures above the critical temperature, the voltage becomes greater than zero and thus the material has resistance.

## CRITICAL CURRENT DENSITY ( $J_c$ )

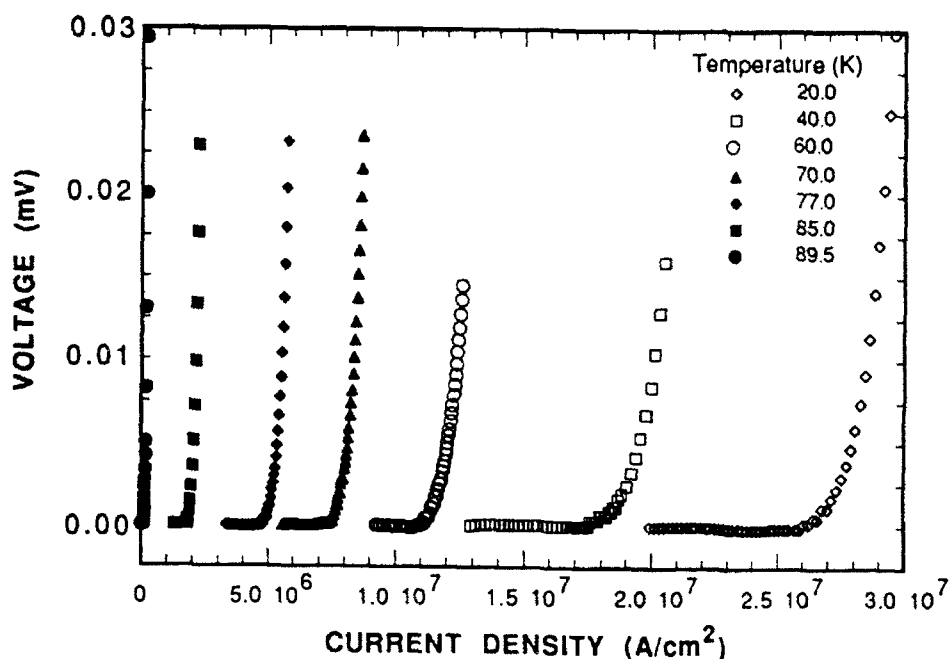


Figure 5. Voltage versus current density.

The critical current density of a sample is calculated as follows :

$$\text{Critical Current Density} = \frac{I_c}{A}$$

where  $I_c$  is the critical current and  $A$  is the cross-sectional area of the sample.

Two other methods were used to determine the quality of the films. One is x-ray diffraction which is used to determine the crystallographic orientation of the films. No phases other than the  $\text{YBa}_2\text{Cu}_3\text{O}_{7-x}$  were observed in any of the films. The x-ray data for the films with high critical current densities show strong peaks of reflections indicating a preferential orientation of the c-axis

perpendicular to the surface of the film. Another method used was scanning electron microscopy which was used to examine the film surface microstructure. Films with high critical current densities have relatively smooth and continuous surfaces with no visible granular features. They also contain surface features which appear to be inclusions about 1 $\mu$ m in diameter. Further investigations of these surface features and methods of avoiding their formation are in progress.

## CONCLUSION

The expanding field of superconductivity has accomplished numerous successes since the first high temperature ceramic superconductor was discovered and developed by Miller. Currently, more and more pressure is placed upon the study of the properties of superconductors in order to learn how they differ and compare to ones made earlier and to be able to apply them to technological uses which will certainly benefit society in the years to come. The WL/MLPO laboratory has expanded into one of the leaders in the field of superconductivity and has by far had some of the best results in its research.

In conclusion, the thin film and bulk sample superconductors produced here at Wright-Patterson Air Force Base have excellent transport properties with an enormous potential for future applications.

## REFERENCES

- [1] D.W. Chung, I. Maartense, T.L. Peterson, P.M. Hemenger, J. Appl. Phys. **68**, 3772 (1990).
- [2] I. Bransky, J. Bransky, I. Maartense, T.L. Peterson, J. Appl. Phys. **66**, 5510 (1989).
- [3] H. Adrian, C. Tome-Rosa, G. Jacob, A Walkenhorst, M. Maul, M. Paulson, M. Schmitt, P. Przyslupski, G. Adrian, M. Huth, T. Becherer, Supercond. Sci. Technol. **4**, 166 (1991).
- [4] G. Adrian, W. Wilkens, H. Adrian, M. Maul, Supercon. Sci. Technol. **4**, 169 (1991).
- [5] G. Deutscher, K.A. Muller, Phys. Rev. Lett. **59**, 1745 (1987).



**COMPUTER RESOURCES  
EXAMINING THE WORKINGS OF A  
COMPUTER NETWORK**

**Daniel J. Kramer**

**Final Report for:  
High School Apprenticeship Program  
Wright Laboratory**

**Sponsored by:  
Air Force Office of Scientific Research  
Bolling Air Force Base, Washington , D.C.**

**August 1992**

COMPUTER RESOURCES  
EXAMINING THE WORKINGS OF A  
COMPUTER NETWORK

Daniel J. Kramer

Abstract

This investigation involved the study and experiences of operating and maintaining a large computer network at a government facility such as Wright Patterson Air Force Base. The work was as varied as assembling computer hardware, to installing computer software, and to backing up computer file systems and disk partitions. While this is just a small part of the overall operations in this facility its importance in keeping the computers running and up to standards is a key to complete performance.

COMPUTER RESOURCES  
EXAMINING THE WORKINGS OF A  
COMPUTER NETWORK

Daniel J. Kramer

INTRODUCTION

The Computer Resources Team works to keep the computer network functioning so that others in the laboratory can accomplish the tasks necessary on the computer system for their research and other projects. Among their responsibilities is experimenting with enhanced computer productivity, finding and fixing bugs in programs and in the network, and developing more effective ways of running and maintaining the computer network. Working with this Team has given new insights into understanding the functions and capabilities of computers by themselves and when working together over a complex network.

DISCUSSION

Working for eight weeks in this setting proved to be a different experience for myself as I had very little in actual computer experience to fall back upon. I knew a little DOS and had experience using word processors but other than that I was off to a fresh start. Add to that the complexities of learning a new operating system, UNIX, and at first I was wondering how long I was going to last.

My first task was working with part of the computer resources team assembling a system of computers. This included installing memory cards and graphic cards, adding disk drives and other external SCSI devices. After the system was completed software was installed on to the computer's hard drive. The software package consisted of MS-DOS, WINDOWS, PCTools, Harvard Graphics, Microsoft Word, Microsoft Power Point, and other software as needed or requested by the user of the new system. There was a total of eight systems, some more complex than others with the number of external devices and amount of software, and assembly and installation was not accomplished without its share of problems, but we finally finished what we had started.

My next major task was to learn how to use UNIX to a point where I could perform some minor tasks on the operating system. After reading manuals, experimenting with the commands on my terminal, and then rereading the manual to find out what I had done wrong, I felt that I had a semblance of what I was doing and more importantly what I was supposed to be doing. Taking self tests with the manuals increased my proficiency and soon I could handle the incoming information as it came to me and could also understand what task I was performing before I executed it, not after it had already started.

Using this new information I was ready to work on a new problem, backing up file systems on part of the network. Backing

up the file systems was necessary to protect against possible loss of files by users or even worse against a possible system crash or an attack by a virus in which most if not all the files could be damaged or destroyed. The files would be backed up on to a cartridge tape according to which disk partition they were located on and the amount of information present in that partition. Each tape could contain up to 150Mb of information so partitions that took up more than that amount of space would require more than one cartridge tape to back up. Using a no rewind option a group of partitions that took up less than 150Mb of information could all be dumped onto one tape. The following is a list of the disk partitions backed up and the number of cartridge tapes required for the dump procedure.

- a. /dev/rsd0a     /
- b. /dev/rsd1g     /home2
- c. /dev/rsd1h     /homepc     1st four on one tape
- d. /dev/rsd2e     /home3
- e. /dev/rsd0g     /usr           2 tapes
- f. /dev/rsd0h     /home1          3 tapes
- g. /dev/rsd2f     /apps1          2 tapes
- h. /dev/rsd2g     /home5          1 tape

The partitions were to be dumped on a weekly basis to insure that an up to date archive of all files would be available for use in case of possible loss. Two sets of tapes were to be used,

one the first week, the second the next week, and from then on alternating on a biweekly basis.

The command used to initiate the dump procedure involved first bringing the entire system down to single-user mode and then entering the following command line.

```
dump 0ucdtsf 1250 18 570 /dev/rst0 /dev/{disk partition}
```

The arguments after the initial dump text specify the dump level, in this case a full dump of all files in the partition, the use of a cartridge tape, the density, tracks, and size of the cartridge tape being used, and to which device the output is being sent to. In the case of the four partitions being dumped to one cartridge tape where the no rewind option was used a small change was entered in the command text. The portion of the text is shown below.

```
570 /dev/nrst0 /dev/r
```

After all the partitions were dumped successfully to the tape the tape must be rewound using the following command line.

```
mt -f /dev/rst0 offline
```

The process of dumping all eight partition took approximately 3.5 to 4 hours to accomplish and many problems initially occurred. Among them were finding cartridge tapes with no write fail errors on them, learning how to successfully use the no rewind option in conjunction with the dump command, and realizing that for a completely successful dump to occur we had to drop the

system down to single user mode.

After the dump procedure was completed The next step was learning how to restore a file, a directory, or a partition in case of a possible accident or system failure. This process was as lengthy and as full of trial and error as was the back up process using the dump command. The final process involved a series of steps to determine where the file, files, or directory was located and then copying them to an existing directory. To list all the files located on a particular cartridge tape insert the tape in the drive and enter the following command.

```
restore tf /dev/rst0
```

To verify that a particular file is located on the cartridge tape the above command was typed followed by the name of the file being searched for.

```
restore tf /dev/rst0 {filename}
```

After verifying the presence of the file, files, or directories, they can be copied to an existing directory. First the directory was changed to that of where the file was to be copied. Then to copy the file the following command line was entered.

```
restore x /dev/rst0 {filename}
```

The "x" tells the restore command to copy the file, files, or directories. After the procedure was completed the tape was rewound and taken offline by using the command from above.

```
mt -f /dev/rst0 offline
```

After the procedures were successfully completed a short, but detailed, instruction manual was written up to be placed in a "bible" of all system procedures for referencing for future use. During the time until I completed my research tenure I was to complete this weekly task. Using the manual as a reference for the first time I also taught a contractor the procedure for after I left the establishment.

This process taught the efforts of trial and error when learning a new procedure for a computer system. Each system is different and the manufacture's manuals do not always have specific instructions for the exact hook-up of hardware that is present on the system being worked on. So through repetition of the procedure with each attempt trying something a little different to accomplish the exact goals. And after time a workable solution is found and can be used for the system.

Upon finally completing this task I went about some smaller projects around the Computer Resources Lab. Among them was installing DOS 5.0 on several of the computers around the High Speed Aeromechanics Division and updating other software to run in conjunction with DOS 5.0. I also spent more time learning about the workings of a UNIX system and also attempted to learn something about C language and UNIX's C shell where script files are developed and written. I did not have time to put to practice the new knowledge I had learned but hopefully in the future



I will have a chance to put this and all the other information that I have gained through this program to good use.

# FORCED LIQUID COOLING OF A NON-FLUSH SIMULATED ELECTRONIC CHIP

Joel Kulesa  
Archbishop Alter High School  
Kettering, OH

John Leland  
Wright Laboratory  
Wright Patterson AFB, OH

Final Report for:  
Summer Research Program  
Wright Laboratory

Sponsored by:  
Air Force Office of Summer Research  
Wright Patterson Air Force Base, Dayton, OH

August 1992

# FORCED LIQUID COOLING OF A NON-FLUSH SIMULATED ELECTRONIC CHIP

Joel Kulesa  
Archbishop Alter High School  
Kettering, OH

and

John Leland  
Wright Laboratory  
Wright Patterson AFB, OH

## Abstract

The properties of forced liquid semiconductor cooling were studied. Previous experiments have shown how the elevation of a semiconductor into a flow channel caused a cooling efficiency change. Initially, when the chip was raised from flush, the efficiency dropped. After a few more millimeters were exposed the efficiency started rising. Eventually the efficiency rose to a higher level than the flush model. To further study this effect and to isolate the physical forces involved, a new heater design was implemented. The new prism shaped foil heater was designed to eliminate the increased surface area caused by the elevation of the IC. Due to the continuing nature of this experiment, results and conclusions have not been reached as to how the new heater affects cooling efficiency.

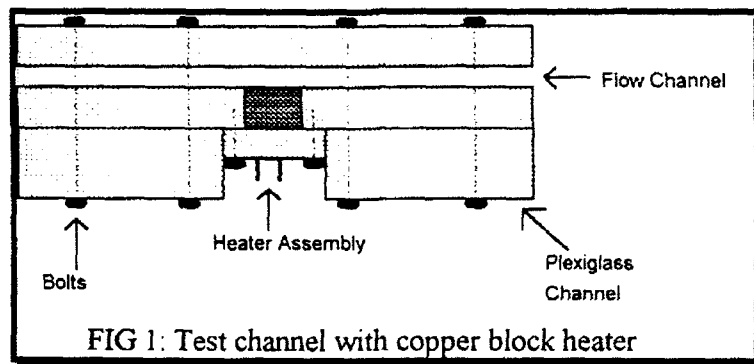
# FORCED LIQUID COOLING OF A NON-FLUSH SIMULATED ELECTRONIC CHIP

Joel Kulesa  
and  
John Leland

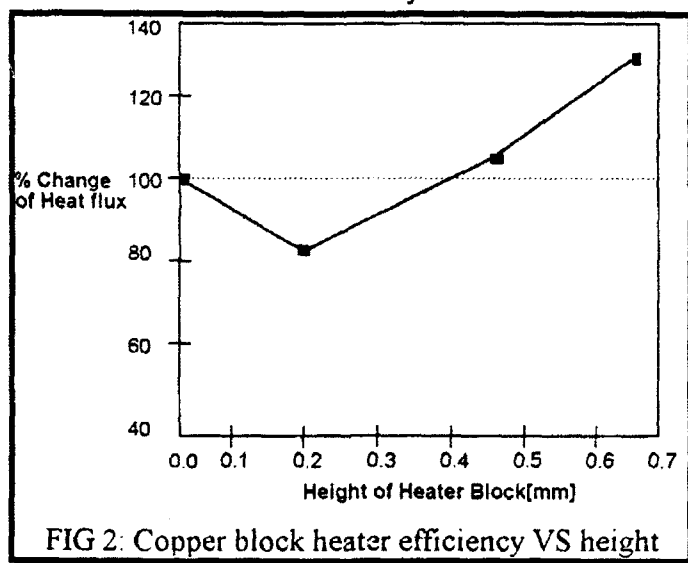
## *Introduction*

Not more than a few years ago, aircraft control systems were primarily mechanical systems that were heavy and cumbersome. Currently, though, these mechanical systems are being phased out and replaced by electrical counterparts. These new electrical components are of great benefit since they are more reliable, more efficient, and much smaller. Unfortunately, electronic devices are not the perfect solution since they create a large amount of heat. This heat, once built up, can cause inaccuracies, component malfunction and system failure. Since the benefit of electronics outweighs the heat problem, the next logical step would be to build some kind of heat transfer system to remove the heat from the electronics and deposit it to the outside shell of the aircraft. One method of heat removal is forced air circulation -- such as commonly used in ground based computer equipment. This method is unsatisfactory due to the low thermal conductivity and heat capacity of air as well as the high density of components in an aircraft. Rather than pumping air over ICs, researchers realized that pumping a high thermal conducting liquid would remove excess heat far more efficiently. Since this liquid may be in contact with live electrical circuits, one property that this kind of liquid must have is a high dielectric constant. In past experiments by John Leland, a 3M product called Fluorinert was used since it exhibited all the desired thermal and electrical properties. In his most recent experiment, John Leland used a simulated IC chip (copper block heater) in a channel to test the effectiveness of forced liquid flow cooling. (See FIG. 1) The chip was placed

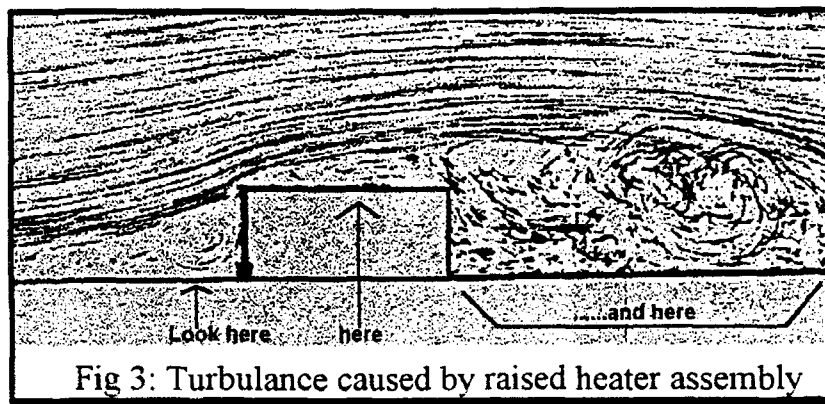
flush with the surface of one side of the channel and Fluorinert was pumped through at 4 m/s at 20°C. However, since achieving a perfect flush fit would not be practical in a real application due to thermal expansion, contraction and vibration; the simulated chip was extended into the channel at various heights to see how height affects cooling efficiency. As FIG. 2 shows, when the



chip was initially nudged out to 0.2 mm the thermal efficiency dropped 20%. But when the simulated IC chip was extended by 0.4 mm the thermal efficiency equaled that of the flush chip. And when the chip was brought out to 0.6 mm the thermal efficiency was 20% higher than the flush model. It would initially



appear that the increased surface area of the simulated chip caused the increase in efficiency. However, that interpretation could not explain the initial drop in efficiency. As well, the increase in efficiency was more than the few millimeters of extra surface area could explain. Not only that but anytime a liquid flows over a projection, such as the simulated IC, chaotic turbulence results. (See FIG. 3) This turbulence could be the cause of the unusual efficiency response. To further understand the forces at work a new experiment was designed to isolate the turbulence.



## Apparatus

The isolation of the turbulence was carried out by implementing a completely new heater design. The design, as shown in FIG. 4, was primarily a prism shaped foil heater with insulators on both sides, mounted on a base piece. These insulators prevented the Fluorinert from being heated from the sides, hence the surface area of the heater was limited to the top. With this configuration the heater could be used solely to test the thermal effects of turbulence in the channel. Before this could happen, though, the performance characteristics of the new heater had to be analyzed.

To analyze and calibrate the foil heater, a software program was written for a newly acquired Hewlett Packard 3852A Data Acquisition unit. The programming of the

HP3852A was done in a modified version of BASIC called HP BASIC. Just like regular BASIC, the language is poorly structured, slow, and inflexible, but it communicated flawlessly with the IEEE interface that the HP 3852A used. The software heater calibration program, once written and debugged, measured the temperature of the foil and related it to the resistance. The foil heater was submerged in a temperature regulated bath along with several thermocouples which monitored the temperature closely. Then the bath controller was linked to the computer through an RS-232 port. As the program slowly increased the temperature of the bath, it monitored the thermocouples and the resistance of the foil heater. This calibration data was written to disk to be used later with the main data acquisition program.

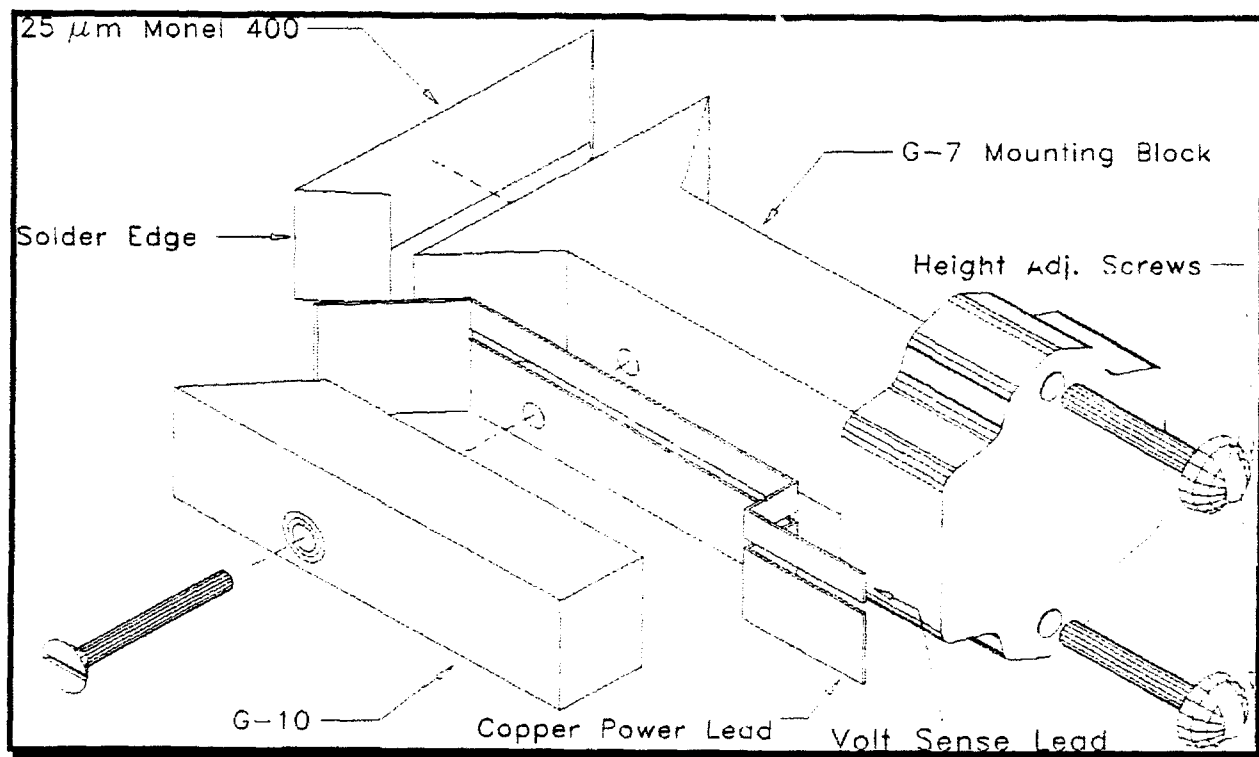


FIG 4: New foil heater design

The use of a foil heater versus a copper block heater caused a significant problem. The copper block had a high heat capacity, so if the experiment thermally "ran away" or was unable to cool the block effectively, at the most, a half-minute could pass before any damage would be done to the heater block. On the other hand, the Monel foil heater had an extremely low heat capacity. If the experiment thermally "ran away" with a foil heater, the heater would last only a few seconds before self-destructing. A half-minute was enough time for one to manually shut down the experiment, but several seconds hardly allowed for human reaction time. An automatic shutdown ability was needed to turn off the foil heater within seconds of a runaway condition.

With the previous experiment using the copper block heater, a Fluke Helios I data acquisition device coupled to LabTech Notebook software, read and stored the experimental data. However, neither the software nor the hardware was capable of shutting down the system as specified. So it was decided to abandon the Fluke device and to use the HP 3852A Data Acquisition Unit with HP BASIC. Virtually no software was written for the HP 3852A so all data acquisition work had to be programmed in HP BASIC before any further experiments could be run. By writing the software in-house, performance and customization (i.e. the auto shutoff routine) could be easily modified and implemented.

The HP BASIC data acquisition program's job was to log and graph real time data from a wide variety of sensors and inputs. The list of sensors included: Four type T thermocouples, two type K thermocouples, three voltmeter readings, and a frequency counter. The raw data from these sensors wasn't of much use(for real time graphing) until it was processed by the program. For example, to find the speed of the Fluorinert passing through the channel, the frequency measurement was interpolated into a flow rate in Gallons Per Minute(GPM). Then that figure was calculated into a measurement



in meters per second. The program then displayed and stored the final calculated value. A similar process was performed for many of the other inputs as well, such as: converting measured voltage into a current, interpolating a voltage into a pressure measurement, or calculating heat flux from several sensors. In addition, the program used data from the foil heater calibration program(above) to determine the foil heater surface temperature. Last but most importantly, the program checked for temperature over range. When any one of the four type T thermocouples exceeded  $100^{\circ}\text{C}$ , the program sent a "CLOSE" command to a relay bank in the HP 3852A. That relay bank, in turn, was hooked to a safety shutoff on the heater power supply. Once the program tripped the power supply, the only way power could be re-applied to the heater would be to manually reset the supply. Upon adding the automatic shutoff, the program was ready to receive data.

## Conclusions

Due to the ongoing nature of this experiment no results or conclusions have been made as of this writing. However, one realization was made during the setup of the experiment. The use of custom computerized data acquisition software made gathering and reducing data quick and powerful. Other acquisition methods such as commercial software programs or data loggers proved to be either too slow or far too inflexible for the demands of this experiment. Computerized data acquisition made this experiment possible by allowing for reasonably fast sampling rates, real-time calculation and graph plotting, accurate data logging, and reliable safety interlocks. These features make computerized data acquisition an important link when running experiments in a modern laboratory.

USING MATHEMATICAL CONCEPTS TO PRODUCE  
THREE DIMENSIONAL COMPUTER GRAPHICS

Allen L. Lefkovitz  
High School Student

Dayton Christian High School  
325 Homewood Avenue  
Dayton, OH 45404

Final Report for:  
High School Apprenticeship Program  
Wright Laboratory

Sponsored by:  
Air Force Office of Scientific Research  
Wright Patterson Air Force Base, Dayton, Ohio

August 1992

# USING MATHEMATICAL CONCEPTS TO PRODUCE THREE DIMENSIONAL COMPUTER GRAPHICS

Allen C. Lefkowitz  
High School Student  
Davton Christian High School

## Abstract

My summer apprenticeship in the Avionics Laboratory involved both the generation and analysis of three dimensional data. Using Mathematica - a system for calculating and graphing numerical, symbolic, and algebraic iterations - I first plotted a three dimensional circle showing a shift in the data and then displayed the data in a graphical image. Also at this time I recorded planes landing and taking off so that another apprentice, Eric Powers, could use this data in his project. After learning the principles of Forlan G. I determined a way to write mathematical data to a file for later use. My first set of mathematical programs created and converted cylindrical data into rectangular or xyz coordinates. The next set of programs detailed the creation and conversion of spherical coordinates into rectangular coordinates. Once I stored rectangular coordinates of a cylinder and a sphere in data files, I reconstructed a graphics project written by my mentor, Eric Powers, so that the data could be plotted onto a screen in a recognizable pattern. My apprenticeship ended with processing longitude and latitude data of a scanned circle into rectangular coordinates so that it could be plotted.

# USING THE BORLAND C++ 3.0 TO VISUAL THREE DIMENSIONAL COMPUTER GRAPHICS

Allen L. Lefkowitz

## Introduction

With the increasing use of computers in business, government, art, entertainment, education, research, training, and medicine, graphical displays are in demand. While most graphics programs can be used to create graphs and charts, their most important use is designing models that quickly and easily display vast amounts of data. Unlike two dimensional graphics, clearly representing a third dimension is quite complicated.

When plotting three dimensional images, there are many possible coordinate reference systems including Cartesian, spherical, and cylindrical. Another consideration of graphics involves the view or perspective of the user. The perspective can be greatly enhanced or hindered by removal, hidden-surface removal, and shading.

## Discussion of Problem

During the first weeks of this summer, I had to use Mathematica to evaluate equations, build arrays, matrices, and tables, and finally, plot the data. As I began to learn C, I noticed many similarities to the computer languages I already knew, and certain basic rudiments frustrated me. The main problem that I dealt with this summer involved how I could use Borland C++ to create and graph data of various

shapes. While I originally wrote programs that would deal with a cylinder or a sphere, eventually I needed a program that could transform real data such as a scan of an engine.

### Methodology

While working with Borland C on a 486dx, I not only had to deal with coordinate conversions, but also I had to revise a graphics program so that it could organize and hold large amounts of data. In order to obtain the various coordinates I had to locate and rearrange various mathematical equations. A key to handling the necessary data not only involved graphic mode commands, but also orderly and recursive loops.

### Results and Conclusions

After rearranging the mathematical equations and writing code that would properly collect, organize, and disperse the data, observation of three dimensional shapes on the screen was finally possible. In order to clarify the image, I worked with various view points, sizes, and region of interests. Even though different parts of the image are extremely clear when they are first drawn, by the time all the points are plotted some of the detail is no longer apparent.

## REFERENCES

- Berry, R.E. and B.A.E. Meekings. A Book on C. London: Macmillan Education, LTD, 1984.
- Hearn, Donald and M. Pauline Baker. Computer Graphics. Englewood Cliffs, New Jersey: Prentice-Hall, Inc., 1986.
- Leestma, Sanford and Larry Nyhoff. PASCAL Programming and Problem Solving. New York: Macmillan Publishing Company, 1987.
- Roberts, Cornel K. and Curtis F. Gerald. Computer Graphics: The Principles Behind the Art and Science. Irvine, California: Franklin, Beedle & Associates, 1989.
- Schildt, Herbert. C Made Easy. Berkeley: McGraw-Hill, 1985.
- Stevens, Roger T.. Graphics Programming in C. Redwood City, California: M & T Publishing, Inc., 1989.
- Swokowski, Earl W.. Calculus With Analytic Geometry. Boston: Prindle, Weber & Schmidt, Incorporated, 1975.
- Waite, Mitchell, Stephen Prata, and Donald Martin. C Primer Plus. Indianapolis: Howard W. Sams & Co., Inc., 1984.
- Wolfram, Stephen. Mathematica - A System for Doing Mathematics by Computer. Reading, MA: Addison-Wesley Publishing Company, Inc., 1988.

IMAGE ANALYSIS: A FRACTAL APPLICATION

Jason Eric Lindsey  
High School Apprentice  
Advanced Guidance Branch

Wright Laboratory Armament Directorate  
WL/MNGA  
Eglin AFB, Florida 32542-5434

Final Report for:  
High School Apprenticeship Program  
Wright Laboratory Armament Directorate

Sponsored by:  
Air Force Office of Scientific Research  
Bolling Air Force Base, Washington, D.C.

August 1992  
IMAGE ANALYSIS: A FRACTAL APPLICATION

Jason Eric Lindsey  
High School Apprenticeship Program  
Advanced Guidance Branch  
Wright Laboratory Armament Directorate

ABSTRACT

Through intense research into the nature and applications of fractals and fractal geometry, it was theorized that fractal geometry may have a useful application to image analysis. By analyzing an image for fractal dimension, areas in the image with low dimension or areas with integral dimension may be isolated. In this way, man-made objects may be isolated from natural background clutter. Code was written to perform this task. The code utilized the Hurst Dimensional Estimation Method and was rendered on Turbo Pascal. The method is intended for use on several types of imagery (LADAR, SAR, IR, etc.) and is a possible candidate to aid in sensor fusion for more efficient, more effective autonomous seeker technology.



## INTRODUCTION

The theories that form the foundation upon which fractal geometry is built would indicate that Euclidean geometry is inadequate to define the vast majority of objects in the chaotic world of nature. On the other hand, man-made objects are quite simply defined by standard euclidean curves and planes. Therefore, by employing fractal dimensioning techniques, one may differentiate between naturally occurring and man-made objects. These ideas were happened upon as we strove to gain an understanding of the ATLAS (Advanced Technology LADAR System) Program and its supplement, LADAR (Laser Radar). Extensive research was done into the area of fractal geometry and an understanding of how fractal geometry could be used in image analysis, and, more specifically, in target acquisition was gained. A code was then developed to perform the necessary analysis on an image file to determine the fractal dimension over the image and to, hopefully, isolate all man-made objects from the naturally occurring background clutter. The research and code development were done under the supervision, and with the aid of, my mentor Lt. Matt Whiteley. Bill Eardley also gave tremendous assistance as I struggled to learn, understand, and implement the Turbo Pascal programming language. The following are explanations of the application of fractal geometry to image analysis and of the code developed as a result of that application.

## APPARATUS

To aid in my project I used a 486 Zenith desktop work station. The pure research portion was achieved using several reference books and articles on fractals and on fractal geometry. The programming was done on the 486 using Turbo Pascal 5.0. The TP resource manual and reference guide were, therefore, among the most extensively utilized sources. Also helping with my project were several individuals who were familiar with fractal geometry, or with Pascal programming, or with the LADAR system, or with all of the above.

## BACKGROUND

To begin the background research to my project, extensive research into the nature of fractal geometry, fractal dimensions, and image processing was done. Much of the theoretical research was accomplished by my research partner and fellow high school apprentice, Lesha Denega. By applying the principle knowledge gained through our research to image processing, a new way to process and analyze a visual image was conceived and subsequently applied to image processing for weapons systems.

Image processing associated with weapons systems is concerned with detecting, acquiring, and recognizing targets for the weapons system. They are, therefore, often

concerned with methods to distinguish man-made objects from natural objects. Kim T. Constantikes, a senior staff engineer in APL's Fleet Systems Department, published an article in The Johns Hopkins APL Technical Digest in November of 1991 entitled "Using Fractal Dimension For Target Detection in Clutter." Constantikes reported on research and experimentation that he had done using fractal dimensioning techniques to analyze images in the infrared form. Notable in his research efforts was the use of fractal dimension imaging to differentiate a T-38 airplane from a background of an ocean surface. This was significant considering the solar glint from the water's surface and the interference that it would cause in the infrared imaging technique.

Inspiration was taken from the article and from Mr. Constantikes' methodology. Although he had used the techniques described to analyze infrared data, it was determined that, with some adaptation, similar techniques could be employed on LADAR returns, which have an x, y, and z value for position in space. Man-made objects, which are made up of Euclidean curves and planes, should exhibit a fairly simple fractal dimension, or one approximately equal to two. Naturally occurring objects, on the other hand, are not adequately defined by simple Euclidean concepts and will, therefore, return a higher, more complex fractal dimension. Thus, relying upon our first principle knowledge of the nature of fractal dimension, an appropriate

thresholding value may be selected to segment the image. The goal of such thresholding and segmentation is to isolate man-made objects from natural objects in the target acquisition stage.

The Hurst Dimensional Estimation Method was selected for further consideration as a candidate to achieve the aforementioned, as per Mr. Constantikes' example. The method involves looking at the same image at several scales of resolution to find the sum of the variations over a series of sub-areas of the image. This is accomplished using a function  $M$ , which is defined at  $A$ : the sub-area being considered, and  $R$ : the resolution of the image within that sub-area. This function,  $M(A,R)$  is related to the dimension  $D$  by the following equation:

$$R \cdot M(A,R) = K \cdot R^D$$

where  $K$  is a constant,  $R$ ,  $A$ , and  $D$  are as above. The resolution and the areas are such that the sub-areas cover the entire original image:

$$A = \{y: iR \leq x < (i+1)R\}$$

where  $A$  and  $R$  are as above and  $i$  is chosen such that the complete area  $A$  is covered. The maximum and minimum values for each area  $A$  is determined and the difference of the maximum value and the minimum value is summed up over all the sub-areas (this is the value of  $M$ ):

$$\text{Calculate } M(A,R): \sum_i (\text{Max}[A_i] - \text{Min}[A_i])$$

The function for Capacity,  $C$ , is thus defined as:

$$C = R \cdot M(A,R) \text{ and (from above) } C = K R^D$$

Now, manipulating the first equation, we divide both sides by the value of R:

$$R * M(A, R) = K R^D$$

$$M(A, R) = K R^{D-1}$$

Then, taking the natural log of each side, remembering that K is a constant, and then taking the partial derivative of the equation with respect to  $\ln R$ , we are left with a value for D-1:

$$\ln M(A, R) = (D-1) * \ln R + \ln K$$

$$\frac{\delta \ln M(A, R)}{\delta \ln R} = D-1$$

Therefore, a log versus log plot of M versus R will yield a linear relationship. A least square fit is utilized to determine the slope of the line formed, and that slope is equal to the value D-1. The dimensional estimate, D, is thereby derived.

Research was done on other dimensional estimators and the Hurst Dimensional Estimator Method (as defined above) was selected for use with the program. By using this method, and given a two-dimensional pixel-registered scalar field, a corresponding image of lower resolution that indicates the fractal dimension variation across the initial image may be developed. The function M is used iteratively at differing resolutions and scales and the least square fit mentioned earlier is used to isolate the fractal dimension at that sub-area of the initial image.

## METHODOLOGY

Once an understanding of fractal dimensions, the Hurst Method, and image analysis had been achieved, we began to formulate a code to perform an appropriate algorithm. The code was developed using Turbo Pascal 5.0 and my rendering of the code relied upon the sagacious guidance of Lt. Matt Whiteley and Bill Eardley. Representing my first major programming effort, the code represents many tedious hours of work and is the culmination of a personal triumph of my own.

Code development took place over the span of approximately four weeks and was an evolutionary process. Following the "top down planning, bottom up programming" doctrine, the code was developed using small, fundamental procedures and functions to constitute the "meat" of the program. Once the minor tools were completed, they were tied into the portions of the code with larger scope, the portions that actually control the code's operation. The final program had three major procedures that utilized the smaller functions and procedures. The three are as follows: a procedure to process imagery to create fractals dimension arrays from the initial image, a procedure to display image files as well as dimensional image arrays, a procedure to convert image files and dimensional image arrays to GrafTool format for 3-dimensional viewing (GrafTool being a commercial software package for 3-D image rendering and

viewing). Among the minor functions and procedures are: functions to get max and get min from area, a procedure to rescale images and arrays to convenient size, a procedure to read data files, a procedure to write output files, a procedure to calculate the value of the function M, a procedure to perform a least squares fit, a function to get the dimensional value from the least squares fit information.

The major procedure, and the actual objective of the program, is the procedure called the "Dimensional Image Generator," which processes images to create the corresponding dimensional image array. Due to memory restrictions, the procedure can take in any square array of resolution 64x64 or less. The image is partitioned and the value of the M function is found for an 8x8 block that traces over the original image one pixel at a time. Thus the resulting dimensional image has a resolution of 50x50. The M function is calculated in each 8x8 at  $R=8$ ,  $R=4$ , and  $R=2$ . The value of M is, therefore, calculated 7500 times as the program is run. The value of  $\ln M$  is plotted against the value of  $\ln R$  for each R on a log-log plot. The least square fit determines the slope of the resulting line and assigns that value to the value of  $D-1$ . The value of D, the dimensional estimation, is thereby calculated for the centroid of each 8x8 block.

The code and the final program were successful. Supplemental programs were written to create images of known

fractal dimension, images of varying dimension, and random image backgrounds that have objects overlaid onto them. All of these images were rendered and treated as if they were of ATLAS format (containing x, y, and z values for position in space). SAR imagery (infrared-based) was also used with the program and the results were encouraging. The type of processing used in this program may be used with any number of imaging techniques (passive IR, LADAR, SAR, Radar, etc.), demonstrating fine credentials as a candidate for sensor fusion technology. Real-time targeting and automated target acquisition may greatly benefit from this sensor fusion capability and from the application of fractal dimensioning to image processing.



# REFERENCES

Briggs, John and F. David Peet. Turbulent Mirror. Harper and Row, New York; 1990.

Constantikes, Kim T. "Using Fractal Dimension for Target Detection in Clutter," The Johns Hopkins APL Technical Digest. Vol. 12, No. 4, 1991.

Gleick, James. Chaos: Making a New Science. Penguin Books, New York; 1987.

# **Analysis of Fractal Image Compression and Decompression**

**Daran J. Mason  
High School Apprenticeship  
Guided Interceptor Technology Branch**

**Wright Laboratory Armament Directorate  
WL/MNSI  
Eglin AFB, FL 32542-5434**

**Final Report for:  
High School Apprenticeship Program  
Wright Laboratory Armament Directorate**

**Sponsored by:  
Air Force Office of Scientific Research  
Bolling Air Force Base, Washington, D.C.**

**August 1992**

## Analysis of Fractal Image Compression and Decompression

Daran J. Mason  
High School Apprenticeship  
Guided Interceptor Technology Branch  
WL/MNSI, Eglin AFB

### Abstract

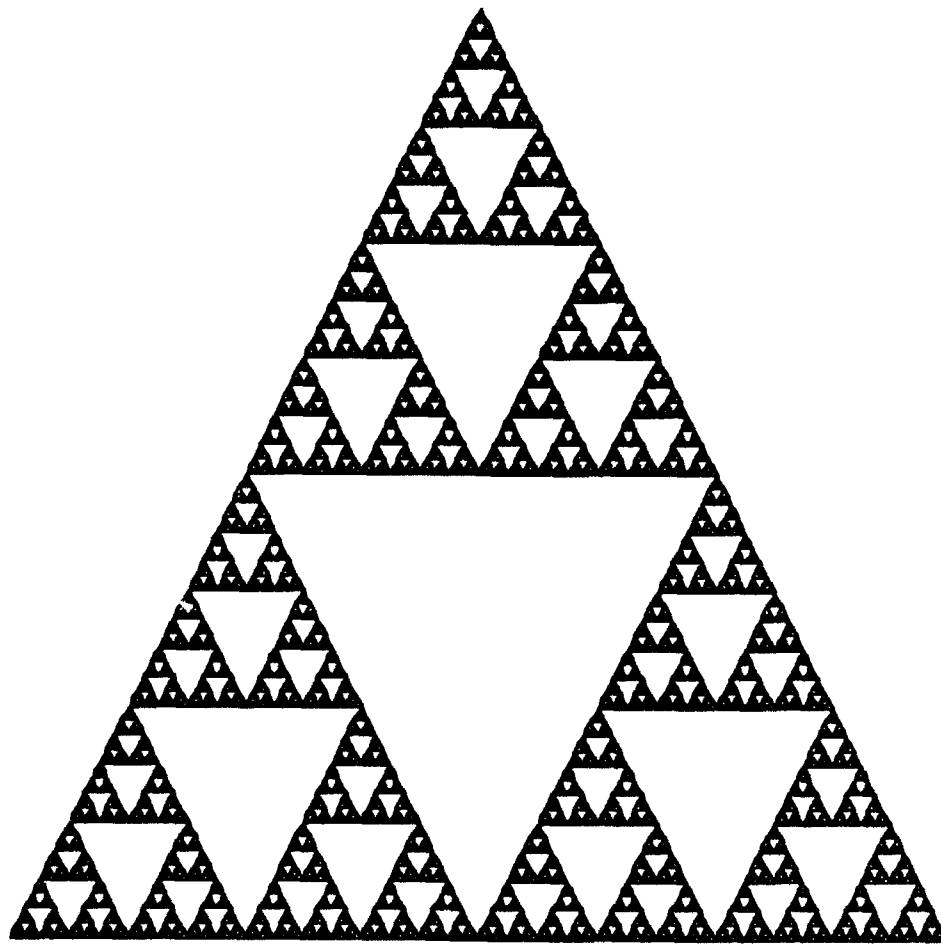
Fractals are a form of higher mathematics and Benoit Mandelbrot described it in its simplest form. He coined the term "fractal" to mean a broken structure possessing similar-looking forms of many different sizes. (Anson) The problem associated with this project was not one that I had to solve, but was given to Iterated Systems Incorporated (ISI) of Atlanta, Georgia. The problem is that image storage on a computer takes up massive amounts of memory. A method was needed to somehow "compress" the storage process to use less space. This was the task of ISI. The exact process of Fractal compression and decompression cannot be released, because it is proprietary to ISI. I didn't have a problem to solve, but two tasks. Task one was to process images through a hardware compression board and decompress images using software. Task two was to validate the results ISI reached and follow-up on some of the conclusions.

Daran J. Mason

### Introduction

It is hard to describe the analysis of fractal image compression and decompression without first understanding fractals. Fractals are a form of higher mathematics and Benoit Mandelbrot described it in its simplest form. He coined the term "fractal" to mean a broken structure possessing similar-looking forms of many different sizes. (Anson) The best way to describe what Mandelbrot said is by using the Sierpinski Triangle (Figure 1). At a glance, this triangle looks like a complex form of triangles, but if you look at the very top, you will notice one very small triangle.

# Sierpiński



# Triangle

Figure 1

This triangle was used as a pattern to create the whole picture. First, you take one triangle and shrink it about fifty percent. Then you triplicate the triangle pattern and place the three new triangles to resemble the original triangle. Repeat this process using the new pattern to create a newer triangle and so on to create a more complex geometrical figure. One of these triangles or group of triangles is a fractal of the whole figure. Fractal theory was used in the compression process by dividing an image into equal square blocks called "domains." The first domain block is compared to the rest of the image for some kind of relationship between them. Once this relationship is found, codes describing it are stored in memory. This process is repeated for every domain square. (figure 2). Until the entire image is compressed. Decompression reverses the process. The image is rebuilt

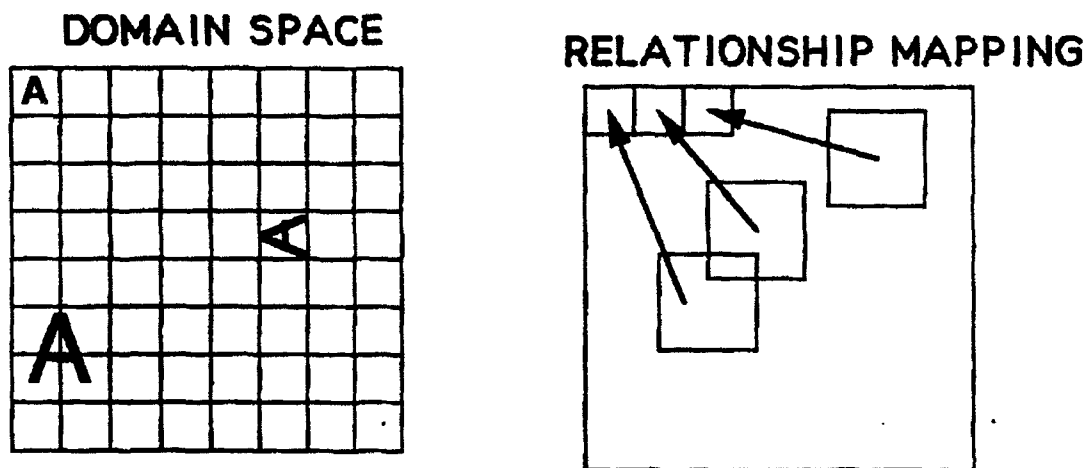


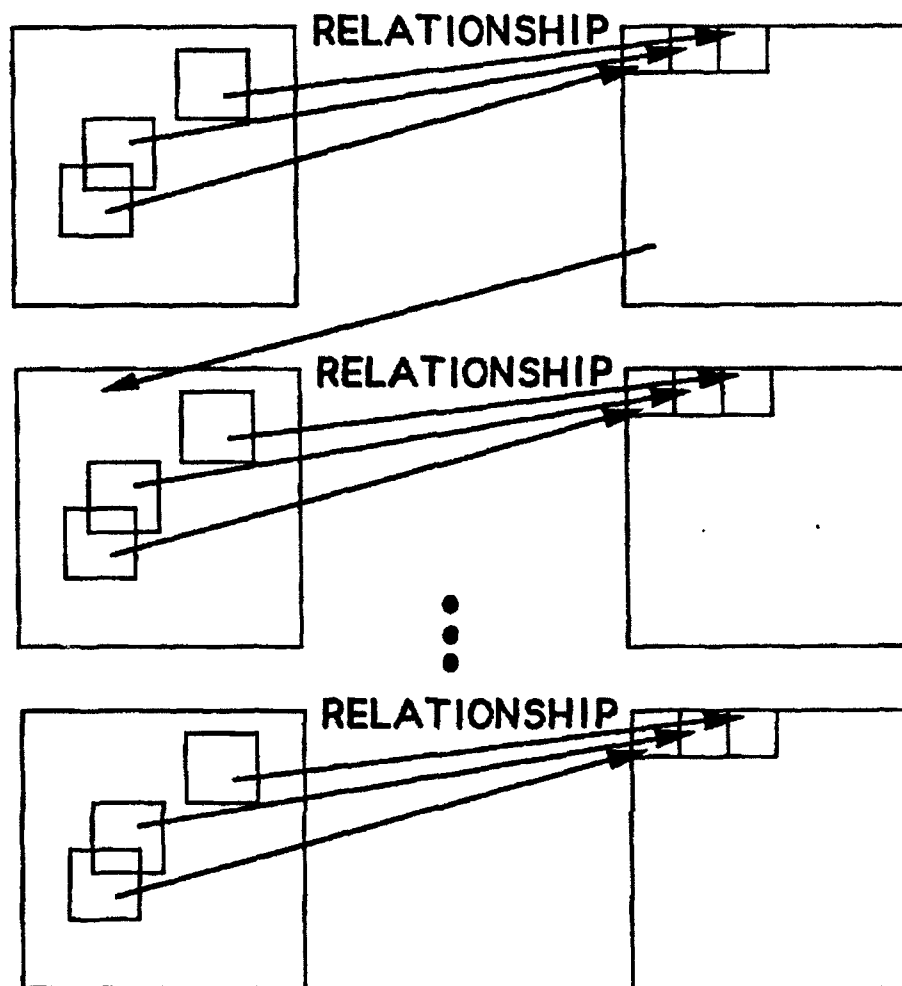
Figure 2

using the stored relationship data by an iterated mathematical scheme (figure 3). The exact process of Fractal compression and decompression cannot be released, because it is proprietary to Iterated Systems Incorporated (ISI) of Atlanta, Georgia.

The problem associated with this project was not one that I had to solve, but was given to ISI. The problem is that image storage on a computer takes up massive amounts of memory. A method was needed to somehow "compress" the storage process to use less space. This was the task of ISI. To give you a simple analogy, a computer monitor display of a straight line about 640 pixels long would usually take 640 bytes of memory, one byte per pixel, but compressed to a 40:1 ratio, it would only take two bytes of memory. This is possible, because the compression scheme would store the line as an equation rather than a line. So, all the computer would store in memory are the coefficients "m" and "b" in the equation  $y = mx + b$ , equation for a straight line (figure 4). This is a simple example. For a more complex example see attachment A, a jet fighter. Before the image was compressed it required 768 kilobytes (kb) of memory for storage, after an 80:1 compression ratio it only required 9.8kb. This picture was compressed by using the method described earlier. All other images that I worked with were compressed in this manner.

INITIAL IMAGE

NEW IMAGE



STOP WHEN DIFFERENCE IS WITHIN DESIRED ACCURACY

Figure 3

Problem

I didn't have a problem to solve, but two tasks. Task one was to process images through a hardware compression board and decompress images using software. Task two was to validate the

$$y = mx + b$$

---

640 bytes: one per pixel

VS

2 bytes: "m" and "b"

Figure 4

results ISI reached and follow-up on some of the conclusions.

### Methodology

Both, the hardware compression board and software used for decompression were developed by ISI and were installed on an IBM 386 computer with a VGA monitor. The compression board was built by ISI as a prototype to process 24 bit color images. This board does not meet the Air Force unique requirements, but serves well as a test board. The program written by ISI to run the compression process was very user friendly. The program allowed the user to select from thirty-five different images. The user could choose one of three different ways of converting a sixteen bit image map to a twenty-four bit image map. First, two color conversion method which divides the image into eight bit words and maps. Second, YUV color method which maps each 16 bit word into a 24 bit bit YUV encoded data word. Finally, eight bit conversion method which divides the 16 bit words into upper and lower eight bit values. YUV conversion was chosen as the best method. The image also had to be converted from a 1280x800 pixel size to four 640x400 images. Dividing the image into four quadrants was necessary to match the existing compression hardware. Speed at which the compression runs was also a choice. The speed varies from one to five. For speeds one through four, the user can select the file size for which the compressed image will be stored. For speed five (quick) which is the fastest, The program selects the file size for the compressed image. Many different analyses can be chosen in the program menu; Sobel analysis (detects boundaries), Roberts analysis (highlights edges), statistical analysis (absolute RMS error, standard deviation, percent RMS error, bias, total intensity difference), signal to noise ratio, spatial filter image, and calculate centroids. The database files outputted by the program were downloaded from the 386 to a Macintosh spreadsheet. Then the data was arranged into bar charts for easier reading. A Tektronics 4693 wax printer was used to print images for comparison since two images could not be brought up at the same time on the computer screen. Also three new images of target vehicles were created in the branch using a SUN computer and then compressed and decompressed for analysis.

### Results

The program written by ISI exported the results of analysis selected in the analysis menu to image files or record sheets in a database file. One option in the compression program was for the computer to make a difference image. The computer made an image of the difference in pixels of the original image compared to the decompressed image. These images were used to help determine in what areas the compression process was having problems. Most of the images did not exhibit any problems. One of the background images that was a problem is shown in figures 6, 7, and 8. These figures show the original image, the compressed/decompressed image and the difference image. Results of the statistical analysis was converted to bar charts comparing the seven groups in different areas (figure 9) Some errors existed in the transfer of data into record sheets by the computer. In most cases it would output three record sheets where there should only be one record sheet. The

first only having the input image file name, the second having the input name and the output name, and the third having all the data requested. Other problems with outputting data was that if you tried to compress two different images at the same time the program would give the same output name for both images in the record sheets. The three new images created in the branch did not have very good results. They did not look the same when displayed on the IBM. Also, there were a lot of differences in the image difference file for these three images.

### Conclusions

Here are some of the conclusions reached by ISI that I validated and some concluded by myself. ISI's conclusion that error increases when compression ratio increases is correct. We also agree that a compression ratio of 37:1 is a good tradeoff between file size and image quality. I disagreed when ISI said that background images compressed well. From my results I concluded that sometimes background images do well and other times they do not. The problems associated with three new target images created on the SUN could not be concluded. Problems found in the output of record files and with the new target images were brought to ISI's attention in a technical discussion the week of 17 august 1992 by my mentor. Their conclusion on average RMS was correct. More detailed description of conclusions cannot be discussed, because the information is either proprietary or export controlled. From my validation I conclude that ISI's compression process works well, but some fine tuning needs to be done.



# Original Background Image

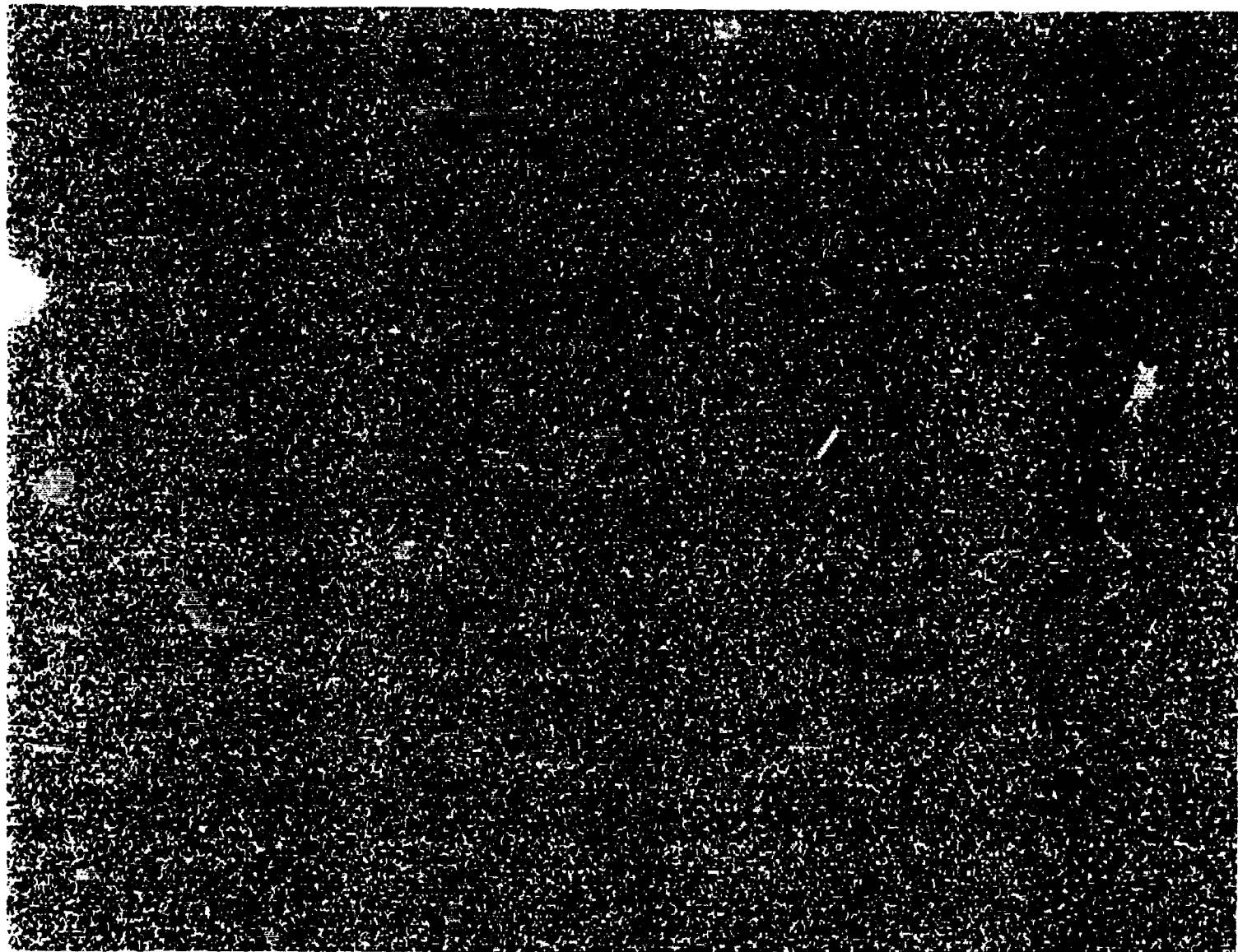


Figure 6

# Compressed/Decompressed Background Image

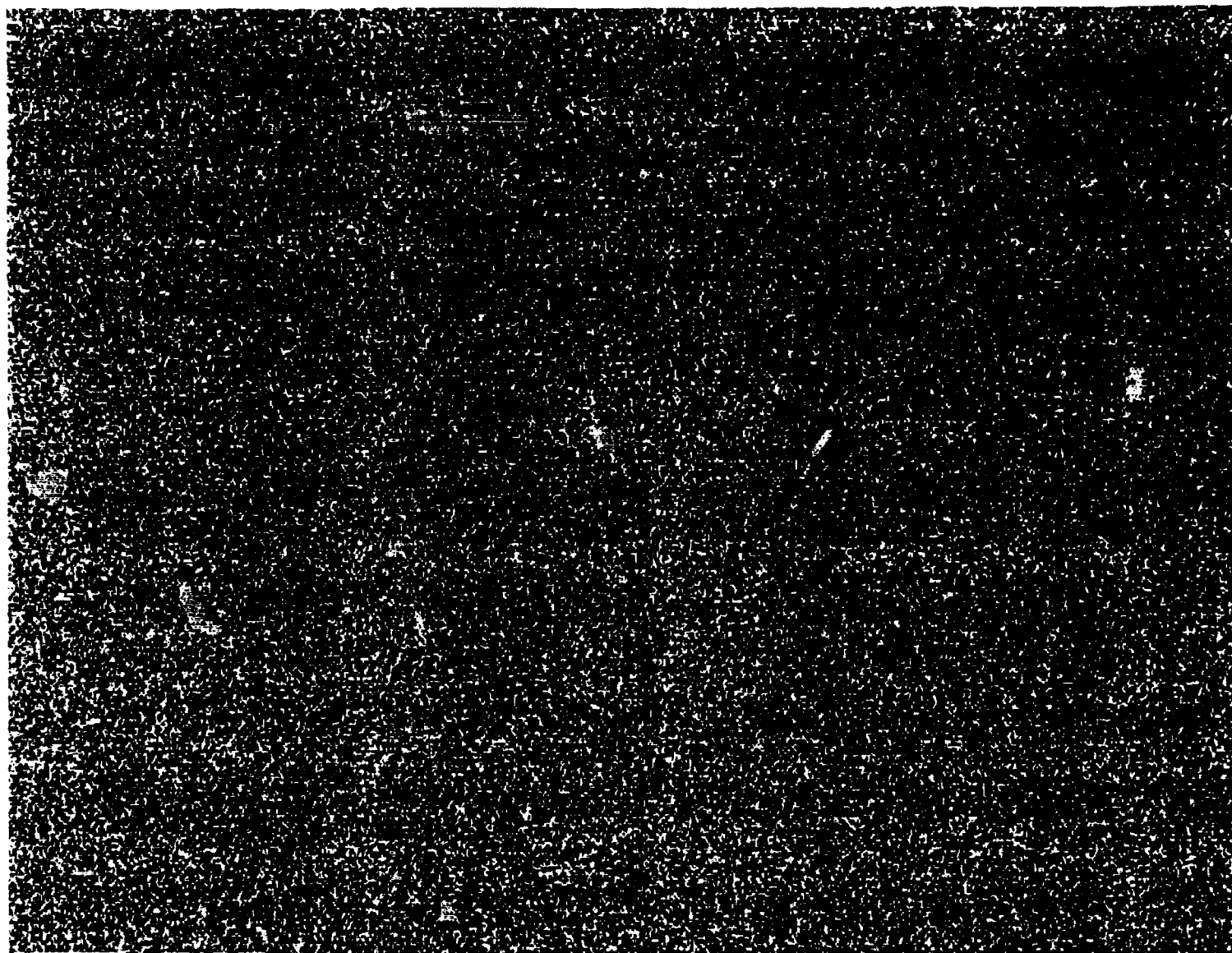


Figure 7

# Background Difference Image

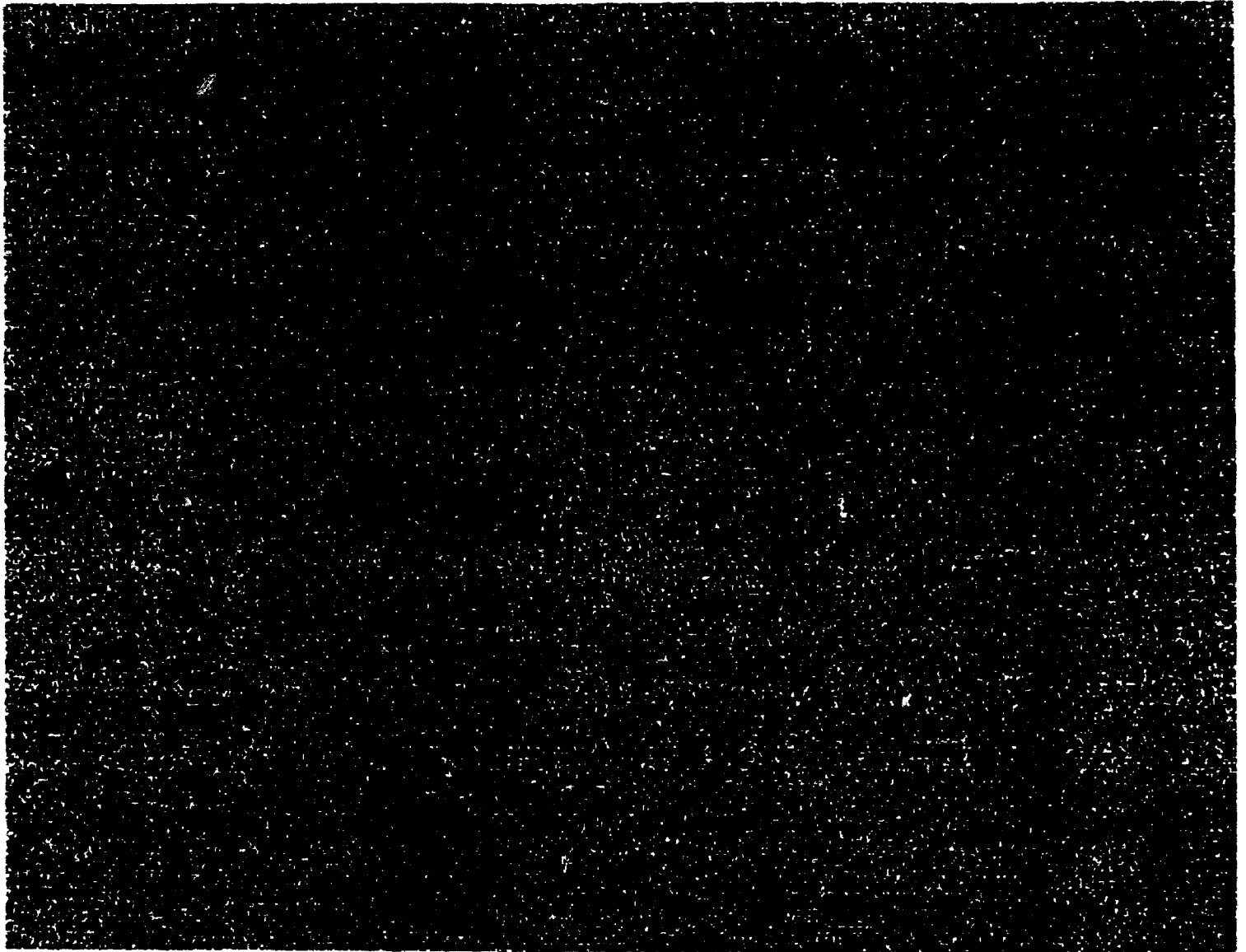


Figure 8

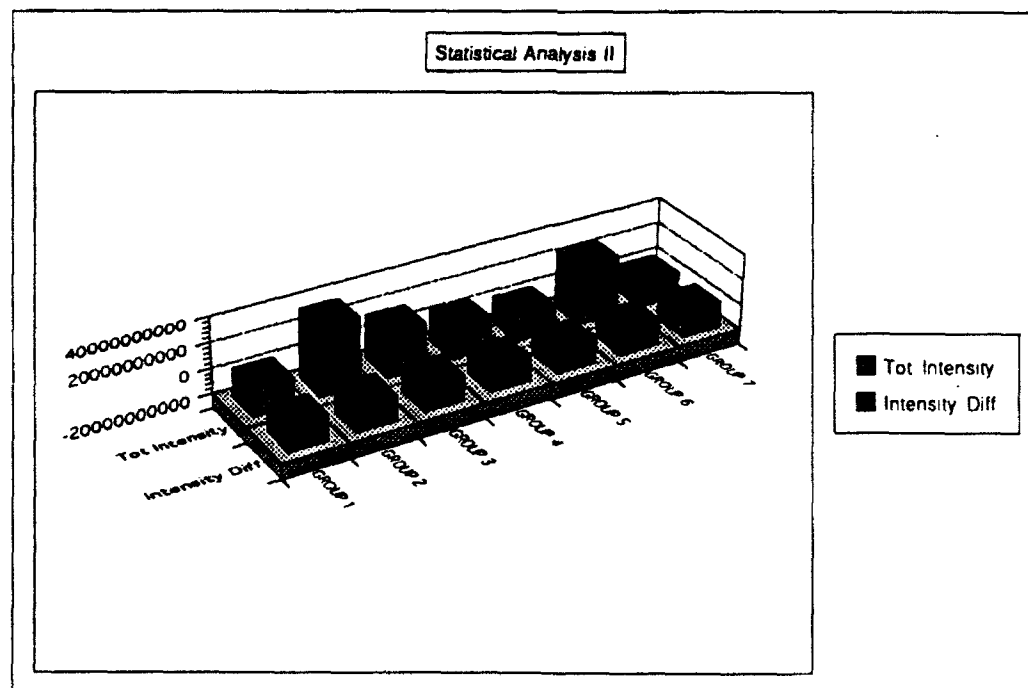
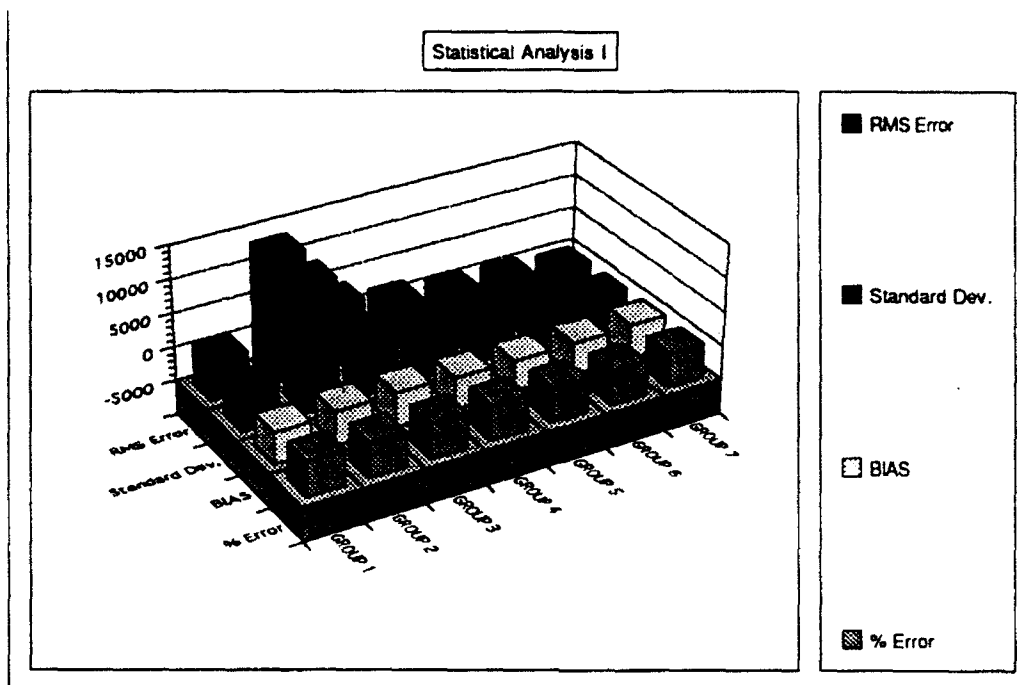


Figure 9

## REFERENCES

Anson, Louisa and Barnsley, Michael, "Graphics Compression Technology", Sunworld: October 1991, p 47.

## ACKNOWLEDGEMENTS

I would like to thank the following people; Mr. Mel Nagel, my mentor, through his teaching, I learned a lot this summer. Not only in the fractal compression field, but also in program management, money management, basic computer use and abuse and many many other useful topics. Capt. Allen Andrews for his great get-aways. "without" him being here I wouldn't have had a place to sit. I also enjoyed an in depth lecture in a variety of topics. Mr. Craig Ewing who was my mentor last year, but that wasn't his fault. But I appreciate him for listening to the noisy wax printer in his office that I used now and then. Lee Murrer for talking to me every week or two, just when I thought I had the hang of it, he would come in and ask me a question that would blow my mind. Tom Rathbun for being my second Macintosh guru, right after Mel. Cliff Nees for being my guru on everything else which I hope will help me in college. Mr. Bob reassuring my thought that there are weird people in science and engineering. Ron Rapp for a great day of basketball. The ultimate frisbee guys who introduced me to some ultimate frisbee. Randy Jones who let me know there are tall people who speak German in electrical engineering. Dennis Garbou who created some more images for me when I thought I was through. Christina Trossbach who would not let me forget the word "pity" and "airhead" this summer. Eric Apfel and JJ Kahrs who taught me how to fix my computer and how to really mess it up. Last but not least Mrs. Debbie Welch, even though she owns two, not one, but two corvettes she is the best imaginary skier in a office that I have ever seen. Keep on hoppin!!

SCANNER NOISE  
ELIMINATED BY  
COMPRESSION  
PROCESS



SCANNER NOISE  
ELIMINATED BY  
COMPRESSION  
PROCESS



Attachment A

VIDEO DOCUMENTATION OF THE  
PATRAN TO EPIC LINK

Elliot Moore II  
High School Apprentice  
Warheads Branch  
Mentor: Mr. Mike Nixon

Wright Laboratory Armament Directorate  
WL/MNMW  
Eglin AFB, FL 32542-5434

Final Report for:  
High School Apprenticeship Program  
Wright Laboratory Armament Directorate

Sponsored by:  
Air Force Office of Scientific Research  
Bolling Air Force Base, Washington D.C.

August 1992

## VIDEO DOCUMENTATION OF THE PATRAN TO EPIC LINK

Elliot Moore II  
High School Apprentice  
Warheads Branch  
Wright Laboratory Armament Directorate

### ABSTRACT

My summer was spent working as an apprentice in the computational mechanics section of the warheads branch in WL/MMW on Eglin Air Force Base. My mentor was Mike Nixon and my project centered around the video representation of EPIC (Elastic Plastic Impact Computations) hydrocode capabilities. The graphics capabilities of PATRAN was used as a post processor. Through the use of various "session" files, several different EPIC sample simulations were demonstrated. Through the use of Silicon Graphics machines, these sample simulations were comprised of various "picture frames", known as RGB files. These files were put together and used to animate the EPIC simulations on videotape.



## VIDEO DOCUMENTATION OF THE PATRAN TO EPIC LINK

Elliot Moore II

### INTRODUCTION

The most essential portion of this paper centers around the use of hydrocodes. Hydrocodes are lengthy and complex computer programs that use continuum mechanics concepts to simulate warhead formation, warhead penetration, and target responses. Graphics software like PATRAN allow output data to be organized and more easily interpreted. The hydrocodes have the capability to simulate an experiment for analysis by the engineer or scientist. EPIC, which stands for Elastic Plastic Impact Computations, is only one type of hydrocode. It contains thirteen different sample problems to demonstrate its abilities. These sample problems are briefly discussed in APPENDIX A. However, it does require a post-processor program for graphic representation. One such program is PATRAN, which can also be used as preprocessor when calculating unique three dimensional geometries.

### METHODOLOGY

The methodology includes creating a series of "snapshots" of a simulation, capturing each of these to a file then transferring these "snapshots" to magnetic tape. These are then replayed in chronological order to give the illusion of motion. These "picture frames" are attained through the use of a "snapshot" function, known as "getit."

The first step in the movie making process is the responsibility of the EPIC. The engineer develops an input file describing the geometry and initial

conditions and then runs EPIC. EPIC can generate neutral files which are files that make data compatible with PATRAN. These can be three different types of files that are generated by EPIC91 for use by PATRAN. There are MODEL Files, ELEMENT Files, and NODE Files. The MODEL Files, as their name suggests, contain the geometry of the object or objects to be simulated. It is a "skeleton" drawing of the object consisting of a number of points called nodes that are connected by lines to form elements. In PATRAN the nodes can be grouped and colored by various parameters. For example, the elements representing the explosive can be colored red, while the elements representing the case wall can be colored white, and so on. The ELEMENT Files contain the data associated with each element such as pressure, stress, or strain.

In order to use these neutral files, a PATRAN Session file is created. A SESSION file is merely a list of PATRAN routines and commands that will allow PATRAN to operate without having a user present. In actuality, a SESSION file is created every time PATRAN is used. Every command that the user executes during the time they are using PATRAN is saved and stored as a "patran.ses". This will allow the user to repeat everything he did before, using the SESSION file. An example of a SESSION file is contained in APPENDIX B. The way to make a SESSION file is to use PATRAN manually first. The user must "act" out what it is he wishes PATRAN to do. It is, in essence, like showing by example. The user must initiate the PATRAN program to begin. When the title screen appears there will be four different commands at the bottom of the screen: "GO, SES, STOP, HELP." The "GO" command will start manual operation of PATRAN. The "SES" command stands for "session" and is used after the

SESSION file has been created. The "STOP" command will end PATRAN and return to the prompt. The "HELP" command will give a list of topics and inquire as to which the user needs assistance with. To begin, the "GO" command is given. From here on, in an effort to be more user friendly, PATRAN offers numbered options at the bottom of the screen for the user to choose from. Therefore, much of the SESSION file is recorded in numbers, as seen in APPENDIX B. It is not necessary to explain the function of each of these numbers. In general, the SESSION file will include an interface with PATRAN that allows for the input of the MODEL file, first (Indicated as E08P01.MDL in APPENDIX B). After the MODEL file is inputted, the ELEMENT file is inputted (Indicated as E08P01.ELE in APPENDIX B). PATRAN will display the results of each function as they are entered. Once the user is satisfied with the graphic display he has on the screen, he must stop PATRAN, thus ending the session. When the current directory is listed, there will be a file named "patran.ses.1", which will contain all of the commands he just implemented in PATRAN. Now, considering that there are, normally, at least 50 different MODEL files, and chances are, the user has only a few in his new SESSION file, he must find a way to extend his file to compensate for the others. On the Silicon Graphics machine, there are two different editor functions that can perform such a job: vi editor and jot. Both of these editing functions can be used to extend the PATRAN session file to compensate for all MODEL and ELEMENT files. Once the SESSION file has been extended to include all of the proper MODEL/ELEMENT files, a command is implemented into the session file to allow for the capturing of the RGB files (picture frames). The entire command is noted in APPENDIX B as "ui\_spawn\_command ("getit 001",true)." The "spawn" command is part of PATRAN's language, and the "getit" function is taking the snapshot of

what is on the computer screen at the time the session reaches that point. Now it is time to reenter PATRAN. When the title screen comes up this time, however, the user will type in "SES", instead of "GO", in order to begin the session. When "SES" is entered, PATRAN will ask for the name of the SESSION file. When the proper name is entered, PATRAN will begin to run the SESSION file, following each command, without need for further user intervention. When PATRAN has completed all of the commands listed in the SESSION file, it will stop and await further instruction from the user. If everything has run correctly, the user will be able to end the use of PATRAN by inputting the "STOP" command. The RGB files are saved in the directory specified by the "getit" function. On the Silicon Graphics machines, the RGB pictures can be redisplayed using the "ipaste" function. The command would be "ipaste 'name'.rgb#". In place of the "#" sign would be the number of the RGB file that is to be seen, because ipaste will only show one RGB at a time. Another feature available on the Silicon Graphics machine is the "movie" function which allows all of the RGB files to be seen in progression, one frame after the other, like a movie. The command for this is "movie 'name'.rgb\*". The star signifies that all of the RGB files are to be used. Once the user decides that the RGB files are all correct, they are all moved onto a tape using the "tar" command. The command is "tar -cv 'name'.rgb". The "-c" means that the RGB files are to be copied or created on the magnetic tape and the "v" tells the computer that the user wishes to see specific information about what is being copied. Once the RGB files are all copied onto the tape it is taken into a room which contains all of the recording equipment necessary to make the movie. This consists of a Silicon Graphics machine, with a video

controller board and a video tape recorder. The RGB files are extracted from the tape onto the Silicon Graphics computer with the board using the command is "tar -xv 'name'.rgb". The "-x" tells the machine to extract the information from the tape into the current directory and the "v" tells the computer to list specific information about the data being extracted. Once the RGB files are in the desired directory, the ANIMATE program can be run. The ANIMATE program, which automatically takes the RGB files and records them onto the video tape in the recorder, was developed by Mr. Randy Anderson, a computer scientist, from TEAS, located in the computation mechanics section. The ANIMATE program will ask a series of questions such as: the name of the RGB files, the directory path in which they are located, the number of RGB files, and how many frames per second the movie will be recorded in. The video tape recorder must be given certain settings before it can run properly. The most obvious is that there must be a tape in the machine. There is also a switch on the machine that allows for "local" or "remote" control of the machine. If the switch is on the "local" setting, this will allow for manual control by the user. On the "remote" setting, the machine operates itself. The machine should be in the "remote" setting in order for the ANIMATE program to work. For recording purposes, there should be a four to six second gap on the video tape between the starting point and the last movie that has been recorded or the beginning of the tape. Also, the counter on the machine should be reset to zero. Once all the preparations have been made, the ANIMATE program can be run, and the end result will be an animated representation of a hydrocode computation.

## **RESULTS AND CONCLUSIONS**

The results of my summer are seven PATRAN representations of EPIC sample

runs. All of the movies are recorded on one videotape to be used to demonstrate the PATRAN to EPIC link. As an addition to the regular movie making, PATRAN possesses the ability to make 3 dimensional representations of EPIC capabilities. The process is similar, yet a little more complex. A brief description of 3 dimensional movie making is contained in APPENDIX C. This summer I turned out 2 different 3-d movies: one of the Explosively Formed Penetrator (EFP) and one of the Shaped Charge. I have learned a great deal this summer. Most obviously, I learned how to use the PATRAN program with the intent to display EPIC capabilities. I also learned how to use some of the UNIX language on the Silicon Graphics Machines. I am also realizing how difficult it can be to work as an engineer sometimes. Things do not always go the way they are expected. And even though the equipment is all very expensive, that does not make it any less capable of breaking down or malfunctioning. This has been the one of the most meaningful summer's of my life.

### ACKNOWLEDGMENTS

I have thoroughly enjoyed myself this summer and that is due to the efforts of many individuals. First, I thank God for granting me the ability to be in this program. Next I really appreciate the efforts of my mentor, Mr. Mike Nixon. His patience and calm demeanor have been a great help in my development this summer. He is an excellent instructor and deserves a pay raise, at the least. Also important in aiding me this summer were Darren Boisjolie, Randy Anderson, Bizhan Aref, and Pamela Cortner, contractors with Sverdrup. Dr. Bill Cook and Tom Byron were also helpful with helping my PATRAN skills. Last of all, but definitely not least, is one of the Co-ops from the University of Florida, by the name of Ken Gage. He has been

extremely helpful to me in my use of Unix on the Silicon Graphics machines, making movies, and so many other things. The summer would have been a lot harder without him. Everyone in the office has been extremely courteous and helpful. I would also like to thank my co-worker Jennifer Bautista for an outstanding summer. I look forward to working with her again. They made the summer a lot more enjoyable. I look forward to the opportunity of working with them again next summer.

## APPENDIX A

### EPIC SAMPLE PROBLEMS

- EXAMPLE 1 - 2D Shaped Charge with Standard Elements
- EXAMPLE 2 - 2D Shaped Charge with PER Option and Shell Elements
- EXAMPLE 3 - 2D Explosively Formed Penetrator
- EXAMPLE 4 - 2D Multi-point Detonation with Wave Shaper
- EXAMPLE 5 - 2D Perforation with Erosion Option and Behind Armor Debris
- EXAMPLE 6 - 2D Perforation with Plugging Option (Not yet Available)
- EXAMPLE 7 - 2D Penetration into a Concrete/Soil Target
- EXAMPLE 8 - 2D Penetration into a Concrete Target with NABOR Nodes
- EXAMPLE 9 - 2D Spaced Plate Perforation in Plane Strain
- EXAMPLE 10 - 3D Perforation with Erosion
- EXAMPLE 11 - 3D Explosively Formed Penetrator (Coarse Grid)
- EXAMPLE 12 - 3D Spaced Plate Perforation
- EXAMPLE 13 - 1D Impact onto Reactive Explosive
- EXAMPLE 14 - 3D Projectile Penetration into a Concrete Target with Reinforcing Bars



GO  
1  
VI  
2  
0/90  
SET,AXES,OFF  
SET,ZNULL,OFF  
SET,LABS,OFF  
SET,LABC,OFF  
SET,SPECTRUM,OFF

APPENDIX B

SESSION FILE

5  
1  
2  
E08P01.MDL  
N  
Y  
NAME,RIGHT  
NAME,LEFT,ROT,0/0/0/0/0/1/180,RIGHT

5  
1  
2  
E08P50.MDL

Y  
A  
Y  
Y  
Y  
RUN,DEL2

Y  
5  
1  
2  
E08P01.MDL

N  
Y  
! ui\_spawn\_command("getit 001",true)  
RUN,DEL2

Y  
END  
END  
SET,NOERASE,OFF  
INT

1  
2  
E08P02.MDL

N  
Y  
END

2  
2  
E08P02.ELE  
ET,XFRINGE,ON  
UN,HIDE,FRINGE  
ND  
ET,AHIDE,OFF

,2000

ND

```

NODE,1T#,ERASE
2
7
SET,NOERASE,ON
NAME,RIGHT
NAME,RIGHT,ROT,0/0/0/0/0/1/180,RIGHT
Y
1
4
2
7
END
NODE,1T#,ERASE
2
7
END
END
END
END
SET,NOERASE,OFF
! ui_spawn_command("getit 002",true)
RUN,DEL2
Y
END
END
SET,NOERASE,OFF
INT
1
2
E08P03.MDL
N
Y
END
4
2
2
1
2
1
1
E08P03.ELE
SET,XFRINGE,ON
RUN,HIDE,FRINGE
END
SET,AHIDE,OFF
3
F
0,2000
2
7
1
END
NODE,1T#,ERASE
2
7
SET,NOERASE,ON
NAME,RIGHT
NAME,RIGHT,ROT,0/0/0/0/0/1/180,RIGHT
Y
1
4
2
7
END
NODE,1T#,ERASE
2

```

```

7
END
END
END
END
! ui_spawn_command("getit 003",true)
RUN,DEL2
Y
SET,NOERASE,OFF
RUN,DEL2
Y
INT
1
2
E08P04.MDL
N
Y
END
4
2
2
1
2
1
1
E08P04.ELE
SET,XFRINGE,ON
RUN,HIDE,FRINGE
END
SET,AHIDE,OFF
3
7
0,2000
ND
ODE,1T#,ERASE
ET,NOERASE,ON
AME,RIGHT
AME,RIGHT,ROT,0/0/0/0/0/1/180,RIGHT
ND
ODE,1T#,ERASE
D
D
D
D
ui_spawn_command("getit 004",true)
N,DEL2
T,NOERASE,OFF
N,DEL2
T
P05.MDL

```

## APPENDIX C

### PATRAN 3-d Movie Making Process

The method of making a movie 3 dimensional in PATRAN is not extremely complex. Only the model files are needed. Remember, the model files consist of hundreds of tiny nodes that connect to define elements. The nodes have specific numbers that distinguish them from the others. PATRAN has the ability to identify each node with the proper command. The command is: "NODE,'n'#,WHO". This asks PATRAN to let the user pick and identify 'n' number of nodes. The best nodes to identify are those that will help separate the MODEL file into its different property identification. When these nodes have identified, they are connected with additional lines using the command: "LI,#,FN,, 'node1'T'node2'". These lines are used to define the edges of patches. Patches are made with the command: "PA,#,EDG,, 'line n'T'line x'." After the patches are made, they are rotated to form hyperpatches, or 3 dimensional entities, using this command: "HP,'n'#,ARC,0/0/0/0/0/1/'x',P'y'T'z'" where 'n' represents the number of hyperpatches to be formed, 'x' represents the number of degrees to rotate the patches, and 'y' and 'z' indicate the number of the patches to be used. PATRAN will then form a 3-dimensional skeleton of the object. The command "RUN,HIDE,SOLID" will provide the proper shading to give the full 3-dimensional effect.

CONSTRUCTION AND DESIGN  
OF A REGULATED POWER SUPPLY

Robert Baird Murray, IV

Final Report for:  
Air Force Office of Scientific Research  
Summer Research Program  
Wright Labs / Solid State Electronics (Optics)

Sponsored by:  
Air Force Office of Scientific Research  
Wright-Patterson Air Force Base, Dayton, Ohio

August 1992

## CONSTRUCTION AND DESIGN OF A REGULATED POWER SUPPLY

Robert Baird Murray, IV

### Abstract

A +/-15 volt 150 milliampere, +5 volt 1.0 Ampere power supply was designed and constructed. In designing the power supply, the circuit schematic was drawn and the values for the necessary components were calculated. After acquiring the components from various sources, the container was chosen and the exterior customized. The components were soldered to the circuit board with high precision and leads were connected to their terminals. The circuit board was then mounted to the customized metal container and output terminals installed for convenient use. After complete construction, the power supply was tested, using a multimeter to determine voltage and amperage output, and an oscilloscope to determine voltage ripple. The power supply's input was from a standard 115 volt, 60 cycles per second output, and is equipped with a lighted switch and fuse to safeguard against a possible short circuit.

# CONSTRUCTION AND DESIGN OF A REGULATED POWER SUPPLY

Robert Baird Murray, IV

## INTRODUCTION

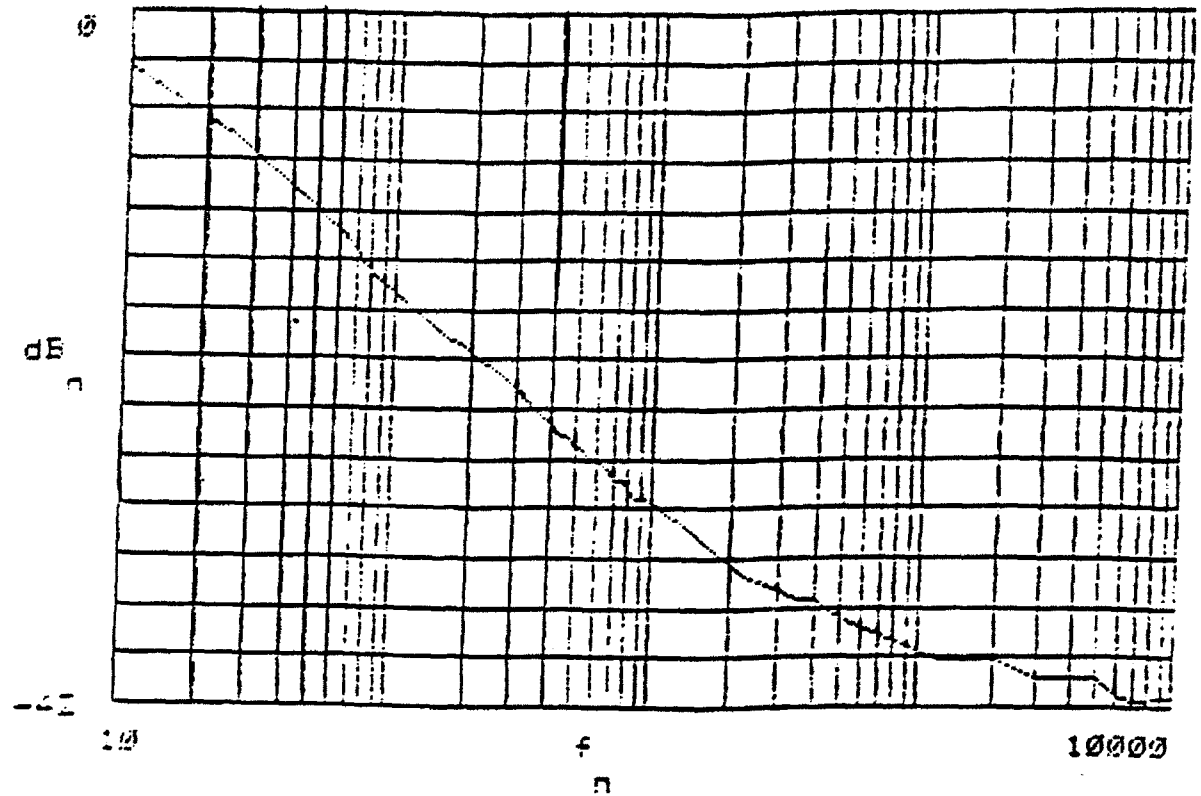
Building a power supply from scratch is quite a task for one who has not been exposed to the various intricacies of electronics. However, any lack of exposure at the beginning of my summer was soon obsolete as I was immediately thrown into working hands-on with high-tech equipment and state-of-the-art materials. At the end of two weeks, I was prepared to design and construct a working power supply. In this particular design, special consideration had to be paid to efficiency, availability, cost, and size of both the components and the abstract parts. Certain standards had to be met in order to ensure safe operation, and the components' cost had to remain as low as possible. Each of these limitations had to be compromised with the others in order to produce an optimum level of manufacturing. In recognizing these parameters, the entire construction of the power supply became similar to that of a commercial product.

## RESEARCH

Before designing a power supply, it was necessary to acquire as much knowledge as possible on circuits and their vital components. First, a simple passive filter was built, using a resistor and capacitor in parallel. A signal was put through the circuit using an wave generator, and the output was displayed on an oscilloscope, to compare with the unfiltered signal. As the frequency of the wave was altered, the change in the output voltage was observed and recorded. Then the input and output voltages were converted into decibels and plotted against frequency on a semi-logarithmic graph to show any attenuation in the signal (See Figure 1). Only a slight attenuation was found. However, the next circuit, an active filter with an operational amplifier IC (See Appendix 1-1), was far more effective in its response to the

Filter Response

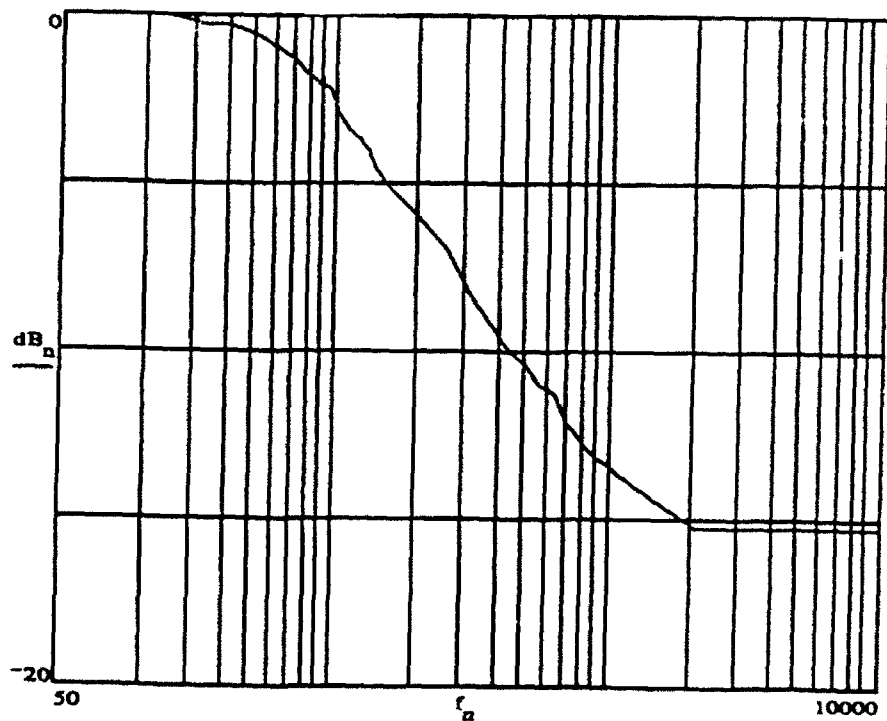
FIGURE 1



$$dB_n = 10 \cdot \log \left[ \frac{V_{o_n}}{V_{i_1}} \right] \quad \text{Voltage to Decibels}$$

FIGURE 2

Filter Response





signal. Again the results were recorded using an oscilloscope and then converted to decibels, which was plotted against a variable frequency (See Figure 2). The response showed a significant attenuation near the 230 Hz range, which indeed was the design cutoff frequency for this filter.

In building these circuits, not only was invaluable hands-on experience gained, but also a working knowledge of the reason behind the behavior of the circuits. This proved to be essential in the design of the power supply, and helped to trouble-shoot and eliminate schematic errors. After experimenting with the circuits, the next step was to explore the basics of the power supply and determine its characteristics. This was done primarily from literature and information given to me by my mentor, who offered a good source of information on the selection of components and calculation of the values for the power supply. After reviewing the literature and conferring with several opinions, I was prepared to begin design.

## DESIGN

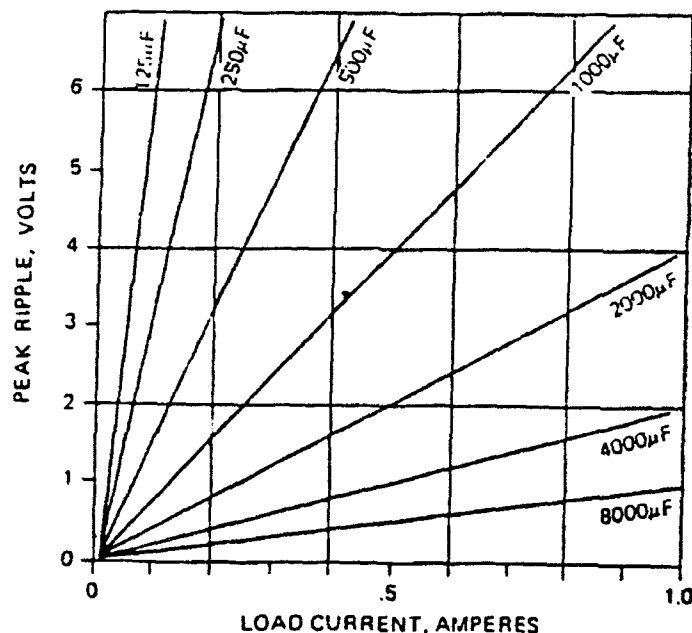
Basically, a power supply is a circuit which takes an input voltage and puts out a certain voltage or range of voltages. This conversion is done mostly through the work of a transformer, with the help of diodes, capacitors, and voltage regulators to fine-tune the desired output. This power supply was to put out  $\pm 15$  volts and 150 milliamperes, and +5 volts and 1.0 ampere, all the while maintaining not more than a .2 volt AC voltage ripple. A three-output transformer was needed to satisfy these requirements. A "STANCOR" PCA-3 8-terminal dual transformer was selected (See Appendix 2-2). The two secondaries were nearly perfect for the desired output values. The secondary #1 center-tapped RMS voltage was 43 volts, yielding 21 volts and .15 amps on the positive and negative terminal. Secondary #2 RMS voltage was an ample 8.5 volts and the current was rated at 2.0 amps.

After the selection of the transformer, the remainder of the circuit could more easily be

determined. The values of the regulators and diodes (and bridge rectifier) were fairly simple to find; the voltage regulators were merely the values of the three voltage outputs, and the diodes need only be twice the voltage and current of that which exited the transformer. The capacitors, especially the filter capacitors, were significantly more difficult to determine and acquire. The size of the filter capacitor and the maximum load current determined the amount of voltage ripple. With simplification, the relationship between the load current and the capacitor size is given by:

$$\text{CURRENT}_{\text{load}} = \frac{V_{\text{load}}}{R_{\text{load}}} = \frac{C \cdot V_r}{8.33 \cdot 10^{-3}}$$

**FIGURE 3**



Above, Figure 3 shows the relationship between load current and peak voltage ripple. This relationship is linear, which allows for simpler calculations and more conservative values. Difficulty arose with these values because they were so large. Obtaining the necessary two 4,500  $\mu\text{F}$  and the 28,000  $\mu\text{F}$  capacitors required commercial purchase, since none existed in working stock at the lab. Nevertheless, we were soon supplied with the capacitors from a local warehouse of "MCM Electronics." The values

chosen for the stabilizing tantalum capacitors were small in comparison to the mammoth filter capacitors, (10 uF) but were still vital to the power supply. Finally, the exterior components - the fuse, the switch - were selected, and the schematic diagram was finalized (See Appendix 2-5).

## CONSTRUCTION

The largest component in this power supply circuit beside the transformer was a 28,000 uF capacitor, and even its dimensions were not difficult to manage. Therefore, the entire circuit and its accessories (i.e. terminals, leads, rubber feet) fit snugly into a box 13 x 15 x 13 (lwh). This size provided not only convenience in usage, but also simplification in construction. With a small container, the leads were short and therefore extraneous loss of power could be avoided. Also, shorts and faulty connections could be detected easier. The soldering of the leads proved to be the most meticulous aspect of the construction. To ensure the absence of cold joints or faulty connections, the solder had to be fused perfectly with the pad and lead. This was the sole drawback in respect to the smallness of the power supply.

The first stage of physical development of the power supply was to select the size of the PC board. Using a stationary power saw, The board was cut to exactly the dimensions needed. All components but the transformer would sit on the board, so it was cut into an 'L' shape to closely fit around the transformer. However, the board had to be elevated off the ground so that no part of the circuit is in contact with the metal box. To accomplish this, four plastic pegs, or "stand-offs," were placed under the board. Significant effort was put into getting the perfect location of the pegs on the board, and then drilling the holes with the drill press (See Appendix 2-7). Once this was completed, the components were installed on the board and the soldering took place.

In soldering the leads to the various components, precautions were taken to make sure the components themselves were not overheated. An error such as that which would not easily be recognized would be detrimental to the circuit. The failed component could cause a short, inflict further damage, and the circuit would be very difficult to correct. This occurred in the -15 volt regulator, and almost resulted in the termination of the bridge rectifier. In addition to overheating, shorts between component leads were also dangerous, and the consequences are similar. Since these leads were often be very close to one another, soldering became very detailed and precise. The bridge rectifier, for example, has four pins, extremely close together. To avoid unwanted connection, the pins were bent in opposite directions, allowing more space to work with each individual pin. The wires between pins were soldered before being attached to provide more stability in the connection. After that, they were bent into a "J-hook" again to stabilize the connection by giving additional solid support to the solder. Each lead and connection was tested for shorts and faulty joints immediately, because testing later would be too tedious with everything in place. After a successful check and double-check, the board was fastened to the stand-offs, and the input wires soldered to the transformer.

The next stage in development was customizing the box to fit the terminals, switch, rubber feet, screws for fastening the interior parts, and input cable. The measurements for the location of the holes had to be highly accurate - the parts could not be shifted - it could disrupt the perfect layout of the parts. The output terminals were each made equidistant from a common (ground) so that a two-pronged plug could be inserted for convenient output use. The switch was installed in the back, next to the input cable to minimize the length of the power cord within the power supply. After the holes were drilled using the drill press, the box was sanded and then painted with two coats of water-proof spray paint. Following that, the interior parts were fastened securely to the chassis and the outer parts were carefully put into

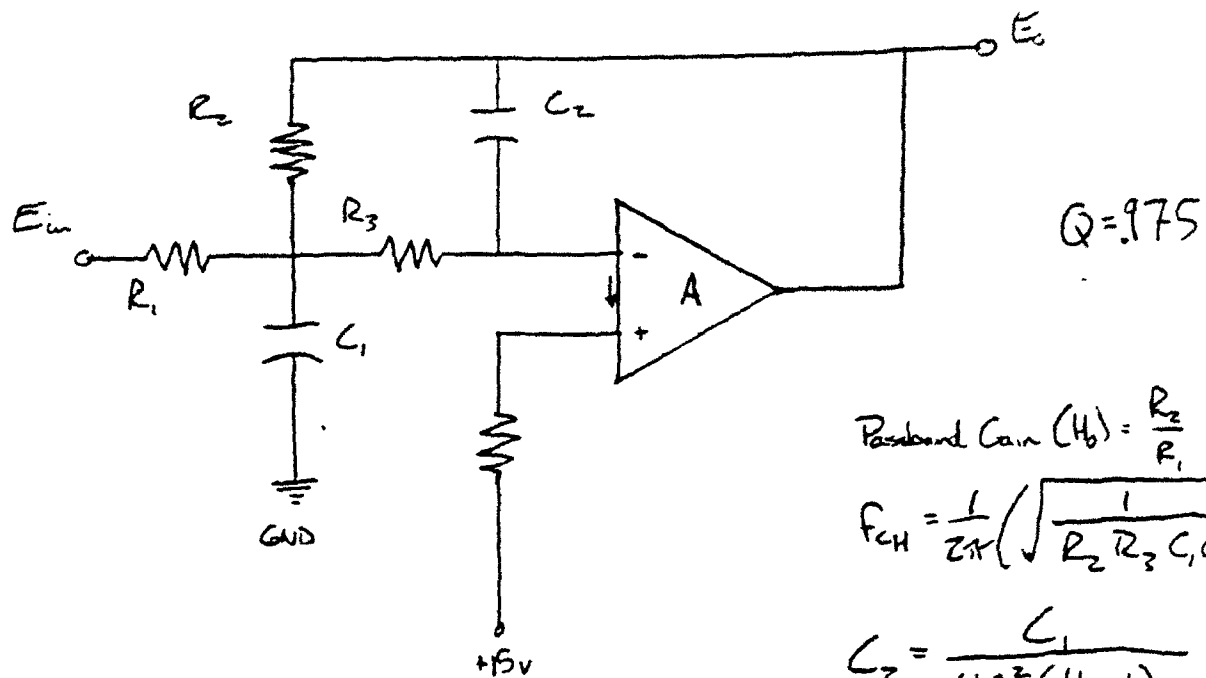
place.

In finalizing the product, the data sheets were completed and the power supply was tested. In testing for voltage output, a multimeter was attached to each output terminal and the ground. The results were on the money, each being within .05 volts of the desired output. To test the current output, a load resistor with a value calculated from Ohm's law,  $V=IR$ , was placed in parallel with an ammeter to draw the current. Again, the results were superb (See Appendix 2-8), with each output easily reaching its theoretical rating. The final analysis, voltage ripple, was tested using an oscilloscope. By feeding the output into the scope and switching the monitor to AC, the ripple could be detected, using the amplitude as the voltage reading. This was the surprise of the project; the ripple was nearly 100 times lower than calculated. Later it was discovered that this was due to the filtering done by the regulator, which was not taken into account when the values were determined. However, because of this minor oversight, the power supply is nothing but more effective. After testing was completed, the data sheets were compiled and the power supply set on a shelf to be used at the disposal of the laboratory.

## CONCLUSION

The power supply which has just been described was an effort to help - even in the most insignificant amount - the engineers and scientists of this laboratory in the achievement of their goals and research. Through patience and perseverance this project was completed with very successful results. I thank my mentor, Antonio Crespo, and various other colleagues, namely Dale Stevens and Jim Grote for their time teaching me the very basics of electrical engineering and helping me through some tough problems. I have learned more these past eight weeks than I learned in High School Physics all last year. I hope any contributions I have made will help the future of technology in any way, no matter how small.

## APPENDIX 1



$$\text{Passband Gain } (H_0) = \frac{R_2}{R_1}$$

$$f_{cH} = \frac{1}{2\pi} \left( \sqrt{\frac{1}{R_2 R_3 C_1 C_2}} \right)$$

$$C_2 = \frac{C_1}{4Q^2(H_0 + 1)}$$

$$R_1 = \frac{R_2}{H_0}$$

$$R_2 = \frac{1}{4\pi f_{cH} Q C_2}$$

$$R_3 = \frac{1}{4\pi f_{cH} Q C_2 (H_0 + 1)}$$

## APPENDIX 2



# POWER SUPPLY DATA SHEET

TRANSFORMER: Stancor PCA-3 dual

Secondary 1: 42V<sub>RMS</sub> (CT) 150mA

Secondary 2: 18V<sub>RMS</sub> (CT) 1.25A

REGULATORS (VOLTAGE):

$V_{R_1}$  : +5V

$V_{R_2}$  : +15V

$V_{R_3}$  : -15V

CAPACITORS (ELECTROLYTIC)

(FILTER)  $C_1$  : 28,000  $\mu$ F

$C_2$  : 4,700  $\mu$ F

$C_3$  : 4,700  $\mu$ F

(STABILIZER)  $C_4$  : 10  $\mu$ F

$C_5$  : 10  $\mu$ F

$C_6$  : 10  $\mu$ F

DIODES

$D_1$  : 100V, 3A

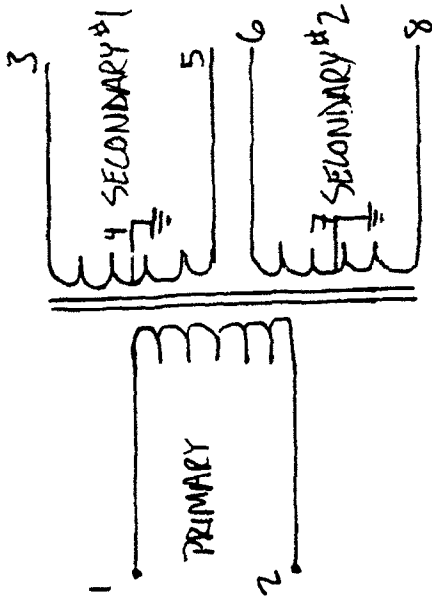
$D_2$  : 100V, 3A

(BRIDGE RECTIFIER): 100V, 1A

FUSE : .8A, 250V

SWITCH : 10A, 175V

# TRANSFORMER     Stancor PCA-3



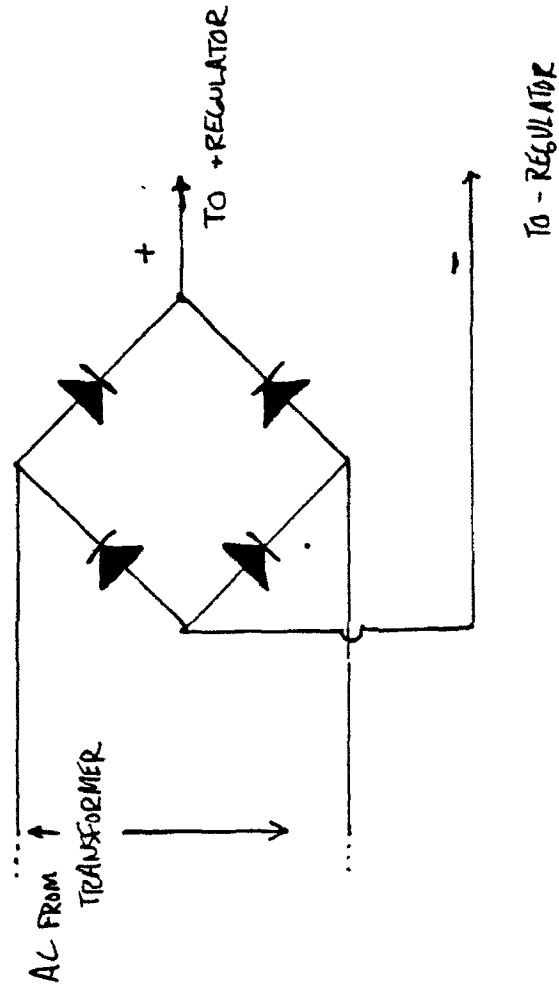
## SECONDARY 1

- Positive 21 V.D.C. at 150 mA
- Negative 21 V.D.C. at 150 mA

## SECONDARY 2

- +8.5 V.D.C. at 2.0 A

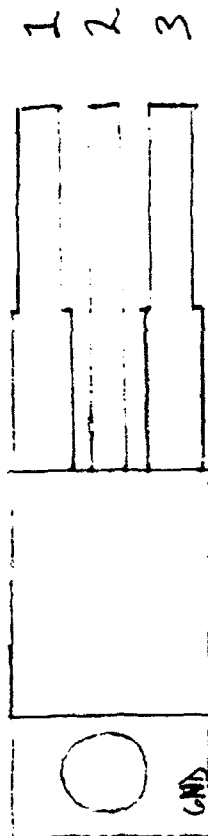
# BRIDGE RECTIFIER



# VOLTAGE REGULATORS

+15v, +5v

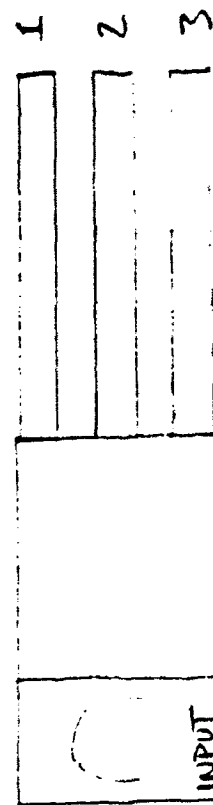
- 1 = output
- 2 = GND
- 3 = input



-15v

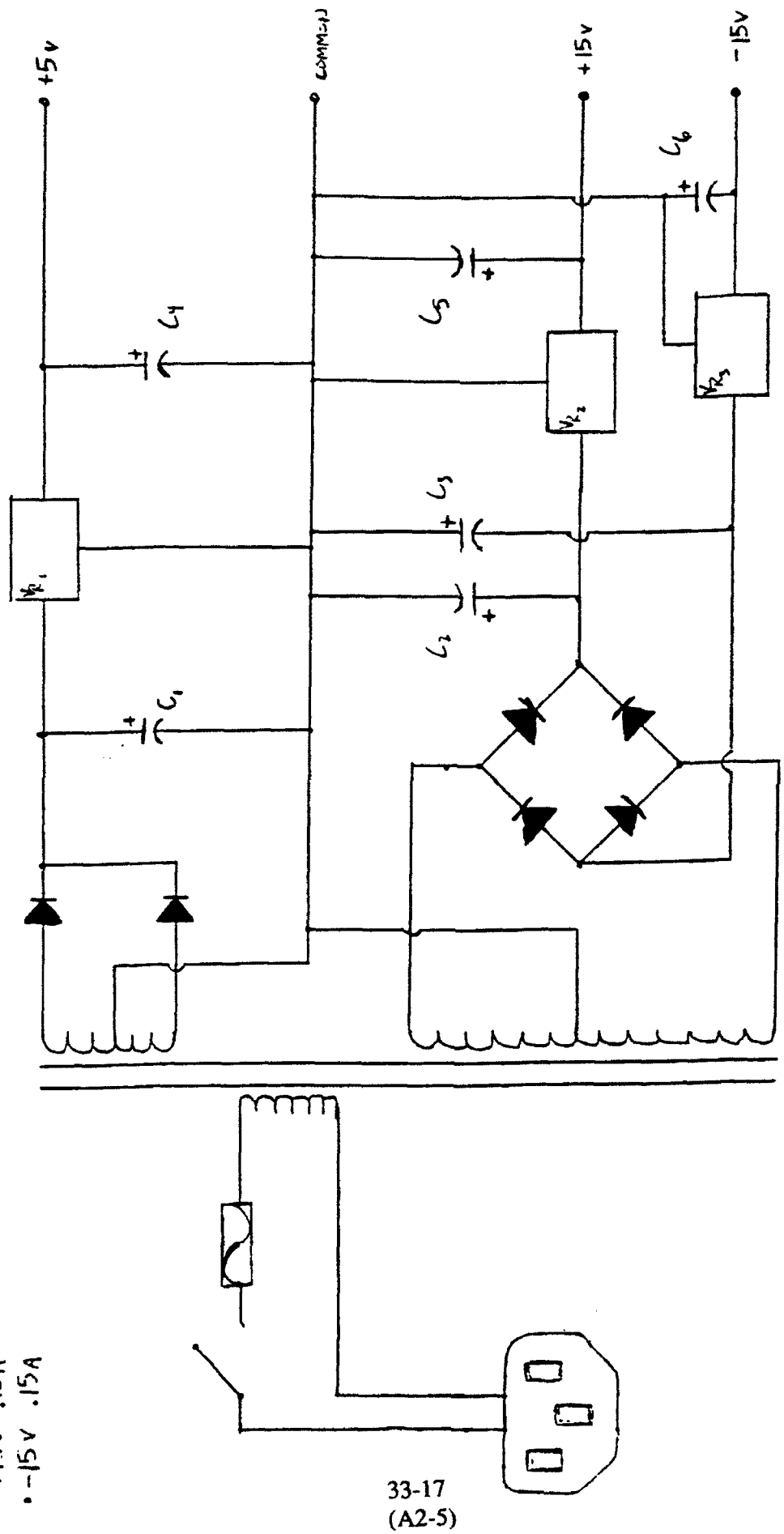
33-16  
(A2-4)

- 1 = input
- 2 = output
- 3 = GND



# DUAL POWER SUPPLY

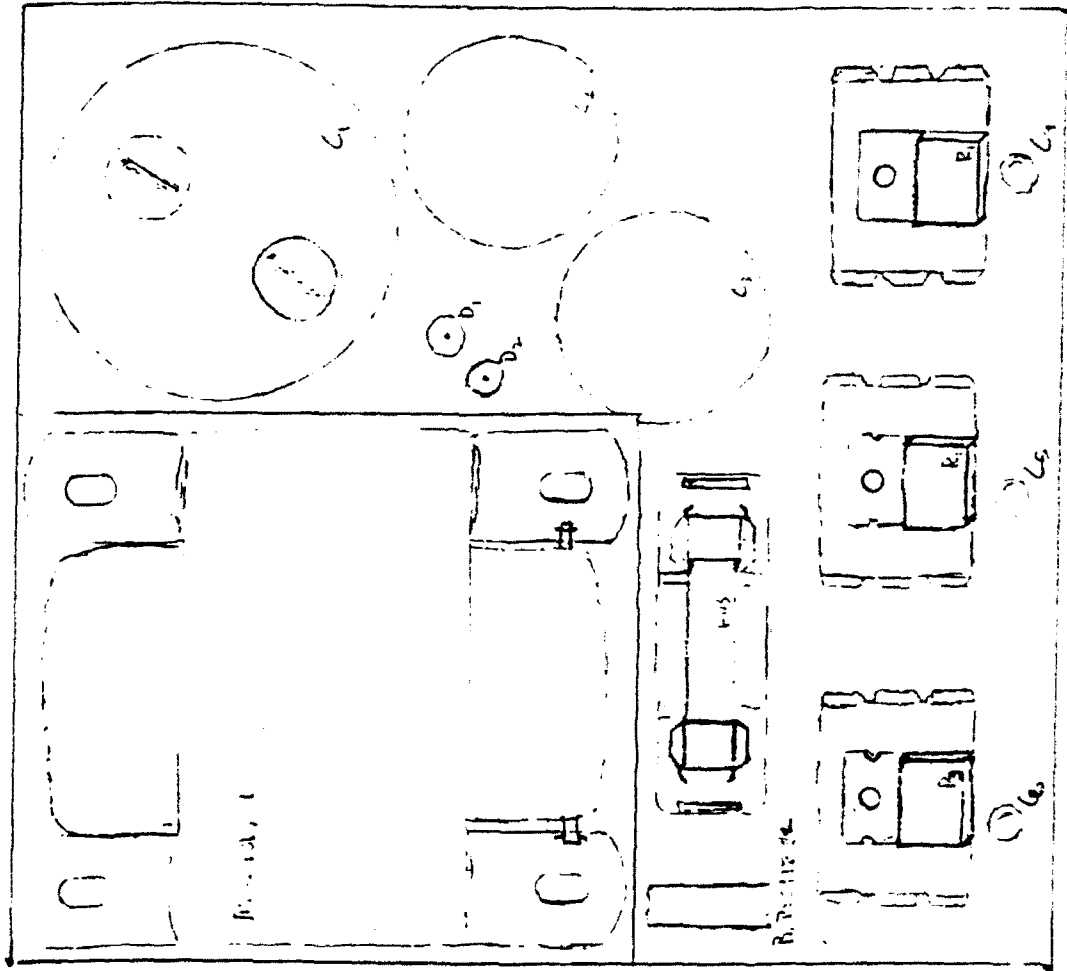
- +5 v 1 A
- +15 v .15 A
- -15 v .15 A



33-17  
(A2-5)

PL DIAGRAM (TOP VIEW)

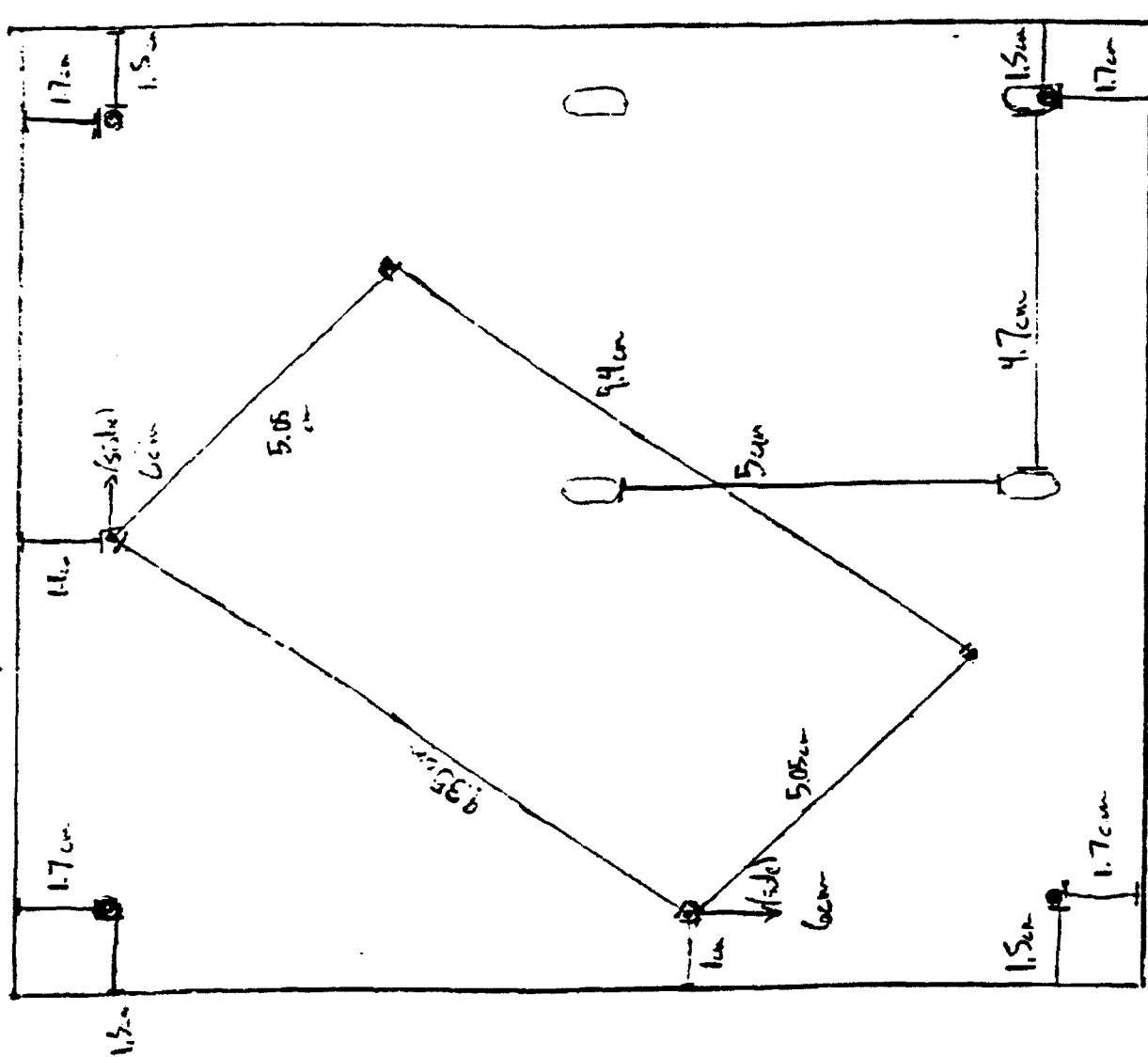
12cm x 13cm (4)



33-18  
(A2-6)

Bottom 13m x 15m

FRONT



Back

42 381	50 SHEETS	5 SQUARE
42 382	100 SHEETS <td>5 SQUARE</td>	5 SQUARE
42 389	200 SHEETS <td>5 SQUARE</td>	5 SQUARE



$\pm 15v$

33-20  
(A2-8)



PREPARING HIGH TECH AIRCRAFT FOR TESTING

Thomas M. Owsley  
Student  
Alter High School

Final Report for:  
High School Apprenticeship Program  
Wright Laboratory

Sponsored by:  
Flight Dynamics Directorate  
Wright-Patterson Air Force Base, Ohio

August 1992

## PREPARING HIGH TECH AIRCRAFT FOR TESTING

Thomas M. Owsley  
Student  
Alter High School

### Abstract

For my eight week tour at Wright-Patterson Air Force Base, I worked in building 65, the Structures Test Branch of the Flight Dynamics Directorate. In this building, high tech aircraft and pieces of high tech aircraft are instrumented and then submitted to heat and stress loads that simulate the expected conditions that will exist in flight. I had the opportunity to help instrument an F-15, the Air Force's current duel role air superiority fighter, a section of the 1995 Supportable Hybrid Fighter, which is a joint effort next generation fighter aircraft, and a piece of the National Aero Space Plane (NASP) X-30 which will carry passengers to the edge of space and yet take off and land on conventional runways.

## PREPARING HIGH TECH AIRCRAFT FOR TESTING

Thomas M. Owsley

### F-15

The F-15 fighter is being tested for the second time at the structure testing facility because this aircraft is being flown four times harder than originally anticipated. In it's test structure, the flight hours of an average F-15, along with the g-loads it will have to sustain, are simulated on the test F-15. By simulating flight hours ahead of what the Air Force's fleet of F-15s is now at, the test facility can detect cracks and stresses in the airframe and report these as trouble spots to watch for in the F-15s currently being flown. For several days I assisted technician Larry Marcum in installing some new strain gages on the wing of the F-15. These gages were added after a major crack was found in the wing. I also, along with fellow high school apprentice Jonathan Servaites, cut cables and soldered connectors to these cables which we then helped run from the new gages to the control room.

### Supportable Hybrid Fighter Structure

The Supportable Hybrid Fighter Structure is a section of the 1995 Air Superiority Fighter. The aircraft is a joint project by General Dynamics, Lockheed, and Boeing. The structure will be tested for signs of stress under low heat and high loads. I did not get to do much work on this project but did assist technician Larry Marcum for a few days in applying some of the gages and solder strips. This involved sanding the area where the gages and solder strips were to be applied, then cleaning the areas with a mild acid, and then carefully attaching the strips and gages with contact cement.

### NASP X-30

The National Aeronautics and Space Administration is working on developing the X-30, a hypersonic passenger aircraft that can take off from a conventional runway, fly up to the edge of space, and then land again on a conventional runway. In a joint project with the Air Force, NASP developed the Lightly Loaded Splice Subcomponent, and it is being instrumented and tested at the Structures Test Branch at Wright-Patterson Air Force Base. The Lightly Loaded Splice Subcomponent is a 27.5 inch by 60.1 inch panel of

titanium matrix composite that consists of two halves joined in the middle by the splice plate. This is one small section of the outer skin of the X-30. This specimen will be heated up to 1500 degrees Fahrenheit and have compression loads of up to 47600 lbs and stretching loads of up to 8900 lbs. To read the heat levels and strains on the specimen, hundreds of thermocouple wires and several types of strain gages have been instrumented on to it. Standard low and high temperature strain gages are being used as well as two types of advanced concept strain gages developed at NASA Lewis and NASA Langley. These two gages are self-compensating, meaning they expand or compress due only to the change of the surface, not just because of the applied heat. All of the high temperature strain gages have been flame sprayed on to the surface. This is an experimental process in which the gage is secured to the surface by being placed between two layers of ceramic that have been melted and sprayed on by the flame spray gun. This process is very new and has been improved upon by the Wright-Patterson technicians working on the project. Most of my time was spent working on the Lightly Loaded Splice Subcomponent. I, along with Jonathan Servaites, assisted technicians Ron Ditmer, Cliff Hitchcock, and Jim Wieher in many ways. One of the first things we did was to cut over 300 thermocouple wires and put connections on them. We also cut and stripped 150 Inconel thermocouple wires and put connections on them too. After the Inconel wires were attached to the specimen, Jon and I checked and labeled all of the them to make sure they worked properly and could be easily identified. I also had the opportunity to do some sand blasting and welding. I sand blasted small areas of the specimen in order to clean the surface so I could then weld to it. I welded hold down straps for the wires to be attached to the NASA Lewis gages and welded the hold down straps for the Teflon wires coming from the standard low temperature strain gages. The most difficult welding I did was for the NASA Lewis strain gages. One millimeter wires had to be welded to another wire end that was a little smaller than the head of a pin. This took steady hands and a lot of patience. Another part of the project that I worked on with Jonathan Servaites was painting the surface of the specimen with black conductive paint which allows for even absorption of the heat that will be applied. The last part Jon and I worked on was testing the resistance of the standard high temperature strain gages to make sure they all functioned properly.

### Conclusion

My eight week tour at Wright-Patterson Air Force Base was a very enjoyable learning experience. I learned how complex it is to test aircraft and learned several of the methods used to do so. I truly enjoyed working on the projects and working with the people who were informative, helpful, and friendly. Thanks to all who helped make my job a success.

Using Computer Applications

M. Cristina Pacheco

Final Report For:  
High School Apprenticeship Program  
Wright Laboratory

Sponsored By:  
Structural Dynamics Branch  
Wright Patterson Air Force Base, Dayton, OH

June 15 - August 7, 1992

## Using Computer Applications

M. Cristina Pacheco

### Abstract

The Structural Dynamics Branch at WPAFB uses many different types of software programs to aid in data presentation. Therefore, by learning to use Harvard Graphics and Microsoft Excel, data processing was made much easier. By putting information collected in experiments into a spreadsheet, calculations could easily be made. When this information was later transferred to Harvard Graphics using a Lotus Data Worksheet, which allowed information from the spreadsheet to be read into Harvard Graphics, it became very easy to make plots.

## Using Computer Applications

M. Cristina Pacheco

During the course of my summer apprenticeship I learned to use various computer applications to process different types of data. Much of my time at WPAFB was spent creating charts from data collected in experiments involving pressure transducer calibration and acoustic modulators. After the data was collected, I used the Microsoft Excel program to create spreadsheets and then transferred the information to Harvard Graphics to make plots.

The largest amount of data that was processed was concerned with creating acoustic modulators with greater efficiency. The project engineer took data from three different modulators in three different configurations resulting in a total of nine separate systems which required analysis. By measuring the first, second, and third pressures, the temperature in degrees Fahrenheit, the current, and the change in pressure; the temperature in degrees Rankin, velocity, mass flow rate, and total pressure were easily calculated using Microsoft Excel. First, the known values were entered into the spreadsheet a column or row form. The cells requiring calculated values were then filled by entering the formulas into the top cell of a column and utilizing the fill down function to make the remaining relative calculations. Once the spreadsheet contained all the desired information, it was saved as a Lotus Worksheet to allow



it to be transferred to Harvard Graphics, an application specializing in data presentation (example 1). However, due to the fact that the information I worked with was sensitive unclassified, I had to make-up data for my sample materials.

The Harvard Graphics application makes it very easy to create graphs of the desired information. By going into the submenu "Create a Chart" and choosing the number as the data type an x,y coordinate plane is quickly made. The program allows for a variety of other graphs to be constructed also. Once the titles of the graph are in place, the information from the Lotus Worksheet can be read into the graph by simply typing in the cell desired ranges in the import/export function. If more than one series of points is to be plotted on the same graph a different symbol for the points can be used or, by using the draw/annotate function, a label can be placed directly onto the graph. Due to the tremendous quantity of graphs needed for the modulator test, a simple way of using the same graph for different information was devised. Since each of the nine modulators needed a plot showing the relationship between current and one of the other variables from the spreadsheet, only one complete chart was necessary for each column. One merely has to clear the data points from the table and import the new data (example 2).

I learned how to use the Harvard Graphics draw/annotate function extensively but found Corel Draw, a graphical presentation package, a bit more difficult to master. However, the draw/annotate function has more limitations as far as the complexity of the drawings one can create. It is better suited

to making one-dimensional drawings with few details (example 3) unlike Corel Draw, which with relative ease, can add perspective and minute detail to practically everything.

Although I found learning the computer applications difficult at first, it was definitely worthwhile because after I got the basics down it became much easier. I undoubtedly benefited from learning about some of the different programs available for computers because in the future, no matter what field I finally decide to study, the computer will most likely play a key role. I also found that even if one application is completely different from another, there are usually similarities between them; it facilitates faster learning to be familiar with the computer in any way.

The samples I have included show:

1. A simple spreadsheet made using the Microsoft Excel program. In column D the multiplication function has been used to find the total from the sale of apples for each particular day. Column G uses the same principle to find the total for bananas. Column H uses the addition function to find the total number of pieces of fruit in columns B and E. Finally, column I also utilizes the addition function finding the total of columns D and G.

2. A graph made using Harvard Graphics. The data plotted on this line graph has been transferred from the Microsoft Excel spreadsheet to Harvard Graphics. When in the import/export function of Harvard, the proper worksheet was selected and cells

I2-I8 were read into the X-axis data and B2-B8 were put into the Series 1 data. By selecting "line" and filling in the graph title and X and Y axis labels, the graph was quickly made. However, one of Harvard Graphics limitations is illustrated in this graph because the points must be sorted before the line is drawn, otherwise the line appears to be zigzagged; therefore, it was necessary to use the control and arrow keys to rearrange the numbers.

3. A drawing created in Harvard Graphics. To make the apple and banana the draw/annotate function was selected, and the add and polyline choices were used to draw the fruit. The labels were added using the add and text selections.

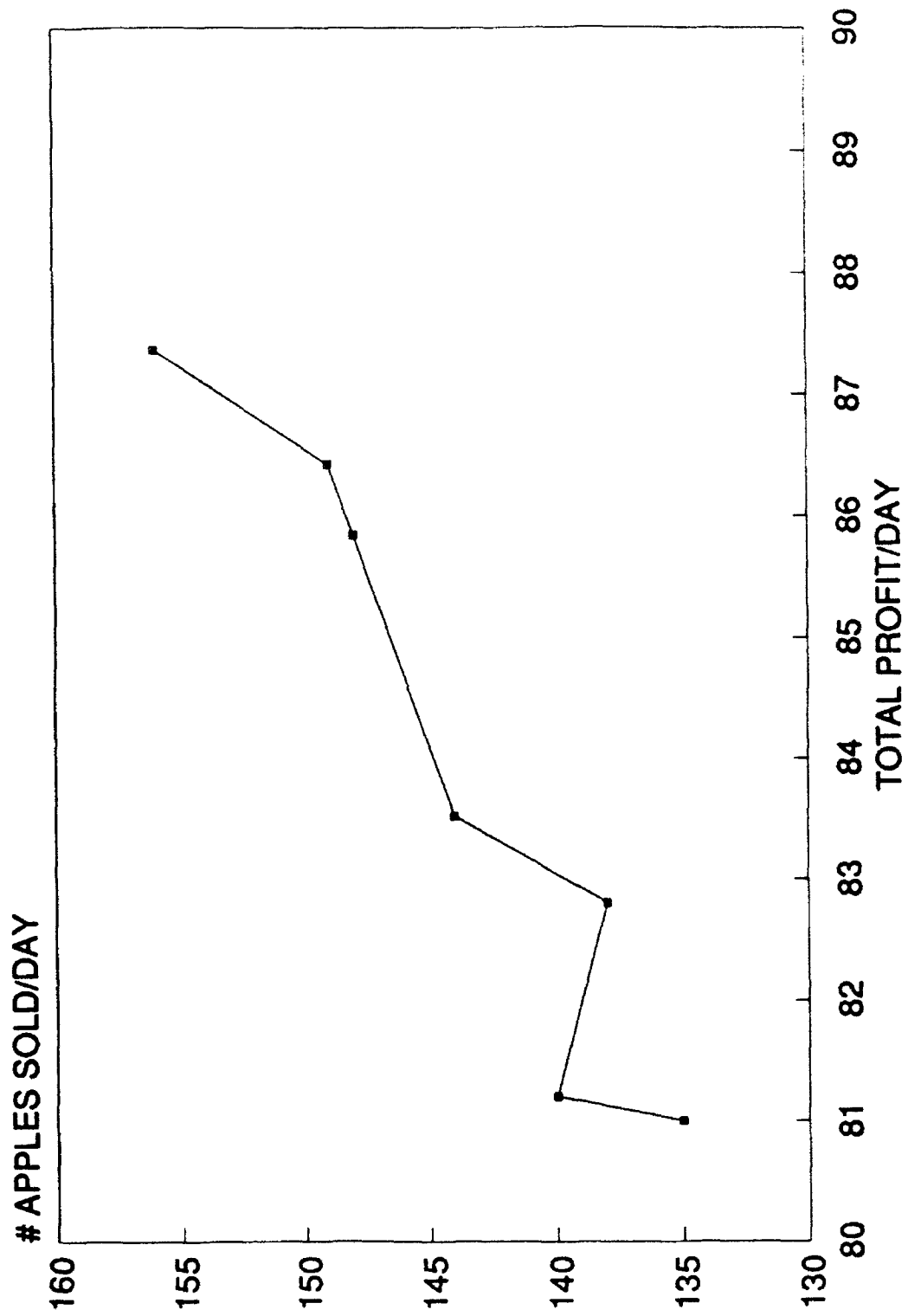
Although these are simple examples, they show what these applications can do, and demonstrate how I was able to use them to process technical data.

# Fruit Sales

	A	B	C	D	E	F	G	H	I
1	day	#apples	price/one	subtotal	#bananas	price/one	subtotal	fruit sold	total
2	Sun	140	\$0.29	\$40.60	325	\$0.24	\$40.60	465	\$81.20
3	Mon	135	\$0.30	\$40.50	317	\$0.25	\$40.50	452	\$81.00
4	Tues	144	\$0.29	\$41.76	345	\$0.23	\$41.76	489	\$83.52
5	Wed	156	\$0.28	\$43.68	333	\$0.24	\$43.68	489	\$87.36
6	Thurs	149	\$0.29	\$43.21	353	\$0.23	\$43.21	502	\$86.42
7	Fri	148	\$0.29	\$42.92	312	\$0.25	\$42.92	460	\$85.84
8	Sat	138	\$0.30	\$41.40	367	\$0.23	\$41.40	505	\$82.80

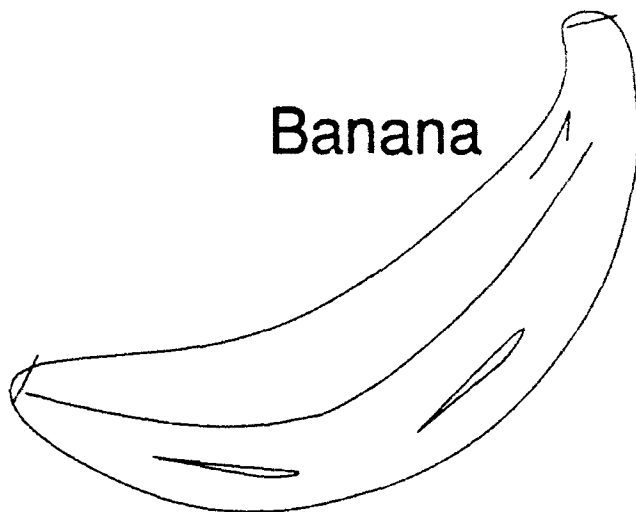
example 1

# APPLES SOLD VERSUS TOTAL PROFIT

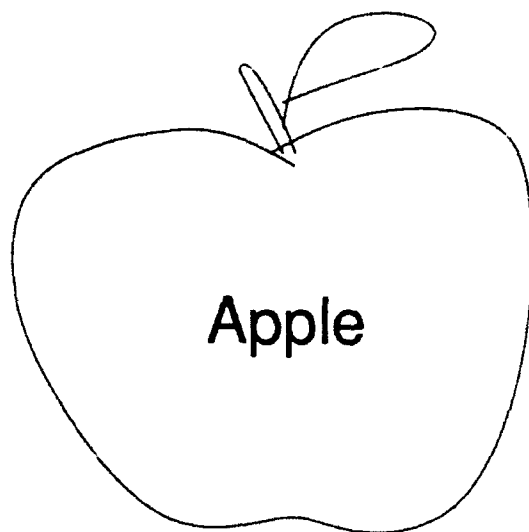


example 2

Banana



Apple



example 3

**THE CREATION OF A  
GRAPHICS WORKSTATION**

**Eric J. Powers  
High School Student**

**Beavercreek High School  
2660 Dayton Xenia Road  
Beavercreek OH, 45434**

**Final Report for:  
Summer Research Program  
Wright Laboratories**

**Sponsored by:  
Air Force Office of Scientific Research  
Bolling Air Force Base, Washington, D.C.**

**August 1992**

# THE CREATION OF A GRAPHICS WORKSTATION

Eric J. Powers  
High School Student

## Abstract

The C programming language along with a special graphics card were used to analyze video of moving objects. Microsoft C v7.0, and compatible libraries were used to write the code. Since the functions required of the application were not totally known, tests were continually conducted. When test results proved to be very encouraging, a demo program was created to graphically display the capabilities of the graphics card and application written. In final, the program consists of around eighty functions.



# THE CREATION OF A GRAPHICS WORKSTATION

Eric J. Powers

## Introduction

In current times, computers are being used for every task possible. In the Air Force, it seems that almost everyone would be lost without their machines. This summer the goal was to take yet another human task and make the machine do it for us.

## Discussion of the Problem

The goal of the summer apprenticeship program was to have a computer through the use of a camera, identify objects. In order to accomplish this task, the Microsoft programming language had to be learned. Camera footage had to be taken. A Professor at Wright State University had to derive mathematical equations, and the C libraries that came with the graphics card, had to be coded.

## Methodology

At the beginning of the summer I worked on learning how to make windows software. Since none of the equipment or books had

arrived yet. Once the 486DX computer arrived, I installed Borland C++ and Applications & Frameworks, Microsoft Windows, Microsoft C, and Microsoft Software Development Kit. With the use of these tools I started programming the graphics workstation. It seemed like an eternity since, so many functions had to be programmed into the code. As soon as the code was up to par, a demo program was created. This demo program showed some of the neater visual effects of the program and gave the group a taste of what the program could actually do.

### Results and Conclusion

After many long hours of work, including some not to fun debugging, the graphics program worked. With the camera footage taken by Allen, another student, and the technical aide of Greg Power, my mentor, we constructed a program that allows graphics capturing and manipulation.

# THE CREATION OF A GRAPHICS WORKSTATION

Eric J. Powers

## References

Microsoft C/C++ v7.0 Manuals, Microsoft Corporation, USA 1991.

Microsoft Software Development Kit Manuals, Microsoft Corporation,  
USA 1991.

Borland C++ and Applications and Frameworks v3.0, Borland  
International, USA 1991.

# A Comparison of Concept Recognition Skills

Melvin K. Richardson

Final Report for:  
High School Apprenticeship Program  
Air Force Office of Scientific Research



System Concepts Group  
Avionics Directorate  
Wright Laboratory

August 7, 1992

A Comparison of  
Concept Recognition Skills

Melvin K. Richardson

Abstract

The abilities of humans and computer software to learn concepts were studied. Patterned after the well-known Minnesota Card Test, ten concepts of four different categories were selected. Fifteen people were tested to determine their ability to learn these concepts; ten random files for each of the ten concepts were ran on two different computer pattern decomposers. The results indicate that no direct correlation exists between the skills of the people and the skills of the decomposers. The results do show, however, that humans are clearly better at recognizing a certain type of concept, while the decomposers are better at others.

## A Comparison of Concept Recognition Skills

Melvin K. Richardson

### Introduction

In 1956, Jerome S. Bruner, Jacqueline J. Goodnow and George Austin published *A Study of Thinking*[3] outlining their landmark study on concept recognition. Included in the series of reports they performed was the Minnesota Card Test using a set of attribute cards shown in Table 1. These cards and this test are quite unique, utilizing 3 values for each of 4 attributes and with these cards and the test, Bruner *et al.* were able to obtain a great deal of insight into how capable humans are at recognizing various types of concepts and proceeded to derive various strategies that humans might use in this task.

Since Bruner *et al.*'s initial findings, colleagues began and present-day scientists have continued to expand on this "classic" series of studies. This well-known card test has been used by many people in many different ways, and in the process, has greatly helped the field of cognitive psychology emerge, becoming a respected, distinct branch of learning.

Recently, this card test has been used by researchers of neural nets and Pattern Theory to test how capable computers are at pattern and concept recognition. A hot field in computer science, pattern recognition is an important subject. Its further development is vital to increase the reality and applications of Artificial Intelligence.

### Discussion of Problem

The Minnesota Card Test has been administered to both humans and computer programs to test their concept recognition skills. But no known study has been made to compare the abilities of the two. Such a study would

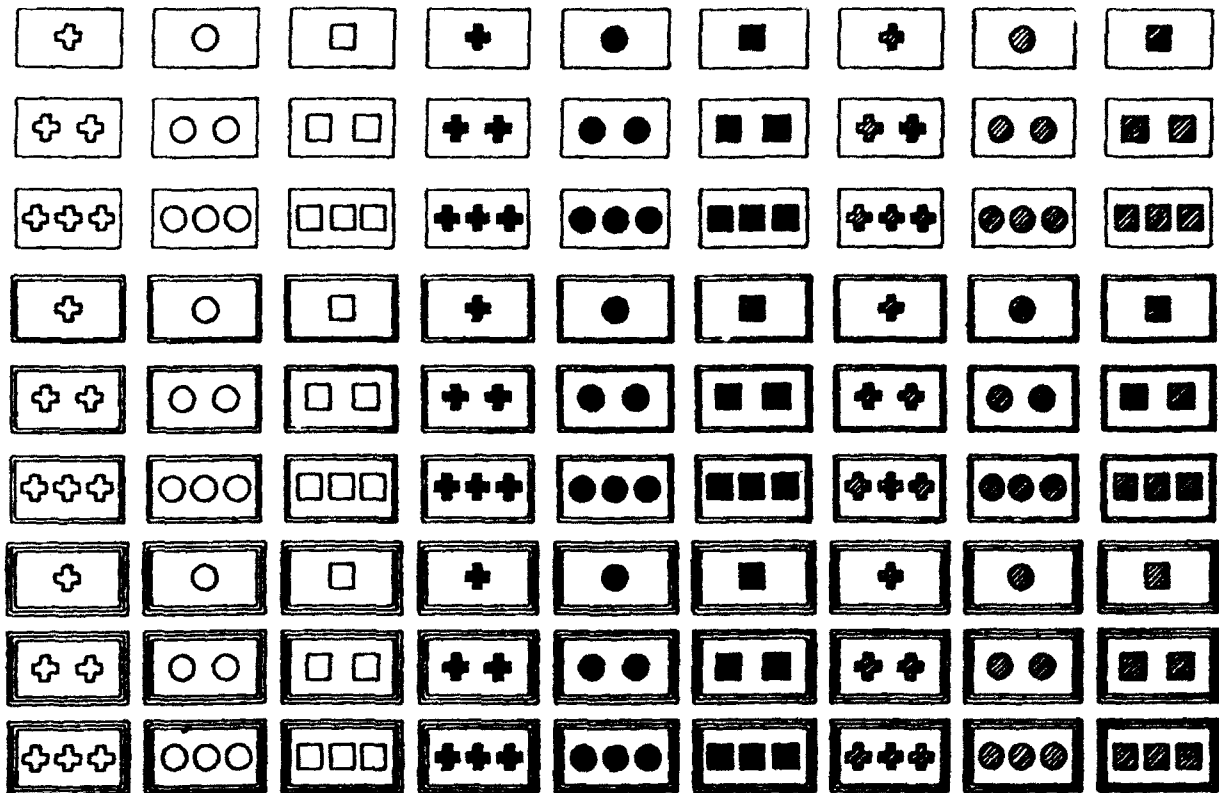


Table 1: The array of cards used. Notice the four attributes with three values each.

be a natural extension to the many studies already performed, answering questions that these previous studies give rise to. Thus, an experiment to do just that, a "man vs. machine" experiment, if you will, was formulated by the Pattern Theory Team, System Concepts Group of the Avionics Directorate of Wright Laboratory, United States Air Force (WL/AART-2). This project utilizes two pattern recognition programs, AFD and FLASH. Both were developed by this team and will be discussed later. The remainder of this paper outlines and discusses the methodology, results and conclusions drawn from this project.

### Methodology

10 concepts were formulated to be tested. These concepts were designed to represent several different types or categories of possible concepts. The four categories or rules used were: simple (a single value for just one attribute), conjunctive (one value and another), disjunctive (one value or another) and relational (if one value, then one other; if another value, then another). There were 2, 3, 3, and 2 concepts used from each category, respectively. Three of these concepts were borrowed from John R. Anderson [1]. The concepts used are located in the appendix.

Humans were tested first. A set of cards was made similar to the cards shown from Bruner *et al.*'s experiment. The subject came to where the test was administered and was given a paper to read. This paper can be found in the appendix, and explained what the test was about and called attention to the various attributes of the cards. After reading this, an example concept was shown so that he could become familiar to the procedure for the experiment. Any last minute questions were answered, the cards were shuffled, as they were several times throughout each experiment, and the test began.

The experimenter flipped through the cards until the first positive example of the first concept came up. This was placed on the table and the subject was told that it was positive. The subject then had a chance to guess the concept. If he was incorrect, the next card from the deck was placed on the table and he was told whether that was positive or negative. The positive cards were placed in one column and the negatives were placed in another. The subject had a chance to guess the rule after each card was placed on the table. This continued until the subject stated a rule consistent with the concept. The experimenter recorded the number of cards needed by the subject to learn the rule and repeated the process for all ten rules. The time



that the subject took was also noted. Although not presented as data, it was used to keep track of the five-minute limit for each rule, needed to keep the experiment moving and maintain the subject's attention and interest.

This process was performed with fifteen subjects. Care was taken to have a good blend of subjects for the test. They varied from engineers to secretaries to a 13-year-old (who, incidentally, had the best total score).

The cards were then converted into 8-variable binary numbers to be entered into the computer. An example of this conversion is in the appendix. Each of the 10 concepts were then entered in their entirety into AFD (Ada Function Decomposer), a machine-learning program that decomposes functions. Version 2A of the AFD Program was used. These concepts were entered with the positives as a 1, the negatives as a 0, and the other numbers, 0-255, that did not represent cards as an X—a "don't care" that the decomposer ignores when decomposing the function. AFD is a first generation function decomposer. It was not originally designed to deal with "don't cares" but can still decompose these functions, despite their presence. It decomposed all 10 concepts, finding the expected structure in the concepts and outputting the correct decomposition and DFC of the functions. DFC (Decomposed Function Cardinality) is a measure of the computational complexity for binary functions.

With the correct decomposition in hand, AFD and FLASH (Function Learning and Synthesis Hotbed), a similar decomposition program were allowed to learn the concepts. FLASH is the second generation program. It is similar to AFD but does directly consider "don't cares" when decomposing functions; it thus can be expected to do better than AFD in this project. The decomposition plan FLASH used is included in the appendix. It must also be mentioned at this time that neither AFD nor FLASH were specifically de-

signed by the Pattern Theory team for use in applications such as this. They are also much different than other machine learning programs. They are not explicitly programmed with every possible type of simple, conjunctive, disjunctive and relational rule possible included in a memory base. No concepts are preprogrammed; rather, they algorithmically search for relationships and patterns. For a detailed description of how these decomposers operate, see [5] on AFD and the upcoming technical report[4] on FLASH.

First, these concepts were transferred to SAMFN4, a program that randomly selected 9 numbers from the 81 numbers representing cards and denoted these as "cares" (positives as a 1 and negatives as a 0), with all the other numbers denoted as "don't cares" (an X). AFD requires that 0 is always a "care," whether positive or negative, so a total of 10 "cares" were selected. It did this 10 times for each of the 10 concepts, creating 100 files. Each file was checked to make sure at least one positive case was a "care," consistent with the human trials. These files were then decomposed on AFD. If AFD correctly learned the concept, with its decomposition the same as that of the original, one "care" was randomly deleted and the file was put back into AFD. If AFD did not learn the concept, a "care" was randomly inserted into the file and also put back into AFD. This process was repeated until the exact number of cards required for AFD to learn the concept was determined for each of the 10 cases for each of the 10 concepts. This process was repeated on FLASH with the same random number files used as for AFD. In the end, the two decomposers were ran a combined total of more than 1000 times.

### Results

Table 2 presents the people's results from the experiment. 'XX' indicates that the person was unable to find the concept in the 5-minute limit.

SUBJECT	CONCEPT									
	1	2	3	4	5	6	7	8	9	10
1	4	20	3	4	15	10	9	10	6	8
2	14	13	16	9	16	XX	15	16	24	25
3	3	24	1	3	2	21	8	18	24	3
4	15	XX	4	6	10	XX	4	14	20	2
5	5	26	2	11	30	20	9	14	3	6
6	5	22	3	14	4	XX	10	12	18	1
7	12	12	3	16	3	XX	7	22	19	4
8	11	XX	5	9	5	8	16	9	XX	12
9	8	XX	2	9	3	XX	16	14	XX	3
10	11	XX	3	12	19	XX	30	21	XX	1
11	19	30	3	8	3	16	6	28	26	1
12	18	23	1	4	15	XX	11	XX	XX	7
13	24	XX	10	18	18	XX	18	12	28	10
14	3	28	2	5	9	16	6	9	19	5
15	2	15	2	3	4	14	8	12	19	4

Table 2: People's Results

CASE	CONCEPT									
	1	2	3	4	5	6	7	8	9	10
1	19	12	14	18	19	14	13	37	7	11
2	21	20	16	33	14	14	5	42	13	13
3	15	27	2	21	13	10	7	37	11	13
4	12	14	4	17	16	13	13	37	12	4
5	16	11	15	19	12	11	11	22	9	8
6	13	13	7	20	15	7	16	32	14	4
7	15	26	6	23	20	14	3	37	12	13
8	16	35	10	30	16	13	13	42	11	10
9	21	15	2	17	20	14	13	23	10	5
10	14	12	19	25	16	16	10	50	13	13

Table 3: AFD Results

Tables 3 and 4, likewise, show the results of AFD and FLASH, respectively.

With these tables in mind, Table 5 shows the DFC for each concept and the averages for each concept for each type of learner (people, AFD, and FLASH).

The overall averages for people, AFD and FLASH were, respectively, 15.1, 15.9 and 12.3. This indicates that FLASH, in general, learned the concepts much faster than people, and that people performed slightly better than AFD. The next table, Table 6, looks for relationships between these numbers, utilizing the appropriate correlation coefficients obtained using the above table as well as the appropriate Hotelling-Pabst test statistics.

The Hotelling-Pabst statistic is used to test the hypothesis that two quantities are positively related [2]. A low number for this statistic indicates a positive correlation. The test concludes that the FLASH and DFC averages are positively correlated at the .001 level of significance (or a 99.9% chance of being correlated) and that the AFD and DFC are positively related at .10 level of significance (a 90% chance). The other tests are inconclusive but the correlation coefficients do not indicate a strong positive linear relation between the variables.

Perhaps one reason for this inconclusiveness is that the concepts involved were necessarily very easy to learn—that is, they had very low DFCs. Therefore, they do not represent a spectrum of all such functions. They are clustered in the “very easy” range. Hence, what may look scattered under the microscope, necessary to discern the points in this narrow range, may in actuality be more regular when viewing the entire picture<sup>1</sup>.

Looking at the results in another way offers another point of comparison.

---

<sup>1</sup>Prof. Mike Breen of Tennessee Tech helped examine these relationships.

CASE	CONCEPT									
	1	2	3	4	5	6	7	8	9	10
1	14	5	2	15	14	13	3	15	5	12
2	22	13	2	30	17	16	3	27	13	13
3	14	14	4	21	14	11	3	14	9	14
4	14	14	4	19	15	16	11	17	11	14
5	15	11	4	15	13	14	3	9	9	8
6	15	10	3	24	12	8	3	20	6	17
7	17	9	2	23	20	14	3	17	11	17
8	16	10	3	15	13	9	3	13	13	17
9	21	15	3	12	21	14	3	21	5	10
10	14	5	2	15	13	11	3	20	13	13

Table 4: FLASH Results

CONCEPT	DFC	People	AFD	FLASH
1	8	10.27	16.2	16.2
2	4	27.87	18.5	10.6
3	0	4.00	9.5	2.9
4	12	9.07	22.3	18.9
5	8	10.40	17.1	15.2
6	8	28.87	8.4	12.6
7	2	11.53	10.4	3.8
8	12	16.80	35.9	19.3
9	4	24.67	11.2	9.5
10	4	6.36	9.4	13.5

Table 5: DFC and Averages

	Correlation Coefficient	Hotelling-Pabst Statistic
(AFD, DFC)	.73	81
(AFD, People)	.03	152
(FLASH, DFC)	.93	17
(FLASH, People)	.04	172
(People, DFC)	.11	137

Table 6: Relationships

Table 7 does just that, comparing FLASH to people by category using the average for each concept and its rank of difficulty.

FLASH found the categories, from easiest to most difficult: simple, disjunctive, conjunctive and relational. The numbers fit perfectly; its easiest two were simple, next three (3,4,5) were all disjunctive, the next three (6,7,8) all conjunctive and its hardest two (9,10) relational. People tended to bounce around quite a bit more, except that their hardest three (8,9,10) were all disjunctive, and the averages indicate that simple was the easiest, closely followed by conjunctive, then relational with disjunctive bringing up the tail-end. Overall, FLASH found the simple and disjunctive concepts easier than people and people found the conjunctive and relational much easier than FLASH.

The greatest disparity between the two was with disjunctive and relational concepts. Why are people able to recognize relational concepts much easier than computers and, by the same token, why are computers much more adept with disjunctive concepts than people? Relational objects seem to be much more visually apparent. In the experiments given, people seemed to notice very quickly that all the positive examples had the same number of objects as borders (Concept #4) and would propose that as the rule even

		FLASH	People
Simple:			
	3	2.9(1)	4.00(1)
	7	3.8(2)	11.53(6)
	Ave.	3.35(1.5)	7.77(3.5)
Conjunctional:			
	1	16.2(8)	10.27(4)
	5	15.2(7)	10.40(5)
	10	13.5(6)	6.36(2)
	Ave.	14.97(7)	9.01(3.7)
Disjunctional:			
	2	10.6(4)	27.87(9)
	6	12.6(5)	28.87(10)
	9	9.5(3)	24.67(8)
	Ave.	10.9(4)	27.13(9)
Relational:			
	4	18.9(9)	9.07(3)
	8	19.3(10)	16.80(7)
	Ave.	19.1(9.5)	12.9(5)

Table 7: FLASH vs. People by Category

before examples of one, two and three objects had been shown, while the computer decomposers were unable to quickly come upon that, even with the three examples as "cares." With the decomposers, so many variables (relational concepts had the highest DFCs) were involved that it just took time to make that connection, while the opposite was true of people.

With disjunctional concepts, people were simply unable, or unwilling, to use the negative cases. Concept #2, disjunctional, is 3 objects or black. After 15 or so cards were shown, it would have been very easy for people to look at the negative column and notice that no black objects were present, then look at the positive column and recognize that those not black all had 3 objects and thus know the rule. But most people paid little to no attention at all to the negative column and failed to learn the disjunctive concepts, while the decomposers did quite well.

### Conclusion

Thus, in summary, FLASH did much better than people recognizing concepts, while AFD did a little worse. No apparent correlation or relationship exists between people's and AFD/FLASH's abilities to recognize and learn concepts. The DFC is a good indicator of how well AFD and FLASH will perform, but not of people. It must be said again, however, that the concepts used were very easy to learn for the computer decomposers. The most complex concept held a meager 4.7% difficulty rate. Perhaps a different test with a wider range of possible concepts will yield a closer, more distinct correlation.

It was also interesting that humans were far superior to FLASH at recognizing relational concepts, while the opposite held true for disjunctive concepts.



## References

- [1] John R. Anderson. *Cognitive Psychology and Its Implications*. W. H. Freeman and Company, San Francisco, 1980.
- [2] James V. Bradley. *Probability; Decisions; Statistics*. Prentice Hall, Englewood Cliffs, New Jersey, 1976.
- [3] Jerome S. Bruner, Jacqueline J. Goodnow, and George Austin. *A Study of Thinking*. Wiley, New York, 1956.
- [4] Timothy D. Ross. *Function Decomposition Strategy for the Function Learning and Synthesis Hotbed*. Technical Memorandum, Wright Laboratory, USAF, WL/AART, WPAFB, OH 45433-6543, August 1992.
- [5] Timothy D. Ross, Michael J. Noviskey, Timothy N. Taylor, and David A. Gadd. *Pattern Theory: An Engineering Paradigm for Algorithm Design*. Final Technical Report WL-TR-91-1060, Wright Laboratory, USAF, WL/AART, WPAFB, OH 45433-6543, August 1991.

## Appendix A

### **Concept Recognition Concepts**

<b>Example:</b>	<b>Squares or three borders</b>
<b>#1:</b>	<b>2 Crosses</b>
<b>#2:</b>	<b>3 Objects or Black</b>
<b>#3:</b>	<b>3 Borders</b>
<b>#4:</b>	<b># of Objects = # of Borders</b>
<b>#5:</b>	<b>1 Border &amp; Squares</b>
<b>#6:</b>	<b>1 Border or Grey</b>
<b>#7:</b>	<b>Odd # of Objects</b>
<b>#8:</b>	<b># of Objects + # of Borders = 4</b>
<b>#9:</b>	<b>2 Borders or Circles</b>
<b>#10:</b>	<b>Black Squares</b>

Appendix B

**Concept Recognition Experiment**

You will be participating in a concept recognition experiment aimed at determining the ability of people to recognize concepts in attribute cards. First, observe the different attributes and values for each card - the number of borders, the shape of the object, the number of objects and the shade of the objects. You will first be shown a card that is a positive example of a predetermined rule. You will be given an opportunity to guess the rule, or pass. You will then be shown cards, randomly ordered, and told whether or not positive or negative until you come up with the rule. You want to find the rule in as few of cards as possible. There will be a 5-minute time limit for each of the 10 rules. Now please observe the example and then take the test. Thank you!

	# of cards	time
# 1	_____	_____
# 2	_____	_____
# 3	_____	_____
# 4	_____	_____
# 5	_____	_____
# 6	_____	_____
# 7	_____	_____
# 8	_____	_____
# 9	_____	_____
# 10	_____	_____

### Appendix C

The cards were coded<sup>2</sup> for entry into the computer as 8-variable binary numbers as follows: The first two digits represented the number of objects on the card. '00' meant 1 object. '01' stood for two and '10' stood for three. '11' was a "don't care," as it represented no type of card. The second two digits represented the number of borders the card had and were numbered in the same fashion as the first two. The third two digits were for the type of object on the card. '00' was a plus, '01' a circle and '10' a square. The final two digits represented the shade of the object—'00' as white, '01' as grey and '10' as black.

Thus, binary number 10010010, or 146, represented a card with two borders and three black crosses, while 01101101, 109, would be a don't care because of the '11' representing the type of object.

---

<sup>2</sup>Dr. Tim Ross developed this coding system.

### Appendix D

The decomposition plan FLASH used is the following:

Decomp Plan:

0 = use partition sets

1 = No. of iterations

Selection Plan:

12 = method

0 = stopping condition

0 = stopping condition parameter

Evaluation Plan:

1 = no of steps

1 = DFC est method

100 = DFC standard

1 = dp\_for\_best\_part\_children\_is\_same

CHARACTERIZATION AND ANALYSIS  
OF  
1,3,5,5-TETRANITROHEXAHYDROPYRIMIDINE

DAVID A. ROSENBAUM

FINAL REPORT FOR:  
HIGH SCHOOL APPRENTICESHIP PROGRAM  
WRIGHT LABORATORY  
HIGH EXPLOSIVES RESEARCH AND DEVELOPMENT FACILITY (HERD)  
WL/MNME  
SPONSORED BY:  
RESEARCH AND DEVELOPMENT LABORATORIES  
CULVER CITY, CA 90230

AUGUST 19, 1992

## CONTENTS

- I. Introduction
- II. Acknowledgments
- III. Background
- IV. Procedures and Results
- V. Conclusions
- VI. Miscellaneous
- VII. References

## INTRODUCTION

### SECTION 1

1,3,3-Trinitroazetidine (TNAZ) is a heterocyclic compound (energetic material) under investigation as a melt cast base for high energy insensitive explosive applications. TNAZ has a high density and high performance level making it suitable for high energy applications. Although TNAZ has a high density and performance level it also has a few disadvantages. It has a high vapor pressure and a moderate melt point of 101 degrees Celsius. The heterocyclic compound 1,3,5,5-tetranitrohexahydropyrimidine (DNNC) is also under investigation. By adding DNNC to TNAZ the vapor pressure, melt temperature, and processing temperature can be lowered. Calculations indicate that TNAZ/DNNC form a low melt eutectic with a 70/30 weight percent and a melt point of 89 degrees Celsius. DNNC was characterized and its compatibility with TNAZ was investigated. The structures of DNNC were verified, its density was determined and its morphology was studied. Thermal analysis was conducted to determine its melt point, heat of fusion, and exothermic onset. Sensitivity of DNNC to impact, pinching, and extrusion was also determined. Calculations were conducted to estimate the performance parameters of DNNC including detonation velocity, detonation pressure, and Gurney energy using Kamlet Finger, Hardesty and Kennedy, Doherty, Short and Kamlet, and Gurney methods.

## ACKNOWLEDGMENTS

### SECTION II

I would like to thank Mr. Stephen Aubert for designing a project that involved hands on chemistry applications. I appreciate all the assistance from employees at the High Explosives Research and Development Facility (HERD). I would like to thank Mr. Don Harrison for managing the HSAP program. Again I appreciate all the time Mr. Stephen Aubert devoted to helping me with my project.



## BACKGROUND

### SECTION III

The military is faced with many problems when developing explosives. They must take into account the explosives performance, insensitivity, cost, and many other factors. The problem the HERD and the military is addressing is the development of a melt cast base using heterocyclic materials for High Energy Insensitive Applications. These high energy applications are for example air-to-air and surface-to-air missiles. Heterocyclic materials possess high density, high energy, and thus high performance. One goal of the problem addressed is to use 1,3,3-Trinitroazetidine (TNAZ) as this high energy melt cast base.

Heterocyclic materials are organic ring compounds containing atoms other than carbon in the skeletal ring. These materials are ideal for high energy insensitive applications. Replacement of carbon with nitrogen provides the advantages of a higher density, favorable oxygen balance, and a positive heat of formation (Ref. 1). High density increases a materials energy per unit volume, and thus its performance. A favorable oxygen balance, where all carbon and hydrogen is combined with oxygen upon reaction, results in a more efficient reactant to product conversion and hence greater energy released (Ref. 1).

TNAZ is a melt castable heterocyclic compound consisting of a four-membered ring (Figure 1) containing one nitrogen in the ring. Two alkyl or geminal nitro functional

groups are attached to the number three carbon and one nitramine functional group is located in the number one position. It has the unique structure of containing both aliphatic nitro and nitramine functional groups (Ref.2).

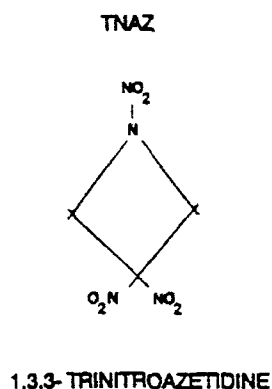


Figure 1

TNAZ is synthesized by nitration of t-Butyl Dinitroazetidiniumtrifluoroacetate, and has a positive heat of formation. The density of TNAZ is 1.85 g/cc(cubic cm) illustrating the high density, high energy heterocyclic. TNAZ has a high performance level with a detonation velocity of 9 km/sec and a detonation pressure of 360 kbar which compares favorably to HMX with a detonation velocity of 9.17 km/sec and a detonation pressure of 400 kbar (Ref. 2). There are also a few disadvantages associated with TNAZ. At 113 Degrees Celsius vapor pressure of 13 torr is considerably higher than TNT's, which is .2 torr at that temperature. The vapor pressure is high and should be lowered to reduce processing related complications in melt cast operations. Its moderate melt point of 101 degrees Celsius compounds its excessive vapor pressure problem. One possible solution to the lowering of the vapor pressure, melt point, and processing temperature is

to combine TNAZ with other explosives but maintain the performance level.

1,3,5,5-Tetranitrohexahydropyrimidine (DNNC) is an explosive under investigation as an additive to resolve the problems associated with TNAZ. DNNC was first synthesized by Dorothy Cichra and Horst Adolph in 1982 at White Oak Naval Center. The synthesis (Figure 2) starts off with 2,2-dinitropropane-1,3-diol in 25 ml of methanol. *t*-Butylamine and paraformaldehyde are added to form the precursor 1,3-diisopropyl -5,5-dinitrohexahydropyrimidine. Through nitration using 99% nitric acid DNNC was produced in a yield of 78%(Ref. 3).

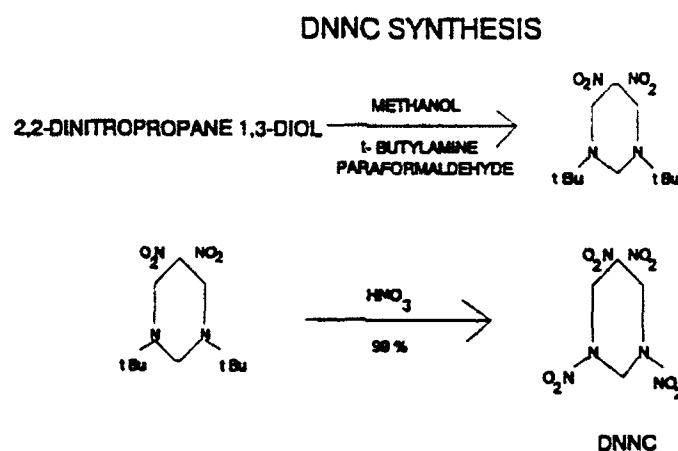
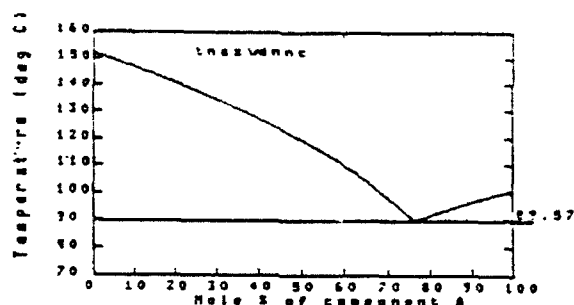


Figure 2

DNNC is a heterocyclic with a density of 1.82 g/cc. Through calculations DNNC appears to be a promising additive to TNAZ.

A possible combination of TNAZ/DNNC was proposed for investigation. The first step of the analysis was to perform calculations on the eutectic composition (Figure 3) to lower the melt point.

# EUTECTIC MELT POINT DIAGRAM



The eutectic is at 75 mole-% of TNAZ,  
which is 63.57 weight-% of TNAZ.  
The calculated eutectic temperature is 89.57 deg C.  
with the difference of the two calculated temperatures at that  
composition being .04 deg C.

Figure 3

A eutectic composition for TNAZ/DNNC of 70/30 weight percent and a melt point of 89 degrees Celsius was estimated by calculation. Next, performance calculations were run on DNNC, TNAZ, and TNAZ/DNNC at a 70/30 weight percent. The results as shown in the following chart.

	DETONATION	DETONATION	GURNEY
	VELOCITY (mm/usec)	PRESSURE (kbar)	ENERGY (KJ/cc)
TNAZ	8.75	375	8.231
DNNC	8.957	353	7.925
TNAZ/DNNC	9.099	366	8.205

This data supported the idea of a possible combination of the two explosives. Differential Scanning Calorimetry was run to determine melt point and chemical compatibility. The measured eutectic melt point was 91 degrees Celsius and no significant evidence of chemical compatibility between the explosives was observed.

The next step in the investigation was to characterize the physical and chemical properties of DNNC. The scientific approach used to study DNNC was divided into three phases. The first phase entailed the verification of structure and examination of the physical morphology using Nuclear Magnetic Resonance Spectrometry (NMR), Fourier Transfer Infrared Spectrometry (FTIR), Mass Spectrometry, Particle Size Analysis, and Scanning Electron Microscopy. Also in the first phase the density of DNNC was determined by gas pycnometry. The second phase included thermal analysis using the DSC/TGA, Henkin Time To Explosion, and Chemical Reactivity Test. Phase three included a sensitivity determination using the Drophammer and the Friction Sensitivity Apparatus. Further compatibility between TNAZ/DNNC was evaluated.

## PROCEDURES AND RESULTS

### SECTION IV

The first phase of characterization of DNNC entailed the verification of structure and morphology. Carbon 13 NMR spectra were obtained using a Bruker AC-300, 300 MHz Fourier Transform Superconducting NMR Spectrometer. One 20 mg sample of DNNC was dissolved in 4 ml of deuterio-acetone. Nuclear magnetic resonance spectrometry measures the applied field strength plotted against the absorption signal. In NMR a superconducting magnet produces a homogenous magnetic field of approximately 7.1 Tesla between its poles. The sample is spun about its mainfield (Z) axis by a stream of air to average out any existing homogeneities in the xy plane. The number of signals in the spectrum tells how many kinds of like atoms there are in the molecule. The position of the signal indicates the electronic environment of each atom. The splitting of a signal into several peaks shows the environment of carbon with respect to other, nearby carbons. The molecule absorbs the magnetic radiation and creates peaks. The peak shifts (Figure 4) are observed and represent the different functional groups of the molecule. (Ref. 1).

The FTIR was also used to confirm the structure of DNNC. As the molecule absorbs the infrared light it bends, stretches, and creates peaks. These peaks are observed and represent the different functional groups of a molecule (Figure 5). A particular group of atoms gives rise to characteristic absorption bands, that is, a particular group absorbs light of frequencies that are much the same from compound to compound. For example, C-N Amine group absorbs strongly at 1180-1360 reciprocal centimeters (Ref. 1).

The Mass Spectrometer was the last instrument used to verify the structure. In the Mass Spectrometer molecules are bombarded with beams of energetic electrons. The molecules are ionized and are broken up into many fragments, some of which are positive ions. As the bonds break, the fragments are recorded on a plot (Figure 6). These peaks are characteristic of the composition of the molecule (Ref. 1). The three charts below illustrate the plots of the verification process.

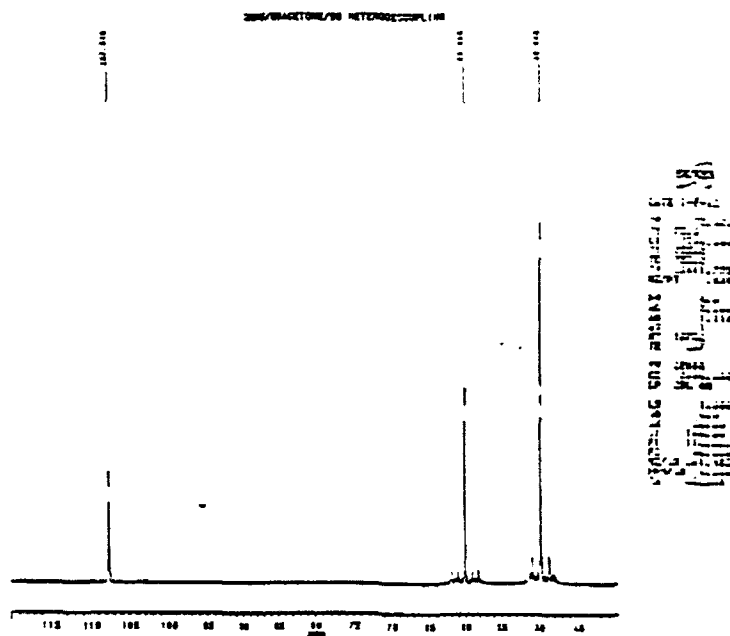


Figure 4

# INFRARED SPECTRUM (FT-IR)

BOND INDICATED	PEAK LOCATION (WAVENUMBERS)
N-H AMINE	3437.4
C-N AMINE	1253.8, 1298.2
C-C	810.2, 885.4, 943.3, 993.4
C-H	2962.8, 1442.8
NO <sub>2</sub>	1575.9, 1379.2

Figure 5

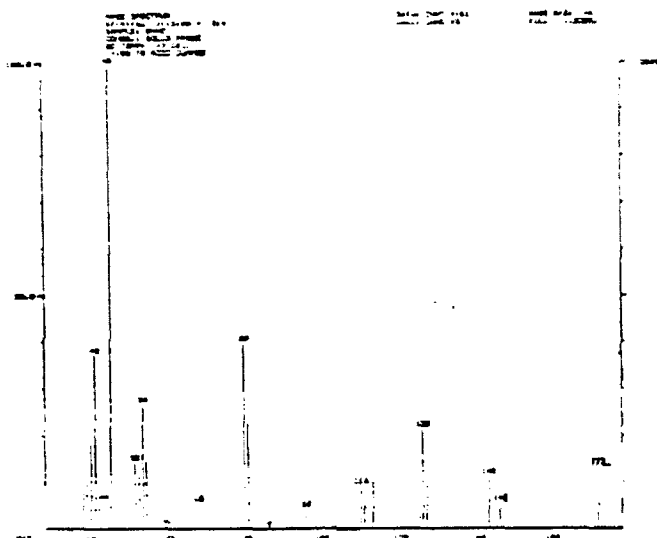


Figure 6

The Carbon-13 NMR Spectrum of DNNC in deuterio-acetone revealed peak shifts of 48.696, 59.999, and 107.646 ppm. The peak at 107.646 ppm represents the germinal carbon groups and the peaks at 59.999 and 107.646 ppm represent the other two carbon groups. All three peaks representing DNNC's different functional groups were recorded. The FTIR was also successful in recording DNNC's functional groups. The Mass Spectrum revealed that the molecules' fragment products were consistent with the composition of DNNC. All three techniques yielded spectra consistent with that expected from DNNC's and confirmed its structure.

The particle size of DNNC was determined using a Brinkman Particle Size Analyzer 2010. The average particle size was 52.91 microns (Figure 7). Scanning Electron Micrographs revealed that DNNC's structure was somewhat pyramidal (Figure 8).



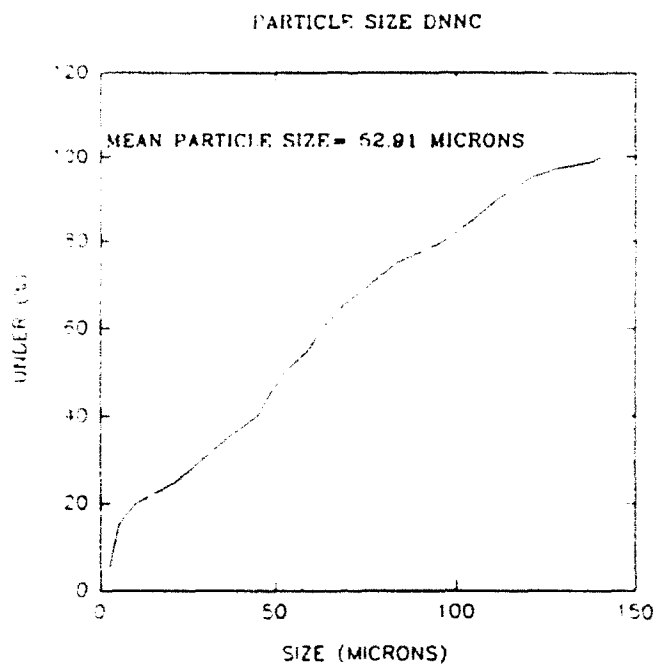


Figure 7



Figure 8

The density of DNNC was determined through gas pycnometry. The average density was found to be 1.76 g/cc. The density results for each run appear in the chart below (Figure 9).

# DENSITY DETERMINATION BY PYCNOMETRY

	VOLUME (cc)	DENSITY (g/cc)
RUN 1	3.790	1.760
RUN 2	3.791	1.763
RUN 3	3.800	1.758
RUN 4	3.802	1.757
RUN 5	3.795	1.761

WEIGHT OF DNNC = 6.683 g

AVERAGE DENSITY = 1.760 g/cc

Figure 9

The second phase of the characterization was to determine DNNC's thermal properties. One milligram samples of DNNC were thermally analyzed by Differential Scanning Calorimetry. Heat was applied at a rate of 10.00 deg C /min. The scan produces a trace of endothermic and exothermic events which take place as the temperature of the sample rises in an inert Nitrogen environment (Ref. 5). The following plot (Figure 10) is an example of an exothermic and endothermic run on DNNC.

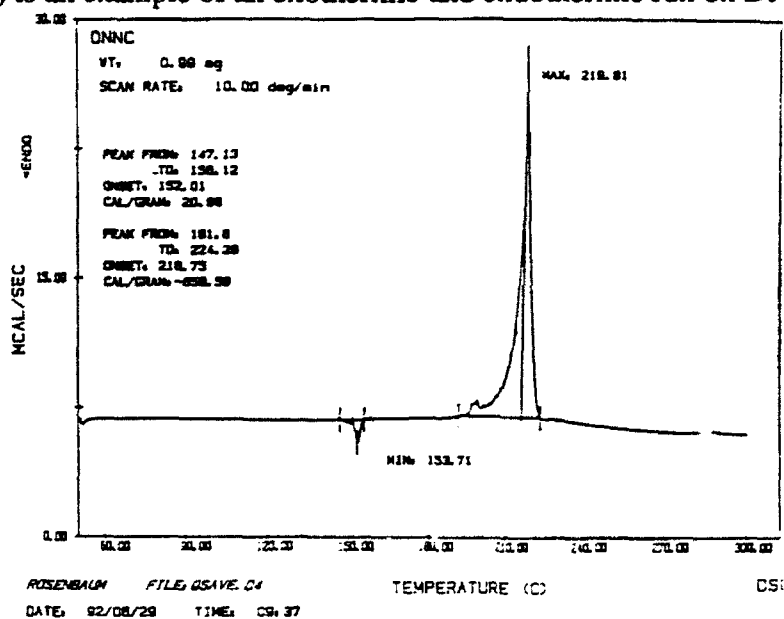


Figure 10

# DIFFERENTIAL SCANNING CALORIMETER RESULTS

MATERIAL	HEATING RATE (DEG/MIN)	MELT ONSET °C	HEAT OF FUSION (cal/g)	KCAL/ MOLE	EXOTHERM ONSET °C
DNNC	10	153.99	20.47	5.4	216.75
DNNC	10	154.72	18.72	5.0	216.16
DNNC	10	152.01	20.88	5.5	—

AVERAGE HEAT OF FUSION = 20.02 cal/g  
5.3 kcal/mole

Figure 11

The DSC results (Figure 11) indicate that DNNC's melt onset ranges from 152-155 Degrees Celsius and the average heat of fusion is 5.3 kcal/mole. The exothermic decomposition remained consistent at 216 degrees Celsius. Variable heating rate experiments were also conducted on the DSC (Figure 12). The Arrhenius Equation of

$$k = Ze^{-E_{act}/RT}$$

was used to find the  $E_{act}$  (Energy of Activation). The energy of activation is the minimum amount of energy that must be provided for reaction to proceed. In the equation  $Z$  is the pre-exponential factor,  $K$  is the reaction rate,  $R$  is the real gas constant, and  $T$  is the temperature in Kelvin (Ref. 4). From the original equation the log of both sides is taken and rearranging is done to form

$$\ln k = -E_{act}/R \cdot 1/T + \ln Z$$

The  $\log B$  (heating rate) is plotted against  $1/T$ . The slope of the line becomes  $-E_{act}/R$ .

Through the Arrhenius Equation the energy of activation was 32.17 kcal/mole.

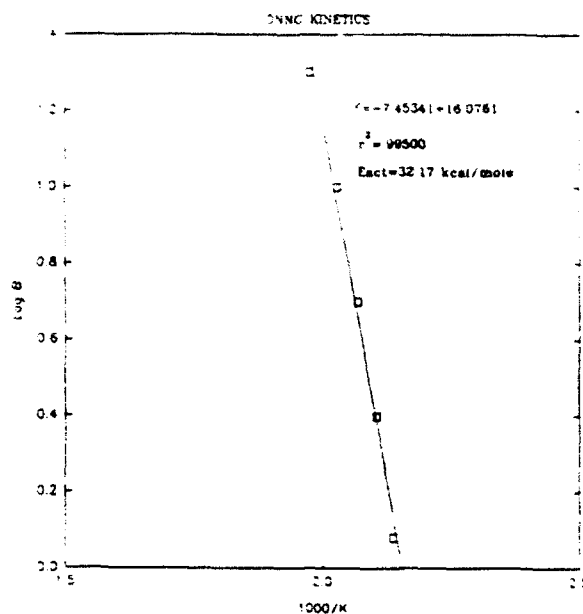


Figure 12

To find the amount of decomposition in DNNC the Thermogravimetric Analyzer was used. The objective of the TGA is to determine whether there are any weight changes in a sample either when it is at a fixed temperature or time. The TGA is useful in obtaining chemical property information such as thermal stability and chemical reaction (Ref. 5). DNNC was run isothermally for 1000 sec. at 120 degrees Celsius and the weight percent lost was 2.585. A question was raised about a possible chemical incompatibility with stainless steel so a sample of DNNC/Stainless Steel 50/50 weight percent was run. Similar results were achieved. A 2.286 percent weight loss was recorded.

The Henkin Time To Explosion was used to determine the critical temperature of DNNC. The critical temperature is the minimum temperature for a given geometry at which an explosive will not react violently. The measured critical temperature of DNNC was 167 Degrees Celsius. The measured energy of activation from the Henkin Time To Explosion was 36.9 kcal/mole. The plots of the Henkin results are shown below (Figure 13 and 14).

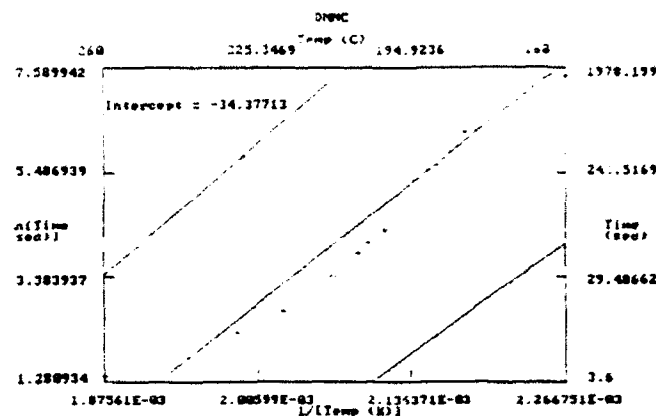


Figure 13

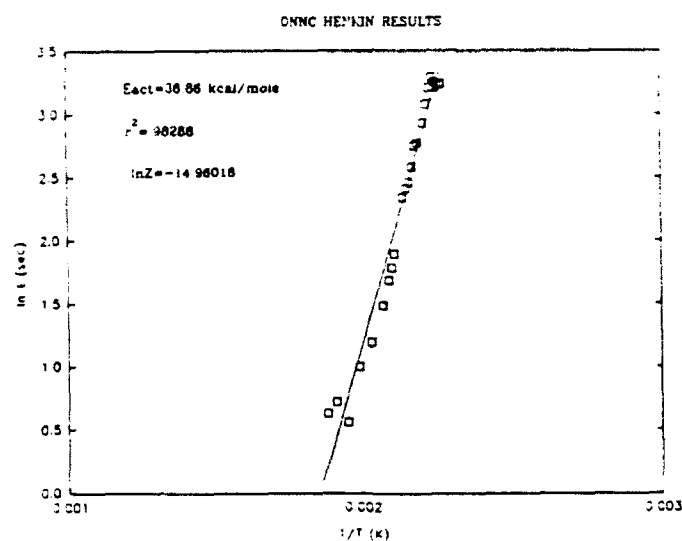


Figure 14

Chemical Reactivity Tests were conducted to find the thermal stability of DNNC. Three 250 mg samples of DNNC, in a Helium environment, were heated for 22 hours at 120 degrees Celsius in a stainless steel and glass tubes. After the sample was heated, analysis was done and revealed that an excessive amount of gasses were released as illustrated by the following chart (Figure 15).

# CHEMICAL REACTIVITY TEST

COMPOUND	CONDITIONS	TOTAL GASES RELEASED (g/cc)
DNNC	GLASS	8.597
DNNC	STAINLESS STEEL	9.454
DNNC	STAINLESS STEEL	10.368
DNNC	STAINLESS STEEL	9.071
TNAZ	STAINLESS STEEL	.576

Figure 15

Phase three included the sensitivity determination using the Bureau of Mines Type 12B Drophammer and BAM Friction Sensitivity Apparatus. The drophammer test measures an explosives sensitivity to impact. Twenty five samples weighing 35 milligram each were placed on pieces of abrasive sandpaper. A 2.5 kg weight was dropped at varying heights registering go's and no go's. The H50% of DNNC was 30 cm compared to RDX which is 22 cm. The friction tester measures an explosives sensitivity to pinching and extrusion. 20 milligram samples are weighed on to porcelain plates. The test records the minimum amount of friction in kilograms needed to produce inflammation in the explosive. DNNC's friction sensitivity was 3.6 kg which is identical to that observed for TNT.

## CONCLUSION

### SECTION V

The characterization of DNNC was successfully completed. The DSC measured the melt point at 152 Degrees Celsius and the heat of fusion at 5.3 kcal/mole. The Carbon NMR, FTIR, and the Mass Spectrometer verified the structure of DNNC. The density determined by pycnometry was 1.76 g/cc. The particles of DNNC averaged 52.91 microns and are pyramidal in shape. The CRT revealed that after 22 hours at 120 degrees Celsius DNNC released an average of 9 g/cc of gasses comparing unfavorably to that of HMX and DATB which are less than .01 g/cc and .03 g/cc respectively (Ref. 6). This amount of decomposition is excessive for use in explosive applications.

## MISCELLANEOUS

### SECTION VI

This summer through HSAP I learned the importance of patience and safety in conducting explosive scientific operations. I have a more complete understanding of organic chemistry and explosive technology. I gained experience with actual chemical engineering which will be useful when I begin to study chemical or environmental engineering.



## REFERENCES

### SECTION VII

1. Morrison, Robert T. and Robert N. Boyd. Organic Chemistry, Third Edition. Boston: Allyn and Bacon, Inc., 1973.
2. Iyor, Dr. Sury, et.al. Scaled-up Preparation of 1,3,3-Trinitroazetidine. Army Armament Research, Development, and Engineering Center. Picatinny Arsenal, NJ.
3. Cichra, D.A. and H.G. Adolph. Synthesis of 1,3,5,5-Tetranitrohexahydropyrimidine. White Oak Naval Facility, Silver Springs, Maryland. 1982.
4. Levine, Ira N. Physical Chemistry. New York: McGraw Hill, 1978.
5. Dobratz, B.M. LLNL Explosives Handbook. Lawrence Livermore National Laboratories. March 16, 1981.

A Study of the Importance of Sled Tests  
To Crew Escape Engineers

Kimberly D. Royalty  
High School Apprentice  
Aircrew Escape Group

Wright Patterson Airforce Base  
Dayton, Ohio  
45404

Final Report For:  
AFSOR Research Program  
Flight Dynamics Laboratory

Sponsored By:  
Air Force Office of Scientific Research

August 1992

A Study of the Importance of Sled Tests  
To Crew Escape Engineers

Kimberly D. Royalty  
High School Apprentice  
Aircrew Escape Group

Abstract

Crew escape engineers use the data they receive from sled test summaries to determine whether the ejection system for a particular aircraft is safe. To be considered safe, a person should be able to eject from an aircraft without cause or harm due to possible deficiencies in the design of the system. Sled track testing is conducted at speeds which are representative of the aircrafts flight envelope. During the test, the acceleration, velocity, and position of the escape system is recorded. Costs and injuries are kept at a minimum by using dummies and models for the test. These facts prove that sled track tests are very important in determining the safety of an escape system.

A Study of the Importance of Sled Test  
To Crew Escape Engineers

Kimberly D. Royalty

INTRODUCTION

For a long time, engineers have been trying to find a way for people to eject safely from airplanes and jets. Escape systems began as parachutes which were sufficient for their time, but as things progressed, something better was needed. As a result, ejection seats came about. They were safer and there was a greater chance of survival when pilots had to eject when they were flying at high speeds and/or low altitudes. Still as time went on, the need for an even better system was evident. This brought about escape capsules which were safer than ejection seats because the pilot is enclosed by the escape system and protected from wind blast, water exposure, cold, etc. (Figs. 1&2). However, there was a big issue about costs and hazards. A cheaper way needed to be found to test these systems without risking human lives in the process.

METHODOLOGY

There are many types of information that can be derived from sled track test data. First of all, the speed at which an aircraft is traveling at the time of ejection is one factor that determines the results of the sled test summary. This also tells you how quickly the aircraft will pass the ejection seat or capsule and allows you to find the minimum speed at which ejections are possible. Secondly is the aircraft's altitude. We can determine just how low a pilot can be flying before it will be dangerous for him to eject. An ejection at a low altitude could pose a number of problems. For example, there could be mountainous terrain and ejecting may throw a pilot into the rocks or maybe into a gorge or ravine. It is also possible that the parachute on the capsule would not have time to deploy and the pilot could fall to the ground or whatever happens to be below him.

FIG 1

# F-111 CREW MODULE

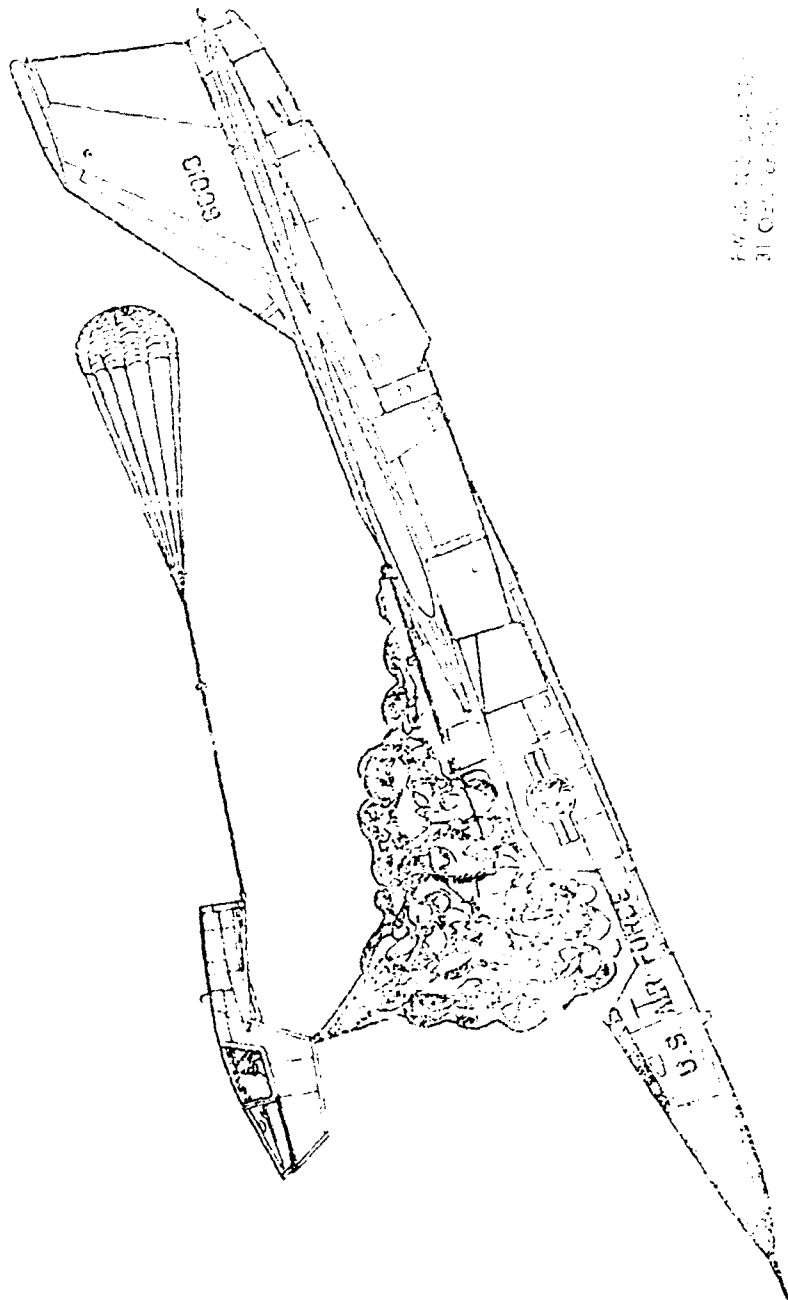
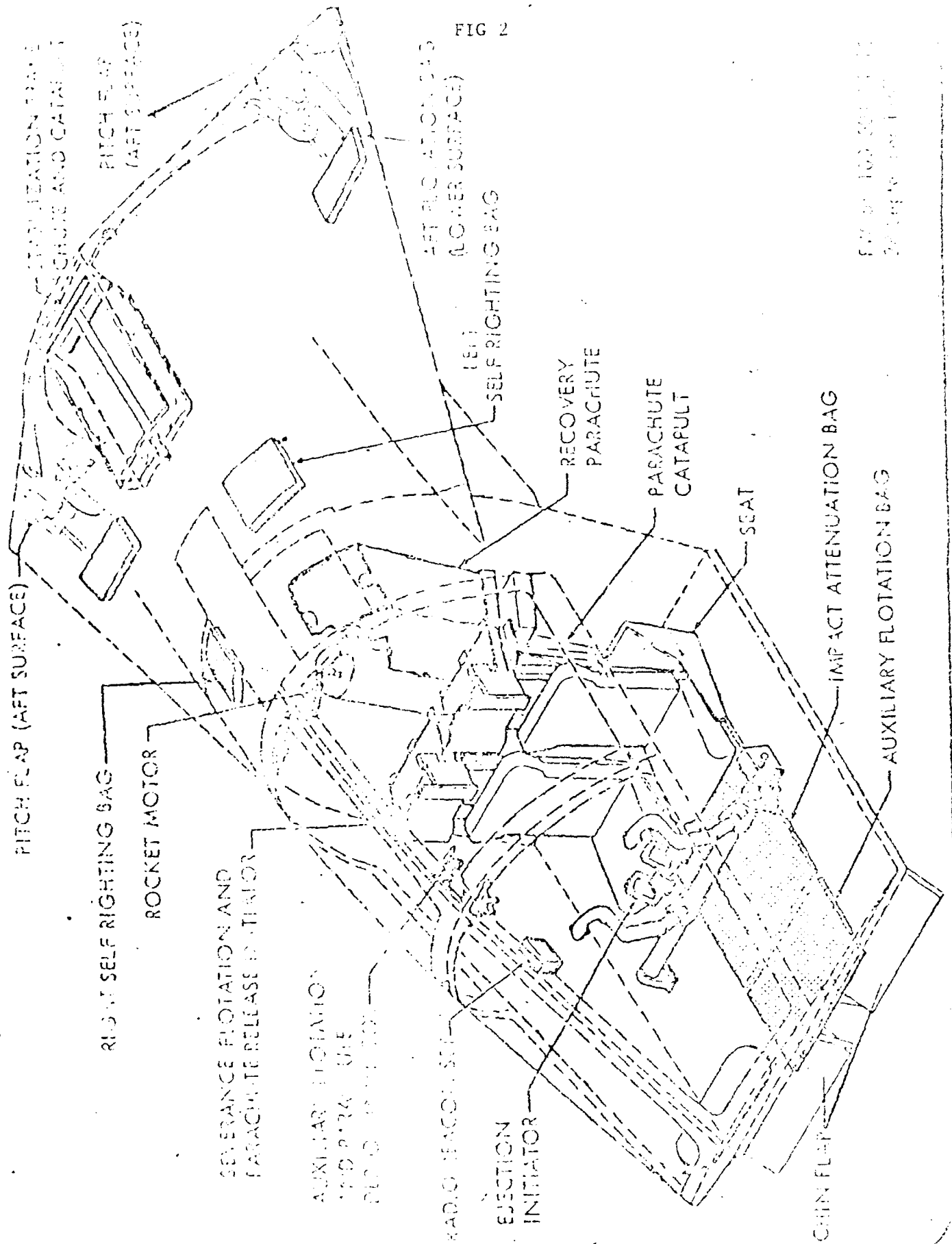


FIG 1  
F-111 CREW MODULE

~~CREW MODULE GENERAL INFORMATION~~

[illegible]

Aircraft altitude is also a very important factor. If an aircraft were upside down and the pilot is flying at a very low altitude, an ejection would probably be fatal unless there was a system that could sense directions and catapult the capsule upward and away from the aircraft. If the pilot were flying sideways, he might end up being thrown into the side of a mountain.

A key problem is how to keep the capsule or ejection seat from coming in contact with the canopy or aircraft in those critical seconds after ejection. If the aircraft were flying at a low speed there would need to be enough time allowed for it to move away from the seat or capsule so that they would not come in contact with each other.

These are some of the problems pilots face when they begin the ejection sequence (Fig. 3). Sled test data provides the information that engineers need to design crew escape systems so they can alleviate these problems.

## RESULTS

Engineers take the data from the sled tests and focus on the problems they find. Then they have to figure out what possible solutions could solve the problems they found. The next step is to use trial and error until they find the best solution to the problem, if any. For example, if a certain system did not have enough power to keep it from colliding with the aircraft after ejection this would show up on the test results. The proper changes could be very minor or they could possibly be so difficult to carry out that a new system may need to be designed instead of changing the old one. One technique that could be used in the future is the use of retrorockets that would let a computer guide the capsule or seat away from danger. The computer would need to have sensors that could find out which direction the seat or capsule was headed, it would have to sense the possible dangers, and then carry out the necessary maneuvers to guide the system away from the danger. The computer would need to have sensors that could find out which direction the seat or capsule was heading, it would have to sense the possible dangers, and then carry out the correct maneuvers to guide the system away from danger (Fig. 4). After finding the direction and dangers the

# CREW MODULE EJECTION SEQUENCE

- 1 • EJECTION HANDLE PULL (1.0 SEC)  
• INERTIA REELS RETRACT  
• EMERGENCY OXYGEN TRIPS  
• ROCKET MOTOR FIRES AND CREW MODULE SEVERS (1.35 SEC)\*  
• STABILIZATION BRAKE CHUTE DEPLOYS (1.5 SEC)

- 2 • MAIN MOTOR FLARES OUT (1.15 SEC)

- 3 • RECOVERY CHUTE DEPLOYS\*\*

- CHAFF DISPENSER AND RADIO BEACON ACTUATES (3.00 SEC)

- 4 • RECOVERY CHUTE LINES STRETCH

- 5 • IMPACT ATTENUATION BAG DEPLOYS (3.00 SEC AFTER RECOVERY CHUTE DEPLOYS)

- RECOVERY CHUTE DISREEFS (2.5 SEC AFTER CHUTE LINES STRETCH)

- 6 • RECOVERY CHUTE FULL OPEN

- IMPACT ATTENUATION BAG INFLATED (4.25 SEC AFTER BAG DEPLOYS)

- CREW MODULE REPOSITIONS AND EMERGENCY UHF ANTENNA EXTENDS (7.00 SEC AFTER RECOVERY CHUTE DEPLOYS)

## Notes

\* AT SPEEDS ABOVE 300 KNOTS, EJECTION MOTOR FIRES AFTER 1.35 SECS

\*\* AFTER DEPLOYMENT, CREW MUST REMAIN IN POSITION UNTIL THE RECOVERY CHUTE IS FULLY OPEN. AFTER THE CHUTE IS FULLY OPEN, THE CREW MAY MOVE TO A MORE COMFORTABLE POSITION.

FIG 3





# STABILIZATION & RECOVERY GROUPS

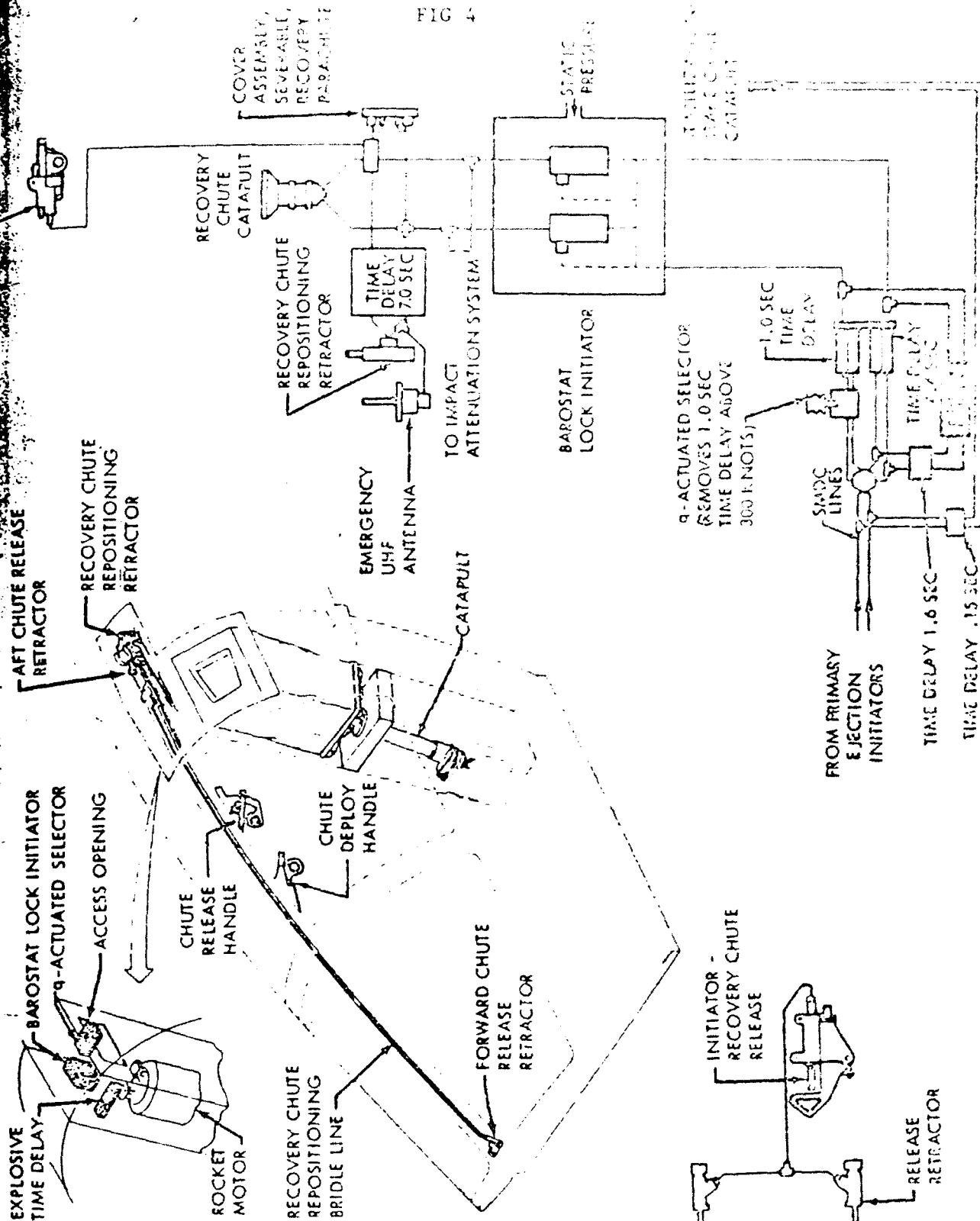


FIG 4

correct maneuvers would ignite these rockets, but it would have to control them as well. This type of system would be very useful, however more problems could arise in the process of designing or testing the system. Advances are being made; a lot of lives and money have been saved by using these sled tests to determine or predict what would happen in certain situations and conditions.

#### CONCLUSIONS

In the near future, we can expect to see a lot of new ideas that could possibly develop into a new generation of escape systems. The need for newer systems and better escape modules has become great. Costs have become so high that it is important to test new ideas at the lowest cost possible, but also to insure accurate results. Sled track tests provide both. They do not cost as much as if someone would actually go out and eject from an aircraft in the middle of a flight. The result would be to build a new aircraft to replace the one destroyed during the test. Sled tests give just as accurate results, do not cost nearly as much as it would to build a new aircraft, and keep from having to place actual humans in the cockpit for the initial testing.

#### REFERENCES

Beasley, M.D., Model F-111A/B Predicted Flight Characteristics, McDonnell Aircraft Corporation, St. Louis, MO, Apr., 1968.

Brinkley, James W., Raddin, J.H., & Others, Evaluation of a Proposed Modified F/FB-111 Crew Seat and Restraint System, Air Force Aerospace Medical Division, Wright-Patterson Airforce Base, Dayton, Ohio, Nov., 1981.

Manufacturing Plan Excerpts F-111 Escape Module Briefing Charts, Convair Airspace Division, Fort Worth, Texas, Oct., 1968.

A SECOND YEAR STUDY ON THE IMPLEMENTATION  
OF THE RECIRCULATING OPTIC DELAY LINE CONCEPT  
IN A COHERENT RADAR SYSTEM

Dennis W. Scott, Jr.  
High School Apprentice  
Seeker Technology Branch

Wright Laboratory Armament Directorate  
WL/MNGS  
Eglin AFB, FL 32542-5434

Final Report for:  
High School Apprenticeship Program  
Wright Laboratory Armament Directorate

Sponsored by:  
Air Force Office of Scientific Research  
Bolling Air Force Base, Washington, D.C.

August 1992

A SECOND YEAR STUDY ON THE IMPLEMENTATION  
OF THE RECIRCULATING OPTIC DELAY LINE CONCEPT  
IN A COHERENT RADAR SYSTEM

Dennis W. Scott, Jr.  
High School Apprentice  
Seeker Technology Branch

Abstract

The concept of the recirculating optic delay line (RODL) used in a coherent radar assembly as a frequency reference unit was the focus of this study. To implement the recirculating optic delay line, a simple coherent radar array was designed and assembled. The entire assembly and its subassemblies were then calibrated in order to define its variables and establish an understanding of the new radar's capabilities before any real world experimentation was conducted. The coherent radar assembly was then tested with real targets so that an idea of the recirculating optic delay line's potential use as a frequency reference unit could be evaluated. The radar performed exceptionally well when not overburdened by clutter, and images could be clearly distinguished in the return. The radar system was linked to both a digitizing oscilloscope and a personal computer so that the images could be seen in real time and stored for further analysis. The results of this study demonstrate that the recirculating optic delay line concept may be feasibly used as frequency memory unit in a coherent radar.

A SECOND YEAR STUDY ON THE IMPLEMENTATION  
OF THE RECIRCULATING OPTIC DELAY LINE CONCEPT  
IN A COHERENT RADAR SYSTEM

Dennis W. Scott, Jr.

INTRODUCTION

The objective of this project was to test and record the virtually unexplored concept of a recirculating fiber-optic delay line as a frequency memory unit, substituting for the conventional frequency reference unit (FRU) in a coherent radar system. The recirculating optic delay line (RODL) concept's intent is aimed at reducing the complexity and expense of the conventional coherent radar such as those which are used and sacrificed in the seeker systems of some missiles. This report describes a coherent radar which uses a fiber-optic delay link to provide the required coherent local oscillator (LO) function. This local oscillator function is one of the several functions conventionally assumed by the frequency reference unit. To perform its functions, the typical frequency reference unit is composed of sophisticated digital subsystems. The complexity of the unit makes it one of the most expensive subsystems in a radar seeker. It is expected that the RODL concept would reduce the number of components and subassemblies as well as the amount of integration and required testing in the radar system. This would further reduce the cost to produce and maintain the radar system.

This report details the concept of the recirculating optic delay line, the system which was constructed to implement the concept, and the results which were gained through the study.

## METHODOLOGY

The coherent radar described in this report works without using the typical frequency reference unit. This is achieved through the use of the recirculating optic delay line. A concept of how the RODL works may be more easily understood with the aid of Figure 1. The RODL is used to mix the radar return with the delayed replica of the signal which was transmitted toward the target. With reference to Figure 1, a small portion of the transmitted RF pulse is coupled to the RODL. This RODL consists of a fiber-optic line (used as the delay link) and RF amplifiers and variable attenuators sufficient to produce a zero round trip insertion loss. The total loop delay  $T_D$  is adjusted to be equal to the length of the RF transmitted pulse  $T_t$ , so that the loop is completely "filled" with the RF transmit pulse. This coupled fraction of the transmit pulse is then allowed to recirculate in the loop. With each completion of the loop a small portion of the recirculating RF energy is coupled off to perform the LO function of the radar.

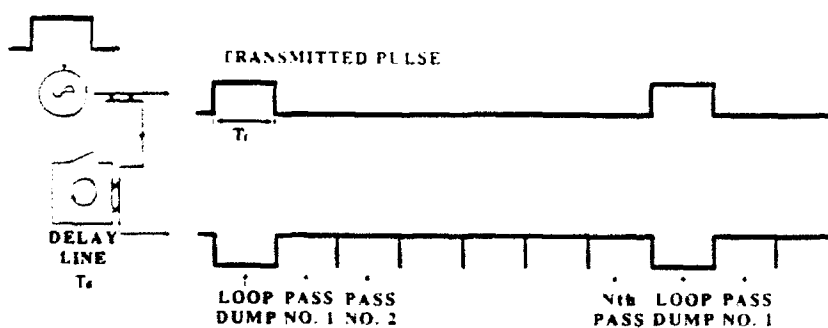


Figure 1

The recirculating optic delay line was incorporated into a simple coherent radar system through a link between the radar's receiving and transmitting subsystems. As Figure 2 shows the signal is first created in a frequency synthesizer and then amplified enough to gain a minimal range over the target area. This signal is directed through a coupler which splits the signal. One of the signals is transmitted through a horn antenna over a target area while the other is attenuated and directed into the RODL circuit. The final version of the recirculating optic delay line circuit carries the virgin RF signal through a directional coupler into a laser transmitter which converts the RF signal into light. The converted signal is delayed as it circulates through a 200 meter spool of fiber-optic line and is then converted by a photodiode into the original RF signal. This signal is amplified and put through a directional coupler which splits the signal. One of the duplicate signals is then amplified again, filtered through a 9.3 GHz band pass filter, attenuated, and recirculated through the RODL circuit until a new signal is entered. The other RF signal is tapped from the directional coupler of the recirculating optic delay line to be used as a local oscillator signal in the receiving circuit. This signal is first put through amplification and a variable attenuator to boost and stabilize the signal. A generated .990 GHz signal is then mixed with the 9.268 GHz signal from the RODL circuit to create an 8.278 GHz RF signal. This new signal is filtered through an 8.3 GHz band pass filter to alleviate some of the noise which might have been acquired in the circuitry and once again is amplified and attenuated to control the signal's power. The 8.278 GHz signal is then mixed with the return signal from any targets. Be reminded that this signal's frequency is no longer 9.268 GHz, but 9.268



GHz plus any doppler shift that the target might have generated. The mixing of the two signals creates a .990 GHz plus doppler shift signal which is amplified and mixed into an in-phase and quadrature port (I and Q port). This I and Q port shifts the signal ninety degrees and mixes it with a .990 GHz signal to reveal the doppler shift which the transmitted signal might have gained. Test couplers were added to the receiving circuit at points before the mixing of the recirculated signal with the return and just after amplifying this mixed signal. These couplers were used for test and data purposes.

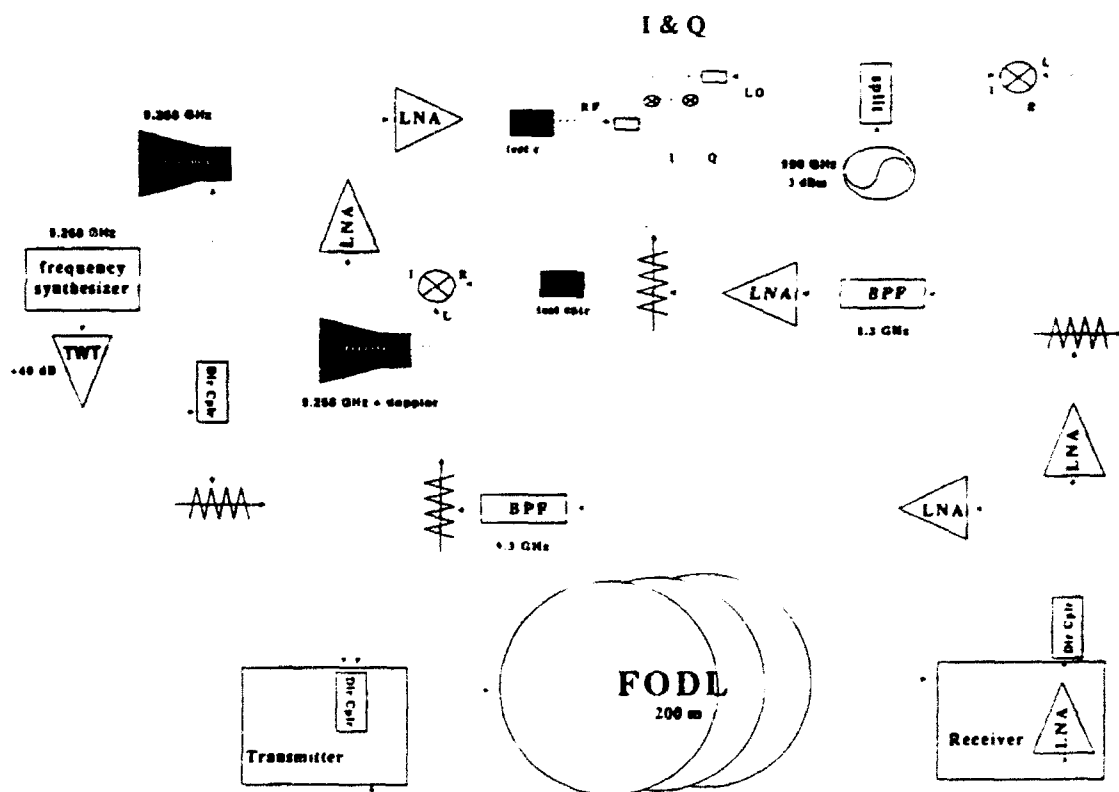


Figure 2

The coherent radar system which was used for this project was designed and constructed during the summer's time specifically to incorporate the RODL circuit. The radar was assembled through the construction and integration of its transmitter, receiver, and RODL subsystems. The recirculating optic delay line circuit was the first of the subsystems to be constructed specifically because detailed plans were already on hand for its construction. The final version of the RODL circuit shown in Figure 2 is a modified version of the original provided drawings. Though the major fiber-optics are unchanged, the smaller components used to stabilize and maintain the RF signal were altered or eliminated to reduce the losses in the circuit and to reduce the complexity of the subsystem. Calibration and trouble-shooting the subsystems was an ongoing process and difficulty arose even before attempts were made at integrating the subsystems. Providing sufficient gain to maintain a stable power of 0 dB in the RF pulse within the RODL provided patient challenges, and timing the pulse length of the signals so that the recirculating and incoming pulses in the recirculating line would not overlap or leave empty spaces also presented hard solved problems.

Once the RODL circuit was satisfactorily operating independently, work began on assembling the receiving subsystem. The receiver was constructed and calibrated independently before being linked to the RODL. Aside from minor incidents relating to the mixers used in the subsystem, relatively few problems occurred with the independent receiver. A simulated return and LO signal was used to test the circuit and calibrate its independent performance. The two existing subsystems were then integrated.

Immediate problems arose with the power and maintenance of the signal

through the joined RODL/receiver circuit. At this point in the assembly of the radar system frequency synthesizers were used to enter signals into the RODL and return ends of the circuit. It was discovered that with certain minor adjustments in the originally planned 9.3 GHz transmitted signal there would be far less loss in the circuitry, thus the output and recirculated signal were toggled to 9.268 GHz. It was then noticed that the signal being coupled from the RODL into the transmitter was not delivering enough power to drive the mixers. An additional amplifier and variable attenuator were thus added to compensate for the low signal. The three variable attenuators throughout the two subsystems were then adjusted in respect to the components of the integration and then to each of the other attenuators.

Finally, the transmitter subsystem was constructed and added to the existing subsystems. With this, the radar was complete. The transmitter subsystem is the simplest of the circuits. It consists of only five components and needed no independent calibration. Once integrated with the entire assembly, adjustments needed only to be made in the transmitter's variable attenuator so that the signal would not be too strong as it entered the recirculating portion of the radar. (The frequency synthesizer in the transmitter circuit needed no calibrating because its standards had been set in the testing of the receiver and RODL subsystems.) The variable attenuators throughout the system were again adjusted to compensate for the newly integrated addition, and the coherent radar system was ready for testing with real world targets.

The radar/recirculating optic delay line was tested with the target area available from the fourth floor of Wright Laboratory on Eglin Air

Force Base in Florida. The radar's horn antennas were directed from the Millimeter Wave Laboratory's east window toward the available target area which included concrete and metal structures, a water tower, fuel storage tanks, a tall metal chimney, tree lines, a rise in the topography, and various types of vehicles moving in various directions. These targets were also available within the radar's range threshold. During the radar's initial real target testings is when problems with the radar's small power capability became apparent. The 40 Db of power provided through the amplifier in the transmitter and the gain of the horn antennas returned only a weak signal and limited the range of the radar. The radar's range was not so much of a problem because the testing was only being conducted on a small scale and to have an extensive range capability was simply unnecessary. The weak signal return, though, did become a problem as the project moved into the stages of needing to record data and the digitizing equipment needed greater power in the return to recognize that there even was a signal. This lead to the addition of an amplifier in the receiving circuit (not shown in Figure 2) just after the receiving horn antenna and before the mixer to boost the return signal. Afterwards little calibration to the radar system was required to view the returns on a digital oscilloscope linked to the radar through one of the test couplers.

The returns from the coherent radar system were also directed through fifty foot co-axial cables to a LeCroy digitizer. The RF returns were digitized and could be viewed and recorded in a personal computer through an existing waveform catalyst program. This meant that data from the radar could be viewed in real time, hard copy still images could be made, and portions of real time data could be stored and transferred to other

personal computers for analysis. An attempt was made during this summer's time to write software in the C programming language which would be better able to manipulate the active radar returns than the waveform catalyst when given a stored image from the waveform catalyst. Unfortunately, time, a lack of C programming knowledge, and an inability to learn the language in the time given finally put this attempt to rest.

## RESULTS

From this project comes a working coherent radar system implementing the recirculating optic delay line concept as a frequency reference unit. The RODL concept worked well and just as expected as shown in Figure 3. The plot shows (from bottom to top) the pulse transmitted pulse, an up-close return and bleed over, and the recirculating pulse in the RODL.

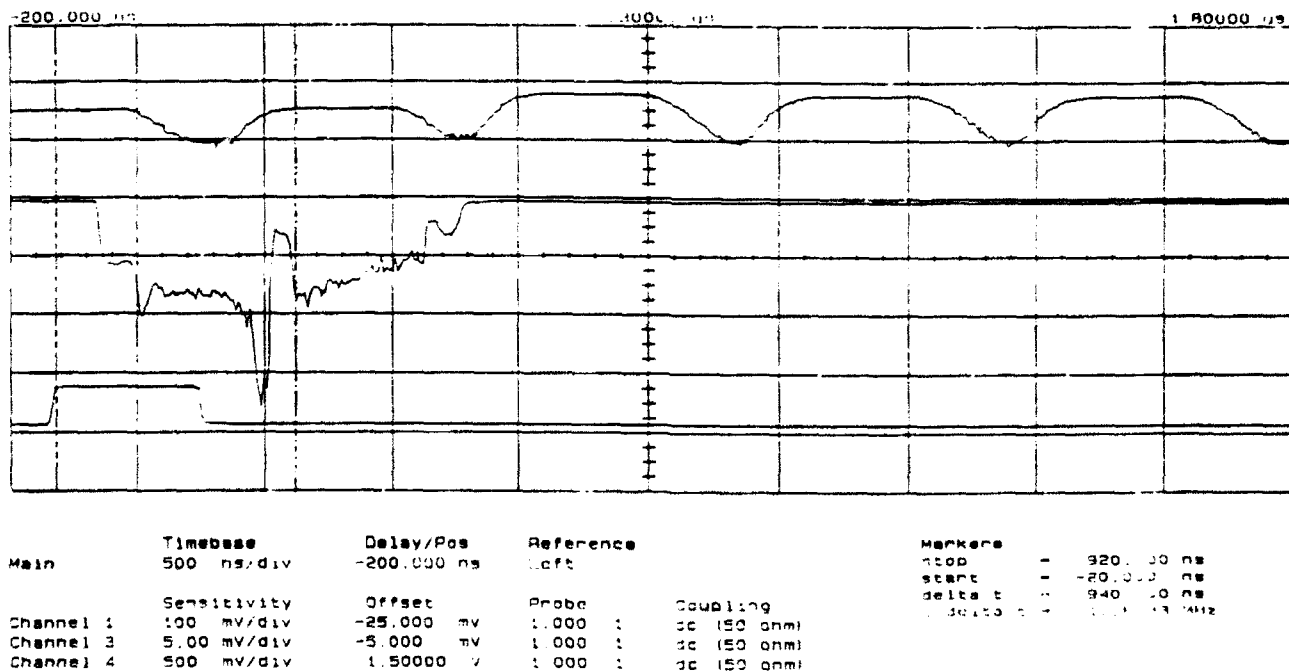
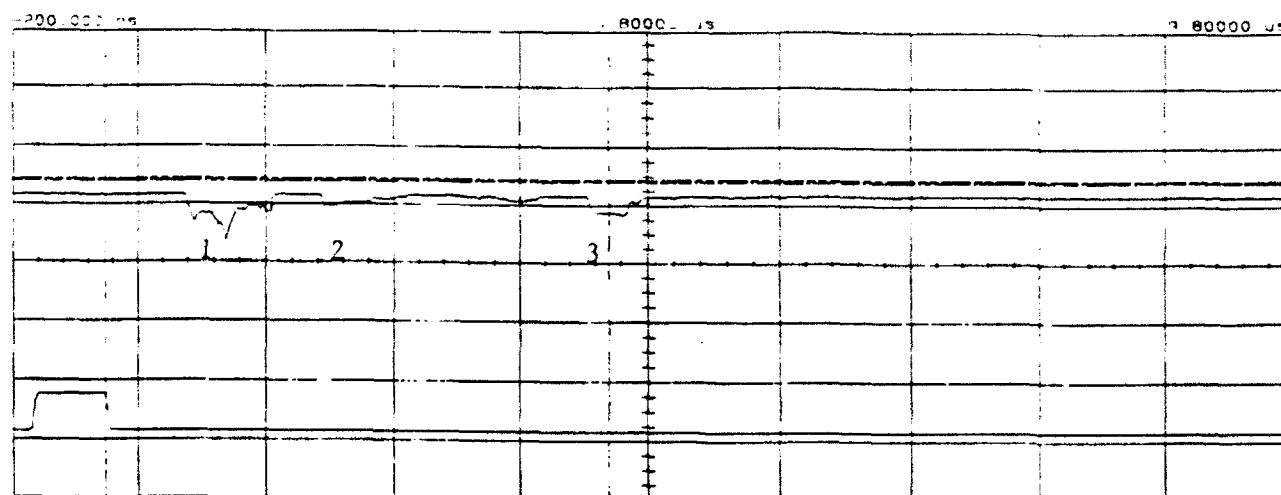


Figure 3

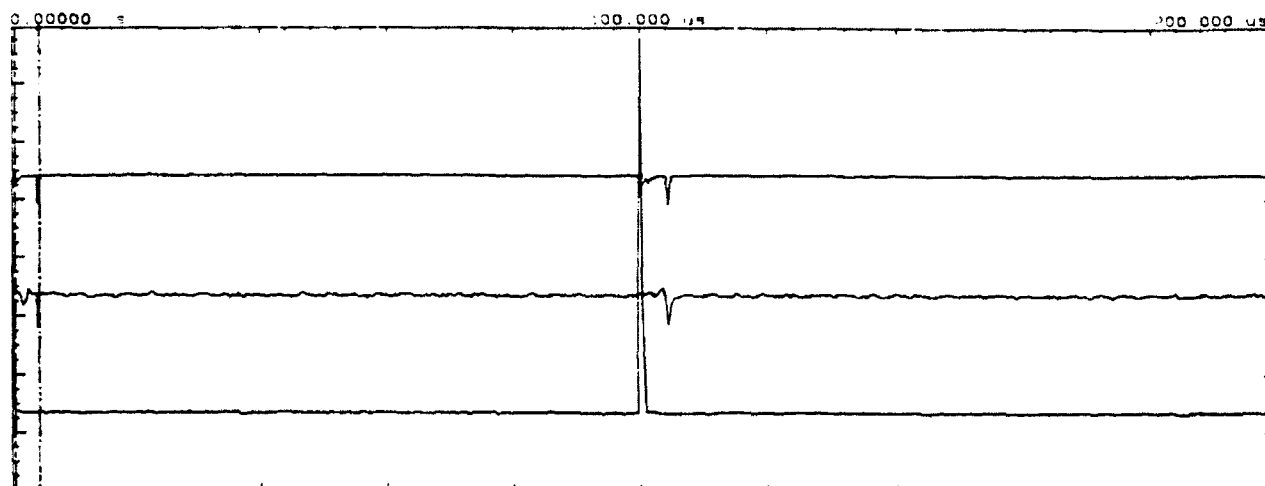
The radar system was still being constantly improved upon through the summer while being tested with real targets. Figure 4 shows the transmitted pulse and the return received from it. From left to right on the return signal there appears targets (dips in the signal) which have been identified as (1) a tree line, (2) a concrete structure, and (3) a water tower.



Main	Timebase	Delay/Pos	Reference			Markers
	1.00 us/div	-200.000 ns	Left			marker2 (ci) = 105.250 mv
						marker1 (ci) = 240.000 mv
						delta V (ci) = 249 mv
Channel 3	Sensitivity	Offset	Probe	Coupling		
	2.00 mv/div	-2.600 mv	1.000 :1	dc (50 ohm)	stop = 4.52000 us	
Channel 4	500 mv/div	1.50000 v	1.000 :1	dc (50 ohm)	start = 540.000 ns	
					delta t = 3.98000 us	
					f delta t = 251.156 kHz	
Trigger mode : Edge						
On Positive Edge Of Chan4						
Trigger level						
Chan4 = 250.000 mv (noise reject OFF)						
Holdoff = 40.000 ns						

Figure 4

To demonstrate the scale at which this radar was operated, Figure 5 shows the exact same targets and full returns as Figure 4. With the time base widened in Figure 5 one may see that the returning images are far within the first five percent of the time before the next transmitted pulse. The targets are within such a short range for easier testing and data collection purposes, and the radar's limited transmit power output also prevents the ability to "see" any further.



Main	Timebase	Delay/Pos	Reference		Markers
	20.0 us/div	0.00000 s	Left		stop - 4.95000 us
					start - 500.000 ns
					delta t - 3.95000 us
					f delta t - 252.925 kHz
	Sensitivity	Offset	Probe	Coupling	
Channel 2	100 mV/div	75.000 mV	1.000 : 1	dc (50 ohm)	
Channel 1	5.00 mV/div	-7.600 mV	1.000 : 1	dc BW lim (50 ohm)	
Channel 4	50.0 mV/div	187.600 mV	1.000 : 1	dc (50 ohm)	

Trigger mode : Edge  
On Positive Edge Of Chan4  
Trigger Level  
Chan4 = 125.000 mV (noise reject OFF)  
Holdoff = 40.000 ns

Figure 5

A somewhat successful attempt was also made to acquiring doppler shifts with the constructed radar. The doppler shifts would have been useful in determining the velocity and direction in which moving targets were moving. The attempts are cited as only "somewhat" successful due to the I and Q ports which were used to measure the doppler shifts. The phase shift in the I and Q ports were crudely constructed and little time or attention was given to them due to the success of other data gathering methods. Shown in Figure 6 (from top to bottom) is the transmitted pulse, the doppler shift from an I and Q port, and the return image. Note how the doppler shift does follow the major dips of the image return. The result of the I and Q ports is that though they do have the ability to determine that a target is there, they are by no means reliable enough to determine accurate conclusions.

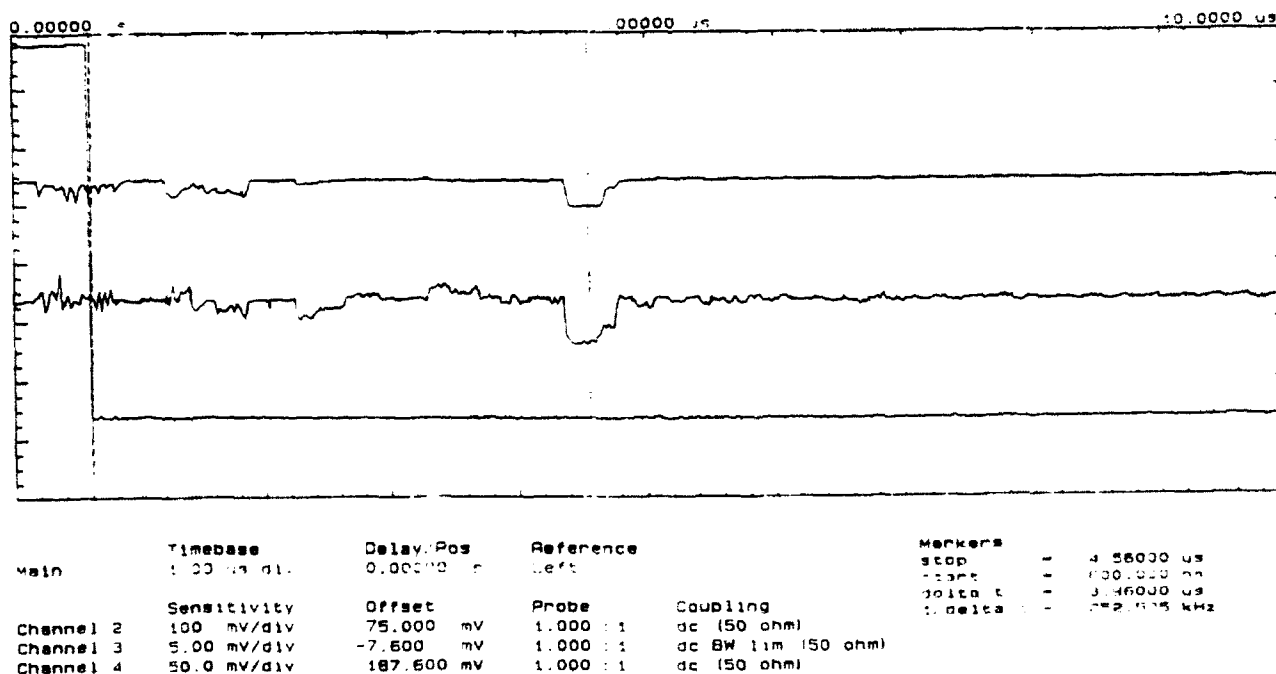


Figure 6



It is important to point out that the major problems encountered in this project were a result of the available hardware or radar configuration used. These problems say little in the terms of the recirculating optic delay line's performance which suitably performed all which was expected of it. The results of the RODL testing and data collection are promising toward its intended use.

#### CONCLUSION

As the results of this project suggest, the recirculating optic delay line concept for use as a frequency reference unit in a coherent radar is concluded to be a feasible alternative to the conventional FRU. Realizing the cost effectiveness of this concept and the capability demonstrated through this project, it becomes a dilemma trying to discover why it is not and has not been given greater attention or why it has not been taken to greater extents.

## REFERENCES AND ACKNOWLEDGMENTS

I would like to thank Frank Arredondo, my mentor, for allowing me to be his apprentice. This, though it may seem a trivial and expected acknowledgment, means a great deal to me. I wanted a chance to learn something and this man has taught me. He also has offered me (as far as I'm concerned) the most interesting project in this High School Apprenticeship Program. For this I want to leave a simple "Thanks!" I'm sorry I couldn't learn C... it was just so boring!!

For help on this project I would again like to thank Frank for doing most of the dirty work, and I would like to thank John R. Walker for adding new insight and trying to word it as simply as possible (and helping with the dirty work). John R. Walker also contributed a great deal expertise when it came to the millimeter wave know-how. Darryl Huddleston deserves a thanks simply for keeping entertaining me. I want Mr. Bruce Quarles to know that I appreciate the use of his lab and I always did try to keep my area clean. Then I would like to thank John P. Walker for helping me out with the manual things (like teaching me how to solder... again), and for keeping me company as I tinkered, and for being a friend. By the way, I wasn't the one who stepped on your paint. Finally, though redundant of past High School Apprentice Derek Holland, I must thank Andrew LLOYD Webber for composing The Phantom of the Opera. Without his music I doubt I would have retained my sanity through the summer of trying to learn C. Besides, it's good stuff!

The people above also serve as the bibliography for this project. They provided, made up, or improvised all of the information that went into this report.

DISCOVERING AND EXPLORING  
SUPERCRITICAL FLUID  
CHROMATOGRAPHY

Tiffany M. Selmon  
Nonmetallic Materials Division  
Wright Patterson Air Force Base, OH

Patterson Career Center  
118 E. First Street  
Dayton, OH 45402

Final Report for:  
Summer Research Program  
Wright Laboratory

Sponsored by:  
Air Force Office of Scientific Research  
Wright Patterson Air Force Base, OH

August 1992

DISCOVERING AND EXPLORING  
SUPERCRITICAL FLUID  
CHROMATOGRAPHY

Tiffany M. Selmon  
Nonmetallic Materials Division  
Wright Patterson Air Force Base  
Patterson Career Center

Abstract

Discovering what supercritical fluid chromatography is and how it works was part of the studies. Supercritical fluid chromatography (SFC) may be defined as a form of chromatography (i.e., a physical separation method based on the interaction of an analyte in a mobile phase with a stationary phase) in which the mobile phase is subjected to pressures and temperatures near or above the critical point for the purpose of enhancing the mobile phase solvating power. In general, three conditions must be met to truly define SFC: (a) the mobile phase must always be at temperatures and pressures near or above their critical point, (b) the mobile phase must possess solvating power and, thus, be able to contribute to selectivity in the chromatographic process, and (c) the mobile phase must be subject to these conditions throughout the full length of the analytical column.

# DISCOVERING AND EXPLORING SUPERCRITICAL FLUID CHROMATOGRAPHY

Tiffany M. Selmon

## INTRODUCTION

The nature of supercritical fluids is such that the mobile phase can easily be varied from gas-like to liquid-like. Based on judicious choice of mobile phase, this may lead to a variety of advantages for SFC over other separation techniques. Fluids with low critical temperatures permit operation at temperatures conducive to the analysis of thermally labile solutes and allow for greater stationary phase selectivity. The higher solvating ability of supercritical fluids permits the analysis of high molecular mass, nonvolatile compounds. SFC is compatible with essentially all detectors commonly used in both gas chromatography (GC) and liquid chromatography (LC).

## METHODOLOGY

Both open tubular and packed columns, with the advantages and disadvantages associated with each column type, are widely used methods. SFC can be conveniently divided into two categories based on column type: open tubular and packed. The choice of column type is due not only to the obvious chromatographic differences (e.g., sample capacity, resolving power, etc.), but also to differences in column pressure drop and volumetric flow, which impose different constraints upon the system. Packed columns for SFC can be classified into three types, borrowing from developments in LC: (a) conventional packed columns that typically are of 2-4.6mm internal diameter (i.d.), (b) 1-mm i.d. "microbore" columns, and (c) packed capillaries that have diameters of

0.2-0.8 mm. To enhance the solvating power of the supercritical mobile phase for polar or high molecular mass analytes, miscible organic dopants or entrainers, known as modifiers, are commonly added to SFC mobile phases.

#### DAILY PERFORMANCE TESTING

It is necessary to occasionally monitor the efficiency of the column and to ensure that the restrictor is not plugged. A test mixture is recommended for daily performance testing. Checking the efficiency of the column (i.e., the number of theoretical plates) is a good way to follow the useful lifetime of the column.

A comparison of retention data usually indicates the performance of the restrictor with time. Increasing retention times are a sign of plugging of the restrictor with high molecular mass material or particles from the sample or the column (if a packed column is used). Sample solutions should be filtered, and in-line micro screens should be installed in the injection valve where sample is injected to avoid these problems.

## FLUID EXTRACTION

Supercritical fluid extraction (SFE) is a relatively new technique in the field of analytical chemistry, having evolved in the last decade as an alternative method of preparing samples prior to analysis. SFE offers many advantages to the analyst that are not inherent in other sample preparation techniques, such as distillation, extraction with liquid solvents, or low resolution liquid chromatography. The most unique property of supercritical fluids for extraction purposes is the ability to adjust their "solubilizing power" primarily *via* mechanical compression (and additionally *via* temperature), thereby providing the possibility of using one supercritical fluid to extract a host of analytes of varying polarity and molecular size.

The closely related technique of supercritical fluid extraction owes its current strong interest to efforts to simplify and increase the speed of sample preparation methods. For most analytical determinations today, sample preparation involves the most time-consuming and laborious steps in the analysis.

## CONCLUSION

The literature relevant to SFC and SFE is widely scattered in various journals and reports. While the chromatographic literature is confined more to chromatographic journals, there is a wealth of related critical state information in the engineering and physical chemistry literature that has been extremely useful for both SFC and SFE. Understanding of critical state phenomena is important to properly and fully utilize supercritical fluids in analytical separations.

### ALSO STUDIED:

#### MOLECULAR MODELING TECHNIQUES

Using a Macintosh IIx computer, I learned how to reconstruct molecules and atoms and collect data from them. One modeling technique used on the computer involved using the menus located on the screen. Another modeling technique used on the computer involved using the command mode. In order to get into the menus on the computer, one must know the password, code for the program, etc. Using this type of program has helped me to recognize how much data and information can be collected with hardly any trouble.



FROM THERMOCOUPLES TO MULTI-MILLION DOLLAR CHUNKS  
OF TITANIUM MATRIX COMPOSITE

Jonathan D. Servaites, high school apprentice under  
Amar A. Bhungalia

Centerville High School  
500 East Franklin St.  
Centerville, OH 45459

Final Report for:  
High School Apprenticeship Program  
Wright Laboratory/Flight Dynamics Directorate/Structures Test Branch

Sponsored by:  
Research and Development Laboratories  
Culver City, CA

August 1992

FROM THERMOCOUPLES TO MULTI-MILLION DOLLAR CHUNKS  
OF TITANIUM MATRIX COMPOSITE

Jonathan D. Servaites  
High School Apprentice  
Centerville High School

Abstract

During the time I spent at the Flight Dynamics Directorate/Structures Test Branch (WL\FIBT) at Wright Patterson Air Force Base, I interacted with various engineers and technicians on several projects. The military fighters and cargo aircraft go through combined environments during their flight mission such as high heat (especially along the leading edges of the craft, ie. wings, nose, etc.), induced static loads, and induced fatigue loads. The Structures Test Branch provides support for static, fatigue, and elevated temperature testing of military aircraft. Throughout my eight week tour, I participated in various tests including: the "Lightly Loaded Splice Structure," "The Elevated Temperature Aluminum Program," heat tests on composites, and F-15 and fuel tank fatigue testing. A large portion of my time at Wright-Pat was spent on the preparation for the test on the "Lightly Loaded Splice Structure," which is a part of the NASP (National Aero Space Plane) program. The structure is composed of one of technology's newest materials, titanium matrix composite or TMC. Furthermore, my involvement in this program allowed me to realize the countless procedures involved in carrying out such a test.

# FROM THERMOCOUPLES TO MULTI-MILLION DOLLAR CHUNKS OF TITANIUM MATRIX COMPOSITE

Jonathan D. Servaites

## THE THERMOCOUPLE

My first day at Wright Patterson AFB introduced to me the inevitable need for the assembly of cables. After an early morning tour of the massive Building 65, I was shown the simple techniques needed in constructing thermocouple cables. However, as I would discover later, thermocouples are much more complex in comparison to their assembly. Thermocouples, which are used to monitor temperature during a test, possess two wires composed of dissimilar metals that are joined at both ends. When heated, a thermoelectric current is established in the circuit. This phenomenon is otherwise known as the Seebeck Effect, which was discovered by Thomas Seebeck in 1821. Then, if the circuit is broken in the center (see figure 1), the net open

circuit voltage (Seebeck voltage) is a function of the junction temperature and a constant established according to the

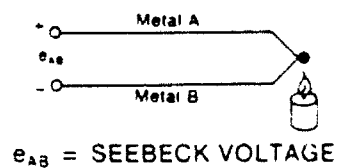


Figure 1

composition of the two metals. Thus, the change in temperature can be calculated by measuring the change in voltage, knowing the two metals' constant, and by applying the equation:

$$\Delta e_{AB} = \alpha \Delta T$$

As it turned out, the assembly of hundreds of thermocouple

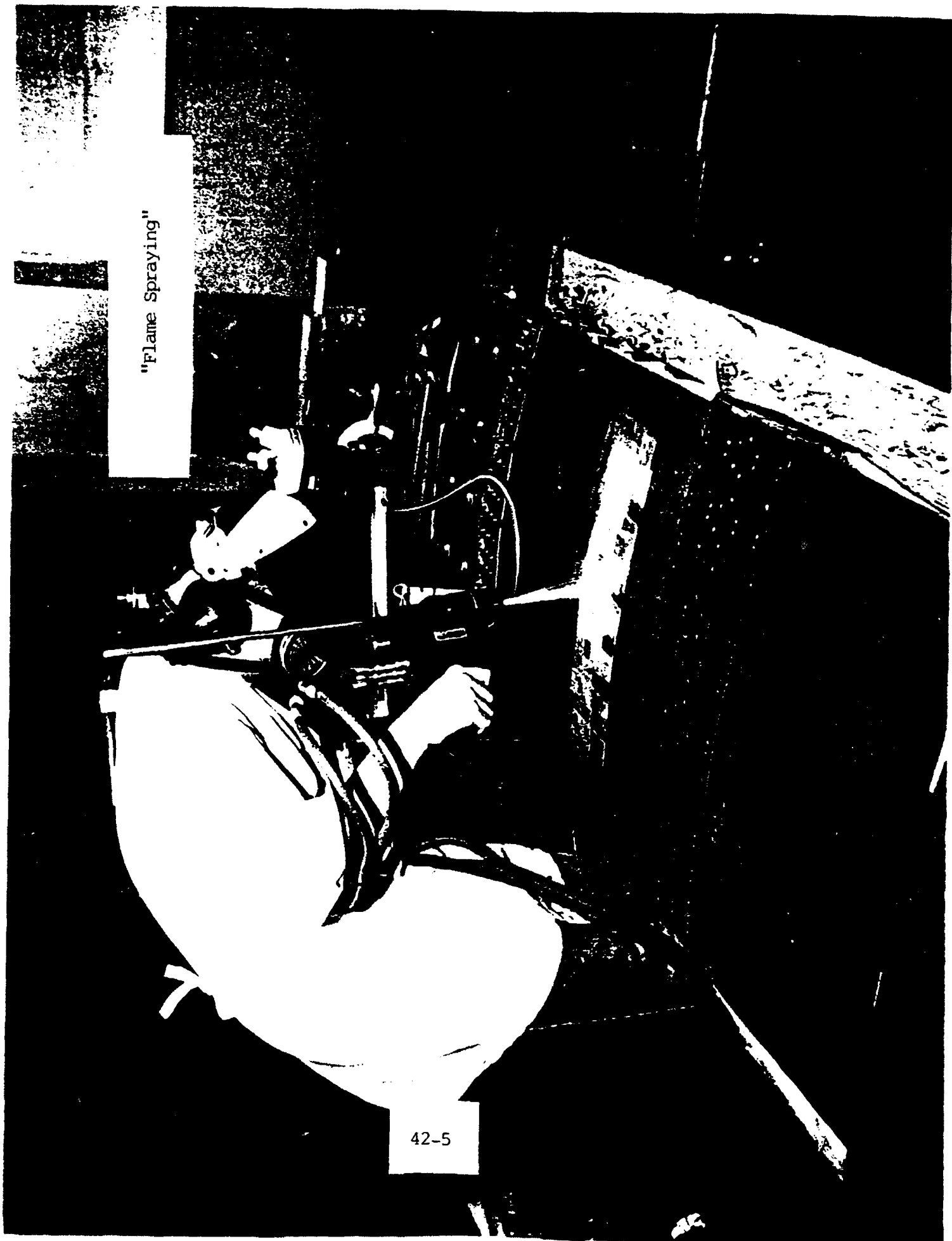
cables was merely one of those innumerable procedures that was required for the preparation of the test on the "Lightly Loaded Splice Structure" (more casually known as the splice plate or splice).

#### OTHER ASPECTS OF THE SPLICE PLATE

Fortunately, my fellow high school apprentice and I were assigned duties on the splice plate other than assembling thermocouples. Even though I did not find the abundance of time to undergo all of the procedures in preparation for testing, my background has become much more complete with several experiences now under my belt. For instance, the opportunity to wire the WK gauges on the splice plate, which was one of my more exciting and educational experiences, contributed to my development. The WK gauge is one of the two standard fatigue gauges used by the Structures Test Branch. The other gauge is known as the NZ. WK's are used to monitor stress at lower temperatures (below 500-600 degrees Fahrenheit). The NZ's, although they are less accurate, are able to monitor stresses at higher temperatures. Even though these gauges are still being used, NASA has proposed two new "compensating" gauges which, accordingly, "compensate" for heat expansion at high temperatures and consequently are accurate at high and low temperatures. These two gauges are also being tested on the splice plate. "Flame spraying" also proved to be an interesting aspect of my tour. As illustrated on page 42-5, aluminum oxide is melted and sprayed from what appears to be flames

"Flame Spraying"

42-5



onto the splice plate. This technique is used in the application of the NZ gauges. Because of flame spraying's hazardous potentials (as you can see in the illustration, the technician must wear a mask and ear protection), I never used the sprayer, but I did view the noisy procedure several times.

As always other cables also had to be made for the gauges. In this case, teflon cables were constructed for the WK gauges, and 3-conductor connector cables were needed for the compensating gauges. Moreover, in order to insure an even heat spread, the entire structure was painted with jet black high temperature paint. From making weld tack-downs and checking thermocouples and gauges for accuracy, there was always busy work to keep everyone's time full.

#### CONCLUSION

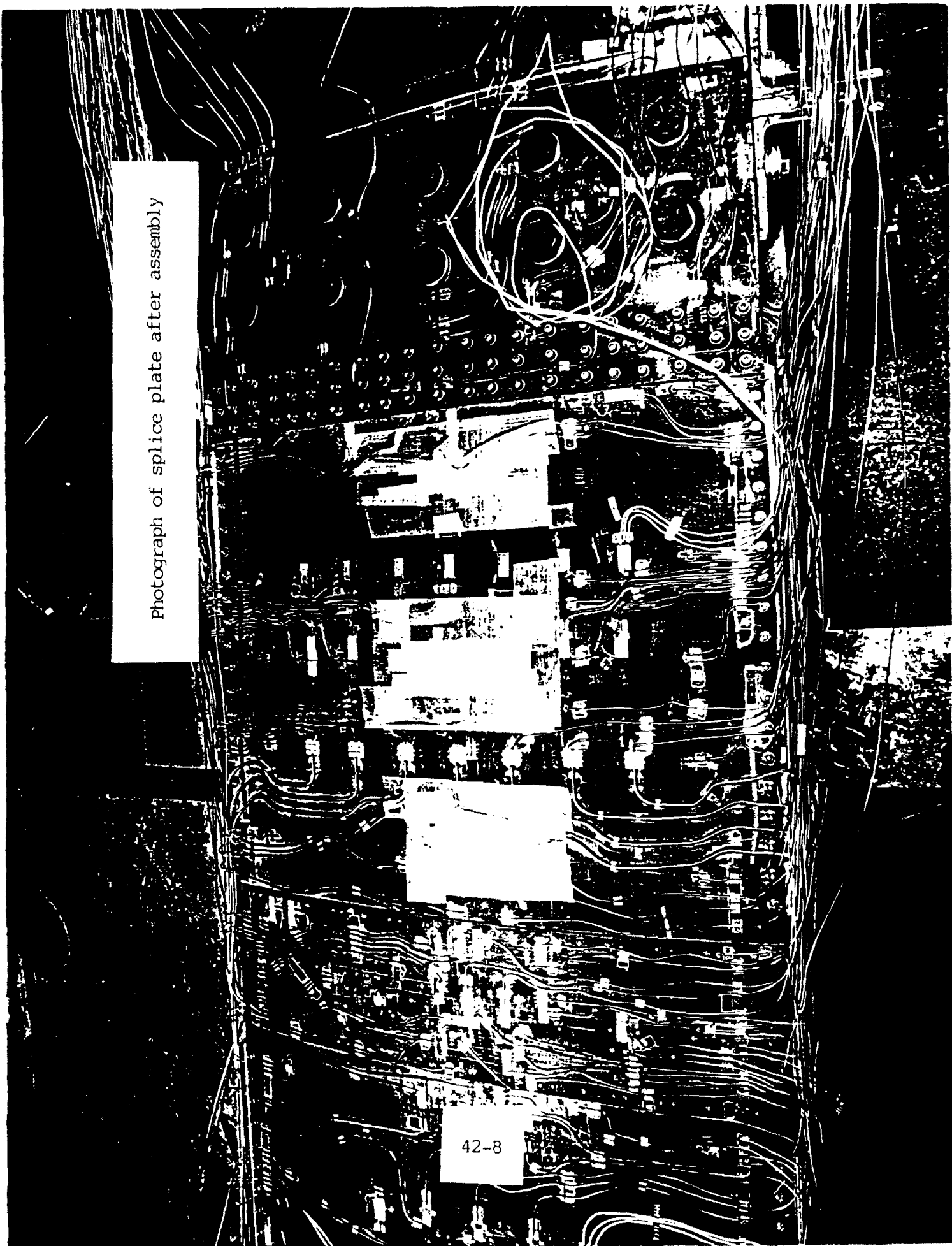
Understanding that projects of such magnitude take a great deal of time, testing had not begun as my eight week stay came to a close. However, I was able to be a part of almost the entire preparation process. Simply put, this experience carries an indispensable lesson of the complexity involved in performing "real-life" work in the field of engineering. This lesson is what separates the HSAP program from life in the classroom.

Photograph of splice plate before assembly

42-7

Photograph of splice plate after assembly

42-8





USING COMPUTERS FOR  
IP-3 INTERMODULATION  
ANALYSIS

Michael A. Shaffer

Final Report for:  
High School Apprenticeship Program  
Wright Patterson Laboratories

Sponsored by:  
Air Force Office of Scientific Research  
Wright Patterson Air Force Base , Dayton , Ohio

August 1992

USING COMPUTERS FOR  
IP-3 INTERMODULATION  
ANALYSIS

Michael A. Shaffer

Abstract

A Hewlett-Packard 300 series computer was used to automate testing of microwave devices (DUT) for third order intercept point intermodulation products. A test box using two programmable attenuators , a sweep oscillator , a power meter , and a spectrum analyzer were all controlled by the computer during testing. Using a HP-IB interface bus that uses IEEE-488-1978 standard language , the computer was able to do everything from capturing and reproducing the image on the spectrum analyzer to setting the power level on the sweep oscillator. An Avantek 4 to 8 gigahertz amplifier was used as a control test. The computer was able to power in , power out , IP-3 measurement , and gain. It was also possible to import data from the Hewlett-Packard to Microsoft Cricket Graph for easier analysis using ASCII format.

USING COMPUTERS FOR  
IP-3 INTERMODULATION  
ANALYSIS

Michael A. Shaffer

INTRODUCTION

What is a microwave? It is more than a helpful kitchen tool. Microwaves are used everyday as a means of communication. In fact , "microwave engineering is the engineering of information-handling systems in the frequency range from about  $10^9$  to  $10^{12}$  cps , corresponding to wavelengths from 30cm down to 0.3mm." (Collin 1) Microwaves can be used for low-energy-loss communication.

For many years , microwave technology and radar have been synonymous. Today , however , the two fields are separating , with microwave technology finding more and more uses. IP-3 intermodulation research , however , does fall under the area of radar research.

Microwave devices are small , thin wafers of electronic components made primarily of Gallium-Arsenide (GaAs). These wafers can hold hundreds of thousands of devices , such as transistors , making them very powerful components.

Microwaves themselves are useful to work with because they are high power and high output. Their short wavelength allows them to be focused into a narrow beam by a small antenna. "The low-frequency boundary of the microwave has not been set officially , but it is usually considered to be the point at which lower-frequency techniques and lumped-circuit elements cannot be used efficiently--generally about 1 gigahertz." (Adam 3) This means that microwaves of even

the lowest frequency are still at an incredibly high relative frequency. This , in turn , means that microwaves can efficiently transmit energy with a minimal loss of that energy because they can be focused into a narrow beam.

As mentioned above , a GaAs wafer can hold many thousands of devices. Testing so many devices manually becomes both tedious and ridiculous. Using a computer to simplify this work helps greatly , but even with a computer testing must be limited to specific areas.

Using computers to control tests allows the user to concentrate on more than one job at a time , with the computer taking over the mundane but necessary testing. A computer also organizes the information more efficiently and quickly than a person could. This allows more information to be gathered.

However , there are a few problems with using a computer for automated testing. The first is determining what kind of a computer to use. Most of the equipment used in testing is made by Hewlett-Packard , which uses the language code known as IEEE-488-1978 , or GP-IB. Obviously, a Hewlett-Packard computer would make control easier. However , it is possible to use an IBM or Macintosh with GP-IB. It is simply a matter of convenience. The Hewlett-Packard has a straight-forward interface while an IBM or Mac would need a translator.

A second concern in computer control is program failure. There is very little software available for instrument control. Even if there was software available , most testing requires specific programming that a general program cannot provide. It wouldn't be of much use to have a spectrum analyzer control program that couldn't read in any data. The GP-IB interface requires BASIC programming , which is notorious for debugging problems. One simple way

mistake , a misplaced comma or an extra space , can cause the entire program to fail. Without an editor , it can literally take hours or days to debug a program.

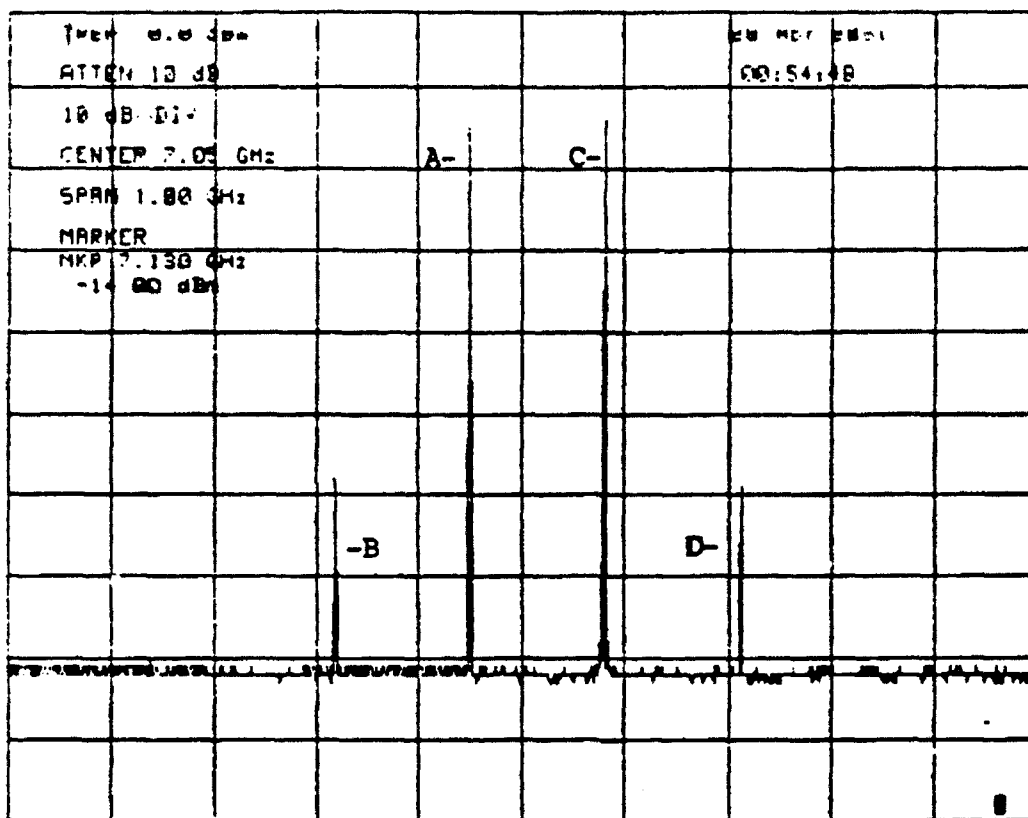
All of this testing is to find the third order intercept point intermodulation product , or IP-3 for short. The IP-3 intermod "occurs when two signals closely spaced together are of large enough amplitude to produce harmonics at twice their frequencies." (Adam 312) (see Fig. 1 for example)

The IP-3 measurement is important in radar detection. The radar requires a filter to remove extraneous signals , like the IP-3 intermod. As power increases , however , the power in vs. IP-3 graph changes from linear to quadratic , and the filter will no longer function properly. These high power IP-3 measurements can better determine where the equation changes , allowing better "tuned" filter capable of functioning at higher power levels.

#### METHODOLOGY

Running an automated IP-3 test requires quite a bit of equipment. A test box (see Fig 2) , which includes two programmable attenuators , a power combiner , a directional coupler , and input and output ports for device testing was used. The attenuators are controlled by an attenuator switch driver which is in turn controlled by the computer. this allows the computer to automatically change the amount of power being sent through the test device.

Another important piece of equipment used in the test set-up is the spectrum analyzer. It , like the switch driver , can be controlled by the computer. Unlike the switch driver , the spectrum analyzer can send its data to the computer. That is , it can "listen" and "talk". Any measurement that can be made using the front panel controls



... Fig. 1

[IP-3 spectrum from the spectrum analyzer. A is F1 , one of the two primary frequencies. B and D are the intermod frequencies, found using the formulas  $2 \cdot F1 - F2$  and  $2 \cdot F2 - F1$ . C is F2 , the other primary frequency. The computer analyzes the spikes in the order. A , B , C , D , isolating each spike before reading its power level.]

can also be made by the computer. The IP-3 graph (Fig. 1) was made from data the computer recieved from the spectrum analyzer and is an accurate , to-scale , representation of the spectrum analyzer screen.

Also note that a power meter can also send its data to the computer. It also tends to be more accurate than a spectrum analyzer. However , the IP-3 measurements require the spectrum analyzer's ability to center different frequencies and isolate those signals.

The final important piece of non-computer equipment in the test is the sweep oscillator. Although the test requires two sweep oscillators , only one programmable unit was available , the other unit was manually controlled. The programmable sweep oscillator was very useful. It , too , could send or receive data from the computer.

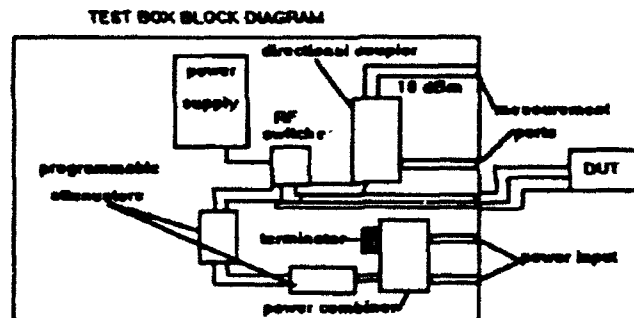


Fig. 2

Obviously , the most important piece of equipment used in testing was the computer. A Hewlett-Packard series 300 computer with HP-IB (same as GP-IB) interface was used as the controller.

The HP-IB itself is "somewhat of an independent entity. It is a communication arbitrator that provides an organized protocol for communications between several devices."

(Programming 12-3) Because of its ability to handle many

devices , it is perfect for test set-ups of any kind. Most importantly , it is standardized , using the IEEE-488-1978 command language for device control.

The actual control program was broken up in to individual programs that can be controlled by a Master Control Program. This allows easier editing and the ability to test each program separately.

The actual testing involves a program that isolates each signal spike on the spectrum analyzer. Given the two primary frequencies from the sweep oscillators , the program then "guesses" the harmonic frequencies using the formulas of  $2 \cdot F_1 - F_2$  and  $2 \cdot F_2 - F_1$  , where  $F_1$  and  $F_2$  are the respective primary frequencies. After isolating a frequency , the computer reduces the frequency span and does ten peak searches. The power readings from these ten searches is then averaged and placed in an array for data handling. The computer steps the attenuation from 10 to 1 dB on one attenuator and from 1 to 0 dB on the other. This means the computer does twenty-two scans in about a fourth of the time a person could do the same number of scans.

#### RESULTS

Many different programs were needed to allow full testing. A program that could isolate each spike on an IP-3 spectrum was the most important program. It would do the actual measurements. This program is listed at the end of this paper as "MEAS1". Other programs were needed for instrument calibration , front panel control , and other power measurements. All of the programs used are cataloged at the end of this paper.

To make test results easier to understand all of the data was save on one disk in ASCII format. This allowed easy transfer of the data to a PC. The PC could then , using CA-Cricket Graph by Computer Associates for Microsoft



Windows , graph the data in an organized fashion. This saved the time and trouble of entering all of the data manually. Presented after the program listings are two data graphs made from actual gathered data. The first is a saturation curve for the Avantek amplifier , and the second is the IP-3 graph of the same Avantek amplifier.

The Avantek amplifier was used as a control to test and calibrate the equipment and the computer. It began to saturate (i.e., it couldn't amplify the power any more) at -8dBm input power with 6dB attenuation. At this point its power output was approximately 12.6 dBm. This is a slight deviation from the given 18 dBm by Avantek. This may have been caused by a faulty sweep oscillator.

However , the computer programs did successfully isolate and measure each spike. The bottom range of the spectrum analyzer for measurement was about -80 dBm , so measurements under that power were unreadable (i.e., they provided false data points). Since the spectrum analyzer could read higher powers , it was still possible to create a good set of data.

As of the writing of this paper there have been no on wafer measurements. However , such measurements are possible and should be as easily done as the Avantek amplifier. The program that actually reads the IP-3 measurement does require over thirty minutes to fully run. This is an improvement over the usual two to two-and-one-half hours that a manual measurement takes. Also , the program does not require any outside monitoring ; it runs completely by itself. This frees-up much valuable time and results in better data.

The computer control succeeded in its goal of automated testing. The computer does just about everything except

turn the switches on! Given the success of this program , it may be possible to automate many other time consuming tests , which would be a help to all engineers.

#### CONCLUSION

Microwave technology is a blossoming field. New discoveries are being made every day. The potential uses of both microwaves and Gallium-Arsenide circuits are expanding. Using these low-energy-loss electromagnetic waves may revolutionize our lives. Just look at how the microwave oven has changed the way we eat. That was just the first benefit of this technology.

Computerized testing will bring those changes sooner. With a more powerful computer and more computer controllable devices , it may be possible to build an entirely automated test lab that would only require the researcher to turn on a switch and insert the test device. With just a few changes to the described test-set up in this paper any number of different tests could have been done. The possibilities are , not to sound too cliché , endless.

One future improvement on the described test set-up would be the incorporation of many of the smaller programs into one large , multi-purpose program. Another improvement would be to use two programmable sweep oscillators , as only one was available for testing. A final improvement would entail building gestalt equipment. That is , building machines designed for a wide range of testing , such as a combination power meter and spectrum analyzer. One such device , a digital signal analyzer , was available in this program , but it proved too hard to interface with.

This research is important and necessary. In a world obsessed with time (and especially the lack of it) , this automation can give engineers more time to do more research and thus improve efficiency.

## PROGRAM CATALOG

"MCP" - Master control program ; calls up all other programs.

"MEAS1" - IP-3 measurement program that uses the spectrum analyzer.

"MIKE2C" - Program that captures spectrum analyzer screen image.

"MIKE3C" - Controls front panel of the spectrum analyzer.

"SPECSWEEP" - Measures power output at different attenuations and output powers.

"POWSWEEP" - Same as "SPECSWEEP" but uses a power meter instead of the spectrum analyzer.

"SPECCAL1" - Similar to "MEAS1" , but this program measures only the two primary frequencies and is used to calibrate the spectrum analyzer.

"FILEREAD" - This program can "read" and printout any ASCII file or program. It is used to check data files before they are sent to Cricket Graph.

"SWEEP1" - Controls front panel of the sweep oscillator (HP83590A).

"DRIVER1" - Controls the attenuator switch driver (HP 11713A).

MEAS1

```

10 Start: CLEAR SCREEN
20  OPTION BASE 1
30  ASSIGN @Ana TO 718 ! Addresses the spectrum analyzer
40  ! The following lines set the spectrum analyzer to test conditions.
50  OUTPUT @Ana: "CF76Z"
60  OUTPUT @Ana: "SP16Z"
70  OUTPUT @Ana: "RB100KZ"
80  OUTPUT @Ana: "VBIKZ"
90  OUTPUT @Ana: "ST1.635C"
100 OUTPUT @Ana: "S1"
110 PRINT "          SPECTRUM ANALYZER METER"
120 INPUT "What is F1?", F18 ! gets the first frequency
130 INPUT "What is F2?", F28 ! gets the second frequency
140 PRINT "Please note that this program will require 31 minutes to run."
150 INPUT "Do you want a print out of the data?", Pos
160 IF Pos="Y" OR Pos="y" THEN PRINTER IS 701 ! turns printer on
170 CLEAR SCREEN
180 Ifs="16Z"
190 F3=2*(VAL(F18))-VAL(F28) ! 'guesses' for the intermods
200 F4=2*(VAL(F28))-VAL(F18)
210 F38=VALS(F3)8"6Z"
220 F48=VALS(F4)8"6Z"
230 ! Arrays for frequency and amplitude are dimensioned.
240 DIM Pa(100), Sa(100), Ffa(100), Sfa(100)
250 DIM Data$(200)
260 DIM A$(32)(25), B$(32)(25), C$(32)(25), D$(32)(25)
270 PRINT "TEST    F1("F18")    F2("F28")    2F1-F2("F38")    2F2-F1("F48"
    ")
280 PRINT "-----"
290 FOR L=1 TO 24 ! Sets up scan loop.
300  Driver(L) ! send the program to the attenuator driver subprogram
310  BEEP 3000, .15
320  DISP "REQUESTING DATA FOR FIRST FREQUENCY"
330  OUTPUT @Ana: "CF" F18 ! Sets initial center frequency.
340  OUTPUT @Ana: "SP15MZ"
350  WAIT 2
360  Cum=0
370  FOR Ls=1 TO 10
380    OUTPUT @Ana: "M2 E1"
390    OUTPUT @Ana: "OT"
400    FOR Z=1 TO 32
410      ENTER @Ana: A$(Z) ! Gets first set of numbers.
420      NEXT Z
430      Cum=Cum+VAL(A$(16))
440      WAIT 1.70
450    NEXT Ls
460    A.g=Cum/(Ls-1)
470    DISP "DATA FOR F1 IN"
480    LET Ffa(L)=A.g
490    IF VALS(Pa(L))=A$(7) THEN
500      OUTPUT @Ana: "PL10DM"
510      GOTO 310
520    END IF

```

```

530 ! First spike measured, on to f3.
540 OUTPUT @Ana:"CF":f3$
550 WAIT 2
560 DISP "REQUESTING DATA FOR 2F1-F3"
570 Cum=0
580 FOR Ls=1 TO 10
590     OUTPUT @Ana:"M2 E1"
600     OUTPUT @Ana:"OT"
610     FOR Z=1 TO 32
620         ENTER @Ana:BS(Z): Scans in second freq. measurement.
630     NEXT Z
640     Cum=Cum+VAL(BS(16))
650     WAIT 1.7
660 NEXT Ls
670 Avg=Cum/(Ls-1)
680 DISP "DATA FOR 2F1-F2 IN"
690 LET Ffa(L)=Avg
700 ! Returns to f2.
710 OUTPUT @Ana:"CF":f2$
720 WAIT 2
730 DISP "REQUESTING DATA FOR F2"
740 Cum=0
750 FOR Ls=1 TO 10
760     OUTPUT @Ana:"M2 E1"
770     OUTPUT @Ana:"OT"
780     FOR Z=1 TO 32
790         ENTER @Ana:CS(Z)
800     NEXT Z
810     Cum=Cum+VAL(CS(16))
820     WAIT 1.7
830 NEXT Ls
840 Avg=Cum/(Ls-1)
850 DISP "DATA FOR F2 IN"
860 LET Sa(L)=Avg
870 IF VALS(Sa(L))=CS(7) THEN
880     OUTPUT @Ana:"RL100M"
890     GOTO 310
900 END IF
910 ! Final measurement.
920 OUTPUT @Ana:"CF":f4$
930 WAIT 2
940 DISP "REQUESTING DATA FOR FOURTH FREQUENCY"
950 Cum=0
960 FOR Ls=1 TO 10
970     OUTPUT @Ana:"M2 E1"
980     OUTPUT @Ana:"OT"
990     FOR Z=1 TO 32
1000         ENTER @Ana:DS(Z)
1010     NEXT Z
1020     Cum=Cum+VAL(DS(16))
1030     WAIT 1.7
1040 NEXT Ls
1050 Avg=Cum/(Ls-1)
1060 DISP "DATA FOR 2F2-F1 IN"
1070 LET Efa(L)=Avg

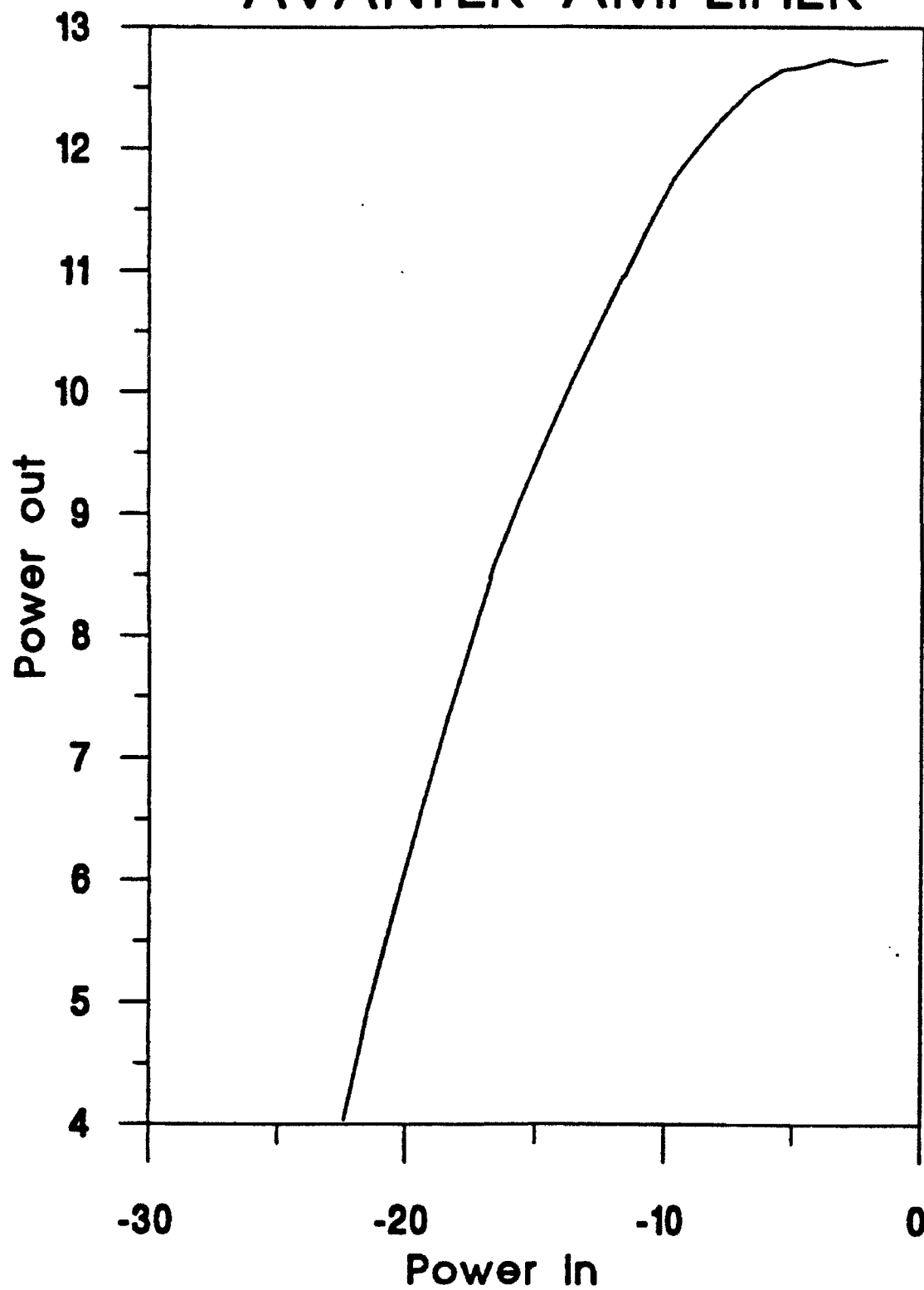
```

```

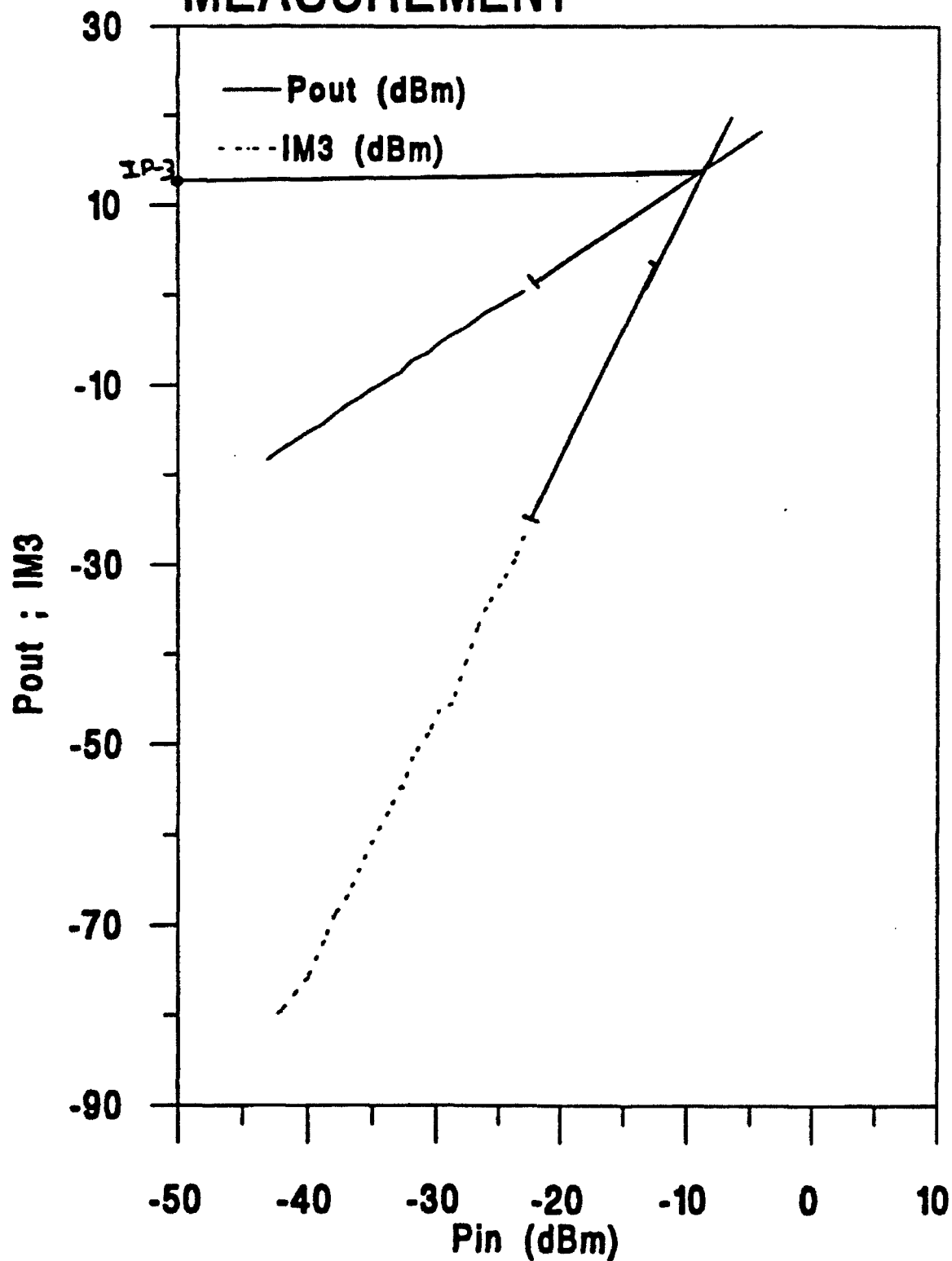
1090  ! All measurements for this loop are now in.
1092  BEEP 3000,.15
1100  PRINT USING "00,0X,0 00.00,9X,00.00,7X,00.00 12,Pa(L),Sa(L),Ffa(L),Sfa
L:  ! prints the data
1110  NEXT L
1120  OUTPUT @Ana:"SP":Ifs$
1130  OUTPUT @Ana:"CF":Fis
1140  OUTPUT @Ana:"SI"
1150  LOCAL @Ana
1160  CLEAR SCREEN
1170  PRINTER IS CRT
1180  INPUT "Do you want to save the data to a data file?",Dfs
1190  IF Dfs="y" OR Dfs="Y" THEN
1200  PRINT "Please insert the disk you want the data saved to into Drive 0 and
press <RETURN>"
1210  INPUT Rs
1220  CLEAR SCREEN
1230  INPUT "What file name do you want to use?",Files$
1240  CREATE ASCII Files$,220 ! creates the file
1250  ASSIGN @Path1 TO Files$
1260  FOR Q=1 TO 24
1270  OUTPUT Datas USING "4:00.00,1A,":Pa(Q),CHR$(9),Sa(Q),CHR$(9),Ffa(Q),CH
Rs,9),Sfa(Q),CHR$(9) ! formatted data string
1280  ! Note that a tab has been placed between the data to allow it to be e
asily converted to Cricket Graph.
1290  OUTPUT @Path1:Datas
1300  NEXT Q
1310  ASSIGN @Path1 TO .
1320  END IF
1330  CLEAR SCREEN
1340  PRINT "Please return the control disk to Drive 0."
1350  End:END
1360  SUB Driver(L) ! This sets the attenuation
1370  REMOTE 7
1380  IF L=1 THEN OUTPUT 729:"A56"
1390  IF L=13 THEN OUTPUT 728:"B5"
1400  IF L=1 OR L=13 THEN OUTPUT 728:"A1234"
1410  IF L=2 OR L=14 THEN OUTPUT 728:"A234B1"
1420  IF L=3 OR L=15 THEN OUTPUT 728:"A134B2"
1430  IF L=4 OR L=16 THEN OUTPUT 728:"A34B12"
1440  IF L=5 OR L=17 THEN OUTPUT 728:"A124B3"
1450  IF L=6 OR L=18 THEN OUTPUT 728:"A24B13"
1462  IF L=7 OR L=19 THEN OUTPUT 728:"A14B23"
1470  IF L=8 OR L=20 THEN OUTPUT 728:"A4B123"
1480  IF L=9 OR L=21 THEN OUTPUT 728:"A12B34"
1490  IF L=10 OR L=22 THEN OUTPUT 729:"A2B134"
1503  IF L=11 OR L=23 THEN OUTPUT 729:"A1B234"
1510  SUBEND

```

# SATURATION CURVE OF AVANTEK AMPLIFIER



# AVANTEK AMPLIFIER IP-3 MEASUREMENT





## REFERENCES

Adam , Stephen F. Microwave Theory and Applications. Englewood Cliffs , NJ:Prentice-Hall Inc. , 1969.

Collin , Robert E. Foundations for Microwave Engineering. New York: McGraw-Hill Inc. , 1966.

Hewlett-Packard. Programming with HP BASIC. Edition 1 , June 1989.

Microwave Training Institute. Microwaves Made Simple:Principles and Applications. Dedham , MA:Staff of Microwave Training Institute , 1985

A MASS SPECTROSCOPIC STUDY OF DIAMOND GROWTH  
FOR LOW-PRESSURE CHEMICAL VAPOR DEPOSITION

David J. Spry  
Summer Apprentice  
Department of the Air Force

Final Report for:  
Summer Research Program  
Propulsion Laboratories WL/POOC-3  
Wright Patterson Air Force Base  
Dayton, OH 45433-6563

Sponsored by:  
Research and Development Laboratories  
5800 Uplander Way, Culver City, CA 90230-6608

August 1992

A MASS SPECTROSCOPIC STUDY OF DIAMOND GROWTH  
FOR LOW-PRESSURE CHEMICAL VAPOR DEPOSITION

David J. Spry  
Summer Apprentice  
Department of the Air Force  
Wright Patterson Air Force Base

**Abstract**

This report discusses the occurrences in a series of diamond chemical vapor deposition (CVD) experiments including some experiments with  $\text{CD}_4$  or  $\text{D}_2$  in replacement of  $\text{CH}_4$  or  $\text{H}_2$ . The data collected for this report was made by a quadrupole mass spectrometer. In order to try to keep methane from reacting with hydrogen or deuterium, a quartz tube was used for direct flow to the substrate. The results of these experiments show that the larger the proportion of hydrogen to methane, the less breaking up of methane by the plasma.

# A MASS SPECTROSCOPIC STUDY OF DIAMOND GROWTH FOR LOW-PRESSURE CHEMICAL VAPOR DEPOSITION

David J. Spry

## Introduction

Diamond is relatively rare in nature, and is in a very difficult form to use, which is why in the past the only main industrial use for diamond has been in the realm of cutting tools. However, diamond has many more attributes which will, in the future, greatly improve the industrial world. One of the excelling characteristics of diamond is that it has an extremely low coefficient of friction which will make it very useful in almost any mechanical machine, anything from turban engine blades to ball berrings. Also, diamond is an excellent thermoconductor which will allow computer components to be packed closer together enabling them to be 60 times smaller and operate four times faster<sup>1</sup>. Being resistant to corrosion enables any material, from steel to plastic coated with diamond, to withstand wearing and weathering. Because diamond is more transparent than glass to many more bands of light, including infrared, it is extremely useful in radomes on missiles and aircraft because the lens would be resistant to all of the environments such as sand, ice and

rain. These characteristics of diamond will make it, in the words of former Norton Vice President Neil Henderson, the "ultimate material of the 21st century"<sup>1</sup>. However, in order to use diamond for these purposes, a way to deposit diamond at low temperatures and low pressures over a large area must be found at relatively reasonable cost.

Before 1977 the only known way to artificially make diamond was to compress carbon under very high temperatures and pressures using very expensive machinery. Fortunately, Russian scientists in 1977 developed a new way of forming diamond by using low-pressure chemical vapor deposition(CVD). This process was later confirmed in 1985 by Japanese scientists Yaichiro Sato and Nobuo Setaka<sup>1</sup>. Many improvements have occurred in this field in recent years producing CVD procedures with temperatures as low as 1300 C<sup>1</sup>. However, the reasons these parameters produce diamond is not truly understood. There are also very many forms of CVD, ranging from torches to power plasma chambers. In this experiment a microwave power deposition chamber with a quadrupole mass spectrometer is used.

Researching nitrides

for the construction of another set up and the assembly of the helical resonator reaction chamber was also very challenging and educational (figure 1).

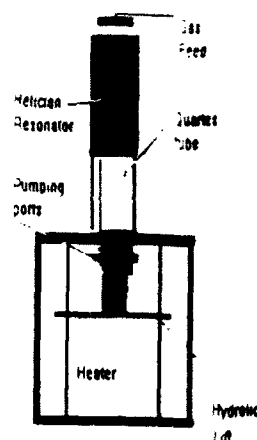


figure 1

### Problem

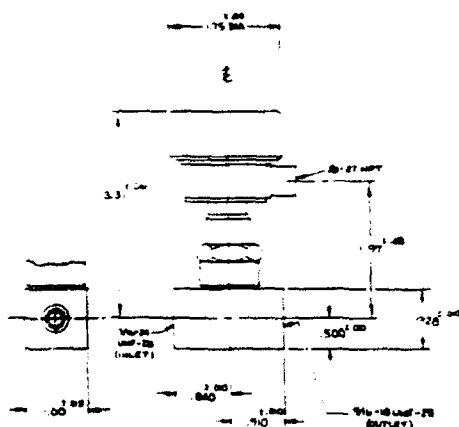
The main problem needing to be solved is why does diamond form in CVD reactions. To solve this problem, several of the questions must be answered. The focus of this report is to trace the different chemicals in the reaction. Another problem is the reliability of the mass spectrometer. Also, many mechanical problems occurred with the machinery that had to be solved.

Using a mass spectrometer, the amounts of most chemicals could be monitored. However, the chemicals that would register on the mass spectrometer are not the same as in the diamond forming part of the reaction because the gasses had to travel about half a foot before making it to the mass spectrometer. Also, some gasses have the same mass, e.g., both methane and atomic oxygen have the mass of 16. Tagging the gasses with isotopes would be difficult

because they would almost spontaneously react with the other gasses making the tagging useless or meaningless.

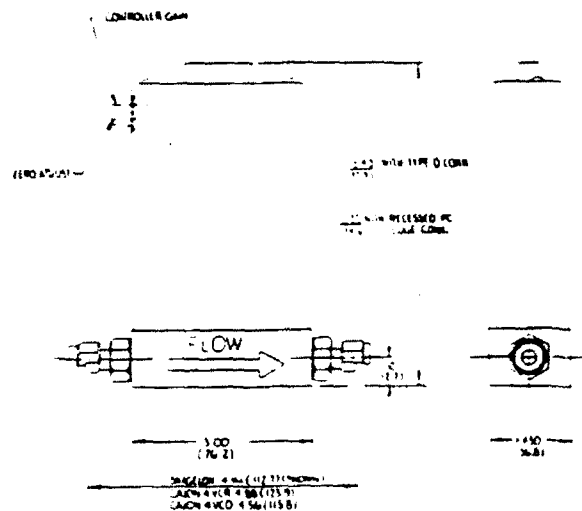
### Methodology

All of the experiments done on diamond deposition were carried out at Wright Patterson AFB. The apparatus used was an Astex high pressure microwave source(H.P.M.S.) source (figure 4) with M.K.S. mass flow controllers model 1159B (figure 2) with a positive shut-off valve (figure 3).



POSITIVE SHUT-OFF VALVE

figure 3



FLOW CONTROLLER

figure 2

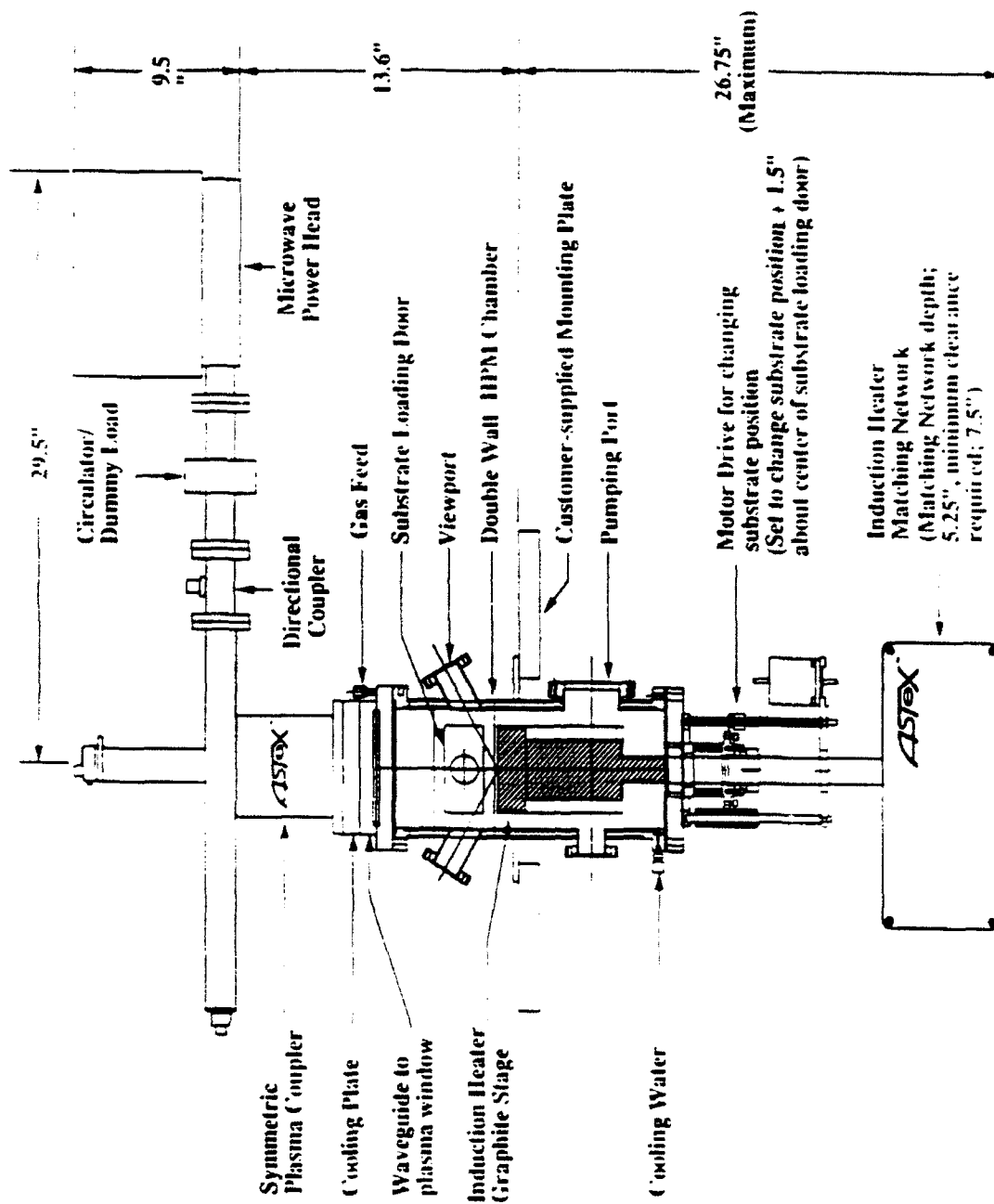


figure 4



The mass controllers used were 10 sccm for all the gasses except  $H_2$  which was a 1000 sccm controller. The quadrupole mass spectrometer was made by Extranuclear Laboratories, but been modified in 1989 with other counters, and was later attached to an IBM 286 clone computer. This set-up is schematically shown in figure 5. The "standard" diamond conditions used in the CVD experiment on this machine were 500 sccm of  $H_2$  and 3.5 sccm  $CH_4$  at 40 torr with 800 W of microwave power on a 800 C substrate. Due to some mechanical difficulties, the wattage of the microwave power supply was increased to 1000 W for the isotopic experiments. In order to isotopically tag the molecules, a quartz tube was place through the flange of the view port. Then the diamond conditions were repeated to see if the quartz had an effect. Next, the  $CH_4$  was sent through the quartz tube but the  $H_2$  through the normal gas feed. Next,  $CD_4$  was sent through the tube and  $H_2$  through the gas feed. Then,  $CH_4$  was sent through the tube and  $D_2$  through the gas feed. The  $CD_2$  was also sent through the tube and  $D_2$  through the gas feed. Last, both the  $CD_4$  and  $D_2$  were sent through the gas tube. Also,  $^{13}CH_4$  was ordered to follow the reaction better, but the gas was not available in time for this report.

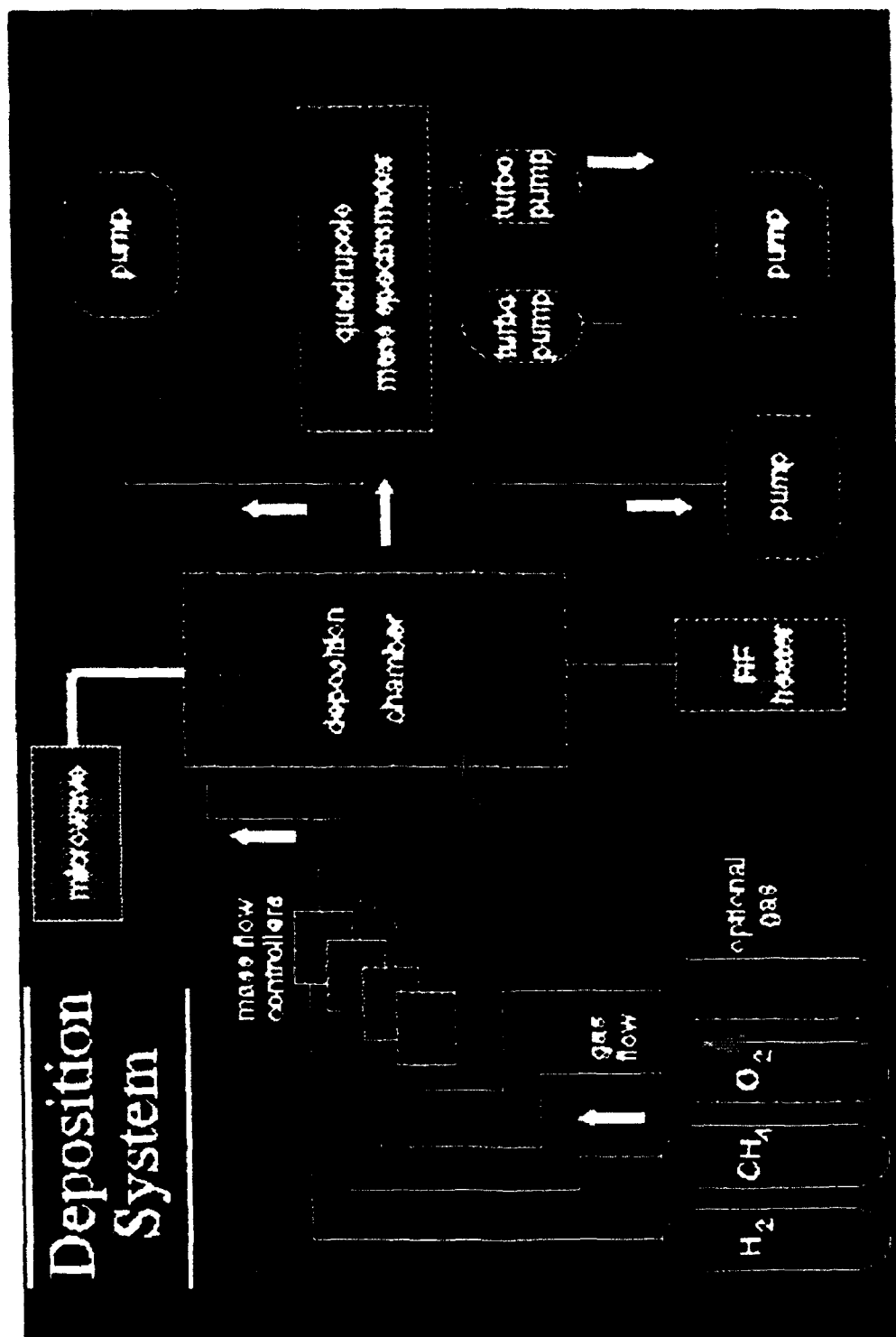


figure 5

Also, I made several pretreatment films and diamond films with oxygen. The pretreatment films are amorphous carbon and diamond like structures used to increase diamond nucleation and growth. The pretreatment films were grown with 7.2 sccm of CH<sub>4</sub>, 7.2 sccm of H<sub>2</sub> and 3.6 sccm of O<sub>2</sub> at a pressure of 3 torr and the substrate at a temperature of 860 C with 290 W of microwave power. The diamond conditions containing oxygen had 4 sccm of CH<sub>4</sub>, 395 sccm of H<sub>2</sub> and 1 sccm of O<sub>2</sub> at a pressure of 5 torr and a substrate temperature of 860 C with 500 W of microwave power. However, it was later discovered that the O<sub>2</sub> MKS mass flow controller had not been letting gas through even though it was registering gas flow.

After doing one of the experiments, the chamber did not keep its normal pressure. I used helium to spray around the chamber and used the mass spectrometer to check if a significant amount of

helium was getting through. It was discovered that the microwave window helix seal was broken. After it was replaced and the chamber continued to leak. Then when the old window was put back with a new helix-ring the leak stopped. The helical resonator originally didn't come with instructions so it had to be put together by what fit and what made sense.

Because the heater is being repaired, a blank off flange had to be made so the system could be run to check if it works. Bob Knight, the support technician, helped with drawing up a schematic (figure 6)

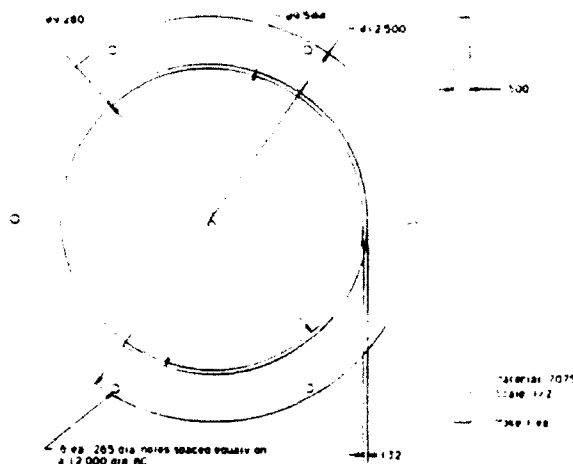


figure 6

for the blank off flange so it could be sent out and made. Assembling the Helical resonator also took a lot of other parts and fittings that were not provided, with the resonator.

## **Results**

The pretreatment films were grown and examined, but the parameters were not changed for experimentation. However, the mass spectroscopic data from the experiments were very educational in what was standard in diamond growth. As previously mentioned there was no oxygen flow so the data is not truly pretreatment film.

The propose of the diamond conditions with oxygen was to see the effects of oxygen on the chemical byproducts. Without the oxygen, the data is basically standard diamond conditions.

On the diamond conditions with the quartz tube the results were very interesting. The names of the different runs are listed in the matrix below in order to more easily keep track of the experiments (figure 7).

Run Name	H <sub>2</sub>	D <sub>2</sub>	CH <sub>4</sub>	CD <sub>4</sub>	Means of input of gas
			sccm		
dia-1, dia-2,	500	--	3.5	--	gas feed
dia-3, dia-4,					
dia-5					
dia-10	500	--	3.5	--	gas feed
dia-11	500	--	3.5	--	CH <sub>4</sub> through tube
					H <sub>2</sub> gas feed
dia-12	500	--	3.5	--	gases feed (deposited for tests)
dia-13	500	--	--	3.5	CD <sub>4</sub> through tube H <sub>2</sub> gas feed
dia-14	--	500	3.5	--	leak in window: not applicable
dia-15	--	500*	3.5	--	CH <sub>4</sub> through tube D <sub>2</sub> gas feed
dia-16	--	500	--	3.5	CD <sub>4</sub> through tube D <sub>2</sub> gas feed

\* The amount of D<sub>2</sub> was purposely change during one part of the run

figure 7

In runs one through five and eleven, the most interesting occurrence was the large proportion of  $C_2H_2$  to  $CH_4$ . In the later diamond conditions, the amount of  $C_2H_2$  is almost undetectable, but in the earlier runs including the pretreatment there was about a six to one ratio of  $CH_4$  to  $C_2H_2$ . This may be due to the adjustments of the controls that occurred when there was trouble with the preamplifier to the mass spectrometer. When the methane was turned on, the  $C_2H_2$  increased and then followed the same form. A graph of this can be seen in figure 8. The constant decrease in gasses is due to the mass spectrometer not being stable and doing what is called drooping.

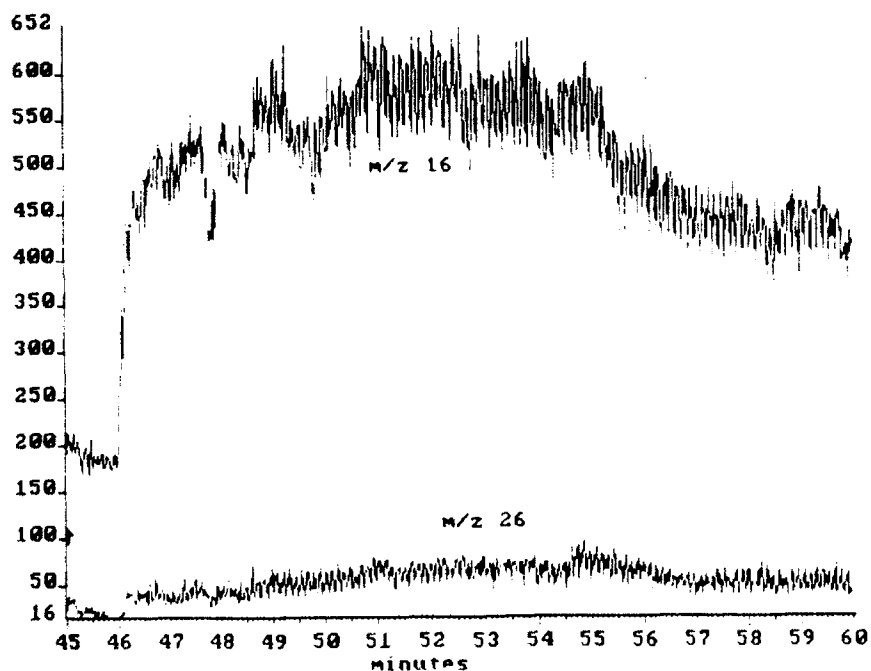


figure 8

In run dia-10, the quartz tube was placed in the chamber, but the gasses were fed through the gas feed in order to see if the quartz tube had an effect on the plasma. From the mass spectroscopic data and the appearance of the tube, it appeared it did not. In dia-11, the methane was sent through the tube. After running for almost two hours the quartz tube was glowing yellow orange hot. Then the RF filter on the mass spectrometer failed, stopping all data acquisition. After the tube was cooled and remove, it was clear that the plasma had etched two holes in the tube. Also the last two inches of the tube was coated with a black film. Between the coated part of the quartz tube and the clear part were rainbow colored bands. The substrate, that the tube was slightly above and was projecting gas on, was a small piece of silicon <111> diamond polished on a four inch silicon <111> wafer. There was a series of rings starting on the edge of the small piece of silicon. The rings that overlapped both the piece of Si and the wafer were white on the piece of Si and black on the wafer. Covering the rest of the wafer were numerous rainbow colored rings. These rings aligned with some of outermost rings on the tube. Both of the piece of Si and the tube will be

looked at under a scanning electron microscope after after this report.

In run dia-12 the tube was removed and the run was under normal conditions to deposit diamond for testing. In dia-13, the  $\text{CD}_4$  was fed through a new quartz tube and  $\text{H}_2$  was fed through the gas feed. When the  $\text{CD}_4$  was turned on after the hydrogen plasma was running at the diamond conditions, masses 3, 4, 13, 15, 16 and 19 increased (figure 9). These masses are most likely  $\text{DH}$ ,  $\text{D}_2$ ,  $\text{CH}$ ,  $\text{CH}_3$ ,  $\text{CH}_4$  and  $\text{CD}_3\text{H}$ .

In run dia-14 there was the leak in the microwave windows so the run was aborted. In run dia-15, when the methane was on and the  $\text{D}_2$  was on for 50 minutes, the amount of  $\text{D}_2$  was lowered to 400 sccm, and then at 56 minutes it was lower to 300 sccm. Then again it was lowered to 200 sccm at 60 minutes. At 64 minutes,  $\text{D}_2$  was raised to 500 sccm and then to 700 and 900 sccm at 67 minutes and 70 minutes respectively. Then the  $\text{D}_2$  was returned to 500 sccm at 72 minutes until  $\text{CH}_4$  was turned off at 75 minutes. This was done to see how the  $\text{D}_2$  effected the other chemicals. As the amount of  $\text{D}_2$  decreased the amount of  $\text{DH}$ ,  $\text{D}_2\text{H}$  and  $\text{C}$  increased. This pattern held true also as the amount of  $\text{D}_2$  increased (figure 10 & 11).



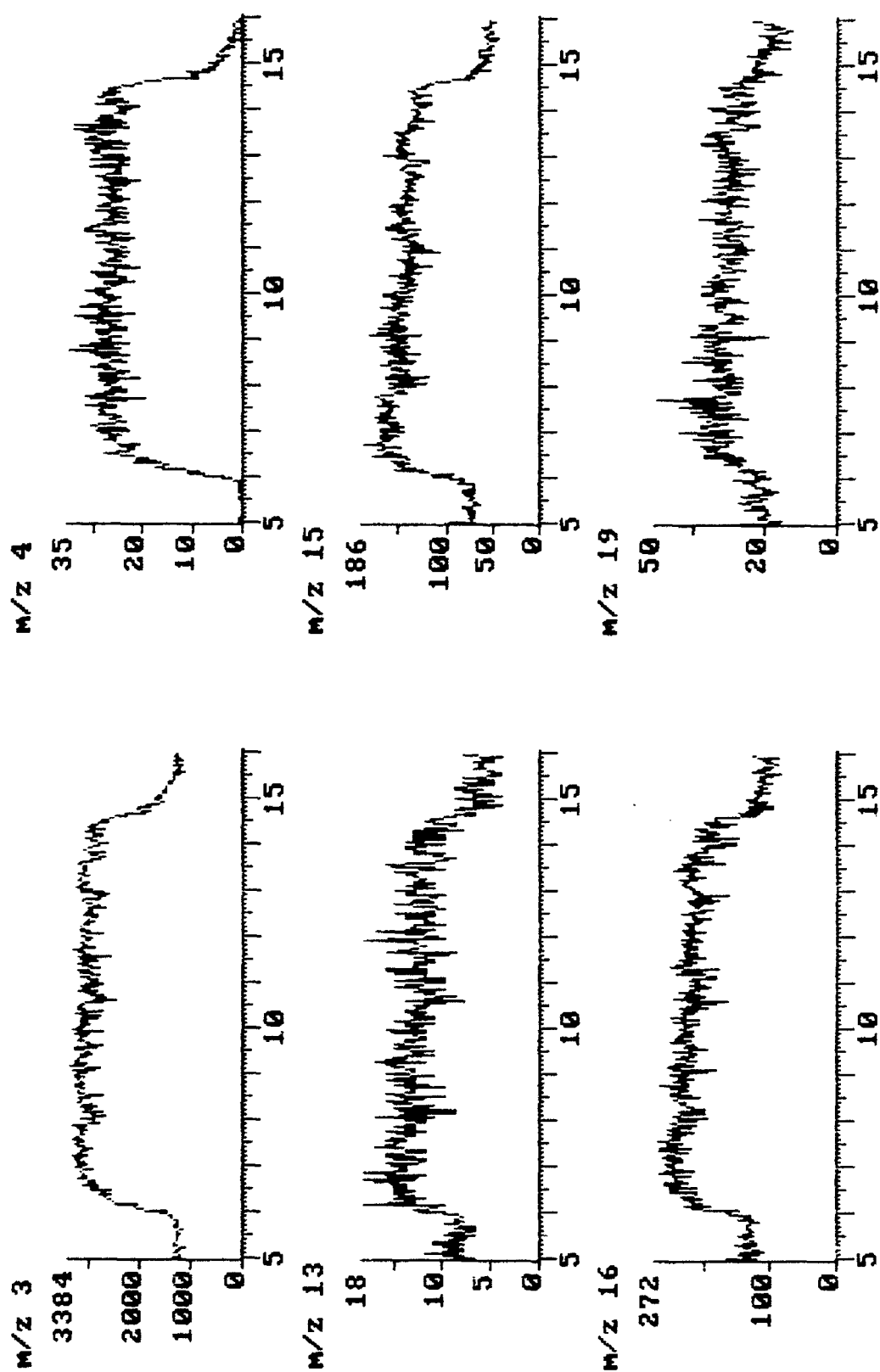


figure 9

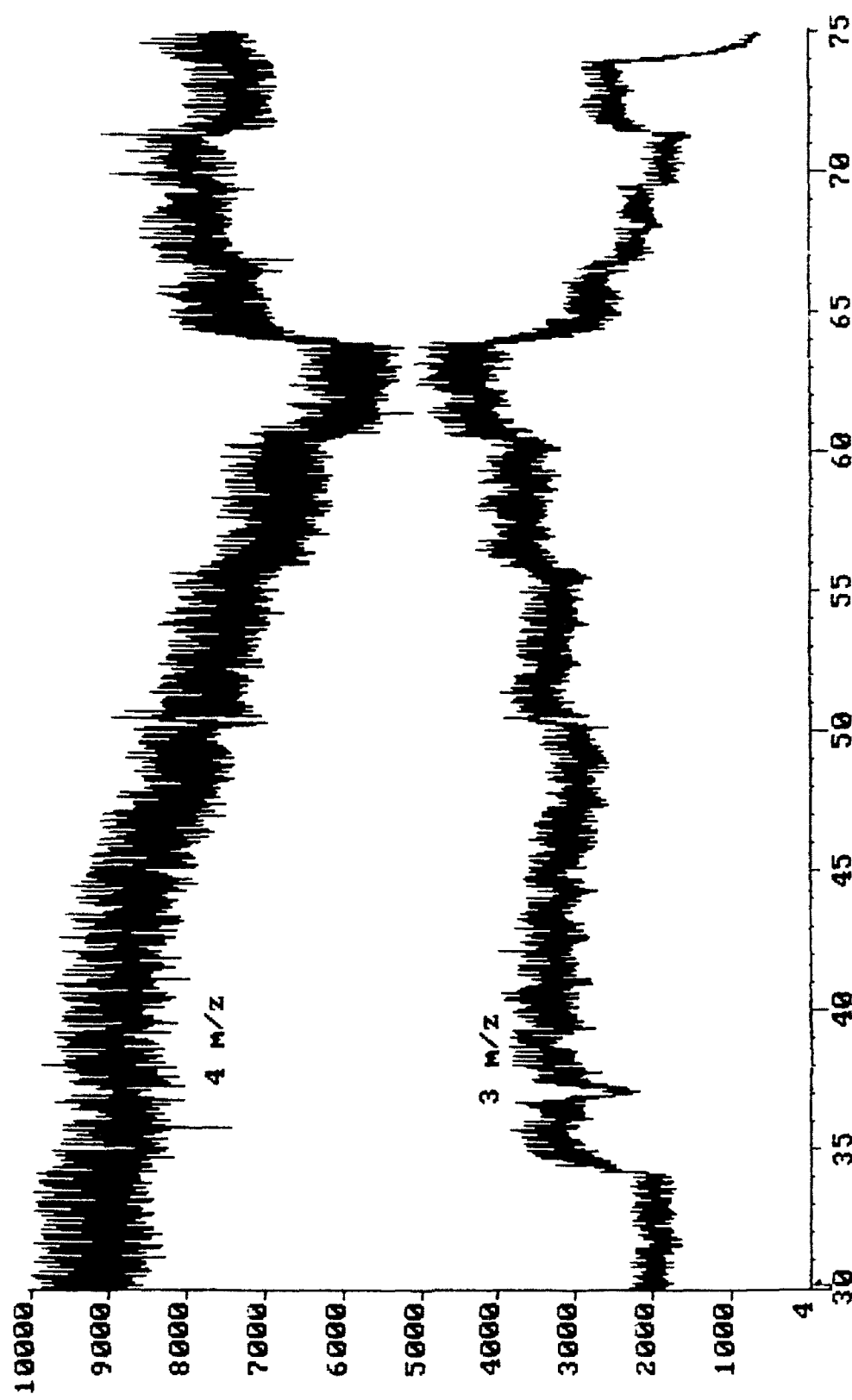


figure 10

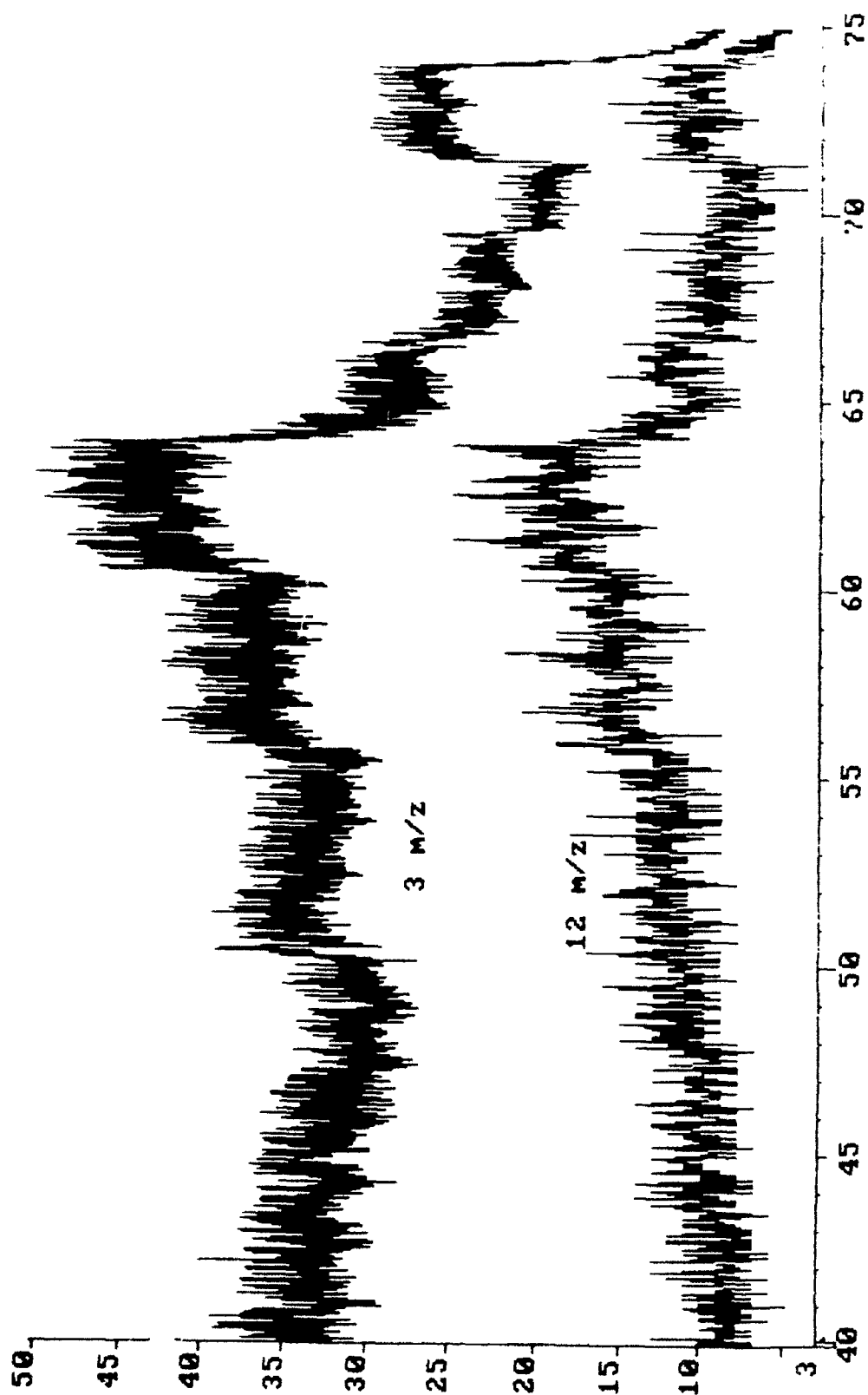


figure 11

In run dia-16 the introduction of  $CD_4$  did not have a significant effect on any of the chemicals.

### **Conclusions**

The results in Dia-13 lead to the conclusion that the hydrogen is replacing the deuterium in  $CD_4$  and then the hydrogen is being removed to form the newly formed  $CH_4$ . This is probable because there is no change in mass 20,  $CD_4^+$ , but there is an increase in mass 19, 4 and 3. Mass 3 is  $H_3^+$  and  $DH^+$ , mass 19 is  $CD_3H$ , and mass 4 is  $D_2$ . This clearly shows that the hydrogen is replacing the deuterium in the methane. The increase in mass 16, 15 and 13 indicate that the hydrogen is also being removed from the methane.

In run dia-15 the inverse proportion of  $D_2$  to  $DH$ ,  $D_2H$  and carbon indicate that the more deuterium that is placed in the chamber the less the amount of breaking up of methane. This would be because the hydrogen needed to form  $DH$  and  $D_2H$  can only come from methane.

### **Acknowledgements**

The author of this report would like to thank Paul Barns, the workers at Wright Patterson AFB and RDL HSAP Program for supporting this project.

### **References**

<sup>1</sup>*Diamonds are technology's best friend.* Aerospace America. **27**, 1991.

<sup>2</sup>*Diamonds Are a Chip's Best Friend.* R & D Magazine **48**, March 1992.

\*

# **SENSOR COMPUTATION ANALYSIS**

**Christina M. Trossbach  
High School Apprentice  
Guided Interceptor Technology Branch**

**Wright Laboratory Armament Directorate  
WL/MNSI  
Eglin AFB, FL 32542 - 5434**

**Final Report for:  
High School Apprenticeship Program  
Wright Laboratory Armament Directorate**

**Sponsored by:  
Air Force Office of Scientific Research  
Bolling Air Force Base, Washington, D.C.**

**August 1992**

# **SENSOR COMPUTATION ANALYSIS**

**Christina M. Trossbach  
High School Apprentice  
Guided Interceptor Technology Branch  
WL/MNSI**

## **Abstract**

The project studied was to determine the computation capability needed to process sensor data at various frame rates. A set of specified algorithms were used to determine the number of operations in each function. A spreadsheet was created to find the operations per second, or computation capability. The experiment consisted of charts comparing millions of operations per second at different frame sizes with the frame rate being the experimental variable.

# SENSOR COMPUTATION ANALYSIS

Christina M. Trossbach

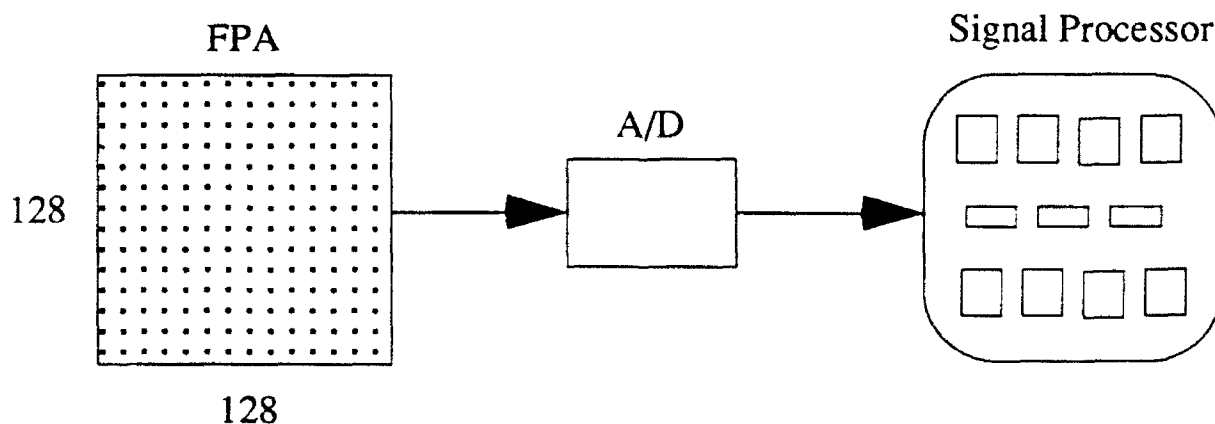
## Introduction

The Strategic Defense Initiative (SDI) is a fairly new mission in the Air Force, first implemented by the Reagan Administration in 1983. Its goal is to provide new technology for strategic defense. Wright Laboratory's role in SDI is to develop components for interceptor missiles. One of these component programs is called SPPD, short for Signal Processor Package Design. I worked in the Signal Processing section of the Guided Interceptor Technology Branch.

Currently, SPPD has a frame size of  $128 \times 128$  with a frame rate of 100 Hz. They hope to develop new technology to increase its capability to a frame size of  $512 \times 512$  or even  $1024 \times 1024$  in the near future, and increase its frame rate to that of 1000 Hz. To develop processors to support this increase in frame size and frame rate, they must determine the computation capability needed to process sensor data at various frame rates.

## Background

SPPD is an example of a signal processor. Together with a sensor, they make up a seeker, which is in the front of an interceptor missile. The sensor absorbs radiation from the target and creates an image. A sensor is an FPA, or focal plane array, which is made up of a matrix of detector elements. Each detector outputs a value, and that is a pixel. The total number of pixels is the image. After this image is created, it is transferred to an analog to digital converter (A/D) which digitizes the image and sends it to the signal processor to process the image and find the target. Sensors and signal processors are two examples of components that are developed by the engineers at MNSI. This is an example of the architecture of a typical seeker.



## Methodology

One method of finding the computation capability is by creating a workable spreadsheet using a set of specified algorithms. These algorithms consist of special functions, such as Gain and Offset or Scene Stabilization, which are required to carry out the task of the sensor. Each function has a certain number of operations per pixel (Example: Gain and Offset has 2 operations), depending on



the frame size, the number of pixels in a frame, and frame rate, the number of frames per second. I counted the total number of operations in each function and with this information I created a spreadsheet using 17 operations. This spreadsheet consisted of the number of operations per pixel, the number of X pixels, the number of Y pixels, the total number of pixels, and the number of frames per second. With this information, I used the formula

$$\frac{\text{Operations}}{\text{Pixel}} \times \frac{\text{Pixels}}{\text{Frame}} \times \frac{\text{Frames}}{\text{Second}} = \frac{\text{Operations}}{\text{Second}}$$

and derived the number of operations per second (or computation capability) for each function. I graphed the results of the total number of millions of operations per second (MOPS) at different frame sizes. I used various frame rates as the experimental variable in this project to show a relative difference between the number of MOPS at 100 Hz and 1000 Hz.

## Results

The results show that there is a relative difference between the computation capability at different frame rates. Currently, SPPD uses a frame size of 128 x 128 and a frame rate of 100 Hz. The data obtained shows that the greater the frame size, such as 1024 x 1024, the greater number of OPS will be needed. The same is true for that of frame rate. I chose to graph the results of the MOPS at 1000 Hz relative to that of the MOPS at 100 Hz because it shows that in the future, technology could increase so greatly that future signal processors could handle a frame rate that great, and the computation capability requirements would tremendously expand by increasing the frame rate to 1000 Hz.

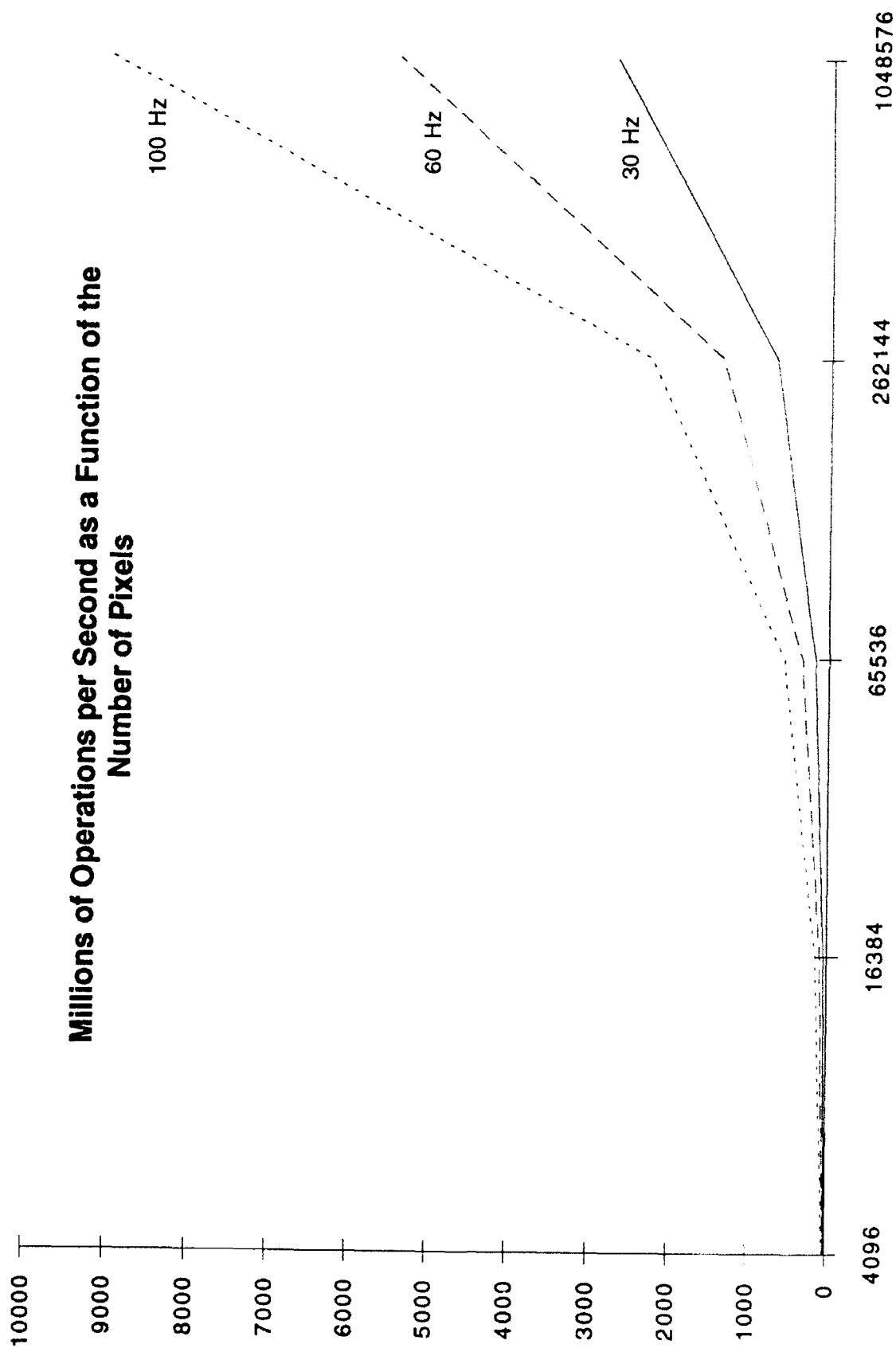
## Conclusions

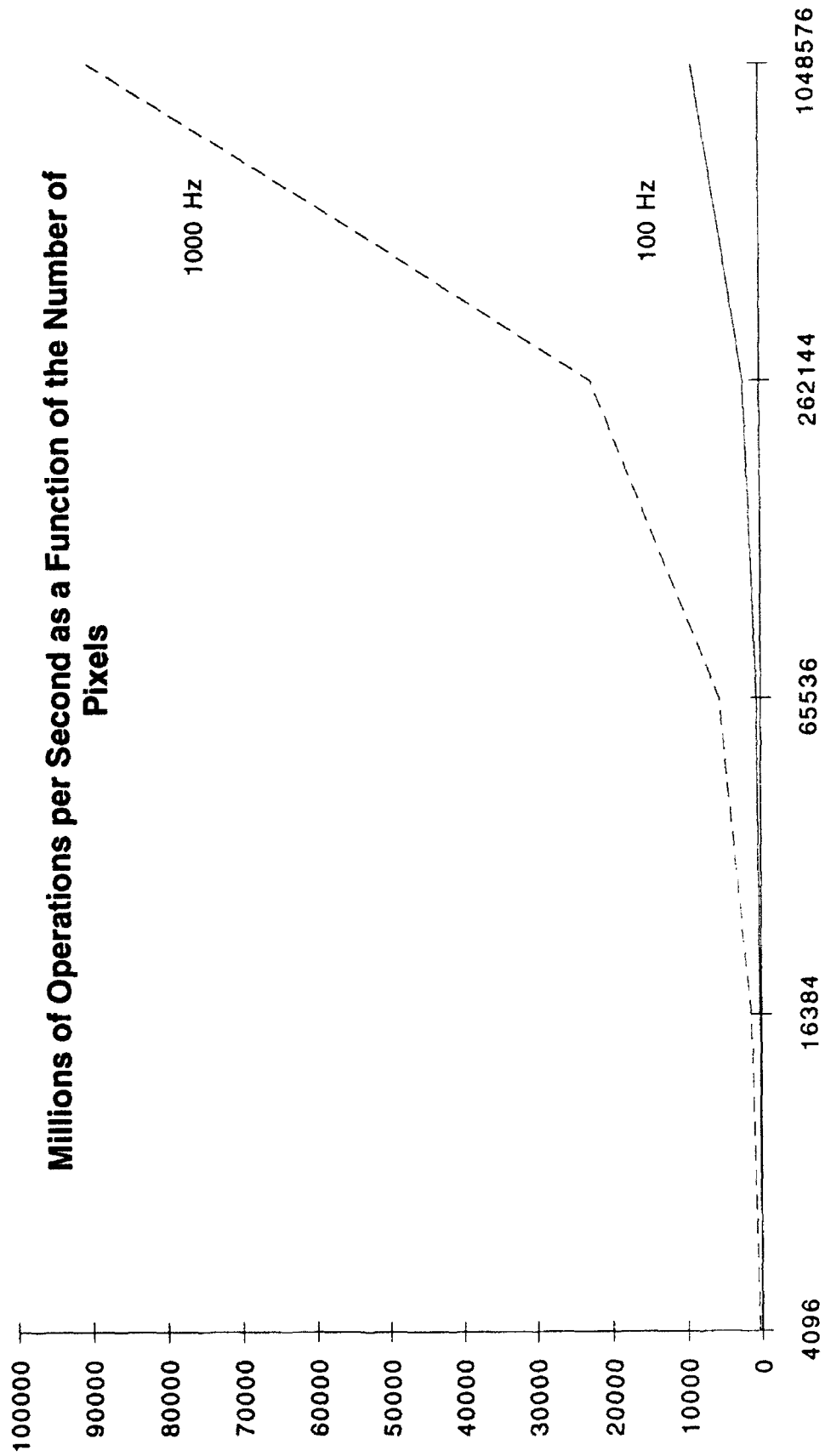
In conclusion, the information gained by this project will be very beneficial to the future engineering world. SDI will be able to use this in their future sensor processors and know exactly what is needed for the amount of computation capability they want. This spreadsheet has projected the data needed for frame sizes as large as 1024 x 1024 with frame rates as high as 1000 Hz which is in the near future for sensor processors. The results show that a signal processor at 1024 x 1024 with a frame rate of 100 Hz has 900 times less the computation capability than that of a signal processor would have at 1000 Hz. These figures are extraordinary. The purpose of this project is to better understand future processing requirements for SDI interceptors, to help SDI determine the maximum frame rate and frame size that their current signal processors can handle, and this EXCEL spreadsheet is an interactive tool for hypothesis testing.

## Acknowledgements

I would like to thank a few people that made my apprenticeship job very fun and extremely beneficial. First I'd like to thank my mentor, Paul McCarley for all of his guidance during the course of the summer. I would have been lost without you! Tom Rathbun - you've been a tremendous help. You were sort of my adopted mentor these last few weeks when Paul was gone. Thanks so much! Ron Rapp - thanks for the tour of KHLS and all your advice about college! Clif Nees - my "debate" partner on controversial issues of life in general. Thanks for the realistic portrayal of college! Mickie Phipps - you weren't here much, but you seem like a real nice person. Bob (Louie) LeBeau - who could forget you? For an old guy, you sure are funny. I guess you proved your competence by knowing that date, but remember, the memory is the first to go! Thanks again for putting up with me. Tim Poth and Mark McClure- you are just a couple of neat guys. I have enjoyed saying "Good Morning" to you guys every day. Daran, Eric and JJ - my fellow apprentices. Thanks for making this whole summer fun! Keep in touch while you're at college. Goodbye Daran (my Crestview buddy), Eric (Wonder Boy), and JJ (Clark Kent). Finally, I'd like to thank all of MNSI for putting up with 4 kids this summer (5, counting Bob). You guys are sure fun to work with. Thanks for treating us as equals.

Signal Processing Algorithms									
Function	Operations/Pixel	X Pixels	Y Pixels	Total Pixels/Frames	Frames/Second	Operations/Second (OPS)			
Gain and Offset	2	128	128	16384	100	3276800			
Scene Stabilization	16	128	128	16384	100	26214400			
Threshold Adjustment	3	128	128	16384	100	4915200			
Threshold	1	128	128	16384	100	1638400			
Clustering	1	128	128	16384	100	1638400			
Peak Intensity	1	128	128	16384	100	1638400			
Area Centroid	4	128	128	16384	100	6553600			
Area Variances	10	128	128	16384	100	16384000			
Area Cross Moment	3	128	128	16384	100	4915200			
Intensity Centroid	4	128	128	16384	100	6553600			
Track Initiation	4	128	128	16384	100	6553600			
Track Maintenance	1	128	128	16384	100	1638400			
Hardbody Selection	1	128	128	16384	100	1638400			
Aimpoint Offset	6	128	128	16384	100	9830400			
Hardbody Detection	2	128	128	16384	100	3276800			
Temporal Filtering	15	128	128	16384	100	24576000			
Spatial Filtering	12	128	128	16384	100	19660800			
<b>Total</b>						<b>140902400</b>			





GaAs OHMIC CONTACTS AT HIGH CURRENTS

Darcie Tutin  
High School Apprentice  
Fuzes Branch

Wright Laboratory Armament Directorate  
WL/MNMF  
Eglin Air Force Base, FL 32542-5434

Final Report for:  
High School Apprenticeship Program  
Wright Laboratory Armament Directorate

Sponsored by:  
Air Force of Scientific Research  
Bolling Air Force Base, Washington, D.C.

August 1992

## GaAs OHMIC CONTACTS AT HIGH CURRENTS

Darcie Tutin  
High School Apprentice  
Fuzes Branch  
Wright Laboratory Armament Directorate

### ABSTRACT

There is a need for ohmic contacts in GaAs photoconductive switches for detonators. These switches employ semi-insulating bulk GaAs in order to hold off high voltage until breakdown is desired. This type of device can be designed to require only small amounts of light triggering energy, thus resulting in a very efficient switch. Ohmic contact data was gathered for the conventional Au:Ge/Ni alloyed contact and a relatively new type of Pd/Ge diffused contact, both pertaining to Si doped GaAs. Unreliability associated with use of Au:Ge/Ni contacts at high currents was found which may limit their application in photoconductive switches. It was determined that Pd/Ge contacts were much more predictable and worthy of operation at high current density (approximately 1 MA/cm<sup>2</sup>).

## GaAs OHMIC CONTACTS AT HIGH CURRENTS

### INTRODUCTION

There is a need for ohmic contacts in photoconductive switches for detonators. These switches employ semi-insulating bulk GaAs die in order to hold off high voltage until breakdown is desired. Only the outer faces of the die are doped and metallized. The entire device becomes conductive only after illumination with photons of the proper wavelength. This type of device can be designed to require only very small amounts of light triggering power in order to operate, thus resulting in a very efficient switch. The research herein relates to the scale-up of GaAs photoconductive switching devices for operation at currents of many kiloamperes.

### DISCUSSION OF PROBLEM

One of the limitations of photoconductive switches is in the ohmic contacts and their inability to withstand large current pulses. In order to deal with this problem the behavior of ohmic contacts at high currents must be examined. The most commonly used contact at low voltages for a Si doped (n-type) GaAs bulk wafer is Au:Ge/Ni. Recently Pd/Ge has also been used effectively for low voltage devices [1]. However, these two types of contacts respond differently to high currents. The microstructures are also significantly different



from each other (Figure 1). The morphology of the Au:Ge/Ni is very non-uniform in comparison with that of the Pd/Ge at the same magnification. It has been shown that such an irregular morphology results in local regions that have large variations in resistivity [2]. The Au:Ge/Ni microstructure suggests that at high current the contact may be more susceptible to current crowding or poorly defined resistivity. Current crowding leads to localized heating and premature failure; lower critical current density will result. This is expected from the Au:Ge/Ni as it is an alloyed contact.

Alloyed contacts actually undergo partial melting during their heat treatment, causing an interfacial non-uniformity. The gold penetrates through several Angstroms and becomes a spike or root in the next layer. Pd/Ge, on the other hand is formed during a solid phase reaction in which Ge is able to diffuse into the substrate and further dope it. The uniform morphology of the Pd/Ge contact results in very small variations in resistivity and we anticipate less tendency towards localized current crowding (Figure 2).

#### METHODOLOGY

The Au:Ge/Ni contacts were all made during the same wafer run and sectioned, with  $2.58\text{cm}^2$  area of GaAs die and a constant etched upper contact area of  $.01533\text{cm}^2$ . The Pd/Ge specimen size varied with sectioning. A caliper was used to measure the size of the Pd/Ge die under a microscope. Of

course, the upper and lower contact area of the Pd/Ge was the same as that of the bulk die.

The dies were then mounted on strip lines. First the die was soldered onto a 1cm x 5cm strip of copper backed with kapton. Next a copper tab (approximately the size of the die) was placed on top of the die. Solder was applied only to the top of the copper tab. Then this tab was connected to a 3mm copper strip surrounded by kapton (Figure 3). With an additional copper tab on the end it was ready to attach to the ERG (extended range gap) fireset.

After the dies had been mounted on strip lines their cold resistance was measured on a Hewlett Packard Precision LCR meter. The measurement of several strip lines with a copper die instead of a GaAs one developed a standard strip line resistance of  $7\text{m}\Omega$ . This allowed for accurate measurements in the thousandths of an ohms range after allowing for a standard strip line.

Strip lines were then hooked up to the ERG fireset and the initial firing voltage was varied in a range of 2 to 5 kV. The fireset was connected to an oscilloscope via a current viewing resistor (CVR) to measure peak current and gain data on the current density of the dies at given voltages. Then an attempt at simulating the circuit was made on PSpice. The circuit was simplified for programming (Figure 4). Parameters were developed with an estimated inductance of  $24\text{nH}$ , resistance in the capacitor and switch of  $50\text{m}\Omega$  and a known capaci-

tance of  $0.4\mu\text{f}$ . Therefore the resistance of the strip line and initial firing voltage can be programmed to model the circuit for a given test.

## RESULTS

After having several problems with the fireset and changing oscilloscopes many times it was possible to come up with some significant results. The differences in Au:Ge/Ni and Pd/Ge were substantial. The critical current density, the location of failure, and the resistance and resistivity measurements exhibit their dissimilarities.

An attempt was made to find the limitations of current density for both Au:Ge/Ni and Pd/Ge. Au:Ge/Ni shows a very irregular pattern of current density which is not consistent from die to die. It was possible to find the critical current density of one die but this would not necessarily remain true for the next (Table 1). With this in mind, it was determined that the best case for critical current density of Au:Ge/Ni was  $841 \text{ kA/cm}^2$  and the worst case was  $211 \text{ kA/cm}^2$ . In each situation the failure took place in the contact region itself. In comparison, Pd/Ge's critical current density could not be determined; failure took place in the GaAs bulk wafer and not in the actual contact (Figure 5).

Resistance of the contacts is another important factor in their use at high current. For dies with a constant area Au:Ge/Ni displayed a large scatter band while Pd/Ge had a very

small one (Figure 6). This once again proves the reproducibility of Pd/Ge and the non-uniformity of Au:Ge/Ni. From the positioning of these scatter bands on the graph it is also possible to see that Pd/Ge for its area shows a closer to ideal resistance than that of the Au:Ge/Ni. Taking into account these results and the critical current densities it is logical to assume that the threshold current of the contact would decrease with an increase in resistance. Therefore a low and constant cold resistance is optimal.

The small scatter characteristic of Pd/Ge makes it possible to study the relationship of resistance as a function of resistivity divided by the area of the die. To do this a constant for resistivity must be met. The way to find this constant is to take an average of the most reliable cold resistance measurements (the  $0.2 \text{ cm}^2$  die measurements are most appropriate) and solve for resistivity. The results of this calculation equals an average resistivity  $\rho = 2.0 \times 10^{-4} \Omega \text{ cm}^2$ . By plotting a simple inverse relationship with  $R = \rho/A$  on an area versus resistance graph, it is shown that the Pd/Ge data can be fit to this curve (Figure 7).

The model of PSpice proved to be an effective way in which to simulate the oscilloscope readings from the fireset. To test the ability of PSpice in modeling the waveforms, the same parameters were set and then a waveform from the oscilloscope was compared with one from the computer. By taking a standard copper stripline with a copper mounted die, instead

of a GaAs one, the first test was done (Figure 8). The waveforms did not display the same peak heights, but this may be due to the fact that resistance had to be estimated within the fireset. By changing the stripline to a slightly higher resistance of  $47\text{m}\Omega$  both on the fireset and PSpice (Figure 9) waveform peak height changed in proportion for each test. This indicates that the oscilloscope readings can be modeled and accurate measurements (this is where current density measurements came from) can be taken from the oscilloscope. PSpice modeling provides additional verification of an earlier result: cold resistance plays a key role in critical current density prior to failure of ohmic contacts subjected to high current pulses.

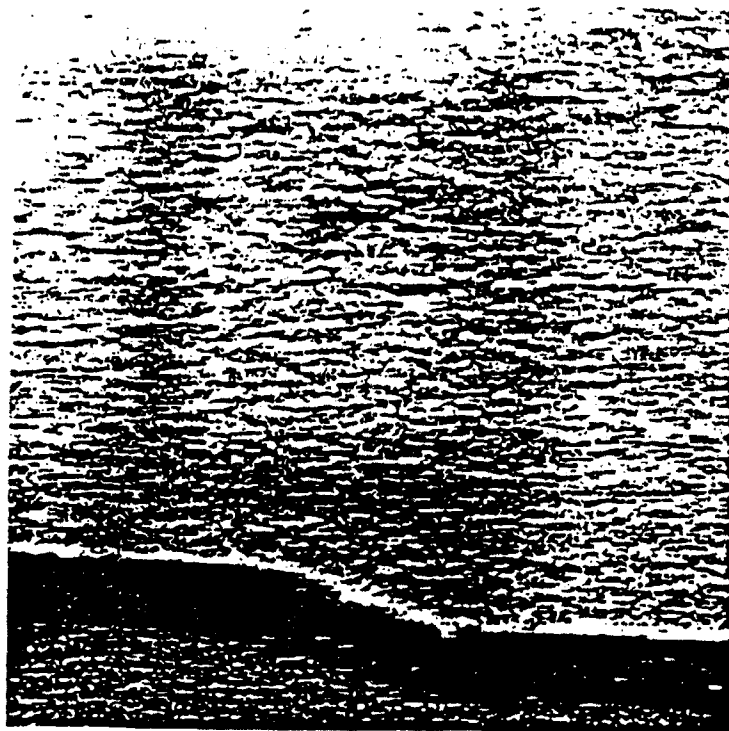
### CONCLUSION

The purpose of this project was to gather data on ohmic contacts of Au:Ge/Ni and Pd/Ge at high currents. Au:Ge/Ni was found to have several inherent problems. These die are harder to reproduce, have a higher resistance and resistivity, do not repeat the same results from die to die, and have limiting critical current density. In comparison the Pd/Ge specimens were found to be much less problematic. These displayed better reproducibility (physically, chemically and electronically from die to die), lower resistance and resistivity, and critical current density beyond the measurable limit of these experiments. The unreliability associated with use of

Au:Ge/Ni contacts at high currents may limit their application in a photoconductive switch; the Pd/Ge would be more predictable and worthy of high current usage.

#### REFERENCES

1. L.C. Wang, PhD Dissertation (1991) , "The Development of Non-spiking Ohmic Contacts Formed by Solid-Phase Reactions to n-type GaAs," University of California, San Diego.
2. P. Gueret, et al, Appl. Phys. Lett. 55 (1989) 1735.
3. L.C. Wang, et al, J. Appl. Phys. 69 (1991) 4364.



SURFACE MORPHOLOGY OF Ge/Pd (TOP)  
AND AuGe/Ni ( BOTTOM)

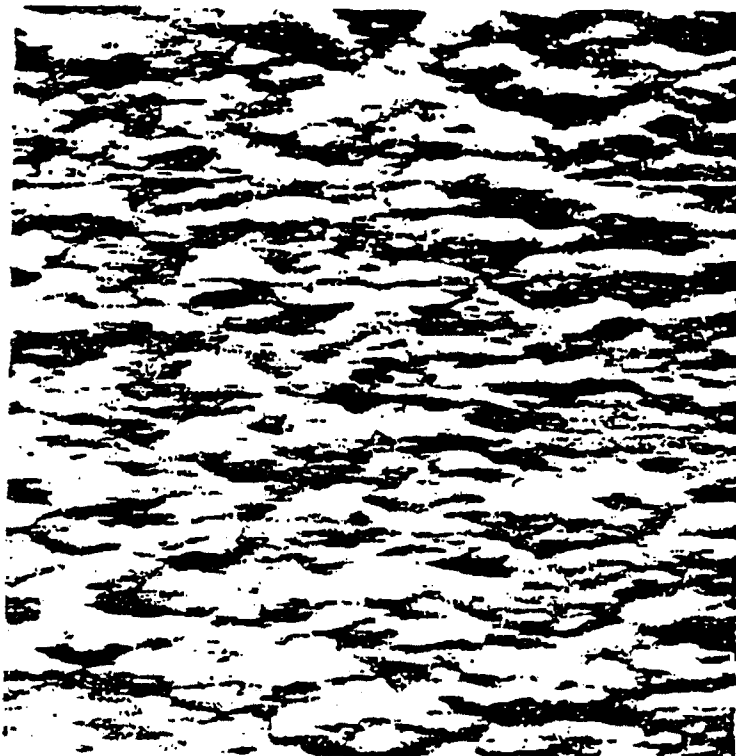


FIGURE 1



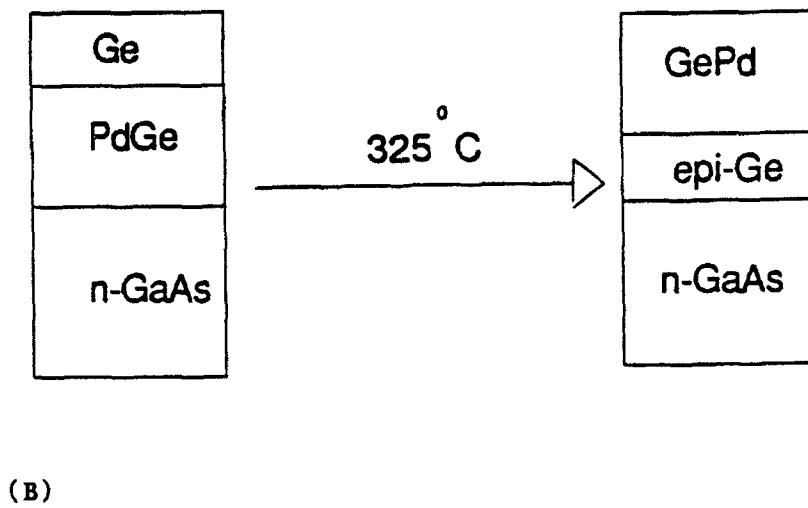
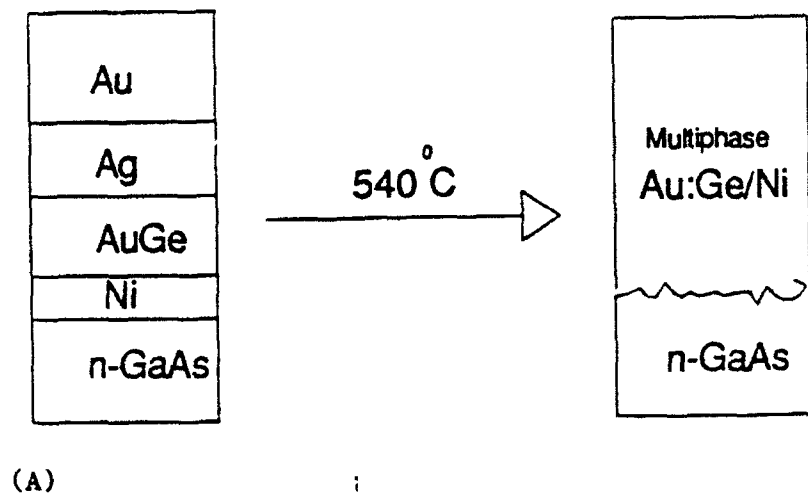


FIGURE 2

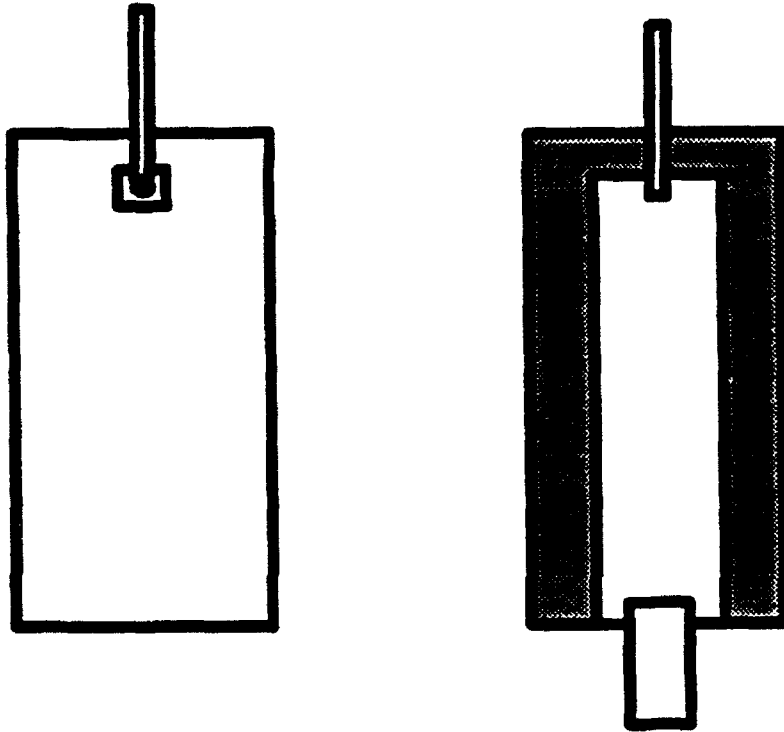
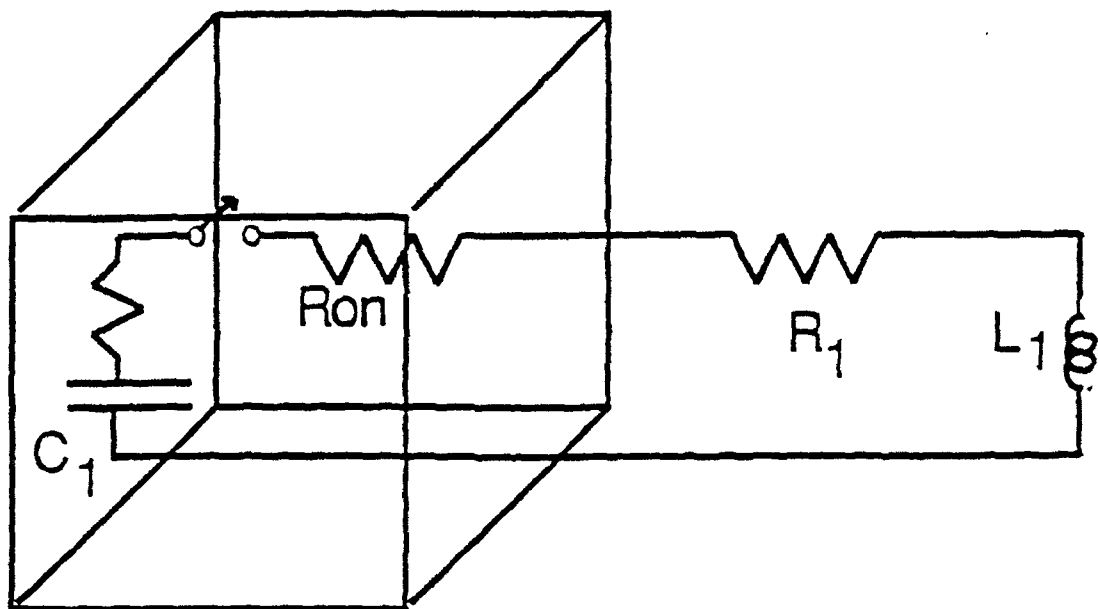


FIGURE 3



```

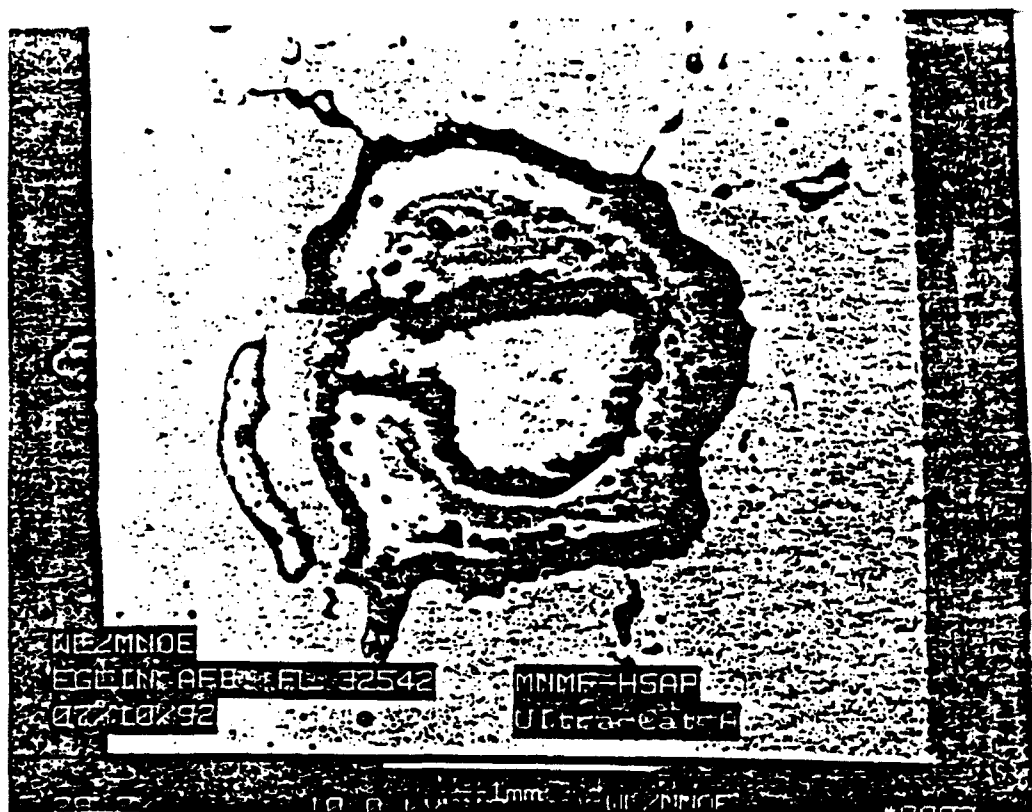
**Darcie circuit
c1 1 0 .4u
s1 1 2 4 5 smodel
.model smodel vswitch (ron=5e-2 roff=1e10 )
r1 2 3 .07
l1 3 0 24n
vsw 4 5 pulse(0v 1v 1.5us 10ns .5us 1.5us 10us)
r2 4 5 10k
r3 4 0 10Meg
.ic V(1) =5000v
.tran 10ns 5us
.probe v(1) v(2) v(3) i(r1)
.end

```

FIGURE 4

# TABLE 1

CONTACT TYPE	AREA (cm <sup>2</sup> )	CURRENT (kA)	CURRENT DENSITY (kA/cm <sup>2</sup> )
Au:Ge/Ni	0.0153	3.23	211
"	"	700	457
"	"	2.9	841
Pd/Ge	0.02	13.5	675



Au:Ge/Ni



Pd/Ge

FIGURE 5

# COMPARATIVE RESISTANCES

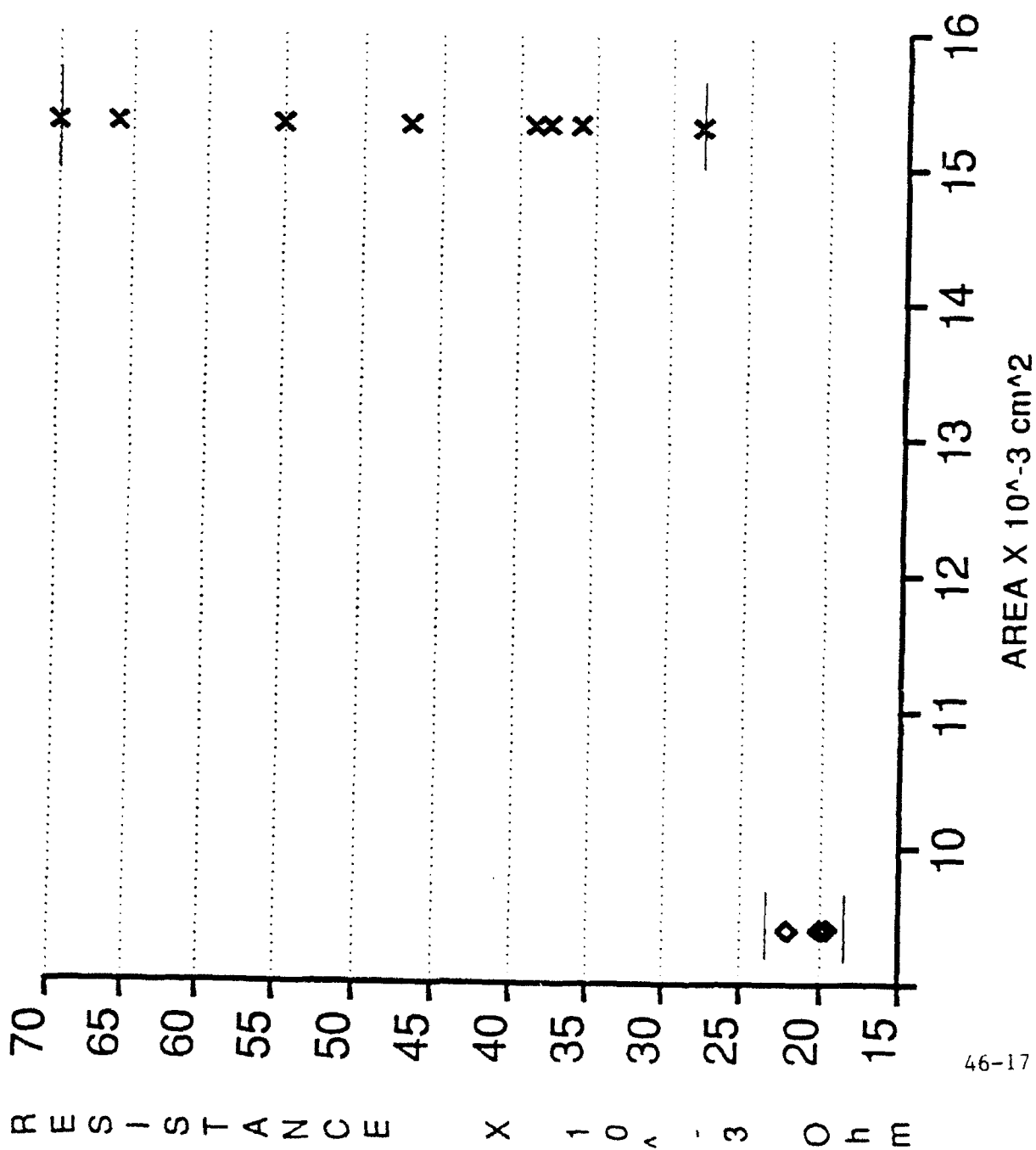


FIGURE 6

# INVERSE FUNCTION FOR $p=2.0 \times 10^{-4}$ CHANGES IN GE/PD AREA

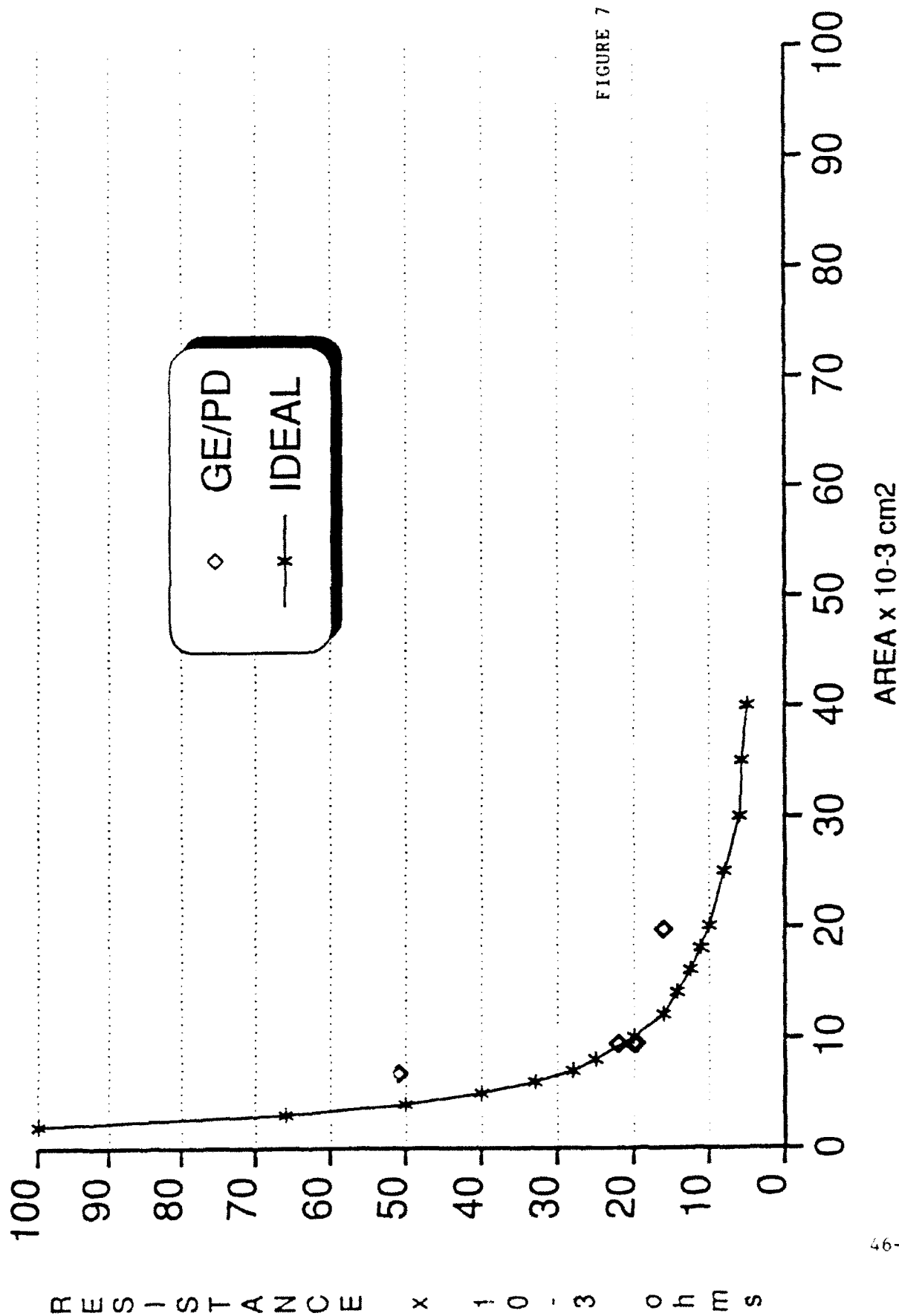
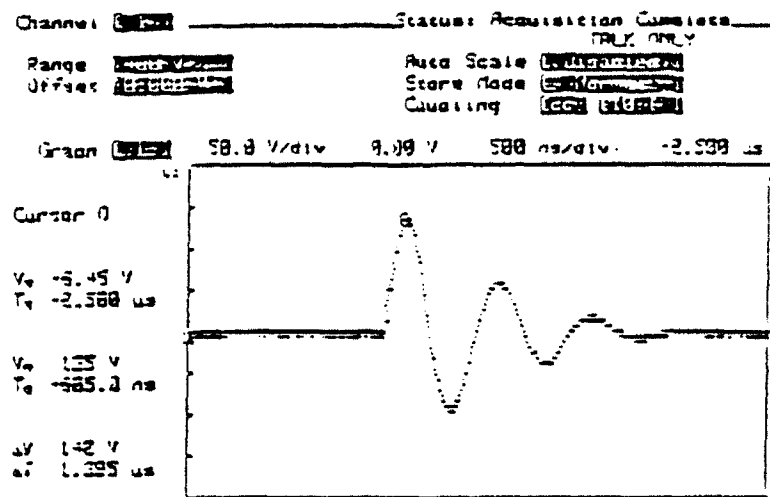
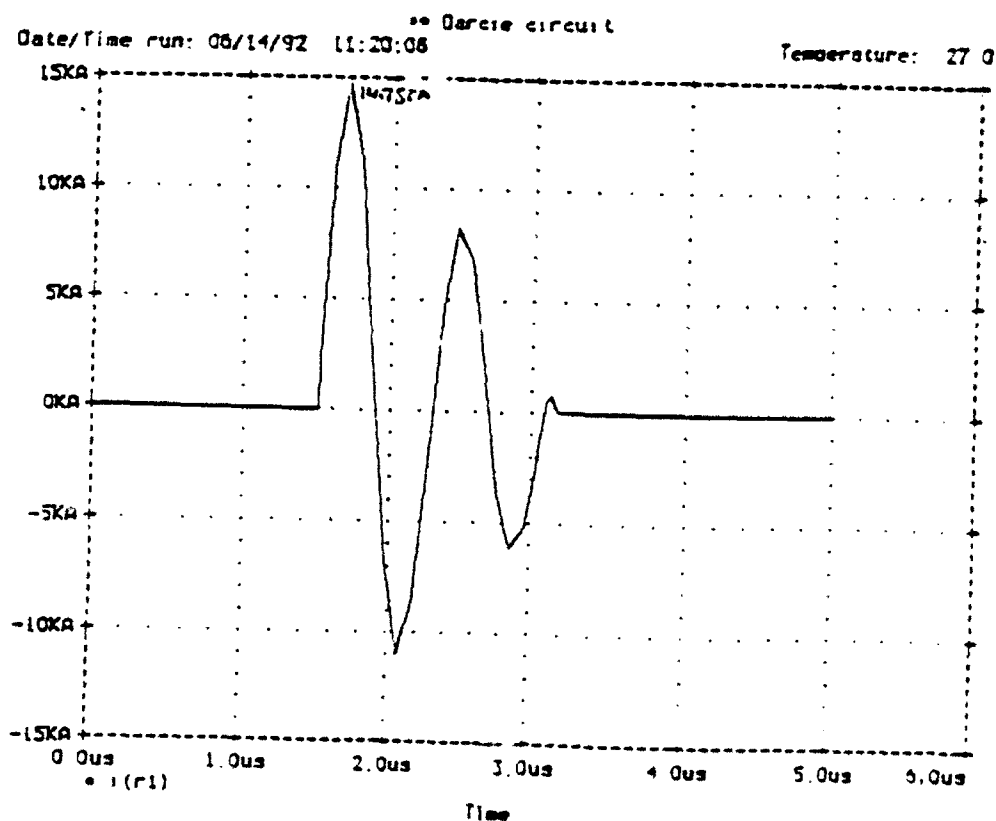


FIGURE 7

# STANDARD COPPER STRIP LINE = 7m OHMS



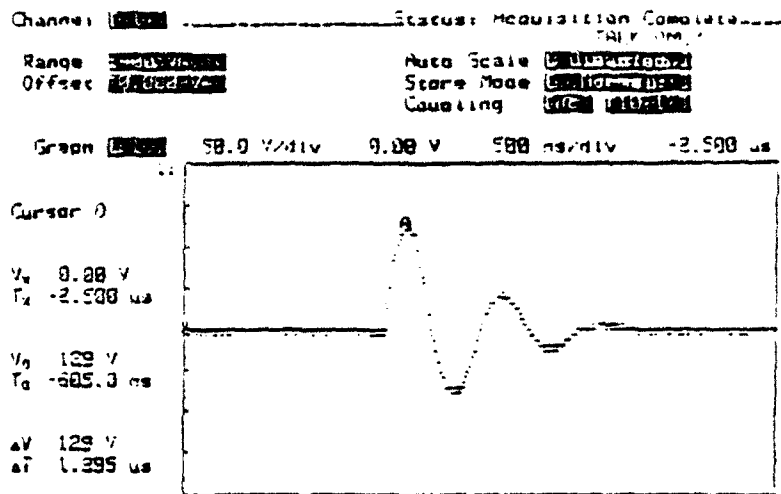
## OSCILLOSCOPE READING AT 5KV



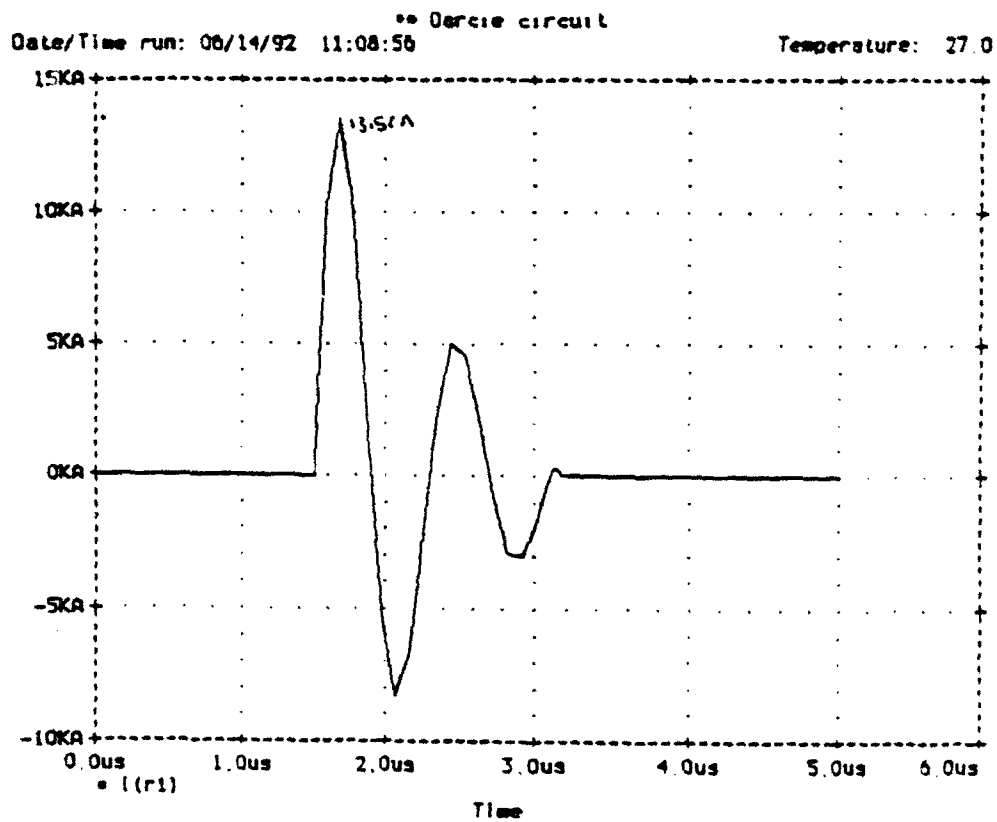
## P-SPICE SIMULATION AT 5KV

FIGURE 8





## OSCILLOSCOPE READING AT 5KV



## P-SPICE SIMULATION AT 5KV

FIGURE 9

**EVALUATION OF ENGINEERING AND SCIENTIFIC SOFTWARE TOOLS FOR USE IN  
ELECTRONIC WARFARE AND DIGITAL SIGNAL PROCESSING APPLICATIONS**

**David L. Watson  
Senior**

**Kettering Fairmont High School  
3301 Shroyer Road  
Kettering, Ohio 45429**

**Final Report for:  
AFOSR Summer Research Program, Wright Laboratory,  
Electronic Warfare Division**

**Sponsored by: Air Force Office of Scientific Research  
Bolling Air Force Base, Washington, D.C.**

**August 1992**

# EVALUATION OF ENGINEERING AND SCIENTIFIC SOFTWARE TOOLS FOR USE IN ELECTRONIC WARFARE AND DIGITAL SIGNAL PROCESSING APPLICATIONS

David L. Watson  
Senior  
Kettering Fairmont High School

## Abstract

Engineering and Scientific software tools were evaluated for their ease of use and utility in electronic warfare and digital signal processing applications. Mathcad, Mathematica, DADiSP, Harvard Graphics and HP Basic were reviewed. Short reviews of Excel and Word Perfect are also presented. Two side projects are discussed: the first involves configuring computers to print to a common printer and the second involves installing a Sun Sparc IPX for use in communication simulations.

# EVALUATION OF ENGINEERING AND SCIENTIFIC SOFTWARE TOOLS FOR USE IN ELECTRONIC WARFARE AND DIGITAL SIGNAL PROCESSING APPLICATIONS

David L. Watson

## Introduction

Computer software has played an increasingly significant role in research and development laboratories as the abilities of computers increases. Engineers and scientists use software for such applications as mathematical analysis, data generation and plotting, digital signal processing, word-processing, presentation of charts, and system modeling and simulation. These applications often require software that is expensive and powerful. This can often lead to the need to spend many hours with the software before it is familiar enough to be useful. Many times good software can remain unused because of a lack of training time.

## Methodology

Each piece of software was evaluated by reviewing all pertinent documentation, running the tutorial and/or demo, and using the software in a specific engineering and scientific application. Special attention was directed towards ease of use, learning time, and utility in the digital signal processing and electronic warfare fields.

## Mathcad, v3.0 PC

Mathcad is a very powerful mathematics package. It works with formulas, numbers, text, and graphs. Mathcad provides a wonderful compromise between power and ease of use. The interface functions as a piece of paper on which equations, text, and even illustrations can be placed. Everything on screen is displayed exactly as it would be if written by hand, while still offering the power found in spreadsheets and programming languages. Mathcad offers many powerful features including two dimensional and surface plots, 15 decimal digits of accuracy, a symbolic processor, matrix operations, and fast Fourier transforms.

The online tutorial permits the user to go through Mathcad in any order. As it demonstrates the program, it lets the user choose between typing the examples or having the program type them in. All demonstrations are done in the actual program, so anything that works in the tutorial will work in real use. The tutorial presents and organizes ideas in a very nice format. Someone somewhat familiar with the Windows interface would have no difficulty doing basic problems in Mathcad after going through the tutorial.

The online help is very extensive. It is based on the basic Windows help interface. Context sensitive help can be reached using the F1 key. Subject help can be accessed through an on-line index.

Context sensitive help is particularly helpful with errors. It reports what the errors mean as well as common mistakes that cause the error. Asking about a selected command, will show what the command is and how to use it. If there are similar commands, their descriptions can be reached by simply clicking on the provided list.

Mathcad's manual provided another easy way to look up information. It contains many examples and screen captures making new ideas easier to understand. With the limited amount I used it, I didn't have any problems.

The first application I tried was a problem from my second year chemistry class (Figure 1). The problem involves taking terms out of the equation to simplify the solving process. The question that arises is how much the removed terms affect the final answer. Using Mathcad's symbolic processor along with the ability to display numbers to thirteen decimal places I determined that the result differed in the fourth decimal place. This is beyond the normal accuracy of classroom equipment, but would not be acceptable in a more accurate laboratory.

The next application was a test of Mathcad's ability to do symbolic calculations. I first solved the formula for a conic section for its x and y components (Figure 2). This worked well and was within Mathcad's ability. Then I tried to solve a third degree polynomial for x (Figure 3). This was too big for Mathcad to handle, it ended up dumping the results into the clipboard. When pasted, the answer was in Mathcad's internal format which was relatively complex to decode. I also tried this problem in Mathematica which returned more favorable results.

Another application was the generation of pseudorandom sequences. This project also used DADiSP and will be discussed later.

The next application was the exploration of a function comprised of even and odd components (Figures 4,5). Figure 4 was done completely in Mathcad. Because of Mathcad's ability to display graphs and functions easily, it worked very well for this problem. The numbers for the graphs in Figure 5 were generated with DADiSP and imported to Mathcad to create a nicer display.

#### Mathematica, v1.2.1 Macintosh

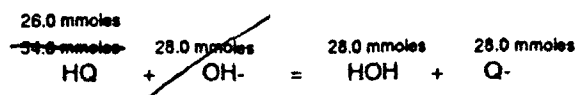
Mathematica is a very powerful mathematics program. It has all the functions that Mathcad has, and many more. It is much more powerful than Mathcad, but doesn't have as nice an interface as Mathcad has. Mathematica takes input one set of commands at a time. Instead of acting like a piece of paper, it acts more like a mail order service where the front end sends it a job and it sends back the results. While this isn't as nice as Mathcad's automatic formatting, it does make some things easier. For example, it permits running the front end on one machine and having all the calculations done on a

This is a standard weak acid-strong base reaction problem taken from my Chemistry 2 class. In solving the problem, I used Mathcad (the right column) to go beyond what was possible in the classroom (the left column). The center column applies to both methods.

A student placed 60.0 ml of .900 M HQ ( $K_a = 1.00 \cdot 10^{-5}$ ) in a container along with 40.0 ml of .700 M NaOH. Determine the pH of the solution.

$$\frac{(60.0 \cdot \text{ml})}{1} \cdot \frac{(.900 \cdot \text{mmoles})}{1 \cdot \text{ml}} = 54 \cdot \text{mmoles} \quad \text{Amount of HQ in solution}$$

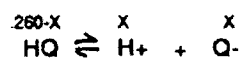
$$\frac{(40.0 \cdot \text{ml})}{1} \cdot \frac{(.700 \cdot \text{mmoles})}{1 \cdot \text{ml}} = 28 \cdot \text{mmoles} \quad \text{Amount of NaOH in solution}$$



26.0 mmoles of HQ and 28.0 mmoles Q- left in beaker

$$[\text{HQ}] = \frac{26.0 \cdot \text{mmoles}}{100.0 \cdot \text{ml}} = 0.26 \cdot \text{M}$$

$$[\text{Q}^-] = \frac{28.0 \cdot \text{mmoles}}{100.0 \cdot \text{ml}} = 0.28 \cdot \text{M}$$



$$K_a = [\text{H}^+][\text{Q}^-] / [\text{HQ}]$$

$$\frac{(x) \cdot (.280)}{(.260)} = 1.00 \cdot 10^{-5}$$

$$\frac{(x) \cdot (.28 + x)}{(.260 - x)} = 1.00 \cdot 10^{-5}$$

In the Classroom the +x and the -x is deleted for simplicity.

$$x_1 := 9.2857142857143 \cdot 10^{-6}$$

$$x_2 := 9.28507477370968 \cdot 10^{-6}$$

This is the equation that Mathcad uses

$$\frac{x \cdot (b + x)}{(c - x)} = k$$

$$x = \left[ \frac{-\frac{1}{2} \cdot b - \frac{1}{2} \cdot k + \frac{1}{2} \cdot \sqrt{b^2 + 2 \cdot b \cdot k + k^2 + 4 \cdot k \cdot c}}{\frac{-1}{2} \cdot b - \frac{1}{2} \cdot k - \frac{1}{2} \cdot \sqrt{b^2 + 2 \cdot b \cdot k + k^2 + 4 \cdot k \cdot c}} \right]$$

$$x = [\text{H}^+]$$

$$\text{pH} = -\log[\text{H}^+]$$

$$-\log[x_1] = 5.0321846833714$$

$$-\log[x_2] = 5.032214594489763$$

Figure 1  
47-5

This is a test of Mathcad's symbolic functions. The first equation is the equation for a conic section. The second equation is a third degree polynomial. The answer to the second problem was too large for Mathcad to handle so it dumped it to the clipboard in it's internal format.

Original Equation

$$a \cdot x^2 + b \cdot x \cdot y + c \cdot y^2 + d \cdot x + e \cdot y + f = 0$$

$$x = \left[ \begin{array}{l} \frac{1}{(2 \cdot a)} \cdot \left[ -b \cdot y - d + \sqrt{b^2 \cdot y^2 + 2 \cdot b \cdot y \cdot d + d^2 - 4 \cdot a \cdot c \cdot y^2 - 4 \cdot a \cdot e \cdot y - 4 \cdot a \cdot f} \right] \\ \frac{1}{(2 \cdot a)} \cdot \left[ -b \cdot y - d - \sqrt{b^2 \cdot y^2 + 2 \cdot b \cdot y \cdot d + d^2 - 4 \cdot a \cdot c \cdot y^2 - 4 \cdot a \cdot e \cdot y - 4 \cdot a \cdot f} \right] \end{array} \right]$$

$$y = \left[ \begin{array}{l} \frac{1}{(2 \cdot c)} \cdot \left[ -b \cdot x - e + \sqrt{b^2 \cdot x^2 + 2 \cdot b \cdot x \cdot e + e^2 - 4 \cdot c \cdot a \cdot x^2 - 4 \cdot c \cdot d \cdot x - 4 \cdot c \cdot f} \right] \\ \frac{1}{(2 \cdot c)} \cdot \left[ -b \cdot x - e - \sqrt{b^2 \cdot x^2 + 2 \cdot b \cdot x \cdot e + e^2 - 4 \cdot c \cdot a \cdot x^2 - 4 \cdot c \cdot d \cdot x - 4 \cdot c \cdot f} \right] \end{array} \right]$$

Figure 2

Original Equation

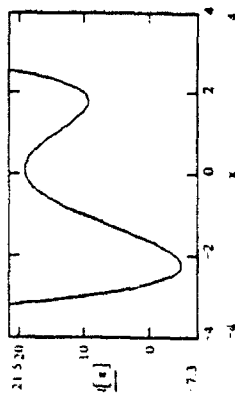
$$a \cdot x^3 + b \cdot x^2 + c \cdot x + d = 0$$

The three roots of x are

$$\begin{aligned} & \left( \frac{1}{6} \cdot \frac{b}{a^{**2}} \cdot c - \frac{1}{2} \cdot \frac{d}{a} - \frac{1}{27} \cdot \frac{b^{**3}}{a^{**3}} + \frac{1}{18} \cdot (4 \cdot a^{**3} \cdot c^{**2} \cdot b^{**2} - 18 \cdot b^{**3} \cdot c \cdot a \cdot d + 27 \cdot d^{**2} \cdot a^{**2} + 4 \cdot d \cdot b^{**3} \right. \\ & \left. )^{** \left( \frac{1}{2} \right) \cdot 3^{** \left( \frac{1}{2} \right) / a^{**2}} \cdot \left( \frac{1}{3} \right)} + \left( \frac{1}{6} \cdot \frac{b}{a^{**2}} \cdot c - \frac{1}{2} \cdot \frac{d}{a} - \frac{1}{27} \cdot \frac{b^{**3}}{a^{**3}} - \frac{1}{18} \cdot (4 \cdot a^{**3} \cdot c^{**2} \cdot b^{**2} - 18 \cdot b^{**3} \cdot c \cdot a \cdot d + 27 \cdot d^{**2} \cdot a^{**2} + 4 \cdot d \cdot b^{**3} \right) \right. \\ & \left. \right)^{** \left( \frac{1}{2} \right) \cdot 3^{** \left( \frac{1}{2} \right) / a^{**2}} \cdot \left( \frac{1}{3} \right)} - \frac{1}{3} \cdot \frac{b}{a} \cdot \\ & - \frac{1}{2} \cdot \left( \frac{1}{6} \cdot \frac{b}{a^{**2}} \cdot c - \frac{1}{2} \cdot \frac{d}{a} - \frac{1}{27} \cdot \frac{b^{**3}}{a^{**3}} + \frac{1}{18} \cdot (4 \cdot a^{**3} \cdot c^{**2} \cdot b^{**2} - 18 \cdot b^{**3} \cdot c \cdot a \cdot d + 27 \cdot d^{**2} \cdot a^{**2} + 4 \cdot d \cdot b^{**3} \right) \right. \\ & \left. \right)^{** \left( \frac{1}{2} \right) \cdot 3^{** \left( \frac{1}{2} \right) / a^{**2}} \cdot \left( \frac{1}{3} \right)} - \frac{1}{2} \cdot \left( \frac{1}{6} \cdot \frac{b}{a^{**2}} \cdot c - \frac{1}{2} \cdot \frac{d}{a} - \frac{1}{27} \cdot \frac{b^{**3}}{a^{**3}} - \frac{1}{18} \cdot (4 \cdot a^{**3} \cdot c^{**2} \cdot b^{**2} - 18 \cdot b^{**3} \cdot c \cdot a \cdot d + 27 \cdot d^{**2} \cdot a^{**2} + 4 \cdot d \cdot b^{**3} \right) \right. \\ & \left. \right)^{** \left( \frac{1}{2} \right) \cdot 3^{** \left( \frac{1}{2} \right) / a^{**2}} \cdot \left( \frac{1}{3} \right)} - \frac{1}{3} \cdot \frac{b}{a} + \frac{1}{2} \cdot 3^{** \left( \frac{1}{2} \right) \cdot \left( \frac{1}{6} \cdot \frac{b}{a^{**2}} \cdot c - \frac{1}{2} \cdot \frac{d}{a} - \frac{1}{27} \cdot \frac{b^{**3}}{a^{**3}} + \frac{1}{18} \cdot (4 \cdot a^{**3} \cdot c^{**2} \cdot b^{**2} - 18 \cdot b^{**3} \cdot c \cdot a \cdot d + 27 \cdot d^{**2} \cdot a^{**2} + 4 \cdot d \cdot b^{**3} \right) \right.} \\ & \left. \right)^{** \left( \frac{1}{2} \right) \cdot 3^{** \left( \frac{1}{2} \right) / a^{**2}} \cdot \left( \frac{1}{3} \right)} - \left( \frac{1}{6} \cdot \frac{b}{a^{**2}} \cdot c - \frac{1}{2} \cdot \frac{d}{a} - \frac{1}{27} \cdot \frac{b^{**3}}{a^{**3}} - \frac{1}{18} \cdot (4 \cdot a^{**3} \cdot c^{**2} \cdot b^{**2} - 18 \cdot b^{**3} \cdot c \cdot a \cdot d + 27 \cdot d^{**2} \cdot a^{**2} + 4 \cdot d \cdot b^{**3} \right) \right. \\ & \left. \right)^{** \left( \frac{1}{2} \right) \cdot 3^{** \left( \frac{1}{2} \right) / a^{**2}} \cdot \left( \frac{1}{3} \right)} \cdot 1, \\ & - \frac{1}{2} \cdot \left( \frac{1}{6} \cdot \frac{b}{a^{**2}} \cdot c - \frac{1}{2} \cdot \frac{d}{a} - \frac{1}{27} \cdot \frac{b^{**3}}{a^{**3}} + \frac{1}{18} \cdot (4 \cdot a^{**3} \cdot c^{**2} \cdot b^{**2} - 18 \cdot b^{**3} \cdot c \cdot a \cdot d + 27 \cdot d^{**2} \cdot a^{**2} + 4 \cdot d \cdot b^{**3} \right) \right. \\ & \left. \right)^{** \left( \frac{1}{2} \right) \cdot 3^{** \left( \frac{1}{2} \right) / a^{**2}} \cdot \left( \frac{1}{3} \right)} - \frac{1}{2} \cdot \left( \frac{1}{6} \cdot \frac{b}{a^{**2}} \cdot c - \frac{1}{2} \cdot \frac{d}{a} - \frac{1}{27} \cdot \frac{b^{**3}}{a^{**3}} - \frac{1}{18} \cdot (4 \cdot a^{**3} \cdot c^{**2} \cdot b^{**2} - 18 \cdot b^{**3} \cdot c \cdot a \cdot d + 27 \cdot d^{**2} \cdot a^{**2} + 4 \cdot d \cdot b^{**3} \right) \right. \\ & \left. \right)^{** \left( \frac{1}{2} \right) \cdot 3^{** \left( \frac{1}{2} \right) / a^{**2}} \cdot \left( \frac{1}{3} \right)} - \frac{1}{3} \cdot \frac{b}{a} - \frac{1}{2} \cdot 3^{** \left( \frac{1}{2} \right) \cdot \left( \frac{1}{6} \cdot \frac{b}{a^{**2}} \cdot c - \frac{1}{2} \cdot \frac{d}{a} - \frac{1}{27} \cdot \frac{b^{**3}}{a^{**3}} + \frac{1}{18} \cdot (4 \cdot a^{**3} \cdot c^{**2} \cdot b^{**2} - 18 \cdot b^{**3} \cdot c \cdot a \cdot d + 27 \cdot d^{**2} \cdot a^{**2} + 4 \cdot d \cdot b^{**3} \right) \right.} \\ & \left. \right)^{** \left( \frac{1}{2} \right) \cdot 3^{** \left( \frac{1}{2} \right) / a^{**2}} \cdot \left( \frac{1}{3} \right)} - \left( \frac{1}{6} \cdot \frac{b}{a^{**2}} \cdot c - \frac{1}{2} \cdot \frac{d}{a} - \frac{1}{27} \cdot \frac{b^{**3}}{a^{**3}} - \frac{1}{18} \cdot (4 \cdot a^{**3} \cdot c^{**2} \cdot b^{**2} - 18 \cdot b^{**3} \cdot c \cdot a \cdot d + 27 \cdot d^{**2} \cdot a^{**2} + 4 \cdot d \cdot b^{**3} \right) \right. \\ & \left. \right)^{** \left( \frac{1}{2} \right) \cdot 3^{** \left( \frac{1}{2} \right) / a^{**2}} \cdot \left( \frac{1}{3} \right)} \cdot 1 \end{aligned}$$

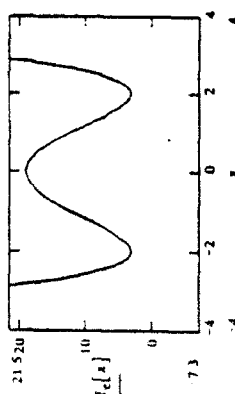
Figure 3

$$f(x) = x^4 + 5x^3 - 8x^2 + 15x + 19$$



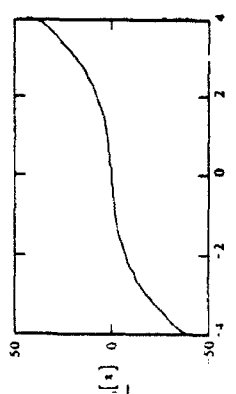
Any function  $f(x)$  can be separated into ...

$$f_e(x) = \frac{1}{2}(f(x) + f(-x))$$



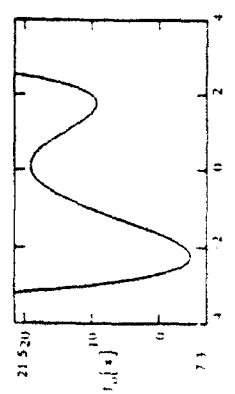
an even function which is symmetric to the y axis...

$$f_o(x) = \frac{1}{2}(f(x) - f(-x))$$



and an odd function which is symmetric to the origin...

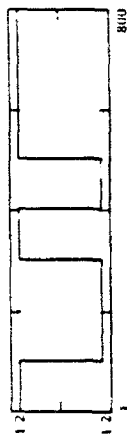
$$f_e(x) + f_o(x)$$



which, when added together re-create the original function.

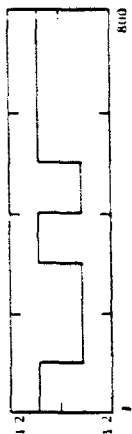
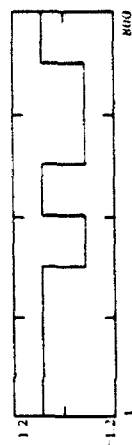
Figure 4

$f(x)$



$$\frac{1}{2}f(-x)$$

$$\frac{1}{2}f(x)$$

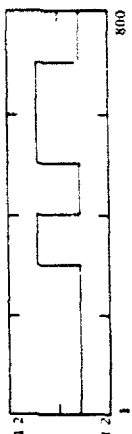
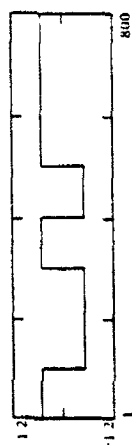


$$+$$

$$+$$

$$\frac{1}{2}f(x)$$

$$\frac{1}{2}f(-x)$$

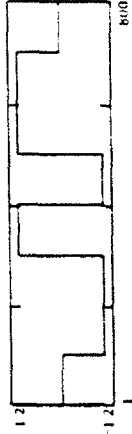
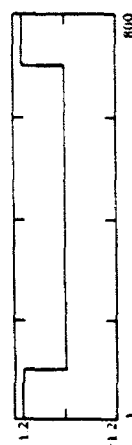


$$=$$

$$=$$

$$f_e(x)$$

$$f_o(x)$$



$f(x)$

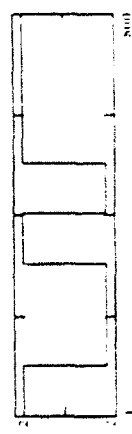


Figure 5



more powerful machine. Mathematica appears to be able to do extremely complex problems, the only restraint is time. It solved a third degree polynomial for  $x$  in about 6.5 seconds. Having Mathematica find the simplest form added about 40 seconds to this time. The interface is a little intimidating for the first time user, but after going through the examples in the book, the program became much easier to use. This isn't the easiest program to use, but its power is unmatched by Mathcad.

There was no tutorial that I saw online. I used the book Mathematica, A System for Doing Mathematics by Computer [1]. It does contain a chapter that gives a basic overview of the program with examples for every explanation. It also contains many sections that look at more specific groups of commands in detail. Once past learning the basic interface to the program, it is relatively easy to use.

Mathematica doesn't contain a lot of online help. Typing a question mark and the name of a command will give a short definition of the command and its usage. It's not enough for the first time user, but it's enough as a reminder for an experienced user. Mathematica will also complete the name of a command that is partially typed in. This is particularly useful when trying to remember the spelling of a command. The book was very useful for looking up commands. Every command is given a short technical explanation in the back of the book. Most, if not all, commands are also given an overview earlier in the book. These usually have helpful examples that show common usage of the commands. Figuring out the usage of a command isn't always easy (even with examples) for a new user. Once the user becomes more experienced with Mathematica, understanding new commands becomes easier.

The first thing I tried to do in Mathematica after figuring out the interface, was to solve a third degree polynomial for  $x$  (Figure 6). I had tried this in Mathcad and it was unable to display the result. Mathematica had no problems, but the answers are so long, they end up being several lines long each, which is a little hard to interpret.

I then explored Mathematica's three dimensional plotting and animation abilities. I generated an animation that showed the development of a  $\sin(X)/X$  function (Figure 7). The top graph is the first frame in the animation while the bottom graph is the last frame. The animation produces an interesting rippling effect. I also generated a series of two dimensional plots that illustrate how the coefficients would affect the rotation of the function  $\text{Cos}[2\pi(ax + by)]$  (Figure 8). The top graph in Figure 8 has  $a=2$  and  $b=3$ . The bottom one has the coefficients reversed.

I was also interested in the accuracy of Mathematica. It doesn't seem to have any limits like Mathcad. I computed  $\pi$  to 2000 places in 37 seconds (Figure 9). The accuracy was verified in a mathematics book.

and degree poly normal

```
in[1]:=
Simplify[ Solve[a x^3 + b x^2 + c x + d == 0, x] ]
Out[1]=
```

$$\{x \rightarrow \frac{-b \sqrt{3} a^2 + (-b^2 - 3 a c + 3 \sqrt{3} a^2 d - 18 a b c d + 27 a^2 d^2) \sqrt{3} a}{27 a^3 + 6 a^2 \sqrt{3} a}, \frac{-b \sqrt{3} a^2 + (-b^2 - 3 a c + 3 \sqrt{3} a^2 d - 18 a b c d + 27 a^2 d^2) \sqrt{3} a}{27 a^3 + 6 a^2 \sqrt{3} a}\}$$

$$\{x \rightarrow \frac{-b \sqrt{3} a^2 + (-b^2 - 3 a c + 3 \sqrt{3} a^2 d - 18 a b c d + 27 a^2 d^2) \sqrt{3} a}{27 a^3 + 6 a^2 \sqrt{3} a}, \frac{-b \sqrt{3} a^2 + (-b^2 - 3 a c + 3 \sqrt{3} a^2 d - 18 a b c d + 27 a^2 d^2) \sqrt{3} a}{27 a^3 + 6 a^2 \sqrt{3} a}\}$$

$$\frac{9 a^3 \left( \frac{-b \sqrt{3} a^2 + (-b^2 - 3 a c + 3 \sqrt{3} a^2 d - 18 a b c d + 27 a^2 d^2) \sqrt{3} a}{27 a^3 + 6 a^2 \sqrt{3} a} \right) + 9 \sqrt{3} a^2 d \left( \frac{-b \sqrt{3} a^2 + (-b^2 - 3 a c + 3 \sqrt{3} a^2 d - 18 a b c d + 27 a^2 d^2) \sqrt{3} a}{27 a^3 + 6 a^2 \sqrt{3} a} \right)}{27 a^3 + 6 a^2 \sqrt{3} a}$$

47-9

$$\frac{18 a^3 \left( \frac{-b \sqrt{3} a^2 + (-b^2 - 3 a c + 3 \sqrt{3} a^2 d - 18 a b c d + 27 a^2 d^2) \sqrt{3} a}{27 a^3 + 6 a^2 \sqrt{3} a} \right) + 18 \sqrt{3} a^2 d \left( \frac{-b \sqrt{3} a^2 + (-b^2 - 3 a c + 3 \sqrt{3} a^2 d - 18 a b c d + 27 a^2 d^2) \sqrt{3} a}{27 a^3 + 6 a^2 \sqrt{3} a} \right)}{27 a^3 + 6 a^2 \sqrt{3} a}$$

$$\{x \rightarrow \frac{-b \sqrt{3} a^2 + (-b^2 - 3 a c + 3 \sqrt{3} a^2 d - 18 a b c d + 27 a^2 d^2) \sqrt{3} a}{27 a^3 + 6 a^2 \sqrt{3} a}, \frac{-b \sqrt{3} a^2 + (-b^2 - 3 a c + 3 \sqrt{3} a^2 d - 18 a b c d + 27 a^2 d^2) \sqrt{3} a}{27 a^3 + 6 a^2 \sqrt{3} a}\}$$

$$\frac{9 a^3 \left( \frac{-b \sqrt{3} a^2 + (-b^2 - 3 a c + 3 \sqrt{3} a^2 d - 18 a b c d + 27 a^2 d^2) \sqrt{3} a}{27 a^3 + 6 a^2 \sqrt{3} a} \right) + 9 \sqrt{3} a^2 d \left( \frac{-b \sqrt{3} a^2 + (-b^2 - 3 a c + 3 \sqrt{3} a^2 d - 18 a b c d + 27 a^2 d^2) \sqrt{3} a}{27 a^3 + 6 a^2 \sqrt{3} a} \right)}{27 a^3 + 6 a^2 \sqrt{3} a}$$

$$\frac{18 a^3 \left( \frac{-b \sqrt{3} a^2 + (-b^2 - 3 a c + 3 \sqrt{3} a^2 d - 18 a b c d + 27 a^2 d^2) \sqrt{3} a}{27 a^3 + 6 a^2 \sqrt{3} a} \right) + 18 \sqrt{3} a^2 d \left( \frac{-b \sqrt{3} a^2 + (-b^2 - 3 a c + 3 \sqrt{3} a^2 d - 18 a b c d + 27 a^2 d^2) \sqrt{3} a}{27 a^3 + 6 a^2 \sqrt{3} a} \right)}{27 a^3 + 6 a^2 \sqrt{3} a}$$

Figure 6

```
Do{Plot3D[Sin[n*Sqrt{x^2+y^2}]/(Sqrt{x^2+y^2})], {n,-10,10},
{y,-10,10}, Boxed->False, Lighting->True, PlotPoints->30,
Axes->None, PlotRange->All}, {n,1,2,.1}]
```

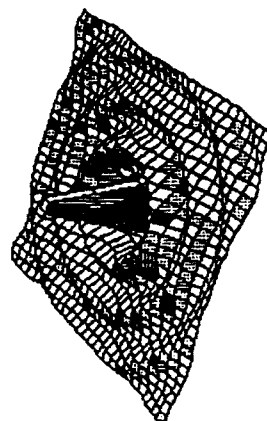
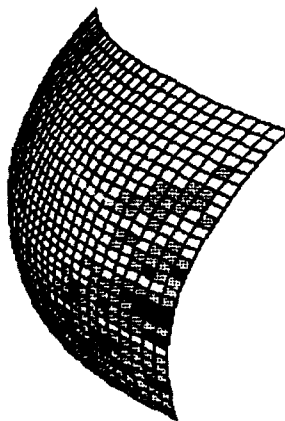
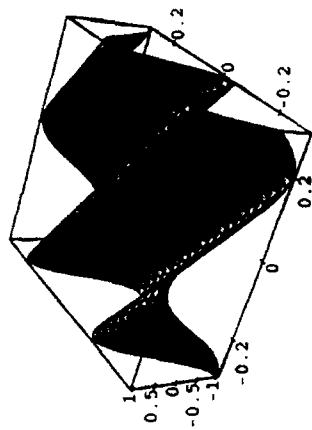


Figure 7

```
Plot3D[Cos[2 Pi (2 x + 3 y) ]], {x, -.3, .3},
{y, -.3, .3}, Lighting->True, PlotPoints->30]
```



```
Plot3D[Cos[2 Pi (3 x + 2 y) ]], {x, -.3, .3},
{y, -.3, .3}, Lighting->True, PlotPoints->30]
```

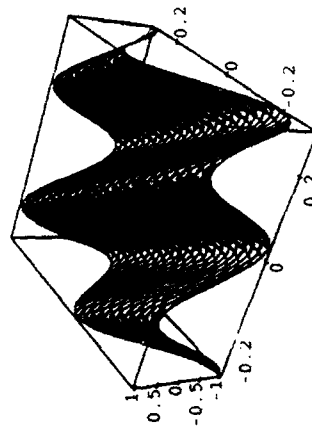


Figure 8

In[3]:=

N[P1, 2000]

Out[3]=

3.141592653589793238462643383279502884197169399375105820974944592307816406286\  
208998628034825342117067982148086513282306647093844609550582231725359408128\  
481117450284102701938521105559644622948954930381964428810975665933446128475\  
648233786783165271201909145648566923460348610454326648213393607260249141273\  
724587006606315588174881520920962829254091715364367892590360011330530548820\  
466521384146951941511609433057270365759591953092186117381932611793105118548\  
074462379962749567351885752724891227938183011949129833673362440656643086021\  
394946395224737190702179860943702770539217176293176752384674818467669405132\  
000568127145263560827785771342757789609175637178721468440901224953430146549\  
585371050792279689258923542019956112129021960864034418159813629774771309960\  
518707211349999998372978049951059731732816096318595024459455346908302642522\  
308253344685035261931188171010003137838752886587533208381420617177669147303\  
598253490428755468731159562863882353787593751957781857780532171226806613001\  
927876611195909216420198938095257201065485863278865936153381827968230301952\  
035301852968995773622599413891249721775283479131515574857242454150695950829\  
533116861727855889075098381754637464939319255060400927701671139009848824012\  
858361603563707660104710181942955596198946767837449448255379774726847104047\  
534646208046684259069491293313677028989152104752162056966024058038150193511\  
253382430035587640247496473263914199272604269922796782354781636009341721641\  
219924586315030286182974555706749838505494588586926995690927210797509302955\  
321165344987202755960236480665499119881834797753566369807426542527862551818\  
417574672890977772793800081647060016145249192173217214772350141441973568548\  
161361157352552133475741849468438523323907394143334547762416862518983569485\  
562099219222184272550254256887671790494601653466804988627232791786085784383\  
827967976681454100953883786360950680064225125205117392984896084128488626945\  
604241965285022210661186306744278622039194945047123713786960956364371917287\  
46776465757396241389086583264599581339047

Figure 9

The last problem I did was to generate a three dimensional representation of a rotating vector in respect to time (Figure 10). In more complex terms, it's the complex exponential equation  $e^{j\omega t}$ . I tried to find a built-in three dimensional parametric plotting command, but nothing I found would do what I wanted. I ended up creating it using the polygon generation command. The result was generated by defining rectangles to plot in three dimensional space to give the function the appearance of having a surface. I did have a problem displaying this function so it wouldn't look distorted.

#### DADiSP, v2.01 PC

DADiSP stands for Data Analysis and Digital Signal Processing. It is a data analysis package based on the principal of a spreadsheet. It has many features that are not included in normal math packages. Data is represented in windows instead of cells, but functions can include window references like cell references in a spreadsheet. All windows can display data in a number of fashions, including several graph formats and a raw data list format. It has a host of digital signal processing functions that are especially useful in communications.

The online demo that comes with DADiSP didn't seem to work on the copy I worked with. It seemed to have been written for an earlier version that was slightly different. There is a tutorial in the manual that demonstrates how to import data and how to manipulate that data. It doesn't show off a lot of the features of DADiSP, but it does give a basic feel of how to use the program. I was shown how to use the program, and from there learned by trial and error.

Pressing F1 in the worksheet displays general interface commands. There is no online help for specific data functions. The manual contains a reference section with a complete description of every command. It does lack examples which would make things easier for a beginning user. Because of the many uses of the program, there are many times when it is necessary to look up commands in the index. While the manual has a very organized reference section, one can't always figure out a particular use of a command, and many times if the exact name for a function is not known, it can't be found in the index. The manual is usable after getting used to the program, but at the start it is rather hard to figure it out.

I generally used DADiSP for problems involving specific communications aspects that were impossible or very difficult to do in Mathcad. There were several instances where I used both programs to take advantage of their individual strengths.

The first problem I did in DADiSP was to generate a maximum length pseudorandom code sequence in Mathcad and import it into DADiSP. From DADiSP I was able to use this sequence as a digital waveform in a communications simulation.

```

Show[
Graphics3D[
Table[
Polygon[
{
{x,0,0},{x-.1,0,0},
{x-.1,Sin[x-.1],Cos[x-.1]},{x,Sin[x],Cos[x]}
}
] , {x, .1,2Pi,.1}
]
, Lighting->False]

```

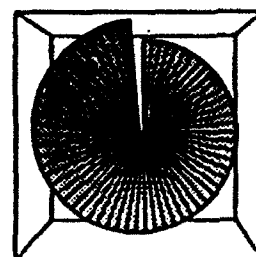
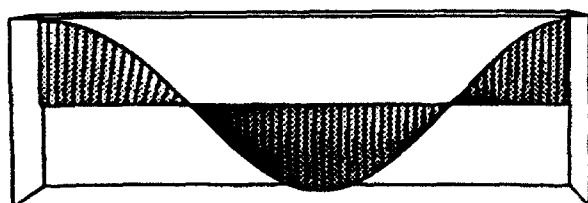
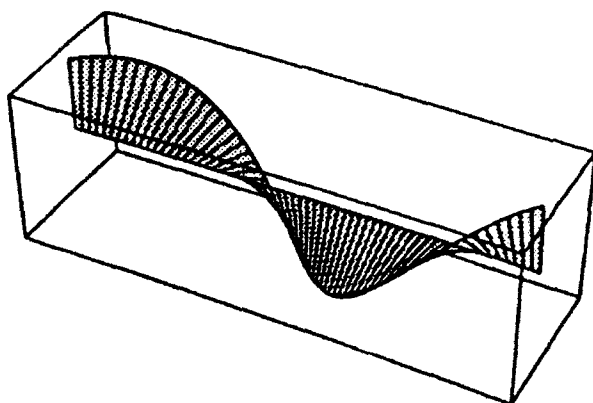


Figure 10

Another joint project I did was to generate a series of square functions that I later imported into Mathcad for display (Figure 5). I generated the functions in DADiSP by creating two line segments, one at -1 and another at 1. I then joined them together to form a basic function. From there it was easy to mathematically manipulate it. Because DADiSP has only basic printing functions, I exported the data into Mathcad. From there it was easy to obtain a good looking printout.

The next project I worked on was to explore amplitude modulation (Figure 11). I generated two sine waves, combined them in various ways to demonstrate different forms of AM modulation. I then took a spectrum of the modulated waveform to look at it in the frequency domain. The top four graphs demonstrate double sideband suppressed carrier modulation and the bottom four represent double sideband large carrier modulation. W1 in each is the signal, W2 is the carrier, W3 is the resulting signal in the time domain, and W4 is the resulting signal in the frequency domain.

The last project I did was shown to me by my mentor to demonstrate the basis behind Fourier transforms (Figure 12). Basically he demonstrated that a square wave is composed of an infinite sum of sine waves having frequencies of the odd harmonics of the square wave. We used the equation for a fourier transform to determine the coefficients of the fundamental and the first three odd harmonics. We then added them together to re-create the square wave. W1 is the DC component of the square wave, W2 is the fundamental frequency, W3-W5 are the first three odd harmonics, and W6 is a combination of the first five and approaches a square wave in shape.

#### Harvard Graphics, v3.0 PC

Harvard Graphics prepares graphs and charts for reports and presentations. The choice of charts include text, pie, xy, organizational, and drawing charts. Harvard Graphics provides a very easy way to prepare almost any kind of information quickly. All functions provide the perfect balance between having enough flexibility and being too complex. Graphs can be easily changed to experiment with different designs. Graphs can be set to a standard template or completely designed by the user.

Harvard Graphics contains a very easy to use online tutorial. The user can choose between the different chart types for instruction. Once in the tutorial, the program steps the user through creating a sample graph. Each type of graph has a basic and advanced tutorial. The tutorial allows the user to follow the instructions and enter all the input to affect the graph. The manual is very complete and would be another way to learn how to use the program. It has the usual chapter to guide a new user through the interface and basic functions of the program.

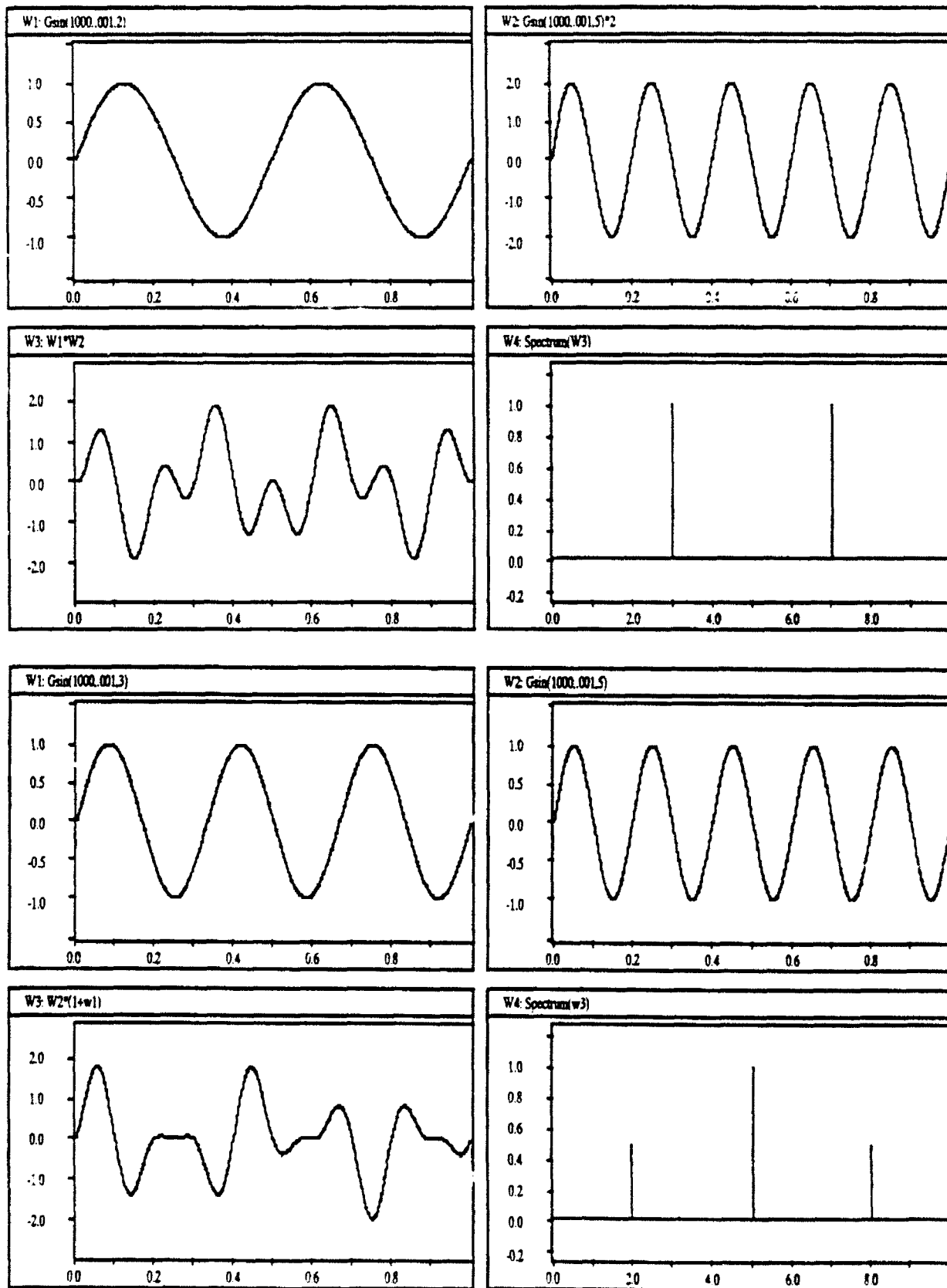


Figure 11  
47-15



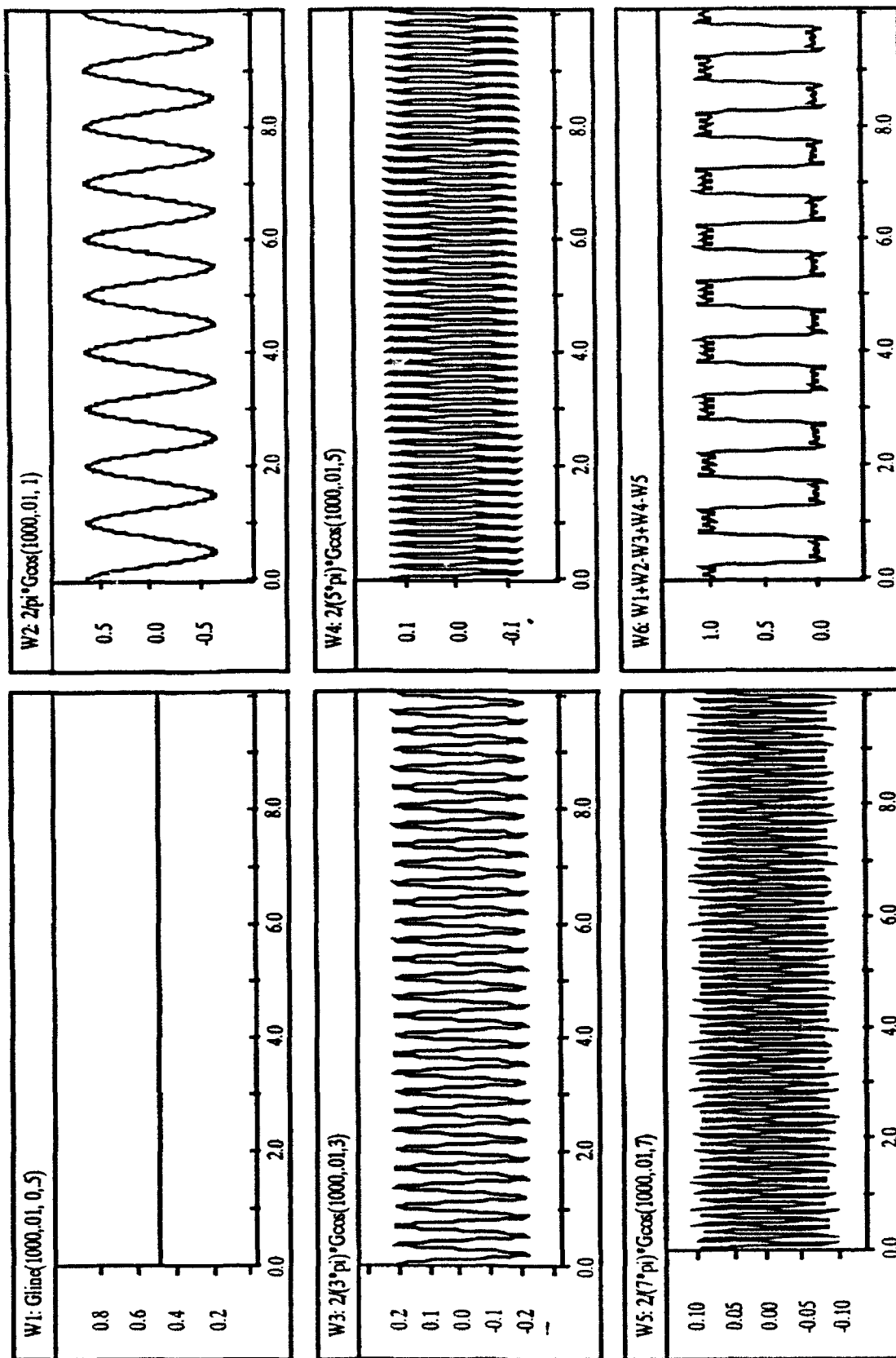


Figure 12

Help is very easy to access inside Harvard Graphics. Pressing F1 from any location provides a small description and helpful information about the current cursor position. Control-F1 provides a list of speed keys arranged alphabetically by description. Shift-F1 provides a set of general help descriptions for general program operation. The help displays are well written and complete enough that the manual is only needed if the user is looking for a specific (usually advanced) topic. The manual, even though not needed much, is well written. Wording is very good and it is one of the most aesthetically pleasing manuals that I have seen. I didn't use it much for looking up how to do things, but the few times I did, I easily understood the examples and could figure out the explanation rather easily. The manual does contain many examples to show the user many advanced features.

I did a couple presentations for my mentor in Harvard Graphics. The program was very easy to learn how to use, and the charts didn't take me very long at all. Combined with a color printer it's very easy to create nice graphs for presentations. It is easy enough to use that the person giving the presentation can easily prepare the charts to his or her style.

#### HP-Basic, v5.0 HP9836C

HP-Basic is a very powerful basic language. It includes some very nice commands such as while loops and multi-line if-then statements.

I used HP-Basic to write a program to control two HP-8770 Arbitrary Waveform Synthesizers through an HP-IB interface bus. The Arbitrary Waveform Synthesizers take input from a computer and output waveforms that can be configured in any shape imaginable. We used HP-Basic to test the synthesizers before they were interfaced to a Sun Sparc workstation. The HP offers a very easy interface through the IEEE 488 port. I was able to generate sine, square, ramp, chirp, and variable frequency sine waves with the setup. We could then look at them on a scope and a spectrum analyzer. This offered a valuable look into real world signals.

#### Other programs

I experimented with Microsoft Excel. It is a nice spreadsheet program. One of its nice features is file compatibility between the Mac and the PC. It also appears to have powerful macro capabilities. I used Excel to create a template for use in satellite link analysis. I also used it to organize data about laser printers when our group was looking for a laser printer for the Macintoshes.

I did several projects in Word Perfect including parts of this report. One of its nice features is its mathematical function writer. I used it to prepare some formulas for my mentor for a technical document.

### Other projects

One of the problems I ran into while working on my main project was the inability to print to the group's laser printer. It was in the computer room which contained a 486, two Macintoshes and the HP LaserJet III which were all tied together via the base network. When I first started working, nothing would print to the laser printer. After about a week, the network was fixed to allow the 486 to print correctly. That solved one problem, but I still wanted to be able to print from the Macintoshes. I then figured out how to configure the Macs so they would print to a PostScript file instead of the printer. PostScript is a page description language somewhat similar to uncompiled Basic or C. All the printer commands and data are in standard English. I could then transfer the PostScript file to the 486 and send it to the printer. The only problem with this method is that it takes quite a while to print documents this way. This method also worked with the individual computers in the group. Most programs on the PC (including all that run using Windows) will output to PostScript files. Then the files could be sent directly to the printer by connecting directly through the network. This made it easy to generate laser quality output from individual computers.

I also worked on setting up a Sun Sparc IPX. Unix was quite a shock after only working with personal computers. The Sparc is set up for multiple users. It likes to run on a network as opposed to a stand alone system as we were trying to do. It made things rather interesting. We were setting up the system for use in communication link simulation. The software is called Signal Processing Workstation by Comdisco. It is able to simulate communications devices as well as manipulate signals. The signals can then be sent to the Arbitrary Waveform Synthesizers to convert them into analog signals. This setup lets the user create virtual systems.

### Conclusions

I reviewed the user interface, available help, learning time and the utility on small projects of five software tools. Mathcad had a very nice interface, extensive online help, a very small learning time, and was very useful in more mathematically related projects. Mathematica had a very intimidating interface, little online help but good manual help, took relatively long to learn but was the most powerful (it had more power than normally needed in the EW and DSP projects on which I worked) which all together made it the least useful in these areas. DADiSP had a moderately easy interface, little help online or in the manual, moderate learning time but was extremely well tailored for digital signal processing. Harvard Graphics had a friendly interface, good online help and manual, small learning time, and was very useful in preparing presentations. HP Basic didn't have anything special

in its interface compared to standard Basic interpreters, had good but not great manual help, didn't take long to learn, and was very useful for the one project for which I used it.

#### References

- [1] Saturnino L. Salas, *Calculus: one and several variables, with analytic geometry*, John Wiley & Sons, Inc., 1986.
- [2] Stephen Wolfram, *Mathematica: A System for Doing Mathematics by Computer*, Addison-Wesley Publishing Company. Inc., 1988.

THE TEMPERATURE DEPENDENCE OF INTRINSIC DEFECT  
LEVELS IN GaAs SEMICONDUCTORS

Jeffrey A. Yerian  
West Carrollton Senior High School  
5833 Student Street  
West Carrollton, Ohio 45449

Final Report for:  
AFOSR Summer Research Program  
Materials Directorate  
Wright Laboratory  
Wright Patterson Air Force Base, Ohio

Sponsored by:  
AFOSR

August 1992

# THE TEMPERATURE DEPENDENCE OF INTRINSIC DEFECT LEVELS IN GaAs SEMICONDUCTORS

Jeffrey A. Yerian  
West Carrollton Senior High School

## ABSTRACT

The temperature dependence of intrinsic defect levels in GaAs semiconductors was studied. In order to investigate the temperature dependence, spectral photoconductivity data of various GaAs semiconductors was taken. Experimental data indicates that the spectral photoresponses of many GaAs semiconductors behave differently and independently of one another. However, two distinct defect levels exist in a majority of the samples. These defect levels occur at 6800 ( $E_i=0.80$  eV) and 3680 ( $E_i=0.43$  eV) wavenumbers, respectively. These two defect levels have been studied in the past, and much research has been documented. Our focus was on the temperature dependence of these defect levels from 9 K to 300 K. The temperature dependence data shows a noticeable decline of peak amplitudes occurring between the temperature range of 130 K to 170 K. From our research, we conclude that at these temperatures another defect level within the structure of the semiconductor is activated which traps free electrons and thus decreases the photoresponse of the entire spectrum. The activation energy of this trap was then calculated from this data.

# THE TEMPERATURE DEPENDENCE OF INTRINSIC DEFECT LEVELS IN GaAs SEMICONDUCTORS

Jeffrey A. Yarian

## INTRODUCTION

Semi-insulating and undoped, conductive  $n$ -type GaAs samples were studied. Undoped  $n$ -type samples are unintentionally grown during the process of growing semi-insulating GaAs. Semi-insulating GaAs materials are used in the ongoing development of compound semiconductor microelectronic devices. The optical and electrical properties of semi-insulating and  $n$ -type GaAs are affected by intrinsic defect levels and impurities which introduce a wide range of energy levels into the GaAs bandgap.<sup>1-2</sup> One method used for studying the optical properties of these defect levels is spectral photoconductivity.

Sharp increases in the photoconductivity spectrum are used to identify the photoionization energies of the intrinsic defect levels in the material. Typically there are two dominate defect levels observed in the photoconductivity spectra of  $n$ -type and semi-insulating GaAs. These two levels are associated with photoresponse peaks at  $3680\text{ cm}^{-1}$  and at  $6800\text{ cm}^{-1}$  respectively. In addition, the photoconductivity experiment can be used to study the temperature dependence of the photoresponse from these levels. Normally, the photoresponse from deep levels would be expected to slightly decrease with temperature until the thermal ionization of these levels occurs diminishing the number of carriers able to make transitions and thus competing with the photoionization process. As the temperature is further increased, the photoresponse will decrease more rapidly as the thermal ionization process dominates the generation of free electrons. Defects with higher photoionization energies would be expected to remain optically active at higher temperatures. However, the photoresponse from both the  $3680\text{ (}E_i=0.43\text{ eV)}$  peak and the  $6800\text{ (}E_i=0.80\text{ eV)}$  peak was observed to simultaneously decrease in the temperature range of 130 K to 170 K. This temperature range is below the expected for the thermal ionization of either defect level. This decreasing photoresponse was seen in both the semi-insulating and  $n$ -type samples and was attributed to a trapping mechanism.

## METHODOLOGY

Semi-insulating and  $n$ -type GaAs samples were cut from wafers grown by several different growth techniques. Indium contacts were placed near the ends of the sample. Gold wires were soldered onto these

contacts using indium. The GaAs samples were mounted onto a beryllium oxide insulator using a varnish and placed on the coldfinger of a cryogenic refrigerator. The coldfinger was set in a Fourier Transform Infrared Spectrometer (FTIR). Using a coldhead compressor, the samples were cooled to 9 K. The samples were allowed to warm as data was collected. Fig. 1 shows a diagram of the mounting components.

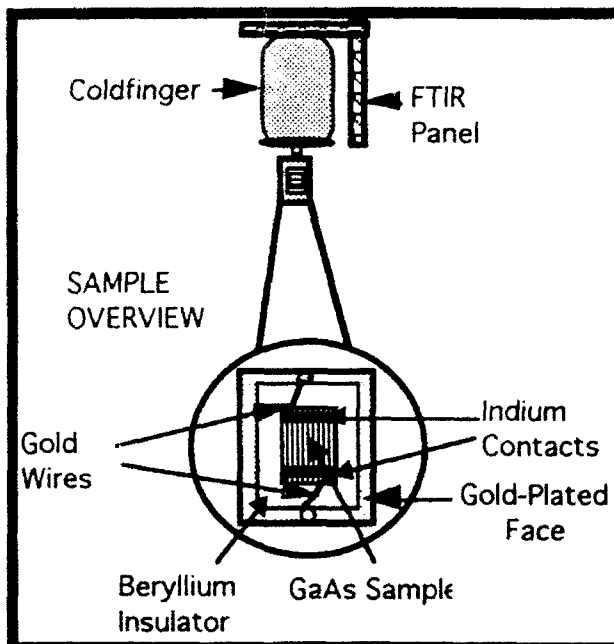


FIG. 1 A schematic drawing of a typical sample set-up.

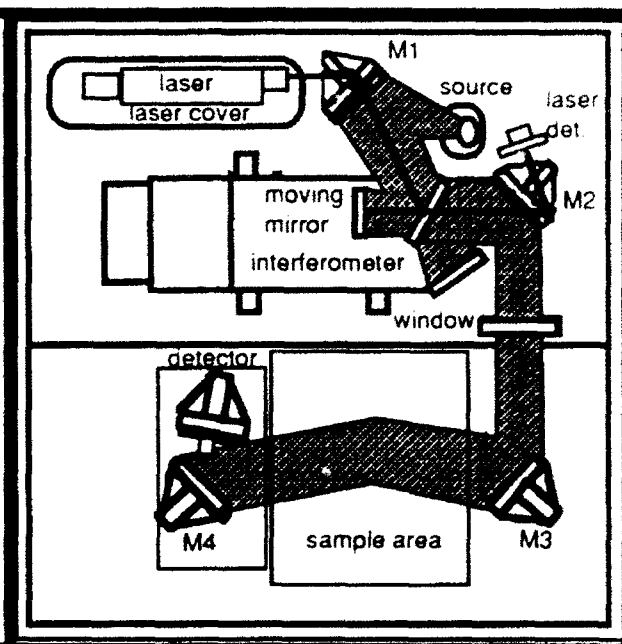


FIG. 2 Optical layout of the FTS-60V Spectrometer. [From "FTS-40V and FTS-60V Users Manual. #091-0410". Digilab. p7.]

The spectral photoresponses were performed on a Digilab model FTS-20CVX mid infrared Fourier Transform Spectrometer. The FTIR consists of two chambers, a sample chamber and an optics chamber. The schematic of the FTIR chambers is shown in Fig. 2. The sample chamber holds the sample and the infrared detector. However, in photoconductivity experiments, the sample, not the infrared detector, serves as the device that measures the signal. The optics chamber has two radiation sources, a laser beam and a high-temperature ceramic light source. The laser beam determines the location of the moving mirror by counting the number of laser wavelengths the mirror has moved from its starting position. The high-temperature ceramic light source provides the broad band of infrared wavelengths used to determine the interferogram. This source light is split into two beams by a beam splitter. One beam is directed toward a stationary mirror, the other is directed toward a moving mirror. A diagram of these paths is shown in



Fig. 3. When the stationary mirror and the moving mirror are equidistant from the beam splitter, the two infrared

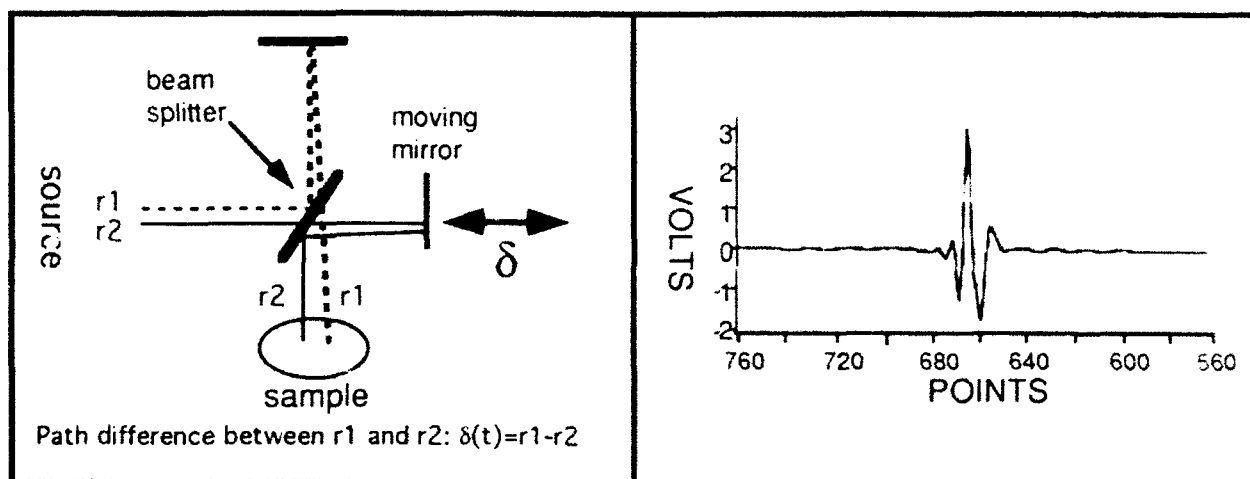


FIG. 3 The necessary paths taken by the photons in order to create an interferogram.

FIG. 4 A graph of the source light interferogram at 660 arbitrary points from where the moving mirror began its scaling.

beams will be in phase and constructive interference will occur. When the two beams are  $1/2$  wavelength out of phase, destructive interference occurs. So as the moving mirror constantly changes the optical path length, the two beams recombine creating a resultant beam with varying intensity. The difference in path intensities, determined by the rapidly changing wavelength, is the basis of the interferogram theory. An example interferogram (intensity in volts vs. points) is shown in Fig. 4.<sup>3</sup> The interferogram is fast-fourier transformed by a computer to produce a spectrum of intensity versus wavelength. In photoconductivity, these increases in intensity are due to increases in the electrical conductivity of a material induced by photo-excitation. For *n*-type and semi-insulating GaAs, electrons are excited by infrared radiation from the ground state of the defect level to the conduction band where these additional electrons change the conductivity of the material. The increased conductivity yields an increase in the measured signal, or photoresponse, of the sample. The resulting spectrum of the sample's photoresponse provides information on the presence of impurities and/or defects. A diagram of a photoresponse spectrum is shown in Fig. 5.

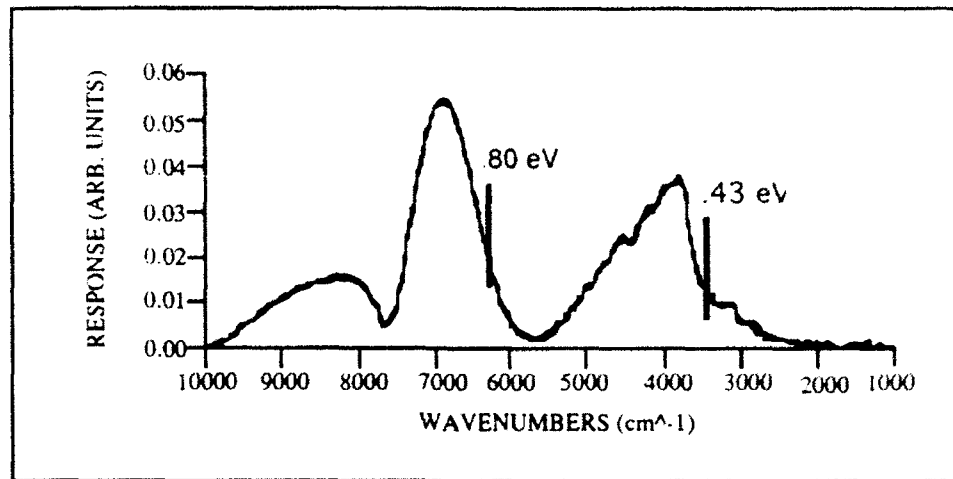


Fig. 5 A typical photoresponse spectrum for GaAs materials.

## RESULTS

Semi-insulating and *n*-type GaAs samples were studied in order to optically characterize them through the use of spectral photoconductivity. From the photoconductivity spectrum, we observed a strong photoresponse from the deeper energy levels at 0.80 eV as well as 0.43 eV (see Fig. 5). In order to further characterize these materials, the temperature dependence of the two dominate defect levels was studied. The temperature dependence results for over ten GaAs samples indicates that the relative photoresponse is dependent on the particular sample and the temperature. A wide variety of intensity versus temperature graphs were observed with little similarity. However, most samples exhibit a simultaneous decrease in the entire photoresponse spectrum between 130 K and 170 K. Spectral photoresponses for the same sample at 131 K and 148 K are shown in Fig. 6, where the simultaneous decrease of the photoresponse for the entire spectrum is clearly evident. As expected, the 6800 ( $E_j=0.80$  eV) and 3680 ( $E_j=0.43$  eV) peaks decrease at the same rate during the temperature range of 130 K to 170 K. The temperature dependence of the dominate defect levels shown in Fig. 7 clearly shows both defect levels experiencing a decrease in photoresponse between the temperature range of 130 K to 170 K. The decrease in photoresponse cannot be attributed to thermal ionization since both peaks have a high activation energy. At these temperatures, the thermal energy is unable to excite the electrons from the energy levels associated with the 6800 and 3680 defect levels to the conduction band. This unexpected decrease indicates that at these temperatures, another intrinsic defect level is activated which traps free electrons causing a universal reduction in photoresponse.

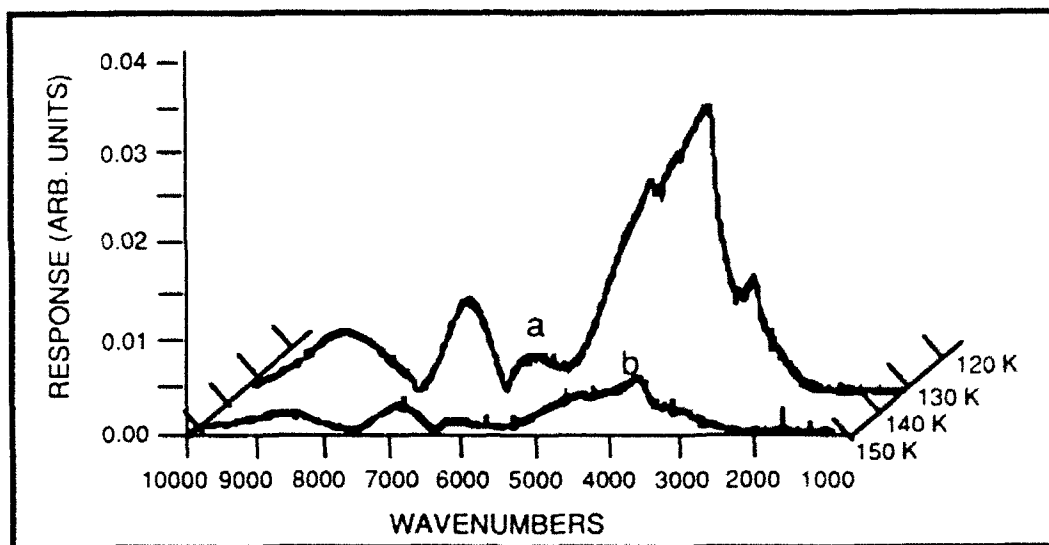


Fig. 6 A graph of the spectral photoresponses at a=131 K, b=148 K.

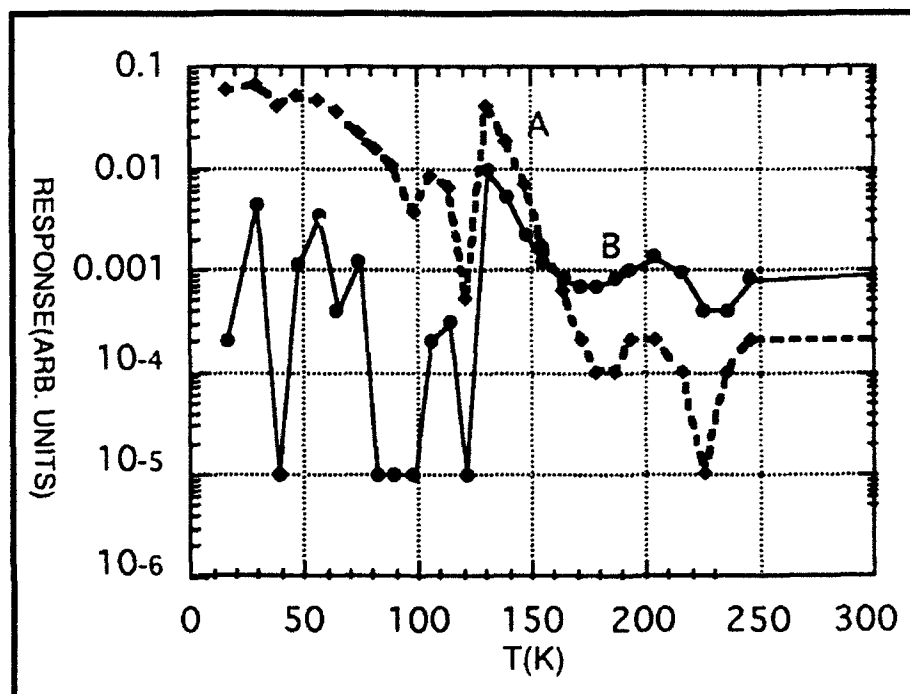


Fig.7 Temperature dependence of the two dominate defect levels: (A)  $\approx 0.43$  eV (B)  $\approx 0.80$  eV.

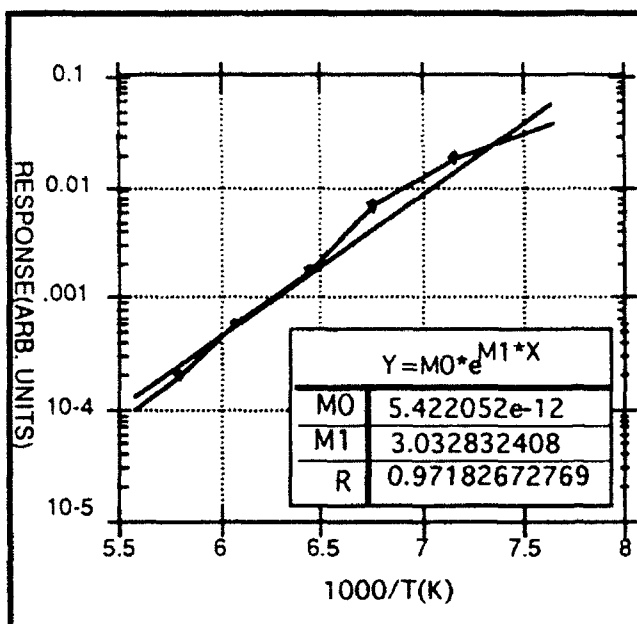


Fig. 8 A graph of the temperature dependence of a semi-insulating GaAs between 130 K and 170 K. A slope of 3.03 was calculated which yields an activation energy of .26 eV.

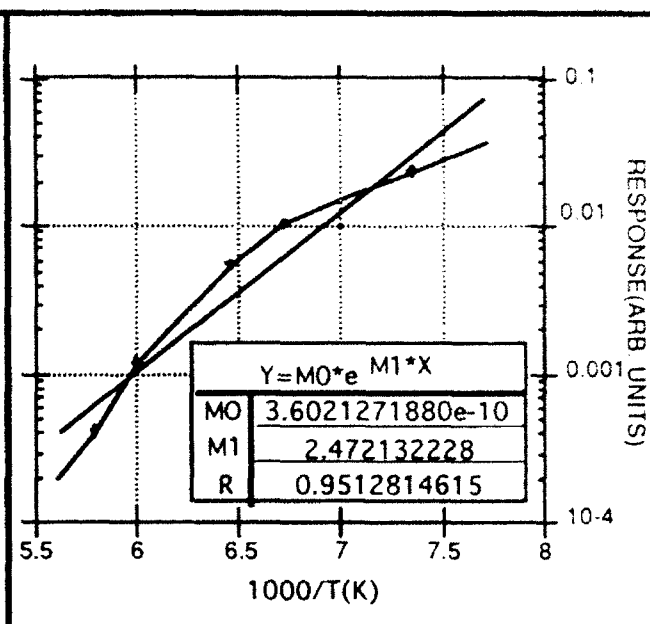


Fig. 9 A graph of the temperature dependence of n-type GaAs between 130 K and 170 K. A slope of 2.47 was calculated which yields an activation energy of .21 eV.

To better analyze this trap, we plotted the photoresponse at the defect levels versus  $1000/T(K)$  for the temperatures between 130 K and 170 K in order to determine the activation energy of the trap. Typical activation energy graphs are shown in Fig. 8 and Fig. 9. A slope was calculated which enabled us to mathematically determine the activation energy of the trap. For the thirteen samples analyzed, the calculated slopes were clustered into two groups. One group had an average slope of 2.12, the other group averaged 2.92. The activation energies associated with these two sets of slopes were calculated to be  $0.18 \pm .03$  eV and  $0.25 \pm .03$  eV. Intrinsic defects with these activation energies have been reported previously for GaAs materials.<sup>4-5</sup> This activation energy would correspond to 1450 and 2015 wavenumbers. For some of the samples studied, photoresponses were observed in the spectrum between 1450 and 2015 wavenumbers. To see if this optically active level was related to the trapping level, comparisons were made between the magnitude of the slope value and the presence of any photoresponse between 1450 and 2015 wavenumbers ( $E_i=0.18$  eV and  $E_i=0.25$  eV). No correlations were discovered, however correlations between other material properties are currently being investigated.

## CONCLUSIONS

A study of the temperature dependence of the photoresponse of the two dominate intrinsic defect levels, the 6800 ( $E_i=.80$  eV) and 3680 ( $E_i=.43$  eV) peaks, of GaAs by Fourier transform photoconductivity has been made. Spectral photoconductivity results confirm that the magnitude of the photoresponse is highly dependent on the sample temperature. The temperature dependence data indicates that the photoresponse of the entire spectrum, including the

two defect levels, decreases in the temperature range of 130 K to 170 K. This unexpected decrease was attributed to a trapping level. Furthermore, we identified this trapping mechanism by calculating its activation energy from the slope of photoresponse versus  $1000/T(K)$  graphs. The slope values clustered into two distinct groups with an average slope of 2.12 and 2.92, respectively. Depending on these slopes, the trapping level has an activation energy of .18 eV or .25 eV. Correlations between the presence of photoresponse between 1450 and 2015 wavenumbers and the magnitude of the slope were unsuccessful. However other correlations relating to properties of the material are being investigated.

#### ACKNOWLEDGEMENTS

I am pleased to recognize the technical, literary, and research assistance of Gail J. Brown. I would also like to acknowledge the Electronic and Optics Materials Branch of the Materials Directorate, especially Dr. Patrick Hemenger, for their support and encouragement of my research. My research was sponsored and funded by the Air Force Office of Scientific Research.

#### REFERENCES

1. G.J. Brown and W.C. Mitchel, Materials Research Society Symposium Proceedings, 163, 157(1989).
2. W.C. Mitchel, G.J. Brown, and Laura S. Rea, J. Appl. Phy. 71, 246 (1992).
3. Ann Maack, "Construction of an Optical Waveguide Between a Superconductive Magnet Dewar and a Fourier Transform Spectrometer", 7-10.
4. D.C. Look, D.C. Walters, and J.R. Meyer, Solid St. Comm. 42, 745 (1982).
5. A.L. Lin and R.H. Bube, J. Appl. Phys. 47, 1867 (1976).

SOFTWARE DEVELOPMENT FOR THE AEROSOL TEST CHAMBER

James E. Youngblood  
High School Apprentice  
Fuzes Branch

Wright Laboratory Armament Directorate  
WL/MNMF  
Eglin Air Force Base, FL 32542-5434

Final Report for:  
High School Apprenticeship Program  
Wright Laboratory Armament Directorate

Sponsored by:  
Air Force Office of Scientific Research  
Bolling Air Force Base, Washington, D.C.

August 1992

## SOFTWARE DEVELOPMENT FOR THE AEROSOL TEST CHAMBER

James E. Youngblood  
*High School Apprentice*  
Fuzes Branch  
Wright Laboratory Armament Directorate

### Abstract

My summer project was to help in the creation of an aerosol chamber that would be used to test optical fuze sensors. I was involved in some of the hardware construction as well as writing the software that will control all of the components. This software was developed using C along with a PC I/O board and LabWindows. The program implements a graphical user interface and, therefore, should be easy to operate. The chamber is still having the final wiring done (at the time of the writing of this paper), but the software controller is finished (although probably not bug free).

## SOFTWARE DEVELOPMENT FOR THE AEROSOL TEST CHAMBER

James E. Youngblood

### INTRODUCTION/DISCUSSION OF PROBLEM

Fuze sensors are currently tested in simulated real-world conditions by using filters or mathematical equations. The filters work well when just testing the power of light that would be reflected by the target through the aerosol; however, they do not consider the light that is reflected off of the aerosol particles back to the sensor. The mathematical testing does a little better but still can not emulate the real-world situations that occur in the operating environment of a fuze.

The solution to testing the optical fuze sensors would be to create a real aerosol inside of a controlled environment. We are creating an aerosol test chamber (see Appendix for diagram) which not only does that but does it automatically. It will be unique (no one else has one similar), because it will be completely computer controlled and will have the ability to run repeatable tests. All the user will have to do is tell the computer what shape of aerosol he/she desires and the software and I/O board combination will do the rest. A controllable pump will be used spray fog oil/diesel fuel on the heater to create the aerosol cloud. The cloud will then be moved down an 18 meter tube by a fan, also controlled by the software. There are fifty sensors (0.3 meters apart) along the tube to test the aerosol density at each location (to ensure that the aerosol profile in the tube is the same as the one the user desired for the test). The fuze sensor will be placed at the end of the tube, and a target will be put close to the front. We can then simulate a cloud moving at a very high relative speed by slowing down the timing of the fuze sensor. The aerosol's desired and actual profiles will be graphed on a monitor real-time as well as recorded on disk for later review.

### METHODOLOGY

After troubleshooting and installing LabWindows onto an IBM AT, I began experimenting with the LabWindows environment, an AT-MIO-16F-5 I/O board (from National Instruments) that was in the computer, and other control hardware that was available. This other hardware included an SC-2062 relay board (to control equip-



ment power), AMUX-64T multiplexer (to connect to the fifty sensors), and SC-2050 connector board (to connect them all together). (All of these boards as well as the LabWindows program were from National Instruments.) Using these boards and LabWindows, I was to write software for controlling a pump, a heater, and a fan, along with collecting data from fifty sensors, a thermocouple, and an emergency shut down switch.

My tasks this summer would include:

1. Manufacturing the case where the boards will be placed, including drilling holes for the cables to be run through.
2. Learning the LabWindows operating environment.

And coding for:

3. Data acquisition from the fifty sensors into arrays that could be manipulated by the software.
4. Graphical User Interface, including graphs of the desired and actual aerosol profiles, indication of equipment faults, and an entry system for the user to easily tell the computer what aerosol is desired.
5. Saving the aerosol data to disk.
6. The error correction of the motion and thickness of the aerosol (to ensure that the aerosol profile would be accurate).

Here I will explain these tasks in more detail:

1. The case that is to be mounted in the bay where the chamber resides was to contain all of the boards used to control the aerosol chamber. It needed a slot for the ribbon cable to be connected to the I/O board in the PC, and 64 cable holes with rubber grommets in them to run the 50 sensor cables through, a thermocouple input, and some relay power wires, as well as a little room for expansion/upgradeability.
2. I basically learned the LabWindows environment as I went along. However, a basic understanding was required from the start of what the environment could do for me and how. This information was found fairly easily by reading the manual and making a few quick programming attempts.
3. The data acquisition was handled by the I/O board through a four to one multiplexer. The multiplexer was required because the I/O board only has the capability to process 16 inputs and we needed 50 just for the sensors

themselves. The software was required to acquire the sensor data (the aerosol profile) at least once every second for graphing and correction purposes. This required some optimization of the code but did not turn out to be a serious problem.

4. A Graphical User Interface was required to display the graphs of the desired and actual aerosol profiles. The interface asks the user for the desired aerosol (either a custom designed one or one that I had already programmed in), and shows him/her what it looks like to confirm that it is indeed what the user desired. The program then initializes all equipment and waits for the user to tell it to start the test. After the user initiates the test, the interface is used to show the graphs of the profiles, progress of the test, and any problems that have occurred.

5. The aerosol profile data with a time tag is saved to disk once per second regardless of how many samples have occurred in that amount of time. This ensures the save file structure regardless of the speed of the computer that the software is running on. The file created can be used for future reference to see what might have gone wrong, or improve the software in some way. However, the main use of this data file will be by the people who want to compare what their fuze sensor was reading to what was actually in the chamber.

6. The data from the sensors is put in an array, which is called Actual (what the sensors are actually reading). The calculated data of what the aerosol should be reading at each location (based on the desired profile) is in an array called Expected. Therefore, if all goes well, the aerosol density stored in Actual should be equal to the aerosol density stored in Expected at all fifty of the sensor locations. We had to allow for problems that could occur, though. Problems that we knew would come about, especially since this system has never been operated before (so we don't know exact settings for the equipment) and no one else has a similar aerosol chamber for a reference.

I thought about possible things that could go wrong in the aerosol chamber:

First the pump may not be putting out the right amount of fuel to the heater. This could be the result of dust or dirt in the nozzle (or it just doesn't pump like it should). This would result in an aerosol that was lower everywhere or higher everywhere (in density) than the desired one (see Appendix). I wrote a routine that would check a sample of the Expected array and compare it to the same sample in the Actual array and determine a multiplier to be used when sending the pump its speed. For example, if the aerosol were only  $4/5$  (or 80 percent) of what it should be then I would multiply the next pump command by  $5/4$ . I also had to keep track of the previous multi-

plier since it needed to be taken into account the next time the pump rate is checked. Also the algorithm adjusts less and less harshly as the test goes on and, therefore, should not overcompensate.

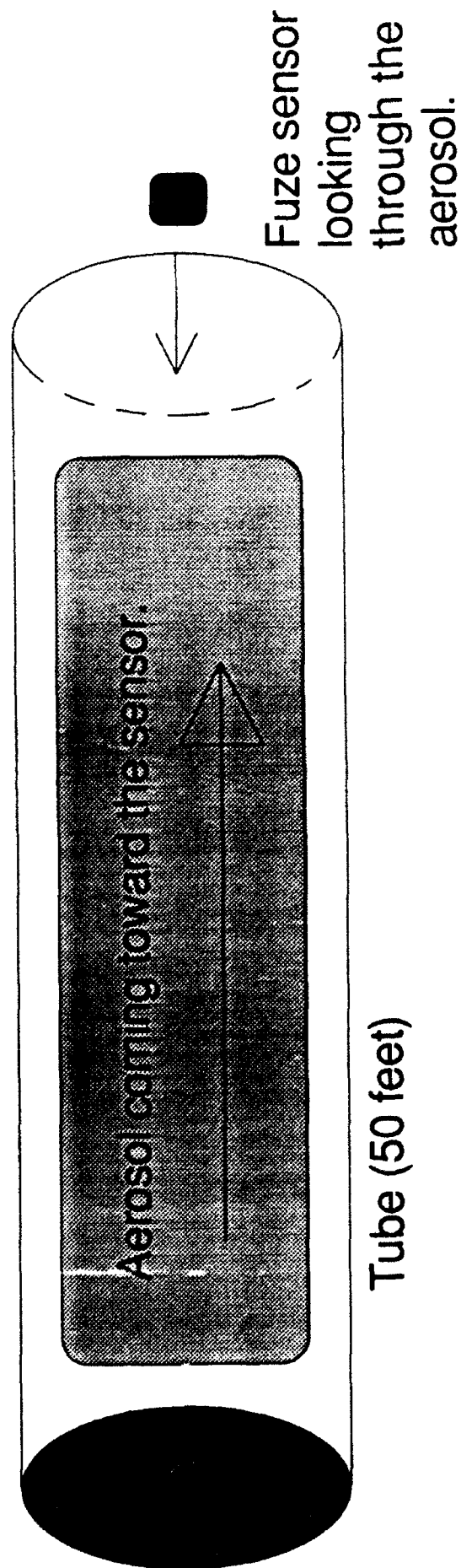
Second, I thought about if the fan were going at an incorrect rate. This would cause the aerosol to be crunched or spread out in the tube (see Appendix). I wrote an algorithm that would check a certain point on the aerosol that it can locate in both the Expected and Actual sensor readings and adjust the fan speed accordingly, once again using a multiplier.

### RESULTS/CONCLUSIONS

The Aerosol Project is still going together. The cables still need to be run from where the computer setup will be to where the sensors are running down the chamber. (This includes over 1200 meters of cable.) The software is completed but has not yet been tested with the actual Aerosol Chamber, so I am sure that there are many bugs yet to be worked out. I learned a lot about the value of commenting my code and am sure that those who will be working with the software that I have written after I leave will be appreciative. I am overjoyed by the standardization of things like GPIB and RS-232. At least the computer industry can agree on a FEW things. I gained the experience of working with engineers and have been able to better see what they really do. Since I believe that I will one day become an engineer, I found that to be especially important. Everyone was helpful. Overall, I had an enjoyable and productive summer.

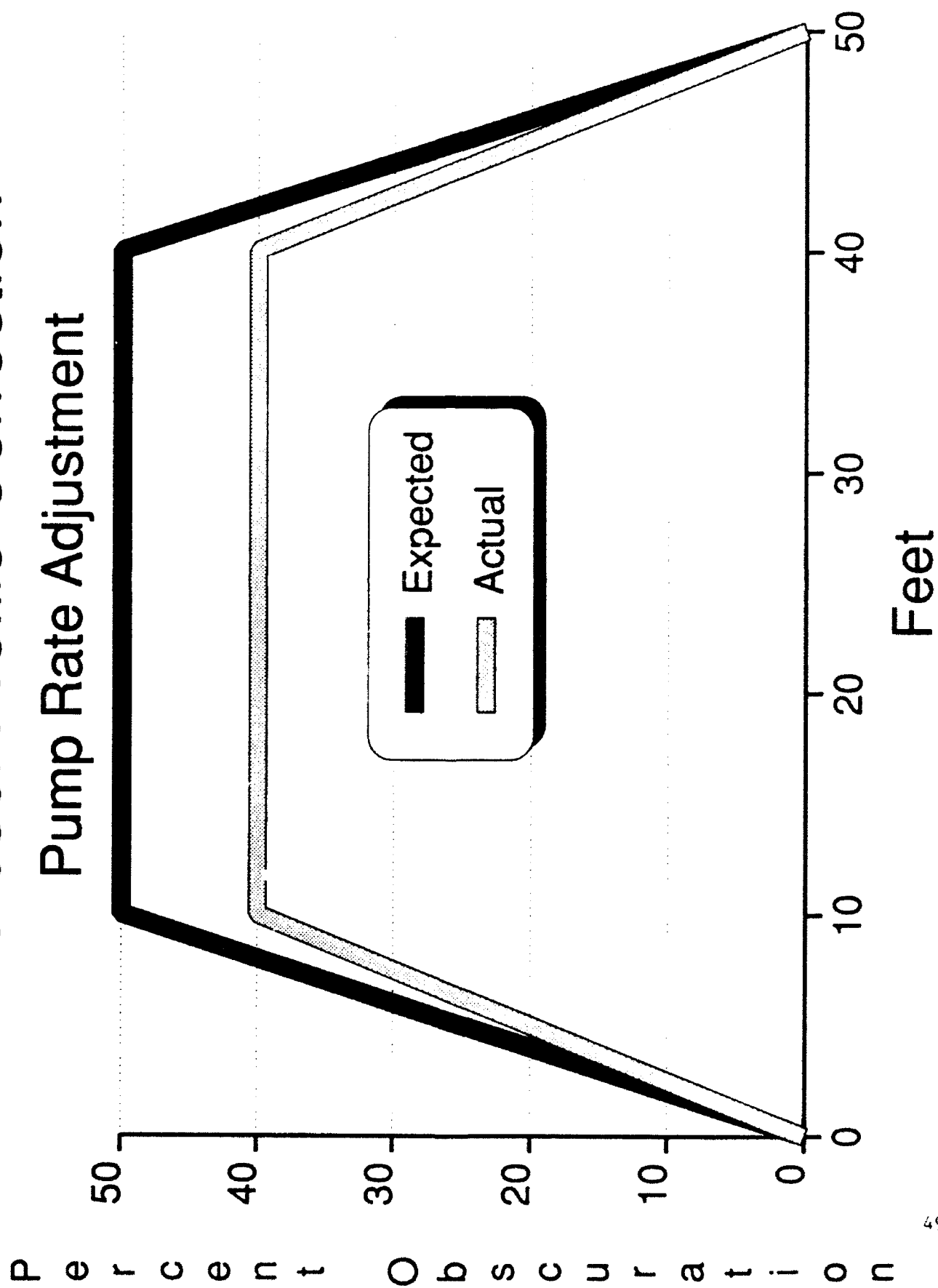
## **APPENDIX**

# Proposed Aerosol Test Chamber

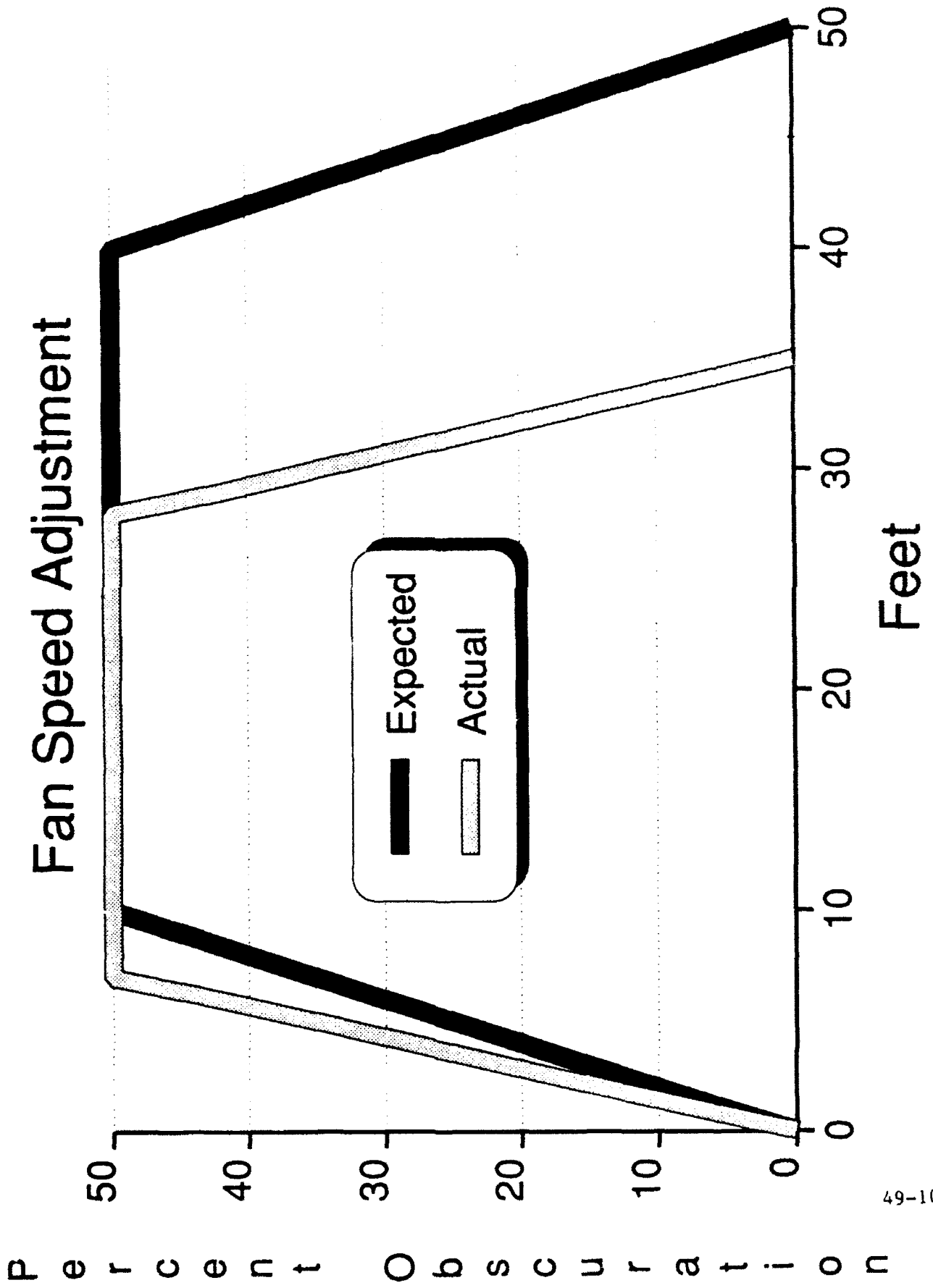


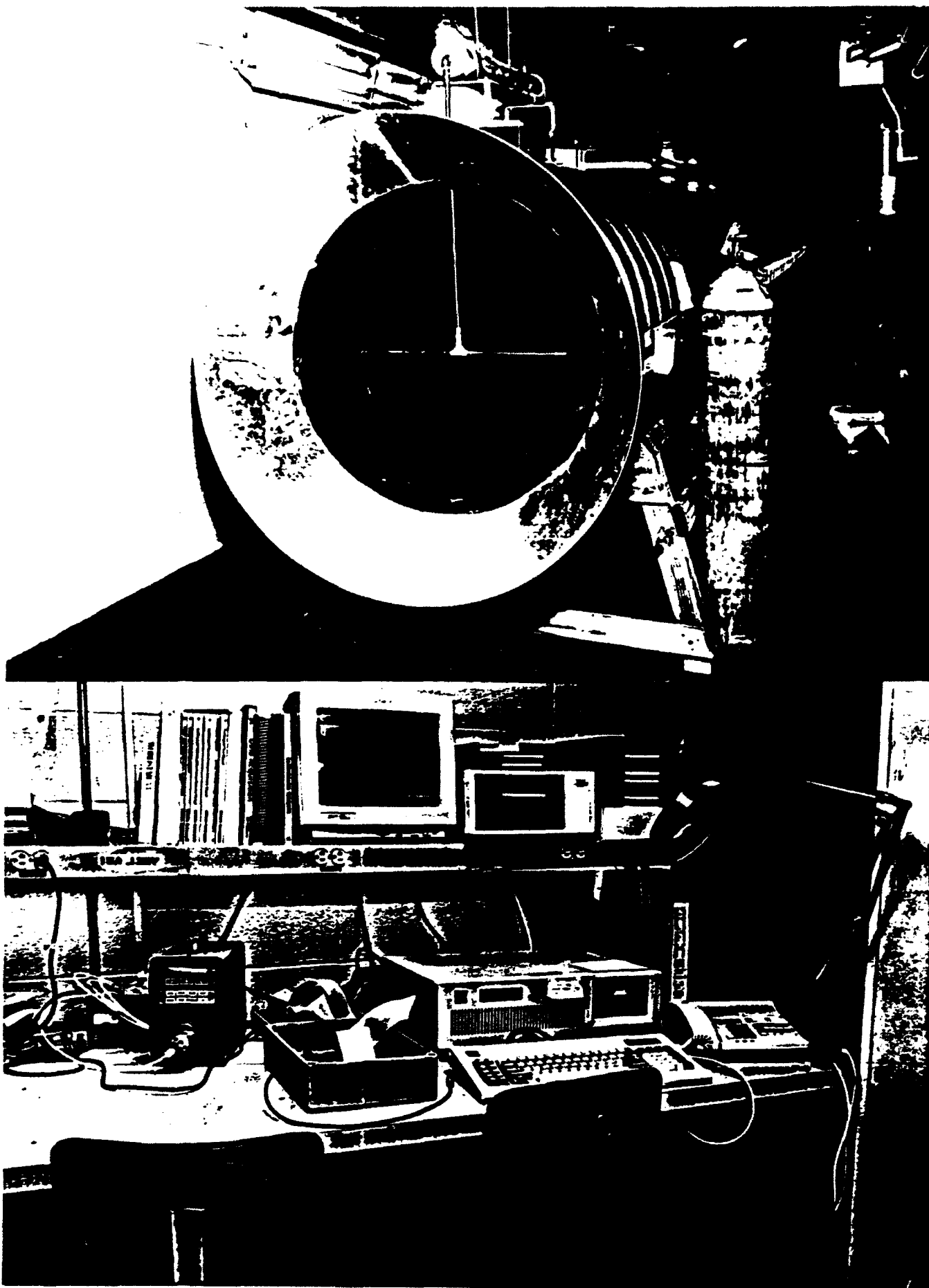
# Aerosol Profile Correction

## Pump Rate Adjustment



# Aerosol Profile Correction





Top: A picture of the Aerosol Chamber. Bottom: The computer that will control it.